FAT METABOLISM AND DEPOSITION IN POULTRY: PHYSIOLOGY, GENETICS, NUTRITION AND INTERDISCIPLINARY RESEARCH, VOLUME I

EDITED BY: Jie Wen, Sami Dridi and Elizabeth Ruth Gilbert

PUBLISHED IN: Frontiers in Physiology

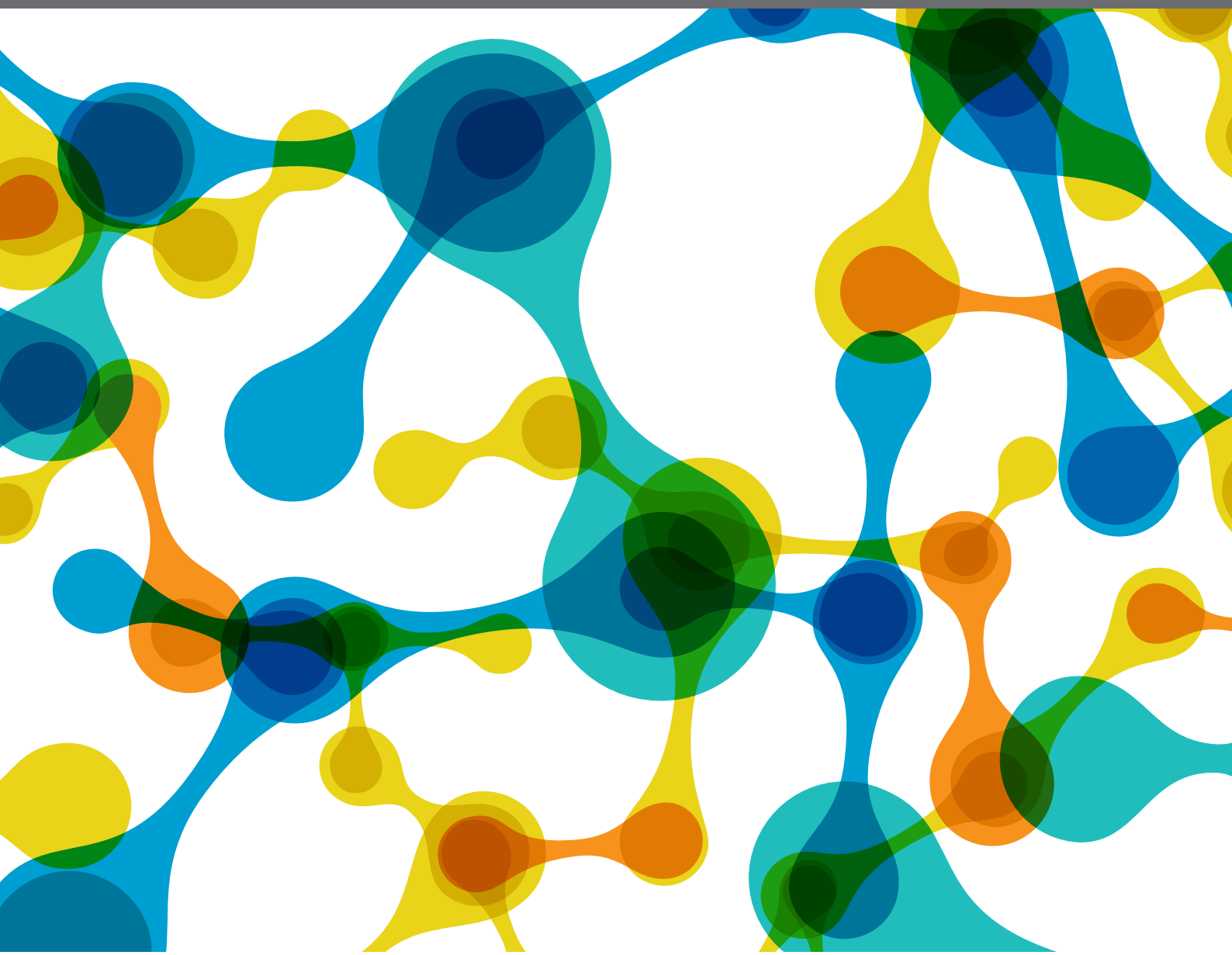

frontiers Research Topics

ISSN 1664-8714
ISBN 978-2-88976-421-1
DOI 10.3389/978-2-88976-421-1

About Frontiers

Frontiers is more than just an open-access publisher of scholarly articles: it is a pioneering approach to the world of academia, radically improving the way scholarly research is managed. The grand vision of Frontiers is a world where all people have an equal opportunity to seek, share and generate knowledge. Frontiers provides immediate and permanent online open access to all its publications, but this alone is not enough to realize our grand goals.

Frontiers Journal Series

The Frontiers Journal Series is a multi-tier and interdisciplinary set of open-access, online journals, promising a paradigm shift from the current review, selection and dissemination processes in academic publishing. All Frontiers journals are driven by researchers for researchers; therefore, they constitute a service to the scholarly community. At the same time, the Frontiers Journal Series operates on a revolutionary invention, the tiered publishing system, initially addressing specific communities of scholars, and gradually climbing up to broader public understanding, thus serving the interests of the lay society, too.

Dedication to Quality

Each Frontiers article is a landmark of the highest quality, thanks to genuinely collaborative interactions between authors and review editors, who include some of the world's best academicians. Research must be certified by peers before entering a stream of knowledge that may eventually reach the public - and shape society; therefore, Frontiers only applies the most rigorous and unbiased reviews.
Frontiers revolutionizes research publishing by freely delivering the most outstanding research, evaluated with no bias from both the academic and social point of view. By applying the most advanced information technologies, Frontiers is catapulting scholarly publishing into a new generation.

What are Frontiers Research Topics?

Frontiers Research Topics are very popular trademarks of the Frontiers Journals Series: they are collections of at least ten articles, all centered on a particular subject. With their unique mix of varied contributions from Original Research to Review Articles, Frontiers Research Topics unify the most influential researchers, the latest key findings and historical advances in a hot research area! Find out more on how to host your own Frontiers Research Topic or contribute to one as an author by contacting the Frontiers Editorial Office: frontiersin.org/about/contact

FAT METABOLISM AND DEPOSITION IN POULTRY: PHYSIOLOGY, GENETICS, NUTRITION AND INTERDISCIPLINARY RESEARCH, VOLUME I

Topic Editors:
Jie Wen, Institute of Animal Sciences, Chinese Academy of Agricultural Sciences, China
Sami Dridi, University of Arkansas, United States
Elizabeth Ruth Gilbert, Virginia Tech, United States

Citation: Wen, J., Dridi, S., Gilbert, E. R., eds. (2022). Fat Metabolism and Deposition in Poultry: Physiology, Genetics, Nutrition and Interdisciplinary Research, Volume I. Lausanne: Frontiers Media SA. doi: 10.3389/978-2-88976-421-1

Table of Contents

frontiers | Frontiers in Physiology

EDITORIAL
published: 26 May 2022
doi: 10.3389/fphys.2022.937081

Editorial: Fat Metabolism and Deposition in Poultry: Physiology, Genetics, Nutrition and Interdisciplinary Research, Volume I

Sami Dridi[1]*, *Craig W. Maynard*[1], *Jie Wen*[2] and *Elizabeth R. Gilbert*[3]

[1]Center of Excellence for Poultry Science, University of Arkansas, Fayetteville, AR, United States, [2]Institute of Animal Sciences, Chinese Academy of Agricultural Sciences, Beijing, China, [3]Department of Animal and Poultry Sciences, Virginia Tech, Blacksburg, VA, United States

Keywords: fat metabolism, chickens, avian, nutrition, omics

Editorial on the Research Topic

Fat metabolism and deposition in Poultry: Physiology, Genetics, Nutrition and Interdisciplinary Research, Volume I

The intensive genetic selection of broiler (meat-type) chickens over the past 80 years has focused narrowly on economically important traits, namely growth rate, feed efficiency, and breast yield (Griffin and Goddard, 1994). Although this has led to spectacular progress in term of productivity and profitability which helped in supporting the livelihoods and food security of billions of people worldwide, there are several unexpected and undesirable changes, including hyperphagia (Denbow, 1994), metabolic disorders such as leg problems (Julian, 1998), breast muscle myopathies (Velleman, 2015), cardiovascular diseases (Olkowski, 2007), and fat deposition (Chen et al., 2017).

Growth rates have dramatically increased by over four times between 1957 and 2005 (Zuidhof et al., 2014) and modern chickens reach the market age in less than half the time that would have taken 60 years ago. This change is associated with hyperphagia and excessive fat deposition mainly in broiler breeders that require feed restriction and feed regimens (de Jong et al., 2002). In broiler breeders, obesity compromises reproductive functions and sexual activity, and thereby alters performance and welfare (De Jong and Guémené, 2011). On the other hand, feed restriction causes chronic hunger, stress, frustration, aggressiveness, cannibalism, and boredom (Decuypere et al., 2010). In commercial broilers, fat deposition reduces meat yield, feed efficiency, and alters meat quality, which all together results in profit margin loss (Lippens et al., 2000).

Generally fat deposition originates from exogenous (diet) and/or endogenous (adipogenesis/lipogenesis) sources. As commercial broilers are fed lipid-poor diets (<10%), the majority of the accumulated fat is derived from the liver, which is the main site for *de novo* lipogenesis (Goodridge and Ball, 1967; Leveille et al., 1968; Yeh and Leveille, 1971). Fat metabolism is modulated through a tight interaction between synthesis and degradation programs, which both are controlled by exogenous factors (diet, environment, etc.,) and endogenous complex molecular mechanisms and pathways that are not fully defined in avian species. In the Research Topic, we invited experts in their fields and gathered outstanding and elegant reviews, case reports, and breakthrough research articles to provide new insights into fat metabolism of various avian species (chickens, quails, ducks) at peripheral and central levels from different, yet complementary disciplines (physiology, genetics, and nutrition).

At the central level, Kato et al. showed that two-week intracerebroventricular infusion of neurosecretory protein GM (NPGM) increased body mass, and the mass of abdominal and gizzard fat in chickens, without effects on feed intake. At molecular levels, they showed that NPGM might induce hepatic fat deposition via down regulation of the hepatic PPARα gene expression.

Edited and reviewed by:
Sandra G. Velleman, The Ohio State University, United States

***Correspondence:**
Sami Dridi
dridi@uark.edu

Specialty section:
This article was submitted to Avian Physiology, a section of the journal Frontiers in Physiology

Received: *05 May 2022*
Accepted: *09 May 2022*
Published: *26 May 2022*

Citation:
Dridi S, Maynard CW, Wen J and Gilbert ER (2022) Editorial: Fat Metabolism and Deposition in Poultry: Physiology, Genetics, Nutrition and Interdisciplinary Research, Volume I. Front. Physiol. 13:937081. doi: 10.3389/fphys.2022.937081

At the peripheral level, the Bonnefont group has used a high throughput metabolomics approach to identify hepatic biomarkers for Foie Gras quality in duck. A total of eighteen quality-associated metabolite signatures were determined, with five specific to liver weight and four specific for technological yield at cooking. Massimino et al., on the other hand, used high throughput real-time quantitative PCR to determine the effect of embryonic thermal manipulation on the hepatic lipid and carbohydrate metabolism, stress, cell proliferation, and thyroid hormone pathways in mule ducks. They identified several key genes that might be involved in thermal long-term programming of hepatic metabolism. Surugihalli et al. used mass spectrometry-based metabolomics to evaluate the rapid remodeling of hepatic mitochondrial and cytoplasmic networks in chicken E18 embryo and d3 post-hatch chicks. Several metabolites were profiled in both plasma and liver showing a transition from lipid oxidation in embryonic liver to *de novo* lipogenesis in neonatal liver. Using forced molting laying hens, cecal metabolomics, and liver transcriptomics, Ruirui (abstract only) identified regulatory intestinal-liver lipid metabolism factors affecting reproductive performance in laying hens.

In adipose tissue, Zhao et al. determined the developmental changes of adipocyte differentiation, lipid synthesis, lipolysis, fatty acid β-oxidation, and lipid content from chicken embryo day 12 to day-9 post hatch. They showed that the mitochondrial copy number and fatty acid β-oxidation increased during the post hatch period, indicating that subcutaneous adipose tissue plays an important role in energy supply. Sun et al. used the Iso-Seq technology and identified several long non-coding RNA and alternative splicing in abdominal and subcutaneous adipose tissues of pekin ducks. Na et al. reported several reference genes for real-time quantitative PCR in chicken adipose tissue and adipocytes. Kim et al. determined the effect of *in ovo* injection of different doses of all-trans retinoic acid on quail embryonic adipogenesis. They found that all-trans retinoic acid promoted hypertrophic fat accretion in quail embryos via upregulation of PPARγ and FABP4 and down regulation of Dlk1. The Gilbert group studied the effect of dietary baicalein supplementation on adipose tissue gene expression profiles during the first week post hatch in chickens. They showed a reduction of growth performance (body weight, feed intake), breast muscle weight, and subcutaneous and abdominal fat weights along with a modulation of several genes involved in adipogenesis and fat storage. In a separate paper, the Cline group reviewed the effects of dietary flavonoids on lipid metabolism in liver, skeletal muscle, and adipose tissue of poultry species. Finally, Kim and Voy provided a thorough review associated with the beneficial effects of n-3 polyunsaturated fatty acids in reducing fat accretion in poultry.

In summary, the papers within the current Research Topic provide new insights and discoveries related to lipid metabolism in various avian species (chicken, quail, and duck) and suggest some solutions and perspectives for future investigations aiming to reduce fat accretion in poultry. It is my fervent hope that this ebook and the Research Topic is a great resource for the readers, and we look forward to a second volume to expand more research and knowledge associated with other molecular pathways of lipid metabolism in various other avian species.

AUTHOR CONTRIBUTIONS

All authors listed have made a substantial, direct, and intellectual contribution to the work and approved it for publication.

REFERENCES

Chen, C. Y., Huang, Y. F., Ko, Y. J., Liu, Y. J., Chen, Y. H., Walzem, R. L., et al. (2017). Obesity-associated Cardiac Pathogenesis in Broiler Breeder Hens: Development of Metabolic Cardiomyopathy ,. *Poult. Sci.* 96 (7), 2438–2446. doi:10.3382/ps/pex016

De Jong, I. C., and Guémené, D. (2011). Major Welfare Issues in Broiler Breeders. *World's Poult. Sci. J.* 67, 73–82. doi:10.1017/s0043933911000067

de Jong, I. C., Voorst, S. V., Ehlhardt, D. A., and Blokhuis, H. J. (2002). Effects of Restricted Feeding on Physiological Stress Parameters in Growing Broiler Breeders. *Br. Poult. Sci.* 43 (2), 157–168. doi:10.1080/00071660120121355

Decuypere, E., Bruggeman, V., Everaert, N., Li, Y., Boonen, R., De Tavernier, J., et al. (2010). The Broiler Breeder Paradox: Ethical, Genetic and Physiological Perspectives, and Suggestions for Solutions. *Br. Poult. Sci.* 51 (5), 569–579. doi:10.1080/00071668.2010.519121

Denbow, D. M. (1994). Peripheral Regulation of Food Intake in Poultry. *J. Nutr.* 124 (8 Suppl. l), 1349S–1354S. doi:10.1093/jn/124.suppl_8.1349S

Goodridge, A., and Ball, E. (1967). Lipogenesis in the Pigeon: *In Vivo* Studies. *Am. J. Physiology-Legacy Content* 213 (1), 245–249. doi:10.1152/ajplegacy.1967.213.1.245

Griffin, H. D., and Goddard, C. (1994). Rapidly Growing Broiler (Meat-type) Chickens. Their Origin and Use for Comparative Studies of the Regulation of Growth. *Int. J. Biochem.* 26 (1), 19–28. doi:10.1016/0020-711x(94)90190-2

Julian, R. J. (1998). Rapid Growth Problems: Ascites and Skeletal Deformities in Broilers. *Poult. Sci.* 77 (12), 1773–1780. doi:10.1093/ps/77.12.1773

Leveille, G. A., O'Hea, E. K., and Chakrabarty, K. (1968). *In Vivo* lipogenesis in the Domestic Chicken. *Exp. Biol. Med.* 128 (2), 398–401. doi:10.3181/00379727-128-33022

Lippens, M., Room, G., De Groote, G., and Decuypere, E. (2000). Early and Temporary Quantitative Food Restriction of Broiler Chickens. 1. Effects on Performance Characteristics, Mortality and Meat Quality. *Br. Poult. Sci.* 41 (3), 343–354. doi:10.1080/713654926

Olkowski, A. A. (2007). Pathophysiology of Heart Failure in Broiler Chickens: Structural, Biochemical, and Molecular Characteristics. *Poult. Sci.* 86 (5), 999–1005. doi:10.1093/ps/86.5.999

Velleman, S. G. (2015). Relationship of Skeletal Muscle Development and Growth to Breast Muscle Myopathies: A Review. *Avian Dis.* 59 (4), 525–531. doi:10.1637/11223-063015-review.1

Yeh, Y.-Y., and Leveille, G. A. (1971). *In Vitro* and *In Vivo* Restoration of Hepatic Lipogenesis in Fasted Chicks. *J. Nutr.* 101 (6), 803–809. doi:10.1093/jn/101.6.803

Zuidhof, M. J., Schneider, B. L., Carney, V. L., Korver, D. R., and Robinson, F. E. (2014). Growth, Efficiency, and Yield of Commercial Broilers from 1957, 1978, and 2005. *Poult. Sci.* 93 (12), 2970–2982. doi:10.3382/ps.2014-04291

Conflict of Interest: The author declares that the research was conducted in the absence of any commercial or financial relationships that could be construed as a potential conflict of interest.

frontiers in Physiology

ORIGINAL RESEARCH
published: 14 May 2021
doi: 10.3389/fphys.2021.676864

Screening of Reference Genes for RT-qPCR in Chicken Adipose Tissue and Adipocytes

Wei Na[1,2,3,4†], Yuxiang Wang[1,2,3†], Pengfei Gong[1,2,3], Xinyang Zhang[1,2,3], Ke Zhang[1,2,3], Hui Zhang[1,2,3], Ning Wang[1,2,3] and Hui Li[1,2,3]*

[1] Key Laboratory of Chicken Genetics and Breeding, Ministry of Agriculture and Rural Affairs, Harbin, China, [2] Key Laboratory of Animal Genetics, Breeding and Reproduction, Education Department of Heilongjiang Province, Harbin, China, [3] College of Animal Science and Technology, Northeast Agricultural University, Harbin, China, [4] College of Animal Science and Technology, Hainan University, Haikou, China

Reverse transcription quantitative real-time PCR is the most commonly used method to detect gene expression levels. In experiments, it is often necessary to correct and standardize the expression level of target genes with reference genes. Therefore, it is very important to select stable reference genes to obtain accurate quantitative results. Although application examples of reference genes in mammals have been reported, no studies have investigated the use of reference genes in studying the growth and development of adipose tissue and the proliferation and differentiation of preadipocytes in chickens. In this study, GeNorm, a reference gene stability statistical algorithm, was used to analyze the expression stability of 14 candidate reference genes in the abdominal adipose tissue of broilers at 1, 4, and 7 weeks of age, the proliferation and differentiation of primary preadipocytes, as well as directly isolated preadipocytes and mature adipocytes. The results showed that the expression of the TATA box binding protein (*TBP*) and hydroxymethylbilane synthase (*HMBS*) genes was most stable during the growth and development of abdominal adipose tissue of broilers, the expression of the peptidylprolyl isomerase A (*PPIA*) and *HMBS* genes was most stable during the proliferation of primary preadipocytes, the expression of the *TBP* and *RPL13* genes was most stable during the differentiation of primary preadipocytes, and the expression of the *TBP* and *HMBS* genes was most stable in directly isolated preadipocytes and mature adipocytes. These results provide reference bases for accurately detecting the mRNA expression of functional genes in adipose tissue and adipocytes of chickens.

Keywords: reference gene, RT-qPCR, adipocytes, adipose tissue, broilers

OPEN ACCESS

Edited by:
Jie Wen,
Institute of Animal Sciences, Chinese Academy of Agricultural Sciences, China

Reviewed by:
Gale Strasburg,
Michigan State University, United States
Rie Henriksen,
Linköping University, Sweden

***Correspondence:**
Hui Li
lihui@neau.edu.cn

† These authors have contributed equally to this work

Specialty section:
This article was submitted to Avian Physiology, a section of the journal Frontiers in Physiology

Received: *06 March 2021*
Accepted: *20 April 2021*
Published: *14 May 2021*

Citation:
Na W, Wang Y, Gong P, Zhang X, Zhang K, Zhang H, Wang N and Li H (2021) Screening of Reference Genes for RT-qPCR in Chicken Adipose Tissue and Adipocytes. Front. Physiol. 12:676864. doi: 10.3389/fphys.2021.676864

INTRODUCTION

Gene expression analysis is an important tool in investigating functional genes. Due to the advantages of simple operation, high sensitivity and good repeatability, reverse transcription quantitative real-time PCR (RT-qPCR) has become the main method to detect gene expression levels (Bustin, 2000; Dheda et al., 2005). To reduce background errors caused by mRNA quality and reverse transcription efficiency (Lekanne Deprez et al., 2002; Sanders et al., 2014), correction factors are usually applied to correct, and standardize experimental results (Huggett et al., 2005;

Hendriks-Balk et al., 2007). The most commonly used correction factor is the reference gene. Reference genes are genes with stable expression levels that are not affected by research conditions and can be used to accurately quantify initial material loads (Dong et al., 2013). The ideal reference genes are stably expressed in all kinds of tissues and cells, and their expression is not influenced by the environment, experimental conditions, or other factors (de Jonge et al., 2007). However, a universal ideal reference gene does not exist (Huggett et al., 2005; Zhang et al., 2014). Even the most versatile reference genes, such as glyceraldehyde-3-phosphate dehydrogenase (*GAPDH*), beta-actin (*ACTB*) and 18S ribosomal RNA (*18S*), are unstable in certain cells, biological processes, or experimental conditions (Barroso et al., 1999; Bas et al., 2004; Ferguson et al., 2010; Stephens et al., 2011). Therefore, the selection of suitable reference genes that are stably expressed in a specific tissue, cell or biological process is very important to accurately quantify the expression level of functional genes.

The stability of reference genes generally requires verification by experiments combined with algorithm analysis. GeNorm is a statistical algorithm developed by Vandesompele et al. (2002) to analyze the expression stability of reference genes in RT-qPCR experiments. The algorithm determines stably expressed reference genes by comparing the *M* value which is defined the average of the pairwise variation of one gene with all the other potential reference genes. The geNorm algorithm can be used to compare and filter the stability of any number of reference genes under any experimental conditions. Additionally, the geNorm algorithm can determine the number of optimal reference genes in the experiment by calculating the ratio of paired variant V_n to V_{n+1}.

At present, the literature on the screening of RT-qPCR reference genes has focused on chicken liver, brain, muscle, heart, lung, ovaries, lymphoid organs, and chicken embryo fibroblasts (Yang et al., 2013; Bagés et al., 2015; Nascimento et al., 2015; Mitra et al., 2016; Staines et al., 2016; Katarzyńska-Banasik et al., 2017; Hassanpour et al., 2018; Simon et al., 2018). No reports have selected RT-qPCR reference genes in the growth and development of abdominal adipose tissue, primary preadipocytes, or mature adipocytes of chickens. Therefore, based on the usage frequency in the literatures on the screening of RT-qPCR reference genes in various tissues and cells of chickens and function of reference genes in the basic cellular processes, 14 commonly used reference genes were proposed as candidates: *ACTB*, tubulin beta class I (*TUBB*), hypoxanthine guanine phosphoribosyl transferase 1 (*HPRT1*), hydroxymethylbilane synthase (*HMBS*), TATA box binding protein (*TBP*), non-POU domain containing, octamer-binding (*NONO*), ribosomal protein L13 (*RPL13*), ribosomal protein S7 (*RPS7*), *18S*, peptidylprolyl isomerase A (*PPIA*), beta-2 microglobulin (β*2M*), tyrosine 3-monooxygenase/tryptophan 5-monooxygenase activation protein zeta (*YWHAZ*), *GAPDH*, and transferrin receptor (*TFRC*). The expression levels of these reference genes in broiler abdominal adipose tissue, the proliferation and differentiation of primary preadipocytes, as well as directly isolated primary preadipocytes and mature adipocytes were detected by RT-qPCR. The expression stability of these reference genes in the above tissues and cells was analyzed by GeNorm statistical algorithms. Finally, we confirmed the most suitable reference genes for detecting functional gene expression levels in broiler adipose tissue and adipocytes.

MATERIALS AND METHODS

Ethics Statement

The study was conducted according to the guidelines for the care and use of experimental animals established by the Ministry of Science and Technology of the People's Republic of China (approval no. 2006–398) and approved by the Institutional Biosafety Committee of Northeast Agricultural University (Harbin, China).

Animals and Tissues

The animals used in this study included 1-, 4-, and 7-week-old birds from generation 19 (G19) of Northeast Agricultural University broiler lines divergently selected for abdominal fat content (NEAUHLF; Guo et al., 2011). All birds were housed under similar environmental conditions with free access to feed and water.

The abdominal fat tissues from each individual male bird were collected and snap-frozen in liquid nitrogen and stored at −80°C for extraction of total RNA. A total of 30 male birds (five birds per line per time point) at 1, 4, and 7 weeks of age were used in this process.

Isolation of Chicken Preadipocytes and Mature Adipocytes

Chicken preadipocytes and mature adipocytes were isolated according to previously reported methods (Wang et al., 2017). Briefly, abdominal adipose tissue was collected from 10- to 14-day-old broilers by sterile dissection following rapid decapitation. Adipose tissue was washed with prewarmed PBS and cut into pieces. Tissue pieces were digested in medium (90 mL DMEM, 1.5 g BSA, and 2.383 g HEPES) containing type I collagenase (0.02 g/mL) for 65 min at 37°C with shaking once per 5 min. After digestion, the cell suspension was filtered through a 165-μm mesh and centrifuged at 2,000 rpm for 10 min at room temperature. The supernatant was collected and centrifuged at 4,000 rpm; the obtained cell precipitates were mature adipocytes. The protocell precipitate was resuspended in complete medium (DMEM/F12, 10% fetal bovine serum, 100 U/mL penicillin, and 100 μg/ml streptomycin) and filtered through a 20-μm mesh. After centrifugation at 2,000 rpm, the precipitates of stromal vascular cells (including preadipocytes) were collected. Some of the preadipocytes were used for gene expression analysis, some of which were seeded at a density of 1×10^6 cells/mL in complete medium and maintained in a humidified atmosphere with 5% CO_2 at 37°C for cell proliferation and differentiation detection.

Induced Chicken Preadipocyte Differentiation

When the confluence of chicken preadipocytes reached 50–60%, culture medium was replaced with an induction medium in

which the final concentration of oleate was 160 μM to induce preadipocyte differentiation. This time was recorded as 0 h. The differentiated preadipocytes were harvested at the following times:12, 24, 48, 72, and 96 h. Three wells of cells were collected at each time point for biological repeats. In the induction process, the induction medium was changed every 24 h.

Staining and Measurement of Lipid Droplet

Lipid droplets were stained with oil red O (Sigma) according to Wang et al. (2017), with some modifications. Briefly, the induced chicken preadipocytes were washed with PBS and fixed with 10% (v/v) formalin at 4°C for 30 min. After washing again with PBS, the cells were stained with oil red O staining solution (oil red O solution: deionized water = 3:2) for 30 min. Then, the cells were immediately washed with ddH_2O and observed and photographed under an inverted fluorescence microscope (Leica).

To accurately quantify lipid droplet accumulation in preadipocytes, an oil red O extraction assay was used. In short, after staining with oil red O, the preadipocytes were washed with PBS. Then, 1 mL 100% (v/v) isopropanol was added to extract oil red O and measured at 510 nm using a plate reader (Synergy H1, BioTek Instruments, Inc, United States).

Correction of Total Cell Protein

The collected cells were added to 150 μL RIPA lysis solution containing 1 mM phenylmethanesulfonyl fluoride (PMSF; Biyuntian) and stirred until there was no cell mass. After lysis for 30 min on ice, the cell solution was centrifuged at 12,000 rpm for 10 min, and the supernatant was taken as total cell protein. The total protein concentration was determined using a bicinchoninic acid kit (Biyuntian). The absorbance value of the oil red O extraction/total protein amount is due to oil red O colorimetry after protein correction.

Detection of Chicken Preadipocyte Proliferation

A CCK-8 assay was used to detect chicken preadipocyte proliferation. When the confluence of the passaged chicken primary preadipocytes reached 30, 50, 70, 90, and 100%, the cells were added to a 10% (v/v) CCK-8 solution (DOJINDO) and incubated for 4 h. Then, the absorbance value of the colored medium was measured at 450 nm by a plate reader (Synergy H1, BioTek Instruments, Inc, United States). Three wells of cells were collected at each time point for biological repetition.

Total RNA Extraction and cDNA Synthesis

Total RNA from tissues and cells was extracted by TRIzol reagent (Invitrogen) following manufacturer instructions. RNA quality was determined by ultraviolet spectrophotometry (Eppendorf) and electrophoresis. Only total RNA of the best quality and purity (absorbance ratio of OD260 to OD280 between 1.8 and 2.2) was intended for further analysis. First-strand cDNA synthesis was performed with 1 μg total RNA using a PrimeScript RT reagent Kit (TaKaRa) and stored at −20°C.

Primer Design and RT-qPCR

In this study, 14 reference genes were selected according to the literature for screening reference genes in chicken tissues and cells as well as their function and usage frequency. The basic information and primer sequences of the 14 reference genes are shown in **Tables 1**, **2**, respectively. Quantitative real-time RT-PCR was performed to detect the expression level of these genes on a QuantStudio™ Real-time PCR system (Applied Biosystems). The reaction procedure was as follows: 1 cycle at 95°C for 10 min, followed by 40 cycles of 95°C for 15 s and 60°C for 1 min, and a melting curve analysis (95°C for 15 s, 60°C for 1 min, and 95°C for 15 s). After amplification, the dissociation curves for each PCR were analyzed using Dissociation Curve 1.0 software (Applied Biosystems) to detect and eliminate possible primer dimer artifacts.

The standard curves of each gene were drawn as follows: first, the cDNA of all samples were mixed together as an initial template, and five gradient cDNA samples were obtained according to a dilution ratio of 5 times the concentration. Second, the concentration of the initial template was defined as 5^0, and the concentrations of the five gradient cDNA samples were named 5^0, 5^{-1}, 5^{-2}, 5^{-3}, and 5^{-4}. Finally, the five gradient cDNA samples were used as templates for qPCR, and a standard curve was prepared. The accuracy of the PCR products was determined by gel electrophoresis and sequencing.

TABLE 1 | Information of the 14 reference genes.

Gene symbol	Full name	Function
ACTB	Actin, beta	Cytoskeletal structural protein
TUBB	Tubulin beta class I	Major constituent of microtubules
HPRT1	Hypoxanthine guanine phosphoribosyl transferase 1	Purine synthesis in salvage pathway
HMBS	Hydroxymethylbilane synthase	Heme synthesis pathway
TBP	TATA box binding protein	Basal transcription machinery
NONO	non-POU domain containing, octamer-binding	Regulation of transcription
RPL13	Ribosomal protein L13	60S ribosomal protein L13
RPS7	Ribosomal protein S7	40S ribosomal protein S7
18S	18S ribosomal RNA	Cytosolic small ribosome subunit, translation
PPIA	Peptidylprolyl isomerase A (cyclophilin A)	Peptidyl-prolyl *cis*-trans isomerase activity
β2M	Beta-2 microglobulin	MHC class I molecules. Defense/immunity protein
GAPDH	Glyceraldehyde-3-phosphate dehydrogenase	Glycolysis
YWHAZ	Tyrosine 3-monooxygenase/tryptophan 5-monooxygenase activation protein zeta	Signal transduction
TFRC	Transferrin receptor (p90, CD71)	Cellular uptake of iron

TABLE 2 | Primer sequences of 14 selected internal control genes.

Gene	Accession number	Exon (*F*)	Exon (*R*)	Length	Sequence (5′>3′)
ACTB	NM_205518	3	4	142 bp	F: TGAACCCCAAAGCCAACAGAG R: TCACCAGAGTCCATCACAATACCA
TUBB	NM_205315	3	4	156 bp	F: GGTAAATATGTGCCACGAGCC R: CTCCGTGTAGTGCCCTTTGG
HPRT1	NM_204848	7	9	157 bp	F: TTGTTGGTCAAAAGAACTCCTCG R: TCTGCTTCCCCGTCTCACTG
HMBS	XM_417846	11	12	118 bp	F: TCGTGCCAAAGACCAAGAAAC R: GACACTACAGCCACCCTCCAA
TBP	NM_205103	4.5	6	122 bp	F: GCGTTTTGCTGCTGTTATTATGAG R: TCCTTGCTGCCAGTCTGGAC
NONO	NM_001031532	6	7	151 bp	F: AGAAGCAGCAGCAAGAAC R: TCCTCCATCCTCCTCAGT
RPL13	NM_204999	3	4	108 bp	F: TCGTGCTGGCAGAGGATTCA R: GATTTGTTTCTTCGCCTGGGAT
RPS7	XM_001234708	5	6	157 bp	F: CTGCCCAAGCCAACGAGAA R: GCCTGCTGCCATCCAGTTTTA
18S	AF173612			96 bp	F: CTCTTTCTCGATTCCGTGGGT R: CATGCCAGAGTCTCGTTCGT
PPIA	NM_001166326	1	2	91 bp	F: CCAACCCCGTCGTGTTCTTC R: GTTATGGGCACCTTGTCAGCG
β2M	NM_001001750	3	4	115 bp	F: ATCCCGAGTTCTGAGCTGTGC R: CCGTCATACCCAGAAGTGCGAT
YWHAZ	NM_001031343	5	6	85 bp	F: AGTCATACAAAGACAGCACGCTA R: GCTTCATCTCCTTGGGTATCCGA
TFRC	NM_205256	10	10.11	137 bp	F: ATCGGTATGTTGTGATTGGAGCC R: CCTCGGTTTGTAGCCCTCGTT
GAPDH	NM_204305	8	9	134 bp	F: CAGAACATCATCCCAGCGTCC R: CGGCAGGTCAGGTCAACAAC

Data Analysis

Based on the correlation coefficient R^2 and slope of the standard curve, the amplification efficiency of each pair of reference gene primers was calculated by the following formula: amplification efficiency (%) = $(10^{(1/-slope)}\text{-}1) \times 100$. The GeNorm algorithm was used to compare the M value to determine the stability of the reference gene. A smaller M value indicates higher stability, and a larger M value indicates lower stability. To test the minimum number of reference genes needed for adequate data normalization, geNorm calculates a pairwise variation (V) between using n (number) and n+1 reference genes (Vandesompele et al., 2002). The ratio of $Vn/Vn+1$ was introduced as a criterion and the default threshold is 0.15, which means the ratio of $Vn/Vn+1$ is greater than 0.15, the most suitable internal reference number is n+1. The original Ct value obtained by RT-qPCR was converted into relative quantitative data by the $2^{-\Delta Ct}$ method, $\Delta Ct = Ct_{sample}\text{-}Ct_{min}$. The difference between groups was analyzed using unpaired Student's t-test. Comparisons with $P < 0.05$ and $P < 0.01$ were considered significant and extremely significant, respectively.

RESULTS AND ANALYSIS

To detect internal gene expression levels more accurately, we first analyzed the specificity of 14 pairs of primers. The results showed that the amplification curves and melting curves of 14 pairs of reference gene primers were all clear and single (**Supplementary Figures 1, 2**). The standard curve correlation coefficients R^2 of 14 reference genes were all greater than 0.99, and the amplification efficiency of primer pairs were 92.943 to 99.76% (**Supplementary Table 1**), which confirmed that the 14 pairs of primers met the quality

TABLE 3 | The average Ct values of the 14 reference genes in the adipose tissue of broilers.

Gene	The average Ct values	Gene	The average Ct values
ACTB	17.07 ± 0.88	*PPIA*	19.60 ± 0.68
TUBB	21.94 ± 0.57	β2M	18.66 ± 0.86
HMBS	22.40 ± 0.75	*GAPDH*	18.18 ± 0.97
TBP	23.36 ± 0.81	*TFRC*	24.75 ± 0.70
NONO	21.53 ± 0.54	*HPRT1*	21.31 ± 0.66
RPL13	17.61 ± 0.69	*18S*	6.59 ± 0.29
RPS7	17.04 ± 0.75	*YWHAZ*	20.44 ± 0.89

ACTB, beta-actin; TUBB, tubulin beta class I; HMBS, hydroxymethylbilane synthase; TBP, TATA box binding protein; NONO, non-POU domain containing, octamer-binding; RPL13, ribosomal protein L13; RPS7, ribosomal protein S7; PPIA, peptidylprolyl isomerase A; β2M, beta-2 microglobulin; GAPDH, glyceraldehyde-3-phosphate dehydrogenase; TFRC, transferrin receptor; HPRT1, hypoxanthine guanine phosphoribosyl transferase 1; 18S, 18S ribosomal RNA; and YWHAZ, yrosine 3-monooxygenase/tryptophan 5-monooxygenase activation protein zeta.

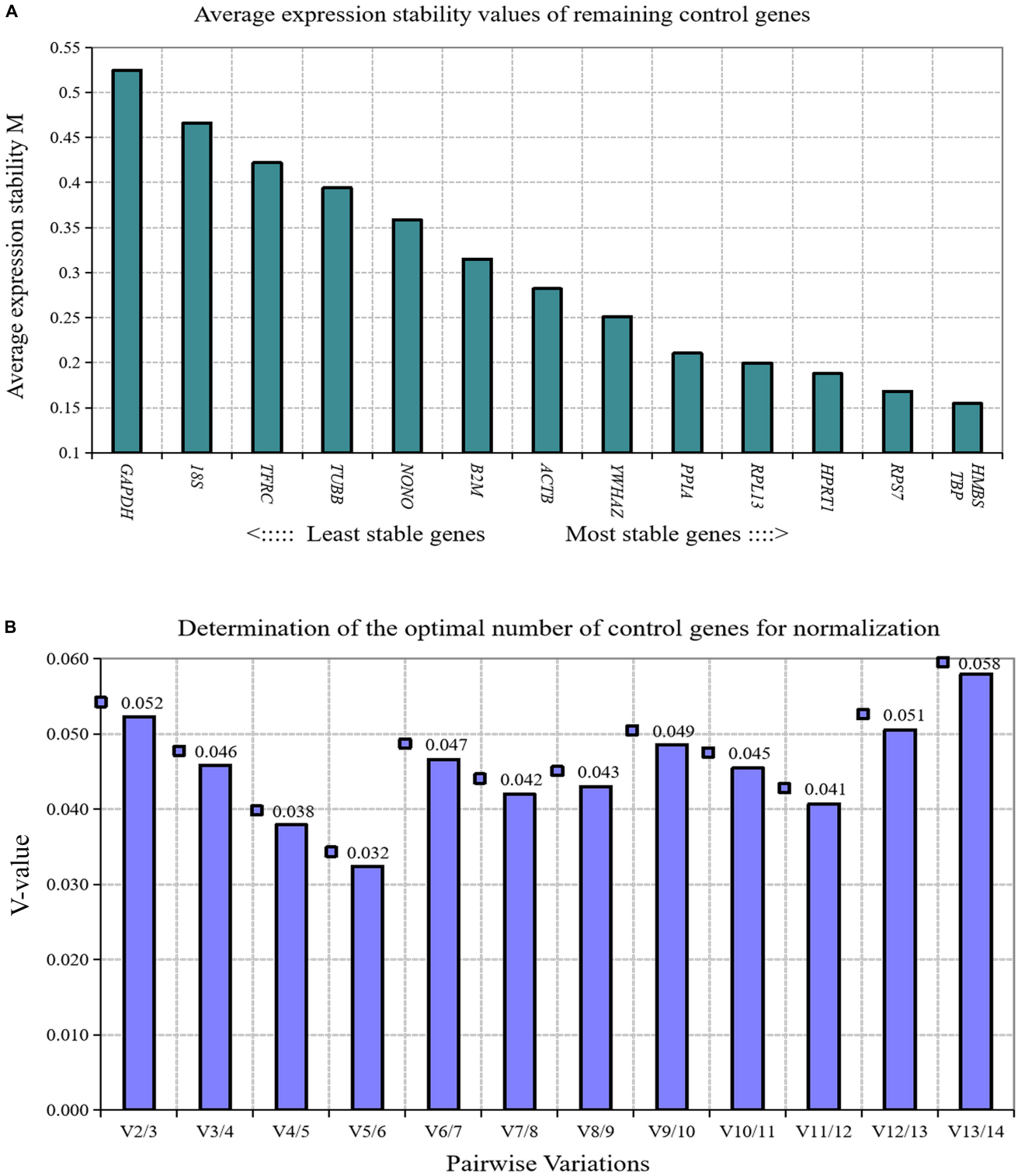

FIGURE 1 | GeNorm analysis of 14 reference genes in broiler abdominal adipose tissue. **(A)** Expression stability analysis. The most stably expressed genes have lower *M* values. *TBP* and *HMBS* were the two best reference genes; **(B)** Pairwise variation analysis. Determination of the optimal number of reference genes required for normalization calculated by pairwise variation analysis between normalization factors NF_n and NF_{n+1}. According to geNorm algorithm, two reference genes were needed.

control standard of RT-qPCR and could be used for follow-up analyses.

Screening of RT-qPCR Reference Genes in Broiler Abdominal Adipose Tissue

Expression Levels Analysis of 14 Reference Genes in Broilers Abdominal Adipose Tissue

We measured the expression levels of 14 reference genes in abdominal adipose tissue of fat and lean line broilers at the ages of 1, 4, and 7 weeks by RT-qPCR. According to the average Ct value of reference genes, the average expression levels of 14 reference genes in broiler abdominal adipose tissues were divided into three categories: high abundance expression, medium abundance expression, and low abundance expression. The *18S* reference gene, with an average Ct value of 6.59, was high abundance expression. *ACTB, RPL13, RPS7, PPIA,* β*2M,* and *GAPDH*, with average Ct values of 17.04 to 19.60, were reference genes expressed in medium abundance. *TUBB, HMBS, TBP, NONO, TFRC, HPRT1,* and *YWHAZ*, with average Ct values of 20.44 to 24.75, were reference genes with low abundance expression (**Table 3**).

Expression Stability Analysis of 14 Reference Genes in Broiler Abdominal Adipose Tissue

We analyzed the expression stability of these 14 reference genes during the growth and development of abdominal adipose tissue of broilers using GeNorm algorithm. The results showed that the expression stability of 14 reference genes from high to low was *TBP* and *HMBS*, *RPS7, HPRT1, RPL13, PPIA, YWHAZ, ACTB,* β*2M, NONO, TUBB, TFRC, 18S,* and *GAPDH* (**Figure 1A**). Paired variation analyses of the reference genes showed that $V_{2/3}$ was 0.052, which was less than the recommended threshold of 0.15, indicating that two reference genes were needed as standardized correction factors in the RT-qPCR experiment with broiler abdominal fat tissue as the experimental material (**Figure 1B**).

Screening of RT-qPCR Reference Genes in Directly Isolated Primary Preadipocytes and Mature Adipocytes

Expression Level Analysis of 14 Reference Genes in Directly Isolated Primary Preadipocytes and Mature Adipocytes

We measured the expression levels of 14 reference genes in directly isolated primary preadipocytes and mature adipocytes. Each kind of cell contained five samples, and every sample came from mixed cells of three chickens. According to the average Ct value of genes, the average expression levels of 14 reference genes in adipocytes can be divided into three categories: high abundance expression, medium abundance expression and low abundance expression. The *18S* gene, with an average Ct value of 6.73, was a reference gene with high abundance expression. *ACTB, RPL13, RPS7, PPIA, GAPDH,* and *YWHAZ*, with average Ct values of 16.80 to 19.86, were reference genes expressed in medium abundance. *TUBB, HMBS, TBP, NONO,* β*2M, TFRC,* and *HPRT1*, with average Ct values of 20.25 to 25.15, were reference genes with low abundance expression (**Table 4**).

Expression Stability Analysis of 14 Reference Genes in Directly Isolated Primary Preadipocytes and Mature Adipocytes

We used GeNorm algorithm to analyze the expression stability of 14 reference genes in directly isolated primary preadipocytes and mature adipocytes. The results showed that the stability of 14 reference genes in directly isolated chicken primary preadipocytes and mature adipocytes from high to low was *TBP* and *HMBS, YWHAZ, GAPDH, RPS7, RPL13, HPRT1, PPIA, ACTB,* β*2M, TUBB, 18S, TFRC,* and *NONO* (**Figure 2A**). Paired variation analyses of reference genes showed that $V_{2/3}$ was 0.028, which was less than the recommended threshold of 0.15, indicating that two reference genes were needed as standardized correction factors in the RT-qPCR experiment with chicken primary preadipocytes and mature adipocytes as the experimental materials (**Figure 2B**).

Screening of RT-qPCR Reference Genes in the Differentiation Process of Chicken Primary Preadipocytes

Differentiation Detection of Chicken Primary Preadipocytes

When primary preadipocytes were induced to differentiate at 96 h, oil red O staining and extraction assays were performed to determine the differentiation status of preadipocytes in the induced group (oleic acid group) and the noninduced group (control group; **Figure 3A**). The results showed that the lipid deposition of cells in the induction group was significantly higher than that in the control group ($P < 0.01$; **Figure 3B**), indicating that chicken preadipocytes were successfully induced to differentiate.

TABLE 4 | The average Ct values of the 14 reference genes in chicken primary preadipocytes and mature adipocytes.

Gene	The average Ct values	Gene	The average Ct values
ACTB	16.80 ± 0.64	*PPIA*	19.06 ± 0.68
TUBB	20.47 ± 0.57	β*2M*	20.25 ± 0.86
HMBS	22.62 ± 0.80	*GAPDH*	17.98 ± 0.77
TBP	23.33 ± 0.82	*TFRC*	25.15 ± 0.60
NONO	21.44 ± 0.59	*HPRT1*	20.73 ± 0.86
RPL13	17.76 ± 0.74	*18S*	6.73 ± 0.33
RPS7	17.78 ± 0.69	*YWHAZ*	19.86 ± 0.76

ACTB, beta-actin; TUBB, tubulin beta class I; HMBS, hydroxymethylbilane synthase; TBP, TATA box binding protein; NONO, non-POU domain containing, octamer-binding; RPL13, ribosomal protein L13; RPS7, ribosomal protein S7; PPIA, peptidylprolyl isomerase A; β*2M, beta-2 microglobulin; GAPDH, glyceraldehyde-3-phosphate dehydrogenase; TFRC, transferrin receptor; HPRT1, hypoxanthine guanine phosphoribosyl transferase 1; 18S, 18S ribosomal RNA; and YWHAZ, yrosine 3-monooxygenase/tryptophan 5-monooxygenase activation protein zeta.*

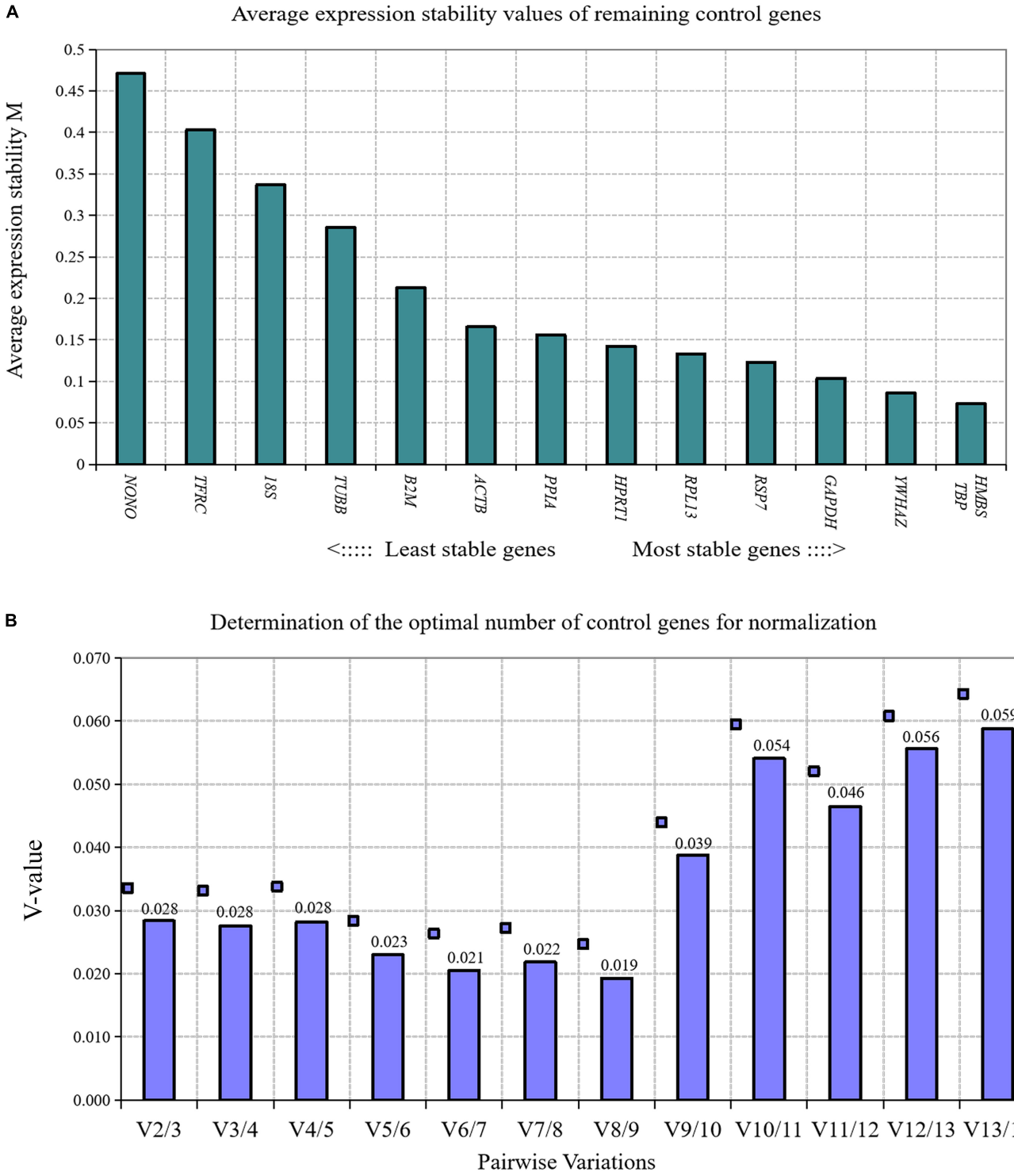

FIGURE 2 | GeNorm analysis of 14 reference genes in directly isolated primary preadipocytes and mature adipocytes. **(A)** Expression stability analysis. The most stably expressed genes have lower *M* values. *TBP* and *HMBS* were the two best reference genes; **(B)** Pairwise variation analysis. Determination of the optimal number of reference genes required for normalization calculated by pairwise variation analysis between normalization factors NF_n and NF_{n+1}. According to geNorm algorithm, two reference genes were needed.

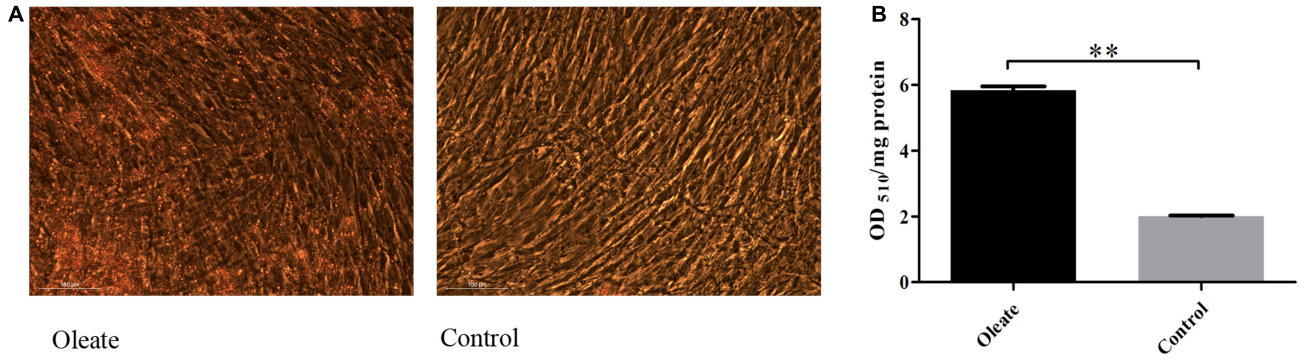

FIGURE 3 | Oil red O staining and content of oil red O at 96 h of induced differentiation. **(A)** Oil red O staining at 96 h of induced differentiation. **(B)** The content of oil red O at 96 h of induced differentiation. **extremely significant ($P < 0.01$).

Expression Stability Analysis of RT-qPCR Reference Genes During Chicken Primary Preadipocyte Differentiation

GeNorm algorithm was applied to analyze the expression stability of 14 reference genes during chicken primary preadipocyte differentiation (0, 12, 24, 48, 72, and 96 h). The results showed that the expression stability of 14 reference genes during the differentiation of chicken preadipocytes from high to low was *TBP* and *RPL13, HMBS, β2M, PPIA, HPRT1, RPS7, GAPDH, 18S, ACTB, TUBB, NONO, TFRC*, and *YWHAZ* (**Figure 4A**). Paired variation analyses of the reference gene showed that the value of $V_{2/3}$ was 0.067, which was less than the recommended threshold of 0.15, indicating that two reference genes were needed as standardized correction factors in RT-qPCR experiments in the process of inducing the differentiation of chicken primary preadipocytes (**Figure 4B**).

Screening of RT-qPCR Reference Genes in the Process of Chicken Primary Preadipocyte Proliferation

Detection of the Proliferation Status of Chicken Primary Preadipocytes

When the confluence of chicken primary preadipocytes reached 30, 50, 70, 90, and 100%, the proliferation status of chicken preadipocytes was measured by the CCK-8 method, and a cell growth curve was prepared. The results showed that the primary preadipocytes of chickens were in a normal proliferative state (**Figure 5**).

Expression Stability Analysis of RT-qPCR Reference Genes During the Proliferation of Chicken Primary Preadipocytes

GeNorm algorithm was used to analyze the expression stability of 14 reference genes in the proliferation process of chicken primary preadipocytes; cell confluence was 30, 50, 70, 90, and 100%. The expression stability of the 14 reference genes in chicken preadipocytes proliferation process from high to low was *PPIA* and *HMBS, RPS7, RPL13, β2M, HPRT1, TBP, GAPDH, ACTB, YWHAZ, TFRC, 18S, NONO*, and *TUBB* (**Figure 6A**). Paired variation analyses of reference genes showed that the value of $V_{2/3}$ was 0.043, which was less than the recommended threshold of 0.15, indicating that two reference genes were needed as standardized correction factors for RT-qPCR data calculation in the proliferation process of chicken preadipocytes (**Figure 6B**).

DISCUSSION AND CONCLUSION

Gene expression analysis plays an important role in understanding the complex network of gene regulation. Commonly used gene expression detection methods include semi-quantitative PCR, Northern blot, Western blot, and sequencing. Although these methods can be used for gene expression analysis, they have different degrees of disadvantages, such as low accuracy of semi-quantitative PCR, high complexity of Northern blot and Western blot methods, and high cost of sequencing. Real-time fluorescence quantitative PCR has become the most widely used technology to detect gene expression due to its high accuracy, good sensitivity, and strong specificity (Bustin, 2000; Dheda et al., 2005). At present, there are two main methods for RT-qPCR to determine gene expression levels: absolute quantitative and relative quantitative. An accurate expression level of genes can be obtained by the absolute quantitative method, but different standard samples are required for different genes, which greatly increases the difficulty and complexity of RT-qPCR experiments. By contrast, the relative quantitative method is simpler, more accurate and efficient and is more widely used. In the relative quantitative detection of RT-qPCR, it is usually necessary to select the corresponding reference genes for calibration and standardization (Huggett et al., 2005; Hendriks-Balk et al., 2007). Therefore, the correct application of reference genes directly affects the accuracy of experimental results (Radoniæ et al., 2004). In Bustin et al. (2009) developed a minimum standard of experimental information for the publication of quantitative PCR experimental data. While aimed at improving the reliability of RT-qPCR experimental results, this guide also emphasized the importance of reference gene selection. A valid reference gene should be constitutively and

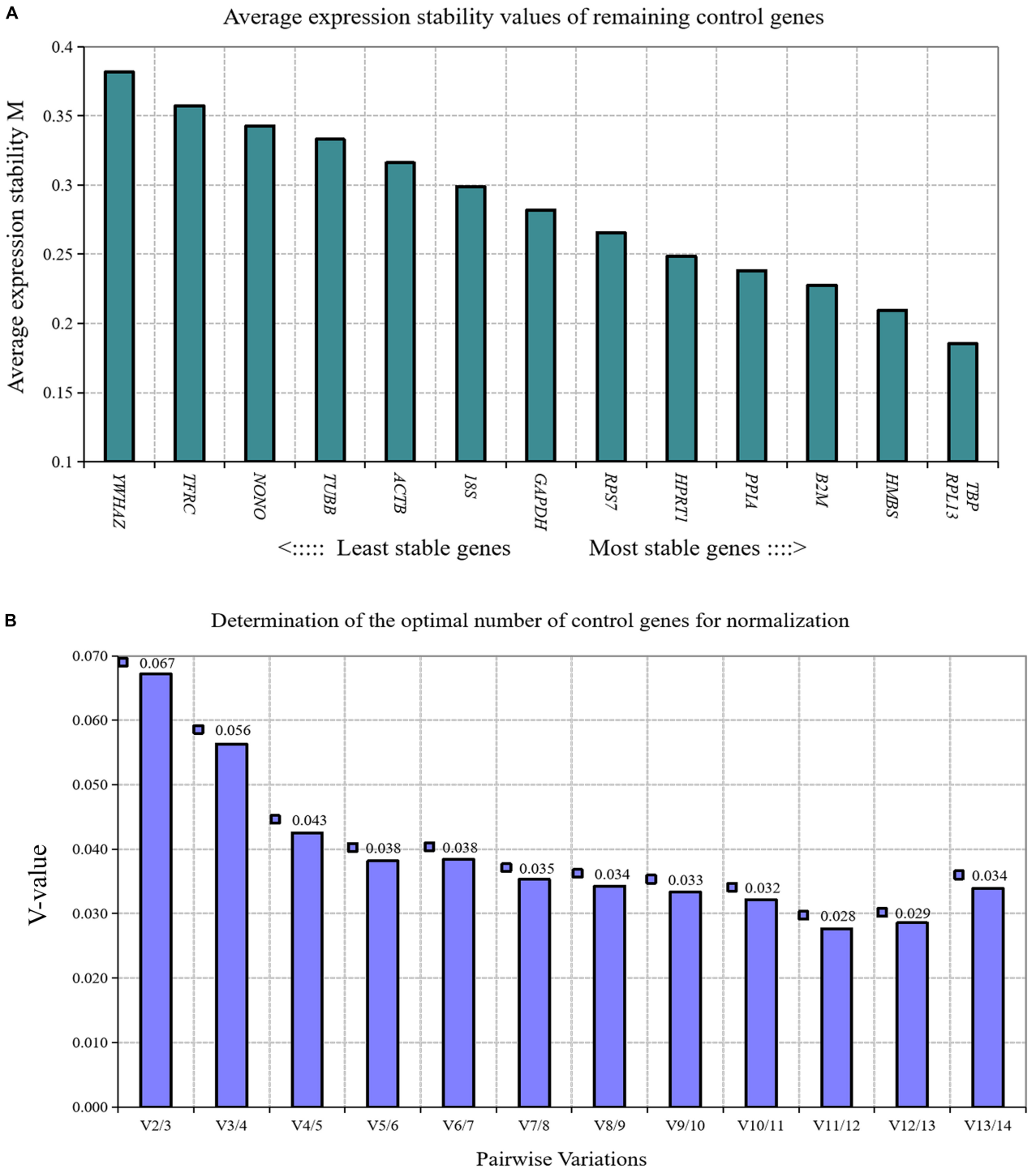

FIGURE 4 | GeNorm analysis of 14 reference genes during chicken primary preadipocyte differentiation. **(A)** Expression stability analysis. The most stably expressed genes have lower *M* values. *TBP* and *RPL13* were the two best reference genes; **(B)** Pairwise variation analysis. Determination of the optimal number of reference genes required for normalization calculated by pairwise variation analysis between normalization factors NF_n and NF_{n+1}. According to geNorm algorithm, two reference genes were needed.

equally expressed in different experimental conditions, tissues or physiological state of the tissue or organism (Kozera and Rapacz, 2013). However, such ideal reference gene is difficult to find. To search reliable reference genes and accurately evaluate the expression stability of these genes, a variety of algorithms, such as GeNorm (Vandesompele et al., 2002), NormFinder

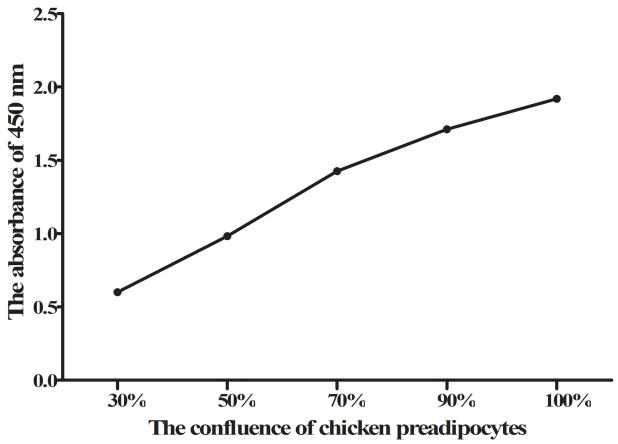

FIGURE 5 | CCK-8 results of chicken primary preadipocyte proliferation. The absorbance of 450 nm gradually increased with the confluence of chicken primary preadipocytes increased, which showed that the primary preadipocytes of chicken were in a normal proliferative state.

(Andersen et al., 2004), and BestKeeper (Pfaffl et al., 2004), have been applied. GeNorm is the most commonly used procedure for calculating a normalization factor based on multiple control genes. This algorithm can calculate the *M* value, which indicates the stability of reference gene expression for a given sample. The higher the *M* value is, the worse the stability of gene expression; in contrast, the lower the *M* value is, the better the stability of gene expression (Vandesompele et al., 2002).

To date, some reference genes have been validated for the standardization of RT-qPCR data in chickens, but these genes are only concentrated in the gene expression analysis of a certain tissue or cell, such as muscle, brain, abdominal fat, heart, lung, ovary, uterus, lymphoid organ, articular cartilage, chicken embryo fibroblasts, IEL-NK cell, and DT40 cell line (Yang et al., 2013; Bagés et al., 2015; Nascimento et al., 2015; Mitra et al., 2016; Staines et al., 2016; Katarzyńska-Banasik et al., 2017; Hassanpour et al., 2018, 2019; Simon et al., 2018; Boo et al., 2020; Dunislawska et al., 2020; Hul et al., 2020; Marciano et al., 2020). Whether these reference genes are also suitable to the study of gene expression during the growth and development of a specific tissue or cell in chickens, such as adipose tissue and adipocyte, still needs to be further determined. In this study, abdominal adipose tissue of broilers at different ages of weeks, primary preadipocytes and mature adipocytes were used as materials to carry out RT-qPCR reference gene screening experiments. This addresses a literature gap on RT-qPCR reference gene screening from the tissue level to the cell level of broilers and provides a reference for the selection of RT-qPCR reference genes in adipose tissue and adipocytes of broilers. The results of this study showed that the *TBP* and *HMBS* genes were stably expressed during the growth and development of broiler abdominal adipose tissue, the *TBP* and *RPL13* genes were stably expressed during the differentiation of chicken primary preadipocytes, the *PPIA* and *HMBS* genes were stably expressed in the proliferation process of chicken primary preadipocytes, and the *TBP* and *HMBS* genes were stably expressed in directly isolated preadipocytes and mature adipocytes. Among them, the *TBP* and *HMBS* genes were stably expressed in many growth and development processes of adipose tissue and cells of broilers, indicating that they can be widely used in the study of gene expression in chickens.

TATA box binding protein can bind to TBP binding factor (TBP-associated factors, TAFs) and combine into transcription factor IID to participate in the transcriptional initiation of genes (Li et al., 2015; Malecova et al., 2016). It has been reported that *TBP* is an reference gene stably expressed in many tissues of chickens in RT-qPCR experiments. Mitra et al. (2016) identified *TBP* as an reference gene stably expressed in spleen, liver, caecum, and caecum tonsil tissues of laying hens using GeNorm, NormFinder, BestKeeper, ΔCt, and RefFinder methods. Simon et al. (2018) analyzed the expression stability of 10 reference genes in the hypothalamus of chickens under three different nutritional conditions using BestKeeper, GeNorm, NormFinder, ΔCt, and a multivariate linear mixed-effect modeling algorithm, and found that *TBP* was one of the most stable reference gene in the hypothalamus of chickens. Bagés et al. (2015) and Hassanpour et al. (2019) also identified *TBP* as an stably expressed reference gene in chicken muscle, liver, ovary, and uterus tissue using GeNorm, NormFinder, CV, and BestKeeper methods. HMBS, the third enzyme in the heme biosynthetic pathway, catalyzes the head-to-tail condensation of four molecules of porphobilinogen to form the linear tetrapyrrole 1-hydroxymethylbilane (HMB; Bung et al., 2018). *HMBS* has been identified as a stably expressing reference gene in many tissues of chickens and is also a commonly used reference gene in chicken RT-qPCR experiments (Cedraz de Oliveira et al., 2017; Lenart et al., 2017; Hassanpour et al., 2019; Boo et al., 2020). Note that only male birds were used in the present study for the selection procedure requirement of the NEAUHLF (Guo et al., 2011). Meanwhile, only juvenile animals were used to more accurately observe the growth and development of abdominal fat tissue in current research. Therefore, our results cannot confirm that *TBP* and *HMBS* genes are still stably expressed during the growth and development of adipose tissue in female birds and adult individuals.

Ribosomal protein L13 is a component of ribosomes and participates in the translation process. The results of this study showed that *RPL13* was stably expressed during the differentiation of chicken primary preadipocytes, which was consistent with the results of human studies. Gentile et al. (2016) showed that ribosomal protein *RPL13A* is the most suitable reference gene to detect the regularity of gene expression during the differentiation of human vascular interstitial cells into adipocytes. *RPL13* also was determined as one of the stable genes in ovary and uterus of laying hens (Hassanpour et al., 2019). PPIA, a multifunctional protein, is the main cytoplasmic binding protein of the immunosuppressive drug cyclosporine A. It has the molecular chaperone activity of peptidyl propyl *cis*-trans isomerase and plays important roles in protein folding, transport, assembly, immunomodulation, and cellular signal transduction (Xu et al., 2010). This study showed that the expression of *PPIA* was stable during the proliferation of chicken primary preadipocytes and relatively stable during the differentiation of primary preadipocytes, which is consistent with the results in

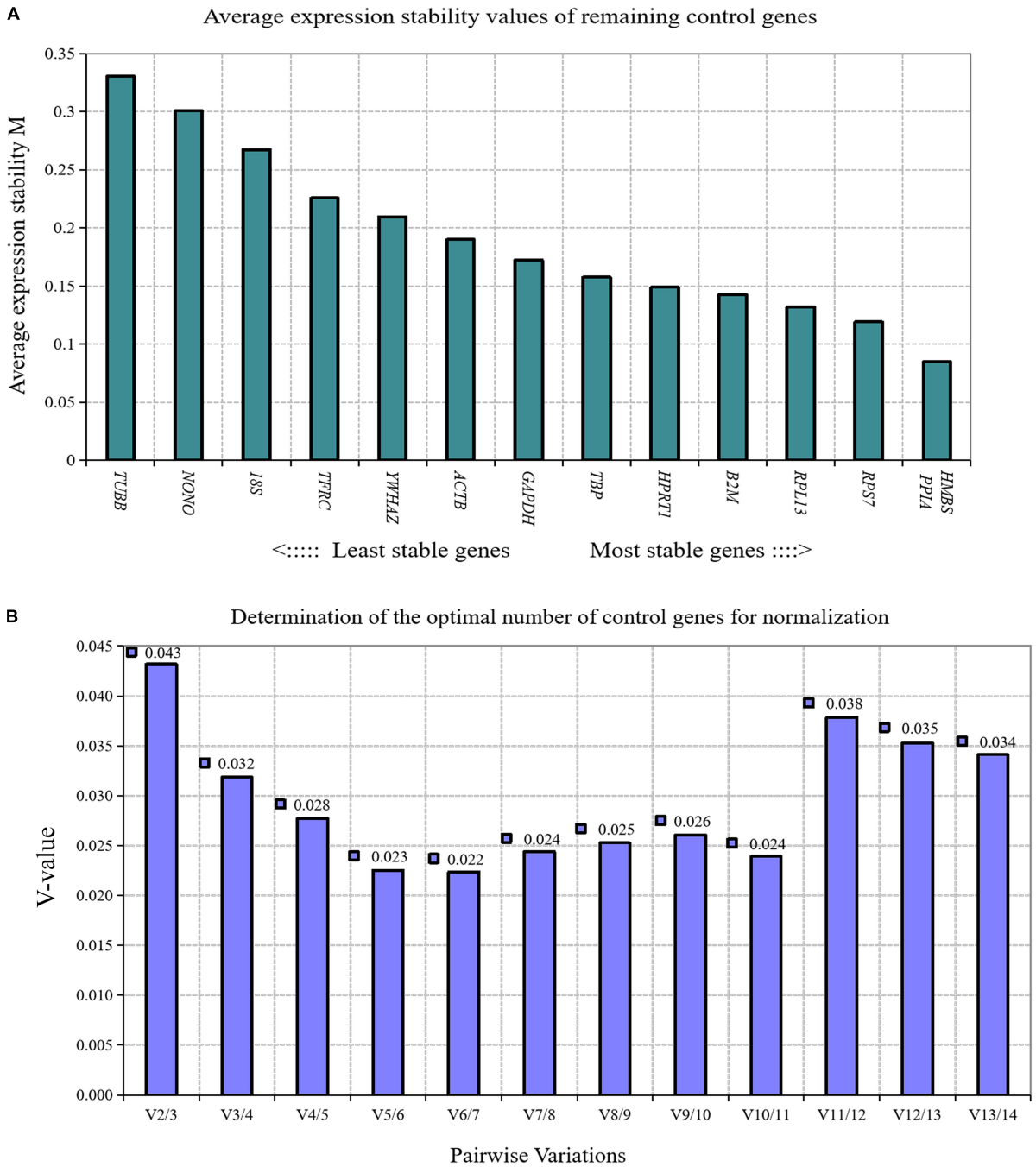

FIGURE 6 | GeNorm analysis of 14 reference genes during the proliferation of chicken primary preadipocytes. **(A)** Expression stability analysis. The most stably expressed genes have lower *M* values. *HMBS* and *PPIA* were the two best reference genes; **(B)** Pairwise variation analysis. Determination of the optimal number of reference genes required for normalization calculated by pairwise variation analysis between normalization factors NF_n and NF_{n+1}. According to geNorm algorithm, two reference genes were needed.

mice: the expression of the *PPIA* gene is relatively stable during the induction of differentiation of mouse 3T3-L1 cells (Zhang et al., 2014). In addition, previous research has shown that the expression of *PPIA* in avian brain tissues and gonads is relatively stable (Zinzow-Kramer et al., 2014). These results indicate that the *RPL13* and *PPIA* genes are more suitable for the study of gene expression levels during the proliferation and differentiation of chicken adipocytes.

In addition, when applying RT-qPCR technology for gene expression analysis, it is often necessary to select multiple reference genes as calibration standards to obtain more reliable results. While analyzing the stability of gene expression, GeNorm

algorithm can also calculate the paired variation V value of the standardized factor after introducing a new reference gene. The default threshold is 0.15. According to the V_n/V_{n+1} ratio, the introduction of a new reference gene can be determined whether to have a significant impact on the standardization factor. If V_n/V_{n+1} is less than 0.15, the number of the best reference genes is n; if the ratio is greater than 0.15, the most suitable internal reference number is n+1. In accordance with this principle, our study found that in RT-qPCR experiments with the above mentioned adipose tissue or cells as the experimental object, two reference genes as correction factors are required to correct the experimental data.

In conclusion, the expression stability of 14 endogenous reference genes in adipose tissue and adipocytes of broilers were evaluated. The optimal number of reference genes required for reliable normalization of RT-qPCR data was also determined. Based on our results, the combination of *TBP* and *HMBS* genes is recommended for studies of gene expression in the growth and development of abdominal adipose tissue of broilers, the combination of *PPIA* and *HMBS* genes is effective for studies of gene expression during the proliferation of primary preadipocytes, the *TBP* and *RPL13* are most stable genes for normalization of gene expression during the differentiation of primary preadipocytes, and the *TBP* and *HMBS* are suitable reference genes for the standardization of RT-qPCR data in studies of directly isolated preadipocytes and mature adipocytes. These findings contribute to selection of optimal reference genes required for normalization of RT-qPCR data in the genes function studies in adipose tissue and adipocytes of chickens.

DATA AVAILABILITY STATEMENT

The original contributions presented in the study are included in the article/**Supplementary Material**, further inquiries can be directed to the corresponding author/s.

ETHICS STATEMENT

The animal study was reviewed and approved by Institutional Biosafety Committee of Northeast Agricultural University (Harbin, China).

AUTHOR CONTRIBUTIONS

WN performed the experiments, analyzed the data, drafted, and edited the manuscript. YW helped design the study, analyzed the data, drafted, and edited the manuscript. PG, XZ, and KZ performed the experiments. HZ and NW participated in designing the study. HL conceived and designed the study, analyzed the data, drafted, and edited the manuscript. All authors read and approved the final manuscript.

FUNDING

This research was funded by the China Agriculture Research System (grant no. CARS-41).

ACKNOWLEDGMENTS

The authors would like to thank members of Poultry Group at Extension Experimental Station of Northeast Agricultural University for assistance with managing the birds.

SUPPLEMENTARY MATERIAL

The Supplementary Material for this article can be found online at: https://www.frontiersin.org/articles/10.3389/fphys.2021.676864/full#supplementary-material

REFERENCES

Andersen, C. L., Jensen, J. L., and Ørntoft, T. F. (2004). Normalization of real-time quantitative reverse transcription-PCR data: a model-based variance estimation approach to identify genes suited for normalization, applied to bladder and colon cancer data sets. *Cancer Res.* 64, 5245–5250. doi: 10.1158/0008-5472.can-04-0496

Bagés, S., Estany, J., Tor, M., and Pena, R. N. (2015). Investigating reference genes for quantitative real-time PCR analysis across four chicken tissues. *Gene* 561, 82–87. doi: 10.1016/j.gene.2015.02.016

Barroso, I., Benito, B., Garcí-Jiménez, C., Hernández, A., Obregón, M. J., and Santisteban, P. (1999). Norepinephrine, tri-iodothyronine and insulin upregulate glyceraldehyde-3-phosphate dehydrogenase mRNA during brown adipocyte differentiation. *Eur. J. Endocrinol.* 141, 169–179. doi: 10.1530/eje.0.1410169

Bas, A., Forsberg, G., Hammarström, S., and Hammarström, M. L. (2004). Utility of the housekeeping genes 18S rRNA, beta-actin and glyceraldehyde-3-phosphate-dehydrogenase for normalization in real-time quantitative reverse transcriptase-polymerase chain reaction analysis of gene expression in human T lymphocytes. *Scand. J. Immunol.* 59, 566–573. doi: 10.1111/j.0300-9475.2004.01440.x

Boo, S. Y., Tan, S. W., Alitheen, N. B., Ho, C. L., Omar, A. R., and Yeap, S. K. (2020). Identification of reference genes in chicken intraepithelial lymphocyte natural killer cells infected with very-virulent infectious bursal disease virus. *Sci. Rep.* 10:8561.

Bung, N., Roy, A., Chen, B., Das, D., Pradhan, M., Yasuda, M., et al. (2018). Human hydroxymethylbilane synthase: molecular dynamics of the pyrrole chain elongation identifies step-specific residues that cause AIP. *Proc. Natl. Acad. Sci. U.S.A.* 115, E4071–E4080.

Bustin, S. A. (2000). Absolute quantification of mRNA using real-time reverse transcription polymerase chain reaction assays. *J. Mol. Endocrinol.* 25, 169–193. doi: 10.1677/jme.0.0250169

Bustin, S. A., Benes, V., Garson, J. A., Hellemans, J., Huggett, J., Kubista, M., et al. (2009). The MIQE guidelines: minimum information for publication of quantitative real-time PCR experiments. *Clin. Chem.* 55, 611–622. doi: 10.1373/clinchem.2008.112797

Cedraz de Oliveira, H., Pinto Garcia, A. A. Jr., Gonzaga Gromboni, J. G., Vasconcelos Farias Filho, R., Souza do Nascimento, C., and Arias Wenceslau, A. (2017). Influence of heat stress, sex and genetic groups on reference genes stability in muscle tissue of chicken. *PLoS One* 12:e0176402. doi: 10.1371/journal.pone.0176402

de Jonge, H. J., Fehrmann, R. S., de Bont, E. S., Hofstra, R. M., Gerbens, F., Kamps, W. A., et al. (2007). Evidence based selection of housekeeping genes. *PLoS One* 2:e898. doi: 10.1371/journal.pone.0000898

Dheda, K., Huggett, J. F., Chang, J. S., Kim, L. U., Bustin, S. A., Johnson, M. A., et al. (2005). The implications of using an inappropriate reference gene for real-time

reverse transcription PCR data normalization. *Anal. Biochem.* 344, 141–143. doi: 10.1016/j.ab.2005.05.022

Dong, E. N., Liang, Q., Li, L., Wang, L. J., Zhong, T., Wang, Y., et al. (2013). The selection of reference gene in real-time quantitative reverse transcription PCR. *Chin. J. Anim. Sci.* 49, 92–96.

Dunislawska, A., Slawinska, A., and Siwek, M. (2020). Validation of the reference genes for the gene expression studies in chicken DT40 cell line. *Genes (Basel)* 11:372. doi: 10.3390/genes11040372

Ferguson, B. S., Nam, H., Hopkins, R. G., and Morrison, R. F. (2010). Impact of reference gene selection for target gene normalization on experimental outcome using real-time qRT-PCR in adipocytes. *PLoS One* 5:e15208. doi: 10.1371/journal.pone.0015208

Gentile, A. M., Lhamyani, S., Coín-Aragüez, L., Oliva-Olivera, W., Zayed, H., Vega-Rioja, A., et al. (2016). RPL13A and EEF1A1 are suitable reference genes for qPCR during adipocyte differentiation of vascular stromal cells from patients with different BMI and HOMA-IR. *PLoS One* 11:e0157002. doi: 10.1371/journal.pone.0157002

Guo, L., Sun, B., Shang, Z., Leng, L., Wang, Y., Wang, N., et al. (2011). Comparison of adipose tissue cellularity in chicken lines divergently selected for fatness. *Poult. Sci.* 90, 2024–2034. doi: 10.3382/ps.2010-00863

Hassanpour, H., Aghajani, Z., Bahadoran, S., Farhadi, N., Nazari, H., and Kaewduangta, W. (2019). Identification of reliable reference genes for quantitative real-time PCR in ovary and uterus of laying hens under heat stress. *Stress* 22, 387–394. doi: 10.1080/10253890.2019.1574294

Hassanpour, H., Bahadoran, S., Farhadfar, F., Chamali, Z. F., Nazari, H., and Kaewduangta, W. (2018). Identification of reliable reference genes for quantitative real-time PCR in lung and heart of pulmonary hypertensive chickens. *Poult. Sci.* 97, 4048–4056. doi: 10.3382/ps/pey258

Hendriks-Balk, M. C., Michel, M. C., and Alewijnse, A. E. (2007). Pitfalls in the normalization of real-time polymerase chain reaction data. *Basic Res. Cardiol.* 102, 195–197. doi: 10.1007/s00395-007-0649-0

Huggett, J., Dheda, K., Bustin, S., and Zumla, A. (2005). Real-time RT PCR normalization, strategies and considerations. *Genes Immun.* 6, 279–284.

Hul, L. M., Ibelli, A. M. G., Peixoto, J. O., Souza, M. R., Savoldi, I. R., Marcelino, D. E. P., et al. (2020). Reference genes for proximal femoral epiphysiolysis expression studies in broilers cartilage. *PLoS One* 15:e0238189. doi: 10.1371/journal.pone.0238189

Katarzyńska-Banasik, D., Grzesiak, M., and Sechman, A. (2017). Selection of reference genes for quantitative real-time PCR analysis in chicken ovary following silver nanoparticle treatment. *Environ. Toxicol. Pharmacol.* 56, 186–190. doi: 10.1016/j.etap.2017.09.011

Kozera, B., and Rapacz, M. (2013). Reference genes in real-time PCR. *J. Appl. Genet.* 54, 391–406.

Lekanne Deprez, R. H., Fijnvandraat, A. C., Ruijter, J. M., and Moorman, A. F. M. (2002). Sensitivity and accuracy of quantitative real time polymerase chain reaction using SYBR green I depends on cDNA synthesis conditions. *Anal. Biochem.* 307, 63–69. doi: 10.1016/s0003-2697(02)00021-0

Lenart, J., Kogut, K., and Salinska, E. (2017). Lateralization of housekeeping genes in the brain of one-day old chicks. *Gene Expr. Patterns* 25–26, 85–91. doi: 10.1016/j.gep.2017.06.006

Li, L., Martinez, S. S., Hu, W., Liu, Z., and Tjian, R. (2015). A specific E3 ligase/deubiquitinase pair modulates TBP protein levels during muscle differentiation. *ELife* 4:e08536.

Malecova, B., Dall'Agnese, A., Madaro, L., Gatto, S., Coutinho Toto, P., Albini, S., et al. (2016). TBP/TFIID-dependent activation of MyoD target genes in skeletal muscle cells. *Elife* 5:e12534.

Marciano, C. M. M., Ibelli, A. M. G., Peixoto, J. O., Savoldi, I. R., do Carmo, K. B., Fernandes, L. T., et al. (2020). Stable reference genes for expression studies in breast muscle of normal and white striping-affected chickens. *Mol. Biol. Rep.* 47, 45–53. doi: 10.1007/s11033-019-05103-z

Mitra, T., Bilic, I., Hess, M., and Liebhart, D. (2016). The 60S ribosomal protein L13 is the most preferable reference gene to investigate gene expression in selected organs from turkeys and chickens, in context of different infection models. *Vet. Res.* 47:105.

Nascimento, C. S., Barbosa, L. T., Brito, C., Fernandes, R. P., Mann, R. S., Pinto, A. P., et al. (2015). Identification of suitable reference genes for real time quantitative polymerase chain reaction assays on pectoralis major muscle in chicken (*Gallus gallus*). *PLoS One* 10:e0127935. doi: 10.1371/journal.pone.0127935

Pfaffl, M. W., Tichopad, A., Prgomet, C., and Neuvians, T. P. (2004). Determination of stable housekeeping genes, differentially regulated target genes and sample integrity: BestKeeper–Excel-based tool using pair-wise correlations. *Biotechnol. Lett.* 26, 509–515. doi: 10.1023/b:bile.0000019559.84305.47

Radonić, A., Thulke, S., Mackay, I. M., Landt, O., Siegert, W., and Nitsche, A. (2004). Guideline to reference gene selection for quantitative real-time PCR. *Biochem. Biophys. Res. Commun.* 313, 856–862.

Sanders, R., Mason, D. J., Foy, C. A., and Huggett, J. F. (2014). Considerations for accurate gene expression measurement by reverse transcription quantitative PCR when analyzing clinical samples. *Anal. Bioanal. Chem.* 406, 6471–6483. doi: 10.1007/s00216-014-7857-x

Simon, Á, Jávor, A., Bai, P., Oláh, J., and Czeglédi, L. (2018). Reference gene selection for reverse transcription quantitative polymerase chain reaction in chicken hypothalamus under different feeding status. *J. Anim. Physiol. Anim. Nutr.* 102, 286–296. doi: 10.1111/jpn.12690

Staines, K., Batra, A., Mwangi, W., Maier, H. J., van Borm, S., Young, J. R., et al. (2016). A versatile panel of reference gene assays for the measurement of chicken mRNA by quantitative PCR. *PLoS One* 11:e0160173. doi: 10.1371/journal.pone.0160173

Stephens, A. S., Stephens, S. R., and Morrison, N. A. (2011). Internal control genes for quantitative RT-PCR expression analysis in mouse osteoblasts, osteoclasts and macrophages. *BMC Res. Notes* 4:410. doi: 10.1186/1756-0500-4-410

Vandesompele, J., de Preter, K., Pattyn, F., Poppe, B., van Roy, N., de Paepe, A., et al. (2002). Accurate normalization of real-time quantitative RT-PCR data by geometric averaging of multiple internal control genes. *Genome Biol.* 3:research0034.1.

Wang, W., Zhang, T., Wu, C., Wang, S., Wang, Y., Li, H., et al. (2017). Immortalization of chicken preadipocytes by retroviral transduction of chicken TERT and TR. *PLoS One* 12:e0177348. doi: 10.1371/journal.pone.0177348

Xu, C., Meng, S., Liu, X., Sun, L., and Liu, W. (2010). Chicken cyclophilin A is an inhibitory factor to influenza virus replication. *Virol. J.* 7:372. doi: 10.1186/1743-422x-7-372

Yang, F., Lei, X., Rodriguez-Palacios, A., Tang, C., and Yue, H. (2013). Selection of reference genes for quantitative real-time PCR analysis in chicken embryo fibroblasts infected with avian leukosis virus subgroup J. *BMC Res. Notes* 6:402. doi: 10.1186/1756-0500-6-402

Zhang, J., Tang, H., Zhang, Y., Deng, R., Shao, L., Liu, Y., et al. (2014). Identification of suitable reference genes for quantitative RT-PCR during 3T3-L1 adipocyte differentiation. *Int. J. Mol. Med.* 33, 1209–1218. doi: 10.3892/ijmm.2014.1695

Zinzow-Kramer, W. M., Horton, B. M., and Maney, D. L. (2014). Evaluation of reference genes for quantitative real-time PCR in the brain, pituitary, and gonads of songbirds. *Horm. Behav.* 66, 267–275. doi: 10.1016/j.yhbeh.2014.04.011

Conflict of Interest: The authors declare that the research was conducted in the absence of any commercial or financial relationships that could be construed as a potential conflict of interest.

frontiers in Physiology

BRIEF RESEARCH REPORT
published: 21 May 2021
doi: 10.3389/fphys.2021.681562

Hypertrophy of Adipose Tissues in Quail Embryos by *in ovo* Injection of All-*Trans* Retinoic Acid

Dong-Hwan Kim[1†], Joonbum Lee[1,2†], Sanggu Kim[3], Hyun S. Lillehoj[4] and Kichoon Lee[1,2]*

[1] Department of Animal Sciences, The Ohio State University, Columbus, OH, United States, [2] The Ohio State University Interdisciplinary Human Nutrition Program, The Ohio State University, Columbus, OH, United States, [3] Department of Veterinary Biosciences, College of Veterinary Medicine, The Ohio State University, Columbus, OH, United States, [4] Animal Bioscience and Biotechnology Laboratory, Beltsville Agricultural Research Center, Agricultural Research Service, United States Department of Agriculture, Beltsville, MD, United States

Excessive adipose accretion causes health issues in humans and decreases feed efficiency in poultry. Although vitamin A has been known to be involved in adipogenesis, effects of all-*trans* retinoic acid (atRA), as a metabolite of vitamin A, on embryonic adipose development have not been studied yet. Avian embryos are developing in confined egg environments, which can be directly modified to study effects of nutrients on embryonic adipogenesis. With the use of quail embryos, different concentrations of atRA (0 M to 10 μM) were injected *in ovo* at embryonic day (E) 9, and adipose tissues were sampled at E14. Percentages of fat pad weights in embryo weights were significantly increased in the group injected with 300 nM of atRA. Also, among three injection time points, E5, E7, or E9, E7 showed the most significant increase in weight and percentage of inguinal fat at E14. Injection of atRA at E7 increased fat cell size in E14 embryos with up-regulation of pro-adipogenic marker genes (*Pparγ* and *Fabp4*) and down-regulation of a preadipocyte marker gene (*Dlk1*) in adipose tissues. These data demonstrate that atRA promotes hypertrophic fat accretion in quail embryos, implying important roles of atRA in embryonic development of adipose tissues.

Keywords: all-*trans* retinoic acid, *in ovo* injection, adipocyte hypertrophy, fat accretion, embryonic development, quail

OPEN ACCESS

Edited by:
Elizabeth Ruth Gilbert, Virginia Tech, United States

Reviewed by:
Woo Kyun Kim, University of Georgia, United States
Yang Xiao, Mayo Clinic, United States

***Correspondence:**
Kichoon Lee
lee.2626@osu.edu

† These authors have contributed equally to this work and share first authorship

Specialty section:
This article was submitted to Avian Physiology, a section of the journal Frontiers in Physiology

Received: *16 March 2021*
Accepted: *14 April 2021*
Published: *21 May 2021*

Citation:
Kim D-H, Lee J, Kim S, Lillehoj HS and Lee K (2021) Hypertrophy of Adipose Tissues in Quail Embryos by in ovo Injection of All-Trans Retinoic Acid. Front. Physiol. 12:681562. doi: 10.3389/fphys.2021.681562

INTRODUCTION

Excessive fat accretion causes obesity and associated diseases in humans. On the agricultural side, excessive fat is undesirable due to economic concerns of animal producers on low feed efficiency associated with fat accretion and health issues of consumers on high fat contents in meat. Discovery and understanding of roles of genetic and nutritional factors in fat regulation will lead to improving health and efficiency of animal production. Different from mammals, avian species depend on the various nutrient contents in the fertile egg for growth and development of embryos. During embryonic development of the chicken, adipose tissues begin to be visible from embryonic day (E) 10 and grown through hyperplasia and hypertrophy (Chen et al., 2014). Chicken embryos at E10–E12 have preadipocytes and multilocular immature fat cells (Chen et al., 2014). These cells are further developed toward more numbers of unilocular fat cells at E14 (Chen et al., 2014). This study showed how rapidly adipocytes are developed during embryonic development.

Vitamin A (retinol) is an essential nutrient in animals and involved in biological processes of adipose development. Retinol can be converted to all-*trans* retinoic acid (atRA), which functions as a key regulatory factor in embryonic development by controlling differentiation of many cell types including adipocytes. Previous studies showed that supplementation of high doses of atRA (over 1 μM) on 3T3-L1 cells blocked lipid accumulation (Mercader et al., 2007; Stoecker et al., 2017), but the supplementation of low concentration (10 nM) had pro-adipogenic effects on Ob1771 cells (Safonova et al., 1994). Our previous study also showed that atRA functions as a positive or negative regulator on adipogenic differentiation of 3T3-L1 cells by supplementation of mild or excessive doses, respectively (Kim et al., 2019). Levels of serum retinol were higher in obese children at the ages of 6–14 years (Aeberli et al., 2007). Supplementation of high levels of dietary vitamin A in obese rats significantly reduced body weight gain and adipose tissue weight (Jeyakumar et al., 2008). In addition, injection of atRA into mice reduced fat mass (Felipe et al., 2005; Mercader et al., 2006), but injection of retinol into new-born Angus cattle increased the ratio of intramuscular fat and marbling score (Harris et al., 2018). However, roles of retinoids in fetal adipose development have not been reported. This might be due to potential difficulties in precisely modulating fetal retinoids such as an uncertain relationship of maternal retinoid levels with fetal levels or issues in direct delivery into fetus.

Avian species are suitable models for the research of developmental origins of health and disease because nutritional, hormonal, and chemical exposures can be strictly modulated by directly injecting exogenous factors into embryos at specific developmental stages, which cannot be easily accomplished in mammalian embryos. In poultry, adipogenic differentiation *in vitro* can be induced by supplementation of atRA (Kim et al., 2020a,b; Lee et al., 2021). Dietary supplementation of vitamin A during early post-hatch period increased fat accretion in broiler chickens (Savaris et al., 2020). The present study aims to investigate the cellular effects of atRA on adipose growth in quail embryos as an animal model.

MATERIALS AND METHODS

Visualization of Embryonic Fat Pads

As described in our previous study (Chen et al., 2014), to visualize fat pads, quail embryo was removed from the egg, and feathers were removed by using forceps during washing with phosphate-buffered saline (PBS) three times. Then, to visualize the fat pads, the embryo was transferred into a 1% potassium hydroxide (KOH) solution after fixing in 70% ethanol because KOH, as a strong alkali, makes tissue soften, digest, and clear. After the skin was cleared, the embryos were visualized using a camera (EOS Rebel T7, Canon, Japan).

In ovo Injection and Tissue Sampling

Experiments using poultry embryos are exempt from requiring University Institutional Animal Care and Use Committee approval, because avian embryos are not considered live animals by the Public Health Service Policy (ILAR News, 1991). All fertile eggs of Japanese quail were obtained from The Ohio State University poultry research farm. atRA (#R2625, Sigma-Aldrich, St. Louis, MO, United States) was diluted with dimethyl sulfoxide (DMSO). Before atRA was injected *in ovo*, the surface of fertile eggs that were confirmed by candling was cleaned with 70% ethanol. Eggshell at the two-thirds point of quail eggs was grinded by twisting with corner tip of blades (#4515, Ettore, Alameda, CA, United States) without disrupting the shell membrane. Two microliters of different concentrations of atRA (final concentrations: 100 nM to 10 μM) was injected through the shell membrane using a micropipette tip (#17000504, Rainin, Columbus, OH, United States), as shown in **Figure 2A**, at different embryonic ages (E5, E7, or E9) and then sealed with parafilm. The injected eggs were incubated at 37.5°C with 60% relative humidity until sampling inguinal fat pads at E12 or E14. DMSO was injected as a control (0 M).

Histological Processing and Measurement of Fat Cell Size

Inguinal fat pads were 1fixed in 10% neutral buffered formalin for 48 h and then processed to embed in paraffin. Paraffin embedded fat tissues were cut into 5-μm slices. To measure fat cell size, serial sections of the embedded samples were de-paraffinized in xylene, re-hydrated in serial diluted ethanol, and then stained with hematoxylin and eosin (H&E). Stained slides were observed and imaged under a microscope (EVOS cell imaging system, Thermo Fisher Scientific, Waltham, MA, United States). ImageJ software (NIH ImageJ 1.52s) was used to determine fat cell size. The average of the adipocyte cross-sectional area was calculated by measuring randomly selected areas having large numbers of cells and dividing this by the total number of cells found within the area. At least 800 cells at E12 and 500 cells at E14 were evaluated per animal.

Analysis of Gene Expression

After extraction of total RNA from inguinal fat tissues and cDNA synthesis by the methods described in our previous study (Kim et al., 2020a), quantitative PCR (qPCR) was performed in duplicate per sample to analyze gene expression associated with adipogenesis with specific primer sets; *Peroxisome proliferator-activated receptor gamma* (*Pparγ*, NCBI Reference Sequence: NM_001001460.1, F: 5′-GTGAATCTTGACCTGAATGATC AGGT, R: 5′-AGATTATCTTGTATATCTTCAATGGGCTTCA CAT), *fatty acid-binding protein 4* (*Fabp4*, NCBI Reference Sequence: XM_015855897.2, F: 5′-CAAGCTGGGTGAAGAGT TTGATG, R: 5′-CTCTTTTGCTGGTAACATTATTCATGGT GCA), and *Delta like non-canonical notch ligand 1* (*Dlk1*, NCBI Reference Sequence: XM_032445023.1, F: 5′-CTGCCATCT CAGGAAAGGACC, R: 5′-ACATGGGTTGGATTCACAGTC ATC). *Glyceraldehyde 3-phosphate dehydrogenase* (*Gapdh*, NCBI Reference Sequence: NM_204305.1, F: 5′-CTCTGTTGTTGAC CTGACCTG, R: 5′-CAAGTCCACAACACGGTTGCT) was used as a reference gene. The expression levels were normalized to those of genes by the 0 M group at E12, and all of the data were analyzed using the ddCt method (Livak and Schmittgen, 2001).

Statistical Analysis

All data were expressed as means ± SEM. The data were analyzed by the Student or multiple *t*-test using GraphPad Prism software, version 6.02. $p < 0.05$ was considered as a statistically significant difference.

RESULTS

Visualization of Developing Adipose Tissues at Different Embryonic Ages

Although adipose tissue in chicken embryos appears around E10 (Chen et al., 2014), embryonic ontogeny of adipose tissues in quail has not been reported yet. Therefore, to investigate the developmental stages of adipose growth during embryonic ages, ontogeny of embryonic adipose development was studied. When adipose tissues begin to appear, they are too small to be visible and distinguished from other tissues. Therefore, intact fat pads in the embryo were visualized using KOH that enables soft tissues transparent by alkaline hydrolysis of proteins and fat tissues distinguishably visible by saponification of lipids (Culling et al., 1974). This method can be applied for visualization of fat pads in various species.

The current study showed that adipose tissues in quail embryos were not found at E8 but initially appeared around the neck at E9 (**Figure 1**). Interestingly, the appearance of fat pads coincided with the time of feather development at E9 in quail and E10 in chickens (Hamburger and Hamilton, 1951; Chen et al., 2014; Nakamura et al., 2019), indicating that fat and feather development might initiate at similar developmental stages. At E10, fat pads around the neck were extended more but did not appear in other areas (**Figure 1**). In addition to neck fat pads, supraclavicular and inguinal fat pads first appeared at E11, and breast and leg fat pads were additionally shown from E12 (**Figure 1**).

Effect of *in ovo* Injection With Different Concentrations of All-*Trans* Retinoic Acid on Adipose Weight

Based on the ontogenetic data showing an appearance of adipose tissues in the neck area from E9, different dosages of atRA (final concentration: 0 M, 100 nM, 300 nM, 1 μM, 3 μM, or

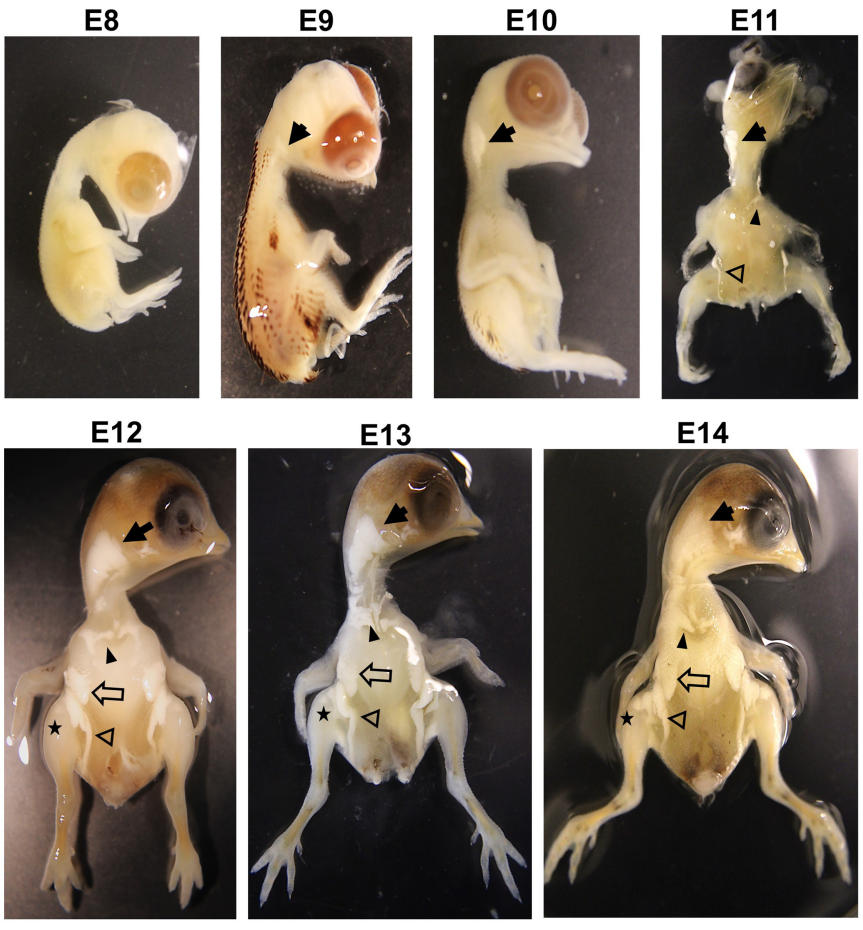

FIGURE 1 | Visualization of fat pad on embryos in quail with 1% KOH at E8, E9, E10, E11, E12, E13, and E14. Solid arrow, neck fat; solid arrowhead, supraclavicular fat; opened arrow, breast fat; opened arrowhead, inguinal fat; star, leg fat. Images are not to scale.

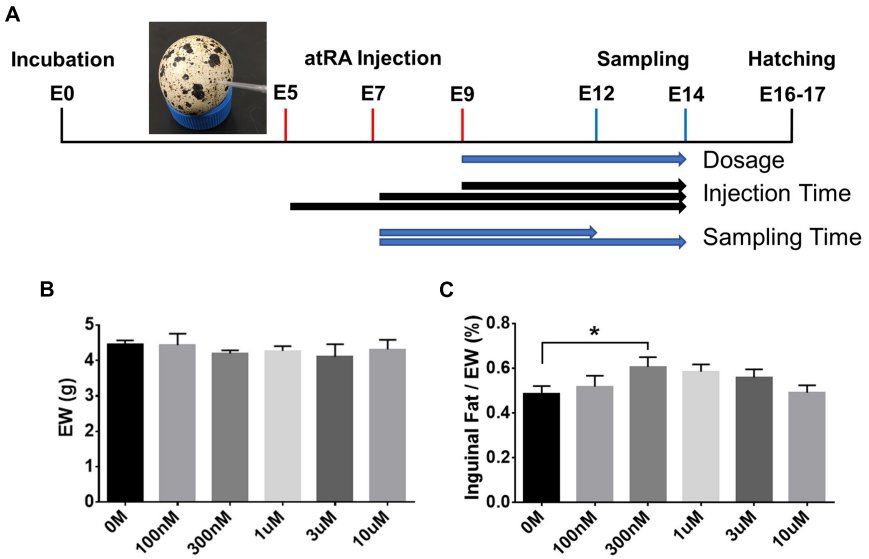

FIGURE 2 | *In ovo* all-*trans* retinoic acid injection. **(A)** Schematic diagram of *in ovo* all-*trans* retinoic acid (atRA) injection. Quail eggs were injected with atRA at embryonic day (E) 5, E7, or E9 and sampled at E12 or E14. Embryo weight (EW, **B**) and percentages of inguinal fat weight in total EW **(C)**. Dose of 0 M, 100 nM, 300 nM, 1 μM, 3 μM, or 10 μM of atRA was injected *in ovo* at E9, and injected embryos were sampled at E14. n = 11, 7, 12, 12, 5, and 7 embryos for 0 M, 100 nM, 300 nM, 1 μM, 3 μM and 10 μM of atRA, respectively. All data were expressed as means ± SEM. The data were analyzed by multiple t-test using GraphPad Prism software, version 6.02. *$p < 0.05$.

10 μM) were injected into quail eggs at E9 to investigate the effect of atRA on embryonic development of adipose tissues (**Figure 2A**). Embryos injected with atRA were sampled at E14 to measure embryo weight (EW) and weight of inguinal fat tissues (**Figure 2A**). Although there was no difference in EW among all groups (**Figure 2B**), the percentages of weight of inguinal fat tissues in EW were gradually increased with increasing concentrations of atRA up to 300 nM and somewhat reduced at higher concentrations from 300 nM to 10 μM (**Figure 2C**). Especially, the group injected with 300 nM atRA showed a significantly increased percentage of inguinal fat tissue compared with those at the 0 M (1.25-fold, $p < 0.05$) (**Figure 2C**). Thus, the current data indicate that adipose growth can be influenced by atRA.

Effect of *in ovo* Injection of All-*Trans* Retinoic Acid at Different Embryonic Ages on Adipose Weight

To investigate to what extent atRA injection at three different ages, before (E5 or 7) and after (E9) appearance of adipose tissues, affects adipose growth, atRA was injected into eggs at those ages and adipose tissues were sampled at E14 (**Figure 3**). Weights of embryos at E14 were not affected by 300 nM of atRA injection at all three ages (**Figure 3A**). Although weights of inguinal fat pads were significantly increased by atRA injection at E5 ($p < 0.05$) and E7 ($p < 0.01$), percentages of inguinal fat weights in EW were significantly increased by injecting at all time points (E5: 1.45-fold, $p < 0.01$; E7: 1.32-fold, $p < 0.01$; E9: 1.25-fold, $p < 0.05$) (**Figure 3C**). These data demonstrated that injecting atRA before the appearance of fat pads is more effective in enhancing embryonic adipose growth.

Hypertrophic Effect of All-*Trans* Retinoic Acid in Fat Tissues

To determine whether the increased fat pad weights by atRA can be attributed to increasing cell size, embryos were sampled at E12 or E14 after injecting atRA at E7, and a histological examination was performed to measure sizes of fat cells. Injection of atRA at E7 resulted in increased percentages of inguinal fat weights in embryos at E12 and E14 (E12: 1.24-fold, $p < 0.05$; E14: 1.32-fold, $p < 0.01$) (**Figure 4A**). The sizes of fat cells at E12 were not significantly different between the two groups (0 M and 300 nM) (**Figures 4B,C**). In the samples that were injected with 300 nM of atRA at E7 and sampled at E14, size of inguinal fat cells was significantly increased compared with the 0 M (1.5-fold, $p < 0.05$) (**Figures 4B,C**). These data clearly showed that atRA injection resulted in increased fat pad weights and cell sizes during embryonic development in quail.

Expression Levels of Genes Involved in Adipogenesis

To further investigate effects of atRA on expression of adipogenic marker genes in embryonic days, expression levels of marker genes for preadipocytes (*Dlk1*) and adipocytes (*Pparγ* and *Fabp4*) were analyzed. Injection of 300 nM atRA at E7 enhanced expression levels of *Pparγ* in E14 inguinal adipose tissues by 75% compared with the 0 M, although the difference was not statistically significant ($p = 0.078$) (**Figure 4D**). Expression of *Fabp4* in E14 adipose tissues was significantly up-regulated (85%,

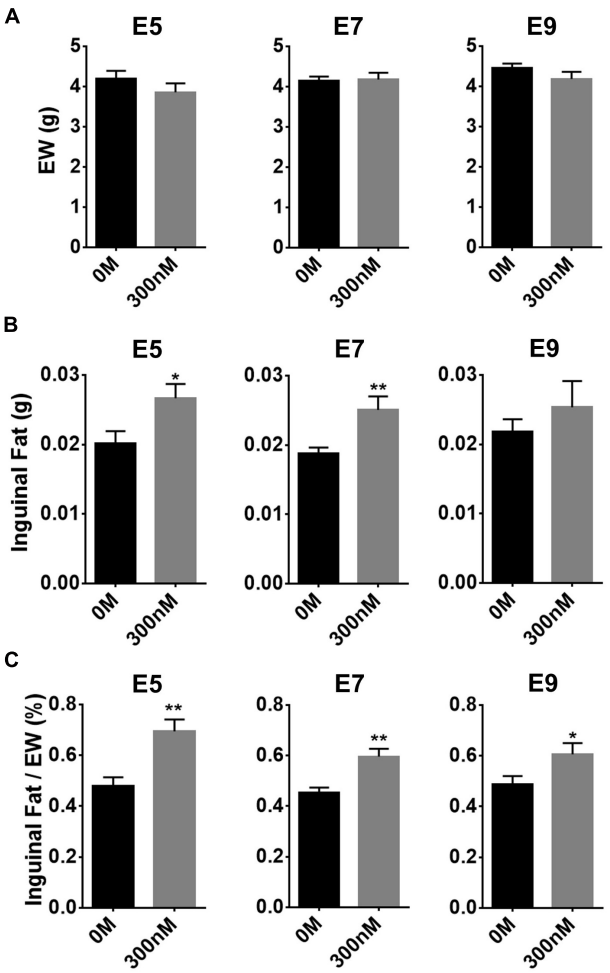

FIGURE 3 | Effect of time of *in ovo* all-*trans* retinoic acid (atRA) injection. Embryo weight (EW) **(A)**, inguinal fat pad weights **(B)**, and percentages of weights of inguinal fat tissues in EW **(C)**. Both 0-M and 300-nM concentrations of atRA were injected *in ovo* at embryonic day (E) 5, E7, or E9; and injected embryos were sampled at E14. For 0 M or 300 nM of atRA, $n = 8$ and $n = 8$ embryos at E5, $n = 9$ and $n = 8$ embryos at E7, and $n = 11$ and $n = 12$ embryos at E9, respectively. All data were expressed as means ± SEM. The data were analyzed by a Student *t*-test using GraphPad Prism software, version 6.02. $^{*}p < 0.05$, $^{**}p < 0.01$.

$p < 0.05$) by the atRA injection at E7 compared with the 0 M (**Figure 4D**). In addition, atRA injection at E7 significantly down-regulated expression levels of *Dlk1* by 68% ($p < 0.05$) in the adipose tissues at E14 compared with the 0 M (**Figure 4D**). These results indicate that *in ovo* injection of atRA caused enhanced expression of adipogenic markers and reduced expression of the preadipocyte marker, suggesting promotion of embryonic adipogenesis by injecting atRA *in ovo* in quail.

DISCUSSION

Avian species, as oviparous animals, have embryonic development within a unique egg environment where nutritional and hormonal factors can be directly injected to study the effect of these factors on processes of embryonic adipogenesis. In addition, different stages of embryos can be obtained from the eggs. However, it is difficult to directly modulate nutritional and hormonal factors in mammalian embryos and to study embryonic development without scarifying dams. For these reasons, chicken embryos have been used to visually aid in presenting embryonic development of adipose tissues (Chen et al., 2014) and to study a nutritional factor, selenium, in adipogenic differentiation by injecting *in ovo* (Hassan et al., 2014). In addition, the current study is the first demonstration that shows the visual evidence of fast-growing adipose tissues during quail embryonic development. Taken together, avian species are suitable models to study for embryonic adipose growth.

Vitamin A and its metabolites such as atRA have been used for the study of adipogenic differentiation in animals. Our previous study (Kim et al., 2019) showed different effects of atRA on differentiation of 3T3-L1 cells depending on atRA concentrations; atRA showed a pro-adipogenic effect at low concentrations but an anti-adipogenic effect at high concentrations. The current study shows the bell-shaped distribution of percentages of fat pad weights in EW with increasing concentrations (0–10 μM) of atRA (**Figure 2C**). The highest fat percentage was shown at 300 nM, and increased fat percentages were gradually diminished by injecting over 300 nM of atRA. These data are somewhat consistent with the previous study by showing anti-adipogenic activities of high concentrations of atRA *in vitro* (Muenzner et al., 2013) and reduced size of fat cells by high levels of atRA administration *in vivo* (Mercader et al., 2006).

The previous study showed that injection of atRA resulted in reduction of adipose tissues in adult mice (Amengual et al., 2010). In newborn Angers calves, injection of vitamin A significantly increased percentages of intramuscular fat (Harris et al., 2018). In broiler chickens, fat deposition rate was increased during 1–21 days after hatching but decreased during 22–42 days by dietary supplementation of vitamin A (Savaris et al., 2020). In the current study, *in ovo* injection of 300 nM atRA at E5–E7 resulted in an increase of weights and percentages of adipose tissues (**Figure 3**). The previous and current studies show that atRA can positively or negatively affect fat deposition in animals. In general, rate of fat accretion in adult animals is determined by a balance of lipolysis and lipogenesis (Cornelius, 1994). However, because avian embryos constantly receive required nutrients from the confined egg environments (Kimura and Warshaw, 1983), both adipocyte differentiation and lipogenesis mainly contribute to growth of embryonic adipose tissues until hatching when lipolysis starts to be active to provide energy for breaking the eggshell (Chen et al., 2014). In the current study, because embryos injected with atRA were sampled at E14 approximately 3 days before hatching in quail, increased fat weights with adipocyte hypertrophy in quail embryos by atRA might be attributed from enhanced lipogenesis rather than changes in lipolysis.

Our previous *in vitro* studies showed that atRA promoted differentiation of murine preadipocyte cell line (3T3-L1) into adipocytes (Kim et al., 2019) and induced adipogenic

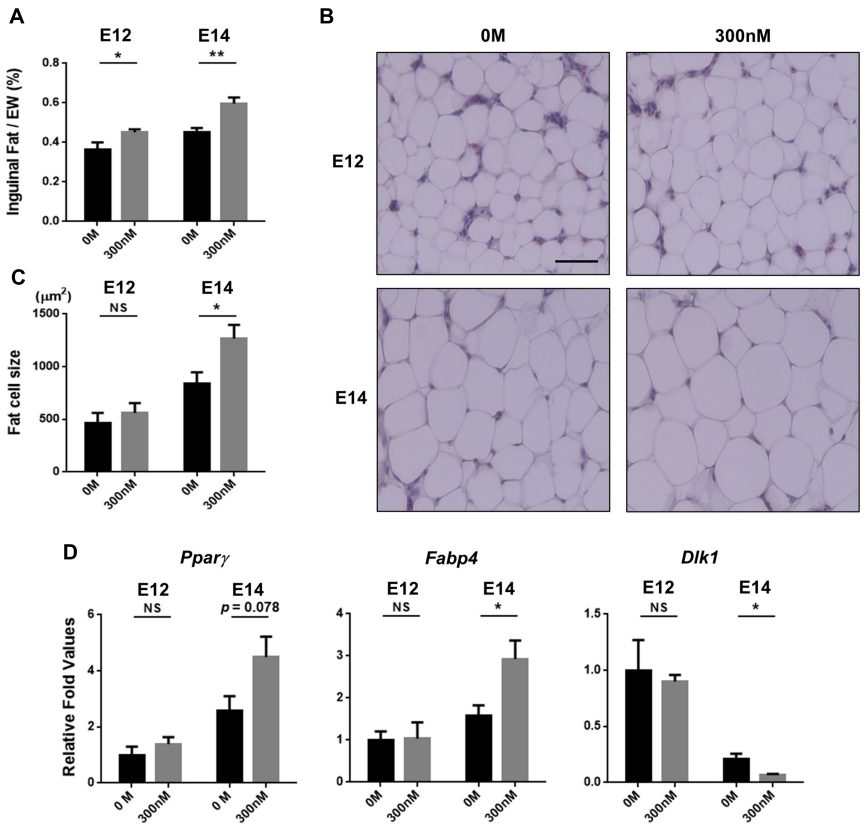

FIGURE 4 | Hypertrophic fat cells by *in ovo* injection of all-*trans* retinoic acid (atRA). Percentages of inguinal fat weights in embryo weight (EW) **(A)**. Embryos were injected with 0 M or 300 nM of atRA at E7 and sampled at E12 or E14. For 0 M or 300 nM of atRA, $n = 9$ and $n = 9$ embryos at E12 and $n = 9$ and $n = 8$ embryos at E14, respectively. Scale bar: 100 μm. H&E stain of inguinal fat tissue **(B)** and comparisons of fat cell size **(C)**. Quantitative analysis of gene expression involved in adipogenesis by qPCR **(D)**. $n = 4$ for 0 M and 300 nM of atRA at E12 and E14, respectively. All data were expressed as means ± SEM. The data were analyzed by Student *t*-test using GraphPad Prism software, version 6.02. NS, no significance; $^{*}p < 0.05$, $^{**}p < 0.01$.

differentiation of chicken embryonic fibroblast (CEF) cell line (Lee et al., 2021) and primary CEFs (Kim et al., 2020a). These pro-adipogenic roles of atRA were also demonstrated by the finding that it increased lipid accumulation by atRA treatment *in vitro*. With the support of these *in vitro* studies, *in ovo* injection of atRA in the current study resulted in adipose hypertrophy. Interestingly, our previous study with a knockout mouse model demonstrated pro-adipogenic function of retinoids by the finding that mice with knockout of the Raldh1 gene, encoding an enzyme producing atRA from retinaldehyde, are lean with less fat (Yasmeen et al., 2013). In addition, Raldh1-deficient cells have impaired adipogenesis *in vitro*, which is rescued by RA supplementation (Reichert et al., 2011). Furthermore, atRA enhanced fat accumulation in zebra fish embryos (Fraher et al., 2015). These previous and current studies support the positive roles of atRA in adipocyte differentiation and fat accretion.

As *Pparγ* and *Fabp4* have been used as well-known adipogenic markers, up-regulation of the two genes suggests promotion of adipocyte differentiation in embryonic adipose tissues by atRA. In general, differentiation potential is negatively correlated with proliferative activities. It is possible that promotion of adipocyte differentiation by atRA may reduce proliferation potential and, consequently, reduce population of preadipocytes in embryonic adipose tissues. In this regard, it is interesting to relate adipogenic potential with population of preadipocytes by assessing a reliable preadipocyte maker. Dlk1, also known as Pref-1, was originally discovered by comparing expression profiles before and after differentiation of 3T3-L1 preadipocytes and identifying Dlk1 as a predominantly expressed gene in preadipocytes (Smas and Sul, 1993). Our previous *in vivo* studies demonstrated anti-adipogenic function of Dlk1 through findings that reduced fat in Dlk1 overexpressed mice (Lee et al., 2003) and obesity phenotype in Dlk1 knockout mice (Moon et al., 2002). Therefore, Dlk1 has been used as a preadipocyte marker in humans (Krautgasser et al., 2019), pigs (Ahn et al., 2013), cattle (Cai et al., 2018), chickens (Shin et al., 2008), and quail (Ahn et al., 2015). In the current study, increased cell size in inguinal adipose tissues with increasing age (E12–E14) is accompanied with up-regulation of *Pparγ* and *Fabp4* and down-regulation of *Dlk1* expression regardless of treatment groups (**Figure 4D**), indicating temporal progresses

of adipogenic differentiation during embryonic development in quail. In addition to up-regulation of *Pparγ* and *Fabp4*, a lesser expression of *Dlk1* by 300 nM atRA compared with the control (0 M) at E14 suggests that adipocyte differentiation might be promoted by atRA and the preadipocyte population might be consequently reduced. In agreement with the current study, supplementation of atRA in 3D cultures of subcutaneous primary human preadipocytes contributed to adipocyte hypertrophy by regulating transcriptional factors involved in adipogenesis (Pope et al., 2020). For these reasons, it is possible that promotion of preadipocyte differentiation by atRA can contribute to increased fat mass in quail embryos. These findings support pro-adipogenic function of atRA during embryonic development.

Our finding showed that *in ovo* injection of 300 nM of atRA resulted in increased fat pad weights and fat cell size. Although the current study supports pro-adipogenic function of atRA in embryos, effects of dietary vitamin A or administration of RA into animals on fat accretion might be variable depending on concentrations of retinoids and ages of animals. Therefore, results from *in vivo* studies with retinoids should be carefully interpreted with consideration of these factors. Our experimental approach with *in ovo* injection in avian species can be applied to investigate effects of nutritional, hormonal, and pharmaceutical factors on embryonic development of various tissues and organs.

DATA AVAILABILITY STATEMENT

The original contributions presented in the study are included in the article/supplementary material, further inquiries can be directed to the corresponding author/s.

ETHICS STATEMENT

Ethical review and approval was not required for the animal study because Experiments using poultry embryos are exempt from requiring University Institutional Animal Care and Use Committee approval, because avian embryos are not considered live animals by the Public Health Service Policy (ILAR News, 1991).

AUTHOR CONTRIBUTIONS

KL: conceptualization and supervision. D-HK: data curation and visualization. D-HK, JL, SK, and HL: formal analysis. D-HK, JL, and KL: investigation. D-HK and JL: methodology and writing—original draft. KL and HL: writing—review and editing. All authors have read and agreed to the published version of the manuscript.

FUNDING

This research was funded by the United States Department of Agriculture National Institute of Food and Agriculture Hatch Grant (Project No. OHO01304).

ACKNOWLEDGMENTS

We are grateful to Michelle Milligan for her invaluable assistance by proofreading this manuscript.

REFERENCES

Aeberli, I., Biebinger, R., Lehmann, R., L'allemand, D., Spinas, G. A., and Zimmermann, M. B. (2007). Serum retinol-binding protein 4 concentration and its ratio to serum retinol are associated with obesity and metabolic syndrome components in children. *J. Clin. Endocrinol. Metab.* 92, 4359–4365. doi: 10.1210/jc.2007-0468

Ahn, J., Oh, S. A., Suh, Y., Moeller, S. J., and Lee, K. (2013). Porcine G0/G1 switch gene 2 (G0S2) expression is regulated during adipogenesis and short-term in-vivo nutritional interventions. *Lipids* 48, 209–218. doi: 10.1007/s11745-013-3756-8

Ahn, J., Shin, S., Suh, Y., Park, J. Y., Hwang, S., and Lee, K. (2015). Identification of the avian RBP7 gene as a new adipose-specific gene and RBP7 promoter-driven GFP expression in adipose tissue of transgenic quail. *PLoS One* 10:e0124768. doi: 10.1371/journal.pone.0124768

Amengual, J., Ribot, J., Bonet, M. L., and Palou, A. (2010). Retinoic acid treatment enhances lipid oxidation and inhibits lipid biosynthesis capacities in the liver of mice. *Cell. Physiol. Biochem.* 25, 657–666. doi: 10.1159/000315085

Cai, H., Li, M., Sun, X., Plath, M., Li, C., Lan, X., et al. (2018). Global transcriptome analysis during adipogenic differentiation and involvement of transthyretin gene in adipogenesis in cattle. *Front. Genet.* 9:463.

Chen, P., Suh, Y., Choi, Y. M., Shin, S., and Lee, K. (2014). Developmental regulation of adipose tissue growth through hyperplasia and hypertrophy in the embryonic leghorn and broiler. *Poult. Sci.* 93, 1809–1817. doi: 10.3382/ps.2013-03816

Cornelius, P. (1994). Regulation of adipocyte development. *Annu. Rev. Nutr.* 14, 99–129. doi: 10.1146/annurev.nutr.14.1.99

Culling, C. F. A., Reid, P. E., Clay, M. G., and Dunn, W. L. (1974). The histochemical demonstration of O-acylated sialic acid in gastrointestinal mucins their association with the potassium hydroxide-periodic acid-schiff effect. *J. Histochem. Cytochem.* 22, 826–831. doi: 10.1177/22.8.826

Felipe, F., Mercader, J., Ribot, J., Palou, A., and Bonet, M. L. (2005). Effects of retinoic acid administration and dietary vitamin a supplementation on leptin expression in mice: lack of correlation with changes of adipose tissue mass and food intake. *Biochim. Biophys. Acta* 1740, 258–265. doi: 10.1016/j.bbadis.2004.11.014

Fraher, D., Ellis, M. K., Morrison, S., McGee, S. L., Ward, A. C., Walder, K., et al. (2015). Lipid abundance in zebrafish embryos is regulated by complementary actions of the endocannabinoid system and retinoic acid pathway. *Endocrinology* 156, 3596–3609. doi: 10.1210/EN.2015-1315

Hamburger, V., and Hamilton, H. L. (1951). A series of normal stages in the development of the chick embryo. *J. Morphol.* 88, 49–92. doi: 10.1002/jmor.1050880104

Harris, C. L., Wang, B., Deavila, J. M., Busboom, J. R., Maquivar, M., Parish, S. M., et al. (2018). Vitamin A administration at birth promotes calf growth and intramuscular fat development in angus beef cattle. *J. Anim. Sci. Biotechnol.* 9, 1–9. doi: 10.1186/s40104-018-0268-7

Hassan, A., Ahn, J., Suh, Y., Choi, Y. M., Chen, P., and Lee, K. (2014). Selenium promotes adipogenic determination and differentiation of chicken embryonic fibroblasts with regulation of genes involved in fatty acid uptake, triacylglycerol synthesis and lipolysis. *J. Nutr. Biochem.* 25, 858–867. doi: 10.1016/j.jnutbio.2014.03.018

ILAR News. (1991). *Office of Laboratory animal Welfare, the Public Health Service Responds to Commonly Asked Questions, Question #1. Accessed Feb. 2021.* Available Online at: https://olaw.nih.gov/guidance/articles/ilar91.html.

Jeyakumar, S. M., Vajreswari, A., and Giridharan, N. V. (2008). Vitamin A regulates obesity in WNIN/Ob obese rat; independent of stearoyl-CoA desaturase-1. *Biochem. Biophys. Res. Commun.* 370, 243–247. doi: 10.1016/j.bbrc.2008.03.073

Kim, D. H., Lee, J., Suh, Y., Cressman, M., and Lee, K. (2020a). Research note: all-trans retinoic acids induce adipogenic differentiation of chicken embryonic fibroblasts and preadipocytes. *Poult. Sci.* 99, 7142–7146. doi: 10.1016/j.psj.2020.09.006

Kim, D. H., Lee, J., Suh, Y., Cressman, M., Lee, S. S., and Lee, K. (2020b). Adipogenic and myogenic potentials of chicken embryonic fibroblasts in vitro: combination of fatty acids and insulin induces adipogenesis. *Lipids* 55, 163–171. doi: 10.1002/lipd.12220

Kim, D. H., Lee, J. W., and Lee, K. (2019). Supplementation of all-trans-retinoic acid below cytotoxic levels promotes adipogenesis in 3T3-L1 cells. *Lipids* 54, 99–107. doi: 10.1002/lipd.12123

Kimura, R. E., and Warshaw, J. B. (1983). Metabolic adaptations of the fetus and newborn. *J. Pediatr. Gastroenterol. Nutr.* 2, S12–S15. doi: 10.1097/00005176-198300201-00003

Krautgasser, C., Mandl, M., Hatzmann, F. M., Waldegger, P., Mattesich, M., and Zwerschke, W. (2019). Reliable reference genes for expression analysis of proliferating and adipogenically differentiating human adipose stromal cells. *Cell. Mol. Biol. Lett.* 24:14. doi: 10.1186/s11658-019-0140-6

Lee, J., Kim, D. H., Suh, Y., and Lee, K. (2021). Research note: potential usage of DF-1 cell line as a new cell model for avian adipogenesis. *Poult. Sci.* 100:101057. doi: 10.1016/j.psj.2021.101057

Lee, K., Villena, J. A., Moon, Y. S., Kim, K.-H., Lee, S., Kang, C., et al. (2003). Inhibition of adipogenesis and development of glucose intolerance by soluble preadipocyte factor–1 (Pref-1). *J. Clin. Invest.* 111, 453–461. doi: 10.1172/jci200315924

Livak, K. J., and Schmittgen, T. D. (2001). Analysis of relative gene expression data using real-time quantitative PCR and the 2-ΔΔCT method. *Methods* 25, 402–408. doi: 10.1006/meth.2001.1262

Mercader, J., Madsen, L., Felipe, F., Palou, A., Kristiansen, K., and Bonet, M. L. (2007). All-trans retinoic acid increases oxidative metabolism in mature adipocytes. *Cell. Physiol. Biochem.* 20, 1061–1072. doi: 10.1159/000110717

Mercader, J., Ribot, J., Murano, I., Felipe, F., Cinti, S., Bonet, M. L., et al. (2006). Remodeling of white adipose tissue after retinoic acid administration in mice. *Endocrinology* 147, 5325–5332. doi: 10.1210/en.2006-0760

Moon, Y. S., Smas, C. M., Lee, K., Villena, J. A., Kim, K.-H., Yun, E. J., et al. (2002). Mice lacking paternally expressed Pref-1/Dlk1 display growth retardation and accelerated adiposity. *Mol. Cell. Biol.* 22, 5585–5592. doi: 10.1128/mcb.22.15.5585-5592.2002

Muenzner, M., Tuvia, N., Deutschmann, C., Witte, N., Tolkachov, A., Valai, A., et al. (2013). Retinol-binding protein 4 and its membrane receptor STRA6 control adipogenesis by regulating cellular retinoid homeostasis and retinoic acid receptor activity. *Mol. Cell. Biol.* 33, 4068–4082. doi: 10.1128/mcb.00221-13

Nakamura, Y., Nakane, Y., and Tsudzuki, M. (2019). Developmental stages of the blue-breasted quail (Coturnix chinensis). *Anim. Sci. J.* 90, 35–48. doi: 10.1111/asj.13119

Pope, B. D., Warren, C. R., Dahl, M. O., Pizza, C. V., Henze, D. E., Sinatra, N. R., et al. (2020). Fattening chips: hypertrophy, feeding, and fasting of human white adipocytes: in vitro. *Lab. Chip* 20, 4152–4165. doi: 10.1039/d0lc00508h

Reichert, B., Yasmeen, R., Jeyakumar, S. M., Yang, F., Thomou, T., Alder, H., et al. (2011). Concerted action of aldehyde dehydrogenases influences depot-specific fat formation. *Mol. Endocrinol.* 25, 799–809. doi: 10.1210/me.2010-0465

Safonova, I., Darimont, C., Amri, E. Z., Grimaldi, P., Ailhaud, G., Reichert, U., et al. (1994). Retinoids are positive effectors of adipose cell differentiation. *Mol. Cell. Endocrinol.* 104, 201–211. doi: 10.1016/0303-7207(94)90123-6

Savaris, V. D. L., Souza, C., Wachholz, L., Broch, J., Polese, C., Carvalho, P. L. O., et al. (2020). Interactions between lipid source and vitamin A on broiler performance, blood parameters, fat and protein deposition rate, and bone development. *Poult. Sci.* 100, 174–185. doi: 10.1016/j.psj.2020.09.001

Shin, J., Lim, S., Latshaw, J. D., and Lee, K. (2008). Cloning and expression of delta-like protein 1 messenger ribonucleic acid during development of adipose and muscle tissues in chickens. *Poult. Sci.* 87, 2636–2646. doi: 10.3382/ps.2008-00189

Smas, C. M., and Sul, H. S. (1993). Pref-1, a protein containing EGF-like repeats, inhibits adipocyte differentiation. *Cell* 73, 725–734. doi: 10.1016/0092-8674(93)90252-l

Stoecker, K., Sass, S., Theis, F. J., Hauner, H., and Pfaffl, M. W. (2017). Inhibition of fat cell differentiation in 3T3-L1 pre-adipocytes by all-trans retinoic acid: integrative analysis of transcriptomic and phenotypic data. *Biomol. Detect. Quantif.* 11, 31–44. doi: 10.1016/j.bdq.2016.11.001

Yasmeen, R., Reichert, B., Deiuliis, J., Yang, F., Lynch, A., Meyers, J., et al. (2013). Autocrine function of aldehyde dehydrogenase 1 as a determinant of diet- and sex-specific differences in visceral adiposity. *Diabetes* 62, 124–136. doi: 10.2337/db11-1779

Conflict of Interest: The authors declare that the research was conducted in the absence of any commercial or financial relationships that could be construed as a potential conflict of interest.

frontiers in Physiology

ORIGINAL RESEARCH
published: 22 June 2021
doi: 10.3389/fphys.2021.684426

Function of Chick Subcutaneous Adipose Tissue During the Embryonic and Posthatch Period

Haidong Zhao[1], Mingli Wu[1], Xiaoqin Tang[1], Qi Li[1], Xiaohua Yi[1], Shuhui Wang[1], Cunling Jia[1], Zehui Wei[1] and Xiuzhu Sun[1,2]**

[1] College of Animal Science and Technology, Northwest A&F University, Xianyang, China, [2] College of Grassland Agriculture, Northwest A&F University, Xianyang, China

Since excess abdominal fat is one of the main problems in the broiler industry for the development of modern broiler and layer industry, the importance of subcutaneous adipose tissue has been neglected. However, chick subcutaneous adipose tissue appeared earlier than abdominal adipose tissue and more than abdominal adipose tissue. Despite a wealth of data, detailed information is lacking about the development and function of chick subcutaneous adipose tissue during the embryonic and posthatch period. Therefore, the objective of the current study was to determine the developmental changes of adipocyte differentiation, lipid synthesis, lipolysis, fatty acid β-oxidation, and lipid contents from E12 to D9.5. The results showed that subcutaneous adipose tissue was another important energy supply tissue during the posthatch period. In this stage, the mitochondrial copy number and fatty acid β-oxidation level significantly increased. It revealed that chick subcutaneous adipose tissue not only has the function of energy supply by lipidolysis but also performs the same function as brown adipose tissue to some extent, despite that the brown adipose tissue does not exist in birds. In addition, this finding improved the theory of energy supply in the embryonic and posthatch period and might provide theoretical basis on physiological characteristics of lipid metabolism in chicks.

Keywords: subcutaneous adipose tissue, chicken, embryonic period, posthatch period, lipometabolism

OPEN ACCESS

Edited by:
Jie Wen,
Institute of Animal Sciences, Chinese Academy of Agricultural Sciences, China

Reviewed by:
Servet Yalcin,
Ege University, Turkey
Xiquan Zhang,
South China Agricultural University, China

***Correspondence:**
Zehui Wei
weizehui7848@163.com
Xiuzhu Sun
sunxiuzhu@nwafu.edu.cn

Specialty section:
This article was submitted to Avian Physiology, a section of the journal Frontiers in Physiology

Received: *23 March 2021*
Accepted: *13 May 2021*
Published: *22 June 2021*

Citation:
Zhao H, Wu M, Tang X, Li Q, Yi X, Wang S, Jia C, Wei Z and Sun X (2021) Function of Chick Subcutaneous Adipose Tissue During the Embryonic and Posthatch Period. Front. Physiol. 12:684426. doi: 10.3389/fphys.2021.684426

INTRODUCTION

For a long period of time, the genetic breeding goal of meat-type chickens was to improve the growth rate, but the rapid growth of body weight is accompanied with the problem of excessive abdominal fat deposition (Moreira et al., 2018; Liu et al., 2020; Mohammadpour et al., 2020). For improve feed conversion rate and grain conservation, many researchers have studied the metabolic mechanism of abdominal fat deposition in chickens, ignoring the significance of subcutaneous adipose tissue (Simon and Leclercq, 1982; Na et al., 2018). Abdominal adipose tissue compared with subcutaneous adipose tissue is more cellular, vascular, innervated, and contains a larger number of inflammatory and immune cells, lesser preadipocyte differentiating capacity, and a greater percentage of large adipocytes, while subcutaneous adipose tissue is more avid in absorption of circulating free fatty acids and triglycerides (Ibrahim, 2010). The significance of subcutaneous fat deposition during the embryonic period is unknown. In the first few days after the hatching of chicks, yolk is rapidly absorbed. Therefore, we hypothesize that the function of

subcutaneous adipose tissue may be associated with absorption of circulating lipid after hatching. The development of digestive system is not complete after hatching; extra energy supply could be an important function of subcutaneous fat deposition during the embryonic and posthatch period (Halevy, 2020; Lu et al., 2020; Nyuiadzi et al., 2020). Chick subcutaneous adipose tissue develops during the embryonic Day 12 and maintains a relatively stable content throughout the lifetime. In contrast, chick abdominal fat develops later than subcutaneous adipose tissue and has a strong relationship with feeding and management (Mellouk et al., 2018; Hicks and Liu, 2021).

During the past two decades, growth and development of white adipose tissue (WAT) and brown adipose tissue (BAT) have been extensively studied in various mammals and humans (Lu et al., 2021; Van Schaik et al., 2021). BAT evolved as a specialized thermogenic organ that is responsible for adaptive non-shivering thermogenesis (NST). For NST, energy metabolism of BAT mitochondria is increased by activation of uncoupling protein 1 (UCP1), which dissipates the proton motive force as heat. There was insufficient evidence to justify the presence of BAT and UCP1 gene in chickens (Mezentseva et al., 2008; Sotome et al., 2021). It is unclear whether subcutaneous adipose tissue is another important source of NST in chickens (Cristina-Silva et al., 2021). It is generally believed that chicken adipose tissue is similar to that of human beings, and neither has a strong ability of *de novo* fat synthesis. This is different from rodents, wherein both liver and adipose tissues have equal importance on *de novo* fat synthesis (Miska et al., 2015; Cogburn et al., 2020). From this point, chickens and humans have higher similarity in adipocyte lipid metabolism, and it is essential to understand the development and function of adipocyte lipid metabolism during the embryonic and posthatch periods. Despite a wealth of data, detailed information is lacking regarding the development of subcutaneous adipose tissue during embryogenesis and after hatching (Mellouk et al., 2018; Xiao et al., 2019).

Therefore, the objective of the current study was to determine the developmental changes of adipocyte differentiation, lipid synthesis, lipolysis, fatty acid β-oxidation, and lipid contents from E12 to D9.5 in chick subcutaneous adipose tissues, aiming to provide theoretical basis on physiological characteristics about lipid metabolism in chicks.

MATERIALS AND METHODS

All experimental procedures were performed in accordance with the Regulations for the Administration of Affairs Concerning Experimental Animals approved by the State Council of People's Republic of China. The study was approved by the Institutional Animal Care and Use Committee of Northwest A&F University (Permit Number: NWAFAC1019).

Sampling Collection

Lohmann pink chicken embryos and chicks used in the current study were bought from the Yangling Julong Poultry Industry Co. Ltd. (Yangling, China). Incubation conditions are as follows: E1∼E19, 37.8℃, E19∼E21, 37 37.5℃ (Qingdao Xinyi Electronic Equipment Co., Ltd. Qingdao, China). Considering that the incubation stage of chicken embryo has certain individual differences, 10 eggs were selected randomly and taken out from the same incubator every 2 days from the embryonic day 12, marked E12, E14, E16, E18, and E20. After hatching, the chicks were allowed *ad libitum* access to water and feed. Considering that the chicks are not hatched at the same time, 10 chicks were selected randomly at the age of 1.5, 3.5, 5.5, 7.5, and 9.5 days after hatching (D1.5, D3.5, D5.5, D7.5, D9.5). Ten stages cover the appearance of subcutaneous adipose tissue to the disappearance of yolk. Chicken embryos and chicks were humanely euthanized by cervical dislocation and weighed after removing surface liquid

TABLE 1 | Primers list in this study.

Genes	Accession number	Sequencing (5′–3′)	Notes
PPARγ	NM_001001460.1	F:AGTCCTTCCCGCTGACCAAA R:TCTCCTGCACTGCCTCCACA	qPCR
C/EBPα	NM_001031459.1	F:TCCCACCTGCAGTACCAGAT R:TTTTGGATTTGCCGCGGTG	qPCR
A-FABP	NM_204290.1	F:GCCAAGCCTAATTTAACTATCA R:CAGCAGGTTCCCATCCAC	qPCR
ACC	NM_205505.1	F:GCTTCCCATTTGCCGTCCTA R:GCCATTCTCACCACCTGATTACT	qPCR
FASN	NM_205155.2	F:TTTGGTGGTTCGAGGTGGTA R:CAAAGGTTGTATTTCGGGAGC	qPCR
LPL	NM_205282.1	F:TTGGTGACCTGCTTATGCTA R:TGCTGCCTCTTCTCCTTTAC	qPCR
ATGL	NM_001113291.1	F:TGCGTGGAGTGAGATATGTTGA R:TTGCGAAGGTTGAATTGGAT	qPCR
HSL	XM_025155301.1	F:GTCTCGGGTTCCAGTTCGTG R:CGTAGGACACCAACCCGATG	qPCR
PPARα	NM_001001464.1	F:CAAACCAACCATCCTGACGAT R:GGAGGTCAGCCATTTTTTGGA	qPCR
CPT1A	NM_001012898.1	F:CTTGCCCTGCAGCTTGCT R:AGGCCTCGTATGTCAAAGAAATT	qPCR
CPT2	NM_001031287.2	F:GCCTTCCCTCTTGGCTACCT R:TCTCAGCAATGCCCACGTATC	qPCR
GAPDH	NM_204305.1	F:AGAACATCATCCCAGCGT R:AGCCTTCACTACCCTCTTG	qPCR
CYTB	YP_009558663.1	F:TCTTACCTGGGTTCTTTCGCC R:AGTAGTAGGCCGGTGAGGAT	mtDNA copy number detection
ACTB	NM_205518.1	F:GACCGGCGGGGTTTATATCTT R:ATTGTCAACAACGAGCGCAG	mtDNA copy number detection

PPARγ, peroxisome proliferator-activated receptor gamma; C/EBPα, CCAAT enhancer binding protein alpha; A-FABP, fatty acid-binding protein 4; ACC, acetyl-CoA carboxylase; FAS: fatty acid synthase; LPL, lipoprotein lipase; ATGL, adipose triglyceride lipase; HSL, hormone-sensitive lipase; PPARα, peroxisome proliferator-activated receptor alpha; CPT1A, carnitine palmitoyltransferase 1A; CPT2, carnitine palmitoyltransferase 2; GAPDH, glyceraldehyde phosphate dehydrogenase; CYTB, cytochrome b; ACTB, actin, beta.

with filter paper. Adipose, intestine, yolk, and liver tissues were rinsed thoroughly with ice-cold phosphate-buffered saline to remove blood contamination on the surface and also weighed for the tissues index calculation. Adipose samples were fixed in 4% formaldehyde for subsequent histological analysis using hematoxylin-eosin (HE) and immunohistochemistry (IHC). Tissues were collected in centrifuge tubes and stored at room temperature. Complete blood was collected in centrifuge tubes, and serum was harvested following centrifugation at 3,000 rpm at 4°C for 10 min until analysis from E20, D1.5, and D9.5. All the samples for RNA and protein analysis were stored at −80°C.

HE and IHC Staining

After fixing, the adipose samples were processed through a series of procedures including dehydration, paraffin embedding, sectioning, and staining. All these procedures were performed by Wuhan Servicebio Technology Co., Ltd. (Wuhan, China). Primary antibody: pref-1 (Sangon, Shanghai, China). According to HE and IHC staining, adipocyte size, preadipocyte number, and cell proportion were calculated. The number of adipocytes per unit area represents the volume of adipocytes. The number of preadipocytes per unit area represents the preadipocyte number. The ratio of adipocyte number and preadipocyte number represents the cell proportion.

Gene Expression

The deposition, decomposition, and utilization of fat are important processes in the function of adipose tissue. The maker genes of adipocyte differentiation (PPARγ, C/EBPα, and FABP4), lipid synthesis (ACC, FAS, and LPL), lipolysis (ATGL and HSL), and fatty acid β-oxidation (PPARα, CPT1A, and CPT2) are then measured from E12 to D9.5 chick adipose tissues. Total RNA extraction and cDNA synthesis from adipose and liver samples were performed according to reagent protocols using TRIzol and Primer Script RT Reagent kits (TaKaRa, Dalian, China). Relative gene expression was quantified by real-time quantitative PCR (qPCR). The assay was carried out *via* SYBR Premix Ex Taq kit (TaKaRa, Dalian, China) on the Y480 (Roche, Basel, Switzerland). Detailed reaction system was referred to our previous research (Zhao et al., 2020). Primer sequences used in the current study were all obtained from GenBank and shown in **Table 1**. All samples were run in triplicate, and the average cycle threshold (Ct) values were calculated for quantification using the $2^{-\Delta\Delta}$Ct method (Livak and Schmittgen, 2001).

Western Blotting

Adipose and liver tissues were lysed with RIPA lysis buffer (1 mM $MgCl_2$, 10 mM Tris-HCl at pH 7.4, 1% Triton X-100, 0.1% sodium dodecyl sulfate (SDS), and 1% Non-idet P40 cocktail). The proteins were separated by 5∼12% SDS polyacrylamide gel electrophoresis and transferred to cellulose membranes. The membranes were incubated overnight with the following primary antibodies: GAPDH (Proteintech, United States), ATGL (Proteintech, United States), PPARα (Sangon, Shanghai, China), FABP4 (Sangon, Shanghai, China), and CPT2 (Sangon, Shanghai, China). They were then immunoblotted with secondary antibody (Immunoway, United States). Immunoreactivity was visualized with enhanced chemiluminescence and analyzed with the Quantity One System (BioRad, United States) (Kim et al., 2020; Liang et al., 2020).

Mitochondrial DNA Copy Number Detection

Fatty acid β-oxidation occurred mainly in mitochondria, and mtDNA copy number is an important index for thermogenesis in adipose tissue (Kavlick, 2019). mtDNA copy number was determined by qPCR as described (Kavlick, 2019; Xia et al., 2020). Briefly, total DNA was isolated from the adipose tissue using column animal genomic DNA purification kit (Sangon, Shanghai, China) according to the manufacturer's instructions. The relative mtDNA copy number was calculated from the ratio of *CYTB* (mitochondrial encoded gene)/*ACTB* (nuclear encoded gene). DNA was homogenized (100 ng/μl) before qPCR (Y480 real-time PCR detection system, Roche, Switzerland) utilizing SYBR detection (Takara, Dalian, China). Amplification protocol was: 95°C for 30 s, 50 cycles at 95°C to denature, and 60°C for 30 s to anneal. Samples were run in triplicate. All data were normalized by *ACTB* and calculated with the $2^{-\Delta\ \Delta}$ Ct method (Livak and Schmittgen, 2001).

Triglyceride and Free Fatty Acid Detection

Blood samples were collected in a vacuum vessel without anticoagulant from jugular vein, and serum was centrifuged at

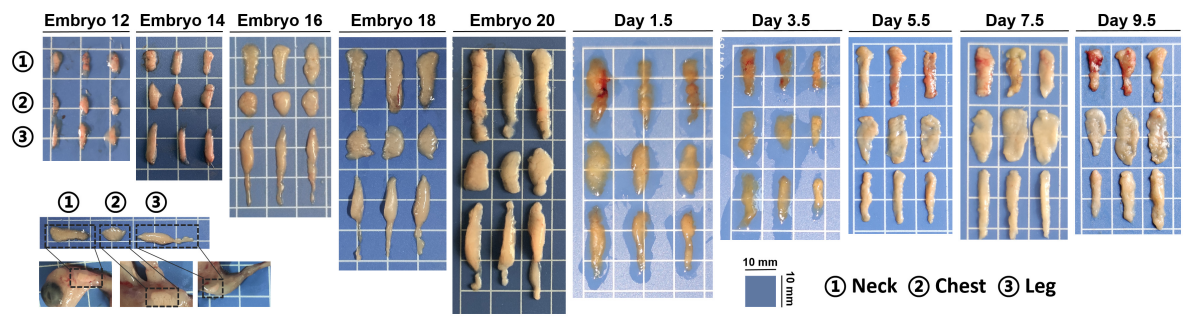

FIGURE 1 | Gross morphology of chick subcutaneous adipose from E12 to D9.5.

2,000 rpm for 10 min at 4°C. Triglyceride (TG) and free fatty acid (FFA) contents in serum were determined using commercial kits (Sangon, Shanghai, China) based on kits' instructions.

Statistical Analysis

All data were shown as means and standard error (SE). Analysis of variance (ANOVA) was used with SPSS software 18.0 (IBM, Chicago, United States). *P*-values of less than 0.05 were considered to be statistically significant, and the notable differences between groups were identified by Duncan's multiple comparisons test. Different tissue parameters were divided into embryo and chick periods, their correlations were calculated by simple linear regression, R^2 and *P*-value represent goodness of fit, and slope is significantly non-zero individually.

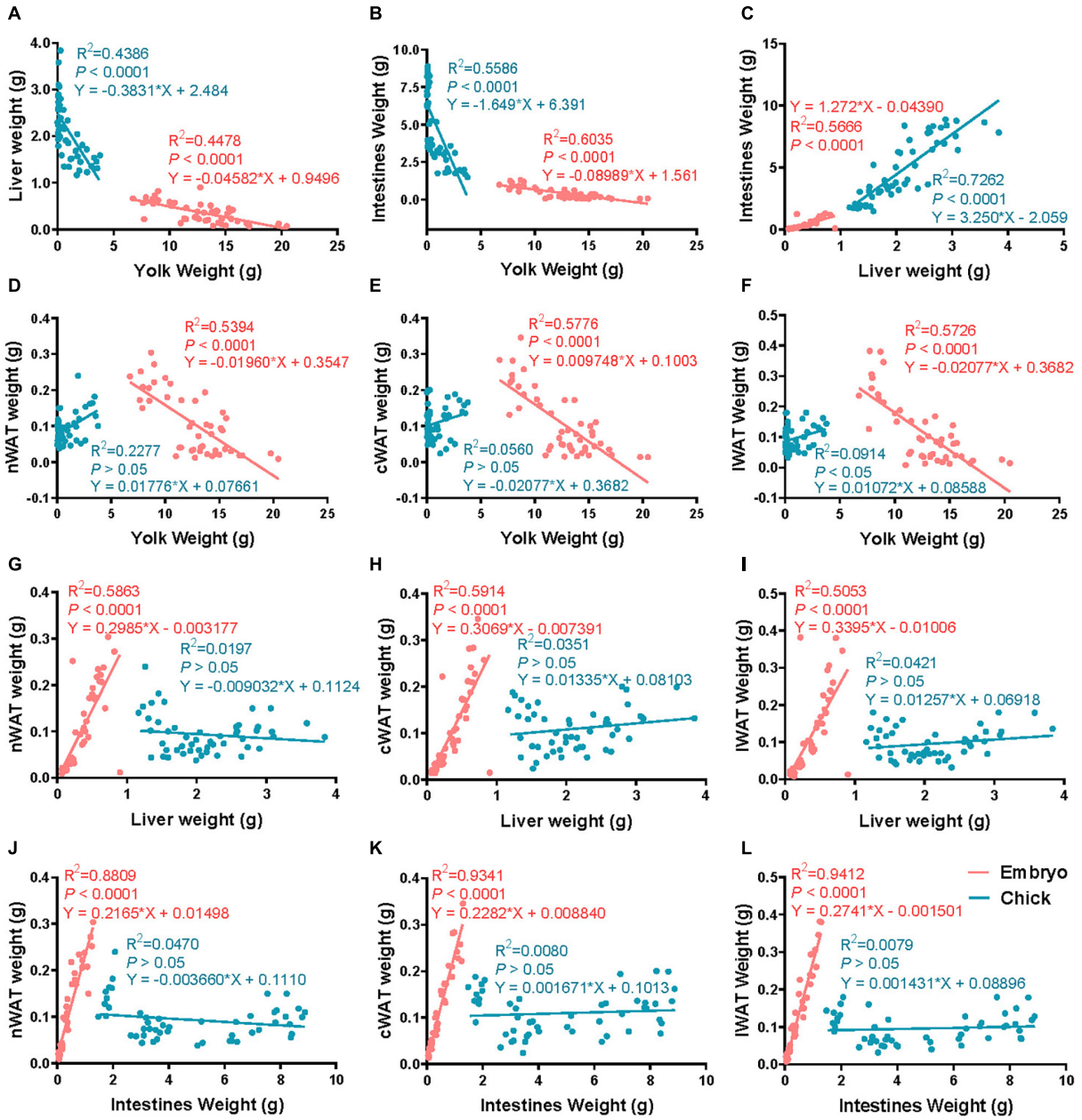

FIGURE 2 | The correlation of subcutaneous fat and related tissues from E12 to D9.5. **(A)** The correlation of liver weight and yolk weight. **(B)** The correlation of intestine weight and yolk weight. **(C)** The correlation of liver weight and liver weight. **(D)** The correlation of nWAT weight and yolk weight. **(E)** The correlation of cWAT weight and yolk weight. **(F)** The correlation of IWAT weight and yolk weight. **(G)** The correlation of nWAT weight and liver weight. **(H)** The correlation of cWAT weight and liver weight. **(I)** The correlation of IWAT weight and liver weight. **(J)** The correlation of nWAT weight and intestine weight. **(K)** The correlation of cWAT weight and intestine weight. **(L)** The correlation of IWAT weight and intestine weight. nWAT, neck white adipose tissue; cWAT, chest white adipose tissue; IWAT, leg white adipose tissue. Pink: embryonic period, blue: posthatch period.

RESULTS

Developmental Changes of Embryo or Chick Growth Parameters and Adipose Contents

As shown in **Figure 1**, subcutaneous adipose tissue of chicks increased gradually during the embryonic period, but the size of the adipose tissue tended to decrease at posthatch period. Neck white adipose tissue (nWAT) is located outside the jugular vein, chest white adipose tissue (cWAT) is located on the surface of pectoralis, and leg white adipose tissue (lWAT) is located in the anterior of the leg. Most adipose tissues of embryo or chick were subcutaneous adipose tissues and little abdominal adipose at this development stage.

The weight data of adipose and related tissues were collected, and their indexes were calculated. As shown in **Supplementary Figure 1**, the weight of the embryo gradually increases during the embryonic period, then decreases briefly after hatching and then begins to rise again. The yolk weight was gradually declining, and the liver weight and intestine weight gradually increased from E14 to D9.5.

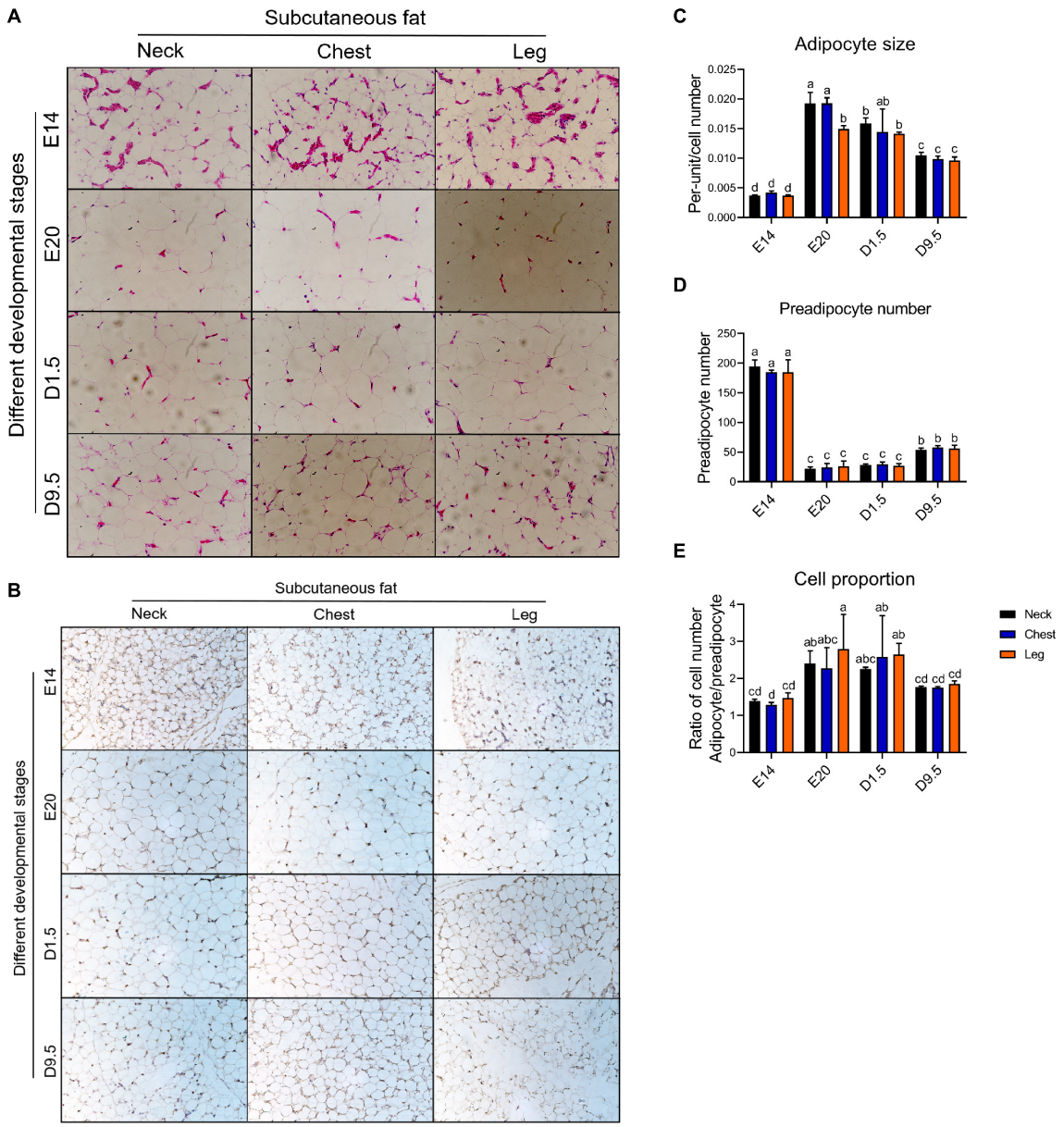

FIGURE 3 | HE and IHC staining analysis of chick adipose. **(A)** HE staining in four development periods. **(B)** IHC staining (pref-1) analysis in four development periods. **(C)** Adipocyte size in four development periods. **(D)** Preadipocyte number in four development periods. **(E)** Ratio of adipocyte to preadipocyte in four developments. HE, hemotoxylin and eosin staining; IHC, immunohistochemical.

Figures 2A–C shows that there was a strong correlation between yolk weight and liver weight, egg yolk weight and intestinal weight, and liver weight and intestinal weight in both embryo and chick. **Figure 2D** shows that nWAT weight was strongly correlated with yolk weight of embryo, but not with yolk weight of chick. **Figure 2E** shows that cWAT weight was strongly correlated with yolk weight in embryo but had no correlation with yolk weight in chick. **Figure 2F** shows that there was a strong correlation between yolk weight and lWAT weight of embryo but had no correlation in chick. **Figure 2G** shows that nWAT weight was strongly correlated with liver weight in embryo but had no correlation with liver weight in chick. **Figure 2H** shows that cWAT weight was strongly correlated with liver weight in embryo, but the cWAT weight had no correlation with liver weight in chick. **Figure 2I** shows that lWAT weight was strongly correlated with liver weight in embryo, while had no correlation with liver weight in chick. **Figure 2J** shows that nWAT weight was strongly correlated with intestine weight in embryo but had no correlation with intestine weight in chick. **Figure 2K** shows that cWAT weight was strongly correlated with intestinal weight in embryo but had no correlation with intestine weight in chick. **Figure 2L** shows that lWAT weight was strongly correlated with intestine weight in embryo but had no correlation with intestine weight in chick.

HE Staining and IHC Analysis of Chick Adipose

Figure 3A shows the HE staining in four development periods. **Figure 3B** shows that the cell that does not have significant lipid can be marked by pref-1, which was recognized as preadipocyte. **Figure 3C** shows the adipocyte size in four development periods. In the case of adipocyte size, E20 was significantly larger than D1.5, D9.5, and E14 in the nWAT and cWAT. D1.5 was significantly larger than D9.5 and E14 in the nWAT and cWAT. D9.5 was significantly larger than E14 in the nWAT and cWAT. There was no significant difference in lWAT between E20 and D1.5, but E20 and D1.5 were significantly larger than D9.5 and E14. D9.5 was significantly larger than E14 in the lWAT. **Figure 3D** shows the preadipocyte number in four development periods. In the case of preadipocyte number, E14 was significantly higher than D9.5, D1.5, and E20. D9.5 was significantly higher than D1.5 and E20. There was no significant difference between E20 and D1.5. **Figure 3E** shows the ratio of adipocyte to preadipocyte in four developments. E20 was significantly higher than D9.5 and E14, and there was no significant difference from

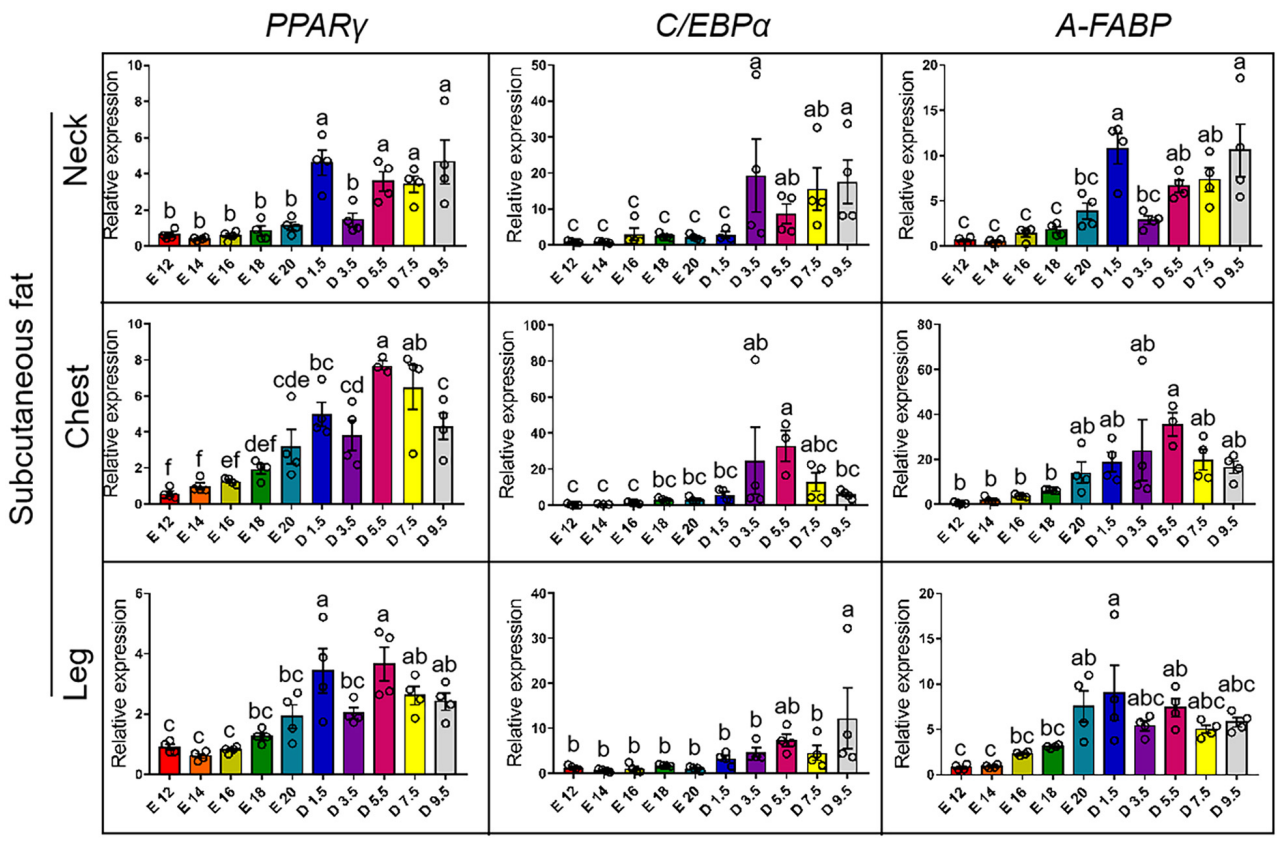

FIGURE 4 | mRNA expression of adipocyte differentiation markers from E12 to D9.5. PPARγ, peroxisome proliferator-activated receptor gamma; C/EBPα, CCAAT enhancer binding protein alpha; A-FABP, fatty acid-binding protein 4.

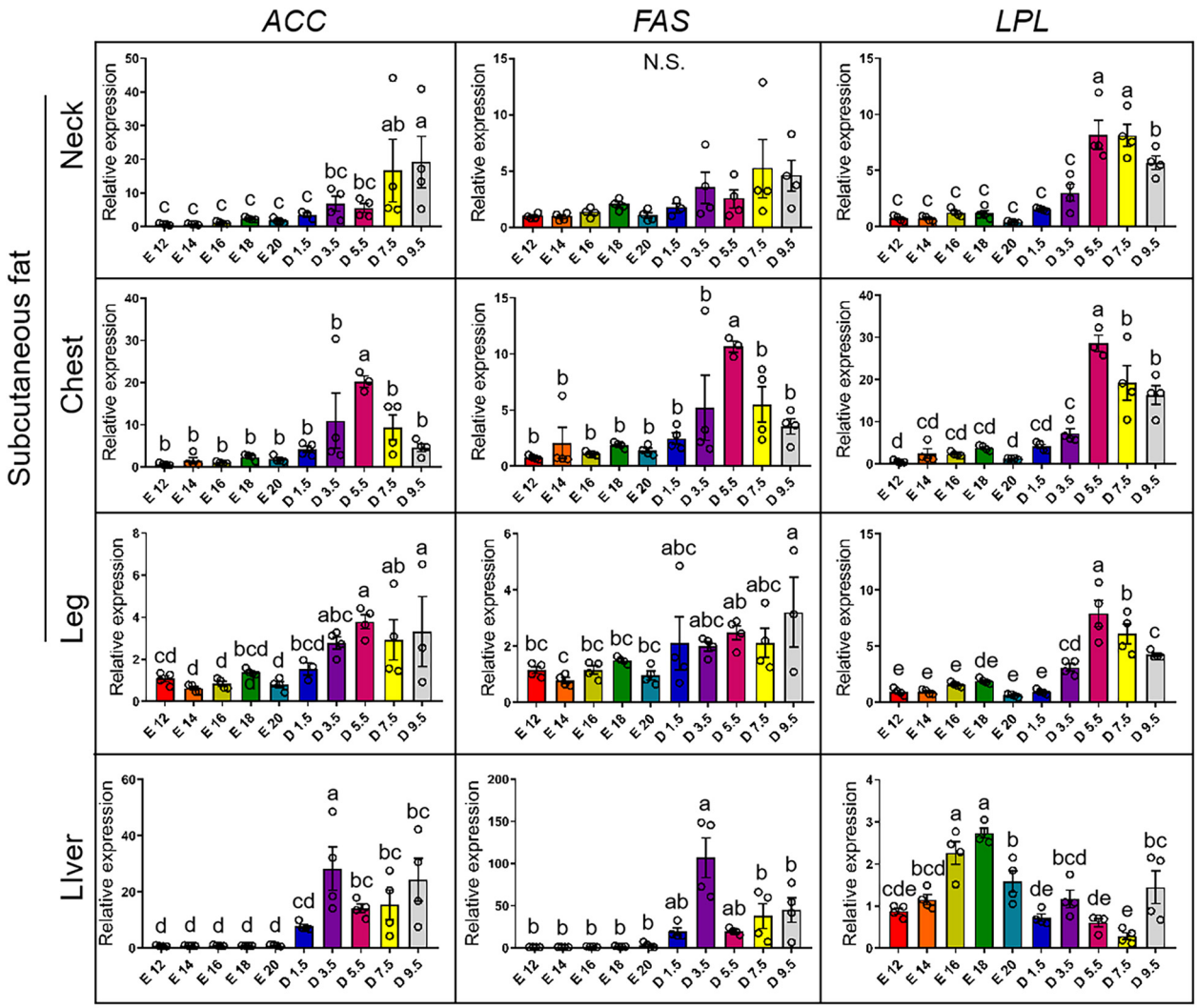

FIGURE 5 | mRNA expression of lipid synthesis genes from E12 to D9.5. ACC, acetyl-CoA carboxylase; FAS, fatty acid synthase; LPL, lipoprotein lipase.

D1.5 in the nWAT and lWAT. E20 was significantly higher than E14, which was not significantly different from D1.5 to D9.5. There were no significant differences between different parts in the same period.

Expression Patterns of Chick Adipose and Liver During Embryonic and Posthatch Periods

Figure 4 shows the expression pattern of adipocyte differentiation marker genes from E12 to D9.5. For the expression of *PPARγ* gene, chicks except D1.5 were significantly higher than embryos in the neck. D5.5 and D7.5 were significantly higher than embryonic stage in the cWAT. D1.5 and D9.5 were significantly higher than E12, E14, E16, and E18 in the cWAT. D1.5 and D5.5 were significantly higher than embryonic stage in the lWAT. For the expression of *C/EBPα* gene, the chicks were significantly higher than embryos in the nWAT, and D5.5 was significantly higher than embryonic stage in the cWAT. D9.5 was the highest in the lWAT and significantly higher than embryonic stage, while D1.5, D3.5, D5.5, and D7.5 were not significantly different from the embryonic stage. For the expression of *A-FABP* (*FABP4*) gene, the expression levels of D1.5 and D9.5 were significantly higher than D7.5, D5.5, D3.5, and embryonic stage in the nWAT. D5.5 was significantly higher than E12, E14, E16, and E18 in the cWAT. D1.5 was the highest in the lWAT and significantly higher than embryonic stage, while D1.5 was not significantly different from other posthatch periods.

Figure 5 shows the expression pattern of lipid synthesis genes from E12 to D9.5. For the expression of *ACC* gene, D9.5 and D7.5 were significantly higher than embryonic stage in the nWAT. D3.5 and D5.5 were not significantly different from the embryonic stage in the nWAT. D5.5 was the highest in the cWAT and significantly higher than other stages. D5.5 and D9.5 were significantly higher than embryonic stage in the lWAT. D3.5 was significantly higher than other stages in the

liver. For the expression of *FAS* gene, there were no significant differences between chicks and embryos in the nWAT. D5.5 was the highest in the cWAT and significantly higher than other stages. D9.5 was the highest in the lWAT and significantly higher than the embryonic stage. D3.5 was the highest in the liver and significantly higher than D7.5, D9.5, and embryonic stage. For the expression of *LPL* gene, D5.5, D7.5, and D9.5 were significantly higher than D3.5 and embryonic stage in the nWAT. D5.5, D7.5, and D9.5 were significantly higher than embryonic stage in the cWAT. D3.5 was significantly higher than E12 and E20 in the cWAT. D5.5 was significantly higher than D7.5, D9.5, D3.5, and embryonic stage in the lWAT. E16 and E18 were significantly

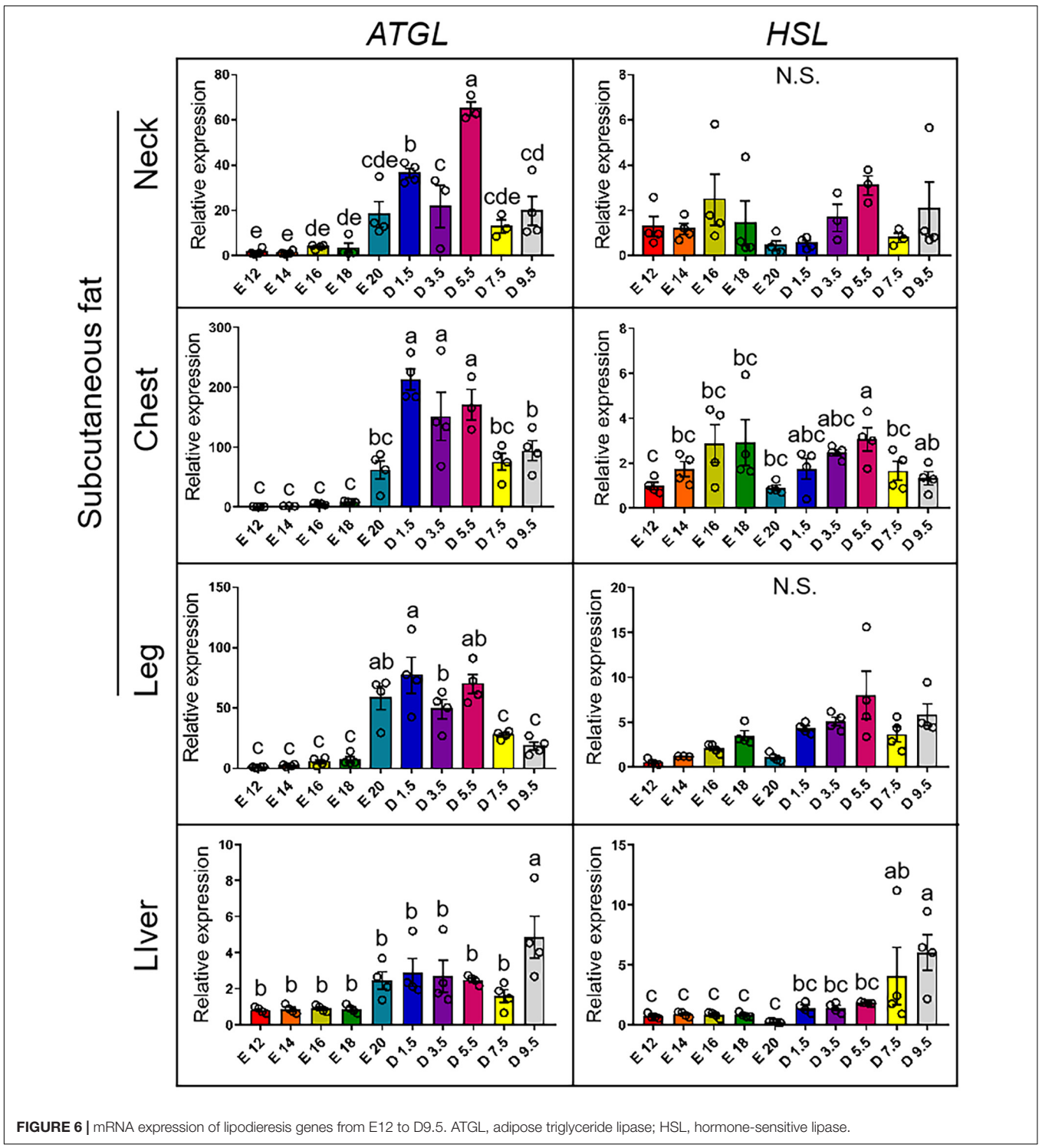

FIGURE 6 | mRNA expression of lipodieresis genes from E12 to D9.5. ATGL, adipose triglyceride lipase; HSL, hormone-sensitive lipase.

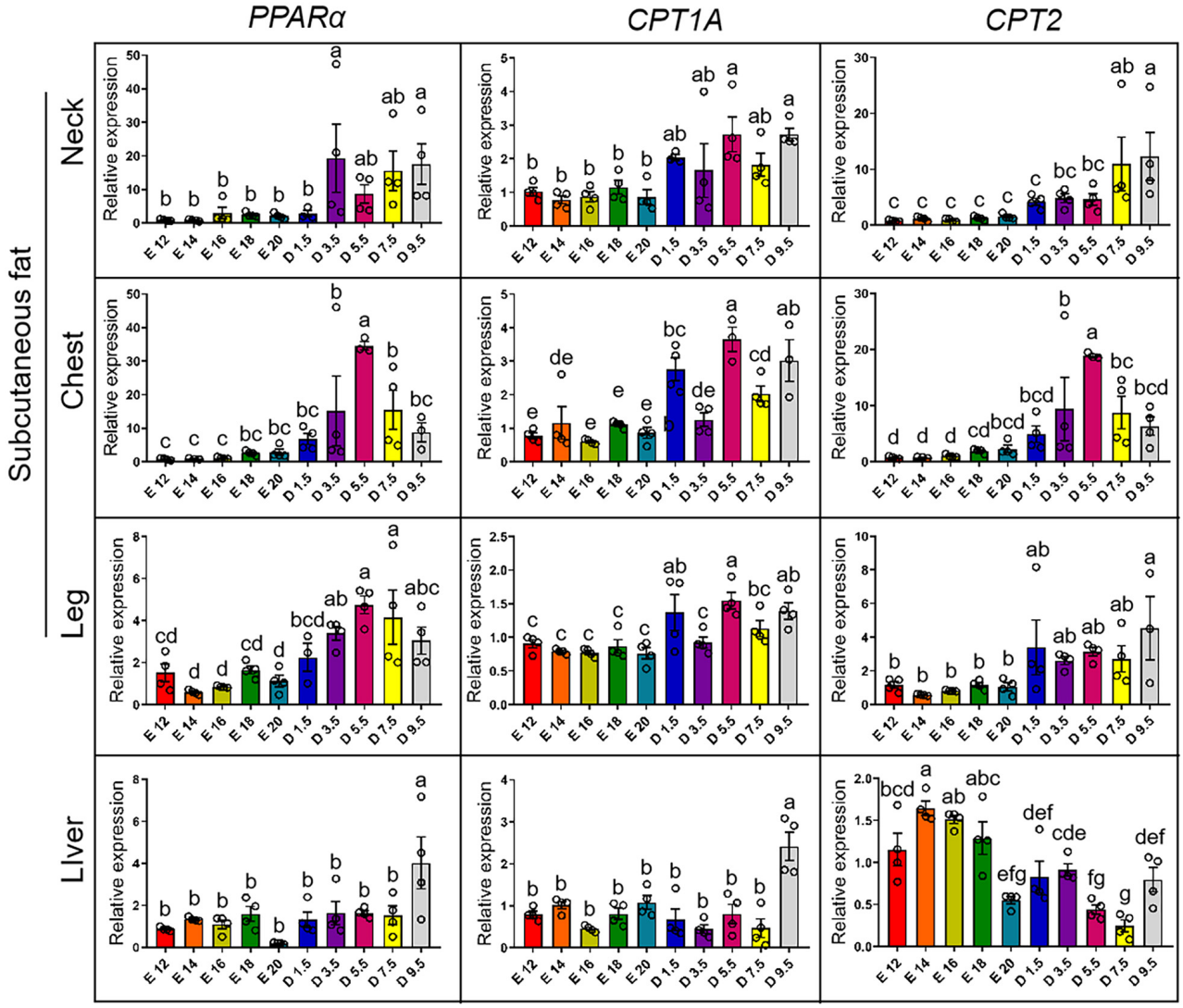

FIGURE 7 | mRNA expression of fatty acid oxidation genes from E12 to D9.5. PPARα, peroxisome proliferator-activated receptor alpha; CPT1A, carnitine palmitoyltransferase 1A; CPT2, carnitine palmitoyltransferase 2.

higher than other stages, and E20 was significantly higher than D1.5, D5.5, and D7.5 in the liver.

Figure 6 shows the expression pattern of lipodieresis genes from E12 to D9.5. In the case of the expression of *ATGL* gene, the chick stages of D1.5, D3.5, and D5.5 were significantly higher than the embryonic stage in the nWAT, cWAT, and lWAT. D9.5 was significantly higher than other stages in the liver. For the expression of *HSL* gene, there was no significant difference in nWAT in different periods. D5.5 in cWAT was significantly higher than the embryonic stage. Except for D5.5, the chick stage was not significantly different with the embryonic stage in the cWAT. The expression level increased from embryonic stage to chick stage, but there was no significant difference between each stage in the lWAT. The chick stage was higher than the embryonic stage in the liver, and D9.5 was significantly higher than other stages.

Figure 7 shows the expression pattern of fatty acid oxidation genes from E12 to D9.5. For the expression of *PPARα* gene, the chick stages of D3.5 and D9.5 were significantly higher than the embryonic stage in nWAT, cWAT, and lWAT. D9.5 was significantly higher than any other stages in the liver, and there was no significant difference between other periods. For the expression of *CPT1A* gene, the chick stages of D5.5 and D9.5 were significantly higher than the embryonic stage in the nWAT and the chick stage was significantly higher than the embryonic stage in the cWAT but D3.5. D5.5, D1.5, and D9.5 were significantly higher than the embryonic stage in the lWAT. D9.5 was significantly higher than other stages in the liver, and there was no significant difference between other periods. For the expression of *CPT2* gene, the chick stage of D7.5 and D9.5 were significantly higher than the embryonic stage in the nWAT. The chick stage of D5.5 was significantly higher than embryonic

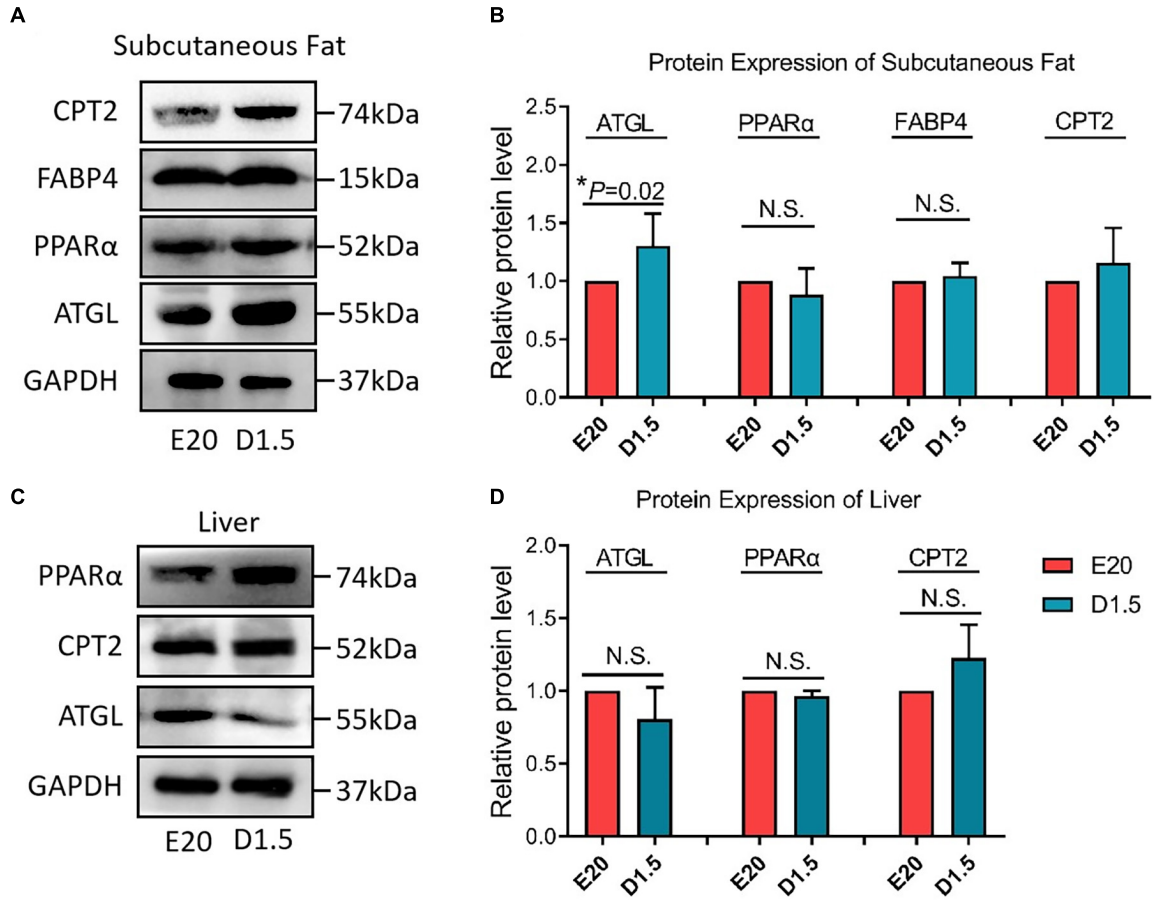

FIGURE 8 | Protein expression of fatty acid oxidation genes in E20 and D1.5. **(A)** Protein expression of subcutaneous adipose in E20 and D1.5. **(B)** Relative protein level expression of subcutaneous adipose in E20 and D1.5. **(C)** Protein expression of liver adipose in E20 and D1.5. **(D)** Relative protein level expression of liver adipose in E20 and D1.5. CPT2, carnitine palmitoyltransferase 2; FABP4, fatty acid binding protein 4; ATGL, adipose triglyceride lipase; GAPDH, glyceraldehyde phosphate dehydrogenase.

stage in the cWAT, and D9.5 was significantly higher than the embryonic stage in the lWAT, but the chick stage was significantly lower than the embryonic stage in the liver and showed a gradual decline from E12 to D9.5.

Figure 8 shows the key protein expression level between E20 and D1.5. For CPT2, there was no significant difference between embryonic and chick period in WAT and liver. For FABP4, the protein expression in D1.5 was higher than E20 in WAT but had no significant difference in liver. For PPARα, there was no significant difference between embryonic and chick period in WAT and liver. For ATGL, the protein expression in D1.5 was higher than E20 in WAT but had no significant difference in liver.

Mitochondrial DNA Copy Number of Subcutaneous Adipose Tissue

To determine whether the massive deposition of subcutaneous adipose tissue in chick embryo was related to thermogenesis, mtDNA copy numbers of E20, D1.5, and D9.5 were measured in nWAT, cWAT, and lWAT. **Figure 9** shows that the mtDNA copy number of E20, D1.5, and D9.5 has no significant difference in nWAT; the mtDNA copy number of D1.5 and D9.5 were significantly higher than E14 in cWAT and lWAT.

TG and FFA Concentration

FFA was the main substrate fatty acid β-oxidation. As the hydrolyzate products of TG, FFA could be used in fatty acid β-oxidation for thermogenesis. **Figure 10** shows that the TG concentration in E20 and D1.5 was significantly higher than D9.5. The FFA concentration in E20 was higher than D9.5, and D9.5 was higher than D1.5.

DISCUSSION

The abdominal fat deposition in chicken is closely related to feed conversion efficiency, so it has attracted more attention in poultry production (Chen et al., 2019; Wu et al., 2019). The study-associated subcutaneous adipose tissue has been neglected to some extent, especially during the embryonic period and after hatching (Xiao et al., 2019). In this study, we described a relatively complete process of subcutaneous adipose tissue development in

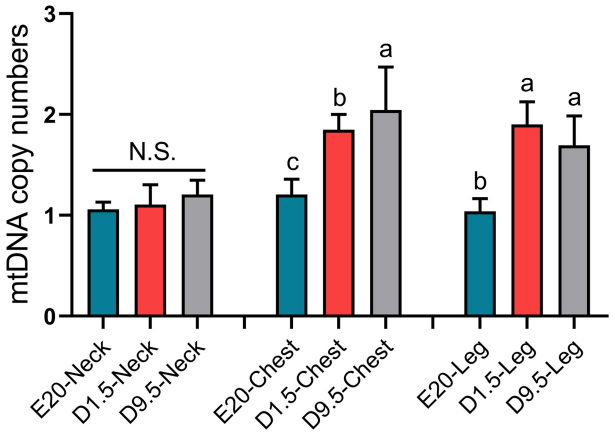

FIGURE 9 | The mitochondrial DNA copy number of subcutaneous fat in E20, D1.5, and D9.5. nWAT, neck white adipose tissue; cWAT, chest white adipose tissue; lWAT, leg white adipose tissue.

the embryonic period and after hatching. Subcutaneous adipose tissue was the main type of abdominal fat at this stage and was mainly distributed in the neck, chest, and leg. It suggested that a large amount of subcutaneous fat deposition at the embryo period is of important physiological significance to chick. During the embryonic and posthatch period, we found that the body weight, liver, and intestine maintained uninterrupted growth and development, and the yolk weight continued to drop. However, the change of WAT weight presented a different trend; it was increasing at embryonic period and decreasing after hatching (**Supplementary Figure 1**). The dynamic changes suggested that subcutaneous adipose tissue may play an important physiological role in chicks after hatching.

Obviously, the explanation that subcutaneous adipose tissue is merely an energy supply organ is illogical; the lipid transferred from yolk to subcutaneous adipose tissue caused a partial loss of energy. Yolk is an important tissue in the first few days after the bird was hatched; on account of insufficient energy supply in the digestive system, yolk provides the main energy for body growth and development (Scanes, 2020; Zhu et al., 2020). More importantly, yolk could be absorbed in two different ways before and after hatching. For the hatching period, the yolk was absorbed by yolk sac membrane, but the yolk contents could pass into the intestine *via* the lumen of the yolk stalk in at least newly hatched to 3-day-old chicken (van der Wagt et al., 2020). The presence of subcutaneous adipose tissue could be an energy supply that helps the chicks survive after hatching.

More than 90% of *de novo* lipogenesis in humans and chickens is undertaken by the liver, which was different from rodent (Na et al., 2018; Hicks and Liu, 2021). Therefore, chicken was considered a more suitable model for non-alcoholic fatty liver disease (NAFLD). Enough studies have revealed the details about lipid synthesis, especially the enzymes of lipid synthesis, such as *ACC*, *FAS*, and *LPL* (Mottillo et al., 2017; Seo et al., 2018; Zhang et al., 2019; Bhat et al., 2021). Meanwhile, many studies have concluded that adult chicken fat tissue has no or very weak lipid synthesis ability (Na et al., 2018). In this study, the expression pattern of *ACC*, *FAS*, and *LPL* was described from E14 to D9.5. It was shown that chick has the ability of *de novo* synthesis of FFA, and the ability has been enhanced a few days after hatching. However, the significance of lipid synthesis in subcutaneous adipose tissue for chick is still incomplete.

The expression of *ATGL* in subcutaneous adipose tissue showed that TG was broken down and FFA was released in blood for other tissue uptake. Comparing the expression pattern of *ATGL* in liver, subcutaneous adipose tissue should have a more important role in FFA supplement. Comparing with abdominal adipose tissue, subcutaneous adipose tissue is more avid in absorption of circulating free fatty acids and triglycerides (Ibrahim, 2010). The results of TG and FFA concentration in D1.5 were extraordinary, the TG concentration was high and the FFA concentration was low. The high concentration of TG was continuously inducted into the fat uptake by the liver after hatching; the remaining TG could be absorbed by the subcutaneous adipose tissue. The special phenomenon may be the reason why hepatocyte was full of lipids in new-hatch chickens, which was generally considered a NAFLD animal model (Liu et al., 2018; Peng et al., 2018). It revealed that the function of subcutaneous adipose tissue were absorbing extra TG in blood and releasing FFA from adipocytes. This finding

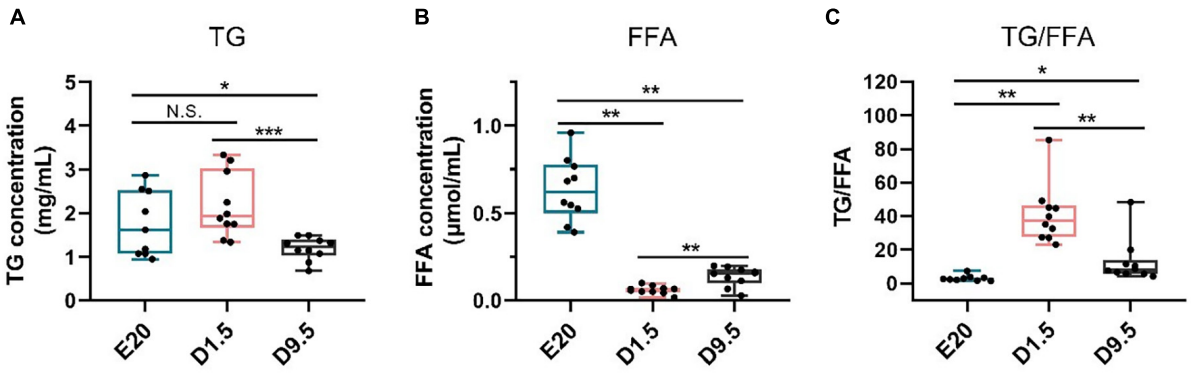

FIGURE 10 | TG and FFA concentration in E20, D1.5, and D9.5. **(A)** TG concentration in E20, D1.5, and D9.5. **(B)** FFA concentration in E20, D1.5, and D9.5. **(C)** Ratio of TG to FFA concentration in E20, D1.5, and D9.5. TG, triglycerides; FFA, free fatty acid. $^{*}P < 0.05$; $^{**}P < 0.01$; $^{***}P < 0.001$.

suggested that large amounts of subcutaneous fat deposition could be the inducement of NAFLD and provided a new idea for human treatment of NAFLD.

It was suggested that the subcutaneous adipose tissue could have other important functions during the special period. The subcutaneous adipose tissue weight was not significantly correlated with liver weight and intestine weight (**Figure 2**). It inferred that the function of adipose tissue may be related to the environmental adaptability of chicks when they were hatched. WAT and BAT are the two main forms of adipose tissue in humans and rodents (Alcalá et al., 2019; Cuevas-Ramos et al., 2019). Thermogenic BAT has never been described in birds or other non-mammalian vertebrates (Mezentseva et al., 2008). Compared with abdominal adipose tissue, the main type of adipose deposition of chicken embryo was subcutaneous adipose tissue (Hicks and Liu, 2021). Interestingly, there were some similarities between the WAT distribution in chickens and the BAT in humans and rodents, and the internal relationship between two adipose tissues needs further study. In this study, it was found that the number of mitochondrial DNA copies in adipose tissue increased significantly within a few days after hatching. The increasing of mitochondrial copy number is an important phenotype of the enhancement of adipose tissue thermogenesis. Due to the loss of *UCP1* gene in chicken, the thermogenesis of subcutaneous adipose tissue depends on *PPARα*, *PPARβ*, *CPT1A*, and *CPT2* genes (Lee et al., 2016; Martos-Sitcha et al., 2019; Kroon et al., 2020). According to the expression pattern of key factors in thermogenesis, the ability of fatty acid β-oxidation in subcutaneous adipose tissue was increasing in new-hatch period. Although birds do not have BAT, subcutaneous adipose tissue partially functions as brown fat during the period before and after hatching, and its oxidative thermogenesis of fatty acids is greatly improved.

CONCLUSION

In this study, the morphology and weight of chick subcutaneous adipose tissue from E14 to D9.5 were characterized, and the expression pattern of adipocyte differentiation, lipid synthesis, lipolysis, and fatty acid β-oxidation from E14 to D9.5 were structured. The results showed that subcutaneous adipose tissue released FFA after hatching and the mitochondrial copy number and fatty acid β-oxidation level significantly increased. It revealed that the function of chick subcutaneous adipose tissue were FFA releasing by lipolysis and thermogenesis by fatty acid β-oxidation. In addition, this finding improved the theory of nutrition supply in embryonic and posthatch period, and might be an important theoretical basis for poultry reproduction.

DATA AVAILABILITY STATEMENT

The original contributions presented in the study are included in the article/**Supplementary Material**, further inquiries can be directed to the corresponding author/s.

ETHICS STATEMENT

The animal study was reviewed and approved by The Institutional Animal Care and Use Committee of Northwest A&F University (Permit Number: NWAFAC1019).

AUTHOR CONTRIBUTIONS

HZ and MW analyzed the data. HZ wrote the manuscript. HZ, QL, MW, XT, and SW collected the samples. QL performed the qPCR. MW, CJ, XT, and XY reviewed and edited the manuscript. HZ, ZW, and XS designed the experiment. All authors contributed to the interpretation of the results and writing of the manuscript.

FUNDING

China Agriculture Research System (CARS-34) supported this work.

ACKNOWLEDGMENTS

We thank JuLong Poultry Industry Co. Ltd. (Yangling, Shannxi, China) for sample collection.

SUPPLEMENTARY MATERIAL

The Supplementary Material for this article can be found online at: https://www.frontiersin.org/articles/10.3389/fphys.2021.684426/full#supplementary-material

Supplementary Figure 1 | The weight of chick subcutaneous fat and related tissues from E12 to D9.5. **(A)** Embryo or chick weight, **(B)** yolk weight, **(C)** liver weight, **(D)** intestine weight, **(E)** nWAT weight, **(F)** cWAT weight, and **(G)** lWAT weight. nWAT, neck white adipose tissue; cWAT, chest white adipose tissue, lWAT, leg white adipose tissue.

REFERENCES

Alcalá, M., Calderon-Dominguez, M., Serra, D., Herrero, L., and Viana, M. (2019). Mechanisms of Impaired Brown Adipose Tissue Recruitment in Obesity. *Front. Physiol.* 10:94. doi: 10.3389/fphys.2019.00094

Bhat, S. F., Pinney, S. E., Kennedy, K. M., McCourt, C. R., Mundy, M. A., Surette, M., et al. (2021). Exposure to high fructose corn syrup during adolescence in the mouse alters hepatic metabolism and the microbiome in a sex-specific manner. *J. Physiol.* 599, 1487–1511. doi: 10.1113/JP280034

Chen, Y., Zhao, Y., Jin, W., Li, Y., Zhang, Y., Ma, X., et al. (2019). MicroRNAs and their regulatory networks in Chinese Gushi chicken abdominal adipose

tissue during postnatal late development. *BMC Genomics* 20:778. doi: 10.1186/s12864-019-6094-2

Cogburn, L. A., Trakooljul, N., Wang, X., Ellestad, L. E., and Porter, T. E. (2020). Transcriptome analyses of liver in newly-hatched chicks during the metabolic perturbation of fasting and re-feeding reveals THRSPA as the key lipogenic transcription factor. *BMC Genomics* 21:109. doi: 10.1186/s12864-020-6525-0

Cristina-Silva, C., Gargaglioni, L. H., and Bícego, K. C. (2021). A thermoregulatory role of the medullary raphe in birds. *J. Exp. Biol.* 2021:234344. doi: 10.1242/jeb.234344

Cuevas-Ramos, D., Mehta, R., and Aguilar-Salinas, C. A. (2019). Fibroblast Growth Factor 21 and Browning of White Adipose Tissue. *Front. Physiol.* 10:37. doi: 10.3389/fphys.2019.00037

Halevy, O. (2020). Timing Is Everything-The High Sensitivity of Avian Satellite Cells to Thermal Conditions During Embryonic and Posthatch Periods. *Front. Physiol.* 11:235. doi: 10.3389/fphys.2020.00235

Hicks, J. A., and Liu, H.-C. (2021). Expression Signatures of microRNAs and Their Targeted Pathways in the Adipose Tissue of Chickens during the Transition from Embryonic to Post-Hatch Development. *Genes* 12:196. doi: 10.3390/genes12020196

Ibrahim, M. M. (2010). Subcutaneous and visceral adipose tissue: structural and functional differences. *Obes. Rev.* 11, 11–18. doi: 10.1111/j.1467-789X.2009.00623

Kavlick, M. F. (2019). Development of a triplex mtDNA qPCR assay to assess quantification, degradation, inhibition, and amplification target copy numbers. *Mitochondrion* 46, 41–50. doi: 10.1016/j.mito.2018.09.007

Kim, M., Lee, S. M., Jung, J., Kim, Y. J., Moon, K. C., Seo, J. H., et al. (2020). Pinealectomy increases thermogenesis and decreases lipogenesis. *Mol. Med. Rep.* 22, 4289–4297. doi: 10.3892/mmr.2020.11534

Kroon, T., Harms, M., Maurer, S., Bonnet, L., Alexandersson, I., Lindblom, A., et al. (2020). PPARγ and PPARα synergize to induce robust browning of white fat in vivo. *Mol. Metab.* 36:100964. doi: 10.1016/j.molmet.2020.02.007

Lee, J., Choi, J., Scafidi, S., and Wolfgang, M. J. (2016). Hepatic Fatty Acid Oxidation Restrains Systemic Catabolism during Starvation. *Cell Rep.* 16, 201–212. doi: 10.1016/j.celrep.2016.05.062

Liang, Y., Alharthi, A. S., Elolimy, A. A., Bucktrout, R., Lopreiato, V., Martinez-Cortés, I., et al. (2020). Molecular networks of insulin signaling and amino acid metabolism in subcutaneous adipose tissue are altered by body condition in periparturient Holstein cows. *J. Dairy Sci.* 103, 10459–10476. doi: 10.3168/jds.2020-18612

Liu, Y., Shen, J., Yang, X., Sun, Q., and Yang, X. (2018). Folic Acid Reduced Triglycerides Deposition in Primary Chicken Hepatocytes. *J. Agric. Food Chem.* 66, 13162–13172. doi: 10.1021/acs.jafc.8b05193

Liu, Y., Zhou, J., Musa, B. B., Khawar, H., Yang, X., Cao, Y., et al. (2020). Developmental changes in hepatic lipid metabolism of chicks during the embryonic periods and the first week of posthatch. *Poult. Sci.* 99, 1655–1662. doi: 10.1016/j.psj.2019.11.004

Livak, K. J., and Schmittgen, T. D. (2001). Analysis of relative gene expression data using real-time quantitative PCR and the 2(-Delta Delta C(T)) Method. *Methods* 25, 402–408. doi: 10.1006/meth.2001.1262

Lu, J., Weil, J., Cerrate, S., and Coon, C. (2020). Developmental changes in physiological amino acids and hepatic methionine remethylation enzyme activities in E10-21 chick embryos and D1-49 broilers. *J. Anim. Physiol. Anim. Nutr.* 104, 1727–1737. doi: 10.1111/jpn.13390

Lu, W. H., Chang, Y. M., and Huang, Y. S. (2021). Alternative Polyadenylation and Differential Regulation of Ucp1: Implications for Brown Adipose Tissue Thermogenesis Across Species. *Front. Pediatr.* 8:612279. doi: 10.3389/fped.2020.612279

Martos-Sitcha, J. A., Simó-Mirabet, P., de Las Heras, V., Calduch-Giner, J. À, and Pérez-Sánchez, J. (2019). Tissue-Specific Orchestration of Gilthead Sea Bream Resilience to Hypoxia and High Stocking Density. *Front. Physiol.* 10:840. doi: 10.3389/fphys.2019.00840

Mellouk, N., Ramé, C., Delaveau, J., Rat, C., Maurer, E., Froment, P., et al. (2018). Adipokines expression profile in liver, adipose tissue and muscle during chicken embryo development. *Gen. Comp. Endocrinol.* 267, 146–156. doi: 10.1016/j.ygcen.2018.06.016

Mezentseva, N. V., Kumaratilake, J. S., and Newman, S. A. (2008). The brown adipocyte differentiation pathway in birds: an evolutionary road not taken. *BMC Biol.* 6:17. doi: 10.1186/1741-7007-6-17

Miska, K. B., Fetterer, R. H., and Wong, E. A. (2015). mRNA expression of amino acid transporters, aminopeptidase, and the di- and tri-peptide transporter PepT1 in the intestine and liver of posthatch broiler chicks. *Poult. Sci.* 94, 1323–1332. doi: 10.3382/ps/pev059

Mohammadpour, F., Darmani-Kuhi, H., Mohit, A., and Sohani, M. M. (2020). Obesity, insulin resistance, adiponectin, and PPAR-γ gene expression in broiler chicks fed diets supplemented with fat and green tea (Camellia sinensis) extract. *Domest Anim. Endocrinol.* 72:106440. doi: 10.1016/j.domaniend.2020.106440

Moreira, G., Boschiero, C., Cesar, A., Reecy, J. M., Godoy, T. F., Pértille, F., et al. (2018). Integration of genome wide association studies and whole genome sequencing provides novel insights into fat deposition in chicken. *Sci. Rep.* 8:16222. doi: 10.1038/s41598-018-34364-0

Mottillo, E. P., Desjardins, E. M., Fritzen, A. M., Zou, V. Z., Crane, J. D., Yabut, J. M., et al. (2017). FGF21 does not require adipocyte AMP-activated protein kinase (AMPK) or the phosphorylation of acetyl-CoA carboxylase (ACC) to mediate improvements in whole-body glucose homeostasis. *Mol. Metab.* 6, 471–481. doi: 10.1016/j.molmet.2017.04.001

Na, W., Wu, Y. Y., Gong, P. F., Wu, C. Y., Cheng, B. H., Wang, Y. X., et al. (2018). Embryonic transcriptome and proteome analyses on hepatic lipid metabolism in chickens divergently selected for abdominal fat content. *BMC Genomics* 19:384. doi: 10.1186/s12864-018-4776-9

Nyuiadzi, D., Berri, C., Dusart, L., Travel, A., Méda, B., Bouvarel, I., et al. (2020). Short cold exposures during incubation and postnatal cold temperature affect performance, breast meat quality, and welfare parameters in broiler chickens. *Poult. Sci.* 99, 857–868. doi: 10.1016/j.psj.2019.10.024

Peng, M. L., Li, S. N., He, Q. Q., Zhao, J. L., Li, L. L., and Ma, H. T. (2018). Based serum metabolomics analysis reveals simultaneous interconnecting changes during chicken embryonic development. *J. Anim. Physiol. Anim. Nutr.* 102, 1210–1219. doi: 10.1111/jpn.12925

Scanes, C. G. (2020). Avian Physiology: Are Birds Simply Feathered Mammals? *Front. Physiol.* 11:542466. doi: 10.3389/fphys.2020.542466

Seo, Y. J., Kim, K. J., Choi, J., Koh, E. J., and Lee, B. Y. (2018). Spirulina maxima Extract Reduces Obesity through Suppression of Adipogenesis and Activation of Browning in 3T3-L1 Cells and High-Fat Diet-Induced Obese Mice. *Nutrients.* 10:712. doi: 10.3390/nu10060712

Simon, J., and Leclercq, B. (1982). Longitudinal study of adiposity in chickens selected for high or low abdominal fat content: further evidence of a glucose-insulin imbalance in the fat line. *J. Nutr.* 112, 1961–1973. doi: 10.1093/jn/112.10.1961

Sotome, R., Hirasawa, A., Kikusato, M., Amo, T., Furukawa, K., Kuriyagawa, A., et al. (2021). In vivo emergence of beige-like fat in chickens as physiological adaptation to cold environments. *Amino Acids* 53, 381–393. doi: 10.1007/s00726-021-02953-5

van der Wagt, I., de Jong, I. C., Mitchell, M. A., Molenaar, R., and van den Brand, H. (2020). A review on yolk sac utilization in poultry. *Poult. Sci.* 99, 2162–2175. doi: 10.1016/j.psj.2019.11.041

Van Schaik, L., Kettle, C., Green, R., Irving, H. R., and Rathner, J. A. (2021). Effects of Caffeine on Brown Adipose Tissue Thermogenesis and Metabolic Homeostasis: A Review. *Front. Neurosci.* 15:621356. doi: 10.3389/fnins.2021.621356

Wu, C., Wang, Y., Gong, P., Wang, L., Liu, C., Chen, C., et al. (2019). Promoter Methylation Regulates ApoA-I Gene Transcription in Chicken Abdominal Adipose Tissue. *J. Agric. Food Chem.* 67, 4535–4544. doi: 10.1021/acs.jafc.9b00007

Xia, B., Shi, X. C., Xie, B. C., Zhu, M. Q., Chen, Y., Chu, X. Y., et al. (2020). Urolithin A exerts antiobesity effects through enhancing adipose tissue thermogenesis in mice. *PLoS Biol.* 18:e3000688. doi: 10.1371/journal.pbio.3000688

Xiao, Y., Wang, G., Gerrard, M. E., Wieland, S., Davis, M., Cline, M. A., et al. (2019). Changes in adipose tissue physiology during the first two weeks posthatch in chicks from lines selected for low or high body weight. *Am. J. Physiol. Regul. Integr. Comp. Physiol.* 316, R802–R818. doi: 10.1152/ajpregu.00017.2019

Zhang, X., Cheng, B., Liu, C., Du, Z., Zhang, H., Wang, N., et al. (2019). A Novel Regulator of Preadipocyte Differentiation, Transcription Factor TCF21, Functions Partially Through Promoting LPL Expression. *Front. Physiol.* 10:458. doi: 10.3389/fphys.2019.00458

Zhao, H., Wu, M., Liu, S., Tang, X., Yi, X., Li, Q., et al. (2020). Liver Expression of IGF2 and Related Proteins in ZBED6 Gene-Edited Pig by RNA-Seq. *Animals* 10:2184. doi: 10.3390/ani10112184

Zhu, W., Zhang, J., He, K., Geng, Z., and Chen, X. (2020). Proteomic analysis of fertilized egg yolk proteins during embryonic development. *Poult. Sci.* 99, 2775–2784. doi: 10.1016/j.psj.2019.12.056

Conflict of Interest: The authors declare that the research was conducted in the absence of any commercial or financial relationships that could be construed as a potential conflict of interest.

frontiers in Physiology

ORIGINAL RESEARCH
published: 25 June 2021
doi: 10.3389/fphys.2021.697384

Dietary Supplementation of Baicalein Affects Gene Expression in Broiler Adipose Tissue During the First Week Post-hatch

*Yang Xiao[1], Bailey Halter[1], Casey Boyer[1], Mark A. Cline[1], Dongmin Liu[2] and Elizabeth R. Gilbert[1]**

[1] Department of Animal and Poultry Sciences, Virginia Polytechnic Institute and State University, Blacksburg, VA, United States, [2] Department of Human Nutrition, Foods and Exercise, Virginia Polytechnic Institute and State University, Blacksburg, VA, United States

Dietary supplementation of baicalein, a flavonoid, has anti-obesity effects in mammals and broiler chickens. The aim of this study was to determine the effect of dietary baicalein supplementation on broiler growth and adipose tissue and breast muscle deposition. Fifty Hubbard × Cobb-500 day-of-hatch broiler chicks were assigned to a control starter diet or control diet supplemented with 125, 250, or 500 mg/kg baicalein and diets were fed for the first 6 days post-hatch. Body weight, average daily body weight gain, and average daily food intake were all reduced by 500 mg/kg baicalein. Breast muscle and subcutaneous and abdominal fat weights were also reduced in chicks that consumed the baicalein-supplemented diets. mRNAs for genes encoding factors involved in adipogenesis and fat storage, 1-acylglycerol-3-phosphate-O-acyltransferase 2, CCAAT/enhancer-binding protein β, perilipin-1, and sterol regulatory element-binding transcription factor 1, were more highly expressed in the adipose tissue of broilers supplemented with baicalein than the controls, independent of depot. Diacylglycerol acyltransferase and peroxisome proliferator-activated receptor gamma mRNAs, involved in triacylglycerol synthesis and adipogenesis, respectively, were greater in subcutaneous than abdominal fat, which may contribute to differences in expansion rates of these depots. Results demonstrate effects of dietary supplementation of baicalein on growth performance in broilers during the early post-hatch stage and molecular effects in major adipose tissue depots. The mild reduction in food intake coupled to slowed rate of breast muscle and adipose tissue accumulation may serve as a strategy to modulate broiler growth and body composition to prevent metabolic and skeletal disorders later in life.

Keywords: flavonoid, baicalein, chicken, adipose tissue, breast muscle

OPEN ACCESS

Edited by:
Mahmoud M. Alagawany, Zagazig University, Egypt

Reviewed by:
Servet Yalcin, Ege University, Turkey
Tatiana Carlesso Santos, State University of Maringá, Brazil

***Correspondence:**
Elizabeth R. Gilbert
egilbert@vt.edu

Specialty section:
This article was submitted to Avian Physiology, a section of the journal Frontiers in Physiology

Received: *19 April 2021*
Accepted: *25 May 2021*
Published: *25 June 2021*

Citation:
Xiao Y, Halter B, Boyer C, Cline MA, Liu D and Gilbert ER (2021) Dietary Supplementation of Baicalein Affects Gene Expression in Broiler Adipose Tissue During the First Week Post-hatch. Front. Physiol. 12:697384. doi: 10.3389/fphys.2021.697384

INTRODUCTION

Excess abdominal fat in broilers, a consequence of selection for growth-related traits, has a negative impact on meat yield and meat quality and contributes to metabolic disorders in the breeders. From 1957 to 2005, there was a greater than 400% increase in the growth rate of broilers (Zuidhof et al., 2014). The 42-day live body weight achieved an increase of 3.3% per year

with a 2.55% per year reduction in feed conversion ratio (grams of feed to grams of body weight). Concurrently, breast meat yield increased by 67%, with breast conversion ratio (grams of feed intake converted into grams of breast meat) decreased from 28 to 9.4 at 22–56 days of age (Zuidhof et al., 2014). Liver, which is critical for lipid and carbohydrate metabolism, also increased in its relative weight during the selection to support rapid growth (Zaefarian et al., 2019), as did the abdominal fat content which is positively correlated with breast weight and food intake (Tavárez and Solis de los Santos, 2016). However, in recent years, the demand for white meat has increased due to the lower fat content, and excess adipose tissue, particularly abdominal fat, is a waste product that represents an economic loss to the poultry industry (Yucel and Taskin, 2018). Moreover, in broiler breeders, maintaining optimum body weights and fat percentages are necessitated to ensure optimal reproductive and metabolic health and controlled feeding protocols are initiated at hatch to restrict growth (De Jong and Guémené, 2011). Thus, feed additives that influence appetite and/or body composition are an attractive strategy to modulate growth and fat accretion in broilers and other species.

The use of naturally occurring chemicals in diets has become a popular area of poultry research with the phasing out of antibiotics in broiler production and the search for growth-promoting alternatives. Feed additives already being used in the broiler industry include herbs, spices, and essential oils. Flavonoids, a class of polyphenolic phytochemicals, are among the natural feed additives investigated (Surai, 2014). Baicalein is one such flavonoid that is derived from a root used in traditional Chinese medicine, *Scutellaria baicalensis Georgi*, which has been studied in mammalian and avian species for its effect on obesity and growth performance, respectively.

Adult C57BL/6J mice with high fat diet-induced metabolic disorders had decreased visceral fat weight and no further metabolic exacerbations through dietary supplementation of either *S. baicalensis* or purified baicalein (Pu et al., 2012; Na and Lee, 2019). Daily intraperitoneal administration of baicalin, which is another major compound in *S. baicalensis* root, also decreased visceral fat weight and improved hepatic steatosis in adult Sprague–Dawley rats with high fat diet-induced metabolic disorders (Guo et al., 2009). Consistent with animal studies, an *in vitro* experiment revealed that baicalein suppressed adipogenesis and lipid accretion in 3T3-L1 pre-adipocytes (Seo et al., 2014). We also demonstrated anti-diabetic effects of baicalein, where hyperglycemia, glucose tolerance, and pancreatic islet function were improved in diabetic mice that were fed a baicalein-supplemented diet, without changes in weekly food intake (Fu et al., 2014).

In 42-day-old broilers, dietary supplementation of *S. baicalensis* improved growth performance (Kroliczewska et al., 2008), while dietary baicalein supplementation was associated with reductions in serum total cholesterol, triglycerides and low-density lipoproteins (Zhou et al., 2019). These data all indicate promise in the use of baicalein as a dietary supplement in the poultry industry to support healthy development while mitigating the development of metabolic disorders. Previous studies determined effects at slaughter age, and broilers have a higher average daily body weight gain, lower feed conversion ratio, and more dynamic metabolism at the early post-hatch stage, especially during the first week, when organ maturation is still occurring (Zuidhof et al., 2014). Also, the specific effect of baicalein on fat and lean mass changes as well as corresponding molecular mechanisms are unknown in chickens. Because other studies involving dietary baicalein supplementation focus on later stages of growth and adult animals, the present study sought to examine effects at an earlier age. The objective of this study was thus to investigate the effects of dietary baicalein supplementation on growth performance, breast muscle and adipose tissue development, and mRNA expression of adipogenesis-associated factors in adipose tissue, in broilers during the first 6 days post-hatch.

MATERIALS AND METHODS

Animals

A total of 50 straight run Hubbard × Cobb-500 broiler chicks were obtained on day of hatch from a nearby commercial hatchery. Chicks were individually caged in a room maintained at 30 ± 2°C and 50 ± 5% relative humidity with free access to feed and water and visual and auditory contact with other chicks. Chicks with evenly distributed body weights were assigned to four dietary groups (n = 12–13 per group): (1) control diet, a corn and soybean meal-based starter diet formulated to meet recommended requirements for Cobb-500 broilers (Cobb-Vantress; detailed formulation in McConn et al., 2018), (2) low baicalein (125 mg/kg), (3) middle baicalein (250 mg/kg), and (4) high baicalein (500 mg/kg). Dietary baicalein inclusion levels were based on our previous work with mice (Fu et al., 2014). Baicalein (98% pure via HPLC) was purchased from Xi'An Yile Bio-Tech Company, China. Experimental procedures were performed according to the National Research Council Publication and were approved by the Virginia Tech Institutional Animal Care and Use Committee.

Growth Performance and Organ Weights

Body weight and food intake was recorded for individuals from the time that the chicks arrived in our facility (approximately 5 h after they hatched) and then every 24 h until day 6 (n = 12–13 per each of the four groups). Feed conversion ratio was calculated by finding the quotient of food intake and body weight gain. On day 6 post-hatch, all chicks were weighed then euthanized by cervical dislocation. Breast muscle, liver, and subcutaneous (visible adipose tissue connected to skin) and abdominal fat (adipose tissue connected to gizzard) tissues were removed and tissue weights were recorded. Subcutaneous and abdominal fat samples from 10 chicks in each dietary group were transferred to vials containing RNA*later* (Invitrogen, Carlsbad, CA, United States) and stored at −80°C until total RNA isolation. Sex was determined by gonadal inspection postmortem.

Total RNA Isolation, Reverse Transcription, and Real-Time PCR

Adipose tissue samples were homogenized in TRI Reagent (Sigma-Aldrich, St. Louis, MO, United States) with 5 mm stainless steel beads (Qiagen, Valencia, CA, United States) using a Tissue Lyser II (Qiagen). After the step of addition to 100% molecular biology-grade ethanol, total RNA was purified using the RNeasy Mini kit (Qiagen, CA, United States) according to the manufacturer's instructions. The eluted total RNA samples were quantified and assessed for purity by spectrophotometry at 260/280/230 nm. First strand cDNA was synthesized from 200 ng total RNA using the High Capacity cDNA Reverse Transcription kit, according to the manufacturer's instructions (Applied Biosystems, NY, United States). Primers for real-time PCR (**Table 1**) were designed in Primer Express 3.0 (Applied Biosystems) and validated for amplification efficiency before use (95–105%). A 10 μL reaction contained 5 μL fast SYBR Green Master Mix (Applied Biosystems), 0.25 μL each of 5 μM forward and reverse primers, 3 μL of 10-fold diluted cDNA, and 1.5 μL of nuclease-free water and was duplicated for all samples with an Applied Biosystems 7500 FAST system as described (Zhang et al., 2015).

Statistical Analysis

The real-time PCR data were analyzed using the ΔΔCT method (Schmittgen and Livak, 2008) with actin as the reference gene and the average of the abdominal adipose tissue from control diet-fed birds as the calibrator sample. The relative quantity ($2^{-\Delta\Delta CT}$) values, growth performance and organ weights were subjected to Fit Model platform in JMP Pro 15 (SAS Ins., Cary, NC, United States). The statistical model for growth performance and organ weights included the main effect of dietary treatment (four doses), time (5 or 6 days) and their interactions. For gene expression, effects included adipose tissue depot (subcutaneous and abdominal), dietary treatment (four doses), and the dietary treatment by adipose depot interaction. Tukey's test was used *post hoc* for pairwise comparisons and results were considered significant at $P < 0.05$. Sex was excluded from the model as initial tests revealed that no effect involving sex was significant.

TABLE 1 | Primers used for real time PCR[1].

Gene	Primers sequence (5′-3′); forward/reverse	Accession no.
β-*Actin*	GTCCACCGCAAATGCTTCTAA/ TGCGCATTTATGGGTTTTGTT	NM_205518.1
AGPAT2	GCCAAACACCGAAGGAACAT/ CCATGGCATCCCCAGAGTT	XM_015279793.1
C/EBPα	CGCGGCAAATCCAAAAAG/ GGCGCACGCGGTACTC	NM_001031459.1
C/EBPβ	GCCGCCCGCCTTTAAA/ CCAAACAGTCCGCCTCGTAA	NM_205253.2
DGAT2	TTGGCTTTGCTCCATGCAT/ CCCACGTGTTCGAGGAGAA	XM_419374.5
PLIN1	GGAGGACGTGGCATGATGAC/ GGCCCTTCCATTCTGCAA	NM_001127439.1
PPARγ	CACTGCAGGAACAGAACAAAGAA/ TCCACAGAGCGAAACTGACATC	NM_001001460.1
SREBP1	CATCCATCAACGACAAGATCGT/ CTCAGGATCGCCGACTTGTT	NM_204126.1

[1]*Primers were designed with Primer Express 3.0 (Applied Biosystems). AGPAT2, 1-acylglycerol-3-phosphate-O-acyltransferase 2; C/EBPα, CCAAT/enhancer-binding protein alpha; C/EBPβ, CCAAT/enhancer-binding protein beta; DGAT2, diacylglycerol acyltransferase; PLIN1, perilipin 1; PPARγ, peroxisome proliferator-activated receptor gamma; SREBP1, sterol regulatory element-binding transcription factor 1.*

RESULTS

Growth Performance

For results involving more than one time point, differences are depicted graphically for *post hoc* pairwise comparisons at time points for which the main effect was significant (**Figures 1**–**4**). The high baicalein (500 mg/kg) diet was associated with a reduction in body weight from days 1 to 6, the middle dose (250 mg/kg) exerted the same effect from days 3 to 6 post-hatch, and the low dose from days 5 to 6, compared to the control group (**Figure 1**). Both middle and high baicalein doses consistently lowered cumulative body weight gain from days 2 to 5, whereas only the high dose had an effect on day 6, compared to the controls (**Figure 2A**). Both middle and high baicalein doses lowered the average daily body weight gain over the 6 days of treatment ($P = 0.003$ for main effect of dietary treatment; **Figure 2B**). Meanwhile, low dose (125 mg/kg) baicalein did not have any effect on body weight or body weight gain.

The high baicalein dose lowered food intake from days 2 to 6 post-hatch, compared to the control group (**Figure 3A**), while the middle dose affected food intake on days 2, 5, and 6, and the low dose reduced food intake on day 2 post-hatch, relative to chicks that were fed the control diet. When calculated as a percentage of body weight, differences were significant on day 2 post-hatch (**Figure 3B**). Over the 6 days of observation,

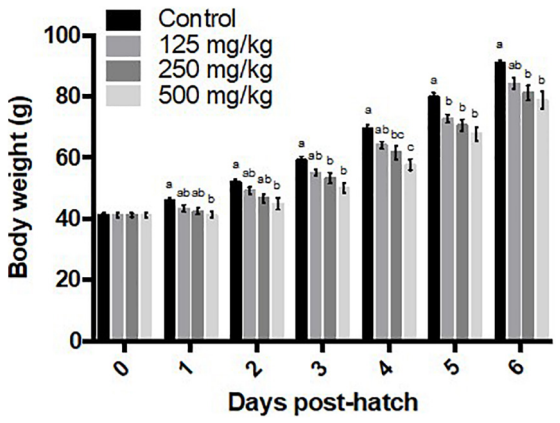

FIGURE 1 | Body weights. Values represent least squares means ± SEM (n = 12–13). Different superscripts within each day indicate a significant difference at $P < 0.05$; Tukey's test.

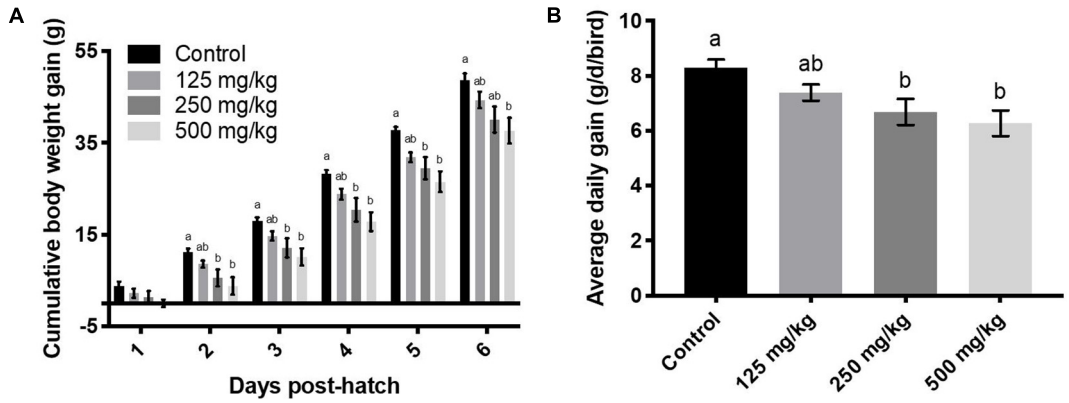

FIGURE 2 | Body weight gain cumulatively **(A)**, and on an average daily basis **(B)**. Values represent least squares means ± SEM (n = 12–13). Different superscripts within each day indicate a significant difference at $P < 0.05$; Tukey's test.

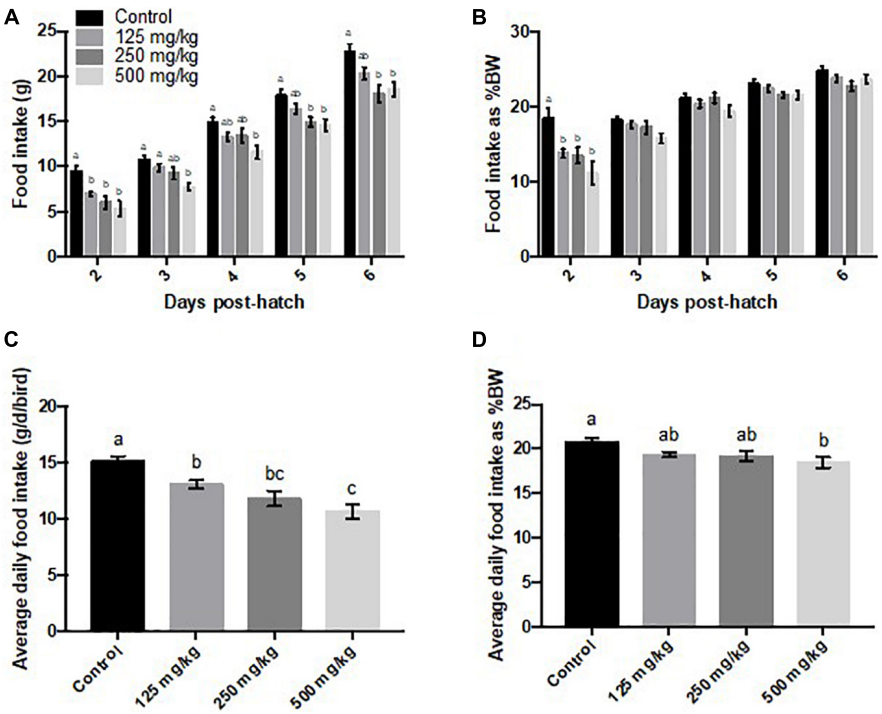

FIGURE 3 | Daily food intake **(A)**, food intake as a percentage of body weight [% body weight (BW)] **(B)**, average daily food intake **(C)**, and average daily food intake as % body weight **(D)**. Values represent least squares means ± SEM (n = 12–13). Different superscripts within each day indicate a significant difference at $P < 0.05$; Tukey's test.

average daily food intake was lowered by all levels of baicalein supplementation ($P < 0.0001$; main effect of dietary treatment; **Figure 3C**), whereas average daily food intake calculated as a percentage of body weight was only lowered in the high baicalein group ($P = 0.009$; main effect of dietary treatment; **Figure 3D**). Feed conversion ratio was increased in the high baicalein group on day 2 post-hatch (**Figure 4**). Although the main effect of treatment was also significant for feed conversion ratio at day 5 ($P = 0.04$), no difference was detected among groups using Tukey's *post hoc* test. The average feed conversion ratio over 6 days of treatment did not differ among the groups (data not shown).

Organ Weights

Relative abdominal fat weight (as % BW) tended to be reduced by baicalein ($P = 0.05$; main effect of dietary treatment; **Table 2**), whereas subcutaneous fat was not affected by treatments. Similarly, relative breast muscle weight was also decreased by the high baicalein dose ($P = 0.005$).

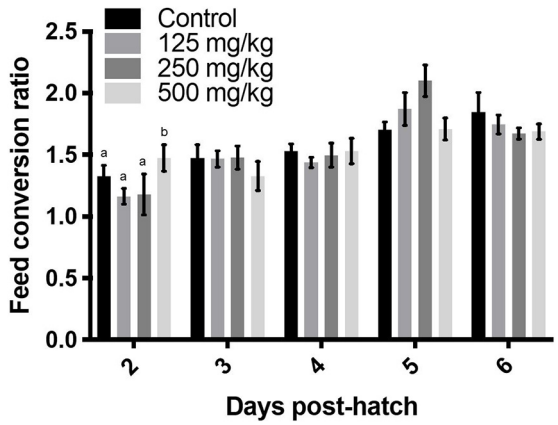

FIGURE 4 | Daily feed conversion ratio over 6 days. Values represent least squares means ± SEM (n = 12–13). Different superscripts within each day indicate a significant difference at $P < 0.05$; Tukey's test.

Adipose Tissue Relative mRNA Gene Expression

There was no treatment by adipose tissue depot interaction for any of the genes that were measured. There was a main effect of treatment on the mRNA abundance of 1-acylglycerol-3-phosphate-O-acyltransferase 2 (*AGPAT2*; P = 0.01), CCAAT/enhancer-binding protein beta (*C/EBPβ*; P = 0.0001), perilipin-1 (*PLIN*; P = 0.001), and sterol regulatory element-binding transcription factor 1 (*SREBP1*; P = 0.03, **Table 3**). Expression of *AGPAT2* mRNA was greater in broilers from the middle baicalein dose group than the control or high dose groups. Abundance of *PLIN1* mRNA was greater in the middle dose group than in all other groups, and *SREBP1* was greater in the middle baicalein dose group than in the control group. Expression of *C/EBPβ* mRNA was greater in the high dose baicalein than low or middle dose groups. Independent of treatment, expression of diacylglycerol acyltransferase (*DGAT2*) and peroxisome proliferator-activated receptor gamma (*PPARγ*) were more highly expressed in subcutaneous than abdominal adipose tissue (P = 0.04 and 0.02, respectively).

TABLE 2 | The effect of dietary baicalein supplementation on organ weights at day 6 post-hatch in Hubbard × Cobb-500 broilers[1].

Treatment	Abdominal fat as % BW	Subcutaneous fat as % BW	Liver as % BW	Breast muscle as % BW
0 mg/kg	0.092	0.32	3.92	8.38^{a}
125 mg/kg	0.092	0.28	4.40	8.02^{a}
250 mg/kg	0.080	0.21	4.25	7.16^{ab}
500 mg/kg	0.055	0.23	4.17	6.67^{b}
SEM	0.01	0.04	0.16	0.34
P-value	0.05	0.18	0.25	0.005

[1]*Values represent least squares means and pooled standard errors of the means with associated P-values for the effect of dietary treatment (n = 10). Different letters within each sampling measurement indicate a significant difference at P < 0.05; Tukey's test.*

DISCUSSION

In this study, we first determined the effect of dietary baicalein supplementation on growth performance and organ weights of broilers during the first week post-hatch. The decrease in body weight and average daily weight gain in response to the middle and high levels of baicalein supplementation was consistent with the observation that 0.5% supplementation of *S. baicalensis* root, which contains 19.3 ± 2.3 mg of baicalein and 214.5 ± 13.3 mg total flavonoids per gram of dry matter, reduced the body weight of 42-day old Hubbard Hi-Y chickens (Króliczewska et al., 2017).

TABLE 3 | Effect of baicalein treatment on relative mRNA abundance of adipogenesis-associated factors.

Effect[1]	*AGPAT2*	*C/EBPα*	*C/EBPβ*	*DGAT2*	*PLIN1*	*PPARγ*	*SREBP1*
Treatment							
0 mg/kg	1.20^{b}	0.93	0.93^{ab}	1.52	1.23^{b}	1.30	1.18^{b}
125 mg/kg	1.75^{ab}	2.00	0.52^{b}	1.80	2.23^{b}	1.21	1.14^{ab}
250 mg/kg	3.17^{a}	1.28	0.53^{b}	1.42	5.27^{a}	1.69	2.40^{a}
500 mg/kg	1.39^{b}	2.13	1.23^{a}	2.24	1.86^{b}	1.47	1.49^{ab}
SEM	0.47	0.48	0.12	0.36	0.79	0.25	0.34
P-value	0.01	0.24	0.0001	0.38	0.001	0.53	0.03
Adipose depot							
Subcutaneous	1.96	1.11	0.72	2.11	2.84	1.72	1.59
Abdominal	1.80	2.05	0.89	1.38	2.45	1.12	1.51
SEM	0.34	0.34	0.08	0.25	0.56	0.18	0.24
P-value	0.74	0.06	0.16	0.04	0.63	0.02	0.83
Treatment × adipose depot	0.25	0.26	0.41	0.66	0.52	0.56	0.42

[1]*Values represent least squares means and pooled standard errors of the means with associated P-values for the effect of dietary treatment, adipose tissue depot, and their interaction (n = 10). Different superscripts within an effect for each gene are significantly different at P < 0.05, Tukey's test.*
AGPAT2, 1-acylglycerol-3-phosphate-O-acyltransferase 2; C/EBPα, CCAAT/enhancer-binding protein alpha; C/EBPβ, CCAAT/enhancer-binding protein beta; DGAT2, diacylglycerol acyltransferase; PLIN1, perilipin-1; PPARγ, peroxisome proliferator-activated receptor gamma; SREBP1, sterol regulatory element-binding transcription factor 1.

In contrast, supplementation of 1.0 and 1.5% of *S. baicalensis* root increased body weight and body weight gain of these birds (Króliczewska et al., 2017), which was similar to what was observed in 42-day old Arbor Acres chickens that were fed diets containing 100 and 200 mg/kg baicalein (Zhou et al., 2019). However, no body weight increase was observed in the same birds at 21 days of age (Zhou et al., 2019).

In the present study, baicalein supplementation was associated with decreased average daily food intake, whereas it was increased in 42-day Hi-Y chickens (Króliczewska et al., 2017) and unchanged in 42-day Arbor Acres broilers (Zhou et al., 2019). Weekly food intake was not affected over the course of 8 weeks of feeding a baicalein-supplemented high-fat diet (500 mg/kg) to middle-aged mice (Fu et al., 2014). Such differences among studies indicate that when interpreting the effect of baicalein on growth performance of broilers, the genetic strains, developmental stage, as well as the form (in flavonoid mixture or purified baicalein), dose, route, and duration of supplementation should all be considered. Also, the results can differ when using an end-point versus day-by-day analysis. The end-point analysis is more reflective of the overall effect at a given time range, whereas it can either bury the significance at a certain time point (like the non-significant average feed conversion ratio versus the significance on day 2 post-hatch in **Figure 4**), or reveal an overall significance by distributing the significance on 1 day to the other days that lack significance (for instance, the daily versus average food intake as percentage of body weight in **Figure 3**). It is worth noting that the two experiments conducted by the same group, using the same strains of birds at the same age, identified different effects of the same doses of *S. baicalensis* root supplementation on body weight, feed conversion ratio, body weight gain, as well as food intake (Kroliczewska et al., 2008; Króliczewska et al., 2017). The disparate effects indicate that boilers may have different sensitivities to flavonoid supplementations over years of selection for rapid growth. It is also possible that the root extracts contain varying amounts of bioactive chemicals that contribute to the biological effects observed, whereas results are expected to be more robust when using a pure chemical.

To our knowledge, there are no reports concerning the effect of baicalein or *S. baicalensis* on body fat mass changes or the corresponding molecular mechanisms, in an avian model. Our results demonstrated that baicalein supplementation reduced absolute abdominal and subcutaneous fat masses (data not shown) and the relative abdominal fat mass in broilers during the early post-hatch stage. Adult C57BL/6J mice with metabolic disorders induced by chronic high fat diet consumption had decreased visceral fat weight (including epididymal, mesentery, and abdominal adipose tissue depots) after 29 weeks of 400 mg/kg baicalein supplementation (Pu et al., 2012). Similarly, adult C57BL/6J mice with high fat diet-induced insulin resistance had reduced epididymal fat weight when supplemented with 500 mg/kg body weight of *S. baicalensis* for 9 weeks (Na and Lee, 2019). Similar to the results of dietary baicalein supplementation, Sprague-Dawley rats with high fat-induced metabolic disorders also showed decreased total visceral (including perirenal and epididymal adipose depots) and epididymal fat masses after 16 weeks of daily 80 mg/kg/d intraperitoneally administered baicalin (baicalein is the aglycone form of baicalin) (Guo et al., 2009). However, in these studies, there was either the lack of a control group fed a normal diet with baicalin/*S. baicalensis* administration/supplementation (Guo et al., 2009; Na and Lee, 2019), or such group showed no difference in adipose tissue depot weights compared to those fed a normal diet that did not contain baicalein (Pu et al., 2012).

To begin to elucidate the molecular mechanisms involved in adipose tissue weight changes during dietary baicalein supplementation, we next determined expression of major genes involved in adipogenesis. Although both abdominal and subcutaneous fat weights were reduced by baicalein treatment, Tukey's test detected pairwise differences only in the abdominal fat depot. Expression of the master regulator of adipogenesis, *PPARγ* (Tontonoz et al., 1994) and the gene encoding the key enzyme in triglyceride biosynthesis, *DGAT2* (Cases et al., 2001), were greater in the subcutaneous than abdominal depot. This is consistent with our previous finding in low- and high-body weight-selected chickens, where during the early post-hatch stage, adipogenesis is more dynamic in the subcutaneous than abdominal adipose tissue depot (Xiao et al., 2019). Possibly, reduced adipogenesis in the abdominal depot contributed to its reduced expansion in chicks fed diets supplemented with baicalein. Interestingly, although the depot weight reduction was only significant at a high level of dietary supplementation, *AGPAT2*, *PLIN1*, and *SREBP1* were more highly expressed in the middle dose of baicalein than control diet group, with levels in the high dose group comparable to the controls. *C/EBPβ* is a transcription factor that is activated during the early stage of adipogenesis, and further activates *C/EBPα* and *PPARγ* (Tang and Lane, 2012). In differentiated 3T3-L1 cells, mRNA expression of *C/EBPβ* and protein expression of C/EBPα, PPARγ, SREBP1, and DGAT1, which are involved in adipogenesis and lipid accumulation, were all decreased by baicalein treatment in a dose-dependent manner (3.125, 6.25, and 12.5 μM) at 6 days post-treatment, which was also confirmed by an *in vivo* study using zebrafish (Seo et al., 2014). Although relative lipid accumulation was also reduced in a dose-dependent manner, when cells were treated with high dose baicalein during differentiation, a significant reduction in lipid accumulation was only observed from day 2 post-differentiation (Seo et al., 2014). Another *in vitro* study using a single dose of 50 μM baicalein with 3T3-L1 cells also demonstrated decreased *C/EBPα, PPARγ*, and *SREBP1* expression on day 6 post-differentiation, whereas lipid content was only decreased during the first 2 days post-differentiation, but not the remaining 4 days, although the overall lipid content over 6 days was also lower than in the control group (Nakao et al., 2016).

These results suggest that adipocytes at various differentiation stages have different sensitivities to baicalein treatment. It is possible that during early development post-hatch, cells in adipose tissue display high rates of hyperplasia (increase in cell number) and hypertrophy (increase in cell volume), whereas at later developmental stages of life, since adipocyte precursor cells are not as adipogenic, hypertrophy predominates as the major contributor to lipid deposition and adipose tissue

expansion (Xiao et al., 2019), which together result in a differential sensitivity to baicalein treatment. Another critical factor pertinent to the present study is that chicks utilize residual yolk as an energy source. Yolk, which contains over 20% of lipids, is essentially absorbed around 4 days post-hatch (Moran, 2007). No research has been conducted on the effect of baicalein on yolk sac resorption in chicks. It is possible that baicalein also interferes with yolk utilization and thereby impacts lipid metabolism in adipose tissue depots, although these data were not collected and beyond the scope of the present study.

In contrast to the findings that 0.5 and 1.5% baical skullcap root supplementation increased dry matter percentage of the breast muscles in Hi-Y broilers at 42 days of age (Kroliczewska et al., 2008), we observed a decrease in absolute and relative breast muscle weight in 7-day old Hubbard × Cobb-500 chicks that consumed a diet containing 500 mg/kg baicalein. The continuous selection for high carcass yield has resulted in an over 80% increase in pectoralis major from 1957 to 2005 (Zuidhof et al., 2014). However, the intense selection also led to an unbalanced body composition, which can cause a plethora of disorders, such as "water belly" (because of the insufficient oxygen supply by relatively small heart and lungs and excessive growth) and "green muscle disease" (also because of the insufficient oxygen supply-induced ischemia and sequential necrosis) (Bailey et al., 2015; Soglia et al., 2019). Therefore, a mild attenuation of breast muscle weight gain through baicalein supplementation may indicate a protective effect of baicalein during early post-hatch broiler development. By slowing down the expansion of breast muscle, the chance for rapid growth-induced body distortion may be prevented as is the sequential induction of the above-mentioned diseases. It is also possible that there is a catch-up growth in response to baicalein supplementation at a later stage of life. Extended feeding experiments should be conducted to illustrate if such a reduction in yield is persistent during later development or if there is compensatory growth leading to comparable or even higher meat yield at 42 days of age.

Our study thus extended the previous research on the effects of baicalein on growth performance in broilers to the early post-hatch stage and for the first time elucidated its effects on major adipose tissue depots as well as associated molecular mechanisms. Such information provides insights on its possible use as a dietary supplement in the poultry industry during early development to modulate rapid growth, slow the accretion of abdominal fat, and to induce a mild reduction in feed intake that circumvents the need to employ a feed restriction protocol early in life. In conclusion, dietary supplementation of baicalein during the early rearing phase may have multi-faceted benefits that improve broiler welfare, health, and overall productivity. For recommended supplementation levels, it is anticipated that further research will reveal the minimum dietary inclusion amount that yields the expected benefits most economically. The present results suggest that the middle dose modulated performance modestly.

DATA AVAILABILITY STATEMENT

The raw data supporting the conclusions of this article will be made available by the authors, without undue reservation.

ETHICS STATEMENT

The animal study was reviewed and approved by the Virginia Tech Institutional Animal Care and Use Committee, Virginia Tech, Blacksburg, VA, United States.

AUTHOR CONTRIBUTIONS

MC and EG contributed to conception and design of the research, interpretation of results, and editing of the manuscript. CB performed the experiments, contributed to statistical analysis, and interpretation of results. YX contributed to statistical analysis, interpretation of results, and drafted the manuscript. BH contributed to interpretation of results and wrote sections of the manuscript. DL contributed to design of the research and interpretation of the results. All authors contributed to manuscript revision, read, and approved the submitted version.

FUNDING

Funding for this work was provided in part by the John Lee Pratt Endowment at Virginia Tech, the Virginia Agricultural Experiment Station and the Hatch Program of the National Institute of Food and Agriculture, U.S. Department of Agriculture.

REFERENCES

Bailey, R. A., Watson, K. A., Bilgili, S., and Avendano, S. (2015). The genetic basis of pectoralis major myopathies in modern broiler chicken lines. *Poult. Sci.* 94, 2870–2879. doi: 10.3382/ps/pev304

Cases, S., Stone, S. J., Zhou, P., Yen, E., Tow, B., Lardizabal, K. D., et al. (2001). Cloning of DGAT2, a second mammalian diacylglycerol acyltransferase, and related family members. *J. Biol. Chem.* 276, 38870–38876. doi: 10.1074/jbc.m106219200

De Jong, I., and Guémené, D. (2011). Major welfare issues in broiler breeders. *World Poult. Sci. J.* 67, 73–82. doi: 10.1017/s0043933911000067

Fu, Y., Luo, J., Jia, Z., Zhen, W., Zhou, K., Gilbert, E., et al. (2014). Baicalein protects against type 2 diabetes via promoting islet β-cell function in obese diabetic mice. *Int. J. Endocrinol.* 2014, 846742–846754.

Guo, H.-X., Liu, D.-H., Ma, Y., Liu, J.-F., Wang, Y., Du, Z.-Y., et al. (2009). Long-term baicalin administration ameliorates metabolic disorders and hepatic steatosis in rats given a high-fat diet. *Acta Pharmacol. Sinica* 30, 1505–1512. doi: 10.1038/aps.2009.150

Króliczewska, B., Graczyk, S., Króliczewski, J., Pliszczak-Król, A., Mišta, D., and Zawadzki, W. (2017). Investigation of the immune effects of Scutellaria baicalensis on blood leukocytes and selected organs of the chicken's lymphatic system. *J. Anim. Sci. Biotechnol.* 8, 1–12.

Kroliczewska, B., Zawadzki, W., Skiba, T., Kopec, W., and Kroliczewski, J. (2008). The influence of baical skullcap root (Scutellaria baicalensis radix) in the diet of broiler chickens on the chemical composition of the muscles, selected performance traits of the animals and the sensory characteristics of the meat. *Veterinarni Med.* 53, 373–380. doi: 10.17221/1994-vetmed

McConn, B. R., Matias, J., Wang, G., Cline, M. A., and Gilbert, E. R. (2018). Dietary macronutrient composition affects hypothalamic appetite regulation in chicks. *Nutr. Neurosci.* 21, 49–58. doi: 10.1080/1028415X.2016.1219103

Moran, E. T. Jr. (2007). Nutrition of the developing embryo and hatchling. *Poult. Sci.* 86, 1043–1049. doi: 10.1093/ps/86.5.1043

Na, H.-Y., and Lee, B.-C. (2019). Scutellaria baicalensis alleviates insulin resistance in diet-induced obese mice by modulating inflammation. *Int. J. Mol. Sci.* 20:727. doi: 10.3390/ijms20030727

Nakao, Y., Yoshihara, H., and Fujimori, K. (2016). Suppression of very early stage of adipogenesis by baicalein, a plant-derived flavonoid through reduced Akt-C/EBPα-GLUT4 signaling-mediated glucose uptake in 3T3-L1 adipocytes. *PLoS One* 11:e0163640. doi: 10.1371/journal.pone.0163640

Pu, P., Wang, X.-A., Salim, M., Zhu, L.-H., Wang, L., Xiao, J.-F., et al. (2012). Baicalein, a natural product, selectively activating AMPKα2 and ameliorates metabolic disorder in diet-induced mice. *Mol. Cell. Endocrinol.* 362, 128–138. doi: 10.1016/j.mce.2012.06.002

Seo, M.-J., Choi, H.-S., Jeon, H.-J., Woo, M.-S., and Lee, B.-Y. (2014). Baicalein inhibits lipid accumulation by regulating early adipogenesis and m-TOR signaling. *Food Chem. Toxicol.* 67, 57–64. doi: 10.1016/j.fct.2014.02.009

Schmittgen, T. D., and Livak, K. J. (2008). Analyzing real-time PCR data by the comparative CT method. *Nat. Protoc.* 3, 1101–1108. doi: 10.1038/nprot.2008.73

Soglia, F., Mazzoni, M., and Petracci, M. (2019). Spotlight on avian pathology: current growth-related breast meat abnormalities in broilers. *Avian Pathol.* 48, 1–3. doi: 10.1080/03079457.2018.1508821

Surai, P. (2014). Polyphenol compounds in the chicken/animal diet: from the past to the future. *J. Anim. Physiol. Anim. Nutr.* 98, 19–31. doi: 10.1111/jpn.12070

Tang, Q. Q., and Lane, M. D. (2012). Adipogenesis: from stem cell to adipocyte. *Ann. Rev. Biochem.* 81, 715–736. doi: 10.1146/annurev-biochem-052110-115718

Tavárez, M. A., and Solis de los Santos, F. (2016). Impact of genetics and breeding on broiler production performance: a look into the past, present, and future of the industry. *Anim. Front.* 6, 37–41. doi: 10.2527/af.2016-0042

Tontonoz, P., Hu, E., and Spiegelman, B. M. (1994). Stimulation of adipogenesis in fibroblasts by PPARγ2, a lipid-activated transcription factor. *Cell* 79, 1147–1156. doi: 10.1016/0092-8674(94)90006-x

Xiao, Y., Wang, G., Gerrard, M. E., Wieland, S., Davis, M., Cline, M. A., et al. (2019). Changes in adipose tissue physiology during the first two weeks posthatch in chicks from lines selected for low or high body weight. *Am. J. Physiol. Regul. Integr. Comp. Physiol.* 316, R802–R818.

Yucel, B., and Taskin, T. (2018). *Animal Husbandry and Nutrition*. London: IntechOpen.

Zaefarian, F., Abdollahi, M. R., Cowieson, A., and Ravindran, V. (2019). Avian liver: the forgotten organ. *Animals* 9:63. doi: 10.3390/ani9020063

Zhang, W., Bai, S., Liu, D., Cline, M. A., and Gilbert, E. R. (2015). Neuropeptide Y promotes adipogenesis in chicken adipose cells in vitro. *Comp. Biochem. Physiol. A Mol. Integr. Physiol.* 181, 62–70. doi: 10.1016/j.cbpa.2014.11.012

Zhou, Y., Mao, S., and Zhou, M. (2019). Effect of the flavonoid baicalein as a feed additive on the growth performance, immunity, and antioxidant capacity of broiler chickens. *Poult. Sci.* 98, 2790–2799. doi: 10.3382/ps/pez071

Zuidhof, M. J., Schneider, B. L., Carney, V. L., Korver, D., and Robinson, F. (2014). Growth, efficiency, and yield of commercial broilers from 1957, 1978, and 2005. *Poult. Sci.* 93, 2970–2982. doi: 10.3382/ps.2014-04291

Conflict of Interest: The authors declare that the research was conducted in the absence of any commercial or financial relationships that could be construed as a potential conflict of interest.

frontiers in Physiology

ORIGINAL RESEARCH
published: 07 July 2021
doi: 10.3389/fphys.2021.694809

Application of Metabolomics to Identify Hepatic Biomarkers of *Foie Gras* Qualities in Duck

Zohre Mozduri[1], Bara Lo[2], Nathalie Marty-Gasset[2], Ali Akbar Masoudi[1], Julien Arroyo[3], Mireille Morisson[2], Cécile Canlet[4,5], Agnès Bonnet[2] and Cécile M. D. Bonnefont[2]**

[1]Department of Animal Science, Faculty of Agriculture, Tarbiat Modares University, Tehran, Iran, [2]GenPhySE, Université de Toulouse, INRAE, ENVT, Castanet Tolosan, France, [3]ASSELDOR, Station d'Expérimentation Appliquée et de Démonstration sur l'oie et le Canard, La Tour de Glane, Coulaures, France, [4]Toxalim, Université de Toulouse, INRA, ENVT, INP-Purpan, UPS, Toulouse, France, [5]Axiom Platform, MetaToul-Me, National Infrastructure for Metabolomics and Fluxomics, Toulouse, France

Foie gras is a traditional dish in France that contains 50 to 60% of lipids. The high-fat content of the liver improves the organoleptic qualities of *foie gras* and reduces its technological yield at cooking (TY). As the valorization of the liver as *foie gras* products is strongly influenced by the TY, classifying the *foie gras* in their potential technological quality before cooking them is the main challenge for producers. Therefore, the current study aimed to identify hepatic biomarkers of *foie gras* qualities like liver weight (LW) and TY. A group of 120 male mule ducks was reared and overfed for 6–12 days, and their livers were sampled and analyzed by proton nuclear magnetic resonance (^{1}H-NMR). Eighteen biomarkers of *foie gras* qualities were identified, nine for LW and TY, five specific to LW, and four specific to TY. All biomarkers were strongly negatively correlated to the liver weights and positively correlated to the technological yield, except for the lactate and the threonine, and also for the creatine that was negatively correlated to *foie gras* technological quality. As a result, in heavy livers, the liver metabolism was oriented through a reduction of carbohydrate and amino acid metabolisms, and the plasma membrane could be damaged, which may explain the low technological yield of these livers. The detected biomarkers have been strongly discussed with the metabolism of the liver in nonalcoholic steatohepatitis.

Keywords: liver, quality, biomarker, metabolomics, *foie gras*

OPEN ACCESS

Edited by:
Elizabeth Ruth Gilbert, Virginia Tech, United States

Reviewed by:
Shaaban Saad Elnesr, Fayoum University, Egypt
Servet Yalcin, Ege University, Turkey

****Correspondence:***
Cécile M. D. Bonnefont
cecile.bonnefont@toulouse-inp.fr
Ali Akbar Masoudi
masoudia@modares.ac.ir

Specialty section:
This article was submitted to Avian Physiology, a section of the journal Frontiers in Physiology

Received: *13 April 2021*
Accepted: *03 June 2021*
Published: *07 July 2021*

Citation:
Mozduri Z, Lo B, Marty-Gasset N, Masoudi AA, Arroyo J, Morisson M, Canlet C, Bonnet A and Bonnefont CMD (2021) Application of Metabolomics to Identify Hepatic Biomarkers of Foie Gras Qualities in Duck. Front. Physiol. 12:694809. doi: 10.3389/fphys.2021.694809

INTRODUCTION

Foie gras is one of the flagship products of French gastronomy. It is the product of hepatic steatosis due to the overfeeding of ducks with an energy-rich feed based on corn. The *foie gras* is the result of the increase in triglyceride storage in the liver. Actually, in the small intestine, the degradation of starch from the corn feed led to an accumulation of carbohydrates absorbed into the hepatic portal vein and carried to the liver. There, the *de novo* lipogenesis process converts carbohydrate precursors into fatty acids. During the overfeeding period, the imbalance between the lipid neosynthesized in the liver and their export in the hepatic vein causes lipids to accumulate as triglycerides in the hepatocytes, conducting to hepatic steatosis. Furthermore, some exported triglycerides go back to the liver and are stored in this organ. The first mechanism consists of exporting the newly formed triglycerides to the peripheral tissues like muscles and

abdominal or subcutaneous tissues for storage or energy utilization. This process is mediated by very low-density lipoprotein (VLDL; Goodridge, 1987). Then, a part of these exported triglycerides is returned to the liver *via* high-density lipoprotein (HDL) and stored in the liver (Tavernier et al., 2018).

The mule duck is the main represented species for *foie gras* production because it has the best ability to hepatic steatosis (Baéza et al., 2005). The duration of fasting before slaughtering and the conditions of evisceration also play important roles in the *foie gras* quality (Auvergne et al., 1998). Indeed, studies have shown that if the liver evisceration occurs 20 min after slaughtering, and if the cooling of livers is quick, the livers have a high technological yield (TY; Bouillier-Oudot et al., 2004). The TY of *foie gras* that is the opposite of the melting rate has strong repercussions on both the organoleptic qualities of *foie gras* and on the performances of the industrial production units. Thus the TY has already been widely studied (Theron et al., 2013). In ducks, there is also a positive correlation between the liver weight (LW) and the melting rate at cooking, especially above 600 g (Blum et al., 1990; Marie-Etancelin et al., 2011). Similarly, the lipid level correlates with the melting rate at cooking (Rousselot-Pailley et al., 1992). Zootechnical factors, pre-, post-mortem conditions, and liver characteristics have already been analyzed to control better the liver melting at cooking, but some individual variabilities persist (Theron et al., 2012).

In a recent study, plasmatic biomarkers of *foie gras* quality (LW and TY) were identified by proton nuclear magnetic resonance (^{1}H-NMR; Mozduri et al., 2021). The plasmatic biomarkers are of main interest because they can bring information of *foie gras* quality before slaughtering the animals. In a second step, hepatic biomarkers of *foie gras* qualities are detected on the same experimental materials. Hepatic biomarkers of crude livers might be very useful to choose the cooking program to apply to livers like pasteurization, sterilization, or emulsion to optimize the *foie gras* products in the industry. Moreover, metabolomics studies with ^{1}H-NMR were already performed on livers at the end of the overfeeding period to distinguish the signaling of livers with high fat loss corresponding to low TY from livers with low-fat loss that corresponded to high TY (Bonnefont et al., 2014). However, the livers weighed around 570 g to 582 g. The strength of the present study was that male mule ducks were overfed for 6 to 12 days which provided a wide variety of liver weights from 300 g to over 900 g.

This study aimed to identify hepatic biomarkers specific to LW and TY by metabolomics approach using ^{1}H-NMR by analyzing the duck livers after 6 to 12 days of overfeeding. This study can also provide information to understand nonalcoholic fatty liver disease in humans better.

MATERIALS AND METHODS

Animal Experimental Design and Liver Characteristics

The animal design was clearly described previously (Bonnefont et al., 2019; Mozduri et al., 2021). Briefly, 120 male mule ducks (*Cairina moschata* × *Anas platyrhynchos*) were reared until 12 weeks and overfed twice a day during 6 to 12 days corresponding to 11 to 23 meals. The feed was composed of 97% corn (38% of grain and 62% of flour) supplemented with 3% of a commercial premix diluted into water. The amount of feed increased gradually from 265 to 420 g by meal (Bonnefont et al., 2019). A total of 30 ducks were slaughtered every other day in the second half of the overfeeding period from the 11th meal on day 6 to the 23rd meal on day 12 (**Figure 1A**). The duck body weight was registered before slaughtering. Then the liver was eviscerated and weighed to obtain LW. Then the livers were cooked as described in Rémignon et al. (2018), and the TY was determined as the ratio between cooked liver weights trimmed of all visible fat and raw liver weights (TY = 100 – % fat loss). At each time point (D6 to D12), 16 ducks were selected among the 30 ducks for liver analyses (n = 64 in total). They were chosen to obtain equivalent means and variabilities of LW and TY in the initial and subgroup groups. The selected samples corresponded to the samples used for identifying plasmatic biomarkers (Mozduri et al., 2021). The body weight, LW, and TY of the selected samples are represented in **Figures 1B–D**.

Liver Sampling and ^{1}H-NMR Analysis

At 20 min *post-mortem*, a sample of 20 g was taken off in the upper part of the main lobe of the liver. All samples were dropped into liquid nitrogen and stored at −80°C for ^{1}H-NMR analyses. They were ground into fine powder. Then, their polar metabolites were extracted with a method adapted from Beckonert et al. (2007) from 0.25 g of the crushed liver with methanol and dichloromethane (Beckonert et al., 2007) and carefully described in Mozduri et al. (2021). The upper phases composed of water and methanol with hydrophilic metabolites were collected in new polypropylene tubes and evaporated with a vacuum concentrator (Concentrator Plus, Eppendorf, Hamburg, Germany) and stored at −80°C until ^{1}H-NMR analysis. Then all samples were diluted into 650 µl of NMR pH7 phosphate buffer in deuterated water (D_2O) with sodium trimethylsilyl propionate (17.2 g TMSP for 100 ml). The tubes were vortexed and then centrifuged for 15 min at 5,350 g. Finally, 600 µl were sampled in NMR tubes of 5 mm. The ^{1}H-NMR analyses were done by Bruker Avance III HD NMR spectrometer operating at 600 MHz for a proton resonance frequency. The first step consisted of acquiring all spectra. For this purpose, the NOESYPR1D spin-echo pulse sequence was used to attenuate signals from water. The spectra were acquired at 300 K with time domain: 32 k, 16 dummy scans, and 512 scans for all samples. After Fourier transformation, using Topspin (V2.1, Bruker, Biospin, Munich, Germany), they were manually phased, corrected for the baseline, and calibrated with chemical shifts of TMSP at 0 ppm.

Spectra Preprocessing and Statistical Analysis

The ^{1}H-NMR spectra were analyzed by two methods: (i) a bucket method and (ii) a metabolite method, both of which

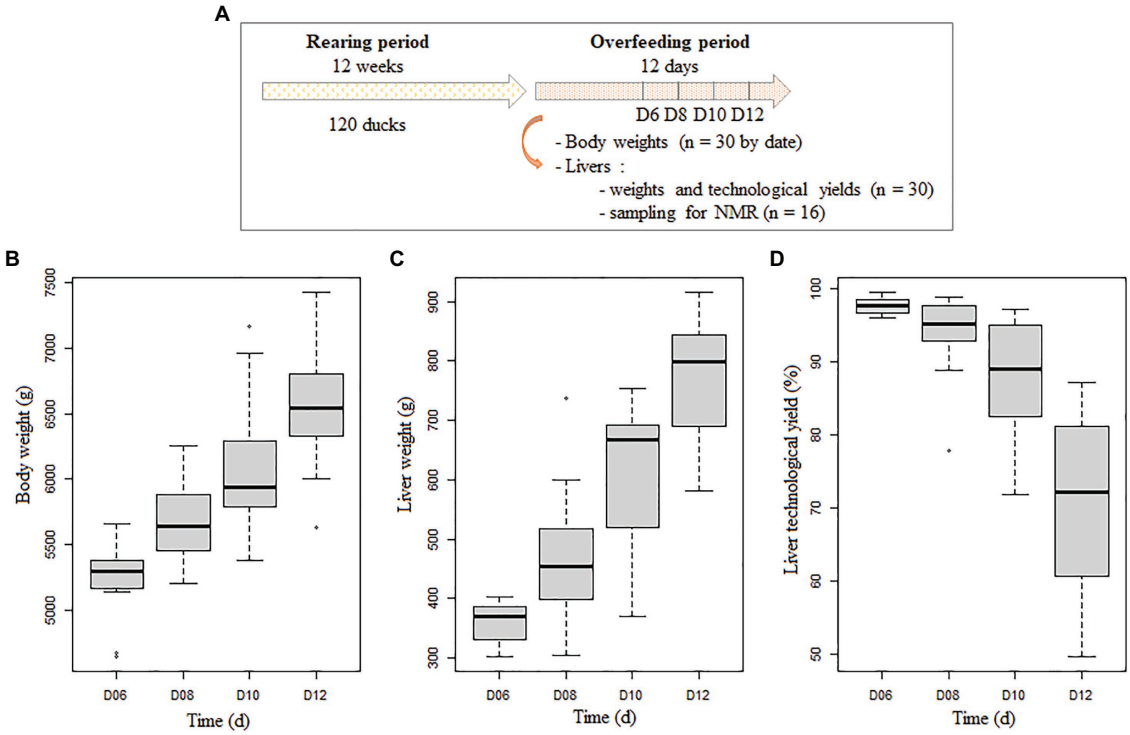

FIGURE 1 | Description of the duck experimental design and the duck characteristics. Experimental design and liver sampling **(A)**, evolution during the overfeeding period of duck body weight before slaughtering **(B)**, of liver weight after eviscerating **(C)** and liver technological yield after cooking (**D**; *n* = 16 or 17 at each time point).

were carefully described previously (Mozduri et al., 2021). (i) Briefly, the traditional bucket method consisted in converting the ^{1}H-NMR spectra into a bucket value table with the Workflow4Metabolomics 3.3 online platform (Giacomoni et al., 2015).[1] After spectra preprocessing (solvent suppression from 5.1 to 4.5 ppm and 3.35 to 3.2, zero-filling, apodization, application of Fourier transform, phasing, baseline correction, and calibration with TSP at 0.0 ppm) and spectra alignment, the spectra were split into buckets with a 0.01 ppm interval from 0.5 to 10 ppm. The raw bucket values were calculated as the integration of the spectrum curves for the corresponding buckets. Then the bucket values were normalized with the integration of the whole spectrum curves as following:

$$\text{Normalized bucket value} = \text{Raw bucket value} / \text{Whole spectrum integration.}$$

A table of bucket values was obtained with 64 rows corresponding to the animals and 714 columns corresponding to the buckets identified by their chemical shifts. (ii) Briefly, the metabolite method converted the ^{1}H-NMR spectra into metabolite relative concentration tables with the ASICS R package (R package version 4.0.2).[2] ASICS package performed an automatic approach to identify and quantify metabolites in complex ^{1}H-NMR spectra from their unique peak pattern (fingerprint; Tardivel et al., 2017; Lefort et al., 2019). The metabolite database used consisted of the spectra of 176 pure metabolites described in Tardivel et al. (2017). A total of 80 metabolites were identified and quantified in at least one sample. The methanol was removed as it was used to extract the metabolites. Then only 41 metabolites were kept for further analyses as they were present in at least 50% of the samples at one time point. Thus, the final table of metabolite relative concentrations contained 64 rows corresponding to the animals and 41 columns corresponding to the metabolites.

The bucket and metabolite relative concentration tables were analyzed with SIMCA P+ software (version 12, Umetrics, AB, Umea, Sweden) for carrying out the multivariate statistical analysis as previously described (Mozduri et al., 2021). Briefly, the variables were preprocessed with Pareto normalizations. Principal component analysis (PCA) was performed for finding outliers. Then partial least square analyses (PLS) were performed to explain Y variables (LW and TY) by the X variables (bucket or metabolite data). The PLS scatter plots were drawn, but as only one latent variable was created, the PLS scatter plot represented the scores (t1) on the vertical axis vs. sample identification on the horizontal axis. The goodness-of-fit of the models were estimated by the proportion of cumulative explained variance (R^2) for both the X variables (X = buckets or metabolites) and the Y variable (Y = LW or TY) and by the predictive ability of the model (Q^2). The root mean square error of estimations (RMSEE) were computed and indicated the fits of the observations to the model. The root mean square

[1]https://workflow4metabolomics.org/
[2]https://bioconductor.org/packages/ASICS/

error after cross-validations (RMSECv) were also computed. The plot of the Y observed vs. Y predicted values were drawn for each PLS model. The validation of the PLS model was evaluated by comparing the goodness of fit (R^2Y and Q^2) of the original model with the goodness of fits of 500 models based on data where the ranks of the Y-observations have been randomly permuted, while the X-matrix (bucket or metabolite) has been kept intact. The permutation plots were drawn. The latent variables associated with interesting axes were analyzed using the variable importance in the projection (VIP) method. The variable (bucket or metabolite) with a VIP superior to 1 was considered as "important." Then a one-by-one regression with either the LW effect or the TY effect was performed on the whole datasets. The *p*-values were corrected for multiple tests with the Benjamini–Hochberg correction using the R software (version 3.6.1) and named "BH *p*-value." A variable was "significant" when the BH *p*-value was inferior to 0.05 and "tended to be significant" when the BH *p*-value was between 0.05 and 0.1.

For the buckets with VIP superior to 1, the corresponding metabolites were identified manually by importing the chemical shift lists into the Human Metabolome Database (Wishart et al., 2009).[3] All carbohydrates identified were D-carbohydrates, and all amino acids were L-amino acids. To simplify the names of the metabolites, the "D-" and the "L-" were removed before the names of the carbohydrates and the amino acids, respectively. To confirm the identification of the metabolites, the ^{1}H-NMR peaks of these metabolites were manually checked on the sample spectra with TopSpin software (version 4.0, Bruker BioSpin, Rheinstetten, Germany). For each metabolite, all ^{1}H-NMR peaks were listed. For each ^{1}H-NMR peak, the VIP values and the BH *p*-values of the corresponding buckets were summarized by the number of buckets with VIP superior to 1 and by the range of BH *p*-values, respectively. The relative concentrations (RC) of a metabolite with the bucket data were estimated with a method adapted from Kostidis et al. (2017) by the following formula (Kostidis et al., 2017):

$$\text{Metabolite RC}_j = \text{mean}\left[\left(\text{intensity Peak}_{ij}\right)/\left(\text{H number Peak}_{ij}\right)\right]$$

where j represented a specific metabolite, i represented each proton peak of the ^{1}H-NMR spectrum of the j metabolite,

[3]http://hmdb.ca/

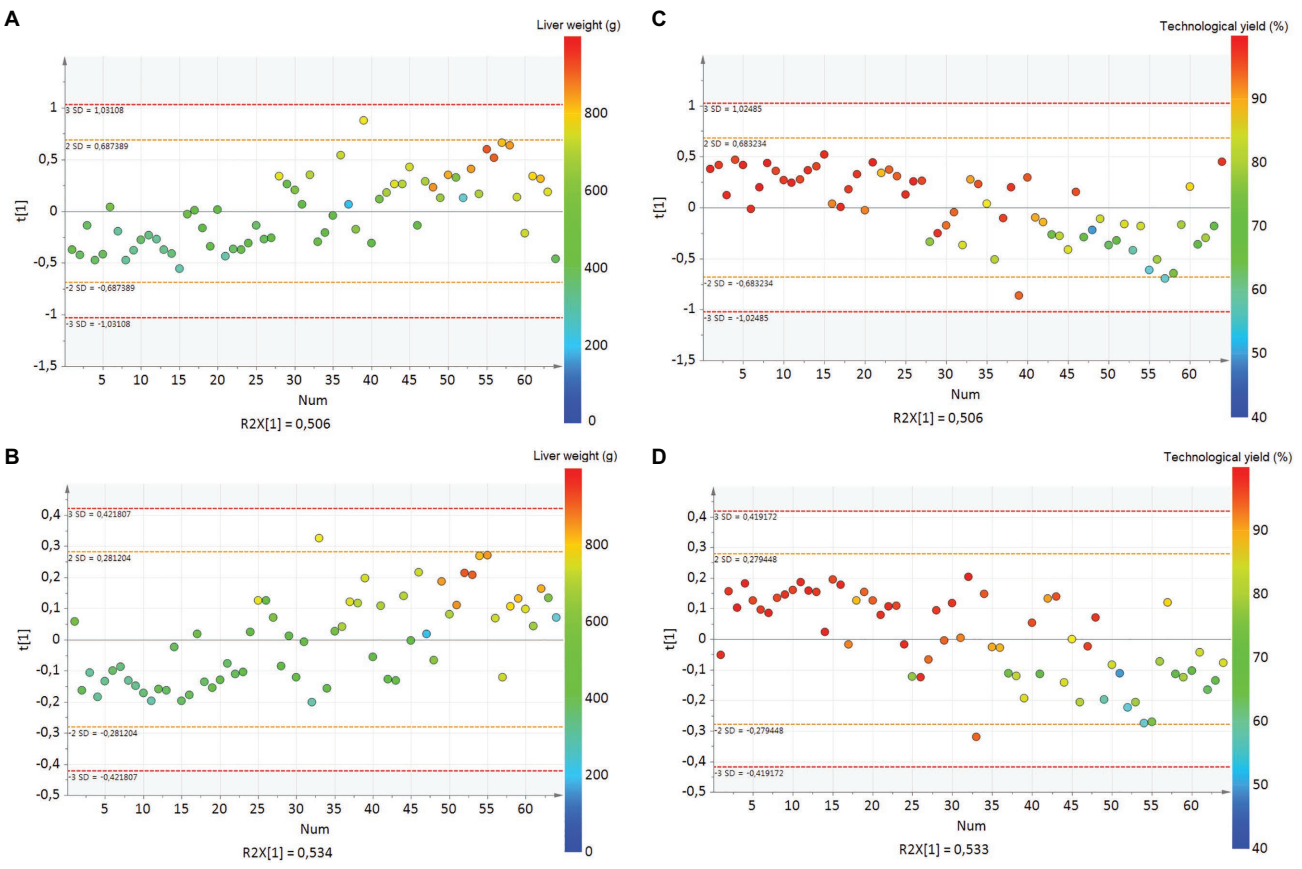

FIGURE 2 | PLS score plots **(A)** for liver weight with the bucket method (R^2X = 0.506, R^2Y = 0.657, Q^2 = 0.633) and **(B)** with the metabolite method (R^2X = 0.534, R^2Y = 0.65, Q^2 = 0.626), **(C)** for liver technological yield with the bucket method (R^2X = 0.506, R^2Y = 0.514, Q^2 = 0.471), **(D)** for liver technological yield with the metabolite method (R^2X = 0.533, R^2Y = 0.522, Q^2 = 0.418). The numbers correspond to the identification of the samples and the colors to the liver weight value. The legend is indicated on the right of the figure. The numbers correspond to the identification of the samples on the X axis and the colors to the liver weight or technological yield values.

"intensity $Peak_{ij}$" was computed as the sum of the bucket intensity of the i peak for the j metabolite, and "H number $Peak_{ij}$" was the number of protons corresponding to the i peak for the j metabolite. Then the lists obtained by the bucket method and the metabolite method were compared with Venn diagrams.[4]

All the biomarkers identified by the bucket method and/or the metabolite method were considered as biomarkers. Network analysis based on the correlation of the biomarker RC and the variable (LW or TY) was performed with the functions pls and network of the MixOmics R package (Lê Cao et al., 2009; Rohart et al., 2017; R package version 4.0.2.).[5]

RESULTS

The overfeeding of male mule ducks from 6 to 12 days enabled to obtain animals with large variability of performances. The body weights of the ducks were between 5 and 7.5 kg, their LW between 302.3 and 914.9 g, and the liver TY between 54.8 and 99.5% (**Figures 1B–D**). This experimental design enabled to obtain livers with strong variabilities like in the *foie gras* industry, and it was suitable to detect hepatic biomarkers of *foie gras* quality by ^{1}H-NMR analysis.

Identification of Hepatic Biomarkers of the Liver Weight of *Foie Gras*

First, a PCA was implemented to observe the data and to find outlier samples, but no outlier was detected (not shown). The partial least squares (PLS) analysis scatter plot had only one latent variable, and the parameters were cumulative $R^2X = 0.506$ and $R^2Y = 0.657$. The projection of the samples highlighted an evolution of LW with the first latent variable on the vertical axis (**Figure 2A**). The prediction of the model was $Q^2 = 0.633$. The original R^2Y and Q^2-values were higher than those obtained after 500 permutations, and the regression line of Q^2-points intersected the vertical axis below zero (−0.126; **Figure 3A**). The RMSEE and the RMSECv were close (109.4 and 111.5, respectively, **Figure 4A**).

A group of 64 buckets with a VIP > 1 explained the first latent variable (**Supplementary Data 1**). For the buckets

[4]https://bioinfogp.cnb.csic.es/tools/venny/index.html
[5]https://CRAN.R-project.org/package=mixOmics

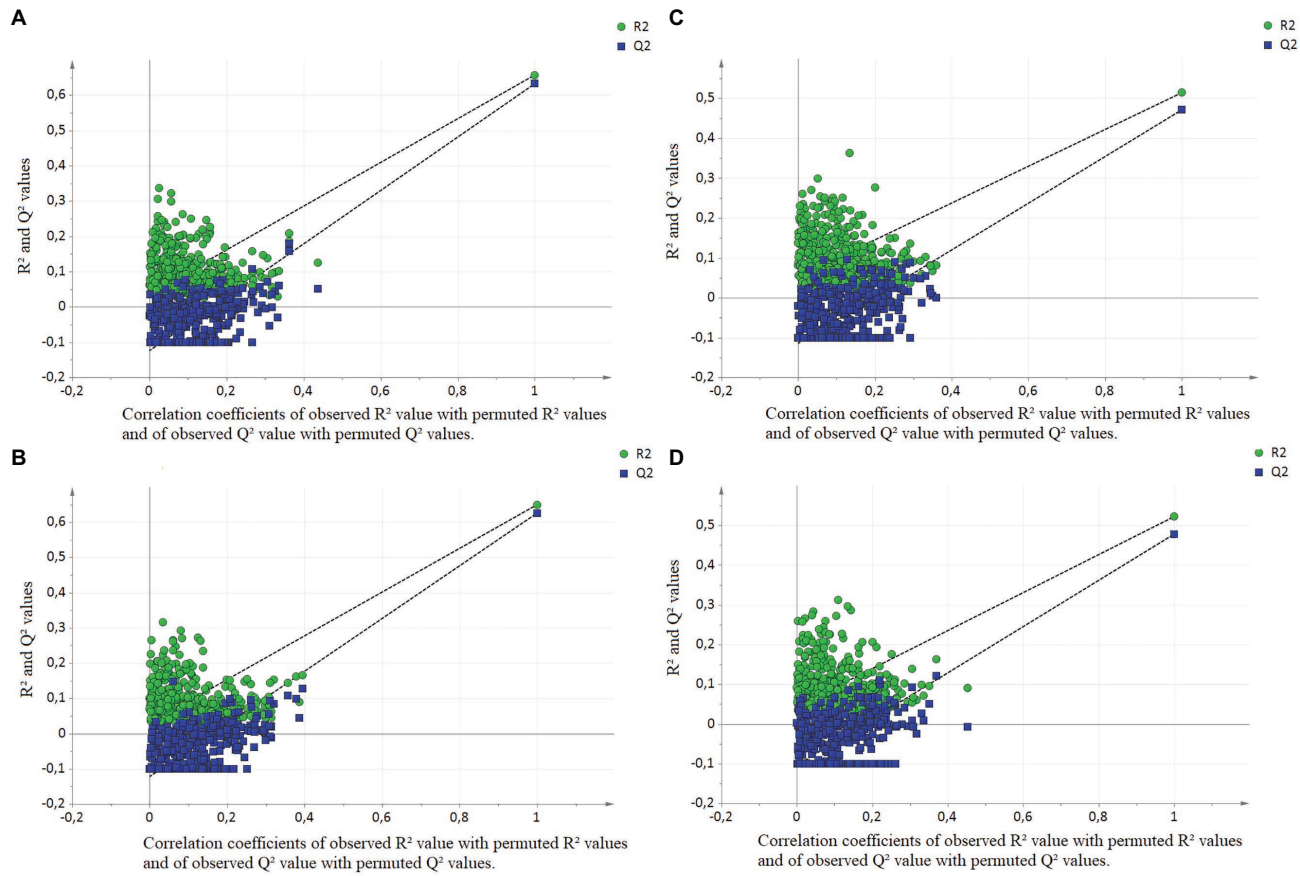

FIGURE 3 | Permutation plots **(A)** for liver weight with the bucket method, **(B)** for liver weight with the metabolite method, **(C)** for liver technological yield with the bucket method, **(D)** for liver technological yield with the metabolite method. 500 permutations were performed. The permutation plot shows, for a selected Y-variable, on the vertical axis the values of R^2Y and Q^2 for the original model and of the Y-permuted models. The horizontal axis shows the correlation between the permuted Y-vectors and the original Y-vector for the selected Y. The original Y has a correlation of 1.0 with itself.

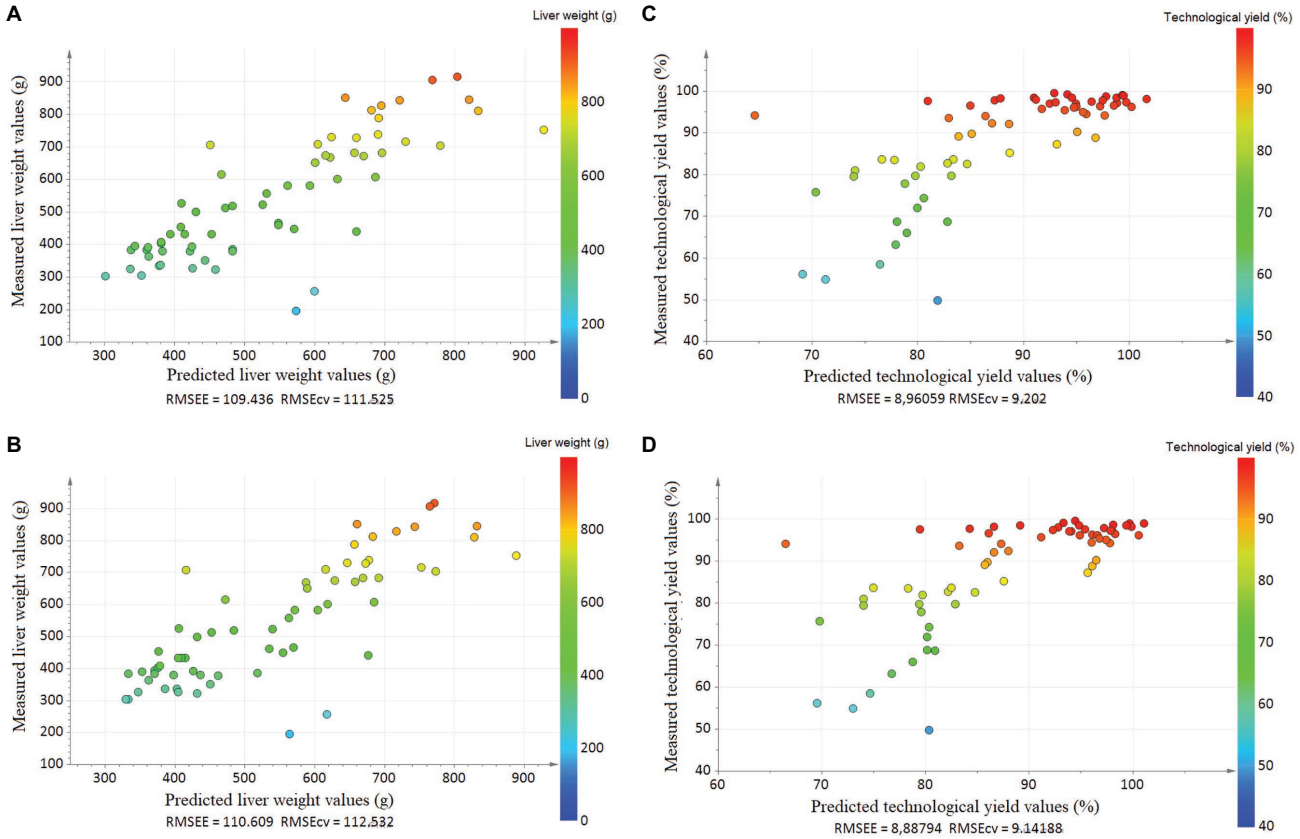

FIGURE 4 | Plots of predicted vs. observed data **(A)** for liver weight with the bucket method, **(B)** for liver weight with the metabolite method, **(C)** for liver technological yield with the bucket method, and **(D)** liver for technological yield with the metabolite method. The Root Mean Square Error of Estimation (RMSEE) and the Root Mean Square Error after cross validation (RMSECv) were indicated.

with VIP > 1 and BH $p < 0.05$, the involved metabolites were identified manually by importing chemical shift lists into the Human Metabolome Database (Wishart et al., 2009; See Footnote 3). They corresponded to 14 metabolites summarized in **Table 1**. There were seven carbohydrates identified as biomarkers for LW. For each metabolite, the number of peaks that contained at least one bucket with VIP > 1 was respectively, seven out of 10 peaks for glucose-6-phosphate (HMDB0001401), six out of eight peaks for glucuronic acid (HMDB0000127), all the two peaks for glyceric acid (HMDB0000139), all two peaks for glycogen (HMDB0000757), all the two peaks for lactate (HMDB0000190), two out of four peaks for malic acid (HMDB0000156), and 12 out of 13 peaks for maltose (HMDB0000163; **Table 1**). There were five amino acids identified as biomarkers of LW. For each metabolite, the number of peaks that contained at least one bucket with VIP > 1 was, respectively, two out of four ^{1}H-NMR peaks for arginine (HMDB0000517), one out of two peaks for N-acetylglycine (HMDB0000532), three out of five peaks for proline (HMDB0000162), all the two peaks for taurine (HMDB0000251) and six out of seven peaks for trans-4-hydroxy-L-proline (HMDB0000725; **Table 1**). There were also two other organic compounds identified as biomarkers of LW. For each metabolite, the number of peaks that contained at least one bucket with VIP > 1 was the one peak for allantoin (HMDB0000462) and three out of four peaks for glycerophosphocholine (HMDB0000086; **Table 1**).

The relative concentrations (RC) of all the 14 metabolites were computed. The BH *p*-values were summarized in **Table 1**. A total of nine metabolites were statistically significant (BH $p < 0.05$) and two tended to be significant ($p < 0.10$). All these 11 metabolites were further considered as LW biomarkers identified by the bucket method. There were six out the seven carbohydrates: glucuronic acid ($p < 0.001$), glyceric acid ($p < 0.001$), glycogen ($p = 0.070$), lactate ($p < 0.001$), malic acid ($p < 0.001$) and maltose ($p < 0.001$) for carbohydrates, three out of five amino acids: arginine ($p < 0.001$), taurine ($p < 0.001$), and trans-4-hydroxy-L-proline ($p = 0.005$) and also allantoin ($p = 0.020$) and glycerophosphocholine ($p = 0.070$; **Table 1**).

In parallel, the metabolite method was applied, and the 64 spectra were converted into a table of 41 metabolite values with the ASICS R package. No outlier was detected by PCA. The PLS scatter plot had only one latent variable, and the parameters of the models were cumulative $R^2X = 0.534$ and $R^2Y = 0.650$ (**Figure 2B**). The prediction of the model was low $Q^2 = 0.626$. The evolution of LW was well represented

TABLE 1 | List of the 14 biomarkers of *foie gras* liver weight identified with the bucket method.

Metabolites	^{1}H-NMR peak[γ]	Chemical shift[δ] (ppm)	number of buckets with VIP > 1[ε]	BH *p*-value[ζ]	BH *p*-value 2[η]
Carbohydrate					
Glucose-6-phosphate					**0.237**
HMDB0001401	multiplet	3.26–3.28	4	<0.001–0.01	
	multiplet	3.47–3.51	7	<0.001–0.004	
	multiplet	3.55–3.59	5	<0.001–0.002	
	triplet	3.70–3.73	4	<0.001	
	doublet	3.87–3.88	0		
	multiplet	3.90–3.94	2	<0.001	
	triplet	3.98–4.00	0		
	multiplet	4.02–4.05	2	<0.001	
	doublet	4.63–4.64	0		
	singlet	5.22	2	<0.001	
Glucuronic acid					**<0.001**
HMDB0000127	multiplet	3.27–3.30	4	<0.001–0.010	
	multiplet	3.49–3.54	7	<0.001–0.004	
	quartet	3.57–3.59	3	<0.001–0.006	
	multiplet	3.72–3.75	8	<0.001–0.040	
	doublet	4.08–4.09	2	<0.001–0.005	
	singlet	4.64	0		
	singlet	4.66	0		
	doublet	5.24–5.25	2	<0.001	
Glyceric acid					**<0.001**
HMDB0000139	multiplet	3.72–3.84	12	<0.001–0.040	
	multiplet	4.12–4.14	2	<0.001	
Glycogen					**0.070**
HMDB0000757	singlet	3.83	3	<0.001	
	singlet	5.39	1	0.030	
Lactate					**<0.001**
HMDB0000190	doublet	1.31–1.32	3	<0.001	
	quartet	4.08–4.12	5	<0.001–0.005	
Malic acid					**<0.001**
HMDB0000156	quartet	2.33–2.38	4	<0.001–0.050	
	doublet	2.64–2.65	0		
	doublet	2.67–2.68	0		
	quartet	4.28–4.31	1	<0.001	
Maltose					**<0.001**
HMDB0000163	singlet	5.40	2	<0.001–0.030	
	doublet	5.22–5.23	2	<0.001	
	doublet	3.96–3.98	1	<0.001	
	doublet	3.93–3.94	1	<0.001	
	doublet	3.89–3.92			
	multiplet	3.81–3.87	5	<0.001	
	multiplet	3.74–3.79	6	<0.001–0.040	
	multiplet	3.69–3.73	4	<0.001	
	quartet	3.65–3.68	1	0.005	
	singlet	3.63	1	0.005	
	multiplet	3.60–3.55	5	<0.001–0.002	
	triplet	3.43–3.39	5	<0.001	
	quartet	3.25–3.28	5	<0.001–0.200	
Amino acids					
Arginine					**0.004**
HMDB0000517	muitiplet	1.605–1.756	1		
	muitiplet	1.874–1.935	0		
	triplet	3.248–3.220	0		
	triplet	3.769–3.744	5	<0.001	
N-acetylglycine					**0.141**
HMDB0000532	singlet	8	0		
	doublet	3.745–3.768	6	<0.001–0.040	
Proline					**0.237**
HMDB0000162	multiplet	1.94–2.09	0		
	multiplet	2.31–2.37	4	<0.001–0.050	
	multiplet	3.30–3.35	2	<0.002	
	multiplet	3.38–3.42	0		
	multiplet	4.11–4.13	1	<0.001	

(Continued)

TABLE 1 | Continued

Metabolites	^{1}H-NMR peak[γ]	Chemical shift[δ] (ppm)	number of buckets with VIP > 1[ε]	BH *p*-value[ζ]	BH *p*-value 2[η]
Taurine					**<0.001**
HMDB0000251	triplet	3.24–3.26	6	<0.001–0.010	
	triplet	3.40–3.43	6	<0.001	
trans-4-hydroxy-L-proline					**0.005**
HMDB0000725	quartet	4.320–4.350	0		
	doublet	3.480–3.490	4	<0.001–0.001	
	singlet	3.46	1	<0.001	
	singlet	3.37	1	<0.001	
	doublet	3.340–3.350	1	<0.001	
	multiplet	2.390–2.450	2	<0.001–0.050	
	multiplet	2.120–2.170	1	<0.001	
Organic compounds					
Allantoin					**0.020**
HMDB0000462	singlet	5.38	1	0.030	
Glycerophosphocholine					**0.070**
HMDB0000086	singlet	3.20	7	<0.001–0.200	
	multiplet	3.59–3.68	4	<0.001–0.006	
	multiplet	3.84–3.95	8	<0.001	
	quartet	4.29–4.33	0		

[γ]For each metabolite, the nature of each ^{1}H-NMR peak is mentioned.
[δ]For each metabolite, the range of chemical shift of each peak is mentioned in ppm.
[ε]The PLS model to describe the liver weight with bucket data was plotted. The first latent variable enabled to separate the fatty livers in function of their liver weight. The VIP of the buckets involved in the first latent were extracted. For each ^{1}H-NMR peak of each metabolite, the number of buckets with VIP > 1 was indicated.
[ζ]For each bucket, the effect of the bucket value on the liver weight was tested by a linear model with R software, and the p-values were corrected with the Benjamini-Hochberg procedure and named BH p-values. For each metabolite, the range of BH p-values of each peak was mentioned.
[η]For each biomarker, the relative metabolite concentration was computed with the bucket data. A linear model with R software tested the effect of the relative metabolite concentration on the liver weight, and the p-values were corrected with the Benjamini-Hochberg procedure and named BH p-values 2.

TABLE 2 | List of the five biomarkers of *foie gras* liver weight identified with the metabolite method.

Metabolites	VIP-values[ε]	BH *p*-values[ζ]	R^2
Lactate	4.11	<0.001	0.65
Glucose	2.87	<0.001	0.51
Threonine	1.72	<0.001	0.62
Alanine	1.55	<0.001	0.35
Taurine	1.29	<0.001	0.26

[ε]The PLS model to describe the liver weight with metabolite data was plotted. The first latent variable enabled to separate the fatty livers in function of the liver weight. The metabolites with VIP superior to 1 were selected. The VIP of the metabolite was indicated.
[ζ]For each biomarker, the effect of their relative concentration on the liver weight was tested by a linear model with R software, and p-values were corrected with the Benjamini-Hochberg procedure and named BH p-values.

on the vertical axis corresponding to the first latent variable (**Figure 2B**). The original R^2Y and Q^2-values were higher than those obtained after 500 permutations, and the regression line of Q^2-points intersected the vertical axis below zero (−0.119; **Figure 3B**). The RMSEE and the RMSECv were close (110.6 and 112.5, respectively, **Figure 4B**). The evolution of LW was well represented on the vertical axis corresponding to the first latent variable (**Figure 2B**). Only five metabolites had a VIP > 1 to explain this axis, of which all had a BH $p < 0.05$ (**Table 2**). Including lactate (VIP = 4.11, BH $p < 0.001$), glucose (VIP = 2.87, BH $p < 0.001$), threonine (VIP = 1.72, BH $p < 0.001$), alanine (VIP = 1.55, BH $p < 0.001$) and taurine (VIP = 1.29, BH $p < 0.001$; **Table 2**).

In conclusion, for LW, there were 14 biomarkers. Two biomarkers were identified by the bucket method and the metabolite method (lactate, taurine), three were identified only by the metabolite method (glucose, alanine, and threonine), and nine metabolites were only identified by the bucket method (glucuronic acid, glyceric acid, glycogen, malic acid, maltose, arginine, trans-4-hydroxy-L-proline, allantoin, and glycerophosphocholine; **Figure 5A**). For the 14 biomarkers, their RCs were computed with the bucket data, and the plots of their RCs in the function of LW were presented in **Figure 6A**. The correlation network between LW and the biomarkers was presented in **Figure 7A**. LW was strongly negatively correlated with glucose (−0.95), glycogen (−0.97), glucuronic acid (−0.93), glyceric acid (−0.89), malic acid (−0.61), and maltose (−0.97) and also to alanine (−0.83), arginine (−0.92), taurine (−0.78), trans-4-hydroxy-L-proline (−0.81), and to allantoin (−0.80) and glycerophosphocholine (−0.84). On the contrary, TY was strongly correlated with lactate (0.98) and threonine (0.98; **Figure 7A**).

Identification of Hepatic Biomarkers of *Foie Gras* Technological Yield

First, the spectra were analyzed with the bucket method. A PCA was first performed, but no outlier was detected (not shown). The PLS scatter plot to explain TY had only one latent variable, and the parameters were cumulative $R^2X = 0.506$ and $R^2Y = 0.514$. The prediction of the model was $Q^2 = 0.471$. The original R^2Y and Q^2-values were higher than those obtained after 500 permutations, and the regression line of Q^2-points intersected the vertical axis below zero (−0.114; **Figure 3C**).

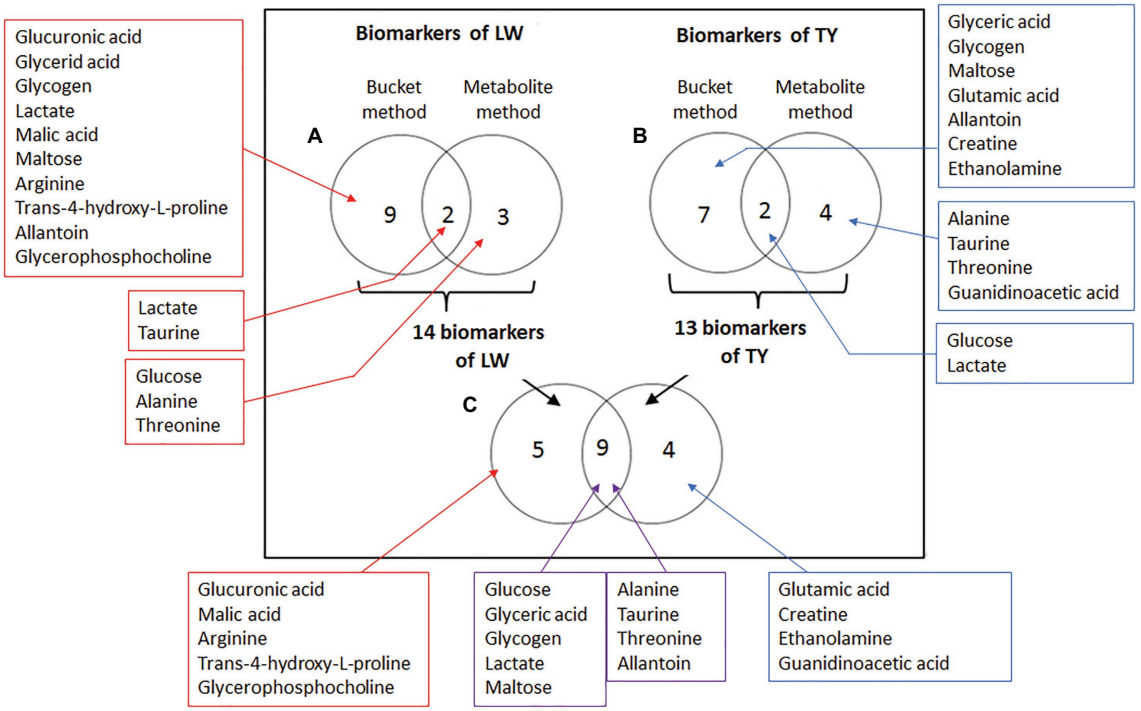

FIGURE 5 | Comparisons of biomarker lists with Venn diagram. **(A)** Biomarkers of liver weight identified by the bucket method and by the metabolite method (with VIP > 1 and BH *p*-value < 0.1). **(B)** Biomarkers of technological yield identified by the bucket method and by the metabolite method. **(C)** Biomarkers of liver weight and technological yield identified by at least one method.

The RMSEE and the RMSECv were close (8.9 and 9.2, respectively; **Figure 4C**). The projection of the samples highlighted an evolution of TY with the first latent variable on the vertical axis (**Figure 2C**). A total of 64 buckets had a VIP value superior to 1 (**Supplementary Data 2**). They corresponded to 14 metabolites. All the buckets corresponding to each 1H-NMR peak were identified for each metabolite, and their VIP values and their BH *p*-values were summarized in **Table 3**. There were six carbohydrates identified as biomarkers for TY. For each metabolite, the number of peaks that contained at least one bucket with VIP > 1 was, respectively, 21 out of 22 peaks for glucose (HMDB0000122), eight out of 10 peaks for glucose-6-phosphate (HMDB0001401), all of the two peaks for glyceric acid (HMDB0000139), all the two peaks for glycogen (HMDB0000757), all the two peaks for lactate (HMDB0000190) and 12 out of 13 peaks for maltose (HMDB0000163). There were also five amino acids identified as biomarkers of TY of *foie gras*. For each metabolite, the number of peaks that contained at least one bucket with VIP > 1 was, respectively, three out four peaks for arginine (HMDB0000517), eight out of nine peaks for glutamic acid (HMDB0000148), one out of two peaks for N-acetylglycine (HMDB0000532), all the five peaks for proline (HMDB0000162) and all the seven peaks for trans-4-hydroxy-L-proline (HMDB0000725). There were also three other organic compounds identified as biomarkers of TY. For each metabolite, the number of peaks that contained at least one bucket with VIP > 1 was, respectively, the only one peak for allantoin (HMDB0000462), all the two peaks for creatine (HMDB0000064), and all the two peaks for ethanolamine (HMDB0000149; **Table 3**).

The RCs of all the 14 metabolites were computed. The BH *p*-values were summarized in **Table 3**. A total of nine metabolites were considered as statistically significant (BH $p < 0.05$) whose glucose, glyceric acid, glycogen, lactate, maltose for carbohydrates, only glutamic acid for the amino acids and allantoin, creatine, and ethanolamine (**Table 2**). All these nine metabolites were further considered as biomarkers of TY.

In parallel, the metabolite method was performed. The individuals were less well represented on the scatter plot than with the bucket data (1 latent variable, cumulative $R^2X = 0.533$, $R^2Y = 0.522$; **Figure 2D**). The prediction of the model was $Q^2 = 0.418$. The original R^2Y and Q^2-values were higher than those obtained after permutation, and the regression line of Q^2-points intersected the vertical axis below zero (−0.104; **Figure 3D**). The RMSEE and the RMSECv were close (8.9 and 9.1, respectively; **Figure 4D**). The latent variable on the vertical axis explained the evolution of TY (**Figure 2D**), and six metabolites had VIP values superior to 1 (**Table 4**). Including glucose (VIP = 2.82, BH $p < 0.001$), lactate (VIP = 4.06, BH $p < 0.001$), alanine (VIP = 1.43, BH $p < 0.001$), taurine (VIP = 1.51, BH $p < 0.001$), threonine (VIP = 1.72, BH $p < 0.001$) and guanidinoacetic acid (VIP = 1.04, BH $p < 0.001$).

In conclusion, for TY, there were 13 biomarkers: two biomarkers were identified by the bucket method and the metabolite method (glucose and lactate), four were identified

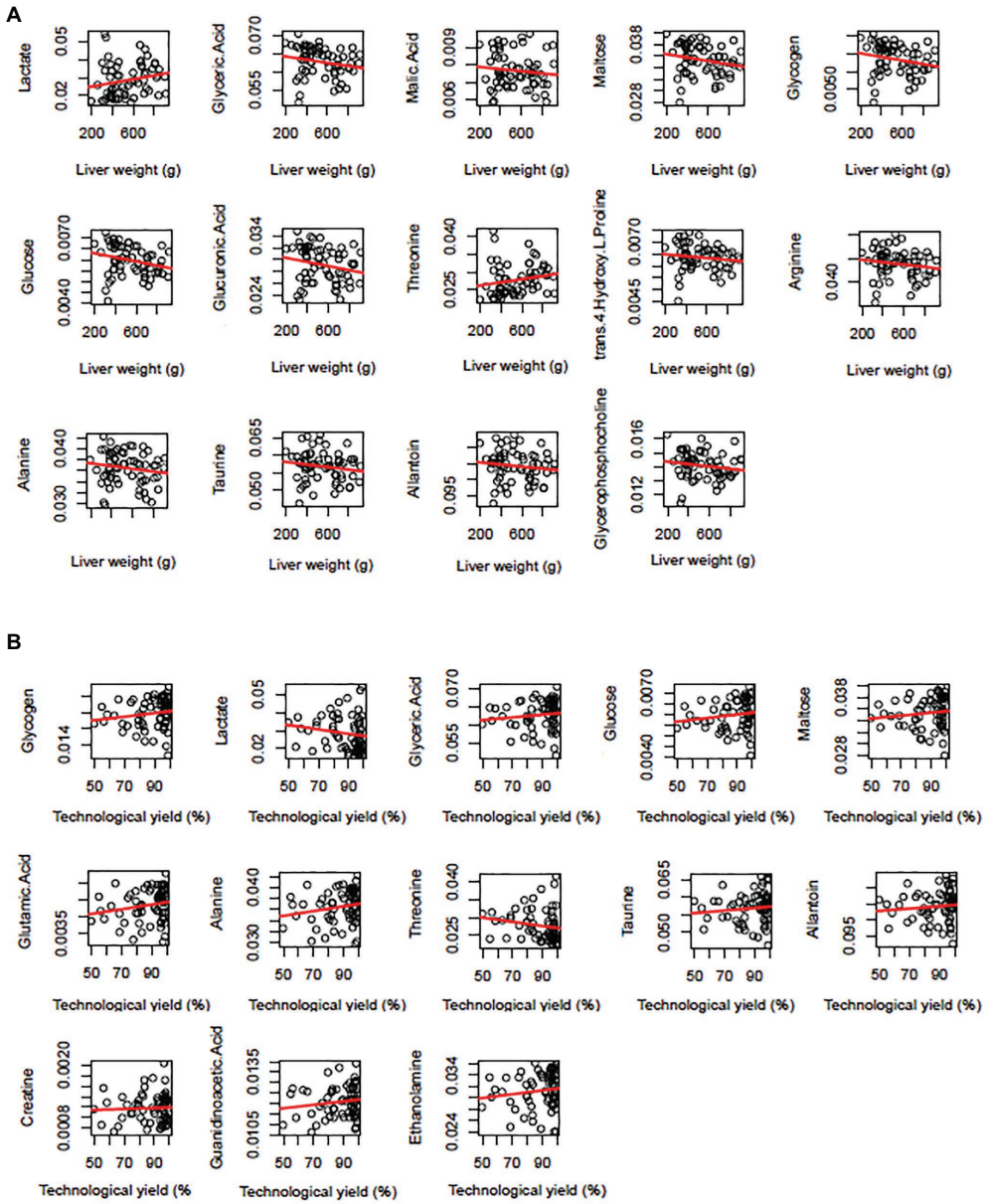

FIGURE 6 | Plots of biomarker relative contents in function of liver weight **(A)** or liver technological yield **(B)**. The metabolite relative contents were computed with the bucket data and had no unit. The regression curves were in red.

only by the metabolite method (alanine, taurine, threonine, and guanidino acetic acid), and seven metabolites were identified by the bucket method (glyceric acid, glycogen, maltose, glutamic acid, allantoin, creatine, and ethanolamine; **Figure 5B**).

For the 13 biomarkers of TY, their RC was computed with the bucket data, and the plots of their RC in the TY function were presented in **Figure 6B**. The correlation network between TY and the biomarker RC was presented in **Figure 7B**. TY was positively correlated with glucose (0.92), glycogen (0.98), glyceric acid (0.9), maltose (0.9), and also to alanine (0.89), glutamic acid (0.93), taurine (0.75), and to allantoin (0.75), ethanolamine (0.95), and guanidinoacetic acid (0.46), whereas TY was negatively correlated with lactate (−0.98), threonine (−0.96) and creatine (−0.57; **Figure 7B**).

Consequently, the results of the ^{1}H-NMR analysis identified 14 hepatic biomarkers for the *foie gras* liver weight and 13 for its technological yield (**Table 5** and **Figures 5A,B**). As the phenotypic correlation between LW and TY was strong (−0.80, $p < 0.001$), nine biomarkers were common to LW and TY (**Figure 5C**), of which five carbohydrates: glucose, glyceric acid, glycogen, lactate, maltose, three amino acids: alanine, taurine, threonine, and allantoin. There were five biomarkers specific to LW: glucuronic acid, malic acid, arginine, trans-4-hydroxy-L-proline, glycerophosphocholine, and four biomarkers specific

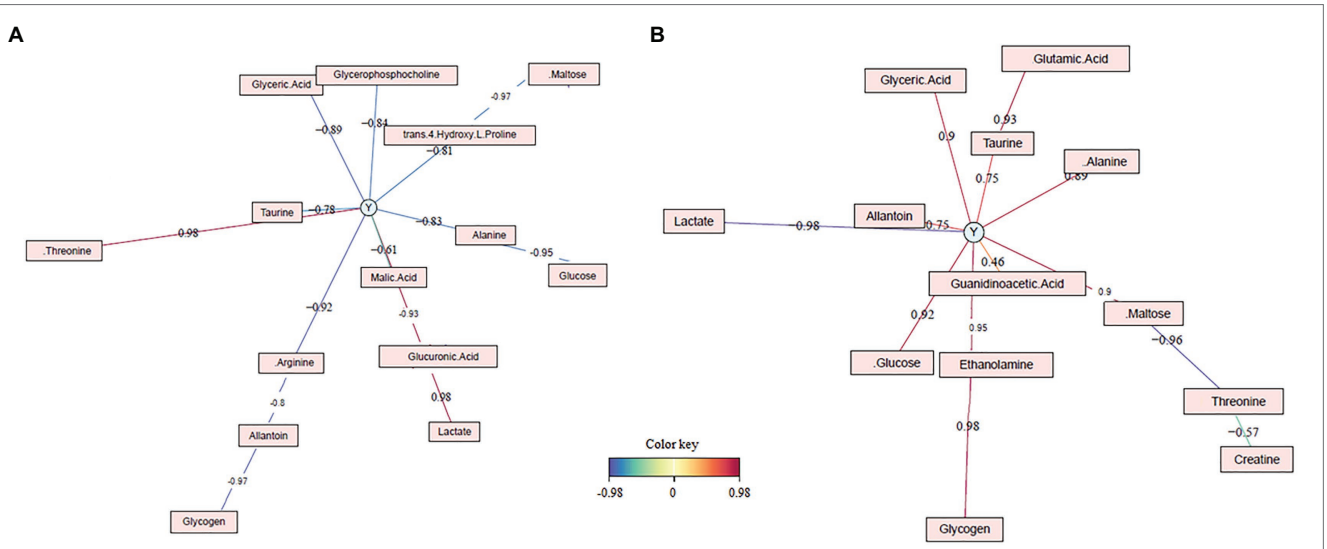

FIGURE 7 | Correlation networks of *foie gras* biomarkers **(A)** of liver weight (Y represents the liver weight) and **(B)** of liver technological yield (Y represents the technological yield). The relative concentration used for the correlations are calculated with the bucket data.

to TY: glutamic acid, creatine, ethanolamine, and guanidinoacetic acid (**Figure 5C**).

DISCUSSION

In this experimental design, the ducks were overfed for 6 to 12 days and received 11 to 23 meals. As a result, large variations in duck body weights, LW, and liver TY occurred, explaining the high correlations observed between the biomarker relative quantities and the liver characteristics.

During the overfeeding, the feed was based on corn. As corn is a cereal, it is rich in starch (around 63% as fed). The ingested starch is converted into glucose in the small intestine. Then the glucose is absorbed into the hepatic portal vein and carry to the liver. There, it can be stored like glycogen or converted into fatty acids by *de novo* lipogenesis. In the study, the liver weight was highly increased (from 80 g on day 0 to more than 750 g on day 12). Thus, the plasmatic glucose contents measured in the carotid artery corresponded to the result of the glucose transfer into the portal vein and the glucose uptake by the liver and other organs. However, the plasmatic glucose content decreased during the overfeeding while LW was increased (correlation of −0.94 in Mozduri et al., 2021) although the ingested starch was strongly increased as the corn quantity meal was increased. That means that the plasmatic glucose content was up-taken more efficiently by the liver during the overfeeding (Pioche et al., 2019). On the contrary, the glucose content in the liver was decreased when LW was increased with a negative correlation of −0.95 between them. So, the glucose was highly metabolized in the liver. At the beginning of the overfeeding period, the liver metabolism was more oriented through glycogenogenesis with strong glycogen storage (until 106 mg of glycogen by grams of the liver after three meals at day 2). In contrast, after seven meals on day 4, the liver metabolism shifted to lipogenesis with a strong triglyceride accumulation (29.5% of lipids at day 4 vs. 4.6 at day 0; Bonnefont et al., 2019). The glycogen content estimated in the liver in the second half of the overfeeding (from day 6 to day 12) was strongly negatively correlated with liver weight (−0.97). Furthermore, in other animal models as rats with hepatic steatosis, the liver glycogen content was lower than in control rats (Kusunoki et al., 2002).

In addition, LW was negatively correlated with TY (−0.82). Thus, the glucose content and the glycogen content were strongly correlated with TY (+0.92 and +0.98). That is consistent with previous results on *foie gras* with livers weighing around 580 g (Bonnefont et al., 2014).

In parallel, the hepatic lactate content was the most important metabolite to discriminate the livers in the function of their LW or TY (VIP values of the O-PLS models of 4.11 and 4.06, respectively). It was positively correlated with LW (+0.98) and negatively correlated with TY (−0.98). Previously, the lactate was the most discriminant metabolite between high TY livers and low TY livers with equivalent weights (Bonnefont et al., 2014). The lactate is the last metabolite of anaerobic glycolysis that converts glucose into pyruvate and then into lactate *via* the lactate dehydrogenase enzyme. In a recent mouse model, it was shown that glucose oxidation in the liver was central in the development of steatosis, as glycolysis metabolizes glucose into pyruvate, which can be anaerobically converted into lactate or aerobically converted into acetyl-CoA. The hepatic lactate in nonalcoholic steatohepatitis (NASH) was primarily diverted toward the production of acetyl-CoA for lipogenesis rather than the production of glucose (Zhu et al., 2018). In addition, Lo et al. (2020b) recently demonstrated in ducks undergoing overfeeding that low LW was associated with aerobic energy metabolism and high weight livers with anaerobic energy metabolism (Lo et al., 2020b). These results suggest that the efficiency of energy metabolism would influence both LW and TY. Therefore, it can be supposed that the increase in LW

TABLE 3 | List of the 14 biomarkers of *foie gras* technological yield identified with the bucket method.

Metabolites	^{1}H-NMR peak[γ]	Chemical shift[δ] (ppm)	number of buckets with VIP > 1[ε]	BH *p*-value[ζ]	BH *p*-value 2[η]
Carbohydrate					
Glucose					**<0.001**
HMDB0000122	quartet	3.22.25	4	<0.001 to 0.005	
	singlet	3.38	1	<0.001	
	doublet	3.39	2	<0.001	
	doublet	3.40–3.41	1	<0.001	
	singlet	3.42	1	<0.001	
	doublet	3.43–3.44	2	<0.001	
	quartet	3.45–3.46	3	<0.001	
	quartet	3.46	1	<0.001	
	singlet	3.48	1	<0.001	
	singlet	3.49	3	<0.001 to 0.030	
	doublet	3.51–3.52	3	<0.001 to 0.050	
	doublet	3.53–3.54	4	<0.001 to 0.050	
	quartet	3.69–3.71	4	<0.001 to 0.030	
	multiplet	3.72–3.77	7	<0.001	
	doublet	3.80–3.81	2	<0.001	
	singlet	3.82	2	<0.001	
	doublet	3.82–3.83	3	<0.001	
	doublet	3.84–3.85	4	<0.001	
	doublet	3.87–3.88	2	<0.001	
	doublet	3.89–3.90	2	<0.001	
	doublet	4.63–4.64	0		
	doublet	5.22	2	<0.001	
Glucose-6-phosphate					**0.490**
HMDB0001401	multiplet	3.26–3.28	4	<0.001 to 0.080	
	multiplet	3.47–3.51	7	<0.001 to 0.030	
	multiplet	3.55–3.59	4	0.005 to 0.040	
	triplet	3.70–3.73	4	<0.001	
	doublet	3.87–3.88	2	<0.001	
	multiplet	3.90–3.94	2	<0.001 to 0.020	
	triplet	3.98–4.00	3	<0.001 to 0.020	
	multiplet	4.02–4.05			
	doublet	4.63–4.64	0		
	singlet	5.22	2	<0.001	
Glyceric acid					**<0.001**
HMDB0000139	multiplet	3.72–3.84	11	<0.001	
	multiplet	4.12–4.14	2	<0.001 to 0.050	
Glycogen					**0.011**
HMDB0000757	singlet	3.83	4	<0.001	
	singlet	5.39	2	0.001 to 0.007	
Lactate					**<0.001**
HMDB0000190	doublet	1.31–1.32	2	<0.001	
	quartet	4.08–4.13	5	<0.001 to 0.050	
Maltose					**<0.001**
HMDB0000163	singlet	5.4	2	0.001 to 0.007	
	doublet	5.22–5.23	2	<0.001	
	doublet	3.96–3.98	2	<0.001 to 0.020	
	doublet	3.93–3.94			
	doublet	3.89–3.92	3	<0.001	
	multiplet	3.87–3.81	5	<0.001	
	multiplet	3.74–3.79	5	<0.001	
	multiplet	3.69–3.73	7	<0.001 to 0.030	
	quartet	3.65–3.68	4	<0.001 to 0.030	
	singlet	3.63	1	0.010	
	multiplet	3.60–3.55	4	0.005 to 0.040	
	triplet	3.39–3.43	5	<0.001	
	quartet	3.28–3.25	5	<0.001 to 0.080	
Amino acids					
Arginine					**0.490**
HMDB0000517	multiplet	1.60–1.75	1	0.002	
	multiplet	1.87–1.93	0		
	triplet	3.22–3.25	6	<0.001 to 0.080	
	triplet	3.74–3.77	5	<0.001	

(Continued)

TABLE 3 | Continued

Metabolites	^{1}H-NMR peak[γ]	Chemical shift[δ] (ppm)	number of buckets with VIP > 1[ε]	BH *p*-value[ζ]	BH *p*-value 2[η]
Glutamic acid					**0.010**
HMDB0000148	quartet	3.73–3.76	5	<0.001	
	multiplet	2.00–2.15	1	0.006	
	singlet	2.29	1	0.005	
	singlet	2.31	1	0.005	
	doublet	2.32–2.33	1	0.005	
	doublet	2.34	1	0.005	
	doublet	2.35–2.36	2		
	singlet	2.38	2	<0.001 to 0.005	
	singlet	2.39	2	<0.001 to 0.110	
N-acetylglycine					**0.495**
HMDB0000532	singlet	8	0		
	doublet	3.75–3.77	5	<0.001	
Proline					**0.286**
HMDB0000162	multiplet	1.94–2.09	1	0.006	
	multiplet	2.31–2.37	3	<0.001 to 0.005	
	multiplet	3.30–3.35	2	<0.001	
	multiplet	3.38–3.42	5	<0.001	
	multiplet	4.11–4.13	3	<0.001 to 0.050	
trans-4-hydroxy-L-proline					**0.147**
HMDB0000725	multiplet	2.12–2.17	2	0.004 to 0.006	
	multiplet	2.39–2.45	3	<0.001 to 0.100	
	doublet	3.34–3.35	1	<0.001	
	singlet	3.37	1	<0.001	
	singlet	3.46	2	0.010	
	doublet	3.48–3.49	4	<0.001 to 0.030	
	quartet	4.32–4.35	1	0.001	
Organic compound					
Allantoin					**0.004**
HMDB0000462	singlet	5.38	2	0.001–0.007	
Creatine					**<0.001**
HMDB0000064	singlet	3.02	1	<0.001	
	singlet	3.92	3	<0.001–0.020	
Ethanolamine					**0.009**
HMDB0000149	triplet	3.12–3.14	1	<0.001	
	triplet	3.80–3.82	3	<0.001	

[γ]*For each metabolite, the nature of each ^{1}H-NMR peak is mentioned.*

[δ]*For each metabolite, the range of chemical shift of each peak is mentioned in ppm.*

[ε]*The PLS model to describe the technological yield with bucket data was plotted. The first latent variable enabled to separate the fatty livers in function of the technological yield. The VIP of the buckets involved in the first latent were extracted. For each 1H-NMR peak of each metabolite, the number of buckets with VIP > 1 was indicated.*

[ζ]*For each bucket, the effect of the bucket value on the technological yield was tested by a linear model with R software, and the p-values were corrected with the Benjamini–Hochberg procedure and named BH p-values. For each metabolite, the range of BH p-values of each peak was mentioned.*

[η]*For each biomarker, the relative metabolite concentration was computed with the bucket data. A linear model with R software tested the effect of the relative metabolite concentration on the technological yield, and the p-values were corrected with the Benjamini–Hochberg procedure and named BH p-values 2.*

could lead to a decrease in the efficiency of this metabolism translated by the increase in hepatic lactate content, which would result in a decrease in TY.

Contrary to hepatic lactate content, the glucuronic acid hepatic content was negatively correlated with LW (−0.93). However, the glucuronic acid can be conjugated to lipophilic substrates *via* UDP-glucuronosyltransferases. These enzymes catalyze phase II biotransformation reactions and promote glucuronidation. Glucuronidation is a major detoxification pathway for endogenous and exogenous compounds, and it is involved in transporter-mediated excretion into bile and urine (Williams et al., 2004). In steatosis livers of mice, the UDP-glucuronosyltransferase expression increased with the increased hepatic triglyceride content and could have a significant impact on determining circulating hormone levels (Xu et al., 2012). Thus, the lower quantity of glucuronic acid in the high-weight liver could be explained using glucuronic acid for glucuronidation.

The amino acid metabolism of duck livers was strongly impacted by the overfeeding period at the same time as the carbohydrate metabolism. The alanine, taurine, and threonine were identified as biomarkers of both LW and TY, whereas arginine and trans-4-hydroxy-proline were only identified as biomarkers of LW and glutamic acid of TY. Briefly, the amino acid liver content was decreased when the LW was increased and/or when the TY was decreased except for the threonine. The reduction of amino acid metabolism in the liver with the enhanced hepatic steatosis was already underlined in overfed ducks (François et al., 2014; Lo et al., 2020b) and other hepatic steatosis models as obese mice (Du et al., 2012; Bruckbauer and Zemel, 2014). Thus, these amino acids were increased in

TABLE 4 | List of the 6 biomarkers of *foie gras* technological yield identified with the metabolite method.

Var ID (Primary)	VIP-values[ε]	BH *p*-values[ζ]	R^2
Glucose	2.8	<0.001	0.39
Lactate	4.06	<0.001	0.50
Alanine	1.43	<0.001	0.24
Taurine	1.51	<0.001	0.28
Threonine	1.72	<0.001	0.49
Guanidinoacetic acid	1.04	<0.001	0.39

[ε]*The PLS model to describe the technological yield with metabolite data was plotted. The first latent variable enabled to separate the fatty livers in function of the liver weight. The metabolites with VIP superior to 1 were selected. The VIP of the metabolite was indicated.*

[ζ]*For each biomarker, the effect of their relative concentration on the technological yield was tested by a linear model with R software, and the p-values were corrected with the Benjamini-Hochberg procedure and named BH p-values.*

low-weight livers. It was shown in rats and mice that a diet supplementation in taurine (Gentile et al., 2011) and arginine (Voloshin et al., 2014; Sellmann et al., 2017) reduced hepatic lipid accumulation. Thus, they were used as a preventative treatment against NASH. The taurine transporter-deficient mice showed strongly decreased taurine levels in various tissues like the liver and developed chronic hepatitis and liver fibrosis during adulthood, accompanied by severe augmentation of hepatocyte apoptosis (Warskulat et al., 2006). In addition, the restriction of lysine and threonine in diets increased the free fatty acid content in the liver of rats (Viviani et al., 1966).

Furthermore, the increase of the activities of the transaminase enzymes alanine aminotransferase (ALT) and aspartate aminotransferase (AST) with liver injury is strongly documented (Pratt and Kaplan, 2000). ALT catalyzes the transfer of an amino group from alanine to α-ketoglutarate to produce pyruvate and glutamate, and AST catalyzes the interconversion of aspartate and α-ketoglutarate to oxaloacetate and glutamate. Both reactions are reversible. Thus, the identification of alanine as a biomarker of both LW and TY and glutamic acid as a specific biomarker of TY should be directly linked to the ALT and AST activities in the liver. Also, the oxaloacetate issued from AST activity is a key intermediate in the citric acid cycle. Actually, in this cycle, the malate dehydrogenase converts the malate into oxaloacetate with the NAD^+ cofactor, and after several reactions, the oxaloacetate is converted again into malate. However, the malate is known to play a role in lipogenesis by furnishing NADPH to reduce acetyl CoA to fatty acids (Wise Jr and Ball, 1964). This may explain the identification of malic acid as a biomarker of LW. In the Poland goose, the activity of ME was correlated positively with the weight of the fatty liver (Mourot et al., 2000).

In addition, glyceric acid was identified as a biomarker of LW and TY. The glyceric acid is a substrate for glycerol synthesis (Feraudi and Bert, 1977), and the glycerol is a substrate for triglyceride synthesis (Tidwell and Johnston, 1961). Thus, the negative correlation of glyceric acid with LW (−0.89) could be explained by using glyceric acid for lipogenesis.

Moreover, in the liver, creatine is synthesized from glycine and arginine. First, both amino acids are combined to form guanidinoacetate which is then methylated using S-adenosyl methionine to synthesize creatine (Rosenberg, 1959). The amount of arginine was negatively correlated with LW (−0.92). The arginine is involved in the process of creatine synthesis (Barcelos et al., 2016). Creatine plays a role in the antioxidant role against aqueous radical and reactive species ions (Lawler et al., 2002). The supplementation in creatine protects the liver from hepatotoxicity by attenuating oxidative stress (Aljobaily et al., 2021). Lo et al. (2020a) showed that, in overfed liver duck, an increase in liver weight resulted in a rise in the cellular oxidative stress level (Lo et al., 2020a). These results corroborated the positive correlation between the level of oxidative stress and LW.

The creatine phosphate serves as a dynamic reservoir of high-energy phosphate in exchange for ATP. The steatosis strongly impacts creatine metabolism as arginine is a specific biomarker of LW, and guanidinoacetate and creatine are specific biomarkers of TY. However, contrary to guanidinoacetate, creatine was negatively correlated with TY. Thus, the creatine content in the liver with low TY may be increased to control oxidative stress. Oxidative stress is defined as the presence of metabolic and radical substances or so-called reactive (oxygen, nitrogen, or chlorine) species (Elnesr et al., 2019; Elwan et al., 2019).

Furthermore, the positive correlation of hepatic amino acid content and TY in *foie gras* was previously underlined in association with a reduction of oxidative stress (Theron et al., 2011; Bonnefont et al., 2014; François et al., 2014). Actually in chronic liver disease there is increased reactive oxygen species production and decreased activity of antioxidant systems (De Minicis et al., 2006). Recently, hypoxic response to severe hypoxia was highlighted in heavy livers of ducks (Lo et al., 2020a).

Moreover, the modification of amino acid metabolism in livers during the overfeeding period corroborates the evolution of amino acid metabolism in plasma of the same ducks (Mozduri et al., 2021) and other hepatic steatosis models, as it was discussed in Mozduri et al. (2021).

Finally, the glycerophosphocholine was identified as a specific biomarker of LW (−0.84), and ethanolamine as a specific biomarker of TY (+0.95). Ethanolamine can be phosphorylated to form phosphoethanolamine. Glycerophosphocholine and phosphoethanolamine are cytosolic intermediates of phospholipids synthesis. In patients with cirrhosis that is considered the most severe stage of liver steatosis disease, the phosphoethanolamine liver content was increased whereas the glycerophosphocholine was decreased compared to controls but not in patients with a lower severe stage of fatty liver disease as NASH (Sevastianova et al., 2010). On the contrary, Kalhan et al. (2011) reported a significantly lower glycerophosphocholine content in steatohepatitis compared with nondiabetic healthy controls in humans (Kalhan et al., 2011). Furthermore, in overfed ducks, a higher glycerophosphocholine content in the low-fat-loss livers that corresponded to high TY livers was underlined (Bonnefont et al., 2014).

The last biomarker of LW and TY was allantoin. It was shown that a supplementation in allantoin in NASH or diabetic mice inhibited the structural damage of the liver concerning fat accumulation (Movahhed et al., 2019; Ma et al., 2020) which explained its lower content in high weight livers.

TABLE 5 | List of the biomarkers of liver weight and technological yield of *foie gras*.

	Biomarkers of liver weight						Biomarkers of technological yield					
	with bucket method			with metabolite method			with bucket method			with metabolite method		
	Important peaks[ε]	BH *p*-Value[ζ]	correlation with LW[η]	VIP[δ]	BH *p*-Value[ζ]	correlation with LW[η]	Important peaks[ε]	BH *p*-Value[ζ]	correlation with TY[η]	VIP[δ]	BH *p*-Value[ζ]	correlation with TY[η]
Biomarkers of LW and TY												
Alanine			−0.83	1.55		−0.9			0.89	1.43	<0.001	0.81
Allantoin	1/1	0.020	−0.8				1/1	0.004	0.75			
Glucose				2.87	<0.001	−0.95	21/22	<0.001	0.92	2.86	<0.001	0.94
Glyceric acid	2/2	<0.001	−0.89				2/2	<0.001	0.90			
Glycogen	2/2	0.007	−0.97				2/2	0.01	0.98			
Lactate	2/2	<0.001	0.98	4.11	<0.001	0.94	2/2	<0.001	−0.98	4.06	<0.001	−0.97
Maltose	12/12	<0.001	−0.97				12/12	<0.001	0.90			
Taurine	2/2	<0.001	−0.78	1.29	<0.001	−0.84			0.75	1.51	<0.001	0.82
Threonine			0.98	1.72	<0.001	0.96			−0.96	1.72	<0.001	−0.95
Biomarkers of LW												
Arginine	2/3	0.004	−0.92									
Glucuronic acid	6/8	<0.001	−0.93									
Glycerophosphocholine	3/4	0.070	−0.84									
Malic acid	2/4	<0.001	−0.61									
Trans-4-hydroxy-L-proline	6/7	0.005	−0.81									
Biomarkers of TY												
Creatine							2/2	<0.001	−0.57			
Ethanolamine							2/2	0.009	0.95			
Glutamic acid							8/8	0.01	0.93			
Guanidinoacetic acid									0.46	1.04	<0.001	0.86

[ε]For each biomarker, the number of important peaks compared with the total number of 1H-NMR peaks is indicated. The important peaks contained at least one bucket with a VIP > 1 to explain the first latent variable of the PLS model of liver weight or technological yield.

[ζ]The models of the effects of the relative metabolite concentration on the liver weight and technological yield were computed. The p-values were corrected with the Benjamini–Hochberg procedure and indicated.

[η]The Pearson correlation of the metabolite relative concentration obtained with bucket data or metabolite data and the liver weight or the technological yield was indicated.

[δ]The PLS model to describe the liver weight or the technological yield with metabolite data was plotted. The first latent variable enabled to separate the fatty livers in function of the liver weight or the technological yield. The metabolites with VIP superior to 1 were selected. The VIP of the metabolite was indicated.

CONCLUSION

To conclude, the analysis of the metabolism of male mule duck livers during the overfeeding period through ^{1}H-NMR analysis enabled the identification of eighteen liver biomarkers of *foie gras* qualities. Nine of them were identified for both LW and TY of *foie gras*: five were carbohydrates like glucose, glyceric acid, glycogen, lactate, and maltose, three were amino acids like alanine taurine and threonine, plus allantoin. Five of them were specific to the LW: two carbohydrates as glucuronic acid, malic acid, two amino acids as arginine, and trans-4-hydroxy-L-proline plus a glycerophosphocholine, a phospholipid. Furthermore, four biomarkers were specific to *foie gras* TY. Two of them were involved in creatine metabolism (creatine and guanidinoacetic acid). One could be an intermediate of phospholipid (ethanolamine) and may be involved in membrane stability. The last one was glutamic acid produced by ALT, whose activity in the liver is enhanced in hepatosteatosis. As a result, in heavy livers, the liver metabolism was oriented through a reduction of carbohydrate metabolism, and the plasma membrane could be damaged, which may explain the low technological yield of these livers.

These findings will be complete if an analysis of the correlation between the plasma and liver metabolisms is made to understand the co-evolution of these tissues during the overfeeding period.

DATA AVAILABILITY STATEMENT

The raw data supporting the conclusions of this article will be made available by the authors, without undue reservation.

ETHICS STATEMENT

The animal study was reviewed and approved by experimental approval A24-137-1.

AUTHOR CONTRIBUTIONS

JA supervised the animal experimental rearing, overfeeding, and slaughtering. BL prepared the liver samples for NMR analysis with the supervision of NM-G. BL, NM-G, and CC performed the NMR analysis. BL and NM-G made the preprocessing of the NMR spectra. ZM, BL, and CB performed the statistical analyses to interpret the data that were helped by AB, MM, and AM, and wrote the paper. All authors contributed to the article and approved the submitted version.

FUNDING

This project was funded by Interprofession *Foie gras* (CIFOG) and Aquitaine Regional and Dordogne Departmental Councils.

ACKNOWLEDGMENTS

The authors thank the staff of the Station d'Expérimentation Appliquée et de Démonstration sur l'oie et le Canard (Dordogne, France) for their excellent supervision of this study, especially Franck Lavigne and Cédric Mondoux. We also thank the staff of the UMR1388 Génétique Physiologie et Systèmes d'Elevage INRAe, in particular Michel Bouillier-Oudot and Caroline Molette for their help in designing the experimental project and getting funding, and Hélène Manse and Stéphane Seidlinger for liver sampling.

SUPPLEMENTARY MATERIAL

The Supplementary Material for this article can be found online at: https://www.frontiersin.org/articles/10.3389/fphys.2021.694809/full#supplementary-material

REFERENCES

Aljobaily, N., Viereckl, M. J., Hydock, D. S., Aljobaily, H., Wu, T.-Y., Busekrus, R., et al. (2021). Creatine alleviates doxorubicin-induced liver damage by inhibiting liver fibrosis, inflammation, oxidative stress, and cellular senescence. *Nutrients* 13:41. doi: 10.3390/nu13010041

Auvergne, A., Candau, M., Babile, R., Manse, H., and Bouillier-Oudot, M. (1998). Relation entre l'état de réplétion digestive et la composition hépatique du canard mulard en gavage. *Reprod. Nutr. Dev.* 38, 39–47. doi: 10.1051/rnd:19980104

Baéza, E., Rideau, N., Chartrin, P., Davail, S., Hoo-Paris, R., Mourot, J., et al. (2005). Canards de Barbarie, Pékin et leurs hybrides: aptitude à l'engraissement. *Prod. Anim.* 18, 131–141. doi: 10.20870/productions-animales.2005.18.2.3516

Barcelos, R. P., Stefanello, S. T., Mauriz, J. L., Gonzalez-Gallego, J., and Soares, F. A. A. (2016). Creatine and the liver: metabolism and possible interactions. *Mini Rev. Med. Chem.* 16, 12–18. doi: 10.2174/1389557515666150722102613

Beckonert, O., Keun, H. C., Ebbels, T. M., Bundy, J., Holmes, E., Lindon, J. C., et al. (2007). Metabolic profiling, metabolomic and metabonomic procedures for NMR spectroscopy of urine, plasma, serum and tissue extracts. *Nat. Protoc.* 2, 2692–2703. doi: 10.1038/nprot.2007.376

Blum, J., Labie, C., and Raynaud, P. (1990). Influence du poids et de la composition chimique du foie gras d'oie sur la fonte mesurée après stérilisation à 104° C. *Sci. Aliment.* 10, 543–554.

Bonnefont, C. M., Guerra, A., Théron, L., Molette, C., Canlet, C., and Fernandez, X. (2014). Metabolomic study of fatty livers in ducks: identification by 1 H-NMR of metabolic markers associated with technological quality. *Poult. Sci.* 93, 1542–1552. doi: 10.3382/ps.2013-03546

Bonnefont, C. M., Molette, C., Lavigne, F., Manse, H., Bravo, C., Lo, B., et al. (2019). Evolution of liver fattening and foie gras technological yield during the overfeeding period in mule duck. *Poult. Sci.* 98, 5724–5733. doi: 10.3382/ps/pez359

Bouillier-Oudot, M., Leprettre, S., Dubois, J., and Babilé, R. (2004). "Evolution de la composition hépatique lors du refroidissement post-mortem de foies gras d'oies dans la carcasse," in *6. Journées de la Recherche sur les Palmipèdes à Foie Gras: Comité Interprofessionnel des Palmipèdes à Foie Gras*; October 07–08, 2004; Arcachon, France.

Bruckbauer, A., and Zemel, M. B. (2014). Synergistic effects of polyphenols and methylxanthines with leucine on AMPK/Sirtuin-mediated metabolism in muscle cells and adipocytes. *PLoS One* 9:e89166. doi: 10.1371/journal.pone.0089166

De Minicis, S., Bataller, R., and Brenner, D. A. (2006). NADPH oxidase in the liver: defensive, offensive, or fibrogenic? *Gastroenterology* 131, 272–275. doi: 10.1053/j.gastro.2006.05.048

Du, Y., Meng, Q., Zhang, Q., and Guo, F. (2012). Isoleucine or valine deprivation stimulates fat loss via increasing energy expenditure and regulating lipid metabolism in WAT. *Amino Acids* 43, 725–734. doi: 10.1007/s00726-011-1123-8

Elnesr, S. S., Elwan, H. A. M., Xu, Q. Q., Xie, C., Dong, X. Y., and Zou, X. T. (2019). Effects of in ovo injection of sulfur-containing amino acids on heat shock protein 70, corticosterone hormone, antioxidant indices, and lipid profile of newly hatched broiler chicks exposed to heat stress during incubation. *Poult. Sci.* 98, 2290–2298. doi: 10.3382/ps/pey609

Elwan, H. A., Elnesr, S. S., Xu, Q., Xie, C., Dong, X., and Zou, X. (2019). Effects of in ovo methionine-cysteine injection on embryonic development, antioxidant status, IGF-I and tlr4 gene expression, and jejunum histomorphometry in newly hatched broiler chicks exposed to heat stress during incubation. *Animals* 9:25. doi: 10.3390/ani9010025

Feraudi, M., and Bert, H. (1977). Role of rat-liver alcohol dehydrogenase in the glycerol pathway to L-lactate in homogenates. *Arch. Int. Physiol. Biochim.* 85, 91–100.

François, Y., Marie-Etancelin, C., Vignal, A., Viala, D., Davail, S. P., and Molette, C. (2014). Mule duck "foie gras" shows different metabolic states according to its quality phenotype by using a proteomic approach. *J. Agric. Food Chem.* 62, 7140–7150. doi: 10.1021/jf5006963

Gentile, C. L., Nivala, A. M., Gonzales, J. C., Pfaffenbach, K. T., Wang, D., Wei, Y., et al. (2011). Experimental evidence for therapeutic potential of taurine in the treatment of nonalcoholic fatty liver disease. *Am. J. Phys. Regul. Integr. Comp. Phys.* 301, R1710–R1722. doi: 10.1152/ajpregu.00677.2010

Giacomoni, F., Le Corguille, G., Monsoor, M., Landi, M., Pericard, P., Pétéra, M., et al. (2015). Workflow4Metabolomics: A collaborative research infrastructure for computational metabolomics. *Bioinformatics* 31, 1493–1495. doi: 10.1093/bioinformatics/btu813

Goodridge, A. G. (1987). Dietary regulation of gene expression: enzymes involved in carbohydrate and lipid metabolism. *Annu. Rev. Nutr.* 7, 157–185. doi: 10.1146/annurev.nu.07.070187.001105

Kalhan, S. C., Guo, L., Edmison, J., Dasarathy, S., Mccullough, A. J., Hanson, R. W., et al. (2011). Plasma metabolomic profile in nonalcoholic fatty liver disease. *Metabolism* 60, 404–413. doi: 10.1016/j.metabol.2010.03.006

Kostidis, S., Addie, R. D., Morreau, H., Mayboroda, O. A., and Giera, M. (2017). Quantitative NMR analysis of intra-and extracellular metabolism of mammalian cells: A tutorial. *Anal. Chim. Acta* 980, 1–24. doi: 10.1016/j.aca.2017.05.011

Kusunoki, M., Tsutsumi, K., Hara, T., Ogawa, H., Nakamura, T., Miyata, T., et al. (2002). Correlation between lipid and glycogen contents in liver and insulin resistance in high-fat [ndash] fed rats treated with the lipoprotein lipase activator NO-1886. *Metabolism* 51, 792–795. doi: 10.1053/meta.2002.32732

Lawler, J., Barnes, W. S., Wu, G., Song, W., and Demaree, S. (2002). Direct antioxidant properties of creatine. *Biochem. Biophys. Res. Commun.* 290, 47–52. doi: 10.1006/bbrc.2001.6164

Lê Cao, K.-A., González, I., and Déjean, S. (2009). integrOmics: an R package to unravel relationships between two omics datasets. *Bioinformatics* 25, 2855–2856. doi: 10.1093/bioinformatics/btp515

Lefort, G., Liaubet, L., Canlet, C., Tardivel, P., Père, M.-C., Quesnel, H., et al. (2019). ASICS: an R package for a whole analysis workflow of 1D 1H NMR spectra. *Bioinformatics* 35, 4356–4363. doi: 10.1093/bioinformatics/btz248

Lo, B., Marty-Gasset, N., Manse, H., Bannelier, C., Bravo, C., Domitile, R., et al. (2020a). Cellular markers of mule duck livers after force-feeding. *Poult. Sci.* 99, 3567–3573. doi: 10.1016/j.psj.2020.03.048

Lo, B., Marty-Gasset, N., Pichereaux, C., Bravo, C., Manse, H., Domitile, R., et al. (2020b). Proteomic analysis of two weight classes of mule duck "foie gras" at the end of an overfeeding period. *Front. Physiol.* 11:569329. doi: 10.3389/fphys.2020.569329

Ma, J., Meng, X., Liu, Y., Yin, C., Zhang, T., Wang, P., et al. (2020). Effects of a rhizome extract of Dioscorea batatas and its bioactive compound, allantoin in high fat diet and streptozotocin-induced diabetic mice and the regulation of liver, pancreas and skeletal muscle dysfunction. *J. Ethnopharmacol.* 259:112926. doi: 10.1016/j.jep.2020.112926

Marie-Etancelin, C., Basso, B., Davail, S., Gontier, K., Fernandez, X., Vitezica, Z.-G., et al. (2011). Genetic parameters of product quality and hepatic metabolism in fattened mule ducks. *J. Anim. Sci.* 89, 669–679. doi: 10.2527/jas.2010-3091

Mourot, J., Guy, G., Lagarrigue, S., Peiniau, P., and Hermier, D. (2000). Role of hepatic lipogenesis in the susceptibility to fatty liver in the goose (*Anser anser*). *Comp. Biochem. Physiol. B Biochem. Mol. Biol.* 126, 81–87. doi: 10.1016/S0305-0491(00)00171-1

Movahhed, T. K., Moslehi, A., Golchoob, M., and Ababzadeh, S. (2019). Allantoin improves methionine-choline deficient diet-induced nonalcoholic steatohepatitis in mice through involvement in endoplasmic reticulum stress and hepatocytes apoptosis-related genes expressions. *Iran. J. Basic Med. Sci.* 22, 736–744. doi: 10.22038/ijbms.2019.33553.8012

Mozduri, Z., Marty-Gasset, N., Lo, B., Masoudi, A. A., Morisson, M., Canlet, C., et al. (2021). Identification of plasmatic biomarkers of foie gras qualities in duck by metabolomics. *Front. Physiol.* 12:628264. doi: 10.3389/fphys.2021.628264

Pioche, T., Skiba, F., Bernadet, M.-D., Seiliez, I., Massimino, W., Houssier, M., et al. (2019). Kinetic study of the expression of genes related to hepatic steatosis, global intermediate metabolism and cellular stress during overfeeding in mule ducks. *bioRxiv* [Preprint]. doi: 10.1101/690156

Pratt, D. S., and Kaplan, M. M. (2000). Evaluation of abnormal liver-enzyme results in asymptomatic patients. *N. Engl. J. Med.* 342, 1266–1271. doi: 10.1056/NEJM200004273421707

Rémignon, H., Yahia, R. B. H., Marty-Gasset, N., and Wilkesman, J. (2018). Apoptosis during the development of the hepatic steatosis in force-fed ducks and cooking yield implications. *Poult. Sci.* 97, 2211–2217. doi: 10.3382/ps/pey054

Rohart, F., Gautier, B., Singh, A., and Lê Cao, K.-A. (2017). mixOmics: An R package for 'omics feature selection and multiple data integration. *PLoS Comput. Biol.* 13:e1005752. doi: 10.1371/journal.pcbi.1005752

Rosenberg, H. (1959). The occurrence of guanidinoacetic acid and other substituted guanidines in mammalian liver. *Biochem. J.* 72:582. doi: 10.1042/bj0720582

Rousselot-Pailley, D., Guy, G., Gourichon, D., Sellier, N., and Blum, J. (1992). Influence des conditions d'abattage et de réfrigération sur la qualité des foies gras d'oie. *INRA Prod. Animal.* 5, 167–172. doi: 10.20870/productions-animales.1992.5.3.4230

Sellmann, C., Degen, C., Jun Jin, C., Nier, A., Engstler, A. J., Alkhatib, D. H., et al. (2017). Oral arginine supplementation protects female mice from the onset of nonalcoholic steatohepatitis. *Amino Acids* 49, 1215–1225. doi: 10.1007/s00726-017-2423-4

Sevastianova, K., Hakkarainen, A., Kotronen, A., Corner, A., Arkkila, P., Arola, J., et al. (2010). Nonalcoholic fatty liver disease: detection of elevated nicotinamide adenine dinucleotide phosphate with in vivo 3.0-T 31P MR spectroscopy with proton decoupling. *Radiology* 256, 466–473. doi: 10.1148/radiol.10091351

Tardivel, P. J., Canlet, C., Lefort, G., Tremblay-Franco, M., Debrauwer, L., Concordet, D., et al. (2017). ASICS: an automatic method for identification and quantification of metabolites in complex 1D 1 H NMR spectra. *Metabolomics* 13:109. doi: 10.1007/s11306-017-1244-5

Tavernier, A., Ricaud, K., Bernadet, M.-D., Gontier, K., and Davail, S. (2018). Pre-and post-prandial expression of genes involved in lipid metabolism at the end of the overfeeding period of mule ducks. *Mol. Cell. Biochem.* 438, 111–121. doi: 10.1007/s11010-017-3118-6

Theron, L., Cullere, M., Bouillier-Oudot, M., Manse, H., Dalle Zotte, A., Molette, C., et al. (2012). Modeling the relationships between quality and biochemical composition of fatty liver in mule ducks. *J. Anim. Sci.* 90, 3312–3317. doi: 10.2527/jas.2011-4945

Theron, L., Fernandez, X., Marty-Gasset, N., Chambon, C., Viala, D., Pichereaux, C., et al. (2013). Proteomic analysis of duck fatty liver during post-mortem storage related to the variability of fat loss during cooking of "foie gras". *J. Agric. Food Chem.* 61, 920–930. doi: 10.1021/jf302979q

Theron, L., Fernandez, X., Marty-Gasset, N., Pichereaux, C., Rossignol, M., Chambon, C., et al. (2011). Identification by proteomic analysis of early post-mortem markers involved in the variability in fat loss during cooking of mule duck "foie gras". *J. Agric. Food Chem.* 59, 12617–12628. doi: 10.1021/jf203058x

Tidwell, H. C., and Johnston, J. M. (1961). Glyceride glycerol utilization in triglyceride formation. *Arch. Biochem. Biophys.* 93, 546–549. doi: 10.1016/S0003-9861(61)80050-7

Viviani, R., Sechi, A., and Lenaz, G. (1966). Lipid metabolism in fatty liver of lysine-and threonine-deficient rats. *J. Lipid Res.* 7, 473–478. doi: 10.1016/S0022-2275(20)39256-7

Voloshin, I., Hahn-Obercyger, M., Anavi, S., and Tirosh, O. (2014). L-arginine conjugates of bile acids-a possible treatment for nonalcoholic fatty liver disease. *Lipids Health Dis.* 13, 1–11. doi: 10.1186/1476-511X-13-69

Warskulat, U., Borsch, E., Reinehr, R., Heller-Stilb, B., Mönnighoff, I., Buchczyk, D., et al. (2006). Chronic liver disease is triggered by taurine transporter knockout in the mouse. *FASEB J.* 20, 574–576. doi: 10.1096/fj.05-5016fje

Williams, J. A., Hyland, R., Jones, B. C., Smith, D. A., Hurst, S., Goosen, T. C., et al. (2004). Drug-drug interactions for UDP-glucuronosyltransferase substrates: a pharmacokinetic explanation for typically observed low exposure (AUCi/AUC) ratios. *Drug Metab. Dispos.* 32, 1201–1208. doi: 10.1124/dmd.104.000794

Wise, E. M. Jr., and Ball, E. G. (1964). Malic enzyme and lipogenesis. *Proc. Natl. Acad. Sci. U. S. A.* 52, 1255. doi: 10.1073/pnas.52.5.1255

Wishart, D. S., Knox, C., Guo, A. C., Eisner, R., Young, N., Gautam, B., et al. (2009). HMDB: a knowledgebase for the human metabolome. *Nucleic Acids Res.* 37, D603–D610. doi: 10.1093/nar/gkn810

Xu, J., Kulkarni, S. R., Li, L., and Slitt, A. L. (2012). UDP-glucuronosyltransferase expression in mouse liver is increased in obesity-and fasting-induced steatosis. *Drug Metab. Dispos.* 40, 259–266. doi: 10.1124/dmd.111.039925

Zhu, L., Baker, S. S., Shahein, A., Choudhury, S., Liu, W., Bhatia, T., et al. (2018). Upregulation of non-canonical Wnt ligands and oxidative glucose metabolism in NASH induced by methionine-choline deficient diet. *Trends Cell Mol. Biol.* 13, 47–56.

Conflict of Interest: The authors declare that the research was conducted in the absence of any commercial or financial relationships that could be construed as a potential conflict of interest.

frontiers in Physiology

MINI REVIEW
published: 29 September 2021
doi: 10.3389/fphys.2021.755317

Fighting Fat With Fat: n-3 Polyunsaturated Fatty Acids and Adipose Deposition in Broiler Chickens

*Minjeong Kim and Brynn H. Voy**

Department of Animal Science, The University of Tennessee, Knoxville, Knoxville, TN, United States

Modern broiler chickens are incredibly efficient, but they accumulate more adipose tissue than is physiologically necessary due to inadvertent consequences of selection for rapid growth. Accumulation of excess adipose tissue wastes feed in birds raised for market, and it compromises well-being in broiler-breeders. Studies driven by the obesity epidemic in humans demonstrate that the fatty acid profile of the diet influences adipose tissue growth and metabolism in ways that can be manipulated to reduce fat accretion. Omega-3 polyunsaturated fatty acids (n-3 PUFA) can inhibit adipocyte differentiation, induce fatty acid oxidation, and enhance energy expenditure, all of which can counteract the accretion of excess adipose tissue. This mini-review summarizes efforts to counteract the tendency for fat accretion in broilers by enriching the diet in n-3 PUFA.

Keywords: adipose development, adiposity, broiler chickens, DHA, EPA, hen diet, omega-3 polyunsaturated fatty acid

OPEN ACCESS

Edited by:
Sami Dridi,
University of Arkansas, United States

Reviewed by:
Michael Babak Papah,
University of Delaware, United States
Yuwares Malila,
National Center for Genetic Engineering and Biotechnology (BIOTEC), Thailand

***Correspondence:**
Brynn H. Voy
bhvoy@utk.edu

Specialty section:
This article was submitted to Avian Physiology, a section of the journal Frontiers in Physiology

Received: *08 August 2021*
Accepted: *09 September 2021*
Published: *29 September 2021*

Citation:
Kim M and Voy BH (2021) Fighting Fat With Fat: n-3 Polyunsaturated Fatty Acids and Adipose Deposition in Broiler Chickens. Front. Physiol. 12:755317. doi: 10.3389/fphys.2021.755317

INTRODUCTION

Poultry meat is a major source of protein for much of the world. Due to population growth, rising incomes, and concerns about both health and sustainability, global demand is expected to continue to grow around the globe. Current projections are that poultry will account for 41% of all protein consumption from meat by 2030 (OECD and FAO, 2021). Broiler chickens are produced for meat, and genetic selection has produced remarkable advances in growth of broilers over the past several decades. For example, a 35 days broiler weighed approximately 1.4 kg in 1985 and more than 2.4 kg in 2010, largely due to increase in muscle mass (Siegel, 2014). Inadvertently, selection of broilers for rapid growth also increased their tendency to accumulate excess adipose tissue (Zuidhof et al., 2014). Adipose tissue in poultry is not commercially valuable, and it effectively wastes feed by allocating it away from muscle. Physiologically, the need for adipose tissue as an energy reservoir is minimal in market birds that have almost constant access to feed. In broiler-breeders, excess fat accretion also compromises fertility and welfare. The tendency to deposit excess adipose has in part been suppressed in commercial lines of broilers through refined approaches to selection (Siegel, 2014; Zuidhof et al., 2014). However, even a modest misallocation of feed, the most expensive component of production, significantly increases costs given the scale of commercial broiler production. The default approach to preventing fat accretion is feed restriction, but this has a negative impact on weight gain and meat yield and is also a welfare concern (Jackson et al., 1982; Lindholm et al., 2018).

Adipose Tissue Basics in Broilers

Chickens store energy as lipids in subcutaneous depots found near the legs and neck, and in a visceral depot in the abdomen. Subcutaneous fat is the first depot to develop and becomes visible in the embryo by embryonic day 12 (E12) (Speake et al., 1993). Adipocytes develop from a mesenchymal stem cell pool that gives rise to preadipocytes, a cell type that is committed to an adipocyte fate. Preadipocytes then differentiate and acquire a mature, lipid-storing adipocyte phenotype through a series of orchestrated changes in gene expression that are similar to those described for mammals (Rosen and MacDougald, 2006). In the embryo, development of subcutaneous fat coincides with a sharp increase in extraction of fatty acids from the yolk (Speake et al., 1998). Subcutaneous adipocytes grow rapidly as these fatty acids are taken up and stored as triacylglycerol until E19, when they are mobilized by lipolysis to provide the energy needed at hatch (Speake et al., 1993). Abdominal fat, which becomes the main site of triglyceride storage in the mature bird, develops after hatch and becomes clearly visible around 7 days of age. Adipose depots grow rapidly in broiler chicks through increases in adipocyte number (hyperplasia), as preadipocytes proliferate and undergo differentiation, and size (hypertrophy) as mature fat cells take up and store fatty acids (Bai et al., 2015). Both processes are very active during the first several weeks of life, after which hypertrophy becomes the dominant mechanism of fat deposition (Cartwright, 1991). Fatty acids that are taken up from the circulation and stored in broiler adipocytes come primarily from the liver, the main site of *de novo* lipogenesis in avians (Leveille et al., 1975). Fatty acids synthesized by the liver from glucose and acetate are packaged into VLDL molecules, which ferry them to adipocytes for uptake and storage. Hepatic synthesis of lipids plays a major role in adipose deposition in broilers. Divergent selection on serum VLDL level has been used to produce lines of broilers that differ significantly in fatness, illustrating the key role of the liver (Leclercq et al., 1980; Whitehead and Griffin, 1984; Baéza and Le Bihan-Duval, 2013; Resnyk et al., 2013). In addition, intrinsic differences in adipose development also contribute to excessive fat accretion in broilers. For example, significant increases in both adipocyte number and size appear as early as 2 weeks of age in broiler lines that have higher fat mass as they mature (Hermier et al., 1989).

Dietary Fatty Acids and Adipose Growth

Paradoxically, certain types of dietary fatty acids have been shown to inhibit accumulation of adipose tissue in a variety of species. Polyunsaturated fatty acids (PUFAs) are classified as n-3 or n-6 based on the position of the first double bond in relation to the methyl end of the molecule. Linoleic acid (LA; 18:2 n-6) and alpha linolenic acid (ALA; 18:3 n-3) are the main dietary n-6 and n-3 fatty acids, respectively. These fatty acids are required for the formation of cell membranes but cannot be synthesized endogenously and therefore must be provided in the diet (Smith and Mukhopadhyay, 2012). Linoleic acid is enriched in a variety of common plant oils, such as those derived from corn, soybean, and safflower. Alpha linolenic acid, which is less abundant than LA, is usually obtained from flaxseed, rapeseed, and walnuts. When taken into the cell, ALA and LA can be used in formation of cell membranes, oxidized for energy, or used to synthesize longer and more highly unsaturated PUFA through a series of sequential elongation and desaturation steps (Jakobsson et al., 2006). Some of these longer chain species have unique bioactive properties through their ability to bind and activate lipid-responsive transcription factors, such as members of the PPAR family of nuclear receptors. In addition, the 20 carbon products of LA (arachidonic acid; ARA, 20:4 n-6) and ALA (eicosapentaenoic acid, EPA; 20:5 n-3) are used as substrates to produce eicosanoids, a broad family of lipid mediators that interact with various cell signaling pathways. The seemingly modest structural difference between LA and ALA has marked effects on the biochemical properties of these fatty acids and their metabolites. For example, eicosanoids produced from ARA are primarily proinflammatory, while those synthesized from EPA tend to be anti-inflammatory (Calder, 2017). The same enzymes catalyze elongation and desaturation of n-3 and n-6 PUFA. As a result, the relative synthesis of longer chain n-3 and n-6 species is determined by the ratio of n-3/n-6 in the diet.

Extensive *in vivo* and *in vitro* studies indicate that n-3 and n-6 PUFA differentially regulate adiposity in multiple species. In particular, diets enriched with n-3 PUFA are associated with reduced fat accretion (Rokling-Andersen et al., 2009; Torres-Castillo et al., 2018; Ballester et al., 2020; Chen et al., 2020; Riera-Heredia et al., 2020). At the cellular level, n-3 PUFA have been shown to suppress adipogenesis, attenuate lipid accumulation in adipocytes, and promote an oxidative adipocyte phenotype (Kim et al., 2006; Manickam et al., 2010; An et al., 2012; Fleckenstein-Elsen et al., 2016). Conversely, n-6 PUFAs tend to be pro-adipogenic (Gaillard et al., 1989; Negrel et al., 1989; Massiera et al., 2003). The anti-obesogenic effects of n-3 PUFA are most strongly associated with actions of EPA and docosahexaenoic acid (DHA, 22:6 n-3), the characteristic fatty acids of marine oils (Flachs et al., 2009). These two fatty acids, which are synthesized in algae and consumed by fish, influence a range of pathways that regulate adipose growth and adipocyte metabolism. Each fatty acid can bind and activate PPARA, a nuclear receptor that transcriptionally increases fatty acid oxidation (Diep et al., 2000; Zúñiga et al., 2011). In addition, EPA and DHA activate signaling through AMPK and promote mitochondrial biogenesis, both of which augment fatty acid oxidation (Siriwardhana et al., 2012). They also increase synthesis of the insulin-sensitizing adipokine adiponectin, which further activates AMPK and amplifies energy expenditure in adipocytes (Itoh et al., 2007; Song et al., 2017). EPA and DHA are also used to synthesize several classes of lipid mediators, including eicosanoids and resolvins as well as other novel metabolites that suppress inflammation and limit metabolic stress in adipose tissue (Kuda et al., 2018). These actions indirectly oppose fat accretion by preventing inflammatory cascades that disrupt the efficient metabolism of glucose and fatty acids in adipocytes. Finally, EPA and DHA promote the browning of white adipocytes, which further enhances oxidative metabolism in adipose tissue and prevents fat accretion (Fleckenstein-Elsen et al., 2016). Browning is the process by which white adipocytes acquire the highly oxidative phenotype associated with mitochondria-rich brown fat cells.

Browning includes induction of uncoupling protein 1 (UCP1), the characteristic protein of brown adipocytes, which uncouples mitochondrial respiration from ATP synthesis. These actions of EPA and DHA may not be relevant to broilers, as they are thought to lack brown adipocytes due to loss of the UCP1 gene from avian genomes (Mezentseva et al., 2008). However, a recent study demonstrates the existence of brown-like fat cells in broiler chicks (Sotome et al., 2021). Collectively, ample evidence from multiple species suggests that dietary n-3 PUFA, particularly EPA and DHA, may be a tool for reducing fat accretion in broilers.

Reducing Fat Accretion in Broilers With n-3 Polyunsaturated Fatty Acids

Broiler diets are typically formulated with 2–5% added fat to support the intense energetic demands of rapid growth. Fat is often supplied using corn or soybean oil, both of which are readily available, cost-effective and enriched in LA. Combined with the use of corn and soybean meals as the diet base, this results in commercial diets that are heavily skewed toward high n-6/n-3 PUFA. In this context, commercial broiler diets are comparable to the modern human diet, in which high n-6/n-3 ratios have been associated with increased prevalence of obesity (Chilton et al., 2017). Considering the beneficial effects on fat accretion in other species, several groups have tested the ability to limit fat accretion in broilers by replacing a portion of LA-rich oils or saturated fat in the diet with sources enriched in n-3 PUFA. These have used a variety of experimental designs, including variation in age at which experimental diets were introduced, different amounts of added fat, and varying duration of feeding (**Table 1**). Nonetheless, they provide evidence that n-3 PUFA are also a promising tool to reduce fat accretion in broilers.

Fish and algal oils are the most direct way to increase dietary delivery of EPA and DHA to broilers. However, they are relatively expensive and more prone to lipid peroxidation than sources of ALA. Newman et al. (2002) replaced tallow (a source of saturated fat) with either fish oil or sunflower oil (as an n-6 PUFA control) in the diets of broiler chicks beginning at 3 weeks of age. After 5 weeks of feeding, fish oil significantly reduced abdominal fat pad weight and increased the breast muscle: abdominal fat ratio in comparison to tallow controls. However, comparable effects were seen with the sunflower oil diet (Newman et al., 2002). Unlike most vertebrates, many types of algae can efficiently synthesize long-chain n-3 PUFA and are thus rich sources of EPA and DHA. Microalgae are microscopic algae species of commercial interest as renewable sources of biofuel production and animal feeds (Khan et al., 2018). Long et al. (2018) used a source of dehydrated microalgal biomass to efficiently deliver DHA in broiler diets. The biomass consisted of 64% fat made up primarily of palmitate (60%) and DHA (29%). Microalgae were added to the diet and 1 and 2% by weight, with the balance of fat (up to 3% total) provided by soybean oil, and chicks were fed from 1 to 42 days. Both the 1 and 2% microalgae diets significantly reduced adiposity at 42 days. In addition, both diets significantly improved feed efficiency and increased weight gain, and improved antioxidant status, resulting in broader effects on performance than just reduced fatness. These results demonstrate that replacing even part of an n-6 PUFA source in the broiler diet with a DHA-rich alternative has beneficial effects on fat accretion.

Flaxseed and other oils rich in ALA provide the substrate for EPA and DHA synthesis, but the efficiency of ALA conversion to longer chain n-3 PUFA is thought to be very low in vertebrates due to catalytic properties of the elongase enzymes in the PUFA synthesis pathway (Arterburn et al., 2006; Brenna et al., 2009; Gregory et al., 2011). However, the chicken elongase enzymes (Elongation of Very Long Chain Fatty Acids-Like 2 and 5 (ELOVL2 and ELOVL5) in this pathway have enhanced ability to synthesize DHA from ALA (Zuidhof et al., 2009; Gregory et al., 2013). ELOVL5 is highly expressed in broiler adipose tissue, including in the embryo (Mihelic et al., 2020). Unlike in most mammals, supplementing broiler diets with ALA significantly enriches tissues in EPA and DHA (Poureslami et al., 2010; Kartikasari et al., 2012). Accordingly, several studies have been reported that linseed oil inclusion in broiler diet suppressed abdominal fat deposition and enhanced growth performance compared with saturated fat sources, such as tallow (Crespo and Esteve-Garcia, 2001, 2002; Ferrini et al., 2010; González-Ortiz et al., 2013) or n-6 PUFA sources such as sunflower oil (Crespo and Esteve-Garcia, 2002; Ibrahim et al., 2018). For example, supplementing broiler diets with flaxseed oil (10%) reduced abdominal fat by 30% compared to equivalent amounts of saturated or monounsaturated fatty acids (Ferrini et al., 2008). Both fish and flaxseed oils have also been shown to reduce adipocyte size in broiler chicks, suggesting that they act relatively early on adipose development (Torchon et al., 2017). The relative effects of fish oil and flaxseed oil as replacements for sunflower oil have also been compared. Broilers were fed diets in which all or part of sunflower oil (4%) was replaced by either flaxseed or fish oil (Ibrahim et al., 2018). Each diet significantly reduced abdominal fat percentage compared to sunflower controls, while feed efficiency, gain, and antioxidant status were significantly improved. The experimental diets also improved muscle tissue weight (breast and thigh) and decreased breast intramuscular fat (IMF) content. The diets that replaced sunflower with flaxseed oil had very low levels of EPA and DHA, as did the sunflower control. However, fatty acid analyses of breast muscle further support the ability for chickens to efficiently synthesize these fatty acids from ALA. Tissue levels of EPA and DHA were significantly increased in all experimental diets, except for the lowest level (5:1, sunflower: flaxseed) of ALA inclusion.

Potential to Reduce Fat Accretion Through n-3 Polyunsaturated Fatty Acids in the Hen Diet

Given the scale of broiler production, replacing standard fat sources with more expensive ones, such as flaxseed or fish oil, would impose a significant cost to the industry. Developmental programming through the diet of the broiler-breeder hen is a potential alternative means to reduce fat accretion in broilers. Developmental programming refers to the ability of embryonic exposures to exert persistent effects on the physiology of offspring after birth. This concept forms the basis of the Barker hypothesis, which was proposed in 1992 to explain the

TABLE 1 | Studies that investigated different dietary sources of n-3 PUFA and fat deposition in broiler chickens.

References	n-3 PUFA source	Experimental diet	Animal (age)	Feeding period	Relevant phenotypes measured	Significant effects
Crespo and Esteve-Garcia, 2001	Linseed oil	(6 or 10%) • Tallow (T) • Olive oil (OO) • Sunflower oil (SO) • Linseed oil (LO)	Broiler chickens (21 days)	22 days/29 days	• Growth performance • Abdominal fat pad	• ↑ feed efficiency • ↓ abdominal fat
Crespo and Esteve-Garcia, 2002	Linseed oil	(10%) • Tallow (SFA) • Sunflower oil (SO) • Linseed oil (LO)	Broiler chickens (27 days)	27 days	• Abdominal fat mass	• ↓ abdominal and body fat deposition in LO compared with SFA or SO
Ferrini et al., 2008	Linseed oil	(10%) • Tallow (T) • Sunflower oil rich in oleic acid (SOO) • SO rich in linoleic acid (SOL) • Linseed oil (LO) • Mix of fats (M: 55% T + 35% LO + 10% SOL)	Female broiler chickens (1 day)	42 days	• Abdominal fat mass	• ↓ abdominal fat% (reduced by 30%) in LO compared to saturated diet
Ferrini et al., 2010	Linseed oil	(10%) • Basal diet (BS) containing 0.5% sunflower oil • Tallow diet (TA) • Linseed diet (LO)	Female broiler chickens (1 day)	36 days	• Growth performance • Abdominal fat mass	• ↑ BWG • ↓ abdominal fat deposition
González-Ortiz et al., 2013	FO and LO mixture	(10%) • Tallow diet (S) • A blend of fish oil and linseed oil (N3 diet)	Female broiler chickens (14 days)	37 days	• Abdominal fat mass • Adipocyte size	• ↓ abdominal fat% • ↓ adipocyte size
Torchon et al., 2017	Fish oil Flaxseed oil	(8%) • Lard (saturated) • Fish oil (FO) • Flaxseed oil • Canola oil	Broiler chickens (7 days)	24 days	• Growth performance • Abdominal fat mass • Adipocyte size	• ↓ adipocyte size • ↑ plasma non-esterified fatty acid levels (lipolysis)
Ibrahim et al., 2018	Fish oil Linseed oil	(4–4.5%) • Sunflower (C) • Fish oil (FO) • C1:FO1 • C3:FO1 • Linseed oil (LO) • C1:LO1 • C3:LO1	Broiler chickens (1 day)	42 days	• Growth performance • Abdominal fat mass	• ↑ BW, BWG/↓ FCR • ↓ abdominal fat% • ↓ TG and total cholesterol/↑ HDL-C/↓ LDL-C and VLDL
Long et al., 2018	Microalgae (MA)	(3%) • Soybean oil (SO) • MA 1: SO 2 • MA 2: SO 1	Male broiler chickens (1 day)	42 days	• Growth performance • Abdominal fat mass	• ↑ BWG/↓ FCR • ↑ liver %, ↓ abdominal fat % • ↑ serum glucose/↓ cholesterol • ↑ superoxide dismutase, ↑ antioxidant capacity

influence of factors during fetal development on the risk of diseases as adults (Barker, 1992). Programming occurs in part through epigenetic mechanisms, in which pre- and perinatal factors modify the genome through methylation, chromatin acetylation, and other non-sequence-based changes. These modifications persist through cell divisions and can influence gene expression and subsequently phenotypes throughout the life of the organism as well as across multiple generations. The concept of developmental programming has been applied to a plethora of embryonic exposures, but it is rooted in the impact of the maternal diet on offspring (Barker and Osmond, 1986). Studies in mammals indicate that energy metabolism and adiposity are especially sensitive to developmental programming by the maternal diet (Holness et al., 2000; George et al., 2012; Du et al., 2013; Lukaszewski et al., 2013; Ong and Guest, 2018). For example, energy deficit in the maternal diet during pregnancy increases adiposity in offspring after birth (Howie et al., 2012). A growing body of evidence from other species suggests that n-3 PUFA can act very early in life to influence adiposity and metabolism through developmental programming. For example, higher maternal blood levels of n-3 vs. n-6 PUFA during pregnancy have been associated with reduced body fat and increased leanness in children (Donahue et al., 2011; Vidakovic et al., 2016a,b). Experimental studies demonstrate that the relative abundance of n-6 vs. n-3 fatty acids in the perinatal period influences adipogenesis and fat accretion. Mice born from

dams with low n-6/n-3 ratios due to genetic manipulation had half the body fat, increased energy expenditure and fatty acid oxidation, and more but smaller adipocytes as adults compared to mice born to wild type dams (Rudolph et al., 2018).

Avians are ideally suited for developmental programming by fatty acids due to the relationship between the hen diet and the yolk, and the role of yolk fatty acids in supporting the developing embryo. Approximately 60% of the yolk's dry mass consists of lipids that are transported to the egg from the hen's liver (Speake et al., 1998). This lipid supply includes triglycerides that provide the embryo with fatty acids needed for energy, and phospholipids that serve as building blocks for cell membranes. Virtually all of the triglyceride and phospholipid pools in the yolk are utilized by the time of hatch (Noble and Moore, 1964). Saturated and monounsaturated fatty acids delivered to the yolk can be synthesized in the liver through *de novo* lipogenesis from carbohydrate, but the PUFA components come directly from the diet. Therefore, the n-3 and n-6 profile of the yolk, and subsequently of the tissues of the developing embryo, is determined almost exclusively by the diet of the hen (Cherian and Sim, 1991, 1993; Cherian et al., 1997). This appears to be particularly true for n-3 PUFA, which are preferentially incorporated into phospholipids of the developing embryo (Speake et al., 1998). Fish oil is the most direct means to enrich eggs and developing embryos in EPA and DHA, as the hen liver directly incorporates these species into phospholipids that are packaged for delivery to the yolk. However, oils such as flaxseed can have similar effects because of the unique properties of PUFA synthesis enzymes in chicken (Cherian et al., 1997; Gregory et al., 2013). The hen liver elongates and desaturates a portion of dietary ALA before packaging for delivery to the yolk. During embryonic development, both the yolk sac and the tissues of the embryo convert additional ALA to EPA and DHA, amplifying the effects of the hen diet (Noble, 1987; Noble and Cocchi, 1990). Therefore, oils that are more affordable and more stable than fish oil could feasibly be used for dietary developmental programming in production. Several studies have utilized the relationship between fatty acids in the hen diet and those of the embryo to demonstrate the potential for developmental programming by n-3 PUFA in chickens. For example, enriching the hen diet in different sources of n-3 PUFA has been shown to influence immunocompetence, synthesis of inflammatory mediators, bone mineralization, and antioxidant status in offspring (Hall et al., 2007; Bautista-Ortega et al., 2009; Bullock et al., 2014; Akbari Moghaddam Kakhki et al., 2020). Readers are referred to a recent review by Thanabalan and Kiarie (2021) for more details.

The ability to developmentally program reduced fat accretion through n-3 PUFA in the hen diet has been demonstrated in broilers. Beckford et al. (2017) fed broiler-breeder hen diets with fat provided from either corn or fish oil (2.3%) for 4 weeks. Chicks hatched from both sets of hens were fed commercial starter diets after hatch, with no modification to the fat source. Those produced from hens fed fish oil had significantly less fat accretion at 7 and 14 days, with no impact on growth or lean tissue mass. Reduced fat accretion was associated with smaller but more abundant adipocytes, consistent with inhibition of late stage of adipogenesis. Transcriptomic and proteomic analyses of adipose tissue indicated that the hen fish oil diet inhibited pathways associated with triacylglycerol synthesis, adipogenesis, mobilization of stored fatty acids from lipid droplets, and fatty acid utilization, all of which likely contributed to reduced adipose mass. This study provides compelling evidence that the broiler hen diet is a potential avenue through which to reduce fat accretion in broilers through developmental programming by n-3 PUFA.

It is important to acknowledge the potential challenges that would result from increasing the relative content of LC n-3 PUFA in production diets. In addition to a higher cost, oils rich in long-chain PUFA species are more prone to oxidation due to increased chain length and numbers of double bonds in their fatty acids. Supplementation with additional antioxidants, such as vitamin E, is often used to suppress oxidation, which can impair taste and meat quality. Alternative sources of LC n-3 PUFA that are naturally enriched in antioxidants may be able to offset this concern. For example, microalgae, a viable and effective alternative to fish oil as a source of EPA and DHA, have been shown to contain antioxidants that markedly reduce lipid peroxidation in broiler tissues (Tao et al., 2018).

SUMMARY

Collectively, these studies demonstrate the ability to reduce the deposition of adipose tissue in broilers by enriching the diet in n-3 PUFA. In particular, the potential to limit fat accretion through developmental programming shows promise for efficiently limiting fat deposition through the diet of the hen. Strategies to continue to improve the utilization of feed for broiler production will be increasingly important as the global population continues to grow and seek affordable sources of complete protein.

AUTHOR CONTRIBUTIONS

MK reviewed the studies described herein, prepared the included table, drafted the initial version of the manuscript, and proofread the final version. BV conceived the overall content, edited the draft, and approved the final version. Both authors contributed to the article and approved the submitted version.

FUNDING

MK was supported as a graduate student by funding to BV from USDA-NIFA (1018835). The general topic of this review is highly relevant to this funding.

ACKNOWLEDGMENTS

We would like to acknowledge UT AgResearch and the Department of Animal Science for supporting efforts to reduce fat accretion in broilers.

REFERENCES

Akbari Moghaddam Kakhki, R., Price, K. R., Moats, J., Bédécarrats, G., Karrow, N. A., and Kiarie, E. G. (2020). Impact of feeding microalgae (*Aurantiochytrium limacinum*) and co-extruded mixture of full-fat flaxseed as sources of n-3 fatty acids to ISA brown and Shaver white breeders and progeny on pullet skeletal attributes at hatch through to 18 weeks of age. *Poult. Sci.* 99, 2087–2099. doi: 10.1016/j.psj.2019.12.016

An, L., Pang, Y. W., Gao, H. M., Tao, L., Miao, K., Wu, Z. H., et al. (2012). Heterologous expression of C. elegans fat-1 decreases the n-6/n-3 fatty acid ratio and inhibits adipogenesis in 3T3-L1 cells. *Biochem. Biophys. Res. Commun.* 428, 405–410. doi: 10.1016/j.bbrc.2012.10.068

Arterburn, L. M., Hall, E. B., and Oken, H. (2006). Distribution, interconversion, and dose response of n-3 fatty acids in humans. *Am. J. Clin. Nutr.* 83, 1467S–1476S. doi: 10.1093/ajcn/83.6.1467S

Baéza, E., and Le Bihan-Duval, E. (2013). Chicken lines divergent for low or high abdominal fat deposition: a relevant model to study the regulation of energy metabolism. *Animal* 7, 965–973. doi: 10.1017/S1751731113000153

Bai, S., Wang, G., Zhang, W., Zhang, S., Rice, B. B., Cline, M. A., et al. (2015). Broiler chicken adipose tissue dynamics during the first two weeks post-hatch. *Comp. Biochem. Physiol. A Mol. Integr. Physiol.* 189, 115–123. doi: 10.1016/j.cbpa.2015.08.002

Ballester, M., Quintanilla, R., Ortega, F. J., Serrano, J. C. E., Cassanyé, A., Rodríguez-Palmero, M., et al. (2020). Dietary intake of bioactive ingredients impacts liver and adipose tissue transcriptomes in a porcine model of prepubertal early obesity. *Sci. Rep.* 10:5375. doi: 10.1038/s41598-020-62320-4

Barker, D. J. (1992). The fetal origins of diseases of old age. *Eur. J. Clin. Nutr.* 46, S3–S9.

Barker, D. J., and Osmond, C. (1986). Infant mortality, childhood nutrition, and ischaemic heart disease in England and Wales. *Lancet* 1, 1077–1081. doi: 10.1016/S0140-6736(86)91340-1

Bautista-Ortega, J., Goeger, D. E., and Cherian, G. (2009). Egg yolk omega-6 and omega-3 fatty acids modify tissue lipid components, antioxidant status, and *ex vivo* eicosanoid production in chick cardiac tissue. *Poult. Sci.* 88, 1167–1175. doi: 10.3382/ps.2009-00027

Beckford, R. C., Howard, S. J., Das, S., Farmer, A. T., Campagna, S. R., Yu, J., et al. (2017). Maternal consumption of fish oil programs reduced adiposity in broiler chicks. *Sci. Rep.* 7:13129. doi: 10.1038/s41598-017-13519-5

Brenna, J. T., Salem, N. Jr., Sinclair, A. J., and Cunnane, S. C. (2009). alpha-Linolenic acid supplementation and conversion to n-3 long-chain polyunsaturated fatty acids in humans. *Prostaglandins Leukot. Essent. Fatty Acids* 80, 85–91. doi: 10.1016/j.plefa.2009.01.004

Bullock, C., Bobe, G., and Cherian, G. (2014). *Gastrointestinal and Hepatic Tissue Fatty Acid Composition and Interleukin-6 Concentration in Broiler Chickens: effect of Maternal Dietary n-3 Fatty Acids*. Corvallis: Oregon State University.

Calder, P. C. (2017). Omega-3 fatty acids and inflammatory processes: from molecules to man. *Biochem. Soc. Trans.* 45, 1105–1115. doi: 10.1042/BST20160474

Cartwright, A. L. (1991). Adipose Cellularity in Gallus domesticus: investigations to Control Body Composition in Growing Chickens. *J. Nutr.* 121, 1486–1497. doi: 10.1093/jn/121.9.1486

Chen, C. Y., Su, C. W., and Kang, J. X. (2020). Endogenous Omega-3 Polyunsaturated Fatty Acids Reduce the Number and Differentiation of White Adipocyte Progenitors in Mice. *Obesity* 28, 235–240. doi: 10.1002/oby.22626

Cherian, G., Gopalakrishnan, N., Akiba, Y., and Sim, J. S. (1997). Effect of maternal dietary n-3 fatty acids on the accretion of long-chain polyunsaturated fatty acids in the tissues of developing chick embryo. *Biol. Neonate* 72, 165–174. doi: 10.1159/000244480

Cherian, G., and Sim, J. S. (1991). Effect of Feeding Full Fat Flax and Canola Seeds to Laying Hens on the Fatty Acid Composition of Eggs, Embryos, and Newly Hatched Chicks. *Poul. Sci.* 70, 917–922. doi: 10.3382/ps.0700917

Cherian, G., and Sim, J. S. (1993). Net transfer and incorporation of yolk n-3 fatty acids into developing chick embryos. *Poult. Sci.* 72, 98–105. doi: 10.3382/ps.0720098

Chilton, F. H., Dutta, R., Reynolds, L. M., Sergeant, S., Mathias, R. A., and Seeds, M. C. (2017). Precision Nutrition and Omega-3 Polyunsaturated Fatty Acids: a Case for Personalized Supplementation Approaches for the Prevention and Management of Human Diseases. *Nutrients* 9:1165. doi: 10.3390/nu9111165

Crespo, N., and Esteve-Garcia, E. (2001). Dietary fatty acid profile modifies abdominal fat deposition in broiler chickens. *Poult. Sci.* 80, 71–78. doi: 10.1093/ps/80.1.71

Crespo, N., and Esteve-Garcia, E. (2002). Dietary linseed oil produces lower abdominal fat deposition but higher *de novo* fatty acid synthesis in broiler chickens. *Poult. Sci.* 81, 1555–1562. doi: 10.1093/ps/81.10.1555

Diep, Q. N., Touyz, R. M., and Schiffrin, E. L. (2000). Docosahexaenoic acid, a peroxisome proliferator-activated receptor-alpha ligand, induces apoptosis in vascular smooth muscle cells by stimulation of p38 mitogen-activated protein kinase. *Hypertension* 36, 851–855. doi: 10.1161/01.HYP.36.5.851

Donahue, S. M., Rifas-Shiman, S. L., Gold, D. R., Jouni, Z. E., Gillman, M. W., and Oken, E. (2011). Prenatal fatty acid status and child adiposity at age 3 y: results from a US pregnancy cohort. *Am. J. Clin. Nutr.* 93, 780–788. doi: 10.3945/ajcn.110.005801

Du, M., Huang, Y., Das, A. K., Yang, Q., Duarte, M. S., Dodson, M. V., et al. (2013). Meat Science and Muscle Biology Symposium: manipulating mesenchymal progenitor cell differentiation to optimize performance and carcass value of beef cattle. *J. Anim. Sci.* 91, 1419–1427. doi: 10.2527/jas.2012-5670

Ferrini, G., Baucells, M. D., Esteve-García, E., and Barroeta, A. C. (2008). Dietary polyunsaturated fat reduces skin fat as well as abdominal fat in broiler chickens. *Poult. Sci.* 87, 528–535. doi: 10.3382/ps.2007-00234

Ferrini, G., Manzanilla, E. G., Menoyo, D., Esteve-Garcia, E., Baucells, M. D., and Barroeta, A. C. (2010). Effects of dietary n-3 fatty acids in fat metabolism and thyroid hormone levels when compared to dietary saturated fatty acids in chickens. *Livest. Sci.* 131, 287–291. doi: 10.1016/j.livsci.2010.03.017

Flachs, P., Rossmeisl, M., Bryhn, M., and Kopecky, J. (2009). Cellular and molecular effects of n-3 polyunsaturated fatty acids on adipose tissue biology and metabolism. *Clin. Sci.* 116, 1–16. doi: 10.1042/CS20070456

Fleckenstein-Elsen, M., Dinnies, D., Jelenik, T., Roden, M., Romacho, T., and Eckel, J. (2016). Eicosapentaenoic acid and arachidonic acid differentially regulate adipogenesis, acquisition of a brite phenotype and mitochondrial function in primary human adipocytes. *Mol. Nutr. Food Res.* 60, 2065–2075. doi: 10.1002/mnfr.201500892

Gaillard, D., Negrel, R., Lagarde, M., and Ailhaud, G. (1989). Requirement and role of arachidonic acid in the differentiation of pre-adipose cells. *Biochem. J.* 257, 389–397. doi: 10.1042/bj2570389

George, L. A., Zhang, L., Tuersunjiang, N., Ma, Y., Long, N. M., Uthlaut, A. B., et al. (2012). Early maternal undernutrition programs increased feed intake, altered glucose metabolism and insulin secretion, and liver function in aged female offspring. *Am. J. Physiol. Regul. Integr. Comp. Physiol.* 302, R795–R804. doi: 10.1152/ajpregu.00241.2011

González-Ortiz, G., Sala, R., Cánovas, E., Abed, N., and Barroeta, A. C. (2013). Consumption of dietary n-3 fatty acids decreases fat deposition and adipocyte size, but increases oxidative susceptibility in broiler chickens. *Lipids* 48, 705–717. doi: 10.1007/s11745-013-3785-3

Gregory, M. K., Geier, M. S., Gibson, R. A., and James, M. J. (2013). Functional characterization of the chicken fatty acid elongases. *J. Nutr.* 143, 12–16. doi: 10.3945/jn.112.170290

Gregory, M. K., Gibson, R. A., Cook-Johnson, R. J., Cleland, L. G., and James, M. J. (2011). Elongase reactions as control points in long-chain polyunsaturated fatty acid synthesis. *PLoS One* 6:e29662. doi: 10.1371/journal.pone.0029662

Hall, J. A., Jha, S., Skinner, M. M., and Cherian, G. (2007). Maternal dietary n-3 fatty acids alter immune cell fatty acid composition and leukotriene production in growing chicks. *Prostaglandins Leukot. Essent. Fatty Acids* 76, 19–28. doi: 10.1016/j.plefa.2006.09.003

Hermier, D., Quignard-Boulangé, A., Dugail, I., Guy, G., Salichon, M. R., Brigant, L., et al. (1989). Evidence of Enhanced Storage Capacity in Adipose Tissue of Genetically Fat Chickens. *J. Nutr.* 119, 1369–1375. doi: 10.1093/jn/119.10.1369

Holness, M. J., Langdown, M. L., and Sugden, M. C. (2000). Early-life programming of susceptibility to dysregulation of glucose metabolism and the development of Type 2 diabetes mellitus. *Biochem. J.* 349, 657–665. doi: 10.1042/bj3490657

Howie, G. J., Sloboda, D. M., and Vickers, M. H. (2012). Maternal undernutrition during critical windows of development results in differential and sex-specific effects on postnatal adiposity and related metabolic profiles in adult rat offspring. *Br. J. Nutr.* 108, 298–307. doi: 10.1017/S000711451100554X

Ibrahim, D., El-Sayed, R., Khater, S. I., Said, E. N., and El-Mandrawy, S. A. M. (2018). Changing dietary n-6:n-3 ratio using different oil sources affects

performance, behavior, cytokines mRNA expression and meat fatty acid profile of broiler chickens. *Anim. Nutr.* 4, 44–51. doi: 10.1016/j.aninu.2017.08.003

Itoh, M., Suganami, T., Satoh, N., Tanimoto-Koyama, K., Yuan, X., Tanaka, M., et al. (2007). Increased adiponectin secretion by highly purified eicosapentaenoic acid in rodent models of obesity and human obese subjects. *Arterioscler. Thromb. Vasc. Biol.* 27, 1918–1925. doi: 10.1161/ATVBAHA.106.136853

Jackson, S., Summers, J. D., and Leeson, S. (1982). Effect of Dietary Protein and Energy on Broiler Carcass Composition and Efficiency of Nutrient Utilization. *Poult. Sci.* 61, 2224–2231. doi: 10.3382/ps.0612224

Jakobsson, A., Westerberg, R., and Jacobsson, A. (2006). Fatty acid elongases in mammals: their regulation and roles in metabolism. *Prog. Lipid Res.* 45, 237–249. doi: 10.1016/j.plipres.2006.01.004

Kartikasari, L. R., Hughes, R. J., Geier, M. S., Makrides, M., and Gibson, R. A. (2012). Dietary alpha-linolenic acid enhances omega-3 long chain polyunsaturated fatty acid levels in chicken tissues. *Prostaglandins Leukot. Essent. Fatty Acids* 87, 103–109. doi: 10.1016/j.plefa.2012.07.005

Khan, M. I., Shin, J. H., and Kim, J. D. (2018). The promising future of microalgae: current status, challenges, and optimization of a sustainable and renewable industry for biofuels, feed, and other products. *Microb. Cell Fact.* 17:36. doi: 10.1186/s12934-018-0879-x

Kim, H. K., Della-Fera, M., Lin, J., and Baile, C. A. (2006). Docosahexaenoic acid inhibits adipocyte differentiation and induces apoptosis in 3T3-L1 preadipocytes. *J. Nutr.* 136, 2965–2969. doi: 10.1093/jn/136.12.2965

Kuda, O., Rossmeisl, M., and Kopecky, J. (2018). Omega-3 fatty acids and adipose tissue biology. *Mol. Aspects Med.* 64, 147–160. doi: 10.1016/j.mam.2018.01.004

Leclercq, B., Blum, J. C., and Boyer, J. P. (1980). Selecting broilers for low or high abdominal fat: initial observations. *Br. Poult. Sci.* 21, 107–113.

Leveille, G. A., Romsos, D. R., Yeh, Y., and O'Hea, E. K. (1975). Lipid biosynthesis in the chick. A consideration of site of synthesis, influence of diet and possible regulatory mechanisms. *Poult. Sci.* 54, 1075–1093.

Lindholm, C., Johansson, A., Middelkoop, A., Lees, J. J., Yngwe, N., Berndtson, E., et al. (2018). The Quest for Welfare-Friendly Feeding of Broiler Breeders: effects of Daily vs. 5:2 Feed Restriction Schedules. *Poult. Sci.* 97, 368–377.

Long, S. F., Kang, S., Wang, Q. Q., Xu, Y. T., Pan, L., Hu, J. X., et al. (2018). Dietary supplementation with DHA-rich microalgae improves performance, serum composition, carcass trait, antioxidant status, and fatty acid profile of broilers. *Poult. Sci.* 97, 1881–1890.

Lukaszewski, M. A., Eberle, D., Vieau, D., and Breton, C. (2013). Nutritional manipulations in the perinatal period program adipose tissue in offspring. *Am. J. Physiol. Endocrinol. Metab.* 305, E1195–E1207.

Manickam, E., Sinclair, A. J., and Cameron-Smith, D. (2010). Suppressive actions of eicosapentaenoic acid on lipid droplet formation in 3T3-L1 adipocytes. *Lipids Health Dis.* 9:57.

Massiera, F., Saint-Marc, P., Seydoux, J., Murata, T., Kobayashi, T., Narumiya, S., et al. (2003). Arachidonic acid and prostacyclin signaling promote adipose tissue development: a human health concern? *J. Lipid Res.* 44, 271–279.

Mezentseva, N. V., Kumaratilake, J. S., and Newman, S. A. (2008). The brown adipocyte differentiation pathway in birds: an evolutionary road not taken. *BMC Biol.* 6:17. doi: 10.1186/1741-7007-6-17

Mihelic, R., Winter, H., Powers, J. B., Das, S., Lamour, K., Campagna, S. R., et al. (2020). Genes controlling polyunsaturated fatty acid synthesis are developmentally regulated in broiler chicks. *Br. Poult. Sci.* 61, 508–517.

Negrel, R., Gaillard, D., and Ailhaud, G. (1989). Prostacyclin as a potent effector of adipose-cell differentiation. *Biochem. J.* 257, 399–405. doi: 10.1042/bj2570399

Newman, R. E., Bryden, W. L., Fleck, E., Ashes, J. R., Buttemer, W. A., Storlien, L. H., et al. (2002). Dietary n-3 and n-6 fatty acids alter avian metabolism: metabolism and abdominal fat deposition. *Br. J. Nutr.* 88, 11–18. doi: 10.1079/BJN2002580

Noble, R. C. (1987). Lipid metabolism in the chick embryo: some recent ideas. *J. Exp. Zool. Suppl.* 1, 65–73.

Noble, R. C., and Cocchi, M. (1990). Lipid metabolism and the neonatal chicken. *Prog. Lipid Res.* 29, 107–140. doi: 10.1016/0163-7827(90)90014-C

Noble, R. C., and Moore, J. H. (1964). STUDIES ON THE LIPID METABOLISM OF THE CHICK EMBRYO. *Can. J. Biochem.* 42, 1729–1741.

OECD and FAO (2021). *OECD-FAO Agricultural Outlook 2021-2030*. Paris: OECD Publishing. doi: 10.1787/19428846-en

Ong, T. P., and Guest, P. C. (2018). Nutritional Programming Effects on Development of Metabolic Disorders in Later Life. *Methods Mol. Biol.* 1735, 3–17.

Poureslami, R., Raes, K., Turchini, G. M., Huyghebaert, G., and De Smet, S. (2010). Effect of diet, sex and age on fatty acid metabolism in broiler chickens: n-3 and n-6 PUFA. *Br. J. Nutr.* 104, 189–197. doi: 10.1017/S0007114510000395

Resnyk, C. W., Carré, W., Wang, X., Porter, T. E., Simon, J., Le Bihan-Duval, E., et al. (2013). Transcriptional analysis of abdominal fat in genetically fat and lean chickens reveals adipokines, lipogenic genes and a link between hemostasis and leanness. *BMC Genomics* 14:557. doi: doi.org/10.1186/1471-2164-14-557

Riera-Heredia, N., Lutfi, E., ánchez-Moya, A. S., Gutiérrez, J., Capilla, E., and Navarro, I. (2020). Short-Term Responses to Fatty Acids on Lipid Metabolism and Adipogenesis in Rainbow Trout (*Oncorhynchus mykiss*). *Int. J. Mol. Sci.* 21:1623. doi: 10.3390/ijms21051623

Rokling-Andersen, M. H., Rustan, A. C., Wensaas, A. J., Kaalhus, O., Wergedahl, H., Røst, T. H., et al. (2009). Marine n-3 fatty acids promote size reduction of visceral adipose depots, without altering body weight and composition, in male Wistar rats fed a high-fat diet. *Br. J. Nutr.* 102, 995–1006. doi: 10.1017/S0007114509353210

Rosen, E. D., and MacDougald, O. A. (2006). Adipocyte differentiation from the inside out. *Nat. Rev. Mol. Cell Biol.* 7, 885–896. doi: 10.1038/nrm2066

Rudolph, M. C., Jackman, M. R., Presby, D. M., Houck, J. A., Webb, P. G., and Johnson, G. C. (2018). Low Neonatal Plasma n-6/n-3 PUFA Ratios Regulate Offspring Adipogenic Potential and Condition Adult Obesity Resistance. *Diabetes* 67, 651–661. doi: 10.2337/db17-0890

Siegel, P. B. (2014). Evolution of the modern broiler and feed efficiency. *Annu. Rev. Anim. Biosci.* 2, 375–385. doi: 10.1146/annurev-animal-022513-114132

Siriwardhana, N., Kalupahana, N. S., and Moustaid-Moussa, N. (2012). Health benefits of n-3 polyunsaturated fatty acids: eicosapentaenoic acid and docosahexaenoic acid. *Adv. Food Nutr. Res.* 65, 211–222. doi: 10.1016/B978-0-12-416003-3.00013-5

Smith, W., and Mukhopadhyay, R. (2012). Essential fatty acids: the work of George and Mildred Burr. *J. Biol. Chem.* 287, 35439–35441. doi: 10.1074/jbc.O112.000005

Song, J., Li, C., Lv, Y., Zhang, Y., Amakye, W. K., and Mao, L. (2017). DHA increases adiponectin expression more effectively than EPA at relative low concentrations by regulating PPARγ and its phosphorylation at Ser273 in 3T3-L1 adipocytes. *Nutr. Metab.* 14:52. doi: 10.1186/s12986-017-0209-z

Sotome, R., Hirasawa, A., Kikusato, M., Amo, T., Furukawa, K., Kuriyagawa, A., et al. (2021). *In vivo* emergence of beige-like fat in chickens as physiological adaptation to cold environments. *Amino Acids* 53, 381–393. doi: 10.1007/s00726-021-02953-5

Speake, B. K., Murray, A. M., and Noble, R. C. (1998). Transport and transformations of yolk lipids during development of the avian embryo. *Prog. Lipid Res.* 37, 1–32.

Speake, B. K., Noble, R. C., and McCartney, R. J. (1993). Tissue-specific changes in lipid composition and lipoprotein lipase activity during the development of the chick embryo. *Biochim. Biophys. Acta* 1165, 263–270. doi: 10.1016/0005-2760(93)90135-V

Tao, L., Sun, T., Magnuson, A. D., Qamar, T. R., and Lei, X. G. (2018). Defatted Microalgae-Mediated Enrichment of n–3 Polyunsaturated Fatty Acids in Chicken Muscle Is Not Affected by Dietary Selenium, Vitamin E, or Corn Oil. *J. Nutr.* 148, 1547–1555. doi: 10.1093/jn/nxy164

Thanabalan, A., and Kiarie, E. G. (2021). Influence of Feeding Omega-3 Polyunsaturated Fatty Acids to Broiler Breeders on Indices of Immunocompetence, Gastrointestinal, and Skeletal Development in Broiler Chickens. *Front. Vet. Sci.* 8:653152. doi: 10.3389/fvets.2021.653152

Torchon, E. T., Das, S., Beckford, R. C., and Voy, B. H. (2017). Enriching the Starter Diet in n-3 Polyunsaturated Fatty Acids Reduces Adipocyte Size in Broiler Chicks. *Curr. Dev. Nutr.* 1:e001644.

Torres-Castillo, N., Silva-Gómez, J. A., Campos-Perez, W., Barron-Cabrera, E., Hernandez-Cañaveral, I., Garcia-Cazarin, M., et al. (2018). High Dietary ω-6:ω-3 PUFA Ratio Is Positively Associated with Excessive Adiposity and Waist Circumference. *Obes. Facts* 11, 344–353.

Vidakovic, A. J., Gishti, O., Voortman, T., Felix, J. F., Williams, M. A., Hofman, A., et al. (2016a). Maternal plasma PUFA concentrations during pregnancy and childhood adiposity: the Generation R Study. *Am. J. Clin. Nutr.* 103, 1017–1025.

Vidakovic, A. J., Jaddoe, V. W., Voortman, T., Demmelmair, H., Koletzko, B., and Gaillard, R. (2016b). Maternal plasma polyunsaturated fatty acid levels during pregnancy and childhood lipid and insulin levels. *Nutr. Metab. Cardiovasc. Dis.* 27, 78–85. doi: 10.1016/j.numecd.2016.10.001

Whitehead, C. C., and Griffin, H. D. (1984). Development of divergent lines of lean and fat broilers using plasma very low density lipoprotein concentration as selection criterion: the first three generations. *Br. Poult. Sci.* 25, 573–582. doi: 10.1080/00071668408454899

Zuidhof, M. J., Betti, M., Korver, D. R., Hernandez, F. I., Schneider, B. L., Carney, V. L., et al. (2009). Omega-3-enriched broiler meat: 1. Optimization of a production system. *Poult. Sci.* 88, 1108–1120.

Zuidhof, M. J., Schneider, B. L., Carney, V. L., Korver, D. R., and Robinson, F. E. (2014). Growth, efficiency, and yield of commercial broilers from 1957, 1978, and 2005. *Poult. Sci.* 93, 2970–2982.

Zúñiga, J., Cancino, M., Medina, F., Varela, P., Vargas, R., Tapia, G., et al. (2011). N-3 PUFA supplementation triggers PPAR-α activation and PPAR-α/NF-κB interaction: anti-inflammatory implications in liver ischemia-reperfusion injury. *PLoS One* 6:e28502. doi: 10.1371/journal.pone.0028502

Conflict of Interest: The authors declare that the research was conducted in the absence of any commercial or financial relationships that could be construed as a potential conflict of interest.

The handling editor declared a past co-authorship with one of the author BV.

frontiers in Physiology

BRIEF RESEARCH REPORT
published: 25 October 2021
doi: 10.3389/fphys.2021.747473

A Novel Hypothalamic Factor, Neurosecretory Protein GM, Causes Fat Deposition in Chicks

Masaki Kato, Eiko Iwakoshi-Ukena, Megumi Furumitsu and Kazuyoshi Ukena**

Laboratory of Neurometabolism, Graduate School of Integrated Sciences for Life, Hiroshima University, Hiroshima, Japan

We recently discovered a novel cDNA encoding the precursor of a small secretory protein, neurosecretory protein GM (NPGM), in the mediobasal hypothalamus of chickens. Although our previous study showed that subcutaneous infusion of NPGM for 6 days increased body mass in chicks, the chronic effect of intracerebroventricular (i.c.v.) infusion of NPGM remains unknown. In this study, we performed i.c.v. administration of NPGM in eight-day-old layer chicks using osmotic pumps for 2 weeks. In the results, chronic i.c.v. infusion of NPGM significantly increased body mass, water intake, and the mass of abdominal and gizzard fat in chicks, whereas NPGM did not affect food intake, liver and muscle masses, or blood glucose concentration. Morphological analyses using Oil Red O and hematoxylin-eosin stainings revealed that fat accumulation occurred in both the liver and gizzard fat after NPGM infusion. The real-time PCR analysis showed that NPGM decreased the mRNA expression of peroxisome proliferator-activated receptor α, a lipolytic factor in the liver. These results indicate that NPGM may participate in fat storage in chicks.

Keywords: neurosecretory protein, chicken, hypothalamus, fat deposition, chronic intracerebroventricular infusion

OPEN ACCESS

Edited by:
Sami Dridi,
University of Arkansas, United States

Reviewed by:
Brian McCabe,
University of Cambridge, United Kingdom
Xiquan Zhang,
South China Agricultural University, China
Shaaban Saad Elnesr,
Fayoum University, Egypt
Elizabeth S. Greene,
University of Arkansas, United States

****Correspondence:***
Kazuyoshi Ukena
ukena@hiroshima-u.ac.jp
Eiko Iwakoshi-Ukena
iwakoshi@hiroshima-u.ac.jp

Specialty section:
This article was submitted to Avian Physiology, a section of the journal Frontiers in Physiology

Received: *26 July 2021*
Accepted: *04 October 2021*
Published: *25 October 2021*

Citation:
Kato M, Iwakoshi-Ukena E, Furumitsu M and Ukena K (2021) A Novel Hypothalamic Factor, Neurosecretory Protein GM, Causes Fat Deposition in Chicks. Front. Physiol. 12:747473. doi: 10.3389/fphys.2021.747473

INTRODUCTION

Energy intake through feeding behavior is a necessary element for the maintenance of animal life and growth. However, excessive food intake can cause diseases, such as obesity (Moore et al., 2014). In general, it is known that animals have a complex endocrine system that controls their appetite to avoid obesity (Lawrence et al., 1999; Geary, 2000). Poultry, especially chickens, are an important agricultural species and have been repeatedly selected for meat and/or egg production, with emphasis on feed efficiency and growth rate (Abo Ghanima et al., 2020; Rehman et al., 2020; Batool et al., 2021). However, there is concern that excessive food intake and fat accumulation in broiler chickens can lead to reduced growth rates and metabolic diseases, resulting in lower meat production (Knowles et al., 2008). For layer chickens, fatty acid is required to product eggs. However, excessive fat accumulation in liver and abdomen may induce several health disorders and lead to a decline of egg production and reproductive performance (Trott et al., 2014; Cherian, 2015; Wang et al., 2019). This problem is undesirable from the standpoint of animal health and production efficiency. Therefore, it is important to control growth and fat accumulation in chickens to enable efficient meat and/or egg production. Understanding the mechanisms of fat accumulation

in birds at the molecular and cellular levels will provide sufficient knowledge to improve these problems. In contrast, chicken fat is also one of healthy foods (Peña-Saldarriaga et al., 2020). Several studies have shown that the nutrient composition of diets affects adipose tissue development and lipid metabolism in chickens (Wang et al., 2017). However, the contribution of hormones to lipid metabolism in chickens and other birds has not yet been revealed. Therefore, it is likely that unknown factors are involved in these processes in avian species.

Recently, we discovered a novel cDNA encoding the precursor of a small secretory protein in the chick hypothalamus (Ukena et al., 2014; Shikano et al., 2018a). We named the small protein of 83-amino acid residues as neurosecretory protein GM (NPGM) (Ukena et al., 2014; Shikano et al., 2018a). The NPGM gene is highly conserved in vertebrates, including chickens, rats, and humans (Ukena et al., 2014). Our previous studies identified the localization of NPGM in the chick brain by *in situ* hybridization and immunostaining. NPGM-producing cells are localized in the infundibular nucleus (IN) and the medial mammillary nucleus (MM) of the hypothalamus in chicks (Shikano et al., 2018a). These nuclei are known to be feeding and metabolic centers in chicks. Furthermore, we found that the expression levels of NPGM mRNA gradually decreased during post-hatching development (Shikano et al., 2018a). These results suggest that NPGM is a novel hypothalamic factor involved in energy metabolism immediately after hatching in chicks. Subsequently, we performed chronic subcutaneous infusion to clarify the physiological functions of NPGM in chicks. Chronic subcutaneous infusion of NPGM for 6 days increased the body mass gain in chicks (Shikano et al., 2018c). It was not clear which parts of the body gained mass, although NPGM seemed to induce the largest increase in abdominal fat mass (Shikano et al., 2018c). In the present study, we analyzed the effects of chronic intracerebroventricular (i.c.v.) infusion of NPGM for 2 weeks on food intake, water intake, and body composition, including fat accumulation and lipid metabolism in the abdominal and gizzard fat and the liver.

MATERIALS AND METHODS

Animals

One-day-old male layer chicks were purchased from a commercial company (Nihon layer, Gifu, Japan) and housed in a windowless room at 28°C on a 20–h light (4:00–24:00)/4–h dark (0:00–4:00) cycle. The chicks had *ad libitum* access to food and water.

Production of Chicken Neurosecretory Protein GM

Chicken NPGM was synthesized using fluorenylmethyloxycarbonyl (Fmoc) and a peptide synthesizer (Syro Wave; Biotage, Uppsala, Sweden) according to our previous method (Masuda et al., 2015; Shikano et al., 2019). The purity of the protein was >95%. Lyophilized NPGM was weighed using an analytical and precision balance (AP125WD; Shimadzu, Kyoto, Japan).

Chronic Intracerebroventricular Infusion of Chicken Neurosecretory Protein GM for 2 Weeks

Chronic i.c.v. infusion of chicken NPGM was performed according to a previously reported method (Shikano et al., 2018b, 2019). NPGM was dissolved in absolute propylene glycol and adjusted to 30% propylene glycol at pH 8.0 as a vehicle solution. The administration period of NPGM was fixed to 13 days because our preliminary study showed that the chemical instability of NPGM occurred in the osmotic pump over 2 weeks. Eight-day-old chicks were i.c.v.-infused with 0 (vehicle control) or 15 nmol/day NPGM. This dose has been reported to be a physiological dose in rats and chicks (Stoyanovitch et al., 2005; Rich et al., 2007; Shikano et al., 2018b, 2019). Body mass, food intake, and water intake were measured daily (between 9:00 and 10:00) throughout the experiment. After 13 days of chronic i.c.v. infusion of NPGM, chicks were euthanized by decapitation, and the masses of the liver, abdominal and gizzard fat, subcutaneous fat, pectoralis major muscle, pectoralis minor muscle, and biceps femoris muscle were measured. Blood samples were taken at the endpoint and centrifuged at 800× *g* for 15 min at 4°C to separate the serum. The blood glucose levels were measured using a GLUCOCARD G + meter (Arkray, Kyoto, Japan). The method for identification and isolation of the mediobasal hypothalamus was performed according to a previously reported method (Ukena et al., 2014). The chicken pituitary gland lies within the sella turcia of the sphenoid bone. We removed sphenoid bone for isolation of the pituitary gland. The mediobasal hypothalamus, pituitary gland, abdominal and gizzard fat, and liver were immediately snap-frozen in liquid nitrogen and stored at −80°C for real-time PCR analysis.

Morphological Analyses

Oil Red O staining of the livers and hematoxylin and eosin staining of the gizzard fat were performed according to a previously reported method (Shikano et al., 2019).

Real-Time PCR

RNA extraction was performed as previously described (Shikano et al., 2019). PCR amplifications were performed using THUNDERBIRD SYBR qPCR Mix (TOYOBO, Osaka, Japan): 95°C for 20 s followed by 40 cycles at 95°C for 3 s and 60°C for 30 s using a real-time thermal cycler (CFX Connect; BioRad, Hercules, CA, United States).

The amplification of the lipid metabolic factors was performed using the primer sets listed in **Supplementary Table 1**. Acetyl-CoA carboxylase (*ACC*), fatty acid synthase (*FAS*), stearoyl-CoA desaturase 1 (*SCD1*), malic enzyme (*ME*), peroxisome proliferator-activated receptor γ (*PPARγ*), and fatty acid transporter 1 (*FATP1*) are lipogenic enzymes and related factors, and peroxisome proliferator-activated receptor α (*PPARα*), carnitine palmitoyltransferase 1a (*CPT1a*), lipoprotein lipase (*LPL*), adipose triglyceride lipase (*ATGL*), and comparative gene identification-58 (*CGI-58*) are lipolytic enzymes and related factors.

Amplification of feeding, water intake, and growth-related factors was performed using the primer sets listed in **Supplementary Table 1**. We chose neurosecretory protein GL (*NPGL*) as a paralogous gene of NPGM; neuropeptide Y (*NPY*) and agouti-related peptide (AGRP) as orexigenic factors; pro-opiomelanocortin (*POMC*), glucagon-like peptide-1 (*GLP-1*), and cholecystokinin (*CCK*) as anorexigenic factors; and angiotensinogen (*AGT*) and angiotensin-converting enzyme (*ACE*) as water intake-related factors in the hypothalamus. In the pituitary gland, we chose growth hormone (*GH*), prolactin (*PRL*), thyroid-stimulating hormone (*TSH*), and *POMC*. The relative quantification for each expression was determined by the $2^{-\Delta\Delta Ct}$ method using β-actin (*ACTB*) as an internal control.

Statistical Analysis

Data were analyzed with Student's *t*-test for endpoint body mass, cumulative food intake, cumulative water intake, tissue mass, blood glucose level, and mRNA expression or two-way repeated-measures analysis of variance (ANOVA) followed by Bonferroni's test for body mass gain and daily food and water intake. The significance level was set at $P < 0.05$. All results are expressed as the mean ± SEM.

RESULTS

Effects of Chronic Intracerebroventricular Infusion of Neurosecretory Protein GM on Body Mass, Food Intake, Water Intake

To investigate the effect of chronic i.c.v. infusion of NPGM on energy metabolism, we measured body mass, food intake, and water intake for 2 weeks. The results showed that chronic infusion of NPGM significantly increased daily body mass gain and final body mass after 2 weeks (**Figures 1A,B**). However, daily and cumulative food intake remained unchanged (**Figures 1C,D**). The daily water intake was almost unchanged, but the cumulative water intake increased after 2 weeks of NPGM infusion (**Figures 1E,F**).

Effects of Chronic Intracerebroventricular Infusion of Neurosecretory Protein GM on Body Composition

When we analyzed the effect of NPGM on body composition and blood glucose level, chronic infusion of NPGM increased the mass of the abdominal and gizzard fat and tended to increase the mass of the subcutaneous fat (**Figure 2B**). On the other hand, no change was observed in the liver mass and the muscle masses of the pectoralis major, pectoralis minor, and biceps femoris muscles after the infusion of NPGM (**Figures 2A,C**). Furthermore, the blood glucose levels were not altered by NPGM (**Figure 2D**).

Effects of Chronic Intracerebroventricular Infusion of Neurosecretory Protein GM on Lipid Deposition in the Liver and Gizzard Fat

We elucidated the effect of fat accumulation by morphological analyses in the liver and gizzard fat. Oil Red O staining of the liver demonstrated that lipid droplets were deposited after chronic i.c.v. infusion of NPGM (**Figure 3A**).

We found an increase in the gizzard fat in NPGM-treated chicks compared with controls (**Figure 3B**, lower left panel). Hematoxylin-eosin staining revealed that the adipocytes in the gizzard fat of the NPGM-treated chicks were larger than those of the control group (**Figure 3B**, lower right panel).

Effects of Chronic Intracerebroventricular Infusion of Neurosecretory Protein GM on the mRNA Expression of Lipogenic and Lipolytic Factors in the Liver and Abdominal and Gizzard Fat

To explore the molecular mechanism of fat accumulation in the liver and the abdominal and gizzard fat by chronic i.c.v. infusion of NPGM, we investigated the mRNA expression levels of the lipid metabolic factors. We analyzed the mRNA expression levels of *ACC, FAS, SCD1, ME, PPARγ, FATP1, PPARα, CPT1a, LPL, ATGL,* and *CGI-58* after chronic infusion of NPGM. In the liver, NPGM decreased the mRNA expression of *PPARα* (**Figure 4A**), whereas in the abdominal and gizzard fat, the mRNA expression levels did not change (**Figure 4B**).

Effects of Chronic Intracerebroventricular Infusion of Neurosecretory Protein GM on the mRNA Expression for Feeding, Water Intake, and Pituitary Hormones in the Hypothalamus and Pituitary Gland

Based on the results of body mass gain and water intake, we investigated the mRNA expression levels of the endocrine hormones and related factors, which are involved in feeding, water intake, and growth in the hypothalamus and pituitary gland after chronic infusion of NPGM. NPGM did not change the mRNA expression levels in the hypothalamus (**Supplementary Figure 1A**), whereas NPGM decreased the expression of *PRL* mRNA in the pituitary gland (**Supplementary Figure 1B**).

DISCUSSION

In this study, we investigated the effects of a novel small protein, NPGM, on the body composition of chicks by chronic i.c.v. infusion for 2 weeks. Our data showed that the infusion of NPGM increased body mass and cumulative water intake without changes in food intake. Furthermore, morphological analyses showed that NPGM induced fat accumulation in the liver and

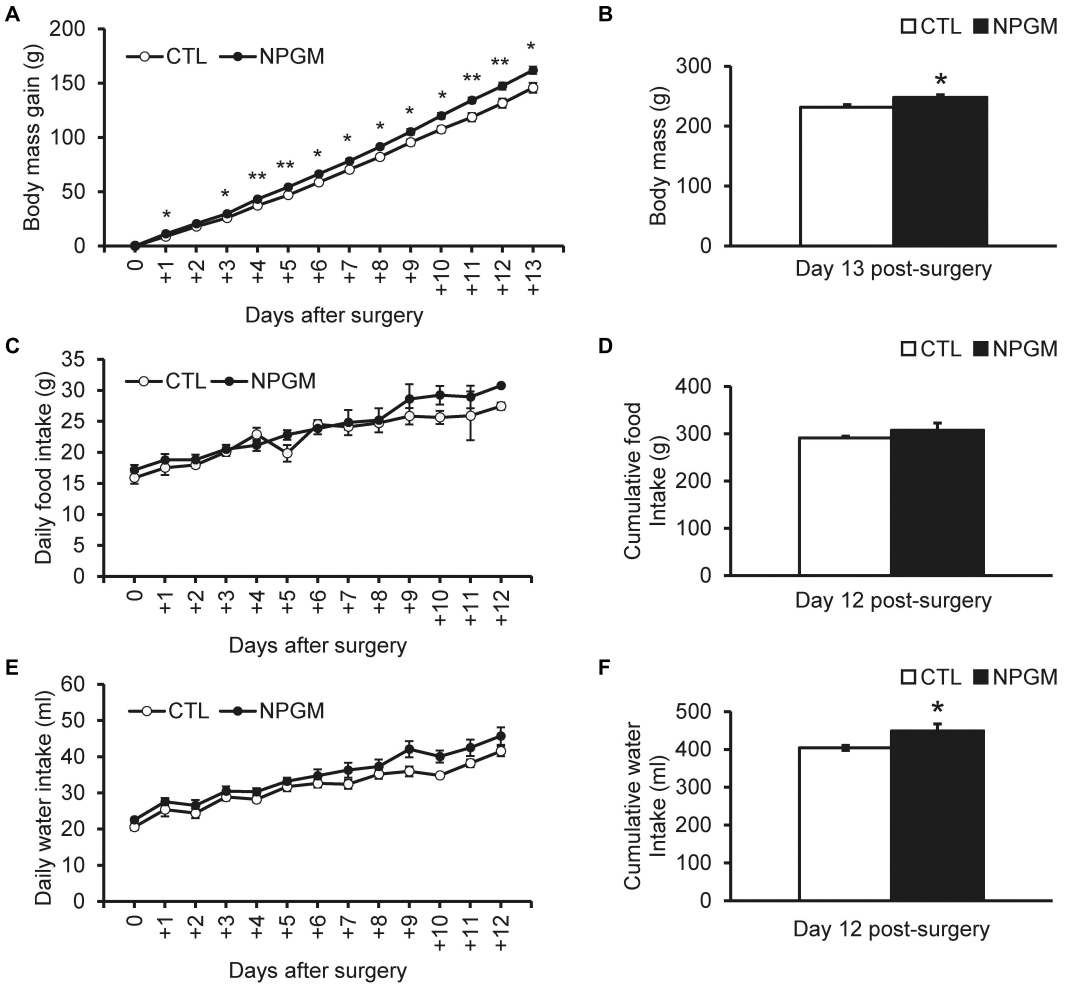

FIGURE 1 | Effect of chronic i.c.v. infusion of NPGM on body mass gain, food intake, and water intake. The results were obtained by the infusion of the vehicle (control; CTL) and NPGM. The change in the body mass gain after surgery **(A,B)**. The daily and cumulative food intake **(C,D)**. The daily and cumulative water intake **(E,F)**. Data are expressed as the mean ± SEM (n = 7–8). Data were analyzed using the student t-test and two-way repeated-measures analysis of variance (ANOVA). An asterisk indicates a statistically significant difference (*$P < 0.05$, **$P < 0.01$).

gizzard fat. This study is the first to show that NPGM induces fat deposition in animals.

Several studies have been conducted on fat accumulation in mammals (Gesta et al., 2007; Peirce et al., 2014). However, the mechanism of lipid metabolism in birds has not been established. The biological structures of birds differ from those of mammals, and their endocrine actions are unique. For example, birds do not have heat-producing brown adipose tissue (BAT) and have only white adipose tissue (WAT) (Johnston, 1971). Moreover, birds are hyperglycemic animals that exhibit insulin resistance despite normal insulin activity (Dupont et al., 2008). In chickens, unlike mammals, insulin has little effect on glucose uptake in adipose tissue and does not inhibit lipolysis (Tokushima et al., 2005). Furthermore, glucagon is thought to be the main lipolytic hormone (Scanes et al., 1994). In mammals, leptin is a hormone secreted by adipocytes and acts on the hypothalamus to suppress eating and obesity (Halaas et al., 1995). Recently, the leptin gene has been identified in some bird and these findings suggest that avian leptin may have a different physiological function from that of lipid metabolism in mammals (Seroussi et al., 2017, 2019; Beauclair et al., 2019; Friedman-Einat and Seroussi, 2019). The present study showed that NPGM is a new player in regulating fat deposition in avian species, chicken.

We have also reported a paralog gene with NPGM, which is named neurosecretory protein GL (NPGL) in vertebrates (Ukena et al., 2014; Ukena, 2018). The NPGL gene is also highly conserved in vertebrates, including chickens, rats, mice, and humans (Ukena et al., 2014; Ukena, 2018). Sequence similarity between mature NPGM and NPGL is 54% in chickens (Shikano et al., 2018c). Our previous studies showed that NPGL-immunoreactive cells were localized in the IN and MM of the hypothalamus, and parts of NPGL-immunoreactive cells were identical to NPGM-immunoreactive cells in the MM in 1- and 15-day-old chicks and the IN in 15-day-old

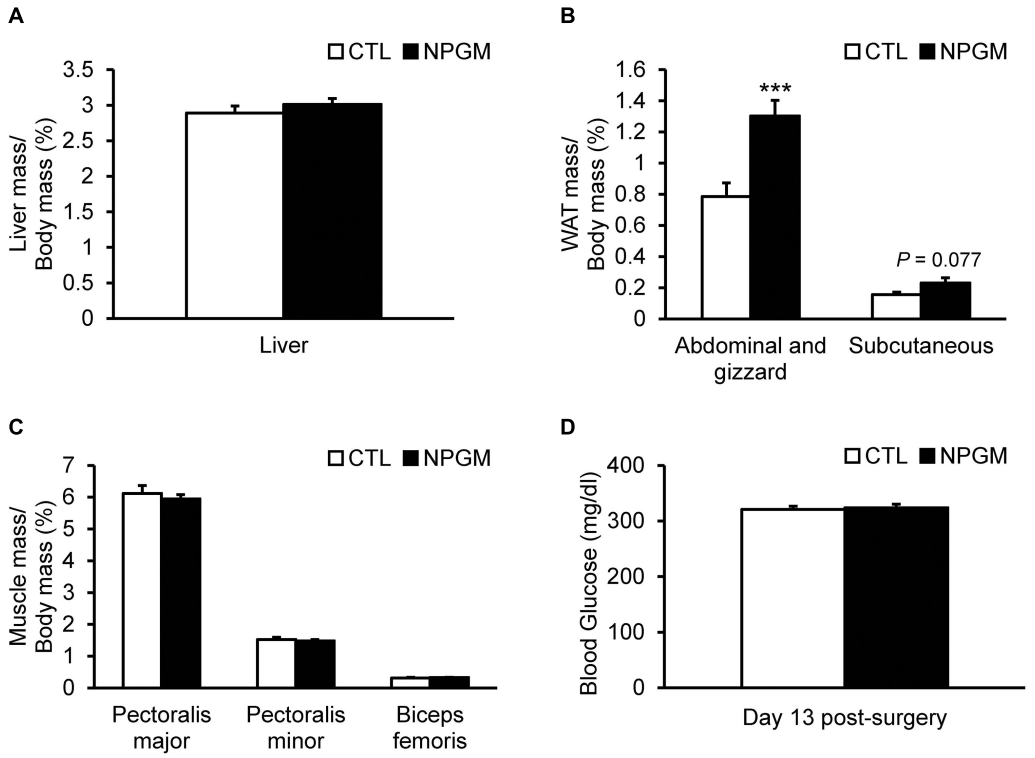

FIGURE 2 | Effect of chronic i.c.v. infusion of NPGM on body composition. The results were obtained by the infusion of the vehicle (control; CTL) and NPGM for 2 weeks. Ratio of the liver mass/body mass **(A)**, ratio of the abdominal and gizzard fat mass/body mass, and the subcutaneous fat mass/body mass **(B)**, ratio of pectoralis major, pectoralis minor, and biceps femoris muscle masses/body mass **(C)**, and blood glucose level **(D)** were measured at the end of the experiment. Data are expressed as the mean ± SEM (n = 7–8). Data were analyzed by the Student's t-test. Asterisks indicate statistically significant differences (***$P < 0.005$).

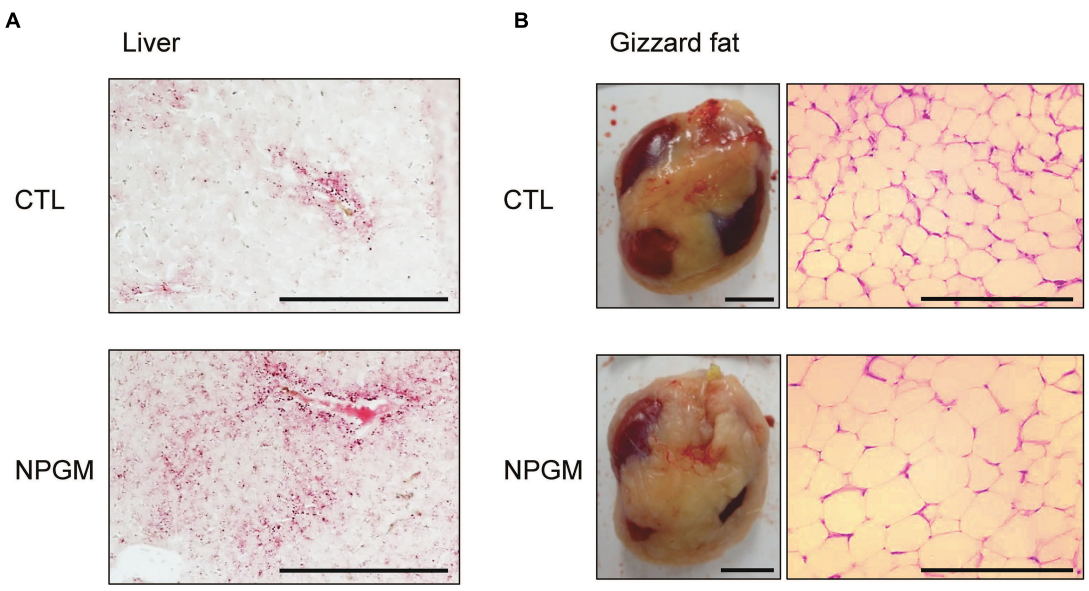

FIGURE 3 | Effect of chronic i.c.v. infusion of NPGM on lipid deposition in the liver and lipid droplets in the gizzard fat. The results were obtained 2 weeks after infusion of the vehicle (control; CTL) and NPGM. In the liver, representative photomicrographs of the sections were stained by Oil Red O (scale bar = 100 μm) **(A)**. For the gizzard fat, exterior photographs around the gizzard (left panel, scale bar = 1 cm) and representative photographs of the sections stained by hematoxylin and eosin (right panel, scale bar = 100 μm) **(B)** were obtained.

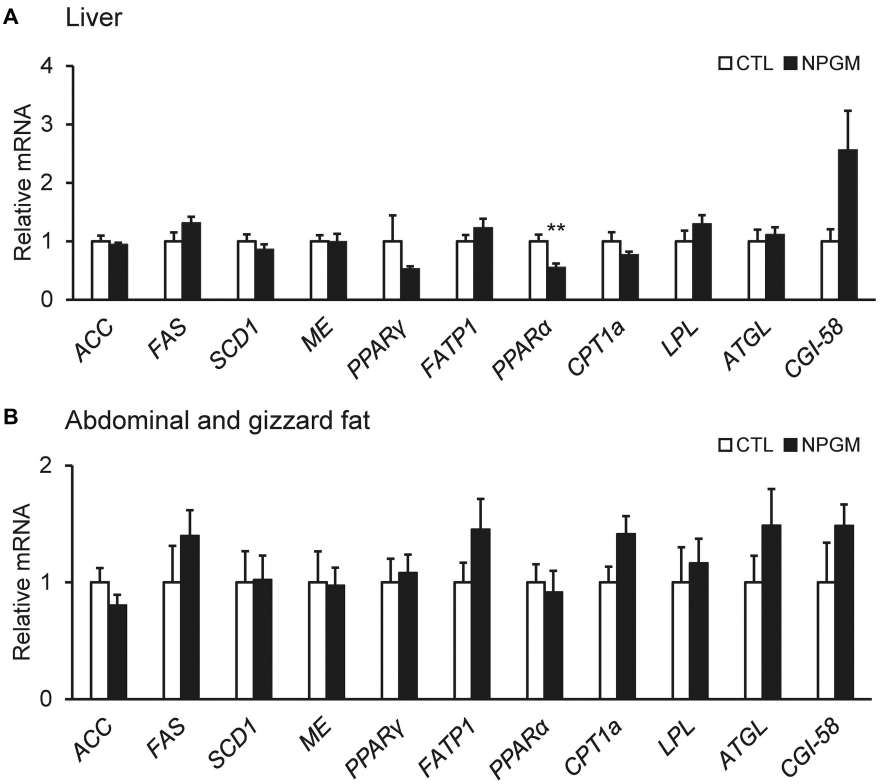

FIGURE 4 | Effect of chronic i.c.v. infusion of NPGM on the mRNA expression of lipogenic and lipolytic factors [acetyl-CoA carboxylase (*ACC*), fatty acid synthase (*FAS*), stearoyl-CoA desaturase 1 (*SCD1*), malic enzyme (*ME*), peroxisome proliferator-activated receptor γ (*PPARγ*), fatty acid transporter 1 (*FATP1*), peroxisome proliferator-activated receptor α (*PPARα*), carnitine palmitoyltransferase 1a (*CPT1a*), lipoprotein lipase (*LPL*), adipose triglyceride lipase (*ATGL*), and comparative gene identification-58 (*CGI-58*)] in the liver **(A)** and the abdominal and gizzard fat **(B)**. The results were obtained 2 weeks after infusion of the vehicle (control; CTL) and NPGM. Data are expressed as the mean ± SEM (n = 7–8). Data were analyzed by Student's t-test. An asterisk indicates a statistically significant difference (**$P < 0.01$).

chicks (Shikano et al., 2018a). The expression levels of NPGL mRNA gradually increased during post-hatching development. In contrast, the expression level of NPGM mRNA gradually decreased after hatching, suggesting that NPGM and NPGL have different timings of action during the growth process (Shikano et al., 2018a). Functional analysis of NPGL has already been demonstrated in rats, mice, and chicks (Iwakoshi-Ukena et al., 2017; Matsuura et al., 2017; Shikano et al., 2018b, 2019, 2020; Fukumura et al., 2021). The results showed that the long-term administration of NPGL stimulated food intake and induced fat accumulation in rats, mice, and chicks. In contrast, NPGM treatment did not change food intake or the gene expression levels of feeding and growth regulators (*NPY, AgRP, POMC, GLP-1, CCK, GH,* and *TSH*) in the hypothalamus and pituitary gland in this study. Therefore, it is likely that NPGM does not directly regulate feeding behavior in chicks. In addition, the expression levels of water intake-regulating factors (*AGT* and *ACE*) did not change, although the amount of drinking water was increased by NPGM infusion. The future study is necessary to elucidate the regulatory mechanism of drinking behavior by NPGM.

In our previous studies, NPGL increased the mass of WAT through *de novo* lipogenesis in rats and chicks, resulting in fast body mass gain (Iwakoshi-Ukena et al., 2017; Shikano et al., 2019). In general, birds are known to use the liver rather than adipose tissue as the primary site of *de novo* lipogenesis (Leveille et al., 1975). Glucose taken up by the liver is converted into fatty acids and cholesterol and, subsequently, fatty acids are converted into triacylglycerols (TAGs). Cholesterol and TAGs are transported by very low-density lipoproteins (VLDL) to the adipose tissue where they are stored (Hermier, 1997). However, we found that *de novo* lipogenesis by NPGL in chicks occurred in the adipose tissue but not in the liver (Shikano et al., 2019). This result indicates that NPGL is a neuropeptide that upregulates *de novo* lipogenesis in the adipose tissues of chicks. In the present study, chronic i.c.v. infusion of NPGM induced body mass gain in chicks, similar to NPGL. However, mRNA expression analysis of lipid metabolism factors involved in lipogenesis and lipolysis showed little change in the expression levels of lipid metabolism factors in the liver and adipose tissue, except for a decrease in the lipolytic factor *PPARα* in the liver. These results suggest that *de novo* lipogenesis by NPGM does not occur in these tissues. Therefore, the mechanism of action of NPGM and NPGL for fat accumulation may differ in the same animals. It is also

known that lipogenesis and lipolysis in the adipose tissue are controlled by the hypothalamus *via* the sympathetic nervous system in mammals (Buettner et al., 2008; Scherer et al., 2011). Therefore, NPGM may be involved in the sympathetic control of fat accumulation in chickens. Future studies are needed to classify the target regions and neural networks of NPGM-producing neurons in chickens.

In this study, *PRL* mRNA expression was decreased in the pituitary gland after NPGM infusion. PRL is known to be involved in more than 300 actions in vertebrates (Bole-Feysot et al., 1998). In birds, the most studied role of PRL is involved in actions during the egg incubation phase (March et al., 1994). In addition, PRL has been reported to increase feeding behavior and activate LPL in adipocytes (Garrison and Scow, 1975; Das, 1991). In the present study, there was no change in food intake or *LPL* mRNA expression levels after NPGM infusion. However, NPGM may inhibit the increase in food intake and the activation of lipolysis through the suppression of PRL expression. In the future, it will be necessary to clarify the exact relationship between NPGM and PRL in chickens.

The present data on NPGM-induced fat accumulation in chickens may facilitate future applications in animal agriculture, such as controlling fat accumulation in poultry. The French food, *foie gras*, is a fatty liver, and the artificial production of *foie gras* is a problem related to animal welfare (Litt et al., 2020). In addition, chicken fat is becoming a healthy food because of the high amounts of unsaturated fatty acids (Peña-Saldarriaga et al., 2020) and these fatty acids are necessary constituents of the cell membrane and represent precursors to numerous different body components (Alagawany et al., 2021a,b). The application of NPGM to fat deposition in the liver and the abdominal and gizzard fat will have an impact on agricultural and livestock industries.

In conclusion, chronic i.c.v. administration of NPGM increased the body mass and caused fat accumulation in both the liver and the abdominal and gizzard fat. This is the first report describing the effect of NPGM on fat deposition in vertebrates, including birds. These results suggested that the biological functions of NPGM might affect egg production and reproductive performance in layers. In the future, we need to analyze the effects of NPGM in broilers for meat production. In addition, to clarify the exact role of NPGM action in the brain, the receptor for NPGM needs to be discovered. However, to date, receptors for NPGM and NPGL have not yet been discovered in vertebrates. It is known that fat accumulation is essential for birds, not only to sustain life but also to maintain bird-specific behaviors such as migration (Price, 2010; Guglielmo, 2018). Therefore, NPGM is considered an important factor in avian survival and reproduction. In the future, comparative analysis using other avian species and other vertebrates will help clarify the physiological role of NPGM in animals.

DATA AVAILABILITY STATEMENT

The raw data supporting the conclusions of this article will be made available by the authors, without undue reservation.

ETHICS STATEMENT

The animal study was reviewed and approved by the Guide for the Care and Use of Laboratory Animals prepared by Hiroshima University (Higashi-Hiroshima, Japan).

AUTHOR CONTRIBUTIONS

MK, EI-U, and KU: conceptualization and writing—review and editing. MK, EI-U, MF, and KU: methodology and investigation. MK: writing—original draft preparation and visualization. EI-U and KU: project administration and funding acquisition. All authors have read and agreed to the published version of the manuscript.

FUNDING

This work was supported by JSPS KAKENHI Grant (JP19K06768 to EI-U and JP19H03258 to KU), the Kieikai Research Foundation (KU).

ACKNOWLEDGMENTS

We would like to thank Kenshiro Shikano, Yuki Narimatsu, and Keisuke Fukumura for the experimental support.

SUPPLEMENTARY MATERIAL

The Supplementary Material for this article can be found online at: https://www.frontiersin.org/articles/10.3389/fphys.2021.747473/full#supplementary-material

REFERENCES

Abo Ghanima, M. M., Alagawany, M., Abd El-Hack, M. E., Taha, A., Elnesr, S. S., Ajarem, J., et al. (2020). Consequences of various housing systems and dietary supplementation of thymol, carvacrol, and euganol on performance, egg quality, blood chemistry, and antioxidant parameters. *Poult. Sci.* 99, 4384–4397. doi: 10.1016/j.psj.2020.05.028

Alagawany, M., Elnesr, S. S., Farag, M. R., El-Sabrout, K., Alqaisi, O., Dawood, M. A., et al. (2021a). Nutritional significance and health benefits of omega-3, -6 and-9 fatty acids in animals. *Anim. Biotechnol.* doi: 10.1080/10495398.2020.1869562 [Epub ahead of print].

Alagawany, M., Elnesr, S. S., Farag, M. R., Abd El-Hack, M. E., Barkat, R. A., Gabr, A. A., et al. (2021b). Potential role of important nutraceuticals in poultry performance and health-A comprehensive review. *Res. Vet. Sci.* 137, 9–29. doi: 10.1016/j.rvsc.2021.04.009

Batool, F., Bilal, R. M., Hassan, F. U., Nasir, T. A., Rafeeque, M., Elnesr, S. S., et al. (2021). An updated review on behavior of domestic quail with reference to the

negative effect of heat stress. *Anim. Biotechnol.* doi: 10.1080/10495398.2021.1951281 [Epub ahead of print].

Beauclair, L., Ramé, C., Arensburger, P., Piégu, B., Guillou, F., Dupont, J., et al. (2019). Sequence properties of certain GC rich avian genes, their origins and absence from genome assemblies: case studies. *BMC Genomics* 20:734 doi: 10.1186/s12864-019-6131-1

Bole-Feysot, C., Goffin, V., Edery, M., Binart, N., and Kelly, P. A. (1998). Prolactin (PRL) and its receptor: actions, signal transduction pathways and phenotypes observed in PRL receptor knockout mice. *Endocr. Rev.* 19, 225–268. doi: 10.1210/edrv.19.3.0334

Buettner, C., Muse, E. D., Cheng, A., Chen, L., Scherer, T., Pocai, A., et al. (2008). Leptin controls adipose tissue lipogenesis via central, STAT3-independent mechanisms. *Nat. Med.* 14, 667–675. doi: 10.1038/nm1775

Cherian, G. (2015). Nutrition and metabolism in poultry: role of lipids in early diet. *J. Anim. Sci. Biotechnol.* 6:28 doi: 10.1186/s40104-015-0029-9

Das, K. (1991). Effects of testosterone propionate, prolactin and photoperiod on feeding behaviours of Indian male weaver birds. *Indian J. Exp. Biol.* 29, 1104–1108.

Dupont, J., Tesseraud, S., and Simon, J. (2008). Insulin signaling in chicken liver and muscle. *Gen. Comp. Endocrinol.* 163, 52–57. doi: 10.1016/j.ygcen.2008.10.016

Friedman-Einat, M., and Seroussi, E. (2019). Avian leptin: bird's-eye view of the evolution of vertebrate energy-balance control. *Trends Endocrinol. Metab.* 30, 819–832. doi: 10.1016/j.tem.2019.07.007

Fukumura, K., Shikano, K., Narimatsu, Y., Iwakoshi-Ukena, E., Furumitsu, M., Naito, M., et al. (2021). Effects of neurosecretory protein GL on food intake and fat accumulation under different dietary nutrient compositions in rats. *Biosci. Biotechnol. Biochem.* 85, 1514–1520. doi: 10.1093/bbb/zbab064

Garrison, M. M., and Scow, R. O. (1975). Effect of prolactin on lipoprotein lipase in crop sac and adipose tissue of pigeons. *Am. J. Physiol.* 228, 1542–1544. doi: 10.1152/ajplegacy.1975.228.5.1542

Geary, N. (2000). Control-theory models of body-weight regulation and body-weight-regulatory appetite. *Appetite* 144:104440. doi: 10.1016/j.appet.2019.104440

Gesta, S., Tseng, Y. H., and Kahn, C. R. (2007). Developmental origin of fat: tracking obesity to its source. *Cell* 131, 242–256. doi: 10.1016/j.cell.2007.10.004

Guglielmo, C. G. (2018). Obese super athletes: fat-fueled migration in birds and bats. *J. Exp. Biol.* 221(Pt Suppl 1):jeb165753. doi: 10.1242/jeb.165753

Hermier, D. (1997). Lipoprotein metabolism and fattening in poultry. *J. Nutr.* 127, 805–808. doi: 10.1093/jn/127.5.805S

Halaas, J. L., Gajiwala, K. S., Maffei, M., Cohen, S. L., Chait, B. T., Rabinowitz, D., et al. (1995). Weight-reducing effects of the plasma protein encoded by the obese gene. *Science* 269, 543–546. doi: 10.1126/science.7624777

Iwakoshi-Ukena, E., Shikano, K., Kondo, K., Taniuchi, S., Furumitsu, M., Ochi, Y., et al. (2017). Neurosecretory protein GL stimulates food intake, de novo lipogenesis, and onset of obesity. *eLife* 6:e28527. doi: 10.7554/eLife.28527

Johnston, D. W. (1971). The absence of brown adipose tissue in birds. *Comp. Biochem. Physiol. A Comp. Physiol.* 40, 1107–1108 doi: 10.1016/0300-9629(71)90298-2

Knowles, T. G., Kestin, S. C., Haslam, S. M., Brown, S. N., Green, L. E., Butterworth, A., et al. (2008). Leg disorders in broiler chickens: prevalence, risk factors and prevention. *PLoS One* 3:e1545. doi: 10.1371/journal.pone.0001545

Lawrence, C. B., Turnbull, A. V., and Rothwell, N. J. (1999). Hypothalamic control of feeding. *Curr. Opin. Neurobiol.* 6, 778–783. doi: 10.1016/S0959-4388(99)00032-X

Leveille, G. A., Romsos, D. R., Yeh, Y., and O'Hea, E. K. (1975). Lipid biosynthesis in the chick. A consideration of site of synthesis, influence of diet and possible regulatory mechanisms. *Poult. Sci.* 54, 1075–1093. doi: 10.3382/ps.0541075

Litt, J., Leterrier, C., Savietto, D., and Fortun-Lamothe, L. (2020). Influence of dietary strategy on progression of health and behaviour in mule ducks reared for fatty liver production. *Animal* 14, 1258–1269. doi: 10.1017/S1751731119003367

March, J. B., Sharp, P. J., Wilson, P. W., and Sang, H. M. (1994). Effect of active immunization against recombinant-derived chicken prolactin fusion protein on the onset of broodiness and photoinduced egg laying in bantam hens. *J. Reprod. Fertil.* 101, 227–233. doi: 10.1530/jrf.0.1010227

Masuda, K., Ooyama, H., Shikano, K., Kondo, K., Furumitsu, M., Iwakoshi-Ukena, E., et al. (2015). Microwave-assisted solid-phase peptide synthesis of neurosecretory protein GL composed of 80 amino acid residues. *J. Pept. Sci.* 21, 454–460. doi: 10.1002/psc.2756

Matsuura, D., Shikano, K., Saito, T., Iwakoshi-Ukena, E., Furumitsu, M., Ochi, Y., et al. (2017). Neurosecretory protein GL, a hypothalamic small secretory protein, participates in energy homeostasis in male mice. *Endocrinology* 158, 1120–1129. doi: 10.1210/en.2017-00064

Moore, J. B., Gunn, P. J., and Fielding, B. A. (2014). The role of dietary sugars and de novo lipogenesis in non-alcoholic fatty liver disease. *Nutrients* 6, 5679–5703. doi: 10.3390/nu6125679

Peirce, V., Carobbio, S., and Vidal-Puig, A. (2014). The different shades of fat. *Nature* 510, 76–83. doi: 10.1038/nature13477

Peña-Saldarriaga, L. M., Fernández-López, J., and Pérez-Alvarez, J. A. (2020). Quality of chicken fat by-products: lipid profile and colour properties. *Foods* 9:1046. doi: 10.3390/foods9081046

Price, E. R. (2010). Dietary lipid composition and avian migratory flight performance: development of a theoretical framework for avian fat storage. *Comp. Biochem. Physiol. A Mol. Integr. Physiol.* 157, 297–309. doi: 10.1016/j.cbpa.2010.05.019

Rehman, A., Arif, M., Sajjad, N., Al-Ghadi, M. Q., Alagawany, M., Abd El-Hack, M. E., et al. (2020). Dietary effect of probiotics and prebiotics on broiler performance, carcass, and immunity. *Poult. Sci.* 99, 6946–6953. doi: 10.1016/j.psj.2020.09.043

Rich, N., Reyes, P., Reap, L., Goswami, R., and Fraley, G. S. (2007). Sex differences in the effect of prepubertal GALP infusion on growth, metabolism and LH secretion. *Physiol. Behav.* 92, 814–823. doi: 10.1016/j.physbeh.2007.06.003

Scanes, C. G., Peterla, T. A., Campbell, R. M. (1994). Influence of adenosine or adrenergic agonists on growth hormone stimulated lipolysis by chicken adipose tissue *in vitro*. *Comp. Biochem. Physiol. Pharmacol. Toxicol. Endocrinol.* 107, 243–248. doi: 10.1016/1367-8280(94)90047-7

Scherer, T., O'Hare, J., Diggs-Andrews, K., Schweiger, M., Cheng, B., Lindtner, C., et al. (2011). Brain insulin controls adipose tissue lipolysis and lipogenesis. *Cell. Metab.* 13, 183–194. doi: 10.1016/j.cmet.2011.01.008

Seroussi, E., Knytl, M., Pitel, F., Elleder, D., Krylov, V., Leroux, S., et al. (2019). Avian expression patterns and genomic mapping implicate leptin in digestion and TNF in immunity, suggesting that their interacting adipokine role has been acquired only in mammals. *Int. J. Mol. Sci.* 20:4489. doi: 10.3390/ijms20184489

Seroussi, E., Pitel, F., Leroux, S., Morisson, M., Bornelöv, S., Miyara, S., et al. (2017). Mapping of leptin and its syntenic genes to chicken chromosome 1p. *BMC. Genet.* 18:77. doi: 10.1186/s12863-017-0543-1

Shikano, K., Bessho, Y., Kato, M., Iwakoshi-Ukena, E., Taniuchi, S., Furumitsu, M., et al. (2018a). Localization and function of neurosecretory protein GM, a novel small secretory protein, in the chicken hypothalamus. *Sci. Rep.* 8:704. doi: 10.1038/s41598-018-24103-w

Shikano, K., Taniuchi, S., Iwakoshi-Ukena, E., Furumitsu, M., Bentley, G. E., Kriegsfeld, L. J., et al. (2018c). Chronic subcutaneous infusion of neurosecretory protein GM increases body mass gain in chicks. *Gen. Comp. Endocrinol.* 265, 71–76. doi: 10.1016/j.ygcen.2017.11.010

Shikano, K., Kato, M., Iwakoshi-Ukena, E., Furumitsu, M., Matsuura, D., Masuda, K., et al. (2018b). Effects of chronic intracerebroventricular infusion of neurosecretory protein GL on body mass and food and water intake in chicks. *Gen. Comp. Endocrinol.* 256, 37–42. doi: 10.1016/j.ygcen.2017.05.016

Shikano, K., Iwakoshi-Ukena, E., Kato, M., Furumitsu, M., Bentley, G. E., Kriegsfeld, L. J., et al. (2019). Neurosecretory protein GL induces fat accumulation in chicks. *Front. Endocrinol.* 10:392. doi: 10.3389/fendo.2019.00392

Shikano, K., Iwakoshi-Ukena, E., Saito, T., Narimatsu, Y., Kadota, A., Furumitsu, M., et al. (2020). Neurosecretory protein GL induces fat accumulation in mice. *J. Endocrinol.* 244, 1–12. doi: 10.1530/JOE-19-0112

Stoyanovitch, A. G., Johnson, M. A., Clifton, D. K., Steiner, R. A., and Fraley, G. S. (2005). Galanin-like peptide rescues reproductive function in the diabetic rat. *Diabetes* 54, 2471–2476. doi: 10.2337/diabetes.54.8.2471

Tokushima, Y., Takahashi, K., Sato, K., and Akiba, Y. (2005). Glucose uptake in vivo in skeletal muscles of insulin-injected chicks. *Comp. Biochem. Physiol. B Biochem. Mol. Biol.* 141, 43–48. doi: 10.1016/j.cbpc.2005.01.008

Trott, K. A., Giannitti, F., Rimoldi, G., Hill, A., Woods, L., Barr, B., et al. (2014). Fatty liver hemorrhagic syndrome in the backyard chicken. *Vet. Pathol.* 51, 787–795. doi: 10.1177/0300985813503569

Ukena, K. (2018). Avian and murine neurosecretory protein GL participates in the regulation of feeding and energy metabolism. *Gen. Comp. Endocrinol.* 260, 164–170. doi: 10.1016/j.ygcen.2017.09.019

Ukena, K., Iwakoshi-Ukena, E., Taniuchi, S., Bessho, Y., Maejima, S., Masuda, K., et al. (2014). Identification of a cDNA encoding a novel small secretory protein, neurosecretory protein GL, in the chicken hypothalamic infundibulum. *Biochem. Biophys. Res. Commun.* 446, 298–303. doi: 10.1016/j.bbrc.2014.02.090

Wang, G., Kim, W. K., Cline, M. A., Gilbert, E. R. (2017). Factors affecting adipose tissue development in chickens: a review. *Poult. Sci.* 96, 3687–3699. doi: 10.3382/ps/pex184

Wang, S. H., Wang, W. W., Zhang, H. J., Wang, J, Chen, Y., Wu, S. G., et al. (2019). Conjugated linoleic acid regulates lipid metabolism through the expression of selected hepatic genes in laying hens. *Poult. Sci.* 98, 4632–4639. doi: 10.3382/ps/pez161

Conflict of Interest: The authors declare that the research was conducted in the absence of any commercial or financial relationships that could be construed as a potential conflict of interest.

Publisher's Note: All claims expressed in this article are solely those of the authors and do not necessarily represent those of their affiliated organizations, or those of the publisher, the editors and the reviewers. Any product that may be evaluated in this article, or claim that may be made by its manufacturer, is not guaranteed or endorsed by the publisher.

frontiers in Physiology

ORIGINAL RESEARCH
published: 10 November 2021
doi: 10.3389/fphys.2021.767739

The Full-Length Transcriptome Provides New Insights Into the Transcript Complexity of Abdominal Adipose and Subcutaneous Adipose in Pekin Ducks

*Dandan Sun†, Xiaoqin Li†, Zhongtao Yin and Zhuocheng Hou**

Department of Animal Genetics, Breeding and Reproduction, College of Animal Science and Technology, China Agricultural University, Beijing, China

Adipose tissues have a central role in organisms, and adipose content is a crucial economic trait of poultry. Pekin duck is an ideal model to study the mechanism of abdominal and subcutaneous adipose deposition for its high ability of adipose synthesis and deposition. Alternative splicing contributes to functional diversity in abdominal and subcutaneous adipose. However, there has been no systematic analysis of the dynamics of differential alternative splicing of abdominal and subcutaneous adipose in Pekin duck. In our study, the Pacific Biosciences (PacBio) Iso-Seq technology was applied to explore the transcriptional complexity of abdominal and subcutaneous adipose in Pekin ducks. In total, 143,931 and 111,337 full-length non-chimeric transcriptome sequences of abdominal and subcutaneous adipocytes were obtained from 41.78 GB raw data, respectively. These data led us to identify 19,212 long non-coding RNAs (lncRNAs) and 74,571 alternative splicing events. In addition, combined with the next-generation sequencing technology, we correlated the structure and function annotation with the differential expression profiles of abdominal and subcutaneous adipose transcripts. This study identified lots of novel alternative splicing events and major transcripts of transcription factors related to adipose synthesis. STAT3 was reported as a vital gene for adipogenesis, and we found that its major transcript is STAT3-1, which may play a considerable role in the process of adipose synthesis in Pekin duck. This study greatly increases our understanding of the gene models, genome annotations, genome structures, and the complexity and diversity of abdominal and subcutaneous adipose in Pekin duck. These data provide insights into the regulation of alternative splicing events, which form an essential part of transcript diversity during adipogenesis in poultry. The results of this study provide an invaluable resource for studying alternative splicing and tissue-specific expression.

Keywords: Pekin duck, abdominal adipose, subcutaneous adipose, full-length transcriptome, alternative splicing, proliferation, differentiation

OPEN ACCESS

Edited by:
Jie Wen,
Institute of Animal Sciences (CAAS), China

Reviewed by:
Hamada A. M. Elwan,
Minia University, Egypt
Mahmoud Madkour,
National Research Centre, Egypt

***Correspondence:**
Zhuocheng Hou
zchou@cau.edu.cn

†These authors have contributed equally to this work and share first authorship

Specialty section:
This article was submitted to Avian Physiology, a section of the journal Frontiers in Physiology

Received: *31 August 2021*
Accepted: *21 October 2021*
Published: *10 November 2021*

Citation:
Sun D, Li X, Yin Z and Hou Z (2021) The Full-Length Transcriptome Provides New Insights Into the Transcript Complexity of Abdominal Adipose and Subcutaneous Adipose in Pekin Ducks. Front. Physiol. 12:767739. doi: 10.3389/fphys.2021.767739

Abbreviations: Iso-Seq, isoform sequencing; AS, alternative splicing; PacBio, Pacific Biosciences; TFs, transcription factors; lncRNAs, long non-coding RNAs; GPDH, glycerol-3-phosphate dehydrogenase; KEGG, Kyoto Encyclopedia of Genes and Genomes; A3, alternative 3′ splice site; A5, alternative 5′ splice site; AF, alternative first exon; AL, alternative last exon, MX, mutual exclusive exon; RI, intron retention; SE, exon skipping; PPARγ, peroxisome proliferative activated receptor, gamma; STAT3, signal transducer and activator of transcription 3.

INTRODUCTION

Duck is one of the most widely distributed waterfowl in the world. After being artificially domesticated, Pekin duck stores a large amount of lipids in abdominal and subcutaneous adipose tissues (Kou et al., 2012; Lin et al., 2018), which is an ideal animal model for studying the fat deposition process of birds. The previous research showed that the lipid deposition patterns of the two tissues were different during the growth periods, the content of subcutaneous adipose tissue was higher than abdominal adipose tissue (Ding et al., 2012). However, the difference of molecular mechanism of lipid deposition with different adipose tissues of Pekin duck is still not clear.

Accompanied by the progress of sequencing technology, single-molecule sequencing was widely used in plant research, such as corn (Guo et al., 2021), rice (Du H. et al., 2017), clover (Chao et al., 2018), bamboo (Wang et al., 2017), etc. highlighting the huge advantages of identification of alternative splicing by full-length transcriptome. Single-molecule sequencing can directly obtain all information of the RNA sequence without assembly. However, there are fewer applications of single-molecule sequencing technology in bird research. For ducks, only PacBio Sequel was used to sequence the full-length transcriptome of eight Pekin duck tissues, and identified 35,031 alternative splicing events among 3,346 genes (Yin et al., 2019).

Fortunately, the assembly of the high-quality Mallard genome provides a vital support for us to accurately identify the isoforms and alternative splicing events of genes (NCBI, 2019). Alignment of different isoforms to the reference genome can effectively identify the modes of alternative splicing of genes, especially to improve the accuracy of long isoforms alignment (Kraft and Kurth, 2020). At present, the process of alternative splicing identification for species with reference genome is mature and reliable (Song et al., 2020; Xu et al., 2021). Combined analysis using transcriptome of short-read and long-read sequencing can further improve gene structure annotation, verify splicing sites, analyze tissue-specific or time-specific expression of different isoforms (Hu et al., 2021).

Another advantage of single-molecule transcriptome sequencing is the identification of TFs (Mazzocca et al., 2021) and lncRNAs (Troskie et al., 2021) in tissues, which is essential for the study of transcriptional regulation of fat-related biological processes. Adipogenesis is a process characterized by a complex network involving many TFs and lncRNAs that regulate gene expression (Squillaro et al., 2020). LncRNAs process multiple cellular functions and regulate chromatin remodeling, transcriptional and post-transcriptional events to affect gene expression. Recent investigations have shown that these molecules play a key role in regulating the development and activity of the white and brown/beige adipogenic process (Squillaro et al., 2020). Overexpression and knockout methods have been widely used to understand the contribution of TFs to adipocyte development, providing a basic strategy for studying the complexity of adipogenesis *in vitro*. So far, more than 12 transcription factors have been shown to play an important role in adipocyte development (Farmer, 2006; Lee et al., 2019; Ambele et al., 2020; Zhang et al., 2020). Comprehensive analysis of different isoforms of TFs during adipocyte multiple developmental time points can broaden our view of regulation of different adipocyte development in birds.

Therefore, we performed ISO-seq and RNA-Seq analysis on abdominal and subcutaneous adipocytes derived from the Pekin ducks. We addressed the proliferation and differentiation of the abdominal and subcutaneous adipocytes to identify potential differences in isoforms. The results of this analysis allowed us to expand our cognition of alternative splicing and differential expression which indicate different regulation modes, and provide a rich resource into the alternative splicing that forms an essential part of transcript diversity and complexity during abdominal and subcutaneous adipose synthesis and deposition. These results will facilitate future functional genomics studies and broaden our horizons of alternative splicing in poultry.

MATERIALS AND METHODS

Cell Culture and Differentiation Induction

The cell samples used in this experiment were primary preadipocytes isolated from the abdominal and subcutaneous adipose tissues of Pekin ducks provided by Beijing Golden Star Ltd. The experimental procedure was in accordance with the guidelines of the China agricultural University Animal Care Committee. The isolation method referred to the method used in our previous study (Wang et al., 2019). Ducks were sacrificed under deep anesthesia with sodium pentobarbital (Sigma). Abdominal and subcutaneous adipose tissue was collected under sterile conditions and washed with PBS. The clean adipose tissue was minced into fine sections and digested with 15 mL of digestion Solution [DMEM/F12 (Dulbecco's modified Eagle's medium/Ham's nutrient mixture F-12), 100 mM HEPES, 4% BSA, 2 mg/mL collagenase I (Invitrogen), pH 7. 4] for 65 min at 37°C in a water bath shaker. After incubation and stop digestion by growth medium (DMEM/F12, 10% FBS, 100 U/mL penicillin, and streptomycin). The mixture was filtered through nylon screens with 70 μm mesh openings to remove undigested tissue and large cell aggregates. The filtered suspensions were centrifuged at 300 × *g* for 10 min to separate floating adipocytes from preadipocytes. The harvested preadipocytes were then re-suspended with 10 mL of Blood Cell Lysis Buffer (Invitrogen), and incubated at room temperature for 10 min. The abdominal and subcutaneous preadipocytes isolated were inoculated in a growth medium. The cell culture was carried out at 5% CO_2 concentration, 37°C and 95% air humidity. Preadipocytes can be induced to differentiate by adding oleic acid to the growth medium (Shang et al., 2014).

Cell Counting Kit-8 Assay

Cell Counting Kit-8 (CCK-8) is a highly sensitive colorimetric assay for cell proliferation. In order to determine the difference of proliferation rate of preadipocytes in different parts of Pekin duck, abdominal and subcutaneous preadipocytes divided into 4×10^3 cells/well were seeded in 96 wells cell culture plate. 100 ul medium was added to each well. After induction for 24 h, 48 h, 96 h, 144 h, 192 h, and 240 h, 10 ul CCK-8 (Dojindo

Laboratories, JP) was added to the sample well, incubated at 37°C for 2 h, and the absorbance value at 450 nm was measured by the multi-function microplate reader (Infinite F200, CH).

Determination of the Activity of Glycerol-3-Phosphate Dehydrogenase

Glycerol-3-phosphate dehydrogenase (GPDH) is a rate-limiting enzyme of fatty acyl-CoA biosynthesis, and its enzyme activity increases significantly in the late stage of adipose differentiation, so it can be an index to characterize the differentiation degree of preadipocytes. In our experiment, abdominal and subcutaneous preadipocytes were selected at 0 h, 48 h, and 96 h after inducing differentiation. GPDH activity was conducted by using GPDH activity detection kit (Sigma, United States). Three biological replicates (n = 3) were included at each time point. Bovine serum albumin was used as the standard, BCA protein detection kit (Sigma, United States) was used to determine the protein concentration of cell culture homogenate (Matsubara et al., 2005).

Determination of Relative Lipid Droplet Content

Oil red O (Sigma, United States) staining could specifically stain the neutral lipid in cells because it can be highly dissolved in lipid. In our study, abdominal and subcutaneous preadipocytes were collected at 0 h, 24 h, 48 h, 72 h, 120 h, and 240 h after induction. Firstly, the cells were washed with PBS for three times, fixed with 10% (v/v) paraformaldehyde at room temperature for 30 min, then washed with PBS, stained with 1% oil red O for 40 min, removed the supernatant, and added 1 mL of 100% (v/v) isopropanol to obtain the extraction. The absorbance of the extraction at 500 nm was measured by the multi-function microplate reader (Infinite F200, CH) to characterize the relative lipid droplet content of each sample (Ramirezzacarias et al., 1992). Three biological replicates (n = 3) were included at each time point. The data were analyzed by independent sample students' test.

Sample Collection and RNA Preparation

All the Pekin duck used in this study were provided by Beijing Golden Star Ltd. Inc. The abdominal and subcutaneous adipose tissues were collected for the primary culture of the preadipocytes. The detailed method of primary cell culture is described in previous research (Matsubara et al., 2005). We collected −48 h (48 h before the initiation of differentiation), 0 h (the initiation of differentiation), 12 h, 24 h, 48 h, and 72 h of abdominal and subcutaneous preadipocytes for RNA extraction respectively. The cleaned adipocytes at all time points were homogenized separately (10 μg per sample) in TRIzol (Invitrogen, United States) and processed according to the manufacturer's protocol. RNA integrity number (RIN) values were calculated using an Agilent 2100 Bioanalyzer (Agilent Technologies, United States), and RNA concentration was assessed using a NanoDrop™ spectrophotometer (Thermo Fisher Scientific, United States). All RNA samples had an RNA integrity number value >8.0, and an optical density 260:280 ratio >1.9. RNA was then used for mRNA-seq using the Illumina sequencing platform.

Library Preparation and Pacific Biosciences Sequencing

Abdominal and subcutaneous preadipocytes at 72 h after differentiation were used for full-length transcriptome sequencing. −48 h, 0 h, 12 h, 24 h, 48 h, and 72 h of abdominal adipocytes were collected for RNA-Seq, and each time point included six biological replicates (n = 6).

We constructed two Iso-seq libraries for abdominal and subcutaneous adipocytes, which mixed equal amounts of RNA from each sample (5 μg per sample). The libraries were generated according to PacBio Iso-seq sequencing protocol. Briefly, qualified RNA was first obtained for sequence library construction, and the Clontech SMARTer cDNA synthesis kit with Oligo-dT primers was used to generate first-strand and second-strand cDNA from polyA mRNA. Size fractionation and selection (<4 kb and >4 kb) were performed using the BluePippin™ Size Selection System (Sage Science, Beverly, MA, United States). The full-length cDNA was repaired to construct the equal-mole hybrid library. The sequences without joints at both ends of the cDNA were removed. Two SMRT bell libraries were constructed with the Pacific Biosciences DNA Template Prep Kit 2.0 and SMRT sequencing was then performed using the Pacific Bioscience Sequel System. Approximately 5 μg of total RNA was used for mRNA-seq using the Illumina sequencing platform. Suitably sized fragments were selected using AMPure XP beads (Beckman Coulter, United States) to construct the cDNA libraries by PCR. Following construction, double-stranded cDNA libraries were sequenced on an Illumina HiSeq X-10 with PE150 mode (Novogene, CA, United States). The methods of library construction and sequencing were as described elsewhere (Wang et al., 2019). All sequencing data were deposited in National Centre for Biotechnology Information (NCBI) under the BioProject ID PRJNA723918. RNA-Seq data of multiple differentiation stages of subcutaneous preadipocytes were downloaded from NCBI (accession number: SRX4646736).

Data Analysis of ISO-Seq Raw Data

We obtained all raw data and processed it according to the Iso-seq standard pipeline[1]. Firstly, the sequence adapters were removed and the sequences shorter than 300 bp in length and less than 0.75 accuracy were filtered to obtain subreads. After quality control, the clean polymerase reads were processed to separate reads of an insert with pass >0 and accuracy >0.75. These reads of insert (ROI) were categorized into full-length, non-full-length, and chimeric reads using the SMRT Iso-Seq analysis pipeline. Full-length reads were determined by detecting poly(A) tails, 5′ primers and 3′ primers. ROI was divided into chimeric transcripts and non-chimeric transcripts according to whether there were sequencing primers in the sequence. The cd-hit-est (Li and Godzik, 2006) were used to remove redundant

[1]https://github.com/PacificBiosciences/IsoSeq_SA3nUP/wiki/Tutorial:-Installing-and-Running-Iso-Seq-3-using-Conda

sequences, and all reserved non-redundant sequences are used for downstream analysis.

Analysis of Transcript Structure and Alternative Splicing Identification

We aligned the non-redundant isoforms to the Mallard reference genome using GMAP (Wu and Watanabe, 2005) software (gmap.avx512), and sorted the aligned sam files and converted it into bam files using Samtools (Pertea et al., 2016) (v1.9). MatchAnnot (2015.06) software was used to compare the sorted alignment files with the annotation files of the Mallard genome. According to the exons information derived from annotation files, the different matching results were scored. The scores were marked into 0, 1, 2, 3, 4, and 5 to show the best matching transcripts.

In order to identify the alternative splicing (AS) events of the genes, firstly, The alignment file was filtered for 90% alignment coverage and 90% alignment identity and corresponding GFF files generated using cDNA_Cupcake (Gordon et al., 2015) (v18.1.0). SUPPA2 (Trincado et al., 2018) (v2.2.1) identified the AS events from annotation files (GFF/GTF format). The AS events were detected by SUPPA2 (v2.2.1), including alternative 5′ splice site or alternative 3′ splice site (A5/A3), skipping exon (SE), first exon/last exon alternative splicing (AF/AL), mutually exclusive exons (MX) and intron retention (RI).

Functional Annotation of the Full-Length Transcriptome

In order to annotate non-redundant full-length transcripts, we used Blast (McGinnis and Madden, 2004) (v2.2.26; e value = 1-e5) to align the sequences with the NT (NCBI nucleotide sequences), Swiss-Prot (A manually annotated and reviewed protein sequence database), and KOG (Karyotic Ortholog Groups) databases, and the results with the highest alignment score were used as the annotation. At the same time, we used the known transcription factors of human in the AnimalTFDB database to annotate full-length non-redundant sequences, which is essential for understanding the diversity of transcription factors in adipose. We performed GO (Gene Ontology) and KEGG (Kyoto Encyclopedia of Genes and Genome) functional annotations on the Metascape website (Zhou et al., 2019).

Differentially Expressed Isoforms in Abdominal and Subcutaneous Preadipocytes Cells

The clean reads of abdominal and subcutaneous preadipocytes cells were mapped to the Mallard reference genome (Anas_platyrhynchos.ASM874695v1.dna.toplevel.fa, Ensembl Release 104, CAU-Wild1.0) by Hisat2 (v2.1.0). Then samtools (v1.9) were used to sort and convert the comparison files. Stringtie (Pertea et al., 2016) (v2.0.6) was used to calculate the abundance of full-length transcripts in each sample by annotation files. The DEseq2 (v1.28.1) was used to analyze differentially expressed transcripts (DETs). Transcripts with the fold change >1.5 and FDR < 0.05 were considered DETs.

RNA Isolation and Real-Time Quantitative RT-PCR

The total RNA of abdominal and subcutaneous preadipocytes were extracted with e.z.n.a. total RNA kit II reaction kit (Omega Bio-Tek, United States). The RNA quality and quantity were determined using 1% agarose gel electrophoresis and NanoDrop 1000 (Thermo Scientific, Wilmington, DE, United States), and 2 μg of total RNA from abdominal and subcutaneous preadipocytes were reverse-transcribed with PrimeScript^{TM} RT reagent Kit with gDNA Eraser reaction kit (Takara bio, CA, United States) (Kang et al., 2017). Using total RNA as template and oligo (DT) primer, the first strand of cDNA was inverted. The specific primer pairs of transcripts were designed using the Primer-BLAST software[2]. We tested different annealing temperatures to optimize each pair of primers using conventional PCR to exclude the presence of unspecific products or primer dimer synthesis; the PCR products were analyzed by 2% agarose gel electrophoresis. Real-time fluorescence quantification PCR (RT-qPCR). Real-time fluorescence quantification PCR (RT-qPCR) was performed using TB green premix Ex Taq^{TM} fluorescence quantitative kit (Takara, CA, United States) and 7500 Fast Real-Time PCR system (Applied Biosystems, v2.0.6). Each qPCR reaction had a final volume of 20 μL of the reaction mixture, which consisted of 10 μL 2X TB Green Premix Ex Taq, 0.4 μL ROX Reference DyeII, 6.8 μL DNase/RNase-Free water, 0.4 μL forward and reverse specific primers for each transcript and 2 μL of cDNA template (Madkour et al., 2021). The PCR reaction conditions were pre denaturation at 95°C for 30 s, using 40 cycles (95°C for 5 s and 60°C for 30 s), and each sample was technically repeated three times. Fluorescence data were acquired at the end of the extension step. The primer sequences used in RT-qPCR reaction are shown in **Supplementary Table S5**. Results of the data were obtained by 7500 fast Real-Time PCR system. GAPDH was used as the internal reference gene in each sample to standardize the expression level of the transcripts, and the relative expression was calculated by $2^{-\Delta\Delta CT}$ relative quantitative method.

RESULTS

Phenotypic Difference of Abdominal and Subcutaneous Preadipocytes in Pekin Duck

Adipogenesis includes the proliferation and differentiation of preadipocytes. In order to compare the phenotypic differences between abdominal and subcutaneous preadipocytes in Pekin duck, the proliferation and differentiation ability of abdominal and subcutaneous preadipocytes in different stages were determined. CCK8 cell proliferation assay results showed that the proliferation rate of abdominal preadipocytes was higher than subcutaneous preadipocytes at 96 h, and the number of living cells in the abdominal preadipocytes group was significantly higher than that of subcutaneous preadipocytes at 144 h, 192 h,

[2]www.ncbi.nlm.nih.gov/tools/primer-blast

and 240 h ($P < 0.05$) (**Figure 1A**). These results show that the proliferation ability of abdominal preadipocytes was significantly stronger than subcutaneous preadipocytes. GPDH activity assay showed that GPDH activity of subcutaneous preadipocytes was significantly higher than abdominal preadipocytes at 0 h and 48 h ($P < 0.05$) (**Figure 1B**). Meanwhile, the relative lipid droplet content of subcutaneous and abdominal preadipocytes at different time points after induction showed that the lipid droplet content of subcutaneous preadipocytes was higher than abdominal preadipocytes at each stage, and the difference was significant at 48 h and 72 h ($P < 0.05$) (**Figure 1C**). These results indicate that the differentiation ability of subcutaneous preadipocytes is stronger than abdominal preadipocytes.

Generating Transcript Isoforms in Duck Adipose Tissues

In order to develop a comprehensive catalog of transcript isoforms, size-fractionated libraries (1–10 kb and 4–10 kb) were constructed. Combining the two libraries, a total of 41.78 GB of raw data was obtained, of which the raw data of abdominal and subcutaneous adipose were both 20.89 GB. For the sequencing data, after filtering and quality control, the number of circulating consensus sequences (CCS) of abdominal and subcutaneous adipose were 240,094 and 184,457, with an average length of 3,858 bp and 3,692 bp. As expected, the average length of these ROI (reads of insert) were consistent with the selected library size. In the study, we classified ROI and obtained full-length non-chimeric transcripts and non-full-length non-chimeric transcripts. 143,931 (59.95%) and 111,337 (60.36%) full-length non-chimeric transcripts of abdominal and subcutaneous adipose were obtained respectively (**Table 1**). The full-length non-chimeric transcripts of abdominal and subcutaneous adipose were combined and subjected to cluster, and 89,289 full-length non-redundant sequences were obtained, with an average length of 3,985 bp (**Figure 2**). All full-length non-redundant sequences were used for downstream analysis (**Supplementary Figure S9**).

Identify the Complex Isoforms of Transcription Factors and Long Non-coding RNAs

The transcription factor annotation of Mallard duck in AnimalTFDB3.0 database contains 865 annotated transcription factors from 71 families. The 4,544 full-length non-redundant transcripts in our study were annotated 527 transcription factors which belong to 64 gene families (**Supplementary Table S1**). In most eukaryotes, long-non-coding RNAs (lncRNAs) play an important role in regulating the protein-coding gene expression. In the study, we evaluated the coding potential of the transcripts and obtained 35,134 potential lncRNAs. Then we filtered the transcripts which have high similarity to the known protein sequences. Finally, 19,212 high-confidence lncRNAs were obtained. The length of most of the lncRNAs was 4,000–6,500 bp

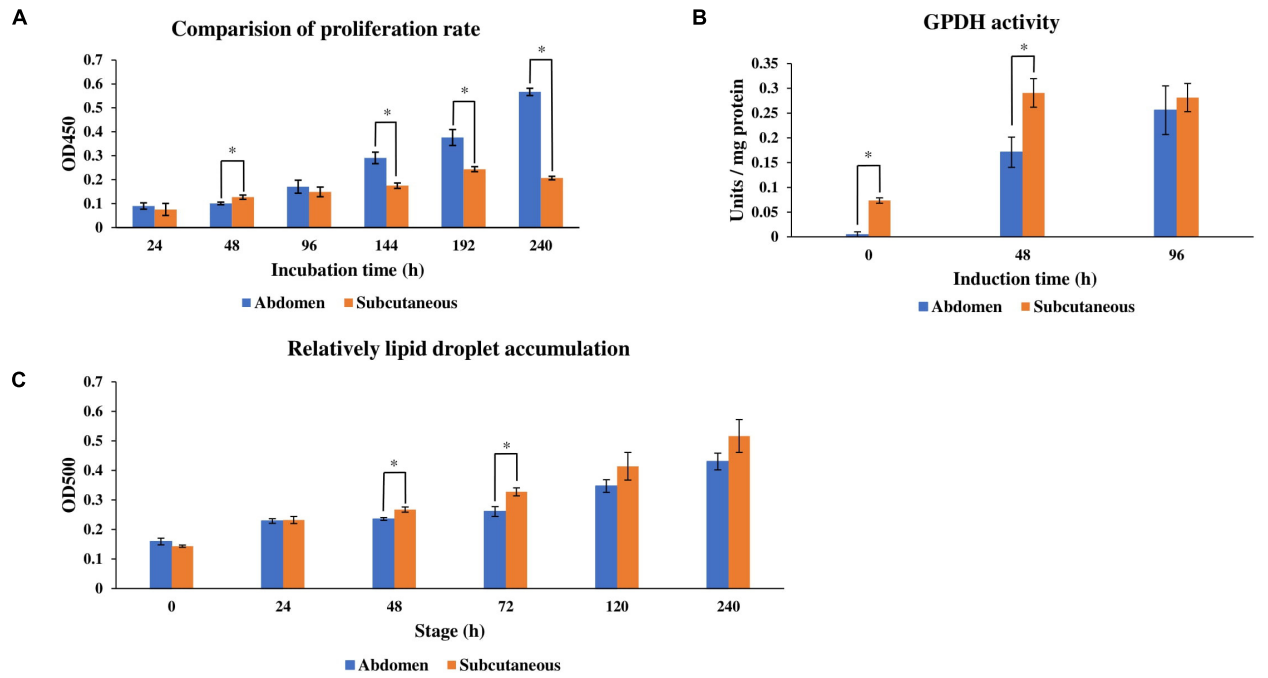

FIGURE 1 | Proliferation rate, GPDH activity, and intracellular lipid droplet accumulation of abdominal adipose and subcutaneous adipose of ducks cultured in differentiation medium (induction). **(A)** Relative quantification of cell proliferation rate within 24–240 h after induction. **(B)** Analysis of GPDH activity at 0 h, 48 h, and 96 h after induction. **(C)** Relative quantification of lipid droplet accumulation within 240 h after induction. The line graph represents the SD of the average ($n = 3$). *Indicates that there is a statistically significant difference between abdominal and subcutaneous preadipocytes at the same time ($P < 0.05$). The statistics data of subcutaneous preadipocytes in panels **(B,C)** were cited by Wang et al. (2019).

TABLE 1 | Full length transcript data information.

Process	Information	Abdominal	Subcutaneous
Sequencing data output	Cell number	1	1
	cDNA size	1–10 k, 4–10 k	1–10 k, 4–10 k
	Polymerase read bases	20.89	20.89
	Polymerase reads	545895	545895
	Polymerase read N50	68983	68983
	Polymerase read length	38266	38266
ROI	cDNA size	1–10 k	1–10 k
	Reads of insert	240094	184457
	Read bases of insert	926290963	681050538
	Mean read length of insert	3858	3692
	Mean read quality of insert	0.9775004	0.9783864
	Mean number of passes	15	16
Classify	cDNA size	1–10 k	1–10 k
	Number of reads of insert	240094	184457
	Number of five–five prime reads	7347	4919
	Number of three–three prime reads	79460	60854
	Number of adaptor reads	65	81
	Number of filtered short reads	65	81
	Number of full-length non-chimeric reads	143931	111337

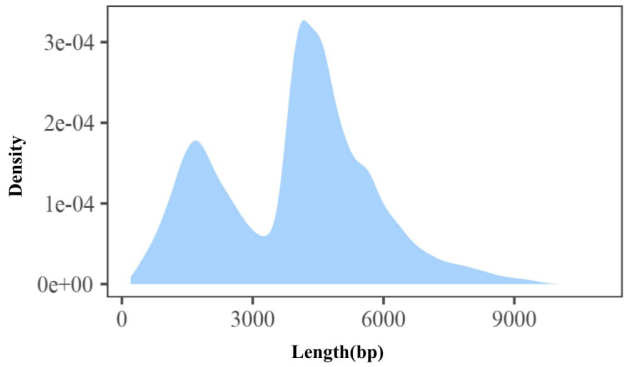

FIGURE 2 | Length distribution of full-length non-redundant transcript.

(**Figure 3A**), with an average length of 4,469 bp, which is significantly longer than the known length of lncRNAs (1,284 bp). Because lncRNAs is involved in a variety of cellular processes, the diversity and expression difference (**Figure 3B**) of lncRNAs reflects the complexity of regulatory processes in adipose tissue.

Structure Annotation

In this study, the amount of multi-exon transcripts were sequenced using PacBio Iso-Seq. At the isoform level, there were 29,320 transcripts from 18,490 wild duck gene models. By comparing with wild duck reference annotation, 62,469 full-length non-redundant transcripts were identified from 11,834 Pekin duck gene models. We found that 71.15% of the genes in the original annotation were defined by a single transcript isoform. After analysis of the Iso-Seq data, only 42.21% of the genes are defined by only a single transcript. The percentage of gene models with at least three isoforms in the full-length non-redundant transcripts was higher than that in the reference transcripts (42.52% vs. 12.83%). On average, there were 5.28 transcripts per gene, compared with 1.59 transcripts in the reference notes (**Figure 4A**). In addition, the full-length non-redundant sequences were annotated in the study. The different scores in the annotation results correspond to the consistency with the known reference transcripts (**Figure 4B**). The sequences with matching degree < 2 were poor matching, accounting for 35.35%, while the sequences with potential alternative splicing (score ≥ 2) accounted for 64.66%. These results indicate that the full-length non-redundant transcripts can predict new transcripts based on known transcripts. The exons differences in the number and structure of transcripts show that the AS increases the transcriptome complexity significantly in Pekin ducks.

Identification of Alternative Splicing Events Based on Mallard Genome

Alternative splicing can increase protein diversity by changing the protein structure. In the full-length non-redundant sequences, 74,571 AS events were identified from 4,046 gene models (**Figure 5** and **Table 2**). The 3′ and 5′ AS (A3/A5) were the main AS events, accounting for 66.59%. The rest AS events included RI (11.80%), SE (5.89%), AF (8.87%), Al (4.51%), and MX (2.33%). A3, A5, IR, and SE AS events are common in genes. Most genes have only one AS type, while only 71 genes have each type. We found that AS events are correlated with the number of exons. With the increase of exons, AS enhanced the diversity and complexity of abdominal and subcutaneous adipose transcripts in Pekin duck.

Functional Annotation of Transcript Isoforms

In order to obtain the annotation of the full-length transcripts, we annotated full-length transcripts of abdominal and subcutaneous adipose of Pekin duck by NT, Swiss-Prot, and KOG databases for further study of gene function (**Figure 6**, **Supplementary Table S2**, and **Supplementary Figures S1, S2**). In NT, Swiss-Prot, and KOG databases, at least 88,388 (98.99%) transcripts were annotated from 89,289 full-length transcripts. The results showed that 88,349 (98.94%) transcripts were annotated in NT database, and 58,149 (65.43%) transcripts were annotated in all databases. The above results show the reliability and accuracy of the full-length transcripts. All genes corresponding to full-length transcripts were subjected to functional annotation, about 9,495 genes were annotated by GO and KEGG. In GO and KEGG databases, the majority gene symbols of abdominal and subcutaneous adipose were represented by protein binding (671), nucleoplasm (379), and protein ubiquitination (42) in 'Molecular Function' category, 'Cellular Component' category, and 'Biological Process' category, analysis

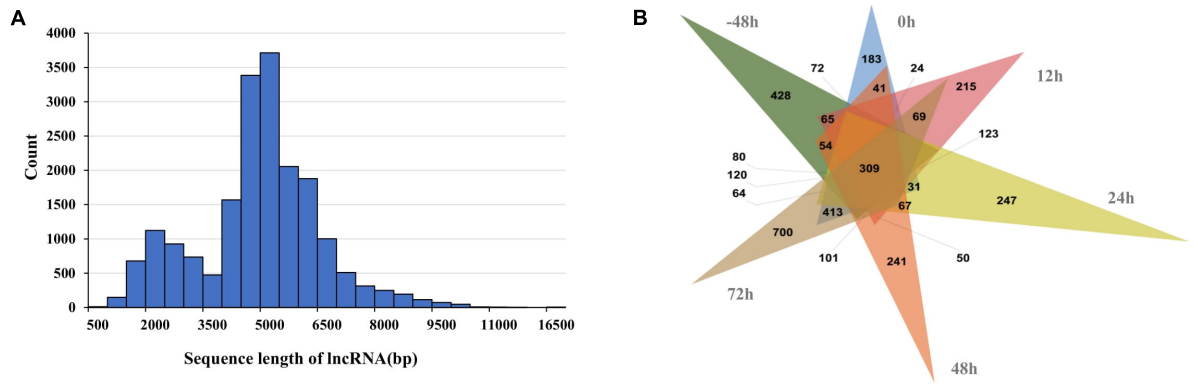

FIGURE 3 | (A) Length distribution and full-length transcripts of lncRNAs in abdominal and subcutaneous adipose. **(B)** The number of DET of lncRNA in abdominal adipose and subcutaneous at each time point.

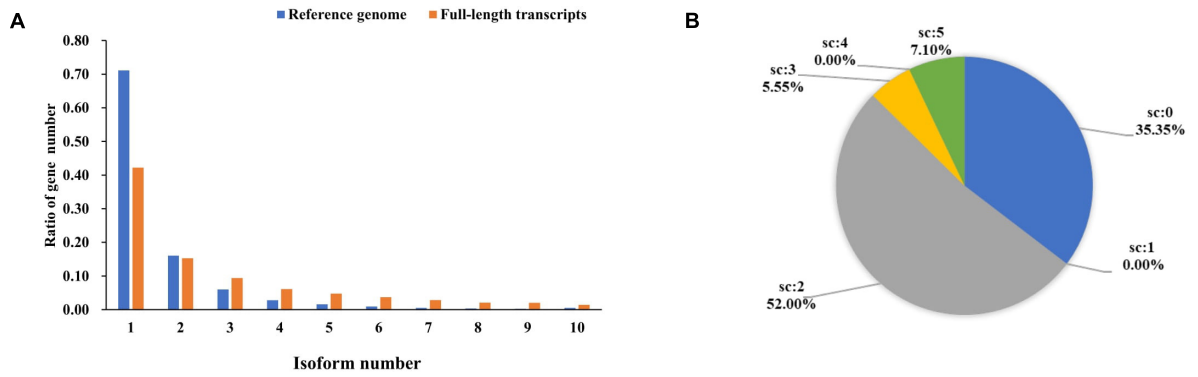

FIGURE 4 | (A) Quantity distribution of mallard duck reference genome and full-length non-redundant transcripts. **(B)** Proportional distribution of structural annotations of full-length transcripts. (Score = 0, isoform overlaps gene, but little or no exon congruence; Score = 1, Some exons overlap, overlaps are 1-for-1 where they exist; Score = 2, The best match among all transcripts with score of 1; Score = 3, One-for-one exon match, but sizes of internal exons disagree; Score = 4, Like 5, but leading and trailing edge sizes differ by a larger amount than the score-5 transcript found for this gene; Score = 5, Iso-Seq exons match annotation exons one-for-one. Sizes agree except for leading and trailing edges).

of the KEGG annotations revealed that most genes were enriched in 'metabolic' pathway (72).

Specific Expression of Isoforms in Different Types of Adipocytes

Our study explored 36 mRNA-Seq libraries to investigate expression level differences between abdominal and subcutaneous adipocytes at six time points. We identified 14054, 12226, 11995, 12854,12255, and 18627 DETs at −48 h, 0 h, 12 h, 24 h, 48 h, and 72 h (**Figure 7**). The data (**Supplementary Table S4**) indicate that there may be differences in the number and function of transcriptional regulators before and after differentiation, which reflects the complexity of the regulation mode in the process of Pekin duck fat deposition.

Discovery of a Specific Transcription Factor During Fat Development

Many transcription factors play vital roles in the regulatory pathways of preadipocyte STAT3 is signal transduction and transcriptional activator. It is a crucial factor for the biological functions of eukaryotes, such as embryonic development, immunity, hematopoiesis, and cell migration (Liu et al., 2021). STAT3 regulates VSTM2A (V-set and transmembrane domain-containing 2A) (Al Dow et al., 2021) and JAK (Janus kinase) (Zhang et al., 2011) in preadipocytes and promotes white adipose tissue development. According to the results of AS events and annotation of full-length transcripts in the study, STAT3 has 17 isoforms and 4 alternative splicing events, including A5, A3, AF, and RI (**Figure 8**). The length and number of exons vary among different transcripts. These transcripts contain 5–26 exons, and the transcript with the largest number of exons has two more exons than STAT3 in the reference genome. The number of STAT3 improved the richness of the transcript AS. For example, STAT3-12 contains 24 exons and 4 types of AS. The main AS events of STAT3 are A3 and A5, which involve trans-activated domain and tandem donor reflecting the diversity of transcripts structure.

Total transcripts of STAT3 show various expression patterns during differentiation (**Figures 9**, **10**). STAT3-2, STAT3-3, and

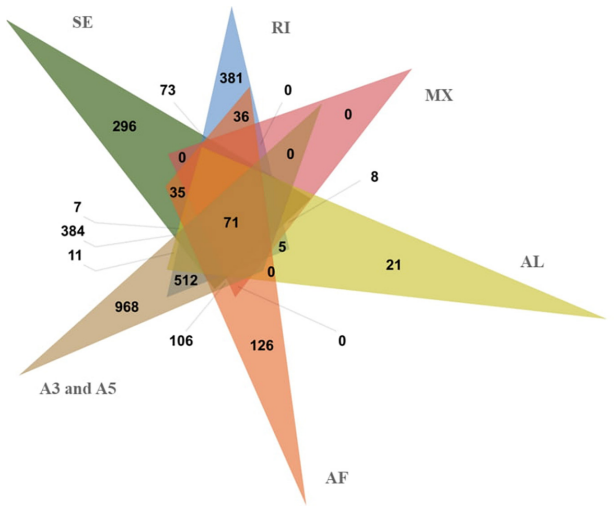

FIGURE 5 | Alternative splice event distribution of abdominal and subcutaneous adipose.

TABLE 2 | The number of alternative splicing (AS) event.

Items	Gene counts (%)	Event counts (%)
A3	2064 (51.01%)	23873 (32.01%)
A5	2283 (56.43%)	25788 (34.58%)
AF	848 (20.96%)	6611 (8.87%)
AL	134 (3.31%)	3362 (4.51%)
MX	198 (4.89%)	1742 (2.33%)
RI	1906 (47.11%)	8802 (11.80%)
SE	1733 (42.83%)	4393 (5.89%)
Total	4046	74571

A3, alternative 3′ splice site; A5, alternative 5′ splice site; AF, alternative first exon; AL, alternative last exon; MX, mutual exclusive exons; RI, intron retention; SE, exon skipping.

STAT3-13 have low-level gene-expression, and STAT3-1 of abdominal and subcutaneous adipocytes are expressed at a considerably higher level than any minor transcripts of the STAT3 during all stages. STAT3-1 has one more exon at the 3′ than the SATA3 in the reference genome. At the early stage of differentiation (12 h, 24 h, and 48 h), the expression level of STAT3-1 in subcutaneous adipocytes was significantly higher than that in abdominal adipocytes ($P < 0.05$). STAT3-10, STAT3-15, STAT3-16, and STAT3-17 have significant difference during preadipocytes differentiation ($P < 0.05$). In abdominal and subcutaneous adipocytes, the expression of STAT3-4, STAT3-8, STAT3-10, STAT3-12, STAT3-16, and STAT3-17 were significantly different at several consecutive stages ($P < 0.05$). These results reflect that the differences in the expression of transcripts lead to the complexity of gene expression among different tissues, which is a potential factor causing the functional complexity of different tissues. Our study analyzed the expression profiles of other transcription factors, such as PPARγ (**Supplementary Figures S3, S4**), BCL6 (**Supplementary Figures S5, S6**), and GATA2 (**Supplementary Figures S7, S8**). The results

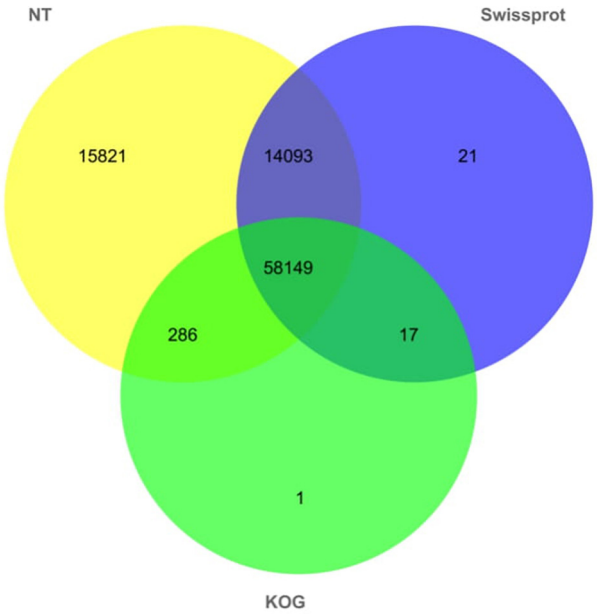

FIGURE 6 | Number distribution of functional notes of full-length non-redundant transcripts of abdominal and subcutaneous adipose in NT, KOG, and Swiss-Prot databases.

indicate that the differences in transcript abundance may be mostly attributed to splicing.

RT-qPCR Assays for Validation of Isoforms

In the current study, three samples of abdominal and subcutaneous preadipocytes from 0 h were randomly selected for RT-qPCR to validate some key genes involved in the proliferation and differentiation of preadipocytes. Including PPARD (Peroxisome Proliferator-Activated Receptor Delta), SMAD3 (SMAD Family Member 3), STAT3, FHL2 (Four and A half LIM domains 2), and SLC16A2 (Solute Carrier Family 16 Member 2) (**Figure 11**). We choose two transcripts with the highest expression (transcript 1) and lower expression (transcript 2) for each gene. The expression patterns of these transcripts were highly consistent with the mRNA-Seq results. The results showed that transcription factors usually have an obvious dominant expression transcript in adipocytes, which may mainly perform gene functions.

DISCUSSION

Duck is an important economic waterfowl, and it is also a model animal for adipose deposition and immune research (Li and Lu, 2011; Zheng et al., 2014). Although the duck genome sequence has been released, its information of genome and transcriptome still needs to be further explored. At present, the research related to transcriptome has been reported in ducks. Wang et al. (2019) analyzed the dynamic transcriptome information of the proliferation and differentiation of subcutaneous preadipocytes,

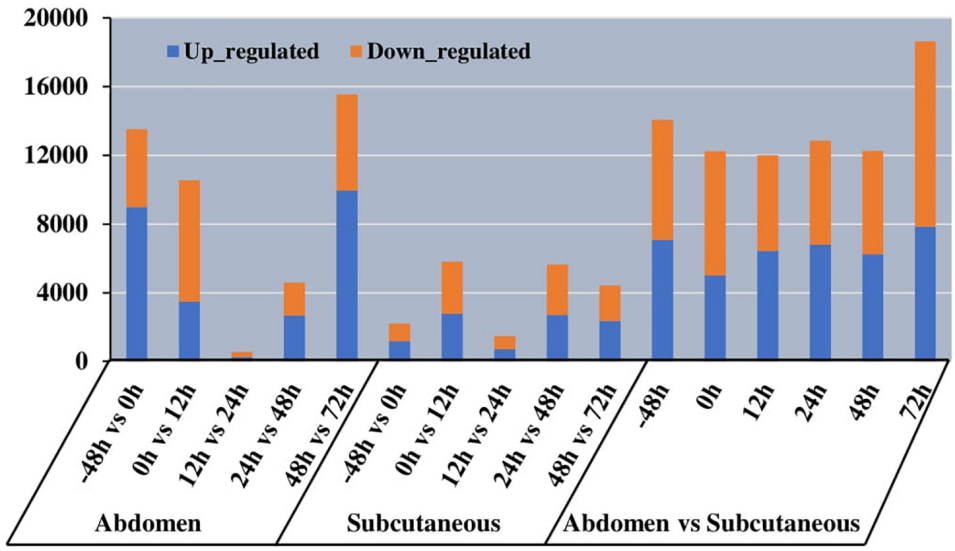

FIGURE 7 | Histogram of the number of different expression transcript (DET) in different tissues at different time of abdominal and subcutaneous adipose.

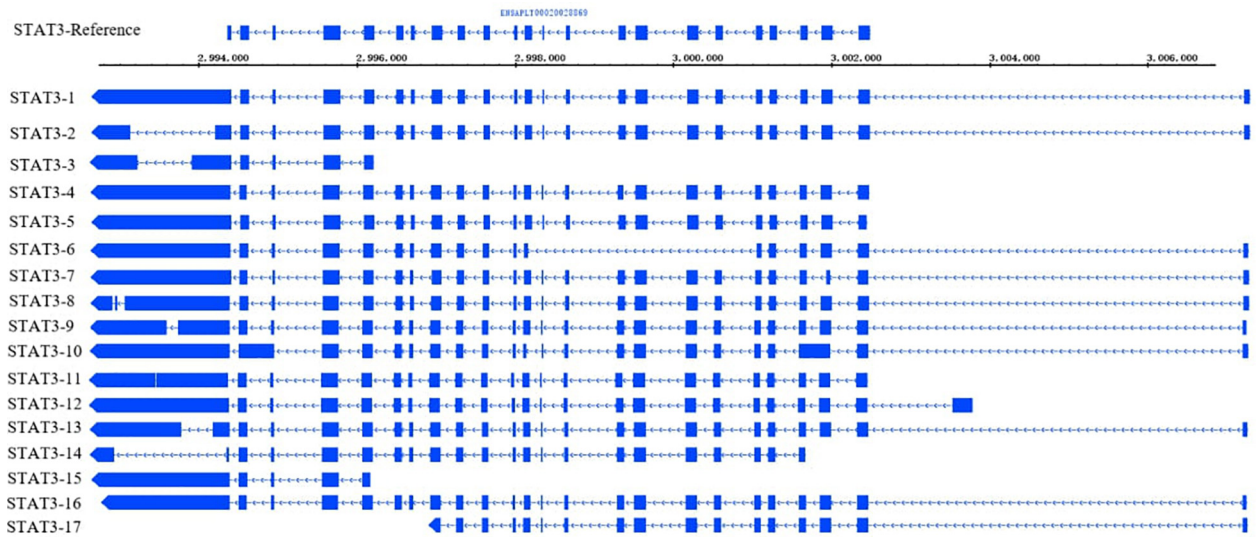

FIGURE 8 | STAT gene transcripts structure diagram.

Qiu et al. (2018) and Xu et al. (2019) discussed the relationship between gene expression and adipose distribution. These findings lay the foundation for understanding duck fat synthesis and deposition. These studies only paid attention to the expression changes of transcripts, but not reported the above alternative splicing and SNP. Yin et al. (2019) published the full-length transcripts information of the pectoral muscle, heart, uterus, ovary, testis, hypothalamus, pituitary gland, and 13-day-old embryos of Pekin duck, and identified lncRNAs and AS events, which improved genome annotations and informative basis with the functional genomics of other birds. The drawback with this study is that it lacks information about the full-length transcripts of adipose, which hinders the accurate analysis of the gene function related to the adipogenesis of Pekin duck. In our study, Iso-seq analysis was performed on the abdominal and subcutaneous adipocytes of Pekin duck, 62,469 full-length transcripts were identified from 11,834 gene models, transcription factors, lncRNAs, and alternative splicing events were identified to facilitate functional genomics in adipose of Pekin duck. The number of transcription factors identified was less than the total transcription factors of wild ducks, which might be due to some transcripts could not be detected because of the specificity of adipose tissue expression (Rodriguez et al., 2020).

Exploring functional differences requires accurate transcript annotations. Alternative splicing increases the richness of transcripts, which has great significance for functional genomics

FIGURE 9 | Expression level of new transcripts of STAT gene at different time points of differentiation. Statistical change was determined by Student's test (two tailed), $*P < 0.05$; $**P < 0.01$; $***P < 0.001$; $****P < 0.0001$ as fat.

research. In this study, 74,571 AS events were identified from 4,046 gene models. A5 and A3 involving 2,283 and 2,064 genes had the highest ratio of alternative splicing events. Xu et al. (2016) used the next-generation sequencing to analyze the AS of breast muscle and subcutaneous adipose. Their results showed that A5 and A3 were the main AS events, which were consistent with the results of our study. But the results of this study are different with Yin et al. (2019). Their main AS types are RI and SE. The results of this study and Yin et al. (2019) reflect the differences in the types of AS between adipose tissue and other tissues. AS increases the complexity and diversity of transcripts, which may be the basis for the inheritance and regulation of tissues and organs performing different functions. The AS events identified in this study provide clues for subsequent studies, such as tissue-specific expression, a difference of homologous genes function in different tissues, and so on.

Transcription factors play an important regulatory role in the process of adipogenesis. As an important transcription factor, STAT3 can be activated under the action of IL-11 (interleukin-11) to promote the proliferation and migration of mouse adipose mesenchymal stem cells (Yang et al., 2020), and can synergistic effect with HMGA2 (High Mobility Group AT-Hook 2) to promote the process of adipogenesis in mice (Yuan et al., 2017). In humans, STAT3 can activate the expression of CD36 (CD36 molecule) and promote preadipocyte differentiation and lipid deposition (Rozovski et al., 2018; Su et al., 2020). In poultry, the JAK-STAT signaling pathway regulates the proliferation and apoptosis of chicken chondrocytes (Chen et al., 2021) and embryo development (Zhang et al., 2017), and STAT3 affects the angiogenesis of chorioallantoic membrane in female chicken embryos by mediating the VEGF/NO (vascular endothelial growth factor/nitric oxide) pathway (Su et al., 2012). STAT3 encodes different transcripts (Qi and Yang, 2014), and it was found that STAT3α2 generated by exon skipping may play a major role in STAT3 signal transduction on grass carp, which is consistent with the function of STAT3α1 (Du L. et al., 2017). In our study, STAT3-1 was the major expression transcript, which was generated by A3 and A5 alternative splicing. Studies have shown that STAT3 can affect preadipocyte differentiation by regulating the activity of the PPARγ promoter and regulate the process of adipogenesis (Su et al., 2020). The specific function of STAT3-1 needs to be further confirmed. For example, the three exons at the 3′ ends of STAT3 of the reference genome belong to the nitrogen-terminal domain affecting protein interaction (Schwalie et al., 2018). Compared with the reference genome, there is an extra exon at the 3′ ends of STAT3 in full-length transcripts, which may affect the binding affinity to the target genes. The expression of STAT3-1 of Pekin duck' s subcutaneous at 12 h, 24 h, and 48 h was higher than that of abdominal fat ($P < 0.05$), which may be one of the factors affecting the differentiation ability of subcutaneous than abdominal preadipocytes. Therefore, in this study, A3 of STAT3-1 was a potential key AS event in the regulation of preadipocyte differentiation. The transcription factors can regulate the binding of other genes, promote or inhibit the differentiation of preadipocytes, but the binding efficiency of

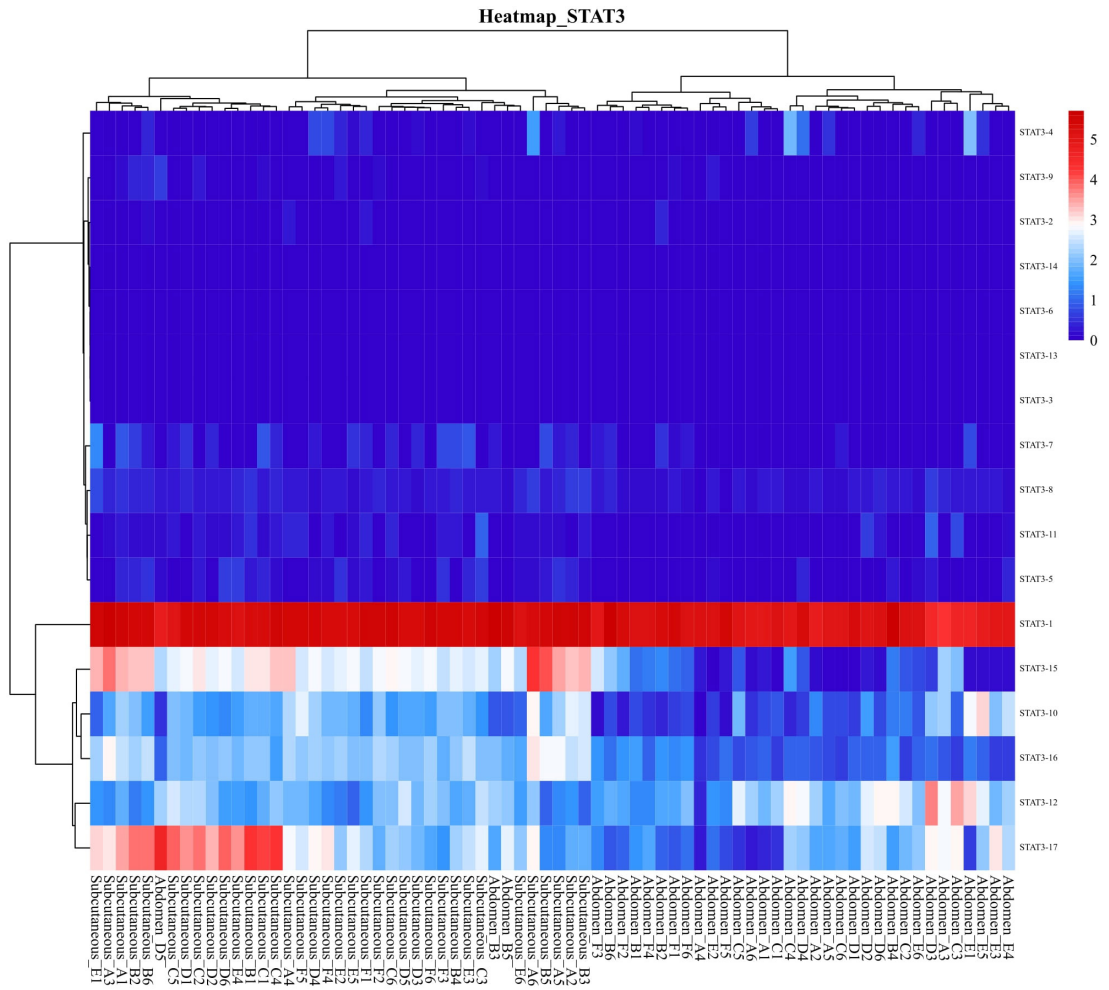

FIGURE 10 | Heatmap of STAT gene transcripts expression.

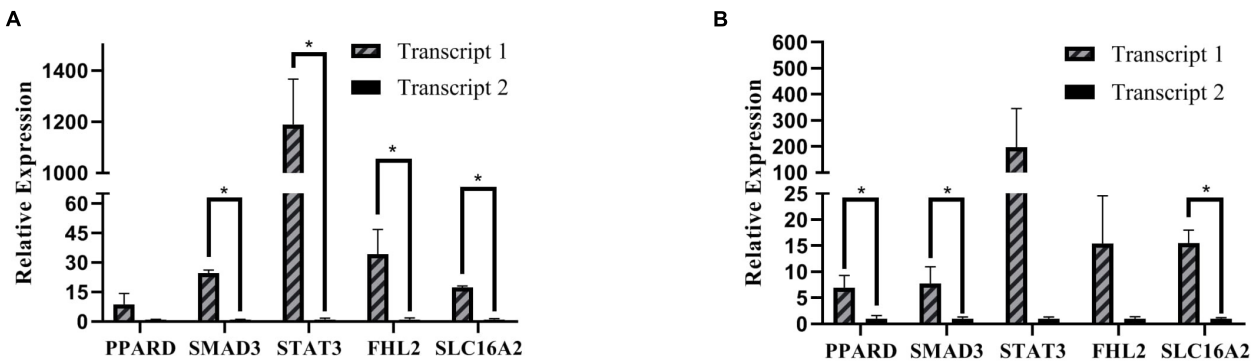

FIGURE 11 | RT-qPCR relative expression. **(A)** Expression of different transcripts of subcutaneous adipose. **(B)** Expression of different transcripts of abdominal adipose, $^*P < 0.05$.

different transcripts of the same gene is also different. Alternative splice-form plays a key role in the process of gene regulation by generating different transcripts. Further studies can be carried out through knockdown, knockout, and overexpression experiments to explore the specific functions of different transcripts in adipogenesis.

Previous studies showed that abdominal and subcutaneous adipose have different transcriptional characteristics

(Burl et al., 2018; Schwalie et al., 2018; Merrick et al., 2019). The process of adipogenesis is characterized by changes in cell morphology (Sebo and Rodeheffer, 2019). The shape of the cells evolves from flat to round cells with triacylglycerol-rich lipid droplets. The material and energy requirements for cytoskeleton reorganization and accumulation of lipids are necessary (Del et al., 2019; Calvo and Izquierdo, 2021; Zhang et al., 2021). Cytoskeleton is composed of protein fibers, which is consistent with the protein binding process in our function annotation study. Subcutaneous and abdominal adipose mediate the adipose synthesis and immune regulation, such as fibrosis, lipid deposition, angiogenesis, and inflammation (Caputo et al., 2021). The above processes are closely related to metabolism, which is consistent with the KEGG annotation results of our study.

In summary, Iso-seq and RNA-Seq conducted a global analysis for the differentiation process of the abdominal and subcutaneous preadipocytes in Pekin duck. This study provided full-length transcripts, AS events, lncRNAs and transcription factors, analyzed expression levels at different stages of preadipocyte differentiation, and initially explored the regulation of AS of abdominal and subcutaneous adipose in Pekin duck. These results definitively provide valuable information for the alternative splicing, gene expression and regulation of adipose tissue in Pekin duck. Furthermore, the information generated will promote future investigations of functional genomics.

DATA AVAILABILITY STATEMENT

The datasets presented in this study can be found in online repositories. The names of the repository/repositories and accession number(s) can be found below: NCBI BioProject PRJNA723918/SRX4646736.

ETHICS STATEMENT

The animal study was reviewed and approved by Committee of China Agricultural University.

AUTHOR CONTRIBUTIONS

ZH conceived and designed the experimental plan. DS and XL collected samples and measurement data. DS and ZY participated in bioinformatics analyses. DS, XL, ZY, and ZH drafted and revised this manuscript. All authors read and approved the final manuscript.

FUNDING

This work was supported by the earmarked fund for Modern-industry Technology Research System (CARS-42-9), the Leading Technology of Modern Agricultural Science and Technology City (Z181100002418008), Future functional food project of CAU (SJ2021002003), and National Natural Science Foundation of China (31972525) awarded to ZH.

ACKNOWLEDGMENTS

We thank Beijing Golden Star Inc. for providing the Pekin ducks. We thank Wang Zheng for providing data on GAPDH activity and lipid droplet accumulation in subcutaneous adipose.

SUPPLEMENTARY MATERIAL

The Supplementary Material for this article can be found online at: https://www.frontiersin.org/articles/10.3389/fphys.2021.767739/full#supplementary-material

REFERENCES

Al Dow, M., Silveira, M. A. D., Poliquin, A., Tribouillard, L., Fournier, E., Trebaol, E., et al. (2021). Control of adipogenic commitment by a STAT3-VSTM2A axis. *Am. J. Physiol.-Endocrinol. Metab.* 320, E259–E269. doi: 10.1152/ajpendo.00314.2020

Ambele, M. A., Dhanraj, P., Giles, R., and Pepper, M. S. (2020). Adipogenesis: a complex interplay of multiple molecular determinants and pathways. *Int. J. Mol. Sci.* 21:4283. doi: 10.3390/ijms21124283

Burl, R. B., Ramseyer, V. D., Rondini, E. A., Pique-Regi, R., Lee, Y. H., and Granneman, J. G. (2018). Deconstructing adipogenesis induced by beta3-Adrenergic receptor activation with Single-Cell expression profiling. *Cell Metab.* 28, 300–309. doi: 10.1016/j.cmet.2018.05.025

Calvo, V., and Izquierdo, M. (2021). Role of actin cytoskeleton reorganization in polarized secretory traffic at the immunological synapse. *Front. Cell Dev. Biol.* 9:629097. doi: 10.3389/fcell.2021.629097

Caputo, T., Tran, V. D. T., Bararpour, N., Winkler, C., Aguileta, G., Trang, K. B., et al. (2021). Anti-adipogenic signals at the onset of obesity-related inflammation in white adipose tissue. *Cell. Mol. Life Sci.* 78, 227–247. doi: 10.1007/s00018-020-03485-z

Chao, Y., Yuan, J., Li, S., Jia, S., Han, L., and Xu, L. (2018). Analysis of transcripts and splice isoforms in red clover (Trifolium pratense L.) by single-molecule long-read sequencing. *BMC Plant Biol.* 18:300. doi: 10.1186/s12870-018-1534-8

Chen, S., Jahejo, A. R., Nabi, F., Ahmed, S., Zhao, J., Yu, J., et al. (2021). Janus kinase/signal transducer and activator of transcription signaling pathway-related genes STAT3, SOCS3 and their role in thiram induced tibial dyschondroplasia chickens. *Res. Vet. Sci.* 136, 25–31. doi: 10.1016/j.rvsc.2021.01.024

Del, C. U., Norkett, R., and Gelfand, V. I. (2019). Unconventional roles of cytoskeletal mitotic machinery in neurodevelopment. *Trends Cell Biol.* 29, 901–911. doi: 10.1016/j.tcb.2019.08.006

Ding, F., Pan, Z., Kou, J., Li, L., Xia, L., Hu, S., et al. (2012). *De novo* lipogenesis in the liver and adipose tissues of ducks during early growth stages after hatching. *Comp. Biochem. Physiol. B Biochem. Mol. Biol.* 163, 154–160. doi: 10.1016/j.cbpb.2012.05.014

Du, H., Yu, Y., Ma, Y., Gao, Q., Cao, Y., Chen, Z., et al. (2017). Sequencing and *de novo* assembly of a near complete indica rice genome. *Nat. Commun.* 8:15324. doi: 10.1038/ncomms15324

Du, L., Zhou, H., Qin, L., Wei, H., Zhang, A., Yang, K., et al. (2017). Identification and functional evaluation of two STAT3 variants in grass carp: implication for the existence of specific alternative splicing of STAT3 gene in teleost. *Dev. Comp. Immunol.* 76, 326–333. doi: 10.1016/j.dci.2017.07.008

Farmer, S. R. (2006). Transcriptional control of adipocyte formation. *Cell Metab.* 4, 263–273. doi: 10.1016/j.cmet.2006.07.001

Gordon, S. P., Tseng, E., Salamov, A., Zhang, J., Meng, X., Zhao, Z., et al. (2015). Widespread polycistronic transcripts in fungi revealed by Single-Molecule mRNA sequencing. *PLoS One* 10:e132628. doi: 10.1371/journal.pone.0132628

Guo, L., Lu, Y., Li, P., Chen, L., Gou, W., and Zhang, C. (2021). Effects of delayed harvest and additives on fermentation quality and bacterial community of corn stalk silage. *Front. Microbiol.* 12:687481. doi: 10.3389/fmicb.2021.687481

Hu, T., Chitnis, N., Monos, D., and Dinh, A. (2021). Next-generation sequencing technologies: an overview. *Hum. Immunol.* 82, 801–811. doi: 10.1016/j.humimm.2021.02.012

Kang, S. W., Madkour, M., and Kuenzel, W. J. (2017). Tissue-Specific expression of DNA methyltransferases involved in Early-Life nutritional stress of chicken, gallus gallus. *Front. Genet.* 8:204. doi: 10.3389/fgene.2017.00204

Kou, J., Wang, W. X., Liu, H. H., Pan, Z. X., He, T., Hu, J. W., et al. (2012). Comparison and characteristics of the formation of different adipose tissues in ducks during early growth. *Poultry Sci.* 91, 2588–2597. doi: 10.3382/ps.2012-02273

Kraft, F., and Kurth, I. (2020). Long-read sequencing to understand genome biology and cell function. *Int. J. Biochem. Cell B* 126:105799. doi: 10.1016/j.biocel.2020.105799

Lee, J., Schmidt, H., Lai, B., and Ge, K. (2019). Transcriptional and epigenomic regulation of adipogenesis. *Mol. Cell. Biol.* 39, e601–e618. doi: 10.1128/MCB.00601-18

Li, G., and Lu, L. (2011). Structural homologies of major immune-related genes between duck and chicken: implications on differential avian resistance against influenza virus. *Braz. J. Poultry Sci.* 13, 1–8.

Li, W., and Godzik, A. (2006). Cd-hit: a fast program for clustering and comparing large sets of protein or nucleotide sequences. *Bioinformatics* 22, 1658–1659. doi: 10.1093/bioinformatics/btl158

Lin, F. B., Zhu, F., Hao, J. P., Yang, F. X., and Hou, Z. C. (2018). *In vivo* prediction of the carcass fatness using live body measurements in Pekin ducks. *Poult Sci.* 97, 2365–2371. doi: 10.3382/ps/pey079

Liu, Y., Liao, S., Bennett, S., Tang, H., Song, D., Wood, D., et al. (2021). STAT3 and its targeting inhibitors in osteosarcoma. *Cell Proliferat.* 54:e12974. doi: 10.1111/cpr.12974

Madkour, M., Aboelenin, M. M., Aboelazab, O., Elolimy, A. A., El-Azeem, N. A., El-Kholy, M. S., et al. (2021). Hepatic expression responses of DNA methyltransferases, heat shock proteins, antioxidant enzymes, and NADPH 4 to early life thermal conditioning in broiler chickens. *Ital. J. Anim. Sci.* 20, 433–446. doi: 10.1080/1828051X.2021.1890645

Matsubara, Y., Sato, K., Ishii, H., and Akiba, Y. (2005). Changes in mRNA expression of regulatory factors involved in adipocyte differentiation during fatty acid induced adipogenesis in chicken. *Comp. Biochem. Phys. A.* 141, 108–115. doi: 10.1016/j.cbpb.2005.04.013

Mazzocca, M., Fillot, T., Loffreda, A., Gnani, D., and Mazza, D. (2021). The needle and the haystack: single molecule tracking to probe the transcription factor search in eukaryotes. *Biochem. Soc. Trans.* 49, 1121–1132. doi: 10.1042/BST20200709

McGinnis, S., and Madden, T. L. (2004). BLAST: at the core of a powerful and diverse set of sequence analysis tools. *Nucleic Acids Res.* 322, W20–W25. doi: 10.1093/nar/gkh435

Merrick, D., Sakers, A., Irgebay, Z., Okada, C., Calvert, C., Morley, M. P., et al. (2019). Identification of a mesenchymal progenitor cell hierarchy in adipose tissue. *Science* 364:eaav2501. doi: 10.1126/science.aav2501

NCBI (2019). *CAU*. Available online at: https://www.ncbi.nlm.nih.gov/assembly/GCA_008746955.1 2019. (accessed January 5, 2020).

Pertea, M., Kim, D., Pertea, G. M., Leek, J. T., and Salzberg, S. L. (2016). Transcript-level expression analysis of RNA-seq experiments with HISAT, StringTie and Ballgown. *Nat. Protoc.* 11, 1650–1667. doi: 10.1038/nprot.2016.095

Qi, Q., and Yang, Z. (2014). Regulation and function of signal transducer and activator of transcription 3. *World J. Biol. Chem.* 5, 231–239. doi: 10.4331/wjbc.v5.i2.231

Qiu, J., Wang, W., Hu, S., Wang, Y., Sun, W., Hu, J., et al. (2018). Molecular cloning, characterization and expression analysis of C/EBP alpha, beta and delta in adipose-related tissues and adipocyte of duck (*Anas platyrhynchos*). *Comp. Biochem. Phys. B.* 221, 29–43. doi: 10.1016/j.cbpb.2018.04.004

Ramirezzacarias, J. L., Castromunozledo, F., and Kuriharcuch, W. (1992). Quantitation of adipose conversion and triglycerides by staining intracytoplasmic lipids with oil red-o. *Histochemistry* 97, 493–497. doi: 10.1007/BF00316069

Rodriguez, J. M., Pozo, F., di Domenico, T., Vazquez, J., and Tress, M. L. (2020). An analysis of tissue-specific alternative splicing at the protein level. *PLoS Comput. Biol.* 16:e1008287. doi: 10.1371/journal.pcbi.1008287

Rozovski, U., Harris, D. M., Li, P., Liu, Z., Jain, P., Ferrajoli, A., et al. (2018). STAT3-activated CD36 facilitates fatty acid uptake in chronic lymphocytic leukemia cells. *Oncotarget* 9, 21268–21280. doi: 10.18632/oncotarget.25066

Schwalie, P. C., Dong, H., Zachara, M., Russeil, J., Alpern, D., Akchiche, N., et al. (2018). A stromal cell population that inhibits adipogenesis in mammalian fat depots. *Nature* 559, 103–108. doi: 10.1038/s41586-018-0226-8

Sebo, Z. L., and Rodeheffer, M. S. (2019). Assembling the adipose organ: adipocyte lineage segregation and adipogenesis *in vivo*. *Development* 146:dev172098. doi: 10.1242/dev.172098

Shang, Z., Guo, L., Wang, N., Shi, H., Wang, Y., and Li, H. (2014). Oleate promotes differentiation of chicken primary preadipocytes *in vitro*. *Biosci. Rep.* 34, 51–57. doi: 10.1042/BSR20130120

Song, H., Wang, L., Chen, D., and Li, F. (2020). The function of Pre-mRNA alternative splicing in mammal spermatogenesis. *Int. J. Biol. Sci.* 16, 38–48. doi: 10.7150/ijbs.34422

Squillaro, T., Peluso, G., Galderisi, U., and Di Bernardo, G. (2020). Long non-coding RNAs in regulation of adipogenesis and adipose tissue function. *eLife* 9:e59053. doi: 10.7554/eLife.59053

Su, L., Rao, K., Guo, F., Li, X., Ahmed, A. A., Ni, Y., et al. (2012). In ovo leptin administration inhibits chorioallantoic membrane angiogenesis in female chicken embryos through the STAT3-mediated vascular endothelial growth factor (VEGF) pathway. *Domest. Anim. Endocrin.* 43, 26–36. doi: 10.1016/j.domaniend.2012.01.007

Su, T., Huang, C., Yang, C., Jiang, T., Su, J., Chen, M., et al. (2020). Apigenin inhibits STAT3/CD36 signaling axis and reduces visceral obesity. *Pharmacol. Res.* 152:104586. doi: 10.1016/j.phrs.2019.104586

Trincado, J. L., Entizne, J. C., Hysenaj, G., Singh, B., Skalic, M., Elliott, D. J., et al. (2018). SUPPA2: fast, accurate, and uncertainty-aware differential splicing analysis across multiple conditions. *Genome Biol.* 19:40. doi: 10.1186/s13059-018-1417-1

Troskie, R., Jafrani, Y., Mercer, T. R., Ewing, A. D., Faulkner, G. J., and Cheetham, S. W. (2021). Long-read cDNA sequencing identifies functional pseudogenes in the human transcriptome. *Genome Biol.* 22:146. doi: 10.1186/s13059-021-02369-0

Wang, T., Wang, H., Cai, D., Gao, Y., Zhang, H., Wang, Y., et al. (2017). Comprehensive profiling of rhizome-associated alternative splicing and alternative polyadenylation in moso bamboo (Phyllostachys edulis). *Plant J.* 91, 684–699. doi: 10.1111/tpj.13597

Wang, Z., Yin, Z. T., Zhang, F., Li, X. Q., Chen, S. R., Yang, N., et al. (2019). Dynamics of transcriptome changes during subcutaneous preadipocyte differentiation in ducks. *BMC Genomics* 20:688. doi: 10.1186/s12864-019-6055-9

Wu, T. D., and Watanabe, C. K. (2005). GMAP: a genomic mapping and alignment program for mRNA and EST sequences. *Bioinformatics* 21, 1859–1875. doi: 10.1093/bioinformatics/bti310

Xu, B., Meng, Y., and Jin, Y. (2021). RNA structures in alternative splicing and back-splicing. *Wiley Interdiscip Rev. RNA* 12:e1626. doi: 10.1002/wrna.1626

Xu, S., Zheng, H., Liu, T., Sun, Y., Cao, J., and Pan, D. (2019). Fat deposition and related gene expression in sheldrake duck of different ages. *Food Sci.* 40, 36–41.

Xu, T., Gu, L., Hou, S., and Ye, B. (2016). Identification and analysis of alternative splicing in duck genome using RNA-seq data. *China Poultry* 38, 10–16.

Yang, W., Zhang, S., Ou, T., Jiang, H., Jia, D., Qi, Z., et al. (2020). Interleukin-11 regulates the fate of adipose-derived mesenchymal stem cells *via* STAT3 signalling pathways. *Cell Proliferat.* 53:e12771. doi: 10.1111/cpr.12771

Yin, Z., Zhang, F., Smith, J., Kuo, R., and Hou, Z. C. (2019). Full-length transcriptome sequencing from multiple tissues of duck, Anas platyrhynchos. Sci. Data 6:275. doi: 10.1038/s41597-019-0293-1

Yuan, Y., Xi, Y., Chen, J., Zhu, P., Kang, J., Zou, Z., et al. (2017). STAT3 stimulates adipogenic stem cell proliferation and cooperates with HMGA2 during the

early stage of differentiation to promote adipogenesis. *Biochem. Biophys. Res. Commun.* 482, 1360–1366. doi: 10.1016/j.bbrc.2016.12.042

Zhang, K., Guo, W., Yang, Y., and Wu, J. (2011). JAK2/STAT3 pathway is involved in the early stage of adipogenesis through regulating C/EBP beta transcription. *J. Cell. Biochem.* 112, 488–497. doi: 10.1002/jcb.22936

Zhang, K., Yang, X., Zhao, Q., Li, Z., Fu, F., Zhang, H., et al. (2020). Molecular mechanism of stem cell differentiation into adipocytes and adipocyte differentiation of malignant tumor. *Stem Cells Int.* 2020:8892300. doi: 10.1155/2020/8892300

Zhang, N., Zhao, C., Zhang, X., Cui, X., Zhao, Y., Yang, J., et al. (2021). Growth arrest-specific 2 protein family: structure and function. *Cell Prolif.* 54:e12934. doi: 10.1111/cpr.12934

Zhang, Y., Zhang, L., Zuo, Q., Wang, Y., Zhang, Y., Xu, Q., et al. (2017). JAK-STAT signaling regulation of chicken embryonic stem cell differentiation into male germ cells. *In Vitro Cell. Dev. Anim.* 53, 728–743. doi: 10.1007/s11626-017-0167-9

Zheng, A., Chang, W., Hou, S., Zhang, S., Cai, H., Chen, G., et al. (2014). Unraveling molecular mechanistic differences in liver metabolism between lean and fat lines of Pekin duck (*Anas platyrhynchos* domestica): a proteomic study. *J. Proteomics* 98, 271–288. doi: 10.1016/j.jprot.2013.12.021

Zhou, Y., Zhou, B., Pache, L., Chang, M., Khodabakhshi, A. H., Tanaseichuk, O., et al. (2019). Metascape provides a biologist-oriented resource for the analysis of systems-level datasets. *Nat. Commun.* 10:1523. doi: 10.1038/s41467-019-09234-6

Conflict of Interest: The authors declare that the research was conducted in the absence of any commercial or financial relationships that could be construed as a potential conflict of interest.

Publisher's Note: All claims expressed in this article are solely those of the authors and do not necessarily represent those of their affiliated organizations, or those of the publisher, the editors and the reviewers. Any product that may be evaluated in this article, or claim that may be made by its manufacturer, is not guaranteed or endorsed by the publisher.

frontiers in Physiology

ORIGINAL RESEARCH
published: 03 December 2021
doi: 10.3389/fphys.2021.779689

Impacts of Embryonic Thermal Programming on the Expression of Genes Involved in *Foie gras* Production in Mule Ducks

*William Massimino[1†], Charlotte Andrieux[1†], Sandra Biasutti[2], Stéphane Davail[1], Marie-Dominique Bernadet[3], Tracy Pioche[1], Karine Ricaud[1], Karine Gontier[1], Mireille Morisson[4], Anne Collin[5], Stéphane Panserat[1] and Marianne Houssier[1]**

[1] Univ Pau & Pays Adour, INRAE, E2S UPPA, UMR 1419, Nutrition, Métabolisme, Aquaculture, Saint-Pée-sur-Nivelle, France, [2] Univ Pau & Pays Adour, E2S UPPA, IUT Génie Biologique, Mont-de-Marsan, France, [3] UEPFG INRAE Bordeaux-Aquitaine, Domaine d'Artiguères 1076, Benquet, France, [4] GenPhySE, Université de Toulouse, INRAE, ENVT, Castanet-Tolosan, France, [5] BOA, INRAE, Université de Tours, Nouzilly, France

OPEN ACCESS

Edited by:
Jie Wen,
Institute of Animal Sciences, Chinese Academy of Agricultural Sciences (CAAS), China

Reviewed by:
Monika Proszkowiec-Weglarz, Agricultural Research Service, United States Department of Agriculture (USDA), United States
Mahmoud Madkour, National Research Centre, Egypt

***Correspondence:**
Marianne Houssier
marianne.houssier@univ-pau.fr

[†] These authors have contributed equally to this work and share first authorship

Specialty section:
This article was submitted to Avian Physiology, a section of the journal Frontiers in Physiology

Received: 19 September 2021
Accepted: 04 November 2021
Published: 03 December 2021

Citation:
Massimino W, Andrieux C, Biasutti S, Davail S, Bernadet M-D, Pioche T, Ricaud K, Gontier K, Morisson M, Collin A, Panserat S and Houssier M (2021) Impacts of Embryonic Thermal Programming on the Expression of Genes Involved in Foie gras Production in Mule Ducks. Front. Physiol. 12:779689. doi: 10.3389/fphys.2021.779689

Embryonic thermal programming has been shown to improve *foie gras* production in overfed mule ducks. However, the mechanisms at the origin of this programming have not yet been characterized. In this study, we investigated the effect of embryonic thermal manipulation (+1°C, 16 h/24 h from embryonic (E) day 13 to E27) on the hepatic expression of genes involved in lipid and carbohydrate metabolisms, stress, cell proliferation and thyroid hormone pathways at the end of thermal manipulation and before and after overfeeding (OF) in mule ducks. Gene expression analyses were performed by classic or high throughput real-time qPCR. First, we confirmed well-known results with strong impact of OF on the expression of genes involved in lipid and carbohydrates metabolisms. Then we observed an impact of OF on the hepatic expression of genes involved in the thyroid pathway, stress and cell proliferation. Only a small number of genes showed modulation of expression related to thermal programming at the time of OF, and only one was also impacted at the end of the thermal manipulation. For the first time, we explored the molecular mechanisms of embryonic thermal programming from the end of heat treatment to the programmed adult phenotype with optimized liver metabolism.

Keywords: embryonic thermal programming, liver, metabolism, gene expression, duck

INTRODUCTION

The concept of early life programming appeared in humans less than 30 years ago with the observation of an association between the size of a child at birth and the risk of developing chronic pathologies in adulthood (Barker et al., 1993). More recently, programming has emerged in farm animals as an effective technique for improving their performances as adults. The principle consists in exposing the organism, during an early period of its life, characterized by a great plasticity, to an environmental stimulus which can thus be "recorded" and which can direct an adapted response to another stimulus, occurring later in its life (Lucas, 1998). In mammals, several types of primary

stimulus have been associated to an alternative phenotype in adulthood such as developmental malnutrition, stress or hypoxia (Tarry-Adkins and Ozanne, 2011).

In birds, since embryogenesis occurs outside the mother's body, many types of environmental factors can be easily applied to "program" the animals. Incubation temperature being one of the easiest parameters to control, embryonic thermal programming is therefore one of the most studied in poultry and has already demonstrated its efficiency in terms of improving adult thermoregulation in multiple species such as chickens (Piestun et al., 2008), ducks (DuRant et al., 2013) or quails (Vitorino Carvalho et al., 2020). Interestingly, changing the incubation temperature can also improve other performances, such as meat production in chicken (Piestun et al., 2013), or even *foie gras* production in mule duck (Massimino et al., 2019). In this last study, our team demonstrated that three different conditions of embryonic thermal programming led to an increase in lipid content in the liver of adult mule ducks after overfeeding (OF) (Massimino et al., 2019). A parallel study, focusing on the ontogeny of mule duck liver (Massimino et al., 2020), demonstrated that these thermal manipulations occurred during a period characterized by high expression of carbohydrate and lipid metabolism genes, suggesting a greater sensitivity of these metabolic pathways to thermal stress applied during this period. Nevertheless, despite the many encouraging results, the molecular mechanisms of programming process remain largely unknown. Modification of hormonal responses, gene expression regulations or epigenetic marks have been studied in the context of increased thermoregulation (Vaiserman et al., 2018; Madkour et al., 2021), but the field concerning hepatic metabolism has been scarcely explored (Loyau et al., 2014).

Overfeeding is a method used to stimulate *de novo* lipogenesis in migratory birds that store their energy in the liver (Leveille et al., 1975). For about 12 days, the ducks are fed corn (grain or meal) twice a day and the excess carbohydrates are converted into lipids by the hepatocytes, resulting in a huge increase in liver weight (Baeza et al., 2013). The metabolic pathways involved in this hepatic steatosis have been more precisely described in the last decades (Herault et al., 2010). First, glucose is taken up by the liver (Annabelle et al., 2017), before being degraded into pyruvate and then into acetyl CoA which is subsequently used for lipid synthesis (Annabelle et al., 2018). These lipids can be transported to peripheral tissues or recaptured by the liver for long-term storage (Tavernier et al., 2017).

The embryonic thermal programming applied to mule ducks that resulted in the increase in liver fattening (Massimino et al., 2019) may have affected each of these metabolic pathways, but also a variety of other pathways such as cell proliferation or thyroid hormone pathway strongly involved in liver metabolism (Sinha et al., 2014). In this study, we examined for the first time the short and long term molecular impacts of a 1°C increase in incubation temperature applied discontinuously (16 h/24 h) between E13 and E27 on mule duck eggs, resulting in the best optimized response to overfeeding (Massimino et al., 2019). We focused our work on the expression of genes involved in liver metabolism, thyroid pathway, cellular stress and cell proliferation at the end of the thermal treatment to study the short term impact, and before and after overfeeding for a longer term study.

MATERIALS AND METHODS

Ethics Approval Statement

All experimental procedures complied with French national guidelines for the care of animals for research purposes. The protocols were approved by the Animal care and Use Committee of the Greater Southwest Region (no. 73) and authorized by the department under the file reference APAFIS14196-201805250850236-v3. Ducks were killed in line with the European Council regulation (European Union, 2009) at the Experimental Station for Waterfowl breeding (INRA, Artiguères, France).

Eggs Incubation and Thermal Treatment

The overall experimental design is shown in **Figure 1**.

A total of 1,000 eggs of mule ducks (genotype H85, provided by Grimaud Frères Selection Company, Roussay, France) were kept at room temperature during 3 days prior to incubation and randomly divided into two incubators (500 eggs each). Control group was maintained at 37.6°C and 47% average relative humidity (RH) during the whole incubation period. Thermal manipulation (TM) was performed during the last 14 days of incubation period, i.e., embryonic day 13 to 27 (E13-E27) at 38.6°C 16 h/day (+1°C 16 h/24 h), RH being adjusted to an average of 63% in order to avoid egg dehydration. This thermal treatment condition was chosen among the three previously studied, for its optimal results, without any negative effect on hatchability or final yield (Massimino et al., 2019).

All eggs were turned through 90° every 3 h. In each incubator, temperature and hygrometry were continuously measured by a sensor equipped with remote probes (KIMO). Unfertile eggs were excluded by candling at E10, with a sliding of remaining eggs to prevent local temperature disturbance caused by the appearance of holes. On embryonic day 27 (E27), 20 embryos per group were collected and then temporarily placed in a small incubator near the dissection table, previously programmed to the incubation temperature, to avoid a long temperature variation before their slaughter by decapitation. Livers were harvested and frozen in liquid nitrogen for RNA extraction. The remaining eggs were placed in the same hatcher at 37.3°C and 80% of RH. Newly hatched ducks were recorded every day from E28 to E31.

Rearing and Force-Feeding Conditions, Sample Collection

Male ducklings were divided into two groups of 70 per treatment and were raised under the same conditions of light and temperature, and fed *ad libitum* from hatching to 4 weeks of age with a starting diet (2,800 Kcal, crude protein 17.5%). From 4 to 8 weeks of age, ducklings were fed *ad libitum* with a growing diet (2,800 Kcal, crude protein 15.5%), and hourly rationed between 8 and 12 weeks of age. At 12 weeks of age (D83) 15 animals per group were slaughtered for liver sampling before overfeeding

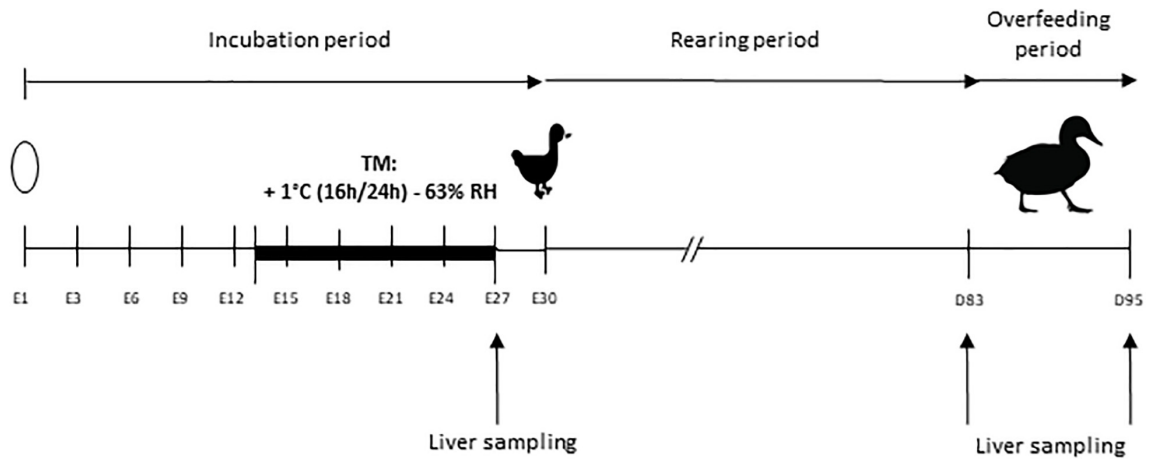

FIGURE 1 | Experimental design. Incubation period extends from embryonic day 1 (E1) to day 30 (E30), day of peak hatching of the ducklings. The thermal manipulation (TM) was performed between E13 and E27, with a temperature increase of 1°C (16 h/24 h) and relative humidity (RH) adjusted to 63%. Overfeeding began at 83 days of age (D83) and ended at 95 days (D95). Liver samplings for RNA extraction are indicated by an arrow at the end of the TM (E27) and before (D83) and after (D95) overfeeding.

period, classically practiced at this age in ducks (Saez et al., 2010; Hérault et al., 2018; Lo et al., 2020). All remaining ducks were overfed with corn meal twice a day (53% corn and 47% water, Palma Maisadour), for 11 days (21 meals) and slaughtered at the end of the OF period (D95). Liver samples from 20 animals per group were collected for gene expression analysis, 10 h after the last meal. In each case, ducks were slaughtered by exsanguination after electronarcosis. After dissection, pieces of liver were sampled in the middle of the large lobe for the study of gene expression and were frozen in liquid nitrogen for RNA analysis.

RNA Extraction and Reverse Transcription

Total RNA was isolated from frozen tissue according to the Ribozol method (VWR Life Science). Total RNA concentration was measured by spectrophotometry (optical density at 260 nm) using a Biotek EPOCH 2 microplate reader (Take 3 plate), and all the samples were normalized at 500 ng/μl. The integrity of total RNA was analyzed by electrophoresis, and the absence of DNA contamination was prevented by DNase treatment. Exogenous RNA of Luciferase (Promega) was added to each sample (100 pg per sample) to ensure the stability of a reference gene to enable data normalization, as described previously (Desvignes et al., 2011). For the RT-PCR, an amount of 3 μg RNA was reverse transcribed to cDNA with Iscript Reverse Transcription Supermix for RTqPCR (Bio-Rad, United States) with duplicate samples. Reverse transcription reaction was done in CFX384 (Bio-Rad, United States) according to this program: 25°C/5 min, 46°C/20 min, 95°C/1 min.

qPCR EvaGreen Using BioMark

The mRNA levels of 45 genes encoding proteins involved in lipid and carbohydrate metabolism, cell stress and proliferation, and the thyroid hormone pathway were quantified in liver from ducks before and after OF (at 83 and 95 days of age). Given the large number of genes and samples, we chose for this part to do a high-throughput expression study. All primer sequences used are listed on the **Supplementary Tables 1–3** and were validated on a concentration range of cDNA pool. Before performing Fluidigm step, a specific target amplification (STA) has been done with 5 ng/μL of cDNA. This step consists in PCR using PreAmp Master Mix and specific primer in order to normalize all samples and to ensure that there are enough copies of cDNA in each well. The manufacturer recommends this step because the method used nanovolumes. After the STA, all target and samples were distributed in a 96 × 96 chip for Fluidigm Gene Expression Array. The primers were provided by Applied Biosystems and were used at a concentration of 100 μM. The reaction was made using 20× EvaGreen dye following the program: holding stage 95°C for 10 min, 35 cycles of amplification: 95°C for 15 s, 60°C for 1 min. All the data were analyzed with the Fluidigm real-time PCR Analysis Software (Fluidigm Corporation v4.1.3). Melting curves were systematically monitored at the end of the last amplification cycle to confirm the specificity of the amplification reaction. Each qPCR run included negative controls (wells without reverse transcriptase, mRNA or cDNA). This part of the work was performed at the platform of quantitative transcriptomic GeT-TQ (GenoToul, Toulouse, France).

Gene Expression Analysis After EvaGreen qPCR

The selectHKgenes function with "Vandesompele" method of the SLqPCR package was used with RStudio (Version 1.2.1335) to choose the 6 most stable housekeeping genes (Pfaffl et al., 2004). The six housekeeping genes for the relative quantification of mRNA levels of target genes were USP9X, beta-actin, EIF3, STAB1, HPRT1 and Luciferase (added during the reverse transcription step), and are listed in the **Supplementary Table 3**. The slope of a standard curve using serial dilutions of cDNA

measured the efficiency (E) of PCR. In all cases, PCR efficiency values ranged between 1.85 and 2. The analyzes were done with RStudio and results were expressed as $2^{-\Delta\Delta Ct}$ with :

$$RQ = 2^{-\Delta\Delta Ct} = \frac{RQ_{target}}{\text{geomean}\,(RQ_{references})}$$

$$RQ = \frac{2^{\Delta Ct_{target}}}{(2^{\Delta Ct_{USP9X}} \times (2^{\Delta Ct_{Actine\beta}} \times 2^{\Delta Ct_{EIF3}} \times 2^{\Delta Ct_{STAB1}} \times 2^{\Delta Ct_{HPRT1}} \times 2^{\Delta Ct_{luciferase}})^{\frac{1}{6}}}$$

$$\Delta Ct_{target} = Ct_{control} - Ct_{sample}$$

$$\Delta Ct_{ref} = Ct_{control} - Ct_{samples}$$

$$Ct_{control} = \text{average Ct of all samples.}$$

Real Time qPCR Using Syber Green

Gene expression levels of embryonic liver samples (E27) were determined by real-time RT-PCR). Primer sequences are listed in the **Supplementary Tables 2, 3**.

The mRNA expression levels of target genes were detected using quantitative PCR with the PerfeCTa SYBR Green FastMix (Quantabio) in the CFX384 qPCR Detection System (Bio-Rad, United States). The reaction volume was 15 μL per sample and included 7.5 μL of SYBR Green FastMix, 2 μL (6 μg/mL) of cDNA and 2.75 μL of each primer (290 nM).

Melting curves were systematically monitored at the end of the last amplification cycle to confirm the specificity of the amplification reaction. Each qPCR run included duplicates of samples and negative controls (wells without reverse transcriptase, mRNA or cDNA).

Gene Expression Analysis After Syber Green qPCR

Relative quantifications of target gene mRNA levels were normalized with exogenous luciferase RNA (Promega), constituting the reference gene (ref). PCR efficiency was measured by the slope of a standard curve using serial dilutions of cDNA. In all cases, PCR efficiency values ranged between 1.85 and 2. Relative quantifications were expressed as $2^{-\Delta\Delta Ct}$ (Livak and Schmittgen, 2001) with:

$$2^{-\Delta\Delta Ct} = \frac{RQ_{target}}{RQ_{ref}}$$

$$RQ_{target} = 2^{\Delta Ct_{(target)}}$$

$$RQ_{ref} = 2^{\Delta Ct(ref)}$$

$$\Delta Ct_{target} = Ct_{control} - Ct_{sample}$$

$$\Delta ref_{target} = Ct_{control} - Ct_{sample}$$

$$Ct_{control} = \text{average Ct of all samples.}$$

Statistical Analyses

Statistical analyses were done using the GraphPad Prism v6 software. For embryonic samples (E27), when data set presented a Normal distribution (assessed by Shapiro–Wilk test), student's *t* tests were performed to compare control and TM groups. If the values did not follow a Normal distribution, the statistical analysis was performed with a non-parametric Mann Whitney test.

For pre-OF and post-OF samples, a two-way analysis of variance (ANOVA) was performed, followed by Sidak's multiple comparison test. The data are presented as the average ± standard error of mean (SEM). In every case, differences between the groups were considered statistically significant if the value of $P < 0.05$.

RESULTS

Expression of Heat Stress Pathway Genes at the End of the Thermal Manipulation

We first checked the expression of genes known to be influenced by heat stress to confirm that the thermal manipulation was indeed perceived by the liver of duck embryos. Relative expressions of three different heat shock proteins (HSP) and one heat shock factors (HSF) were analyzed in **Figure 2** at the end of the TM (E27). We measured a strong increase in gene expressions of HSP70 and HSP90 in the TM group compared to the control group. In contrast, the expressions of DNAJB12 (HSP40) and HSF3 were significantly reduced in the TM group compared to the control group. These results confirm the molecular perception of the thermal stimulus by duck embryos.

Impact of Early Thermal Manipulation and Overfeeding on Gene Expression of Metabolic Pathways

The **Table 1** lists the relative expression values of genes involved in lipid and carbohydrate metabolisms. All these genes were significantly modulated by OF, with an overall increase in carbohydrate transport and oxidation, and lipid synthesis. The two main regulators ChREBP and PPARG were also increased at the end of the OF period compared to before this feeding challenge. On the contrary, lipid oxidation was strongly down-regulated after the last meal of the OF period compared to the pre-OF period. As shown in the right panel of the table, only two genes were significantly altered by the TM during this period: GPAT1 and APOB. The increase in GPAT1 expression was significantly higher in the TM group compared with the control group after the OF period (significant interaction between both factors), whereas APOB expression was decreased by both OF and TM, without significant interaction between both nutritional and incubation factors.

Impact of Early Thermal Manipulation and Overfeeding on Gene Expression of Thyroid, Cellular Stress and Proliferation Pathways

The **Table 2** shows the relative expression of genes involved in various cellular pathways before and after OF in the liver. Most

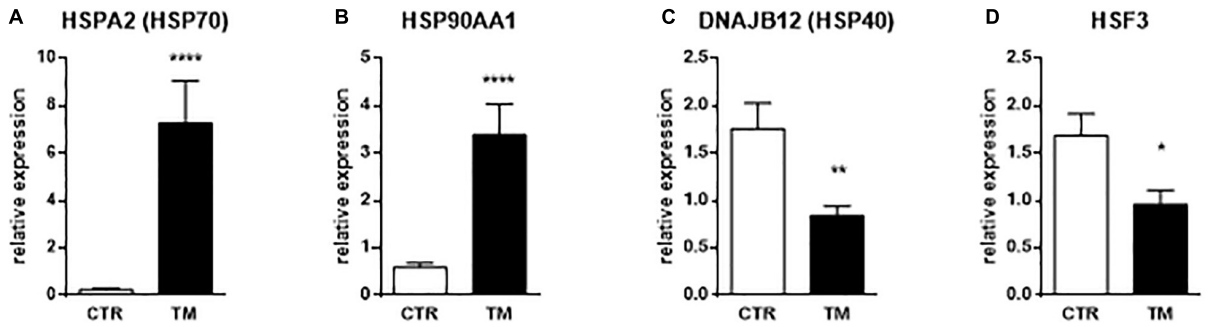

FIGURE 2 | Hepatic relative expression of genes directly influenced by heat treatment at E27. Column representation of the relative expression of HSPA2 **(A)**, HSP90AA1 **(B)**, DNAJB12 **(C)**, and HSF3 **(D)** at the end of the thermal manipulation in the liver of control (CTR) or thermal manipulated (TM) duck embryos. Data are presented as mean +/– SEM (n = 18–19). *P < 0.05, **P < 0.01, ****P < 0.0001.

TABLE 1 | Hepatic relative expression of genes involved in the lipid and carbohydrate pathways depending on incubation conditions before and after overfeeding.

			Control		TM		Effects			
Metabolic pathway		Gene	pre-OF	post-OF	pre-OF	post-OF	OF	TM	Interaction	n
Carbohydrates	Transport	GLUT1	0.44 ± 0.06	0.75 ± 0.06	0.33 ± 0.05	0.68 ± 0.09	**	ns	ns	5-19
		GLUT2	0.56 ± 0.06	0.95 ± 0.08	0.55 ± 0.04	0.83 ± 0.03	****	ns	ns	14-19
		GLUT3	0.26 ± 0.05	0.48 ± 0.05	0.27 ± 0.06	0.41 ± 0.03	***	ns	ns	12-19
	Oxidation	PDHA1	0.59 ± 0.06	0.78 ± 0.05	0.48 ± 0.04	0.78 ± 0.05	****	ns	ns	14-19
		ENO1	0.62 ± 0.04	0.87 ± 0.07	0.59 ± 0.04	0.88 ± 0.06	****	ns	ns	14-19
		HK1	0.54 ± 0.10	0.96 ± 0.08	0.47 ± 0.07	0.95 ± 0.07	****	ns	ns	14-19
Lipids	Synthesis	FASN	0.39 ± 0.06	2.07 ± 0.15	0.45 ± 0.09	1.93 ± 0.07	****	ns	ns	14-19
		DGAT2	0.11 ± 0.01	0.50 ± 0.06	0.19 ± 0.03	0.56 ± 0.10	****	ns	ns	14-18
		ACC	0.51 ± 0.04	1.02 ± 0.05	0.47 ± 0.06	0.92 ± 0.05	****	ns	ns	14-19
		SCD1	0.26 ± 0.06	1.63 ± 0.08	0.20 ± 0.05	1.73 ± 0.08	****	ns	ns	12-19
		ACLY	0.37 ± 0.05	1.28 ± 0.11	0.37 ± 0.06	1.47 ± 0.11	****	ns	ns	14-19
		PLIN2	0.31 ± 0.04	0.62 ± 0.05	0.28 ± 0.05	0.59 ± 0.04	****	ns	ns	14-19
		ELOV6	1.11 ± 0.08	2.18 ± 0.10	1.06 ± 0.10	2.20 ± 0.08	****	ns	ns	14-19
		GPAT1	0.50 (b) ± 0.07	0.84 (b) ± 0.08	0.48 (b) ± 0.08	1.41 (a) ± 0.16	****	*	*	14-19
	Oxidation	ACOX1	1.60 ± 0.14	0.71 ± 0.07	1.43 ± 0.11	0.66 ± 0.06	****	ns	ns	13-19
		ACAD11	1.38 ± 0.18	0.53 ± 0.06	1.01 ± 0.16	0.51 ± 0.06	****	ns	ns	14-19
		ACSL1	1.85 ± 0.19	0.80 ± 0.07	1.68 ± 0.15	0.83 ± 0.07	****	ns	ns	14-19
		LIPC	1.80 ± 0.31	0.98 ± 0.11	1.85 ± 0.31	0.76 ± 0.08	****	ns	ns	14-19
		CPT1	2.32 ± 0.26	0.80 ± 0.08	2.15 ± 0.17	0.87 ± 0.09	****	ns	ns	14-19
	Transport	APOB	1.16 ± 0.10	0.83 ± 0.07	0.88 ± 0.08	0.79 ± 0.06	**	*	ns	14-19
		FABP4	0.13 ± 0.02	1.02 ± 0.16	0.11 ± 0.02	1.24 ± 0.20	****	ns	ns	14-19
		VLDLR	1.02 ± 0.20	1.43 ± 0.13	0.83 ± 0.17	1.19 ± 0.15	*	ns	ns	14-19
		LDLR	1.48 ± 0.20	1.07 ± 0.10	1.54 ± 0.13	0.86 ± 0.06	****	ns	ns	13-19
Regulators		ChREBP	0.42 ± 0.04	1.33 ± 0.09	0.46 ± 0.07	1.23 ± 0.10	****	ns	ns	14-19
		PPARG	0.53 ± 0.06	0.99 ± 0.09	0.42 ± 0.04	0.90 ± 0.05	****	ns	ns	13-19

*Data are presented as mean +/– SEM. TM, thermal manipulation; pre-OF, before overfeeding period; post-OF, after overfeeding period. ns, non significant, *P < 0.05, **P < 0.01, ***P < 0.001, ****P < 0.0001. Different letters in parentheses indicate significant differences measured between each group when there is an interaction between the OF and TM factors. n, number of samples.*

of these genes were significantly modified by OF. All profile types were represented in the thyroid pathway, with OF-induced increases in SPOT14 and THRB expression, decreases in NCOR and DIO3, and no OF effect for DIO1. Similarly, the cellular stress pathway was variously affected by OF, with an increase in HSP70, HSP90, HSF3 and ST13, and a decrease in UBQLN1, HSF2 and HSBP1 whereas PSMD12 were not altered at all by the nutritional challenge. The impact of OF on the cell proliferation pathway in the liver was more homogeneous with an increase in all relative expression values, except for HGF and MAPK1, which were not affected at all.

None of the genes involved in cell proliferation were influenced by the TM unlike the stress pathway that involved two genes whose expression was significantly decreased by

TABLE 2 | Hepatic relative expression of genes involved in the thyroid, stress and cell proliferation pathways depending on incubation conditions before and after overfeeding.

		Control		TM		Effects			
Pathway	**Gene**	**pre-OF**	**post-OF**	**pre-OF**	**post-OF**	**OF**	**TM**	**Interaction**	**n**
Thyroid Hormone Signaling	SPOT14	0.09 ± 0.02	0.83 ± 0.05	0.08 ± 0.01	0.90 ± 0.05	↑ ****	ns	ns	13-19
	THRB	0.35 ± 0.06	0.78 ± 0.05	0.24 ± 0.03	0.77 ± 0.04	↑ ****	ns	ns	14-19
	NCOR	1.56 ± 0.13	1.25 ± 0.07	1.70 ± 0.10	1.28 ± 0.08	↓ ***	ns	ns	14-19
	DIO3	1.37 ± 0.15	0.53 ± 0.07	1.92 ± 0.30	0.77 ± 0.11	↓ ****	* ↑	ns	12-19
	DIO1	1.11 ± 0.09	1.10 ± 0.06	0.94 ± 0.08	1.09 ± 0.06	ns	ns	ns	14-19
Cellular Stress	UBQLN1	4.28 ± 0.44	2.91 ± 0.16	3.41 ± 0.19	2.78 ± 0.11	↓ ****	* ↓	ns	14-19
	PSMD12	1.28 ± 0.12	1.18 ± 0.05	0.92 ± 0.10	1.14 ± 0.05	ns	* ↓	ns	14-19
	HSP70	0.40 ± 0.04	0.92 ± 0.21	0.54 ± 0.07	1.66 ± 0.44	↑ **	ns	ns	13-19
	HSP90AA1	0.78 ± 0.08	0.98 ± 0.13	0.75 ± 0.09	1.04 ± 0.13	↑ *	ns	ns	14-19
	DNAJB12	0.38 (ab) ± 0.10	0.36 (a) ± 0.07	0.11 (b) ± 0.02	0.37 (a) ± 0.04	ns	ns	*	8-19
	HSF3	0.73 ± 0.10	0.91 ± 0.07	0.65 ± 0.07	0.84 ± 0.04	↑ *	ns	ns	14-19
	HSF2	1.40 ± 0.21	1.11 ± 0.05	1.53 ± 0.25	0.99 ± 0.04	↓ **	ns	ns	14-19
	HSBP1	2.52 (a) ± 0.28	1.33 (c) ± 0.05	1.90 (b) ± 0.13	1.33 (c) ± 0.04	↓ ****	* ↓	*	14-19
	ST13	0.78 ± 0.08	1.70 ± 0.11	0.63 ± 0.04	1.63 ± 0.09	↑ ****	ns	ns	12-19
Cell Proliferation	HNF4	0.66 ± 0.11	1.15 ± 0.10	0.50 ± 0.10	1.16 ± 0.07	↑ ****	ns	ns	10-19
	MAPK1	0.35 ± 0.06	0.35 ± 0.05	0.26 ± 0.04	0.32 ± 0.05	ns	ns	ns	14-19
	MED21	0.54 ± 0.08	0.66 ± 0.05	0.52 ± 0.06	0.71 ± 0.03	↑ **	ns	ns	13-19
	TUBa1C	0.36 ± 0.05	0.88 ± 0.06	0.37 ± 0.06	0.96 ± 0.06	↑ ****	ns	ns	14-19
	HGF	2.05 ± 0.47	1.72 ± 0.18	1.84 ± 0.35	1.40 ± 0.17	ns	ns	ns	11-18
	POLR2C	0.59 ± 0.06	0.79 ± 0.04	0.65 ± 0.06	0.86 ± 0.04	↑ ****	ns	ns	14-19

*Data are presented as mean +/− SEM. TM, thermal manipulation; pre-OF, before overfeeding period; post-OF, after overfeeding period. ns, non significant, *P < 0.05, **P < 0.01, ***P < 0.001, ****P < 0.0001. Different letters in parentheses indicate significant differences measured between each group when there is an interaction between the OF and TM factors. n, number of samples.*

embryonic thermal treatment (UBQLN1 and PSMD12), and two for which a significant interaction between feeding and incubation conditions was found: it concerned DNAJB12 for which an increase was observed post-OF only in the TM group, and HSBP1, for which the decrease post-OF was most pronounced in the control group. Concerning the hormonal pathway, only the expression of DIO3 showed a significant increase in the TM group compared to the control group during this period.

The Genes Influenced by Thermal Manipulation During Overfeeding Are Not Affected at the End of the Thermal Stimulus, Except One

As indicated above, only 6 genes (out of a total of 45) were significantly modulated by embryonic thermal treatment during the OF period. To see if this programming was already measurable at the end of the heat treatment, we measured the expression of these 6 genes in the liver of embryos at E27. The results presented in **Figure 3** show that only DIO3 expression was already increased by TM at this stage, with the other five being not affected by the thermal treatment.

DISCUSSION

This study follows the demonstration that embryonic thermal programming can induce an optimization of liver fattening in mule ducks (Massimino et al., 2019). In this previous work, we used three different thermal stimuli during the incubation period to program the liver metabolism of adult ducks to respond more strongly to OF. Although all three programming resulted in larger and fatter livers than the control group, only one had no negative impact on hatchability or finished product quality. This condition consisted of a 1°C increase in incubation temperature, 16 h/24 h, from embryonic day 13 to embryonic day 27. We therefore chose to analyze the expression of genes in the liver of the animals from this condition in order to study the molecular mechanisms at the origin of this metabolic programming.

Expected Molecular Perception of Heat Treatment at E27 Using Genes Known to Be Sensitive to Temperature

We began by studying the expression of genes belonging to the heat shock protein (HSP) family, themselves members of the chaperone protein superfamily (Morimoto, 1993; Vos et al., 2008). These proteins (including HSPA and DNAJ members) play a crucial role in stress conditions but also in normal physiological conditions requiring protein quality control for cellular homeostasis. Their binding to substrates at risk, i.e., in a degraded folding state, allows them to be directed toward a folding or degradation pathway. Although initially identified as heat stress-induced proteins, not all are regulated in the same way, and some not even by temperature (Vos et al., 2008).

In the first step of our experiment, we focused on three members of HSPs that are obviously altered by temperature:

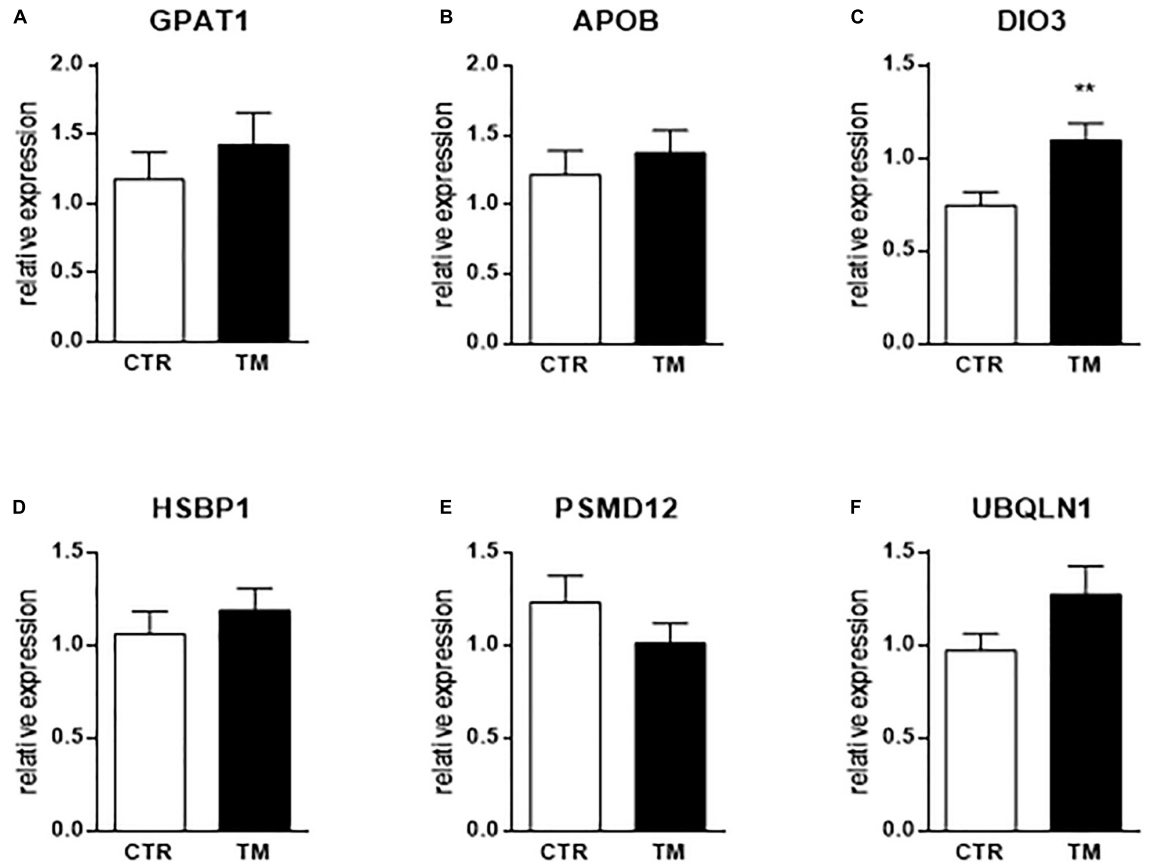

FIGURE 3 | Hepatic relative expression at the end of the heat treatment (E27) of genes influenced by TM before or after overfeeding. Column representation of the relative expression of GPAT1 **(A)**, APOB **(B)**, DIO3 **(C)**, HSBP1 **(D)**, PSMD12 **(E)** and UBQLN1 **(F)** at the end of the thermal manipulation in the liver of control (CTR) or thermal manipulated (TM) duck embryos. Data are presented as mean +/– SEM (n = 16–19). $^{**}P < 0.01$. The absence of a star means that there is no statistical difference between the groups.

HSP70 (HSPA2), HSP90AA1 and HSP40 (DNAJB12). We measured a significant increase in the expression of the first two at the end of the heat treatment (E27) in the TM group compared to the control group, confirming what has already been well described in different tissues of heat-stressed chicken (Wang and Edens, 1998; Al-Zhgoul et al., 2013; Al-Zghoul et al., 2015; Cedraz et al., 2017; Albokhadaim et al., 2019; Madkour et al., 2021). More surprisingly, we also measured a significant decrease in HSP40 (DNAJB12) at E27 in the TM group compared to control. Mostly up-regulated after heat stress (Dong et al., 2006; Neal et al., 2006; Chen et al., 2018), down-regulation of that chaperone has, however, already been measured immediately after a transport stress in the spleen of hens (Li et al., 2021). These data suggest that the type of stress, the targeted tissue, or the time of stress exposure may have a different impact on the expression of different HSP family members.

Heat shock factors (HSFs) on the other hand are transcription factors induced after heat stress that bind to heat shock promoters to modulate the expression of target proteins (Westwood et al., 1991; Morimoto, 1993). HSF3 has been shown to regulate the production of HSP70 and HSP90 proteins under heat stress conditions (Tanabe, 1998). The decrease in its expression measured at the end of the heat treatment, in parallel with the strong increase of HSP70 and HSP90, could reflect the existence of a negative feedback after some time of heat exposure (14 days here), as already suggested in other types of stress responses and involving the glucocorticoid receptor (Wadekar et al., 2001, 2004; Kang et al., 2017).

However, all these changes in HSP and HSF gene expression confirm that the thermal stimulus used for embryonic programming was well perceived and measured at the molecular level in the liver of duck embryos.

Molecular Impact of Overfeeding on Carbohydrate and Lipid Metabolisms but Also on the Thyroid Pathway, Stress and Cell Proliferation in the Liver

As explained above, this thermal embryonic programming has already been shown to increase *foie gras* production in ducks submitted to overfeeding between 83 and 95 days of age (Massimino et al., 2019). To understand the mechanisms behind this increase in fattening, we first explored the expression level of genes involved in lipid and carbohydrate metabolisms in

duck livers before and after OF. As previously described, OF induced a strong increase in the expression of genes involved in carbohydrate transport to the liver (GLUT family), then in carbohydrate oxidation for pyruvate (HK1 and ENO1) and acetyl-CoA (PDHA1) production (Herault et al., 2010; Annabelle et al., 2017). These substrates can then be used by the pathway of lipid synthesis, strongly induced by OF in parallel with a decrease in their oxidation, as also observed previously (Tavernier et al., 2017; Annabelle et al., 2018). ChREBP and PPARG, key regulators of these pathways, are also strongly increased by OF. For lipid transport-related genes, the relative expressions of APOB and LDLR are decreased by OF, whereas those of FABP4 and VLDLR are increased. We propose two ways to explain these opposite regulations: first, depending on the direction of lipid transport through the liver cells (in or out), their expression can be either increased or decreased by the OF; second, the timing of RNA collection after the last OF meal can have a significant impact on the expression level, as demonstrated by a kinetic study of these same genes (which sometimes show opposite regulation at 2 h and at 5 h after the last meal) (Annabelle et al., 2018).

We then turned our attention to the thyroid hormone signaling pathway since it has been shown that, both in mammals (Danforth et al., 1979; Katzeff, 1990) and ducks (Massimino et al., 2019), OF induces an increase in plasma triiodothyronine (T3). The blood concentration in T3 is mainly dependent on the peripheral conversion of T4 in T3 by deiodinases. Especially, T4 can be converted into T3 by deiodinases 1 and 2, but into the inactive hormone rT3 by DIO1 and DIO3 (Darras et al., 2006). This active form T3 of thyroid hormone (TH) is able to bind a nuclear receptor (thyroid hormone receptor beta, THRB, being the predominant form in the liver) to modify the gene expression of a wide spectrum of genes involved in lipid metabolism (Sinha et al., 2018; Ritter et al., 2020). TH can induce the expression of fatty acid transporters, resulting in increased uptake of fatty acids in the liver, enzymes of lipolysis and beta-oxidation, but also *de novo* lipogenesis (Sinha et al., 2018). However, the circulating level of THs (T3 and T4) does not directly reflect their impact on tissue function, since they must first be captured by membrane receptors, then can be altered by deiodinases (DIO) and finally coregulators in the nucleus can regulate their activity (Mendoza and Hollenberg, 2017). Therefore, we were interested in measuring at the transcriptional level the hepatic regulation of their activity. Our expression data seem to confirm a global activation of T3 in the liver of overfed ducks, since we measured an increase in THRB and SPOT14 (involved in T3-induced lipid synthesis) expressions, in parallel with a decrease in NCOR (corepressor) and DIO3 (deiodinase responsible for TH inactivation) (Kinlaw et al., 1995; Mendoza and Hollenberg, 2017; Sinha et al., 2018; Ritter et al., 2020). This increase in T3 activity during overfeeding has been proposed as a protective mechanism to limit weight gain by increasing lipid catabolism in favor of energy expenditure through thermogenesis (Oppenheimer et al., 1991; Almeida et al., 1996; Silvestri et al., 2005). These regulations therefore suggest a protective mechanism for liver cells to limit OF-induced lipid overload, which may alter cell physiology over time.

To further assess the physiological status of liver cells during OF, we were then interested in the genes related to stress. We first notice that half of the chaperones involved in protein folding (HSP70, HSP90AA1, HSF3, ST13) are increased by OF, suggesting that protein quality control processes are globally activated. Decreased expression level of HSBP1 (in the control group, and to a lower extent, in the TM group) as an inhibitor of HSF (Cotto and Morimoto, 1999) could be interpreted as cellular protections. The decrease in HSF2 expression could, in another way, indicate that the transcriptional modulation of these factors does not always reflect their DNA-binding activity, as previously demonstrated (Sarge et al., 1991; Ding et al., 1996), although a negative feedback cannot be excluded in this global activation of protein protection. In another category, PSMD12 is a proteasome subunit that plays a role in global protein homeostasis by clearing misfolded or damaged protein (Du et al., 2020). Here, OF did not affect its expression, although it is downregulated in the liver of obese individuals with an increased fat content, as well as many genes involved in protein catabolism (Pihlajamäki et al., 2009). On the contrary, UBQLN1, also involved in protein degradation *via* proteasome or autophagy (Rothenberg et al., 2010; Kurlawala et al., 2017), is strongly decreased by OF, confirming at least a partial decrease in protein catabolism under these conditions.

Finally, since the role of hyperplasia in the fattening of duck livers after force-feeding has been recently put forward (Hérault et al., 2019), we measured the expression of genes involved in cell proliferation. Our results confirm a general increase in the expression of proliferation-related genes, with the exception of MAPK1, whose activation may be more reflected by the phosphorylation status (Nishida and Gotoh, 1993) and the hepatocyte growth factor (HGF) not affected at all. These observations suggest that hyperplasia may indeed play a role in duck liver fattening during OF, which should be further investigated by histological studies.

Impact of Embryonic Thermal Manipulation During the Overfeeding Period – Evidence of Real Programming

Since ducks in the TM group had larger and fatter livers than controls at the end of OF (Massimino et al., 2019), we were first interested in the impact of TM on the expression of genes involved in the two main pathways directly implicated in liver fattening. Consistently with the study of Loyau et al. (2014) that had highlighted very low effect of TM in the hepatic expression of metabolic genes in the liver, none of the genes related to carbohydrate metabolism were significantly modulated by TM, and only 2 genes related to lipid metabolism were affected, and this at a relatively low level ($P < 0.05$), and only in case of overfeeding for GPAT1 (due to a significant interaction of the incubation and the nutritional factors for this gene expression). Located in the outer membrane of mitochondria, GPAT1 is involved in the first step of triacylglycerol esterification (Coleman, 2019) and has been shown to play critical role in hepatic steatosis (Yu et al., 2018). The second, APOB, is a structural protein of Very-Low-Density Lipoproteins (VLDL), and low-density lipoprotein (LDL) produced by the liver for lipid export to peripheral tissues (Gruffat et al., 1996; Bagherniya et al., 2021). Indeed, a greater increase in a crucial lipogenic enzyme

or a decrease in a key factor involved in lipid export may both play a role in the increased liver fattening of our programmed animals. However, this relatively weak response led us to measure the impact of TM on the expression of other factors, possibly involved in liver metabolism.

Regarding the thyroid hormone signaling pathway, DIO3, considered to be the major TH-inactivating enzyme (Bianco et al., 2002), was significantly increased by TM before and after OF. This result contrasts with the study of Loyau et al. (2014) in the chicken liver who had found no change in this gene expression in slightly different conditions of TM. The expression of the activating enzyme DIO1 was not affected in both studies. The programming effect of TM on the regulation of the hepatic T4 to T3 or rT3 conversion might therefore be slightly different in the two species. Although no impact of thermal programming could be measured on plasma T3 and T4 levels in our overfed ducks (Massimino et al., 2019), increased expression of this deiodinase in the TM group suggests that embryonic thermal programming may induce a slight TH inactivation in the liver. These data support the hypothesis that embryonic thermal manipulation could have increased the lipid content in the liver by decreasing energy expenditure *via* thermogenesis (Almeida et al., 1996). Even though we did not measure a difference in surface temperature after the OF period in our programmed ducks, it is not impossible that internal temperature and thus thermogenesis was affected, reducing energy expenditure and thus promoting liver fattening.

Interestingly, the greatest impact of TM measured during the OF period was on the cellular stress pathway, with half of the significantly impacted genes belonging to this group. All of these genes were down-regulated in the TM group compared to the control group. Decreased expression of HSBP1, which is a negative regulator of the HSP family (Satyal et al., 1998), before OF, could be interpreted as a "protein quality control readiness," preparing the liver to cope with OF and thus promoting improved cellular physiology during this challenge. TM also significantly decreases the expression of PSMD12 and UBQLN1, both involved in protein catabolism (Kurlawala et al., 2017; Du et al., 2020). As this metabolic pathway is decreased in the liver of obese patients with increased fat content (Pihlajamäki et al., 2009), this could represent a kind of predisposition to liver fattening.

Lastly, since it has been shown that embryonic thermal manipulation in chickens can stimulate cell proliferation in an immediate but also delayed manner (Piestun et al., 2009), we wondered whether TM could modulate liver cell proliferation during the OF period and thus contribute to liver fattening. Eventually, none of the genes we measured were affected by TM during this period. However, it might be interesting to measure the impact of TM on liver cell proliferation directly at the end of the thermal stimulus to see if baseline fattening potential is increased from birth by increasing cell numbers.

Finally, only six genes (out of 45) were significantly regulated by the embryonic TM during the OF period. However, these specifically targeted genes represent evidence of long-term programming at the molecular level in duck liver and may all support the hypothesis of optimized metabolism for *foie gras* production. Nevertheless, we do not rule out the possibility of having missed TM-induced transcriptional modulations during OF, especially because RNA samples were taken 10 h after the last feeding. It has been well demonstrated that the expression of metabolic genes during OF (Tavernier et al., 2017) but also according to the time of collection of liver samples after the last meal follow their own kinetics (Annabelle et al., 2017, 2018). Since most of the metabolic genes have a peak of expression about 2 h after the last meal, it would be interesting to study the impact of TM at this precise moment. In addition, the timing of the embryonic thermal stimulus may be optimized based on a recent study showing hepatic gene expression profiles during embryogenesis (Massimino et al., 2020), and may allow measurement of larger expression differences during the OF period. It is also important to note that all of these modulations are measured only at the mRNA level, and do not necessarily predict the activity of associated proteins, which is especially relevant for deiodinases for instance (Darras et al., 2006). It will be interesting during the next studies to confirm and deepen these results at the level of proteins and their activity.

Genes Thermally Programmed to Respond Optimally to the Overfeeding Are Not Affected at the End of the Embryonic Stimulus, Except One

In the last part, we measured the direct impact of TM (at E27) on the six genes that were significantly impacted by long-term programming. We showed that the expression of only one of these genes was directly influenced by the TM at the end of the stimulus, suggesting that programming is registered through other pathways than direct modulation of expression. However, we observe that DIO3 is always up-regulated by TM both at the end of the thermal stimulus and before and after the OF period, suggesting a powerful and continuous mechanism to modulate this pathway which thus seems to have a key role in hepatic metabolism in ducks. Precisely how the expression of these genes is modulated by temperature, and how the information is recorded to program the response of hepatocytes to a dietary challenge much later in the life of the animal, however, are questions that remain to be explored.

CONCLUSION

This study is the first to explore the molecular mechanisms involved in the long-term programming of liver metabolism in ducks by an embryonic thermal stimulus. We have identified a handful of genes that represent prime targets of this programming and may direct hepatic metabolism toward increased lipid storage during overfeeding. However, understanding the precise mechanisms behind programmed phenotypes will therefore require many more studies to be apprehended.

DATA AVAILABILITY STATEMENT

The original contributions presented in the study are included in the article/**Supplementary Material**, further inquiries can be directed to the corresponding author.

ETHICS STATEMENT

The animal study was reviewed and approved by the Animal Care and Use Committee of the Greater Southwest Region (n° 73).

AUTHOR CONTRIBUTIONS

MH, SP, AC, MM, and WM conceived and designed the study. WM and CA conducted all the experiments and analyses with the help of SB, MH, TP, KR, KG, SD, and M-DB. M-DB supervised the whole breeding, overfeeding, and slaughtering phases. All authors reviewed the manuscript and approved the final manuscript.

FUNDING

This work was supported by grants from the "Comité Interprofessionnel des Palmipèdes à Foie Gras" (CIFOG-Agreement 2018-01) and from "Comité Départemental des Landes" (CD40).

ACKNOWLEDGMENTS

We thank all the technicians of the Experimental Station for Waterfowl Breeding (INRAE, Artigueres, France) for the daily care given to the animals and the monitoring of the good conditions for the experiments.

SUPPLEMENTARY MATERIAL

The Supplementary Material for this article can be found online at: https://www.frontiersin.org/articles/10.3389/fphys.2021.779689/full#supplementary-material

REFERENCES

Albokhadaim, I. F., Althnaian, T. A., and El-Bahr, S. M. (2019). Gene expression of heat shock proteins/factors (HSP60, HSP70, HSP90, HSF-1, HSF-3) and antioxidant enzyme activities in heat stressed broilers treated with vitamin C. *Pol. J. Vet. Sci.* 22, 565–572. doi: 10.24425/pjvs.2019.129965

Almeida, N. G., Levitsky, D. A., and Strupp, B. (1996). Enhanced thermogenesis during recovery from diet-induced weight gain in the rat. *Am. J. Physiol.* 271(5 Pt 2), R1380–R1387. doi: 10.1152/ajpregu.1996.271.5.R1380

Al-Zghoul, M.-B., Ismail, Z. B., Dalab, A. E. S., Al-Ramadan, A., Althnaian, T. A., Al-ramadan, S. Y., et al. (2015). Hsp90, Hsp60 and HSF-1 genes expression in muscle, heart and brain of thermally manipulated broiler chicken. *Res. Vet. Sci.* 99, 105–111. doi: 10.1016/j.rvsc.2014.12.014

Al-Zhgoul, M.-B., Dalab, A. E. S., Ababneh, M. M., Jawasreh, K. I., Busadah, K. A. A., and Ismail, Z. B. (2013). Thermal manipulation during chicken embryogenesis results in enhanced Hsp70 gene expression and the acquisition of thermotolerance. *Res. Vet. Sci.* 95, 502–507. doi: 10.1016/j.rvsc.2013.05.012

Annabelle, T., Karine, R., Marie-Dominique, B., Karine, G., and Stéphane, D. (2018). Pre- and post-prandial expression of genes involved in lipid metabolism at the end of the overfeeding period of mule ducks. *Mol. Cell. Biochem.* 438, 111–121. doi: 10.1007/s11010-017-3118-6

Annabelle, T., Karine, R., Marie-Dominique, B., Stéphane, D., and Karine, G. (2017). Kinetics of expression of genes involved in glucose metabolism after the last meal in overfed mule ducks. *Mol. Cell. Biochem.* 430, 127–137. doi: 10.1007/s11010-017-2960-x

Baeza, E., Marie-Etancelin, C., Davail, S., and Diot, C. (2013). La stéatose hépatique chez les palmipèdes. *INRA Prod. Anim.* 26, 403–414.

Bagherniya, M., Johnston, T. P., and Sahebkar, A. (2021). Regulation of apolipoprotein B by natural products and nutraceuticals: a comprehensive review. *Curr. Med. Chem.* 28, 1363–1406. doi: 10.2174/0929867327666200427092114

Barker, D. J. P., Medical Research Council (Great Britain), and Environmental Epidemiology Unit (1993). *Fetal and Infant Origins of Adult Disease: Papers Written by the Medical Research Council Environmental Epidemiology Unit, University of Southampton*. London: British Medical Journal.

Bianco, A. C., Salvatore, D., Gereben, B., Berry, M. J., and Larsen, P. R. (2002). Biochemistry, cellular and molecular biology, and physiological roles of the iodothyronine selenodeiodinases. *Endocr. Rev.* 23, 38–89. doi: 10.1210/edrv.23.1.0455

Cedraz, H., Gromboni, J. G. G., Garcia, A. A. P., Farias Filho, R. V., Souza, T. M., de Oliveira, E. R., et al. (2017). Heat stress induces expression of HSP genes in genetically divergent chickens. *PLoS One* 12:e0186083. doi: 10.1371/journal.pone.0186083

Chen, T., Lin, T., Li, H., Lu, T., Li, J., Huang, W., et al. (2018). Heat shock protein 40 (HSP40) in Pacific white shrimp (*Litopenaeus vannamei*): molecular cloning, tissue distribution and ontogeny, response to temperature, acidity/alkalinity and salinity stresses, and potential role in ovarian development. *Front. Physiol.* 9:1784. doi: 10.3389/fphys.2018.01784

Coleman, R. A. (2019). It takes a village: channeling fatty acid metabolism and triacylglycerol formation *via* protein interactomes. *J. Lipid Res.* 60, 490–497. doi: 10.1194/jlr.S091843

Cotto, J. J., and Morimoto, R. I. (1999). Stress-induced activation of the heat-shock response: cell and molecular biology of heat-shock factors. *Biochem. Soc. Symp.* 64, 105–118.

Danforth, E., Horton, E. S., O'Connell, M., Sims, E. A., Burger, A. G., Ingbar, S. H., et al. (1979). Dietary-induced alterations in thyroid hormone metabolism during overnutrition. *J. Clin. Invest.* 64, 1336–1347. doi: 10.1172/JCI109590

Darras, V. M., Verhoelst, C. H. J., Reyns, G. E., Kühn, E. R., and der Geyten, S. V. (2006). Thyroid hormone deiodination in birds. *Thyroid* 16, 25–35. doi: 10.1089/thy.2006.16.25

Desvignes, T., Fauvel, C., and Bobe, J. (2011). The NME gene family in zebrafish oogenesis and early development. *Naunyn Schmiedeberg's Arch. Pharmacol.* 384, 439–449. doi: 10.1007/s00210-011-0619-9

Ding, X., Smallridge, R., Galloway, R., and Kiang, J. (1996). Rapid assay of HSF1 and HSF2 gene expression by RT-PCR. *Mol. Cell. Biochem.* 158, 189–192. doi: 10.1007/BF00225845

Dong, C., Zhang, Y., Zhang, Q., and Gui, J. (2006). Differential expression of three *Paralichthys olivaceus* Hsp40 genes in responses to virus infection and heat shock☆. *Fish Shellfish Immunol.* 21, 146–158. doi: 10.1016/j.fsi.2005.11.002

Du, X., Shen, X., Dai, L., Bi, F., Zhang, H., and Lu, C. (2020). PSMD12 promotes breast cancer growth *via* inhibiting the expression of pro-apoptotic genes. *Biochem. Biophys. Res. Commun.* 526, 368–374. doi: 10.1016/j.bbrc.2020.03.095

DuRant, S. E., Hopkins, W. A., Carter, A. W., Stachowiak, C. M., and Hepp, G. R. (2013). Incubation conditions are more important in determining early thermoregulatory ability than posthatch resource conditions in a precocial bird. *Physiol. Biochem. Zool.* 86, 410–420. doi: 10.1086/671128

European Union (2009). *Council Regulation (EC) No 1099/2009 of 24 September 2009 on the Protection of Animals At the Time of Killing Text with EEA Relevance 30*. Brussels: European Union.

Gruffat, D., Durand, D., Graulet, B., and Bauchart, D. (1996). Regulation of VLDL synthesis and secretion in the liver. *Reprod. Nutr. Dev.* 36, 375–389. doi: 10.1051/rnd:19960404

Hérault, F., Duby, C., Baéza, E., and Diot, C. (2018). Adipogenic genes expression in relation to hepatic steatosis in the liver of two duck species. *Animal* 12, 2571–2577. doi: 10.1017/S1751731118000897

Hérault, F., Houée-Bigot, M., Baéza, E., Bouchez, O., Esquerré, D., Klopp, C., et al. (2019). RNA-seq analysis of hepatic gene expression of common Pekin, Muscovy, mule and hinny ducks fed ad libitum or overfed. *BMC Genomics* 20:13. doi: 10.1186/s12864-018-5415-1

Herault, F., Saez, G., Robert, E., Al Mohammad, A., Davail, S., Chartrin, P., et al. (2010). Liver gene expression in relation to hepatic steatosis and lipid secretion in two duck species. *Anim. Genet.* 41, 12–20. doi: 10.1111/j.1365-2052.2009.01959.x

Kang, S. W., Madkour, M., and Kuenzel, W. J. (2017). Tissue-specific expression of DNA methyltransferases involved in early-life nutritional stress of chicken, *Gallus gallus*. *Front. Genet.* 8:204. doi: 10.3389/fgene.2017.00204

Katzeff, H. L. (1990). Increasing age impairs the thyroid hormone response to overfeeding. *Proc. Soc. Exp. Biol. Med.* 194, 198–203.

Kinlaw, W. B., Church, J. L., Harmon, J., and Mariash, C. N. (1995). Direct evidence for a role of the "spot 14" protein in the regulation of lipid synthesis. *J. Biol. Chem.* 270, 16615–16618. doi: 10.1074/jbc.270.28.16615

Kurlawala, Z., Shah, P. P., Shah, C., and Beverly, L. J. (2017). The STI and UBA domains of UBQLN1 are critical determinants of substrate interaction and proteostasis: U BQLN1 M EDIATED P ROTEOSTASIS. *J. Cell. Biochem.* 118, 2261–2270. doi: 10.1002/jcb.25880

Leveille, G. A., Romsos, D. R., Yeh, Y., and O'Hea, E. K. (1975). Lipid biosynthesis in the chick. A consideration of site of synthesis, influence of diet and possible regulatory mechanisms. *Poult. Sci.* 54, 1075–1093. doi: 10.3382/ps.0541075

Li, C., Zhang, R., Wei, H., Wang, Y., Chen, Y., Zhang, H., et al. (2021). Enriched environment housing improved the laying hen's resistance to transport stress *via* modulating the heat shock protective response and inflammation. *Poult. Sci.* 100:100939. doi: 10.1016/j.psj.2020.12.036

Livak, K. J., and Schmittgen, T. D. (2001). Analysis of relative gene expression data using real-time quantitative PCR and the $2-\Delta\Delta CT$ method. *Methods* 25, 402–408. doi: 10.1006/meth.2001.1262

Lo, B., Marty-Gasset, N., Manse, H., Bannelier, C., Bravo, C., Domitile, R., et al. (2020). Cellular markers of mule duck livers after force-feeding. *Poult. Sci.* 99, 3567–3573. doi: 10.1016/j.psj.2020.03.048

Loyau, T., Métayer-Coustard, S., Berri, C., Crochet, S., Cailleau-Audouin, E., Sannier, M., et al. (2014). Thermal manipulation during embryogenesis has long-term effects on muscle and liver metabolism in fast-growing chickens. *PLoS One* 9:e105339. doi: 10.1371/journal.pone.0105339

Lucas, A. (1998). Programming by early nutrition: an experimental approach. *J. Nutr.* 128, 401S–406S.

Madkour, M., Aboelenin, M. M., Aboelazab, O., Elolimy, A. A., El-Azeem, N. A., El-Kholy, M. S., et al. (2021). Hepatic expression responses of DNA methyltransferases, heat shock proteins, antioxidant enzymes, and NADPH 4 to early life thermal conditioning in broiler chickens. *Ital. J. Anim. Sci.* 20, 433–446. doi: 10.1080/1828051X.2021.1890645

Massimino, W., Davail, S., Bernadet, M.-D., Pioche, T., Tavernier, A., Ricaud, K., et al. (2019). Positive impact of thermal manipulation during embryogenesis on foie gras production in mule ducks. *Front. Physiol.* 10:1495. doi: 10.3389/fphys.2019.01495

Massimino, W., Davail, S., Secula, A., Andrieux, C., Bernadet, M. D., Pioche, T., et al. (2020). Ontogeny of hepatic metabolism in mule ducks highlights different gene expression profiles between carbohydrate and lipid metabolic pathways. *BMC Genomics* 21:742. doi: 10.1186/s12864-020-07093-w

Mendoza, A., and Hollenberg, A. N. (2017). New insights into thyroid hormone action. *Pharmacol. Ther.* 173, 135–145. doi: 10.1016/j.pharmthera.2017.02.012

Morimoto, R. (1993). Cells in stress: transcriptional activation of heat shock genes. *Science* 259, 1409–1410. doi: 10.1126/science.8451637

Neal, S. J., Karunanithi, S., Best, A., So, A. K.-C., Tanguay, R. M., Atwood, H. L., et al. (2006). Thermoprotection of synaptic transmission in a *Drosophila* heat shock factor mutant is accompanied by increased expression of Hsp83 and DnaJ-1. *Physiol. Genomics* 25, 493–501. doi: 10.1152/physiolgenomics.00195.2005

Nishida, E., and Gotoh, Y. (1993). The MAP kinase cascade is essential for diverse signal transduction pathways. *Trends Biochem. Sci.* 18, 128–131. doi: 10.1016/0968-0004(93)90019-j

Oppenheimer, J. H., Schwartz, H. L., Lane, J. T., and Thompson, M. P. (1991). Functional relationship of thyroid hormone-induced lipogenesis, lipolysis, and thermogenesis in the rat. *J. Clin. Invest.* 87, 125–132. doi: 10.1172/JCI114961

Pfaffl, M. W., Tichopad, A., Prgomet, C., and Neuvians, T. P. (2004). Determination of stable housekeeping genes, differentially regulated target genes and sample integrity: best keeper–excel-based tool using pair-wise correlations. *Biotechnol. Lett.* 26, 509–515.

Piestun, Y., Druyan, S., Brake, J., and Yahav, S. (2013). Thermal manipulations during broiler incubation alter performance of broilers to 70 days of age. *Poult. Sci.* 92, 1155–1163. doi: 10.3382/ps.2012-02609

Piestun, Y., Harel, M., Barak, M., Yahav, S., and Halevy, O. (2009). Thermal manipulations in late-term chick embryos have immediate and longer term effects on myoblast proliferation and skeletal muscle hypertrophy. *J. Appl. Physiol.* 106, 233–240. doi: 10.1152/japplphysiol.91090.2008

Piestun, Y., Shinder, D., Ruzal, M., Halevy, O., Brake, J., and Yahav, S. (2008). Thermal manipulations during broiler embryogenesis: effect on the acquisition of thermotolerance. *Poult. Sci.* 87, 1516–1525. doi: 10.3382/ps.2008-00030

Pihlajamäki, J., Boes, T., Kim, E.-Y., Dearie, F., Kim, B. W., Schroeder, J., et al. (2009). Thyroid hormone-related regulation of gene expression in human fatty liver. *J. Clin. Endocrinol. Metab.* 94, 3521–3529. doi: 10.1210/jc.2009-0212

Ritter, M. J., Amano, I., and Hollenberg, A. N. (2020). Thyroid hormone signaling and the liver. *Hepatology* 72, 742–752. doi: 10.1002/hep.31296

Rothenberg, C., Srinivasan, D., Mah, L., Kaushik, S., Peterhoff, C. M., Ugolino, J., et al. (2010). Ubiquilin functions in autophagy and is degraded by chaperone-mediated autophagy. *Hum. Mol. Genet.* 19, 3219–3232. doi: 10.1093/hmg/ddq231

Saez, G., Baéza, E., Bernadet, M. D., and Davail, S. (2010). Is there a relationship between the kinetics of lipoprotein lipase activity after a meal and the susceptibility to hepatic steatosis development in ducks? *Poult. Sci.* 89, 2453–2460. doi: 10.3382/ps.2010-00683

Sarge, K. D., Zimarino, V., Holm, K., Wu, C., and Morimoto, R. I. (1991). Cloning and characterization of two mouse heat shock factors with distinct inducible and constitutive DNA-binding ability. *Genes Dev.* 5, 1902–1911. doi: 10.1101/gad.5.10.1902

Satyal, S. H., Chen, D., Fox, S. G., Kramer, J. M., and Morimoto, R. I. (1998). Negative regulation of the heat shock transcriptional response by HSBP1. *Genes Dev.* 12, 1962–1974.

Silvestri, E., Schiavo, L., Lombardi, A., and Goglia, F. (2005). Thyroid hormones as molecular determinants of thermogenesis. *Acta Physiol. Scand.* 184, 265–283. doi: 10.1111/j.1365-201X.2005.01463.x

Sinha, R. A., Singh, B. K., and Yen, P. M. (2014). Thyroid hormone regulation of hepatic lipid and carbohydrate metabolism. *Trends Endocrinol. Metab.* 25, 538–545. doi: 10.1016/j.tem.2014.07.001

Sinha, R. A., Singh, B. K., and Yen, P. M. (2018). Direct effects of thyroid hormones on hepatic lipid metabolism. *Nat. Rev. Endocrinol.* 14, 259–269. doi: 10.1038/nrendo.2018.10

Tanabe, M. (1998). Disruption of the HSF3 gene results in the severe reduction of heat shock gene expression and loss of thermotolerance. *EMBO J.* 17, 1750–1758. doi: 10.1093/emboj/17.6.1750

Tarry-Adkins, J. L., and Ozanne, S. E. (2011). Mechanisms of early life programming: current knowledge and future directions. *Am. J. Clin. Nutr.* 94, 1765S–1771S. doi: 10.3945/ajcn.110.000620

Tavernier, A., Davail, S., Ricaud, K., Bernadet, M.-D., and Gontier, K. (2017). Genes involved in the establishment of hepatic steatosis in Muscovy, Pekin and mule ducks. *Mol. Cell. Biochem.* 424, 147–161. doi: 10.1007/s11010-016-2850-7

Vaiserman, A., Koliada, A., and Lushchak, O. (2018). Developmental programming of aging trajectory. *Ageing Res. Rev.* 47, 105–122. doi: 10.1016/j.arr.2018.07.007

Vitorino Carvalho, A., Hennequet-Antier, C., Crochet, S., Bordeau, T., Couroussé, N., Cailleau-Audouin, E., et al. (2020). Embryonic thermal manipulation has short and long-term effects on the development and the physiology of the Japanese quail. *PLoS One* 15:e0227700. doi: 10.1371/journal.pone.0227700

Vos, M. J., Hageman, J., Carra, S., and Kampinga, H. H. (2008). Structural and functional diversities between members of the human HSPB, HSPH, HSPA,

and DNAJ chaperone families. *Biochemistry* 47, 7001–7011. doi: 10.1021/bi800639z

Wadekar, S. A., Li, D., and Sánchez, E. R. (2004). Agonist-activated glucocorticoid receptor inhibits binding of heat shock factor 1 to the heat shock protein 70 promoter *in Vivo*. *Mol. Endocrinol.* 18, 500–508. doi: 10.1210/me.2003-0215

Wadekar, S. A., Li, D., Periyasamy, S., and Sánchez, E. R. (2001). Inhibition of heat shock transcription factor by GR. *Mol. Endocrinol.* 15, 1396–1410. doi: 10.1210/mend.15.8.0674

Wang, S., and Edens, F. W. (1998). Heat conditioning induces heat shock proteins in broiler chickens and turkey poults. *Poult. Sci.* 77, 1636–1645. doi: 10.1093/ps/77.11.1636

Westwood, J. T., Clos, J., and Wu, C. (1991). Stress-induced oligomerization and chromosomal relocalization of heat-shock factor. *Nature* 353, 822–827. doi: 10.1038/353822a0

Yu, J., Loh, K., Song, Z., Yang, H., Zhang, Y., and Lin, S. (2018). Update on glycerol-3-phosphate acyltransferases: the roles in the development of insulin resistance. *Nutr. Diabetes* 8:34. doi: 10.1038/s41387-018-0045-x

Conflict of Interest: The authors declare that the research was conducted in the absence of any commercial or financial relationships that could be construed as a potential conflict of interest.

Publisher's Note: All claims expressed in this article are solely those of the authors and do not necessarily represent those of their affiliated organizations, or those of the publisher, the editors and the reviewers. Any product that may be evaluated in this article, or claim that may be made by its manufacturer, is not guaranteed or endorsed by the publisher.

frontiers | Frontiers in Physiology

ORIGINAL RESEARCH
published: 21 April 2022
doi: 10.3389/fphys.2022.870451

Remodeling of Hepatocyte Mitochondrial Metabolism and *De Novo* Lipogenesis During the Embryonic-to-Neonatal Transition in Chickens

Chaitra Surugihalli[1], Linda S. Farley[1], Ronique C. Beckford[1], Boonyarit Kamkrathok[2], Hsiao-Ching Liu[2], Vaishna Muralidaran[1], Kruti Patel[1], Tom E. Porter[1] and Nishanth E. Sunny[1]**

[1]Department of Animal and Avian Sciences, University of Maryland, College Park, MD, United States, [2]Institute of Research and Development, Suranaree University of Technology, Nakhon Ratchasima, Thailand, [3]Department of Animal Science, NC State University, Raleigh, NC, United States

OPEN ACCESS

Edited by:
Elizabeth Ruth Gilbert, Virginia Tech, United States

Reviewed by:
Stephanie Wesolowski, University of Colorado, United States
Laura Ellestad, University of Georgia, United States

***Correspondence:**
Tom E. Porter
teporter@umd.edu
Nishanth E. Sunny
nsunny@umd.edu

Specialty section:
This article was submitted to Avian Physiology, a section of the journal Frontiers in Physiology

Received: *06 February 2022*
Accepted: *28 March 2022*
Published: *21 April 2022*

Citation:
Surugihalli C, Farley LS, Beckford RC, Kamkrathok B, Liu H-C, Muralidaran V, Patel K, Porter TE and Sunny NE (2022) Remodeling of Hepatocyte Mitochondrial Metabolism and De Novo Lipogenesis During the Embryonic-to-Neonatal Transition in Chickens. Front. Physiol. 13:870451. doi: 10.3389/fphys.2022.870451

Embryonic-to-neonatal development in chicken is characterized by high rates of lipid oxidation in the late-term embryonic liver and high rates of *de novo* lipogenesis in the neonatal liver. This rapid remodeling of hepatic mitochondrial and cytoplasmic networks occurs without symptoms of hepatocellular stress. Our objective was to characterize the metabolic phenotype of the embryonic and neonatal liver and explore whether these metabolic signatures are preserved in primary cultured hepatocytes. Plasma and liver metabolites were profiled using mass spectrometry based metabolomics on embryonic day 18 (ed18) and neonatal day 3 (nd3). Hepatocytes from ed18 and nd3 were isolated and cultured, and treated with insulin, glucagon, growth hormone and corticosterone to define hormonal responsiveness and determine their impacts on mitochondrial metabolism and lipogenesis. Metabolic profiling illustrated the clear transition from the embryonic liver relying on lipid oxidation to the neonatal liver upregulating *de novo* lipogenesis. This metabolic phenotype was conserved in the isolated hepatocytes from the embryos and the neonates. Cultured hepatocytes from the neonatal liver also maintained a robust response to insulin and glucagon, as evidenced by their contradictory effects on lipid oxidation and lipogenesis. In summary, primary hepatocytes from the embryonic and neonatal chicken could be a valuable tool to investigate mechanisms regulating hepatic mitochondrial metabolism and *de novo* lipogenesis.

Keywords: chicken, liver metabolism, mitochondria, lipid oxidation, *de novo* lipogenesis, metabolomics

INTRODUCTION

The United States has one of the world's largest poultry production systems, producing over 9.2 billion broilers and 9.3 billion dozen eggs in 2020 (USDA, 2018). Together, there is a burden on the industry and the farmers to meet the expected demand for 128 million tons of poultry meat by 2022 (Davis et al., 2013). In this regard, early hatchling mortality (which ranges between 0.5 and 2%)

during first 10 days after hatch is one of the major factors affecting broiler performance, quality and the economics of poultry industry (Noble et al., 1986; Wilson, 1991; Xin et al., 1994; Peebles et al., 2004; Pedroso et al., 2005; Yassin et al., 2009). The late embryonic and early neonatal development period in chicken is associated with dynamic developmental and metabolic changes in order to facilitate the rapid and healthy transition of the embryo to a hatchling, while simultaneously getting accustomed to the new carbohydrate rich dietary environment (Hicks et al., 2017; Surugihalli et al., 2019). Considering the relevance of this embryonic-to-neonatal period towards the overall health of the chicken, identifying nutritional and metabolic factors influencing this transition and in turn reducing mortality rates after hatch, is of significant interest to the poultry production systems.

The late term chicken embryo extensively relies on the yolk (>45% lipids) to derive over 90% of its energy, while the neonatal chicken has to rapidly transition to a carbohydrate rich starter diet (Hicks et al., 2017; Surugihalli et al., 2019). Thus, the embryonic liver in the chicken is programed to utilize free fatty acids through upregulation of the lipid oxidation networks. However, once exposed to a carbohydrate rich environment, the neonatal chicken liver undergoes a rapid metabolic switch from lipid utilization/oxidation to *de novo* lipogenesis from carbohydrates (Hicks et al., 2017). Such extremes of high rates of lipid oxidation and high rates of *de novo* lipogenesis, as evident during the embryonic-to-neonatal transition in chicken, is also a central feature of the mitochondrial co-morbidities in the liver of mice and humans with non-alcoholic fatty liver disease (NAFLD) (Sunny et al., 2011; Lambert et al., 2014; Patterson et al., 2016; Sunny et al., 2017). Such metabolic milieu could also be a contributing factor to the onset of fatty liver hemorrhagic syndrome (FLHS) in older layer and broiler flocks (Walzem et al., 1993; Lee et al., 2010; Pan et al., 2012; Trott et al., 2013; Liu et al., 2016). Furthermore, during these co-morbidities, high rates of lipid oxidation and high rates of *de novo* lipogenesis in the liver co-exist with inflammation and indices of hepatocellular stress (Nakamura et al., 2009; Satapati et al., 2016; Sunny et al., 2017). Interestingly, despite the lipid overburden associated with the high rates of lipid oxidation and high rates of *de novo* lipogenesis, the embryonic-to-neonatal transition occurs without any major evidence of cellular stress and inflammation in the liver (Surugihalli et al., 2019). Thus, while the existence of this dynamic "metabolic switch" during embryonic-to-neonatal transition is well known (Hicks et al., 2017; Cogburn et al., 2018; Surugihalli et al., 2019), the nutritional, metabolic and molecular factors mediating this transition in chicken remain unclear.

Mitochondrial oxidative networks in the liver, which include β-oxidation, ketogenesis, tricarboxylic acid (TCA) cycle and electron transport chain, adapt and remodel in response to different nutrient and hormonal cues under normal physiological states and during stages of insulin resistance (Satapati et al., 2012; Koliaki et al., 2015; Sunny et al., 2017). Indeed, dysfunctional mitochondrial metabolism is a central feature in rodent and human models of metabolic diseases such as insulin resistance, type-2 diabetes (T2DM) and fatty liver disease (Jelenik et al., 2017; Sunny et al., 2017) and could be a contributing factor to FLHS onset in older layer and broiler flocks (Walzem et al., 1993; Trott et al., 2013). Remodeling of mitochondrial metabolism during insulin resistance and fatty liver disease is characterized by selective activation of certain mitochondrial and cytoplasmic networks, which include the TCA cycle and *de novo* lipogenesis, respectively (Sunny et al., 2011; Lambert et al., 2014; Patterson et al., 2016; Surugihalli et al., 2019). The chronic induction of these networks is thought to aggravate hepatic stress and inflammation during fatty liver disease (Sunny et al., 2011; Satapati et al., 2016). The metabolic milieu in the liver during the embryonic-to-neonatal transition in the chicken allows us to investigate the relevance of the remodeling of mitochondrial networks and lipogenesis towards preserving hepatocyte function.

Our primary objective was to characterize the metabolic profiles of the plasma and liver in chicken embryos and neonatal chicks, in order to demonstrate the dramatic transition from lipid utilization in the embryos to lipid synthesis in the neonates. We further tested whether isolated primary hepatocytes from embryos and neonatal chicks accurately reflect the metabolic adaptation from embryonic-to-post hatch, in order to validate its utility as an *in vitro* system to probe factors regulating mitochondrial function and *de novo* lipogenesis.

MATERIALS AND METHODS

Experimental Plan

Eggs (64 g ± 0.6 standard error of means; SEM) were obtained from Perdue Farms Inc. (Salisbury, MD) from a broiler flock (Ross 708), and were incubated at 37°C and 45% relative humidity. On the day of hatch (day 21), neonatal chicken were transferred to floor pens maintained at 37°C and were provided a starter diet (Diet S-G 5065; ASAP Feed and Bedding, Quakertown, PA) *ad libitum*. The day-18 embryos (ed18) were sacrificed by decapitation, and the neonatal day-3 chicken (nd3) were decapitated following cervical dislocation. Plasma and tissue samples were collected from mixed-sex birds and frozen at −80°C for future analyses. Livers from a subset of day-18 embryos and day-3 neonatal chicken were utilized for the isolation of primary hepatocytes as detailed below. All the experiments were conducted in accordance with Institutional Animal Care and Use Committee protocols approved at the University of Maryland, College Park. All experiments were performed in accordance with relevant guidelines and regulations described by our institutional animal care and use committee. The methods and protocols in this study is reported in accordance with ARRIVE guidelines.

Isolation and Culturing of Primary Hepatocytes

In a separate set of experiments, livers from embryonic day-18 and neonatal day-3 broiler chickens were utilized of isolation of the hepatocytes. Following euthanasia by cervical dislocation and

decapitation, the birds were cut open to expose the heart and the liver. The left ventricle was infused with a perfusion media (10 ml basic SMEM and 20 µl 0.5 M EGTA) and the hepatic vein was severed. Following this, 20 ml SMEM media with collagenase and 0.1% bovine serum albumin (BSA) was infused. This media consisted of 500 ml SMEM (Minimal Essential media for Suspension cultures, Gibco); 57 ml 10X HBSS (Hank's Buffered Salt Solution, Gibco); 5.7 ml PenStrep (10,000 U/ml penicillin, 10,000 U/ml streptomycin) and 7.6 ml of BSA with Collagenase (0.12%) and 4 mM calcium. The perfused liver was collected and minced into small pieces in SMEM media with collagenase in a petri dish and incubated for 10 min at 37°C in a CO_2 incubator. The minced liver pieces were then filtered through a 70 µM filter into a 50 ml centrifuge tube and an additional 20 ml of SMEM media with EGTA was added to it. Later, 10 ml of 50% percol (in SMEM media with EGTA) was added and centrifuged. The cells were then pelleted by centrifuging and washed to remove any dead cells and debris. This was repeated three times. One experimental unit consisted of pooled cells from 2–3 livers, in order to obtain optimal hepatocyte cell counts for seeding the plates. Cells were then re-suspended in Williams' media [500 ml Williams' E media with 5.2 ml 1 mM HEPES (10 mM final concentration), 5.2 ml 100X L-glutamine (1X final concentration), 5.2 ml PenStrep and 7 ml 7.5% BSA (0.1% final concentration)] at 10^6 cells/ml. The cells were plated in 6-well culture plates pre-coated with 0.1% gelatin, and the hormonal treatments were added after 3 h. The cells were either treated with the basal media, corticosterone, growth hormone, glucagon or insulin for 24-h. All hormonal treatments were added at a final concentration of 10^{-9} M. Following 24-h of treatment, the cells were washed twice with ice-cold PBS and harvested using 1X RIPA and frozen at −80°C for further metabolic analysis. All the media were filtered and gassed for 30 s with 95% oxygen and 5% carbon dioxide. Following overnight culture, a set of basal hepatocytes from ed18 and nd3 were treated with 0, 25, and 100 nM insulin for 10 min, to determine the insulin signaling response of the hepatocytes. Following 10 min of insulin incubation, the cells were washed with cold phosphate buffered saline two times, collected and frozen in a lysis buffer for western blot analysis.

Analysis of TCA Cycle Organic Acids and Amino Acids by Gas Chromatography-Mass Spectrometry

Serum (25 µl) collected from ed18 and nd3 broiler birds were spiked with an equal volume of stable isotope-labelled internal standards and were deproteinized with 700 µl of 70% acetonitrile. The samples were centrifuged at 13,500 rpm for 15 min at 4°C, and the supernatant was transferred to a 1 ml v-vial and dried under a stream of nitrogen gas. The metabolites were then converted to their oximes with the addition of 20 µl of 2% methoxamine hydrochloride in pyridine (W/V) and microwaving at 350 W for 90 s. The samples were then derivatized with TBDMS (Tert-butyldimethylsilyl) at 90°C for 1 h. The metabolites were separated on a HP-5MS UI column (30 m × 0.25 mm × 0.25 µm; Agilent, CA, United States) and the ion fragments determined by single ion monitoring (SIM) under electron ionization mode using a GC-MS (5973N, Mass Selective Detector coupled to a 6890 Series GC System, Agilent, CA, United States). Metabolite concentrations were determined in relation to their respective stable isotope-labelled internal standard. For primary hepatocytes, the cells were collected in 1X RIPA and were deproteinized with 700 µl of 70% acetonitrile. The samples were spiked with a known volume of stable isotope-labeled organic acid and amino acid internal standards and sonicated for 10-min to extract the cellular contents. This extract was processed similar to the serum samples for GC-MS analysis.

Analysis of Triglyceride-Fatty Acids in Primary Hepatocytes

GC-MS analysis of the fatty acid methyl esters was performed as previously described (Surugihalli et al., 2019). Briefly, hepatocytes were collected using 1X RIPA and lipids were Folch extracted with 750 µl chloroform: methanol (2:1) after the addition of a mixed $U^{13}C$ fatty acid internal standard (Cambridge isotopes, MA, United States). The lipid layer was dried and saponified with 0.5 N methanolic NaOH for 30 min at 50°C. The samples were treated with 1 ml of 2% methanolic sulphuric acid and incubated at 50°C for 2-h to form fatty acid methyl esters (FAMEs). The FAMEs were then extracted with hexane, dried and re-suspended in 50–100 µl of hexane for GC-MS analysis. The FAMEs were separated on a VF 23 ms column (30 m × 0.25 mm × 0.25 µm; Agilent, CA, United States), followed by fragmentation under electrical ionization on a 5973N-Mass Selective Detector, 6890-Series GC, (Agilent, CA, United States). Concentrations of individual FAMEs were determined relative to their respective stable isotope-labeled internal standard.

Western Blot Analysis

Primary hepatocytes treated under basal and insulin-stimulated conditions were collected in 100 µl of 1x RIPA containing protease and phosphatase inhibitor and incubated for 1 h on ice to extract proteins. The cells were then centrifuged at 13,500 rpm for 15 min at 4°C. The protein content of the supernatant was determined using BCA protein assay (Thermo Fischer Scientific. Waltham, MA, United States). Proteins (10 µg) were separated on 8% tris bolt gels (Invitrogen, Carlsbad, CA, United States), and were transferred to a nitrocellulose membrane and incubated with primary antibodies Akt, pAkt and GAPDH (Cell Signaling Technology Inc., Danvers, MA, United States) to evaluate the response of the primary hepatocytes to insulin treatment.

Global Metabolomics and Lipidomics of Liver Tissue

Liver tissue from a previously published set of studies (Hicks et al., 2017) were utilized for global metabolomics and lipidomics. In this previously published study, eggs from specific pathogen-free (SPF) leghorn chickens (layers) were obtained from Charles River Laboratories (Wilmington, MA, United States) and

incubated at 37.5°C and 60% relative humidity with rotation every hour. Livers from embryonic day 18 (ed18; $n = 9$) and neonatal day 3 (nd3: $n = 9$) chickens (mixed-sex) were utilized for global metabolomics and lipidomics. For the metabolomic and lipidomic analyses, the liver tissues were pre-normalized for mass spectrometry at a protein concentration of 500 µg/ml. Liver samples (25 mg) underwent Folch extraction and the aqueous and lipid layers were was dried and reconstituted for LC-MS/MS based metabolomics and lipidomics, respectively. Global metabolomics and lipidomics was performed on a Thermo Q-Exactive Oribtrap mass spectrometer with Dionex UHPLC and autosampler. All samples were analyzed in positive and negative heated electrospray ionization with a mass resolution of 35,000 at m/z 200 as separate injections. Separation was achieved on an ACE 18-pfp 100 × 2.1 mm, 2 µm column for polar metabolites. Separation was achieved on Acquity BEH C18 1.7 µm, 100 mm × 2.1 mm column for lipid metabolites.

Gene Expression Profiles From RNA Sequencing

RNA sequencing data from SPF leghorn chicken layer livers, a previously published data set (Hicks et al., 2017), were utilized to evaluate changes in expression levels of specific genes involved in mitochondrial metabolism and lipogenesis. In brief, total RNA was isolated and purified using Tri-Reagent (Sigma) per manufacturer's protocol from the liver tissue of e18 and nd3 chicken ($n = 4$ per group). Small RNA libraries (1 µg/each library) were developed at using TruSeq Small RNA sample preparation kit (Illumina) per manufacturer's protocol. The diluted library (10 nM) from each bird was pooled and sequenced with Illumina Genome Analyzer IIx (GAIIx) (NCSU Genomic Sciences Laboratory). The mRNA libraries were generated using TruSeq RNA library preparation kit v2 (Illumina) and barcode indices following the manufacturer's instructions and were assessed using high sensitivity DNA chip on a Agilent Technologies 2100 Bioanalyzer. Further a 50 bp single end of each library was sequenced at DHMRI (Kannapolis, NC) using an Illumina HiSeq 2500. The sequencing data was processed and analyzed CLC genomics workbench (Qiagen).

Gene Expression Analysis Using RT-qPCR

Gene expression analysis performed as previously described (Beckford et al., 2020). Total RNA from primary hepatocytes, derived from broiler chicken livers, was isolated using the RNeasy mini kit (Qiagen, Hilden, Germany) following the manufacturer's protocol. Before elution of RNA, an on-column deoxyribonuclease digestion was done to remove genomic DNA. Total RNA was quantified using Quant-iT RiboGreen RNA Quantification reagent (Invitrogen, Carlsbad, CA, United States). Following which cDNA was prepared from1 µg of total RNA in 20 µl reactions using M-MLV RT kit (New England Biolabs, Ipswich, MA) following the manufacturer's instructions. Quantitative real-time PCR was performed using 20 ng of cDNA, 10 µM of each primer, and 7.5 µl of 2X master mix [PCR buffer (50 mM KCl, 10 mM Tris–HCl, 0.1% triton-X-100), 0.12 U/µl Taq

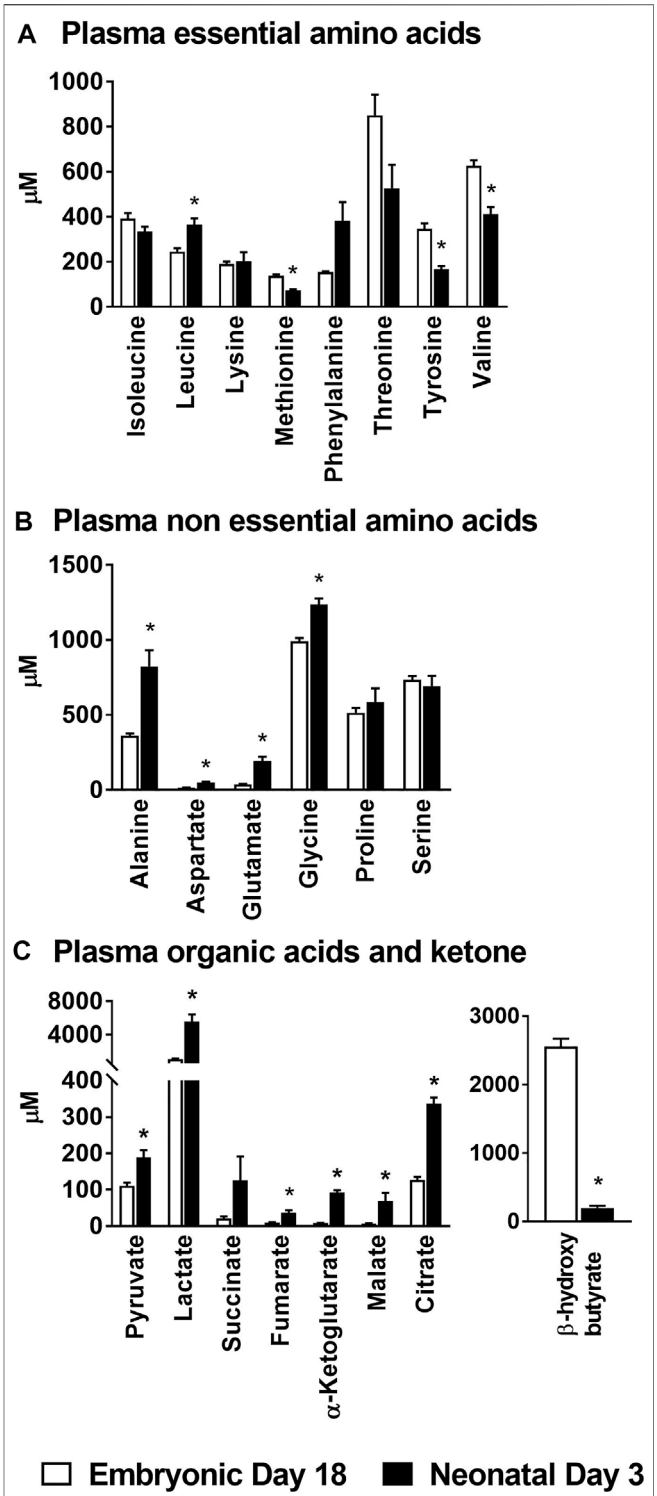

FIGURE 1 | Changes in plasma amino acids, organic acids and β-hydroxybutyrate during embryonic-to-neonatal development. Plasma concentrations of **(A)** Essential amino acids; **(B)** Non-essential amino acids; **(C)** Organic acid intermediates of the TCA cycle and β-hydroxybutyrate in broiler embryos and neonates. All the values are represented as means ± SEM with $n = 6$–9 birds/group. Results were considered significant at $p \leq 0.05$ (*) following a Student t-test between embryonic day 18 and neonatal day 3.

Polymerase, 0.2 μM dNTPs, 40 nM fluorescein (Invitrogen, Waltham, MA, United States), and SYBR Green I Nucleic Acid Gel Stain diluted 1:10,000 (Invitrogen, Waltham, MA, United States), and 4.3 μl of water. Samples were run in duplicate and PCR was performed for 40 cycles under the following conditions: 95°C for 15 s, 60°C for 30 s, and then 72°C for 30 s. Target genes were normalized to the expression of *GAPDH* in the same samples and then expressed relative to the basal treatment (untreated cells). Primers (**Supplementary Table 1**) for real time quantitative PCR. The genes were designed using Primer Express 2.0 (Applied Biosystems, Waltham, MA, United States) and validated according to the procedures previously described (Ellestad et al., 2011).

Statistical Analysis

All the data reported are presented as means ± standard error of means (SEM). Results were analyzed using unpaired *t*-tests for comparisons between e18 and nd3. The responses to hormonal treatments were analyzed using one-way ANOVA followed by Tukey's pair-wise means comparisons. Means were considered significantly different at $p \leq 0.05$. All the statistical analysis were conducted and the graphs were plotted utilizing Prism 7 (GraphPad software Inc., San Diego, CA, United States).

RESULTS

Alterations in Plasma Metabolites Highlight the Major Metabolic Shift During Embryonic-to-Neonatal Development

The circulating concentration (μM ± SEM) of the essential amino acid leucine (ed18: 246 ± 15 vs. nd3: 365 ± 28) was significantly higher ($p \leq 0.05$) in the neonatal chicks; while those of methionine (ed18: 138 ± 6 vs. nd3: 73 ± 5), tyrosine (ed18: 347 ± 24 vs. nd3: 166 ± 15) and valine (ed18: 626 ± 25 vs. nd3: 411 ± 32) were significantly lower ($p \leq 0.05$) than their embryonic counterparts (**Figure 1A**). Plasma non-essential amino acids alanine (ed18: 363 ± 13; nd3: 825 ± 107), aspartate (ed18: 15 ± 2; nd3: 49 ± 7), glutamate (ed18: 38 ± 2; nd3: 194 ± 27), and glycine (ed18: 991 ± 22; nd3: 1,236 ± 42), were significantly higher ($p \leq 0.05$) in the neonatal chicken compared to their embryonic counterparts (**Figure 1B**). There was also a parallel increase in plasma organic acids pyruvate (ed18: 111 ± 8 vs. nd3: 189 ± 20), lactate (ed18: 1,042 ± 71 vs. nd3: 5,573 ± 831), and all the mitochondrial TCA cycle intermediates, succinate (ed18: 21 ± 5 vs. nd3: 126 ± 65), fumarate (ed18: 9 ± 1 vs. nd3: 36 ± 7), α-ketoglutarate (ed18: 8 ± 1 vs. nd3: 92 ± 7), malate (ed18: 7 ± 1 vs. nd3: 68 ± 23), and citrate (ed18: 127 ± 9 vs. nd3: 336 ± 17), in the neonatal chicken ($p \leq 0.05$, **Figure 1C**). On the contrary, there was a dramatic decrease in the plasma β-hydroxybutyrate levels in the neonatal chicks compared to their embryonic counterparts (ed18: 2,556 ± 116 vs. nd3: 200 ± 31; $p \leq 0.05$) (**Figure 1C**). These observed differences in circulating levels of amino acids, organic acids and β-hydroxybutyrate point to significant remodeling of energy metabolism between embryonic and neonatal stages in chicken.

Remodeling of Hepatic Metabolism during Embryonic-to-Neonatal Development

There was a significant decrease ($p \leq 0.05$) in the levels of the essential amino acids isoleucine, leucine, methionine and tyrosine in the liver of the neonatal chicks compared to their embryonic counterparts (**Figure 2A**). While the levels of the non-essential amino acid alanine was significantly lower ($p \leq 0.05$) in neonatal chicks, aspartate, glutamine, glycine and serine were significantly higher ($p \leq 0.05$) in neonatal chicken liver compared to the embryonic liver (**Figure 2B**). Pyruvate and lactate levels were significantly higher ($p \leq 0.05$) in the neonatal liver whereas the mitochondrial TCA cycle intermediates remained unchanged between the two groups (**Figure 2C**). Concurrently, profiling of various triglycerides in the liver demonstrated a 2–10 fold increase ($p \leq 0.1$) in their abundances in the neonatal chicken liver compared to their embryonic counterparts (**Figure 2D**). Considering the dramatic differences in the total liver weight and the total protein content of the liver between the ed18 and nd3 livers (Surugihalli et al., 2019), tissue samples were pre-normalized based on a known amount of liver protein, before liquid chromatography-mass spectrometry (LC-MS/MS) analysis, for the analysis and comparison of triglycerides between the two groups.

Hepatic Gene Expression Profiles Clearly Illustrate the Metabolic Shift From Lipid Oxidation in the Embryonic Liver to New Lipid Synthesis in the Neonatal Liver

The lipid oxidation gene carnitine palmitoyl transferase 1a (*CPT1A*), which is involved in the formation of fatty acyl-carnitines and facilitate the movement of fatty acids in to the mitochondria for β-oxidation was downregulated 2–3 fold ($p \leq 0.05$) in the neonatal chicken liver (**Figure 3A**). Similarly, Carnitine palmitoyl transferase 2 (*CPT2*), which converts fatty acyl-carnitine to fatty acyl-CoA and carnitine, for the breakdown of free fatty acids through β-oxidation, was also suppressed ~2-fold ($p \leq 0.05$) in the neonatal liver (**Figure 3A**). Furthermore, the gene expression of peroxisome proliferator activator receptor 1a (*PPARA*), a transcription factor which is a master regulator of lipid oxidation and hydroxyacyl-CoA dehydrogenase subunit A (*HADHA*) an enzyme involved in mitochondrial β-oxidation were also downregulated ~2–3 fold ($p \leq 0.05$) post-hatch (**Figure 3A**). The decrease in mitochondrial fat oxidation was associated with higher expression of certain mitochondrial complex genes such as succinate dehydrogenase subunit a (*SDHA*) and NADH dehydrogenase (*ND2*) in neonatal chicken liver (**Figure 3B**). However, hepatic gene expression of *PGC1A*, a gene that codes for mitochondrial biogenesis was lower in the neonatal liver ($p \leq 0.05$; **Figure 3B**). The lower expression of the lipid oxidation genes in the liver of the neonatal chicken was accompanied by a ~100–200 fold increase in the expression of genes involved in lipogenesis (**Figure 3C**) including fatty acid synthase (*FASN*), steroyl-Coenzyme A destaurase1

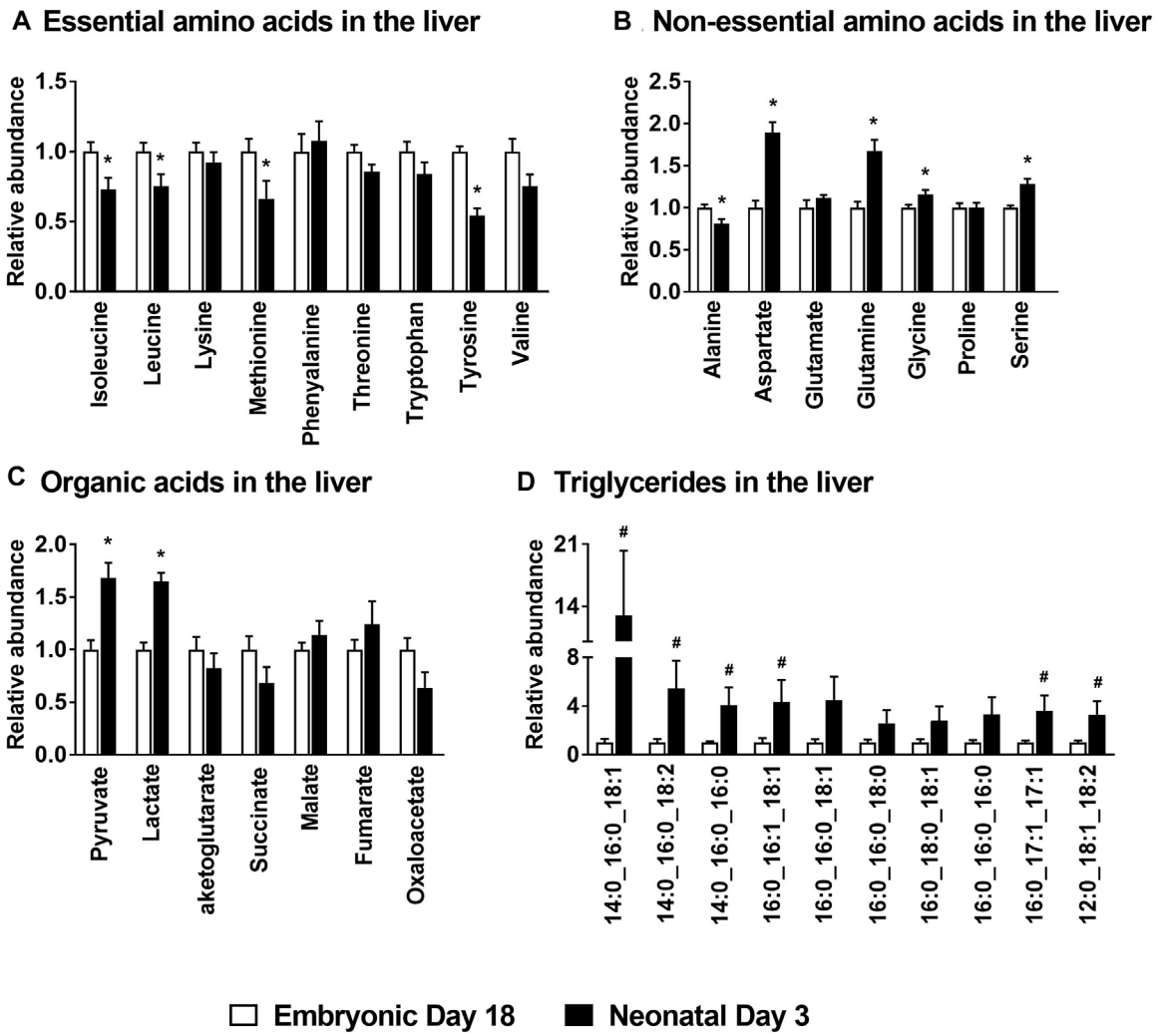

FIGURE 2 | Metabolite profile of the embryonic and neonatal chicken liver. Changes in neonatal liver metabolites are presented relative to those of embryonic day 18. Profiles of **(A)** Essential amino acids; **(B)** Non-essential amino acids; **(C)** Organic acids associated with mitochondrial TCA cycle and **(D)** Hepatic triglycerides in embryos and neonates from leghorn layer flock. All the values are represented as means ± SEM with $n = 6–9$ birds/group. Results were considered significant at $p \leq 0.05$ (*) or a trend at $p \leq 0.1$ (#) following a Student *t*-test between embryonic day 18 and neonatal day 3.

(*SCD1*), elongation of long-chain fatty acids family member 6 (*ELOVL6*), fatty acid desaturase 2 (*FADS2*) and lanosterol synthase (*LSS*). Taken together, these data highlight the metabolic transition from high rates of lipid oxidation and free fatty acid utilization by the embryonic liver, to high rates of *de novo* lipogenesis by the neonatal liver.

Isolated Primary Hepatocytes From the Neonatal Chicken Accumulated More Lipids and Displayed a Robust Response to Insulin Treatment

Triglycerides were isolated from primary hepatocytes and converted to their fatty acid methyl esters for gas chromatography-mass spectrometry (GC-MS) analysis. The concentrations (μg/mg ± SEM) of triglyceride-fatty acid methyl ester of palmitate (ed18: 123 ± 21 vs. nd3: 1,284 ± 320), palmitoleate (ed18: 4.0 ± 0.40 vs. nd3:; 96.7 ± 15.9), stearate (ed18: 88 ± 14 vs. nd3: 809 ± 196), oleate (ed18: 139 ± 6 vs. nd3: 1,519 ± 403) and linoleate (ed18: 51 ± 3 vs. nd3: 272 ± 66) were significantly higher ($p \leq 0.05$) in the hepatocytes isolated from neonatal day 3 chicks (**Figure 4A**). For the organic acid intermediates of the TCA cycle, the lactate content (μg/mg ± SEM; ed18: 7.45 ± 1.02 vs. nd3: 17.15 ± 3.73) was significantly higher ($p \leq 0.05$) in hepatocytes from neonatal chicks (**Figure 4B**), while fumarate, α-ketoglutarate and malate were significantly lower ($p \leq 0.05$) in the neonatal hepatocytes (**Figure 4B**). The concentration of all amino acids remained similar between groups (**Figure 4C**), except for methionine which was significantly higher ($p \leq 0.05$) in the neonatal chick hepatocytes (ed18: 1.51 ± 2.52 vs. nd3: 2.83 ± 0.41) (**Figure 4C**). Further, there was a robust response of the

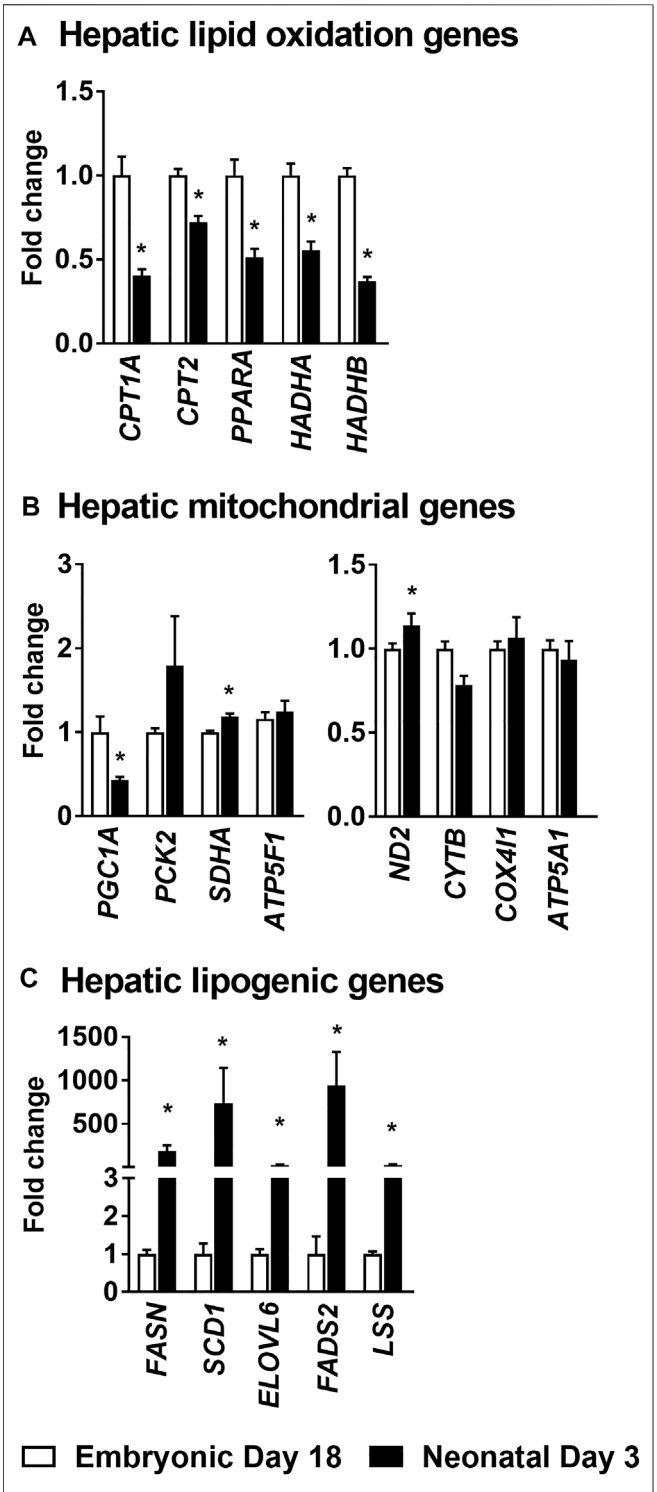

FIGURE 3 | Changes in hepatic gene expression profiles during embryonic-to-neonatal development. The fold changes in the expression profiles of genes involved in **(A)** Lipid oxidation; **(B)** Mitochondrial metabolism and **(C)** Lipogenesis, between the embryonic and neonatal liver. RNA sequencing data from a previously published data set, from a leghorn layer background, were utilized for these analysis (Hicks et al., 2017). All the values are represented as means ± SEM with $n = 4$ birds/group. Results were

(*Continued*)

hepatocytes from both the embryonic and neonatal groups to insulin treatment, as detected by the phosphorylation of AKT (protein kinase B) at serine 473 (**Figure 4D**). The accumulation of lipids by the neonatal primary hepatocytes and their response to insulin were similar to those observed in an *in vivo* embryonic-to-neonatal transition setting. Thus, the primary hepatocyte model system could have utility towards exploring factors regulating lipid accumulation, mitochondrial metabolism and insulin signaling.

Impact of the Hormonal stimuli on Hepatocyte Mitochondrial Lipid Metabolism and Lipogenesis

Isolated primary hepatocytes were incubated with four hormones whose levels are known to dynamically change during embryonic-to-neonatal development and in turn affect major metabolic events during development. The major changes in gene expression profiles in response to the hormonal treatments are highlighted below. The mRNA levels of *CPT1A* were lower ($p \leq 0.05$) in the hepatocytes isolated from the neonatal livers treated with insulin (INS) when compared to the basal treatment (**Figure 5A**). Expression of the cytosolic Phosphoenolpyruvate carboxykinase (*PCK1*) was downregulated ($p \leq 0.05$) in both the embryonic and neonatal hepatocytes in response to INS, compared to the basal treatment (**Figure 5B**). Glucagon treatment did not produce any significant effects on the mRNA profiles, compared to the basal treatment of the hepatocytes. Expression of mRNA for lipogenic genes *FASN* and *LSS* were significantly upregulated ($p \leq 0.05$) upon INS treatment in the embryonic liver, compared to the basal treated groups (**Figure 5C**). In the neonatal hepatocytes, only *FASN* showed significant upregulation ($p \leq 0.05$) upon INS treatment, compared to basal (**Figure 5C**). While the GCG induced changes in lipogenic gene expression of *FASN*, *SCD1* and *LSS* were lower than their corresponding expression in the embryonic hepatocytes treated with INS, the GCG induced changes in gene expression remained similar to basal treatment. Overall, these results suggest that insulin had the most prominent impact on hepatocyte lipid metabolism and lipogenesis in both the embryonic and neonatal stages.

FIGURE 3 | considered significant at $p \leq 0.05$ (*) following a Student *t*-test between embryonic day 18 and neonatal day 3. ***CPT1A***, Carnitine palmitoyl transferase 1a. ***CPT2***, Carnitine palmitoyl transferase 2. ***PPARA***, Peroxisome proliferator activator receptor 1a. ***HADHA***, Hydroxyacyl-CoA dehydrogenase subunit A. ***PGC1A***, Peroxisome proliferator-activated receptor gamma coactivator 1-alpha. ***PCK2***, Phosphoenolpyruvate carboxykinase 2. ***SDHA***, Succinate dehydrogenase flavoprotein subunit A. ***ATP5F1***, ATP synthase F (0) complex subunit B1. ***ND2***, NADH dehydrogenase subunit 2. ***CYTB***, Cytochorome b. ***COX4I1***, Cytochrome c oxidase subunit 4. ***ATP5A1***, ATP synthase alpha subunit. ***FASN***, Fatty acid synthase. ***SCD1***, Steroyl-CoenzymeA desaturase1. ***ELOVL6***, Elongation of very long chain fatty acids protein. ***FADS2***, Fatty Acid Desaturase 2. ***LSS***, Lanosterol synthase.

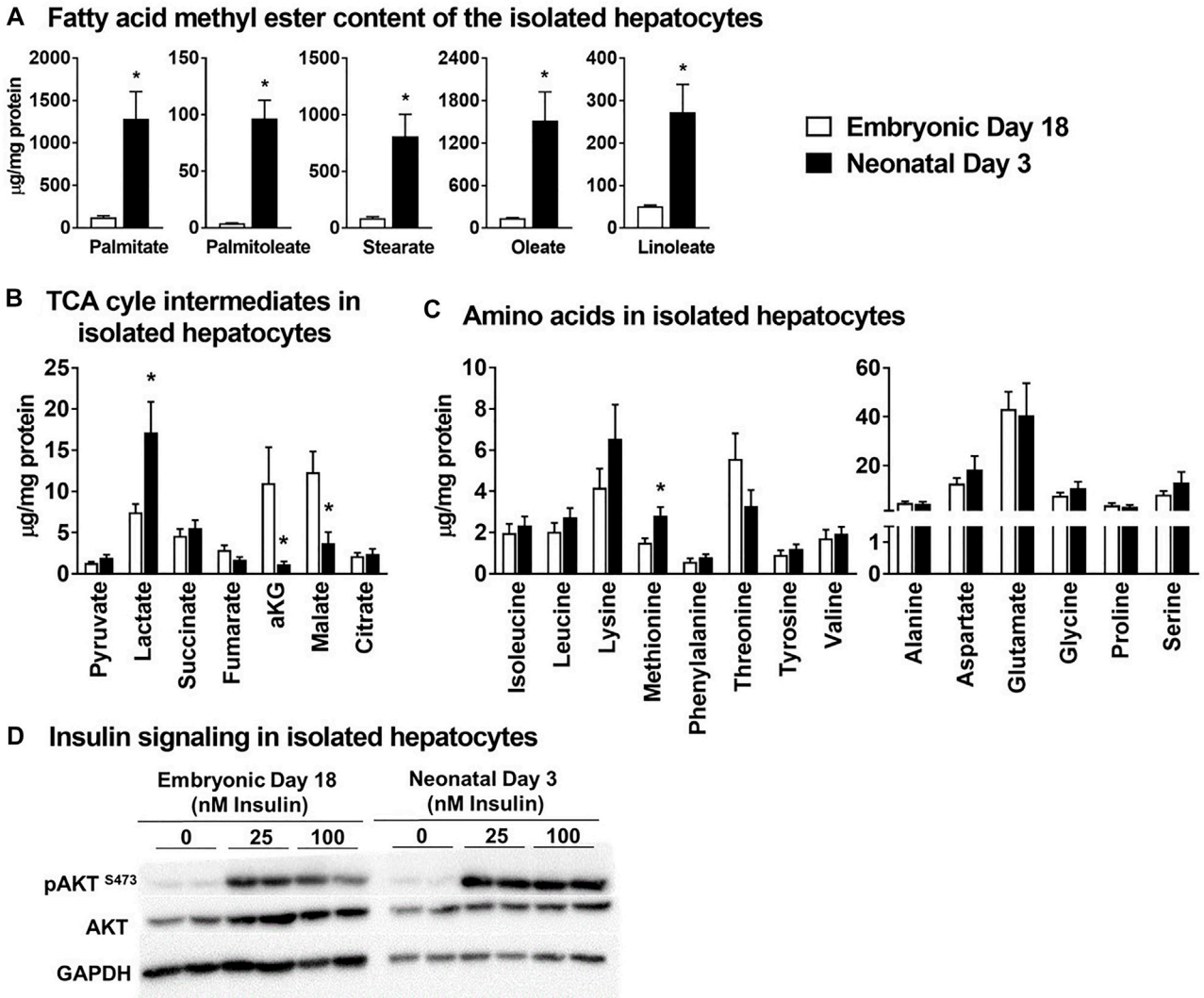

FIGURE 4 | Primary isolated hepatocytes from broiler chicken embryos and neonates - a metabolic model to investigate mitochondrial metabolism and lipid accumulation. All metabolite concentrations were normalized to the cell protein content of the isolated hepatocytes. **(A)** Concentrations of triglyceride derived fatty acid methyl esters in the hepatocytes, **(B)** Levels of TCA cycle intermediates in the isolated hepatocytes **(C)** levels of essential and non-essential amino acids in the isolated hepatocytes and, **(D)** western blot analysis of pAKT at Ser-473 as an index of insulin signaling. All the values are represented as means ± SEM with n = 4–6 independent replicates/group. Each replicate consisted of pooled hepatocytes isolated from 2–3 birds. Results were considered significant at $p \leq 0.05$ (*) following a Student t-test between embryonic day 18 and neonatal day 3. AKT, Protein kinase B.

Impact of the Hormonal Stimuli on the Essential Amino Acid Content of Isolated Hepatocytes

Hormonal treatments did not alter the levels of any of the essential amino acids in the hepatocytes isolated from embryonic day 18 liver (**Figure 6**). Interestingly, there was a significant increase in the levels of all the essential amino acids following growth hormone (GH) and INS treatments ($p \leq 0.05$), compared to the basal treatment in neonatal hepatocytes. Contrary to the higher levels of all the essential amino acids in INS and GH treated hepatocytes, corticosterone (CORT) and GCG treatments resulted in lower levels of these amino acids in the neonatal hepatocytes ($p \leq 0.05$). Considering the anabolic roles of INS and GH, these results could indicate the pivotal roles these essential amino acids are playing to support the active anabolic milieu in the neonatal hepatocyte, including rates of protein synthesis.

DISCUSSION

The embryonic-to-neonatal transition period in chicken provides a unique window to understand the metabolic mechanisms that help to promote rapid and healthy tissue development. Specifically in the liver, this window is unique because, the late

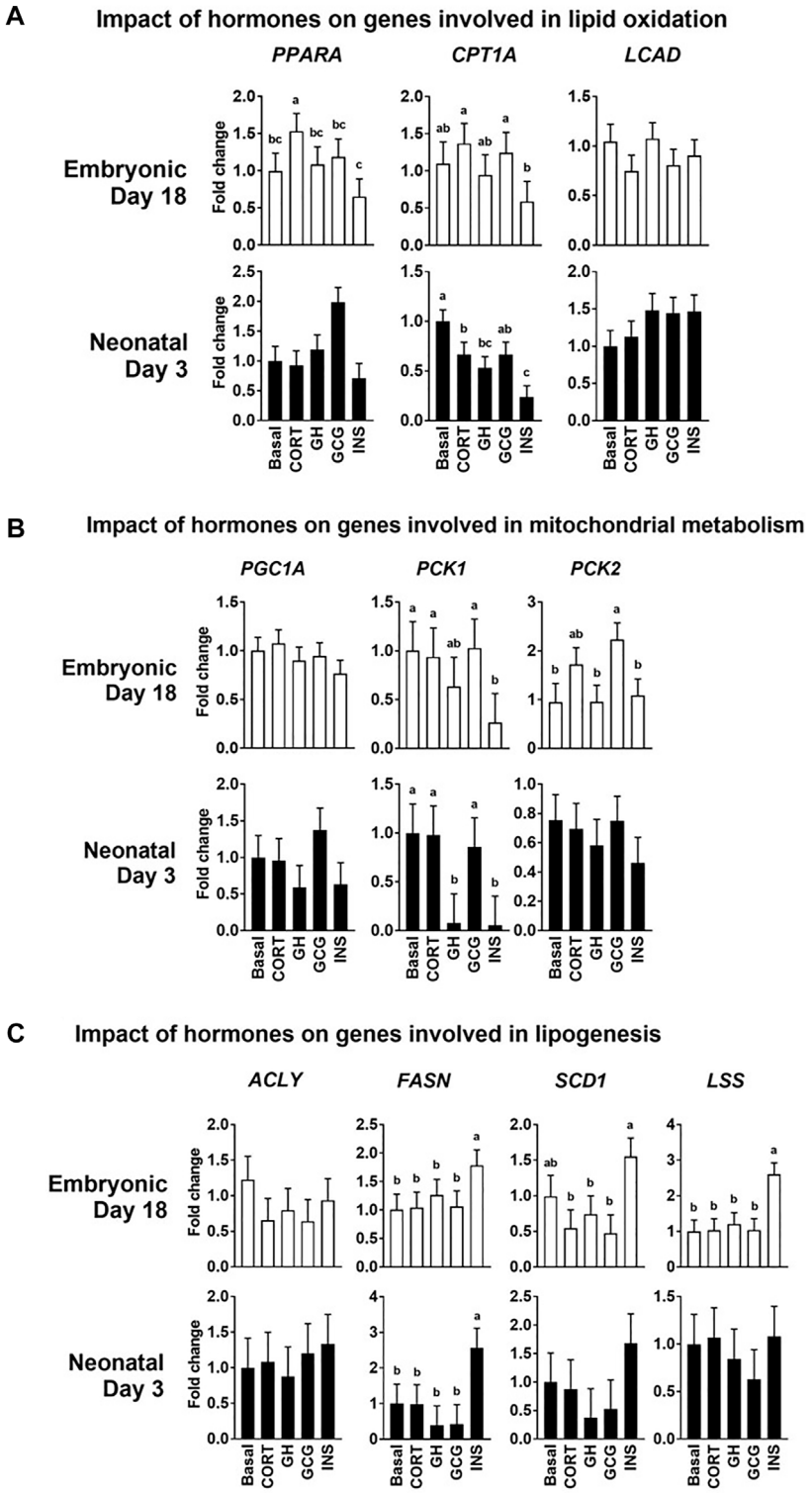

FIGURE 5 | Impact of the hormonal stimuli on hepatocyte metabolism. Quantitative PCR analysis was performed to determine the impact of four major hormones on hepatocyte metabolism. Fold changes in the expression patterns of genes involved in the regulation of **(A)** Lipid oxidation **(B)** Mitochondrial metabolism and **(C)** Lipogenesis in the liver were determined. All the values are Means ± pooled SE of four independent replicate experiments/age. Each independent replicate experiment was performed on pooled hepatocytes isolated from 2–3 birds. Results are considered significant at $p \leq 0.05$ following one way ANOVA. Different superscripts between bars in a panel indicates statistical significance from other treatments. CORT, Corticosterone; GH, Growth hormone; GCG, Glucagon; INS, Insulin; *PPARA*, Peroxisome proliferator activator receptor 1a; *CPT1A*, Carnitine palmitoyl transferase 1a; *LCAD*, Long-chain fatty acyl, *PGC1A*, Peroxisome proliferator-activated receptor gamma coactivator 1-alpha; *PCK1/2*, Phosphoenolpyruvate carboxykinase 1 and 2; *ACLY*, ATP citrate lyase; *FASN*, Fatty acid synthase; *SCD1*, Steroyl-CoA desaturase; *LSS*, Lanosterol synthase.

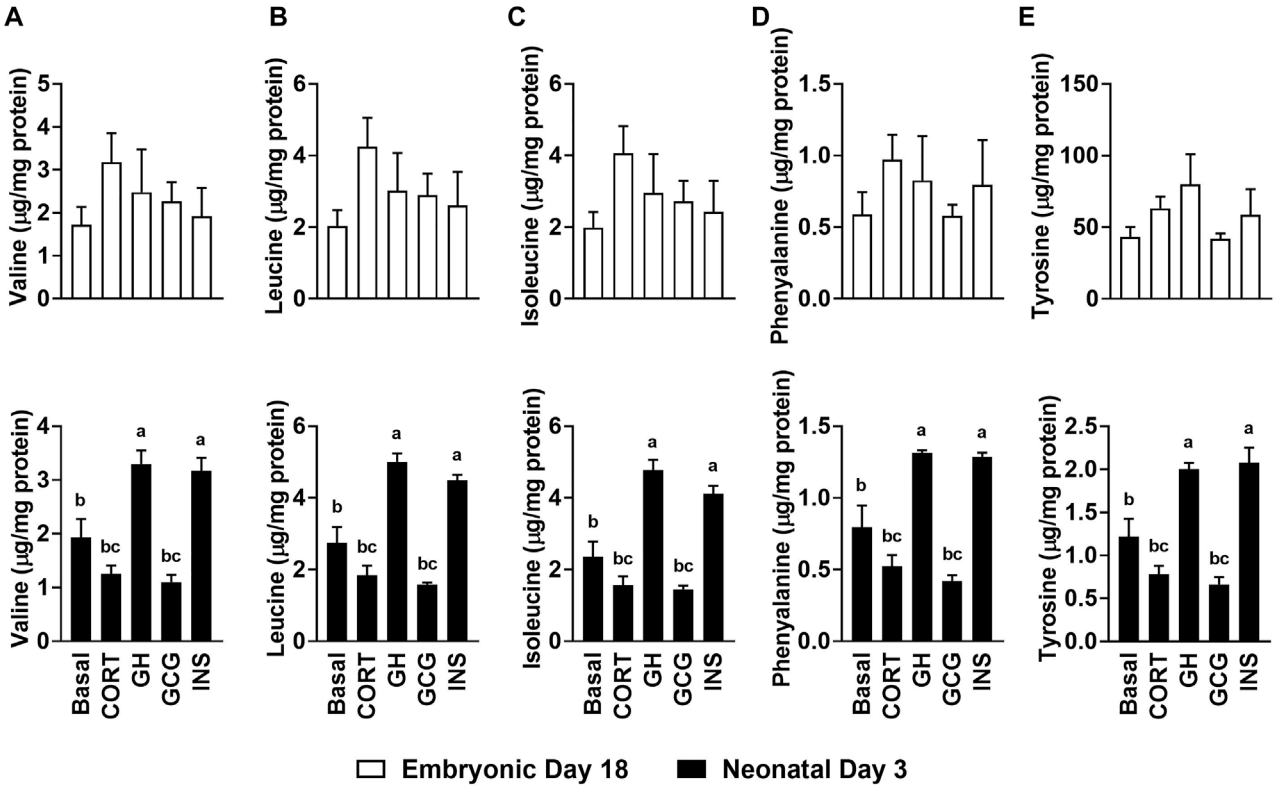

FIGURE 6 | Impact of the hormonal stimuli on the essential amino acid content of isolated hepatocytes. Impact of hormones on levels of branched-chain amino acids, **(A)** Valine, **(B)** Leucine and **(C)** Isoleucine and the essential amino acids **(D)** Phenylalanine and **(E)** Tyrosine. All the values are Means ± SEM of four independent replicates/group. Each replicate consisted of pooled hepatocytes isolated from 2–3 birds. Results are considered significant at $p \leq 0.05$ following one way ANOVA. Different superscripts between bars in a panel indicates statistical significance from other treatments. CORT, Corticosterone; GH, Growth hormone; GCG, Glucagon; INS, Insulin.

term embryonic chicken liver (>day-16 of incubation) derives >90% of its energy through the oxidation of yolk lipids (Hazelwood, 1971; Noble and Cocchi, 1990; Moran Jr, 2007). Further, immediately after hatch, hepatic *de novo* lipogenesis is dramatically upregulated several hundred fold in response to the carbohydrate rich environment provided by the diet (Hicks et al., 2017; Surugihalli et al., 2019). This is interesting considering the fact that the lessons from mouse models and human subjects provide contrary evidence. In these species, a metabolic environment favoring high rates of lipid accumulation and high rates of lipid oxidation contributes to the etiology of fatty liver disease syndrome (Lambert et al., 2014; Patterson et al., 2016; Satapati et al., 2016; Kattapuram et al., 2021). However, during embryonic-to-neonatal transition in chicken, mitochondrial lipid oxidation is optimally coupled with *de novo* lipogenesis, in turn abating the onset and progression of hepatocellular stress (Surugihalli et al., 2019). Understanding mechanisms contributing to this synergy is of great significance to optimize embryonic-to-neonatal development and towards the management of fatty liver syndromes. This makes the embryonic-to-neonatal transition period in chicken is an attractive metabolic model to probe mechanisms regulating hepatocellular function, and thus warranting a detailed characterization of liver metabolism during this unique developmental period.

The embryonic-to-neonatal transition period is a period of active growth and metabolic development. With this in mind, we first profiled the circulating levels of amino acids and organic acid TCA cycle intermediates in embryos and neonatal chicken. The higher levels of circulating non-essential amino acids we observed in the neonatal chicken (e.g., alanine, aspartate and glutamate, **Figure 1B**) could point to their higher requirement as metabolic substrates to support the rapid growth of the hatchlings. There was also a parallel increase in the plasma organic acid TCA cycle intermediates (e.g., pyruvate, lactate, fumarate, α-ketoglutarate, malate and citrate, **Figure 1C**) in the neonatal circulation, many of which are carbon substrates for amino acid synthesis and transamination reactions. In the neonatal chicken liver, significant increases, relative to their embryonic counterparts, were only observed for aspartate, glutamate and serine. While pyruvate and lactate levels were higher in the neonatal liver, potentially a reflection of high rates of carbohydrate oxidation, the levels of other TCA cycle intermediates remained similar between groups. In spite of this, there was a more than 10-fold

drop in circulating β-hydroxybutyrate levels from the embryonic-to-neonatal stage, clearly demonstrating the switch from free fatty acid utilization in the embryos to lipid synthesis in the neonates (Surugihalli et al., 2019). This metabolic switch was further substantiated by the higher rates of triglyceride accumulation along with the dramatic upregulation of lipogenic gene expression in the neonatal liver. The higher lipid accumulation in the neonatal liver occurred simultaneously with the lower expression profiles of genes involved in lipid oxidation. Liver is the primary lipogenic organ in the chicken (Zaefarian et al., 2019; Liu et al., 2020) and the metabolic milieu in the liver is primed to upregulate *de novo* lipogenesis immediately after hatch and on exposure to a carbohydrate rich dietary environment (Hicks et al., 2017; Surugihalli et al., 2019). The cytoplasmic network of *de novo* lipogenesis relies on and shares metabolic and molecular mediators of mitochondrial function, to upregulate its activity. In fact, the dramatic upregulation of *de novo* lipogenesis in the neonatal liver occurs simultaneously and in the presence of active TCA cycle metabolism (Surugihalli et al., 2019). Interestingly, such a metabolic milieu is also evident during NAFLD, which promote the onset of hepatocellular stress (Patterson et al., 2016; Satapati et al., 2016). The apparent absence of hepatocellular stress in the neonatal chicken liver points to the metabolic synergy between the mitochondrial oxidative networks, the cytoplasmic lipid synthesis machinery and the antioxidant defense systems during embryonic-to-neonatal transition (Surugihalli et al., 2019).

Isolated primary hepatocytes are widely utilized as an *in vitro* model system to investigate several facets of hepatic function, including lipid accumulation, mitochondrial function and insulin signaling in a variety of species (Nussler et al., 2001; Soldatow et al., 2013; Nagarajan et al., 2019). Based on this premise, we tested whether the primary hepatocytes isolated from the embryonic and the neonatal liver were able to reproduce the characteristics of the metabolic shift that we observed in the liver tissue. Indeed, the hepatocytes isolated from the neonatal liver had significantly higher triglyceride accumulation compared to their embryonic counterparts, as indicated by the significantly higher levels of fatty acid methyl esters in the nd3 hepatocytes. While the lactate content of the neonatal hepatocytes were significantly higher, the TCA cycle intermediates α-ketoglutarate and malate were significantly lower compared to the embryonic hepatocytes. Along with these differences in lipid accumulation and TCA cycle intermediates, the hepatocytes isolated from both the embryonic and neonatal liver elicited a robust response to insulin stimuli, indicated by the higher rates of AKT phosphorylation in both groups. More importantly, the AKT phosphorylation rates are significantly higher in the nd3 livers, illustrative of robust induction of insulin signaling, and further, coordinating the higher rates of lipid accumulation in these neonatal livers. Considering the significance of identifying mechanisms regulating mitochondrial function and its cross talk with cytoplasmic networks including lipogenesis, cultured primary hepatocytes could be a valuable model system.

We further tested the impact of the hormonal stimuli (insulin, glucagon, growth hormone and corticosterone) on the intermediary metabolism of cultured primary hepatocytes. It is well known that these hormones are major players in the remodeling of growth and intermediary metabolism during embryonic-to-neonatal development, with abundant expression of their respective receptors in the liver tissue (Hazelwood, 1971; Langslow et al., 1979; Jenkins and Porter, 2004; Lu et al., 2007; Wang et al., 2014). We tested the responsiveness of the primary hepatocytes to these hormones, by evaluating changes in expression of genes related to lipid oxidation and lipogenesis. While the response of several of the genes to these four hormonal stimuli presented a complex story, it revealed the major impact of insulin. Insulin stimuli resulted in lower mRNA levels of multiple genes involved in lipid oxidation, while increasing the mRNA levels of multiple genes involved in lipogenesis. The impact of glucagon on expression of genes involved in lipid oxidation and lipogenesis was not significantly different from that of the basal treatment. Overall, these results provided validation towards the utility of embryonic and neonatal derived primary hepatocytes as a potential metabolic model for probing changes in mitochondrial metabolism and lipogenesis, especially under insulin action.

The impact of these studies can be summarized towards addressing two major areas. 1) Outbreak of metabolic disorders like FLHS is one of the major causes of death in poultry flocks with over 5% mortality, especially during the laying cycle (Julian, 2005; Trott et al., 2013). Outbreak of hepatic lipidosis in turkey causes 0.7–17% mortality (Julian, 2005). Fatty liver and kidney disease (FLKS) is another known metabolic disorder that affects broiler chicken (2–3 weeks of age) and is associated with excess lipid deposition in kidney and liver and increased weight (Julian, 2005). Further, loss of chicken due to sudden deaths caused from FLHS/FLKS would affect the quality and quantity of meat and eggs produced (Trott et al., 2013). The etiology of these liver disorders warrants further investigations, and we believe the embryonic-to-neonatal transition period could hold clues to how the synergy between the intermediary metabolic networks in the liver can help prevent the negative outcomes associated with fatty liver syndromes. 2) Losses in productivity from high morbidity and mortality rates during the first week post-hatch is also a significant economic burden to the poultry industry (Noble and Cocchi, 1990; Wilson, 1991; Xin et al., 1994; Peebles et al., 2004). Avenues to optimize embryonic-to-neonatal transition, including the use of *in ovo* nutrient injection strategies (Kadam et al., 2013; Peebles, 2018; Neves et al., 2020), early post-hatch dietary modifications (Jha et al., 2019; Ravindran and Abdollahi, 2021) etc., are being investigated to optimize this critical transition of the embryo to the neonate. In summary, isolated hepatocytes from embryonic and neonatal chicken can be a reliable metabolic model to investigate the optimal remodeling of mitochondrial metabolism and its synergy to accommodate rapid rates of lipogenesis, while avoiding mechanisms promoting hepatocellular stress.

DATA AVAILABILITY STATEMENT

The raw data supporting the conclusion of this article will be made available by the authors, without undue reservation.

ETHICS STATEMENT

The animal study was reviewed and approved by Institutional Animal Care and Use Committee protocols approved at the University of Maryland, College Park.

AUTHOR CONTRIBUTIONS

TP and NS conceived and designed the study; CS, LF, RB, BK, TP, and NS performed the experiments; CS, LF, RB, NS, TP, and H-CL analyzed the data; NS, TP, and CS wrote the manuscript; NS, TP, and H-CL acquired funding. All authors read and approved the final manuscript.

FUNDING

The work was supported in part by USDA National Institute of Food and Agriculture, Agriculture and Food Research Initiative (AFRI) grants 2021-67015-33387 (to NS and TP) and 2018-67015-27480 (to H-CL and TP).

ACKNOWLEDGMENTS

The authors are grateful to Timothy J. Garrett and Joy G. Cagmat at the Southeast Center for Integrated Metabolomics at University of Florida, Gainesville for the help with the LC-MS/MS analysis of metabolites.

SUPPLEMENTARY MATERIAL

The Supplementary Material for this article can be found online at: https://www.frontiersin.org/articles/10.3389/fphys.2022.870451/full#supplementary-material

REFERENCES

Beckford, R. C., Ellestad, L. E., Proszkowiec-Weglarz, M., Farley, L., Brady, K., Angel, R., et al. (2020). Effects of Heat Stress on Performance, Blood Chemistry, and Hypothalamic and Pituitary mRNA Expression in Broiler Chickens. *Poult. Sci.* 99 (12), 6317–6325. doi:10.1016/j.psj.2020.09.052

Cogburn, L. A., Trakooljul, N., Chen, C., Huang, H., Wu, C. H., Carré, W., et al. (2018). Transcriptional Profiling of Liver during the Critical Embryo-To-Hatchling Transition Period in the Chicken (Gallus gallus). *BMC Genomics* 19 (1), 695. doi:10.1186/s12864-018-5080-4

Davis, C. G., Harvey, D., Zahniser, S., Gale, F., and Liefert, W. (2013). *Assessing the Growth of US Broiler and Poultry Meat Exports. A Report From the Economic Research Service*. Washington DC: USDA, 1–28.

Ellestad, L. E., Saliba, J., and Porter, T. E. (2011). Ontogenic Characterization of Gene Expression in the Developing Neuroendocrine System of the Chick. *Gen. Comp. Endocrinol.* 171 (1), 82–93. doi:10.1016/j.ygcen.2010.12.006

Hazelwood, R. L. (1971). Endocrine Control of Avian Carbohydrate Metabolism ,. *Poult. Sci.* 50 (1), 9–18. doi:10.3382/ps.0500009

Hicks, J. A., Porter, T. E., and Liu, H.-C. (2017). Identification of microRNAs Controlling Hepatic mRNA Levels for Metabolic Genes during the Metabolic Transition from Embryonic to Posthatch Development in the Chicken. *BMC Genomics* 18 (1), 687. doi:10.1186/s12864-017-4096-5

Jelenik, T., Kaul, K., Séquaris, G., Flögel, U., Phielix, E., Kotzka, J., et al. (2017). Mechanisms of Insulin Resistance in Primary and Secondary Nonalcoholic Fatty Liver. *Diabetes* 66 (8), 2241–2253. doi:10.2337/db16-1147

Jenkins, S. A., and Porter, T. E. (2004). Ontogeny of the Hypothalamo-Pituitary-Adrenocortical axis in the Chicken Embryo: a Review. *Domest. Anim. Endocrinol.* 26 (4), 267–275. doi:10.1016/j.domaniend.2004.01.001

Jha, R., Singh, A. K., Yadav, S., Berrocoso, J. F. D., and Mishra, B. (2019). Early Nutrition Programming (In Ovo and Post-hatch Feeding) as a Strategy to Modulate Gut Health of Poultry. *Front. Vet. Sci.* 6, 82. doi:10.3389/fvets.2019.00082

Julian, R. J. (2005). Production and Growth Related Disorders and Other Metabolic Diseases of Poultry - A Review. *Vet. J.* 169 (3), 350–369. doi:10.1016/j.tvjl.2004.04.015

Kadam, M. M., Barekatain, M. R., K Bhanja, S., and Iji, P. A. (2013). Prospects of in Ovo Feeding and Nutrient Supplementation for Poultry: the Science and Commercial Applications-A Review. *J. Sci. Food Agric.* 93 (15), 3654–3661. doi:10.1002/jsfa.6301

Kattapuram, N., Zhang, C., Muyyarikkandy, M. S., Surugihalli, C., Muralidaran, V., Gregory, T., et al. (2021). Dietary Macronutrient Composition Differentially Modulates the Remodeling of Mitochondrial Oxidative Metabolism during NAFLD. *Metabolites* 11 (5), 272. doi:10.3390/metabo11050272

Koliaki, C., Szendroedi, J., Kaul, K., Jelenik, T., Nowotny, P., Jankowiak, F., et al. (2015). Adaptation of Hepatic Mitochondrial Function in Humans with Non-alcoholic Fatty Liver Is Lost in Steatohepatitis. *Cel Metab.* 21 (5), 739–746. doi:10.1016/j.cmet.2015.04.004

Lambert, J. E., Ramos–Roman, M. A., Browning, J. D., and Parks, E. J. (2014). Increased De Novo Lipogenesis Is a Distinct Characteristic of Individuals with Nonalcoholic Fatty Liver Disease. *Gastroenterology* 146 (3), 726–735. doi:10.1053/j.gastro.2013.11.049

Langslow, D. R., Cramb, G., and Siddle, K. (1979). Possible Mechanisms for the Increased Sensitivity to Glucagon and Catecholamines of Chicken Adipose Tissue during Hatching. *Gen. Comp. Endocrinol.* 39 (4), 527–533. doi:10.1016/0016-6480(79)90241-7

Lee, B. K., Kim, J. S., Ahn, H. J., Hwang, J. H., Kim, J. M., Lee, H. T., et al. (2010). Changes in Hepatic Lipid Parameters and Hepatic Messenger Ribonucleic Acid Expression Following Estradiol Administration in Laying Hens (*Gallus domesticus*). *Poult. Sci.* 89 (12), 2660–2667. doi:10.3382/ps.2010-00686

Liu, Y., Zhou, J., Musa, B. B., Khawar, H., Yang, X., Cao, Y., et al. (2020). Developmental Changes in Hepatic Lipid Metabolism of Chicks during the Embryonic Periods and the First Week of Posthatch. *Poult. Sci.* 99 (3), 1655–1662. doi:10.1016/j.psj.2019.11.004

Liu, Z., Li, Q., Liu, R., Zhao, G., Zhang, Y., Zheng, M., et al. (2016). Expression and Methylation of Microsomal Triglyceride Transfer Protein and Acetyl-CoA Carboxylase Are Associated with Fatty Liver Syndrome in Chicken. *Poult. Sci.* 95 (6), 1387–1395. doi:10.3382/ps/pew040

Lu, J. W., McMurtry, J. P., and Coon, C. N. (2007). Developmental Changes of Plasma Insulin, Glucagon, Insulin-like Growth Factors, Thyroid Hormones, and Glucose Concentrations in Chick Embryos and Hatched Chicks. *Poult. Sci.* 86 (4), 673–683. doi:10.1093/ps/86.4.673

Moran, E. T., Jr (2007). Nutrition of the Developing Embryo and Hatchling. *Poult. Sci.* 86 (5), 1043–1049. doi:10.1093/ps/86.5.1043

Nagarajan, S. R., Paul-Heng, M., Krycer, J. R., Fazakerley, D. J., Sharland, A. F., and Hoy, A. J. (2019). Lipid and Glucose Metabolism in Hepatocyte Cell Lines and Primary Mouse Hepatocytes: a Comprehensive Resource for *In Vitro* Studies of Hepatic Metabolism. *Am. J. Physiology-Endocrinology Metab.* 316 (4), E578–E589. doi:10.1152/ajpendo.00365.2018

Nakamura, S., Takamura, T., Matsuzawa-Nagata, N., Takayama, H., Misu, H., Noda, H., et al. (2009). Palmitate Induces Insulin Resistance in H4IIEC3 Hepatocytes through Reactive Oxygen Species Produced by Mitochondria. *J. Biol. Chem.* 284 (22), 14809–14818. doi:10.1074/jbc.M901488200

Neves, D. G. D., Retes, P. L., Alves, V. V., Pereira, R. S. G., Bueno, Y. D. C., Alvarenga, R. R., et al. (2020). In Ovo Injection with Glycerol and Insulin-like Growth Factor (IGF-I): Hatchability, Intestinal Morphometry, Performance, and Carcass Characteristics of Broilers. *Arch. Anim. Nutr.* 74 (4), 325–342. doi:10.1080/1745039X.2020.1747377

Noble, R. C., and Cocchi, M. (1990). Lipid Metabolism and the Neonatal Chicken. *Prog. Lipid Res.* 29 (2), 107–140. doi:10.1016/0163-7827(90)90014-c

Noble, R. C., Lonsdale, F., Connor, K., and Brown, D. (1986). Changes in the Lipid Metabolism of the Chick Embryo with Parental Age. *Poult. Sci.* 65 (3), 409–416. doi:10.3382/ps.0650409

Nussler, A. K., Wang, A., Neuhaus, P., Fischer, J., Yuan, J., Liu, L., et al. (2001). The Suitability of Hepatocyte Culture Models to Study Various Aspects of Drug Metabolism. *Altex* 18 (2), 91–101.

Pan, Y.-E., Liu, Z.-C., Chang, C.-J., Xie, Y.-L., Chen, C.-Y., Chen, C.-F., et al. (2012). Ceramide Accumulation and Up-Regulation of Proinflammatory Interleukin-1β Exemplify Lipotoxicity to Mediate Declines of Reproductive Efficacy of Broiler Hens. *Domest. Anim. Endocrinol.* 42 (3), 183–194. doi:10.1016/j.domaniend.2011.12.001

Patterson, R. E., Kalavalapalli, S., Williams, C. M., Nautiyal, M., Mathew, J. T., Martinez, J., et al. (2016). Lipotoxicity in Steatohepatitis Occurs Despite an Increase in Tricarboxylic Acid Cycle Activity. *Am. J. Physiology-Endocrinology Metab.* 310 (7), E484–E494. doi:10.1152/ajpendo.00492.2015

Pedroso, A. A., Andrade, M. A., Café, M. B., Leandro, N. S., Menten, J. F., and Stringhini, J. H. (2005). Fertility and Hatchability of Eggs Laid in the Pullet-To-Breeder Transition Period and in the Initial Production Period. *Anim. Reprod. Sci.* 90 (3-4), 355–364. doi:10.1016/j.anireprosci.2005.03.001

Peebles, E. D. (2018). In Ovo Applications in Poultry: A Review. *Poult. Sci.* 97 (7), 2322–2338. doi:10.3382/ps/pey081

Peebles, E. D., Keirs, R. W., Bennett, L. W., Cummings, T. S., Whitmarsh, S. K., and Gerard, P. D. (2004). Relationships Among Posthatch Physiological Parameters in Broiler Chicks Hatched from Young Breeder Hens and Subjected to Delayed Brooding Placement. *Int. J. Poult. Sci.* 3 (9), 578–585. doi:10.3923/ijps.2004.578.585

Ravindran, V., and Abdollahi, M. R. (2021). Nutrition and Digestive Physiology of the Broiler Chick: State of the Art and Outlook. *Animals* 11 (10), 2795. doi:10.3390/ani11102795

Satapati, S., Kucejova, B., Duarte, J. A. G., Fletcher, J. A., Reynolds, L., Sunny, N. E., et al. (2016). Mitochondrial Metabolism Mediates Oxidative Stress and Inflammation in Fatty Liver. *J. Clin. Invest.* 126 (4), 1605. doi:10.1172/jci86695

Satapati, S., Sunny, N. E., Kucejova, B., Fu, X., He, T. T., Méndez-Lucas, A., et al. (2012). Elevated TCA Cycle Function in the Pathology of Diet-Induced Hepatic Insulin Resistance and Fatty Liver. *J. Lipid Res.* 53 (6), 1080–1092. doi:10.1194/jlr.M023382

Soldatow, V. Y., Lecluyse, E. L., Griffith, L. G., and Rusyn, I. (2013). *In Vitro* models for Liver Toxicity Testing. *Toxicol. Res.* 2 (1), 23–39. doi:10.1039/C2TX20051A

Sunny, N. E., Bril, F., and Cusi, K. (2017). Mitochondrial Adaptation in Nonalcoholic Fatty Liver Disease: Novel Mechanisms and Treatment Strategies. *Trends Endocrinol. Metab.* 28 (4), 250–260. doi:10.1016/j.tem.2016.11.006

Sunny, N. E., Parks, E. J., Browning, J. D., and Burgess, S. C. (2011). Excessive Hepatic Mitochondrial TCA Cycle and Gluconeogenesis in Humans with Nonalcoholic Fatty Liver Disease. *Cel Metab.* 14 (6), 804–810. doi:10.1016/j.cmet.2011.11.004

Surugihalli, C., Porter, T. E., Chan, A., Farley, L. S., Maguire, M., Zhang, C., et al. (2019). Hepatic Mitochondrial Oxidative Metabolism and Lipogenesis Synergistically Adapt to Mediate Healthy Embryonic-To-Neonatal Transition in Chicken. *Sci. Rep.* 9 (1), 20167. doi:10.1038/s41598-019-56715-1

Trott, K. A., Giannitti, F., Rimoldi, G., Hill, A., Woods, L., Barr, B., et al. (2013). Fatty Liver Hemorrhagic Syndrome in the Backyard Chicken. *Vet. Pathol.* 51 (4), 787–795. doi:10.1177/0300985813503569

USDA (2018). *Chicken and Eggs 2017 Summary*. Washington DC: National Agricultural Statistics Service.

Walzem, R. L., Simon, C., Morishita, T., Lowenstine, L., and Hansen, R. J. (1993). Fatty Liver Hemorrhagic Syndrome in Hens Overfed a Purified Diet. Selected Enzyme Activities and Liver Histology in Relation to Liver Hemorrhage and Reproductive Performance. *Poult. Sci.* 72 (8), 1479–1491. doi:10.3382/ps.0721479

Wang, X., Yang, L., Wang, H., Shao, F., Yu, J., Jiang, H., et al. (2014). Growth Hormone-Regulated mRNAs and miRNAs in Chicken Hepatocytes. *PLoS One* 9 (11), e112896. doi:10.1371/journal.pone.0112896

Wilson, H. R. (1991). Interrelationships of Egg Size, Chick Size, Posthatching Growth and Hatchability. *World's Poult. Sci. J.* 47 (1), 5–20. doi:10.1079/wps19910002

Xin, H., Berry, I. L., Barton, T. L., and Tabler, G. T. (1994). Feed and Water Consumption, Growth, and Mortality of Male Broilers. *Poult. Sci.* 73 (5), 610–616. doi:10.3382/ps.0730610

Yassin, H., Velthuis, A. G. J., Boerjan, M., and van Riel, J. (2009). Field Study on Broilers' First-Week Mortality. *Poult. Sci.* 88 (4), 798–804. doi:10.3382/ps.2008-00292

Zaefarian, F., Abdollahi, M., Cowieson, A., and Ravindran, V. (2019). Avian Liver: The Forgotten Organ. *Animals* 9 (2), 63. doi:10.3390/ani9020063

Conflict of Interest: The authors declare that the research was conducted in the absence of any commercial or financial relationships that could be construed as a potential conflict of interest.

Publisher's Note: All claims expressed in this article are solely those of the authors and do not necessarily represent those of their affiliated organizations, or those of the publisher, the editors and the reviewers. Any product that may be evaluated in this article, or claim that may be made by its manufacturer, is not guaranteed or endorsed by the publisher.

frontiers | Frontiers in Physiology

REVIEW
published: 25 April 2022
doi: 10.3389/fphys.2022.863860

Dietary Flavonoids as Modulators of Lipid Metabolism in Poultry

*Zhendong Tan[1], Bailey Halter[1], Dongmin Liu[2], Elizabeth R. Gilbert[1] and Mark A. Cline[1]**

[1]Department of Animal and Poultry Sciences, Blacksburg, VA, United States, [2]Department of Human Nutrition, Foods, and Exercise, Blacksburg, VA, United States

Flavonoids, naturally-occurring compounds with multiple phenolic structures, are the most widely distributed phytochemicals in the plant kingdom, and are mainly found in vegetables, fruits, grains, roots, herbs, and tea and red wine products. Flavonoids have health-promoting effects and are indispensable compounds in nutritional and pharmaceutical (i.e., nutraceutical) applications. Among the demonstrated bioactive effects of flavonoids are anti-oxidant, anti-inflammatory, and anti-microbial in a range of research models. Through dietary formulation strategies, numerous flavonoids provide the ability to support bird health while improving the nutritional quality of poultry meat and eggs by changing the profile of fatty acids and reducing cholesterol content. A number of such compounds have been shown to inhibit adipogenesis, and promote lipolysis and apoptosis in adipose tissue cells, and thereby have the potential to affect fat accretion in poultry at various ages and stages of production. Antioxidant and anti-inflammatory properties contribute to animal health by preventing free radical damage in tissues and ameliorating inflammation in adipose tissue, which are concerns in broiler breeders and laying hens. In this review, we summarize the progress in understanding the effects of dietary flavonoids on lipid metabolism and fat deposition in poultry, and discuss the associated physiological mechanisms.

Keywords: lipid, poultry, adipose tissue, flavonoid, feed additive, phytochemical, polyphenols, broiler

OPEN ACCESS

Edited by:
Xiquan Zhang,
South China Agricultural University, China

Reviewed by:
Nilva Sakomura,
São Paulo State University, Brazil
Gale Strasburg,
Michigan State University, United States

****Correspondence:***
Mark A. Cline
macline2@vt.edu

Specialty section:
This article was submitted to Avian Physiology, a section of the journal Frontiers in Physiology

Received: *27 January 2022*
Accepted: *07 March 2022*
Published: *25 April 2022*

Citation:
Tan Z, Halter B, Liu D, Gilbert ER and Cline MA (2022) Dietary Flavonoids as Modulators of Lipid Metabolism in Poultry. Front. Physiol. 13:863860. doi: 10.3389/fphys.2022.863860

INTRODUCTION

Phytochemicals are natural compounds that are obtained from plants. Phytochemicals are classified into the alkaloids, polyphenols, terpenoids, carotenoids, organo-sulfurs, phytosterols, limonoids, glucosinolates, and fibers, which are further divided into many subtypes according to their chemical structures and characteristics (González-Castejón and Rodriguez-Casado, 2011). Flavonoids are functional derivatives of polyphenols which are the most abundant phytochemicals and are considered to have the greatest health benefits. Results from clinical studies have shown that polyphenols are potent at preventing or slowing the onset of chronic diseases, especially those induced by oxidative stress such as cardiovascular diseases (CVD) and metabolic disorders (Manach et al., 2005).

Flavonoids are a category of plant-derived low-molecular weight secondary metabolites with diverse structures and chemistries. Different from the function of primary plant metabolites (e.g., protein, fat, and carbohydrates which mainly regulate energy metabolism and cell physiology), secondary metabolites are associated with non-nutritive dietary fiber, and are important for interactions between plants and the environment, for instance in conferring resistance to parasites, fungi, and other microorganisms (Leitzmann, 2016). For a long time, flavonoids were

considered to be natural toxins. Considering that many flavonoids indeed have adverse effects which depend on their concentration and form in the feed, such as decreasing nutrient availability and inhibiting digestive enzyme activities, they were long characterized as "anti-nutritive" metabolites by nutritionists (Salunkhe et al., 1982). However, through in-depth studies involving high-precision analytical methods and a comprehensive array of cell and tissue culture and animal models, the beneficial bioactive effects of flavonoids have been increasingly recognized and exploited for nutritional and pharmaceutical purposes (Dillard and German, 2000).

Flavonoids constitute a major family of phytochemicals and are generally used as nutraceuticals in foods and food supplements, or exist in a low-concentration form in herbs, teas, beans, vegetables, and fruits where they still have the potential to exert a physiological effect. The majority of research on flavonoids is conducted to explore antioxidant and anti-inflammatory activities. Although flavonoids are considered to be anti-nutritive agents, there is a strong relationship between these phytochemicals and chronic diseases, especially obesity, CVD, and cancer (Craig, 1997; Dillard and German, 2000; González-Castejón and Rodriguez-Casado, 2011). Consumption of vegetables and fruits is linked to a lower risk of obesity and cancer, and some of the underlying mechanisms may involve bioactive flavonoids (He et al., 2004; McMillan et al., 2006; Key, 2011). For instance, there has been much research on the use of dietary phytochemicals as an anti-obesity strategy, as many of them are known to prevent the expansion of adipose tissue through inhibition of the differentiation of preadipocytes into adipocytes, and promotion of lipolysis and apoptosis in mature adipocytes. Among them, flavonoids targeting the adipocyte life cycle decrease preadipocyte proliferation (Rayalam et al., 2008). In addition, the phenolic constituents of flavonoids are known to inhibit the growth of adipose tissue via anti-angiogenesis and metabolic-regulating pathways in various cells (Ejaz et al., 2009; González-Castejón and Rodriguez-Casado, 2011; Sakuma et al., 2017).

In recent years, there has been a growing awareness of the purported health benefits of plant-based foods. However, the benefits of dietary supplementation of polyphenols in agriculturally-relevant species, particularly in commercial poultry production, have not been as well studied. In this review we summarize the known effects of flavonoids, a sub-class of polyphenols, on lipid metabolism and deposition in poultry, and discuss the proposed physiological mechanisms and practical applications.

LIPID METABOLISM AND ADIPOSE TISSUE PHYSIOLOGY IN POULTRY

The poultry industry is mainly focused on producing eggs and meat. These products are closely related to lipid metabolism and deposition. In nearly half a century, poultry producers, especially of broiler chickens, have shortened the amount of time required to achieve the desired final body weight (BW), and increased the final body weight for slaughter from 1.5 kg in 70 days to 2.5 kg in 42 days (Havenstein et al., 2003). Modern poultry production drastically increased the body weight gain (BWG), carcass yield, breast weight, and egg production of poultry to satisfy the increasing consumer demand (Wang et al., 2012; Fouad and El-Senousey, 2014), but fat deposition in the abdomen was initially ignored in some breeding schemes, which resulted in high rates of lipid biosynthesis and accumulation as adipose tissue. This seems to be universal that selection of BWG leads to an increase in fat deposition. The modern strains of broilers, for example, contain 15–20% of their BW as fat, more than 85% of which is not required for physiological function (Choct et al., 2000). Nowadays, reducing fat content can be achieved by changing the selection strategy in feed conversion ratio (FCR). Selection for BWG leads to a higher fat content of the carcass, whereas lower FCR tends to produce carcasses with lower fat and higher water content (Pym and Solvyns, 1979; Tůmová and Teimouri, 2010). Although reducing fat content during the selection and breeding process can improve reproductive traits of broilers (Zhang et al., 2018), the disadvantages are also obvious. Since fat is a high heritability trait, excessive pursuit of reduced fat during production has adverse effects on live performance of chickens, especially during the chick-rearing stage (Tůmová and Teimouri, 2010). Thus, excess fat deposits, consequently, remain a major problem in modern poultry production. For producers, excess fat content is sometimes unacceptable, as it is considered to be a waste of dietary energy, while reducing carcass yield and affecting meat quality (which may or may not be acceptable to consumers) (Rabie and Szilágyi, 1998; Fouad and El-Senousey, 2014). As for laying hens and broiler breeders, excess fat deposition significantly impacts metabolic health and reproductive performance (Xing et al., 2009). It is important to note that excess energy acquisition is directly related to food intake, which also continues to be a concern in poultry production. Broiler breeders, in particular, are feed-restricted to achieve target BW's and fat percentages in order to slow growth and prevent the onset of metabolic disorders which would adversely affect bird health and reproductive output.

Research on lipid metabolism and adipose tissue physiology in poultry has mainly focused on the conversion of feed energy to fat deposition in meat and eggs, and at present, lipid metabolism and related mechanisms are still popular areas of research because fat deposition in poultry products directly affects production efficiency and profitability. The fat content of poultry products, as well as the fatty acid composition, are particularly important to the health of consumers and poultry (Hargis and Van Elswyk, 1993). Because high fat, saturated fatty acids (SFA), and cholesterol are linked to chronic diseases and cancer (Cross et al., 2010; Ferguson, 2010; Santarelli et al., 2010), there is increasing focus on health outcomes associated with consuming poultry meat and products.

For avian species, the main factors affecting lipid deposition include dietary energy, protein, amino acids, and mineral levels. Oils and fats are the most concentrated sources of energy, which lower heat increment, increase the absorption of fat-soluble vitamins, enhance gastrointestinal passage, and can improve palatability (Krogdahl, 1985). The amount of body fat that poultry species accumulate depends on the availability of

plasma lipid substrates available from feed and those synthesized in the liver via *de novo* lipogenesis (D'Mello, 2000). Moreover, for laying hens, dietary reductions in fat may lower the cholesterol content of egg yolk and thereby lower the risk of cardiovascular diseases in consumers (Han et al., 1993). Thus, dietary lipid sources and quantity can directly affect fat deposition and composition in poultry. In addition, hormones like insulin regulate lipid metabolism in poultry liver and adipose tissue (Goodridge, 1973; Gross and Mialhe, 1984; Wilson et al., 1986), which coordinately determine the amount of fat that is stored and oxidized in the body.

The liver is the one of the most important organs for lipid metabolism in the body, and is responsible for fatty acid synthesis (in birds and humans), bile synthesis, packaging of lipids for transport, lipid storage and oxidation, and also ketogenesis from lipid substrates when glucose is scarce (Bickerstaffe et al., 1970; Griminger, 1986; Nguyen et al., 2008). Hepatic fatty acid metabolism has been recognized as a major determinant of the changes in blood triglyceride levels and fat deposition in poultry (Guillou et al., 2008).

Adipose tissue, on the other hand, is primarily used for fat storage in birds, and plasma non-esterified fatty acids generally represent liberation of fatty acids from adipose tissue triacylglycerol (TG) stores when the animal is in a fasting state (Griffin et al., 1992). In chicken embryos, the subcutaneous depot is the first to arise during development, and at hatch subcutaneous and neck fat (including above the breast) are relatively well-developed and available as a source of energy and insulation, whereas abdominal fat is largely absent. The abdominal fat pad has a faster growth rate compared to other fatty tissues and ultimately becomes a direct determinant of body fat content (Butterwith, 1989).

In most mammals, there are two types of adipose tissue according to their physical function and color, white and brown, with brown associated with non-shivering thermogenesis due to the action of uncoupling protein-1 (UCP-1) (Oelkrug et al., 2015). Due to the lack of orthologous UCP-1 in the avian genomes, the presence of an equivalent brown fat in birds has been questioned and generally thought to not exist (Saarela et al., 1991). White adipocytes are characterized by the presence of a single, large lipid droplet containing TGs that are liberated via the sequential activation of lipases in the cell (Reue, 2011). Adipocytes originate from mesenchymal stem cells that can be committed to become preadipocytes which are then stimulated to differentiate into the mature adipocyte. There are a multitude of transcription factors and enzymes that are associated with cellular differentiation and the accompanying lipid synthesis, respectively, and these encoded genes tend to be the target of research studies aimed at evaluating how various factors, including dietary supplements, influence adipose tissue development and maintenance (Varga et al., 2011). For brevity, this review will mainly focus on the effects of dietary flavonoids on lipid metabolism and adipose tissue physiology in chickens, with an emphasis on the physiological mechanisms. It should also be recognized that these compounds may also exert direct or indirect effects on appetite regulation, which would in turn influence body composition. Where relevant, such mechanisms will be discussed.

FLAVONOIDS

Flavonoids are a group of polyphenols that have been widely used in the pharmaceutical and cosmetic industries because of their antioxidant, anti-inflammatory, anti-microbial, and anticarcinogenic effects, (Panche et al., 2016). In the plant kingdom, flavonoids are essential for plant growth, pigmentation, and resistance to plaques, and represent one of the most common groups of compounds in higher plants (Havsteen, 2002). In addition to plants, flavonoids are commonly found in plant-derived foods and beverages, such as fruits, vegetables, tea, cocoa, and red wine (Panche et al., 2016).

Flavonoids are a general term for a series of compounds with a c6-c3-c6 structure (A, B, C ring, **Figure 1**), which consists of two benzene rings (A, B) linked via a heterocyclic pyrane C-ring (Pietta, 2000). Flavonoids can be divided into various subgroups according to the degree of heterocyclic pyrane C-ring oxidation and the substitution pattern of a functional group on the C ring with a methyl, hydroxyl, glycan, acetyl or other group, the location of the B ring connection (position 2, 3, or 4 of the C ring), and whether the heterocyclic pyrane C-ring forms a ring. The connections of the B ring to the position 3 of the C ring are called isoflavones, and the connections to the position 4 of the C ring are called neo-flavonoids. Those in which the B ring connects to position 2, can be divided into seven subclasses: flavones, flavonols, flavanones, flavanonols, flavanols or catechins, anthocyanins, and chalcones (Panche et al., 2016).

Challenge conditions like oxidative stress (including that caused by heat stress) and diseases have a series of negative impacts on the production performance and welfare of poultry. In environments outside of the comfort zone, birds experience reductions in food intake and depending on the level of severity, cellular dysfunction and lipid peroxidation, leading to associated pathologies (Puthpongsiriporn et al., 2001; Silva et al., 2002). Biological activities of flavonoids have aroused interest for alleviating the detrimental effects of oxidative stress. For example, Peña et al. evaluated the effects of citric flavonoids (quercetin and rutin) combined with ascorbic acid (AA) on the performance and meat quality characteristics of broilers under heat stress for 32 days. They found that the addition of graded AA and citric flavonoids did not affect meat production and quality. However, FCR was improved during the first week post-hatch with 0 and 250 g/ton AA+ citric flavonoids (Peña et al., 2008). The beneficial mechanism is thought to be the stimulation of the expression of stress response proteins and antioxidant enzymes, thereby offsetting production of reactive oxygen species (ROS). Treatment with some flavonoids, like epigallocatechin gallate (EGCG), upregulated the expression of superoxide dismutase to improve the antioxidant capacity and mitigate the influence of heat stress (Hu et al., 2019).

Two major challenges associated with using dietary flavonoids as a strategy to modulate bird health and growth are 1) that the *in vivo* targets are still unclear for many of these chemicals and

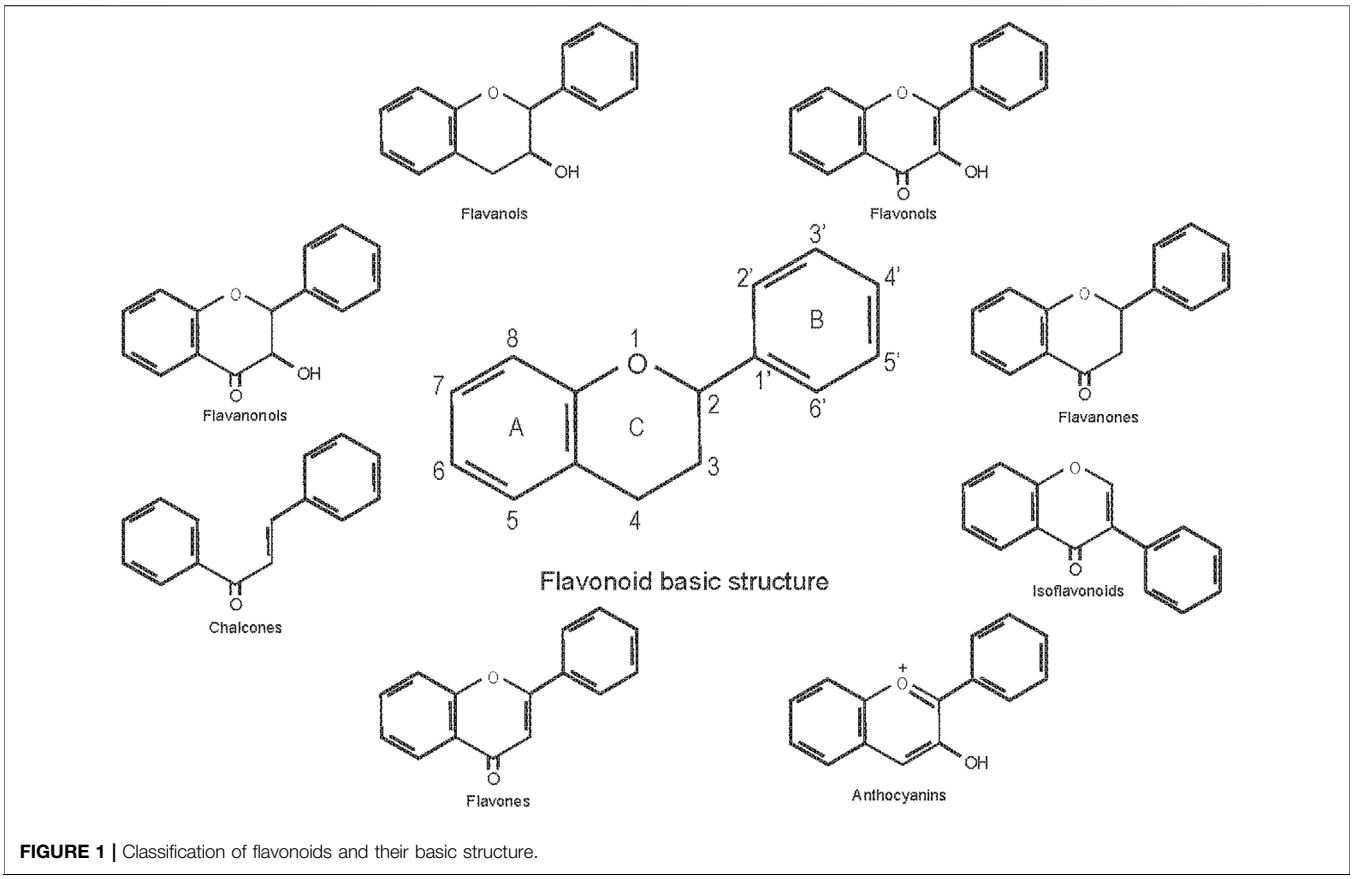

FIGURE 1 | Classification of flavonoids and their basic structure.

results from controlled cell culture studies may not be physiologically relevant and 2) despite much research on their biochemistry, bioavailability continues to be poor. In terms of bioavailability, flavonoids are subject to modification by the intestinal microflora and typical modifications include methylation, glucuronidation, sulfonation and others, as reviewed in (Hu et al., 2017). It is thought that flavonoids exploit nutrient transporters for uptake across the mucosal layer and that following uptake, flavonoids enter the portal circulation and are thus subjected to first-pass metabolism by liver Phase II metabolic enzymes, leading to further modification and potential reductions in cellular bioavailability. Improving bioavailability and absorption are the ultimate goals for utilizing flavonoids as feed supplements. The majority of flavonoids in plants are bound to sugars through a glycosidic bond, known as a glycoside. The glycoside form of flavonoids is not absorbed and must be hydrolyzed in the host intestine. In poultry, flavonoids are mostly absorbed in the ileum at pH 5.0 to 6.8 (Kamboh et al., 2019), although the chemical structure affects their bioavailability, absorption, interaction with cell receptors and enzymes, etc (Abdel-Moneim et al., 2020). Dietary supplementation of exogenous enzymes (e.g., carbohydrases and tannases) facilitates the breakdown of catechins into smaller monomeric and dimeric units at the cost of reduced digestibility of monomeric and dimeric catechins, suggesting that polymeric structures can improve intestinal utilization of monomeric and dimeric catechins (Chamorro et al., 2017). Among all flavonoids, isoflavones have the highest bioavailability. Anthocyanins are rapidly absorbed, but their bioavailability is the lowest of all flavonoids (Rafiei and Khajali, 2021). Aglycones (non-sugar moiety) tend to be more bioavailable than the corresponding glycoside form (Thilakarathna and Rupasinghe, 2013). For instance, Steensma et al. found that aglycone genistein is more bioavailable compared to glycoside genistein in rats (Steensma et al., 2006). Thus, an important consideration for dietary supplementation of flavonoids is the potential for transformation into chemically distinct molecules with different bioavailabilities and pharmacodynamic properties in the body than the chemicals that were present in the diet. Despite these limitations, there are a plethora of data demonstrating beneficial effects on poultry growth and health, and in particular regulation of lipid metabolism and fat deposition (**Table 1**). In the remainder of this review, where appropriate, cellular targets of flavonoids will be described and the current state of knowledge discussed, including gaps in our current understanding of flavonoid biology (**Figure 2**).

Flavones

Flavones are characterized by a double bond at positions 2 and 3 of the C ring, and a ketone group at position 4 (**Figure 1**). Most flavones in nature have a hydroxyl group in the A ring at position 5, and depending on the classification of fruits and vegetables, may also have hydroxyl groups in ring A at position 7 and in the B

TABLE 1 | Flavonoids and effects on body fat, meat quality/composition and egg quality in poultry.

Species	Chemical class	Results of supplementation	References
Broiler	Flavones	Flavones of sea buckthorn fruits at 0.05, 0.10, and 0.15%, ↓ abdominal fat pad weight, ↑ intramuscular fat in breast	Ma et al. (2015)
		0.1 and 0.2% sea buckthorn flavones ↓ abdominal fat %, drip loss of breast and thigh muscle, and serum triglycerides	Li et al. (2008)
	Flavonols	0.3% or 0.6% kaempferol ↓ abdominal and subcutaneous fat, and plasma and hepatic cholesterol and triglycerides	Xiao et al. (2012)
		0.5 and 1 g/kg quercetin ↑ meat lightness (L*), redness, and oxidative stability during refrigeration for 3 and 9 days	Goliomytis et al. (2014b)
		Quercetin at 200 mg/kg ↓ oleic, palmitic, linoleic, and stearic acid in breast	Oskoueian et al. (2013)
	Isoflavones	5 mg of genistein and 20 mg of hesperidin/kg ↓ muscle fat	Kamboh et al. (2018)
		20 mg/kg of genistein and hesperidin ↑ meat-holding capacity and ↓ lipid oxidation of breast at 0 and 15 days of refrigeration	Kamboh and Zhu, (2013a)
		40 and 80 mg/kg soy isoflavones ↑ L*, water-holding, pH, and catalase and superoxide dismutase activity in breast, and ↓ lipid peroxidation	Jiang et al. (2007)
		Genistein (5 mg/kg) ↓ ratio of 14:0, 18:0, and ΣSFA and cholesterol in breast muscle	Kamboh and Zhu, (2013b)
	Anthocyanins	Anthocyanin fortified barley at 5% ↑ abdominal fat	Park et al. (2012)
		10 and 20% *Tridax procumbens* powder ↑ breast meat juiciness and flavor	Ahossi et al. (2016)
		Konini wheat (~14 mg/g of anthocyanin) ↑ BWG.	Stastnik et al. (2016)
		Cranberry fruit extract (40, 80, or 160 mg/kg anthocyanin) ↑ feed efficiency and BW.	Leusink et al. (2010)
	Flavanones	Hesperidin and naringenin at 0.75 or 1.5 g/kg ↑ PUFA and n-6, while ↓ SFA in abdominal fat, breast and thigh muscles	Hager-Theodorides et al. (2021)
		0.75 and 1.5 g/kg hesperidin and naringin ↑ breast muscle redness (a*), and ↓ lipid oxidation for 9 days at 4°C and for 120 days at -20°C	Goliomytis et al. (2015)
		Hesperidin and naringenin at 0.75 and 1.5 mg/kg ↑ content of PUFA, omega n-6, and PUFA/SFA ratio in breast muscle and fat	Hager-Theodorides et al. (2021)
		Hesperidin at 20 mg/kg ↓ cholesterol and changed fatty acids (proportions of 18:0, 9c18:1, 20:4n-6 and Σn-3 were ↓) in breast	Kamboh and Zhu, (2013b)
	Flavanols	Green tea powder (0.5, 1 and 1.5%) ↓ % of abdominal fat	Hrnčár and Bujko, (2017)
		Green tea powder at 0.5, 0.75, 1.0 or 1.5% ↓ liver and serum cholesterol and abdominal fat	Biswas and Wakita, (2001b)
	Flavanonols	120 mg/kg taxifolin ↓ lipid peroxidation in fresh meat and during refrigerated storage for 1 month at -18°C	Bakalivanova and Kaloyanov, (2012)
Layer	Flavonols	Quercetin at 0, 0.2, 0.4, or 0.6 g/kg ↑ laying rate and ↓ feed-egg ratio. Haugh unit, eggshell strength and thickness, and yolk protein ↑, while yolk cholesterol ↓	Liu et al. (2013)
	Isoflavones	10, 50, and 100 mg/kg daidzein for 8 weeks ↑ eggshell thickness, percentage, strength, and egg yolk superoxide dismutase	Cai et al. (2013)
	Anthocyanins	8 weeks anthocyanin-fortified barley ↑ laying performance and egg quality	Choe et al. (2013)
		Purple wheat grain at end of laying period in 69 weeks ↑ eggs and yolk weight	Roztočilová et al. (2018)
	Flavanones	0.05% hesperetin, 0.05% naringenin, and 0.5% galacturonic acid ↓ egg yolk cholesterol and ↑ yolk weight and ratio of yolk weight/egg weight	Lien et al. (2008)
		9% dried orange pulp (0.767 g hesperidin and 0.002 g naringin) for a month ↑ yolk oxidative stability and egg shelf life. ↓ performance and egg quality parameters	Goliomytis et al. (2018)
	Flavanols	0.2 and 0.4% green tea catechins ↓ egg weight, specific gravity, thickness and yolk malondialdehyde	Kara et al. (2016)
		Green tea powder (2, 4, 6, 8 g/kg) or tea catechins (0.5, 1, 1.5, 2 g/kg) for 60 days ↓ total cholesterol, triglyceride, and LDL levels in plasma and breast and thigh meat	Zhou et al. (2012)
	Chalcones	5 or 10 g tomato powder/kg ↑ egg production, egg weight and yolk color	Akdemir et al. (2012)
		Pre-injection of 25 mg chalcones ↓ eggs with blood spots	Bigland et al. (1964)
Quail	Flavones	0.1, 1.0 and 10.0 mg morin/scaled quail/day for 8 weeks: no effect on reproduction	Cain et al. (1987)
	Isoflavones	400 or 800 mg of genistein/kg for 90 days ↑ egg production, egg weight, Haugh unit, shell thickness and weight, while ↓ yolk malondialdehyde	Akdemir and Sahin, (2009)
		400 or 800 mg of soy isoflavones/kg ↑ egg quality	Sahin et al. (2007)
	Anthocyanins	Purple field corn ↑ egg quality, performance and carcass quality	Amnueysit et al. (2010)
	Flavanols	0.25, 0.50 and 0.75% powdered green tea flowers ↑ FCR.	Abdel-Azeem, (2005)

ring at positions 3 and 4. Flavones are abundant in plant branches, leaves and fruits, in the form of glucosides. Celery, parsley, red peppers, ginkgo biloba, and herbs are the main plant sources, and examples of flavones include baicalein, baicalin, diosmetin, luteolin, apigenin, and tangeritin.

Ma et al. (Ma et al., 2015) found that adding different levels (0, 0.05, 0.10, or 0.15%) of sea buckthorn fruits (FSBF), which are rich in flavones, to broiler diets from 1 to 42 days of age, effectively reduced the final abdominal fat pad weight by nearly 20%, while increasing intramuscular fat (IMF) content in breast muscle. Cholesterol, TG, and low-density lipoprotein cholesterol (LDL-C) levels were also reduced. These findings are consistent with those of Li et al. (Li et al., 2008), who also reported that flavone supplementation reduced abdominal fat percentage

in chickens. Body weight gain increased and FCR decreased (increased efficiency) from 7 to 42 days when broilers were fed diets supplemented with 100 and 200 mg/kg flavone baicalein (Zhou et al., 2019). Meanwhile, the serum levels of total cholesterol (TC), the ratio of non-high density lipoprotein (HDL)-C/HDL-C, LDL-C/HDL-C, TC/HDL-C, LDL-C, and TGs were decreased after baicalein treatment (Zhou et al., 2019).

Numerous anti-obesity effects have been attributed to flavone bioactivity. Flavone luteolin is a potent TG lipase inhibitor in preadipocytes and enhances insulin sensitivity through activation of peroxisome proliferator-activated receptor γ (PPARγ) (Zheng et al., 2010). Additionally, flavones can suppress obesity-associated inflammation by blunting the nuclear factor kappa-B (NF-κB)-mediated pathway (González-Castejón and Rodriguez-Casado, 2011). Another flavone, baicalein, also functions as an antioxidant and anti-lipase agent. Xiao et al. (Xiao et al., 2021) supplemented the starter diet of Hubbard × Cobb-500 day-of-hatch broiler chicks with 125, 250, or 500 mg/kg baicalein for 6 days, which significantly reduced chick breast muscle and subcutaneous and abdominal fat weights. Expression of mRNAs for factors involved in adipogenesis and fat storage (PPARγ, diacylglycerol acyltransferase; DGAT2) were more highly expressed in the subcutaneous than abdominal fat depot but were not affected by diet. In cell culture studies, mRNA expression of genes related to adipogenesis and lipid accumulation (CCAAT/enhancer-binding protein beta; C/EBPβ, CCAAT/enhancer-binding protein alpha; C/EBPα, sterol regulatory element-binding transcription factor 1; SREBP1, Diacylglycerol acyltransferase; DGAT1, and PPARγ) were generally decreased after baicalein treatment in a dose-dependent manner (3.125, 6.25, and 12.5 μM) or in response to a single dose (50 μM) (Seo et al., 2014; Nakao et al., 2016).

Flavonols

Flavonols have a C2-C3 double bond, a ketone group in the fourth position of the C ring, and an additional hydroxyl group in the C-ring at position 3. Flavonols, which have the 3-hydroxyflavone backbone, are found in a variety of vegetables and fruits. They are abundant in apples, grapes, lettuce, broccoli, and onions. In addition to vegetables and fruits, other important sources include tea, red wine, and medicinal herbs. Flavonols that have been extensively studied for biological effects in animals are quercetin, kaempferol, myricetin, and fisetin. Because of diverse patterns of methylation and hydroxylation, flavonols are considered to be the most common and largest subgroup of flavonoids (El Gharras, 2009).

Quercetin is reported to exert a variety of biological effects, such as growth promotion, anti-infection, antioxidant, and antiviral, in livestock and poultry species (Comalada et al., 2006; Goliomytis et al., 2014a; Saeed et al., 2017a). It is worth noting that quercetin has anti-obesity effects that are mediated through several pathways that collectively reduce fat accumulation: 1) enhancement of cyclic adenosine monophosphate (cAMP) levels by inactivating phosphodiesterase, to prolong lipolysis in adipocytes; 2) inhibition of insulin receptor and SREBP-1, thereby repressing lipoprotein lipase (LPL), acetyl-CoA carboxylase (ACC), glucose uptake and fatty acid synthesis, and reducing fatty acid absorption and lipid accumulation in tissue; 3) at the transcriptome level, increasing mRNA expression of *Caspase3* and decreasing *PPARγ*, resulting in the apoptosis of adipocytes and inhibition of adipogenesis, respectively, collectively resulting in a reduction in the number of adipocytes (Saeed et al., 2017a). In primary human adipocytes and 3T3-L1 murine adipocytes, quercetin alone or in combination with genistein (isoflavone) and resveratrol (stilbene) reduced the activity of glucose 3-phosphate dehydrogenase (contributor of the glycerol backbone to TG synthesis), thereby inhibiting the late-stage differentiation of adipocytes and promoting the apoptosis of mature adipocytes (Park et al., 2008).

In poultry, dietary supplementation of quercetin was associated with changes in broiler growth and meat composition. Sohaib et al. (Sohaib et al., 2015) showed that adding quercetin to broiler feed reduced the concentration of fatty acids and improved the quality and consumer acceptance of meat products. In addition, quercetin in combination with α-tocopherol significantly increased BWG and reduced SFA while monounsaturated fatty acid (MUFA) content was not significantly altered (Sohaib et al., 2015). Consistent with these findings, Oskoueian et al. (Oskoueian et al., 2013) reported that dietary quercetin supplementation at 200 mg/kg reduced oleic (18:1n-9), palmitic (16:0, 26.1–27.9%), linoleic (18:2n-6) and stearic acid (18:0) in broiler pectoralis major muscle. While it is unclear how quercetin modulates fatty acid composition in the meat, the results from these studies suggest that quercetin has the potential to be used as a dietary additive for broilers to improve growth performance and meat quality.

Quercetin is also an effective functional dietary additive for laying hens. At a concentration of 0.4 g/kg of the basal diet, quercetin not only improved the laying rate, reduced the feed-egg ratio, but also increased the shell strength, shell thickness, and egg yolk protein content throughout the 8 weeks experimental period (Liu et al., 2013). Notably, quercetin has been shown to lower cholesterol and TG levels in the yolk. Kim et al. (Kim et al., 2003) believed that the reduction of cholesterol in egg yolk by quercetin treatment might be due to the inhibition of the activity of HMG-CoA reductase, the rate-limiting enzyme in endogenous cholesterol synthesis. It was also suggested that quercetin modulates intestinal function, altering the composition of the gut microbiome and the luminal microenvironment proximal to the absorption of nutrients (Saeed et al., 2017a). Liu et al. (Liu et al., 2014) studied the effects of quercetin supplementation on the cecal microflora of laying hens, and observed that quercetin (0.2, 0.4, and 0.6 g/kg of diet for 8 weeks) reduced the total number of aerobe and coliform bacteria, whereas the number of beneficial *bifidobacterium* was increased. The results showed that quercetin may function as a metabolic prebiotic and exert important influences on the intestinal environment by regulating the composition of the cecal microflora. Although beyond the scope of this review, it is important to acknowledge the contribution of the gut-microbiome-brain axis to physiology and that dietary changes that influence the microbiome have the potential to in turn influence physiology because of the contribution of bacterial metabolites to host cellular function. Indeed, in both

avian and mammalian models, important links have been established between obesity, metabolic syndrome, and the structure and composition of the gut microflora.

Other flavonol compounds also influence fat deposition in poultry. For example, supplementation of kaempferol, which is derived from the rhizome of *Kaempferol galanga L*, inhibited the expression of angiogenesis gene angiopoietin-like 3 (ANGPTL3) in the liver tissue of broilers, while the content of LPL in adipose tissue was elevated (Xiao et al., 2012). As ANGPTL3 inhibits LPL in peripheral tissues and has hypolipidemic effects (Kersten, 2017), it is conceivable that kaempferol could modulate lipid profiles and reduce obesity in broilers. Myricetin, which has insulin-like functions in the body, affects lipid-protein interactions and membrane fluidity, promotes glucose absorption, and stimulates fat generation, and could thus be of therapeutic value in the management of diabetes (Ong and Khoo, 1996). In the study of poultry, myricetin not only accelerated growth, but also acted as a potent antioxidant to protect lipids in the body and post-mortem tissue from oxidation (King et al., 2014).

Flavanones

Flavanones, also known as dihydroflavones, are ubiquitous in almost all citrus fruits such as oranges, lemons, and pomelos, and are the main source of the bitter taste in the juice. The difference from flavones is that the C ring of flavanones is saturated (**Figure 1**). Citrus flavanones, like other flavonoids, also possess antioxidant and lipid-lowering properties, and examples in this subclass include naringin, naringenin, hesperidin, and hesperetin.

Addition of hesperidin to the poultry diet can improve antioxidant capacity, health and egg production, reduce serum and yolk cholesterol content in laying hens (S.Ting et al., 2011), and improve the fatty acid profile by reducing SFA and increasing polyunsaturated fatty acids (PUFA) content in broilers (Hager-Theodorides et al., 2021), and bolster the immune response against lipopolysaccharide (LPS) (Kawaguchi et al., 2004). Fotakis et al. (Fotakis et al., 2017) demonstrated that when supplemented in the broiler diet (0.70–1.5 g/kg), hesperidin reduced serum lipid content and significantly increased plasma alanine. Hager-Theodorides et al. (Hager-Theodorides et al., 2021) also found that the addition of hesperidin and naringenin to the broiler diet increased omega n-6 FA and PUFA/SFA ratios in breast muscle and fat pads. An explanation for these observed effects on fatty acid composition is that hesperidin and naringenin can enhance the expression of genes encoding factors related to fatty acid β-oxidation as well as fatty acid synthesis.

In a study with laying hens, Lien et al. (Lien et al., 2008) extracted crude hesperidin (31.5%), crude naringenin (39%), and crude pectin (60%) from citrus and grapefruit peels for supplementation into the diet at concentrations of 0.05, 0.05, and 0.5%, respectively. The results showed that the extracts did not significantly change some traits like egg production, eggshell strength, and eggshell thickness. The concentrations of egg yolk cholesterol, and serum cholesterol and TGs, however, were reduced. Excreta cholesterol levels in the hesperidin (14.18 mg/100 g) and naringenin (16.73 mg/100 g) groups were about double that of the control group (7.43 mg/100 g).

At the transcriptional level, flavanones enhance adipogenesis. Hager-Theodorides et al. (Hager-Theodorides et al., 2021) supplemented 240-day-old Ross 308 broiler chickens with hesperidin (0.75 or 1.5 g/kg feed) and naringenin (0.75 or 1.5 g/kg feed) for a month. They analyzed the fatty acid profile of the abdominal fat pad, and breast and thigh muscles, and found that both hesperidin and naringenin significantly reduced SFA and increased PUFA and n-6 content. They suggested that these effects might be attributed to increased expression of fatty acid β-oxidation related genes (*PPARα* and Acyl-CoA Oxidase 1; *ACOX1*) and the fatty acid synthase (*FASN*) gene. Interestingly, there are two forms of citrus flavanones, the glycosides form (naringin, narirutin, hesperidin) and aglycone form (naringenin, hesperetin). Both forms can be bioconverted through cytolase treatment and have different effects on adipogenesis. Lim et al. (Lim et al., 2015) found that cytolase-treated citrus flavanone, which increased the aglycone form while decreasing the glycosides form, markedly inhibited the differentiation of 3T3-L1 preadipocytes, and naringenin and hesperetin suppressed the protein and mRNA expression of CEBPα, PPARγ, as well as the mRNA levels of SREBP1c. This is inconsistent with the results of Saito et al. (Saito et al., 2009) that flavanone (CAS No. 487-26-3) promoted the differentiation of 3T3-L1 preadipocytes via acting as a PPARγ ligand. Yoshida et al. (Yoshida et al., 2010) showed that naringenin and hesperetin inhibit the ERK and NFκB pathways and reduced free fatty acid (FFA) release and prevented FFA-induced insulin resistance in mouse adipocytes. Thus, multiple studies demonstrate effects of flavonones on lipid metabolism in adipocytes and varying results could be explained by multiple factors, including form and purity of the chemical used, time of treatment application and treatment duration, endpoints for molecular analyses, and passage number and other characteristics of the cell line used.

Flavanonols

Flavanonols are 3-hydroxyl derivatives of flavanones and are also referred to as dihydroflavones because the double bond between the C ring positions 2 and 3 is hydrogenated. Red onion, vinegars, and red wine contain large amounts of flavanonols.

In cell, *in vivo* animal, and human volunteer health studies, taxifolin shows a wide range of health-promoting effects and biological activities including anti-inflammatory, anti-cardiovascular and anticancer, etc. In a cell culture study using HepG2 (hepatocyte) cells, taxifolin supplementation (200 μM) inhibited cholesterol synthesis, possibly by suppressing HMG-CoA reductase activity (Theriault et al., 2000). A more in-depth study in HepG2 cells found that taxifolin treatment limited the extracellular availability of TGs by inhibiting diacylglycerol acyltransferase (DGAT) and microscopic TG transfer protein (MTP) activities, resulting in a decrease in apolipoprotein B secretion, which is positively correlated with the development of cardiovascular artery disease (Casaschi et al., 2004; Sunil and Xu, 2019). Zhao et al. (Zhao et al., 2018) used streptozotocin-induced diabetic rats as a model and found that taxifolin

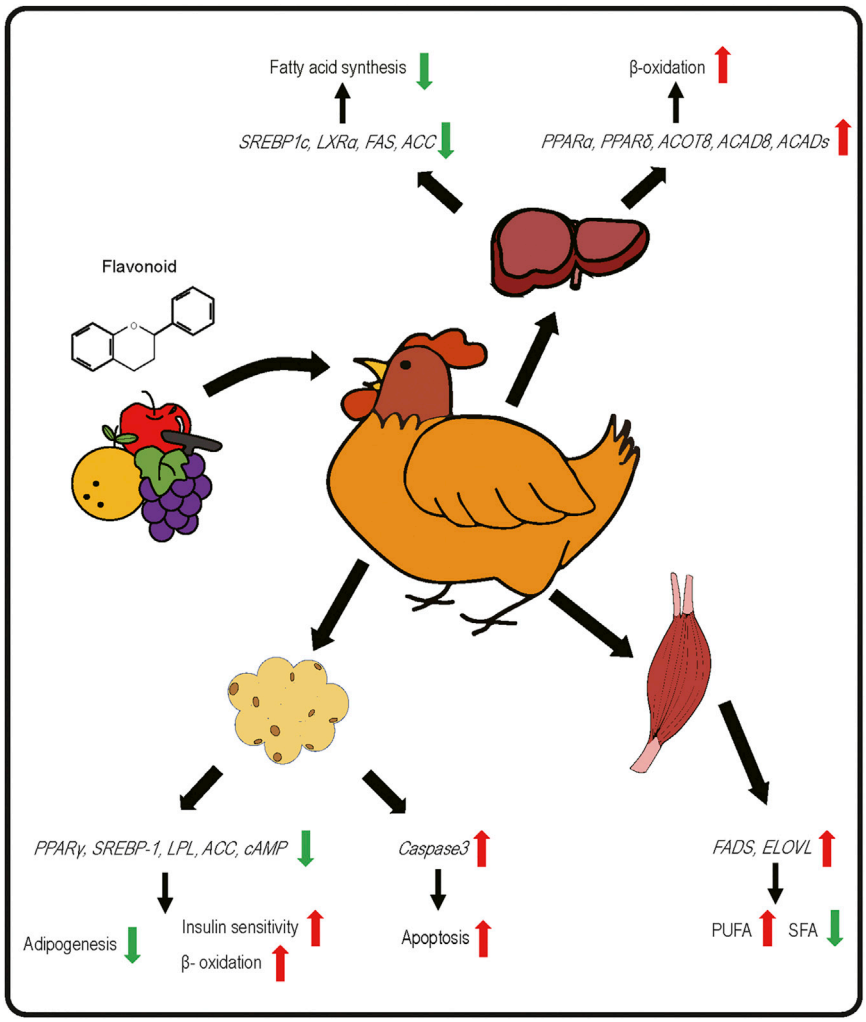

FIGURE 2 | Effects of dietary flavonoids on gene expression related to lipid metabolic pathways in liver, skeletal muscle, and adipose tissue of poultry species.

treatment was associated with a reduction in adipocyte size in the adipose tissue. Studies in poultry have shown that taxifolin (dihydroquercetin) has protective effects on the heart, kidneys, and liver (Saeed et al., 2017b; Cai et al., 2019; Zhang et al., 2019). However, studies regarding the effects of taxifolin on lipid metabolism and adipose tissue physiology in poultry are scarce, and taxifolin appears to function as an antioxidant. Pirgozliev et al. (Pirgozliev et al., 2018) found that feeding taxifolin did not improve the production performance of broilers, except for increasing the redness index of breast meat. Balev et al. (Balev et al., 2015) also found no significant changes in the growth performance of hybrid "Ross" broilers whose diets were supplemented with taxifolin (40 mg/kg body weight) for 49 days.

Flavanols

Flavanols can also be referred to as flavan-3-ols, which contain a hydroxyl group on the C-ring, however there is no double bond and ketone group at position 4 of the C ring. Flavanols can exist as monomers (catechins) or polymers (pro-anthocyanidins). Flavanols are common in many fruits such as bananas, apples, pears, and a variety of drinks and food such as green tea, red wine, and chocolate. Application of dietary flavanols in poultry production can effectively reduce lipid and cholesterol content in blood and yolk as well as improve production performance, carcass, and meat quality (Aziz and Karboune, 2018; Ogbuewu et al., 2019).

Catechins, which are abundant in green tea, and which include epicatechin (EC), epicatechin gallate (ECG), and EGCG, are well studied for their anti-inflammatory, antioxidant, and anti-obesity effects. Studies in mammalian cell culture and animal obesity models have shown that catechins inhibited adipocyte proliferation and differentiation, lipogenesis, and fat deposition (Wolfram et al., 2006; Abd El-Hack et al., 2020). Kim et al. (Kim et al., 2010) demonstrated that EGCG reduced glycerol-3-phosphate dehydrogenase activity, which hindered TG production because of the lack of a glycerol backbone for esterification. Additionally, EGCG treatment inactivated

forkhead transcription factor class O1 (FoxO1) and SREBP1c, which are transcription factors involved in adipocyte differentiation and lipid synthesis. Friedrich et al. (Friedrich et al., 2012) demonstrated that short-term supplementation (up to 1% for 4–7 days) of dietary EGCG to mice inhibited SREBP1c and downregulated its downstream genes *FAS* and stearoyl-coa desaturase (*SCD*) in liver. In cell culture, EGCG at 5 μM inhibited the expression of *PPARγ2* and *C/EBPα* during 3T3-L1 adipocyte differentiation (Furuyashiki et al., 2004). Hung et al. (Hung et al., 2005) found that EGCG (20~50 μM) also inactivated extracellular signal regulated kinase 1 (*ERK1*) and *ERK2* and arrested 3T3-L1 preadipocytes at the G0/G1 phase. Moreover, EGCG promoted β-oxidation and thermogenesis. Dulloo et al. (Dulloo et al., 2000) demonstrated the synergistic effect of green tea extract (GTE; containing 200 μM EGCG) and caffeine on increasing interscapular BAT thermogenesis. The authors speculated that catechins and caffeine may play important roles in the sympathetically released noradrenaline (NA)-cAMP axis, which may also be responsible for the pronounced effect of GTE on BAT thermogenesis. EGCG directly inhibited catechol-O-methyl-transferase, which catalyzes the degradation of NA, thereby prolonging the action of sympathetically released NA. Caffeine, however, inhibited phosphodiesterase, an enzyme that breaks down cAMP. Thus, EGCG and caffeine synergistically increased the intracellular cAMP levels, which then increased activated PKA-dependent phosphorylation of hormone-sensitive lipase and subsequently free fatty acid release for oxidation. However, this might not be as relevant to the discussion of poultry, because it is questioned whether birds have cells that are analogous to brown adipocytes, due to the absence of uncoupling-protein 1 (UCP-1) in the genome.

It is generally accepted that dietary supplementation of catechins affects gastrointestinal tract absorption of water, glucose, fats, minerals, and amino acids (Koo and Noh, 2007; Frejnagel and Wroblewska, 2010). Plant catechins inhibit the activity of digestive enzymes such as α-amylase, trypsin, chymotrypsin and lipase (Salunkhe, 1982) and also interact with proteins to render them insoluble (Kumar and Singh, 1984). *In vitro* studies have shown that green tea catechins interfere with lipid emulsification, digestion and micelle solubilization, which are key steps involved in the intestinal absorption of dietary fatty acids, cholesterol and other lipids. Green tea or its catechins may also reduce the absorption and tissue accumulation of other lipophilic organic compounds (Koo and Noh, 2007). A number of studies have shown that supplementation of catechins from GTE did not affect broiler FCR or BWG. Kaneko et al. (Kaneko et al., 2001) found that 10 weeks of treatment with dietary inclusion levels of GTE at 1, 2.5 and 5% significantly reduced broiler BWG. Yang et al. (Yang et al., 2003) concluded that antibiotic-free green tea (0.5, 1 and 2%) intake for 6 weeks in Ross broilers did not improve feed intake and feed efficiency, but increased BWG. Shomali et al. (Shomali et al., 2012) noted that 1, 2 and 4% of green tea powder (GTP) in the diet for 2 weeks produced no difference in FCR. However, Erener et al. (Erener et al., 2011) showed that 6 weeks of 0.1 or 0.2 g/kg feed GTE improved feed efficiency and increased BW of 42-day-old broilers. Abdel-Azeem (Abdel-Azeem, 2005) also observed that the addition of 0.25, 0.50 and 0.75% powdered green tea flowers in Japanese quail feed increased FCR. The inconsistent results, which apparently are in contradiction with the well-established effects of GTE's on nutrient digestion and absorption, may be related to the different catechin components in green tea and the relative abundance of each in various extracts. It is worth noting that differences in broiler strains, inclusion levels, and treatment times between different studies can also lead to significant differences in final results.

In relation to layers, the results of catechin research have also yielded conflicting results. Ariana et al. (Ariana et al., 2011) observed that 0.5% GTE or 1.5% GTP improved egg yield during the later stage of egg production (64–75 weeks of age). Yamane et al. (Yamane et al., 1999) found that 0.67% GTE reduced egg weight, where Biswas and Wakita (Biswas and Wakita, 2001a) observed similar results when utilizing 0.3% GTP. Others have reported that 0.2% green tea leaves improved egg production and egg mass of laying hens aged 20–44 weeks (Al-Harthi, 2004). Again, this could be due to differences in active ingredients and concentrations in green tea, as well as differences in experimental design such as dietary inclusion level, duration of the study, genetic background of the bird, etc. A challenge in implementing GTP additives in poultry is establishing the optimal level of inclusion to promote the desired effects on animal performance. In addition, when using plants (or derivatives), physiological effects can be attributed to multiple chemicals, whose interactions, metabolism, and effects on cells are complex, making it difficult to define the specific "cocktail" of supplements that will yield optimum results.

Notably, addition of green tea catechins to poultry feed can significantly reduce fat accumulation. Hrnčár (Hrnčár and Bujko, 2017) found that 6 weeks of dietary GTP supplementation at 0.5, 1 and 1.5% decreased abdominal fat pad weights in broilers. Biswas and Wakita (Biswas and Wakita, 2001b) studied the growth performance of broilers that were fed *ad libitum* with starter and finisher diets containing 0.5, 0.75, 1.0 or 1.5% GTP. Feed intake was decreased by about 5.1–15.9% in the 1.0% GTP feeding group, while feed conversion in the 5.0–1.0% GTP feeding groups was improved by 4.1–11.4%. The levels of liver cholesterol, liver fat, and serum cholesterol were decreased in GTP treatment groups. The most significant change observed was a 1.65% loss of relative weight of abdominal fat in a dose-dependent manner. Raederstorff et al. (Raederstorff et al., 2003) concluded that green tea's ability to lower cholesterol was mainly due to EGCG, which could interfere with the micelle dissolution of cholesterol in the digestive tract to regulate lipid digestion, absorption and availability to the liver for bile and lipoprotein synthesis.

Beyond the small intestine, catechin treatment was associated with reduced cholesterol synthesis in the liver (Yousaf et al., 2014). Broilers treated once daily via oral administration of GTP at 50 or 100 mg/kg of BW for a total of 20 days had reduced body fat (Huang et al., 2013). This is partially due to reduced fatty acid

synthesis and enhanced β-oxidation. When EGCG was dissolved in water and orally administered to broilers at 80 mg/kg BW for 4 weeks, there was a reduction in serum TGs and LDL, but an increase in HDL cholesterol (Huang et al., 2015). Supplementation of laying hens diet with 1 g/kg green tea catechins for 60 days reduced plasma total cholesterol, TGs, LDL, and body fat content (Zhou et al., 2012). Collectively, data demonstrate that catechins can reduce lipid accumulation in poultry and potentially improve poultry health and meat quality.

Proanthocyanidins, the most structurally complex and abundant dietary flavonoids that are oligomers of epicatechins or catechins, are found in many plants such as apples, grape seeds and skins, cocoa beans, cranberries, and more (de la Iglesia et al., 2010). Such compounds account for the astringent and bitter taste characteristics of fruit (Lesschaeve and Noble, 2005). Although there are large amounts of proanthocyanidins in the diet, it is important to note that they neutralize proteins in the gut to form tannin-protein complexes that reduce nutrient digestion and absorption (Hagerman and Butler, 1981). In terms of lipid metabolism and adipocyte function, grape seed proanthocyanidins can activate the cAMP signaling pathway in 3T3-L1 adipocytes, thereby inducing lipolysis (Pinent et al., 2005). El-Damrawy (El-Damrawy, 2014) observed that 100 and 200 mg/kg grape seed extract (GSE) supplementation for 3 weeks mitigated some of the negative effects of heat stress in broilers. For example, liver superoxide dismutase and glutathione concentrations were increased and heterophil/lymphocyte ratio, plasma corticosterone, TGs, LDL, HDL and liver malondialdehyde were decreased in broilers fed the GSE-supplemented feed. Farahat et al. (Farahat et al., 2017) reported on the effects of grape seed extract (125, 250, 500, 1,000, and 2000 ppm in diet) in broilers from hatch to 42 days. Although there were no differences in growth performance, total lipids, and high and very low-density lipoprotein cholesterol when compared with control groups, the TC and LDL-C levels were decreased after feeding diets that were supplemented with GSE. Roy and Schneeman (Roy and Schneeman, 1981) suggested that proanthocyanidins can bind and inhibit intestinal absorption of cholesterol, thereby reducing cholesterol levels in the body.

Anthocyanins

Anthocyanins, the glycoside forms of anthocyanidins, are the principal constituent of phyto-pigments of fruits, vegetables, and flowers. The different colors of anthocyanins are usually determined by pH and the methylation or acylation of hydroxyl groups in the A and B rings. They mainly exist in outer cell layers of various fruits such as grapes, strawberries and blueberries, etc. The C ring of anthocyanins has two double bonds, and anthocyanins usually exist in different chemical forms (**Figure 1**). Cyanidin, delphinidin, peonidin, pelargonidin, and petunidin are common anthocyanidins.

Anthocyanins have various bioactive effects such as inhibiting lipid peroxidation, anti-inflammation, improving cell viability, boosting immunity responses and DNA damage repair (Tsuda et al., 2006; Sivamaruthi et al., 2020). Thus, dietary supplementation of these compounds in animals could potentially achieve many physiological benefits, including protective effects against pathogens and mitigating deleterious effects of chronic heat stress. Csernus et al. (Csernus et al., 2020) reported that 0.5% dietary addition of anthocyanins for 26 days improved the BW, average daily gain and average daily feed intake. In chickens that were fed the supplemented diet and challenged with LPS, there was decreased mRNA expression of splenic and ileal interleukin-1β, increased villus height: crypt depth ratios, and thickened mucosa, indicative of increased absorptive surface area. Stantnik et al. (Stastnik et al., 2014a; Stastnik et al., 2014b) found that Konini wheat containing about 14.01 mg/g anthocyanins and milk thistle seed cakes containing 129.83 mg/kg cyanidin-3-glucoside promoted BWG and improvements in meat quality traits of broilers, respectively. Leusink et al. (Goliomytis et al., 2015) noted that 40, 80, or 160 mg/kg anthocyanins from cranberry fruit extract, supplemented for 5 weeks, had no effects on broiler bird performance, meat properties, general health or intestinal integrity. However, treatment lowered the mortality rate, the populations of *Enterococcus spp*. in cecal and cloacal samples, and had positive effects on feed efficiency and BW. Aditya et al. (Aditya et al., 2018) examined the growth performance of broiler chickens treated with grape pomace (*Vitis vinifera*) (containing 1,134 mg/kg anthocyanin). At different concentrations, grape pomace did not affect BWG, feed intake, or FCR. In addition, serum glucose, TGs, and HDL-C were not affected, but total cholesterol content was significantly decreased and some meat quality parameters were improved.

Although there are no detailed experimental data for poultry adipose tissue, anthocyanins show strong anti-lipid production properties in other experimental models. In obesity-related human studies, consuming red (red-flesh) orange juice that contained large amounts of cyanidins reduced risk factors associated with being overweight or obese, for instance insulin resistance, systolic and diastolic blood pressure that were reduced in volunteers after intervention (Azzini et al., 2017; Sivamaruthi et al., 2020). Silveira et al. (Silveira et al., 2015) found that human subjects who consumed 750 ml of red orange juice per day for 8 weeks showed decreases in serum levels of TC and LDL-C. In the diet of obese individuals, 50 g of carbohydrates were substituted with blueberries which contain large amounts of delphinidin, malvidin, and petunidin. After 12 weeks of nutritional therapy, the blueberry-supplemented group lost weight and had less body fat (Istek and Gurbuz, 2017). In addition, anthocyanins inhibited pro-inflammatory markers in obese subjects (Hogan et al., 2010; Santamarina et al., 2020). The reduction in inflammation is particularly appealing, as persistent low-grade chronic inflammation associated with obesity can cause a number of chronic metabolic diseases. Anthocyanin treatment inhibited the expression of *PPARγ* and *FAS* in high-fat diet-induced obese mice (Wu et al., 2016). *In vitro*,

accumulation of TGs in 3T3-L1 preadipocytes was reduced after grape anthocyanin treatment in a dose-dependent manner, due to changes in lipogenic genes such as *LXRα* (*Liver X receptor α*), *SREBP-1c*, *PPARγ*, *C/EBPα*, *FAS*, *SCD-1* and *ACCα* (Lee et al., 2014).

Chalcones

Chalcones are characterized by the absence of the C ring in the basic flavonoid skeleton structure and are also classified as open-chain flavonoids (**Figure 1**). Chalco-naringenin, phlorizin, arbutin, and phloretin are the major examples of chalcones. Chalcones are found in tomatoes, pears, apples, strawberries, as well as in wheat products, red wine, and herbs. Chalcones have important pharmacodynamic significance as they are described as potent anti-inflammatory, antioxidant, anti-proliferative, anti-infective, anticancer, and anti-microbial agents in various animal species, including chickens. For example, over 50 years ago, poultry researchers began to inject chalcones into laying hens in order to eliminate the number and size of blood spots present in eggs (Bigland et al., 1965).

The dihydrochalcone phlorizin is abundant in the leaves of sweet tea and is perhaps most well-known to researchers as a competitive inhibitor of the sodium-glucose transporters (SGLT1 and 2). Phlorizin has thus been studied for managing diabetes mellitus and obesity by inhibiting glucose uptake and resorption (Ehrenkranz et al., 2005; Vaidya and Goyal, 2010), but it can be rapidly hydrolyzed into phloretin in the small intestine of mammals, limiting its potential as a therapeutic agent for diabetes. However, Awad et al. (Awad et al., 2007) reported that phlorizin had the same effect on reducing glucose absorption in the jejunum as deoxynivalenol, a common mycotoxin in feedstuffs. Glucose uptake in laying hens was reduced after treatment with 100 μl/ml phlorizin, consistent with Bierbach (Bierbach et al., 1979), where 1 mM phlorizin also reduced glucose absorption in isolated chicken intestinal epithelial cells.

Chalco-naringenin is mainly found in tomatoes and possesses strong anti-inflammatory properties which can be beneficial for relieving chronic inflammation in obese individual adipose tissue. In obesity-associated adipose tissue, chalco-naringenin inhibited proinflammatory cytokines like monocyte chemoattractant protein 1 (MCP1) and TNF-α in the paracrine loop between adipocytes and macrophages, and decreased overall inflammation as well as insulin resistance (Hirai et al., 2010). There is little known on the precise quantification of chalcone and its subclass in feed additives for poultry, and this review discusses relevant additives rich in chalcone, such as tomato powder. In Japanese quail exposed to heat stress-induced conditions, feed intake, BWG, and FCR all increased when fed a diet supplemented with either 2.5 or 5.0% tomato powder for 3 weeks (Sahin et al., 2008). Similarly, laying hens that were fed a diet containing 5 or 10 g/kg of tomato powder for 90 days, displayed significant increases in feed intake yet a decrease in FCR. Other factors such as egg production, egg weight, yolk color (darker color), and duration of egg production were all increased, while there was also a decrease in egg yolk lipid peroxidation (Akdemir et al., 2012). Omri et al. (Omri et al., 2019) reported that the dietary incorporation of 1% tomato paste, 4.5% linseed, and 1% red pepper in Novogen White laying hen feed for 47 days reduced egg yolk content of palmitic acid and stearic acid. Moreover, SFA and the ratio of omega 6- to 3-PUFAs were decreased, and the total content of PUFAs increased. Thus, dietary chalcones may serve as an attractive strategy to mitigate obesity and associated inflammation and metabolic disorders in broiler breeders and laying hens, while also favorably modulating lipid composition in meat and eggs.

Isoflavones

Isoflavones are unique isomers of flavones, with both glycoside and aglycone forms. Isoflavones are not widely distributed within the plant kingdom, their main presence being in soybean and leguminous plants. Isoflavones in soybeans include genistein, daidzein and glycitein and their respective glycoside forms, with the concentration ratio being about 1:1:0.2 (Manach et al., 2004). Genistein is structurally similar to estrogen and can bind to estrogen receptors, particularly estrogen receptor-beta. Thus, genistein may have weak estrogenic (or antiestrogenic depending on its concentration) properties and is hence referred to as phytoestrogen.

Isoflavones, as a feed supplement, reduced fat deposition, an effect that was attributed to its estrogen-like properties. Gou et al. (Gou et al., 2020) reported that corn–soybean meal-based diets supplemented with linseed oil (2% or 4%) and 30 mg/kg soybean isoflavones reduced the abdominal fat percentage of broilers aged 29–66 days. Adding soybean isoflavones also increased the content of α-linolenic acid (C18: 3n-3), EPA (C20:5n-3) DHA (C22:6n-3) and total n-3 PUFA in breast muscle, while the addition decreased palmitic acid (C16:0), lignoceric acid (C24: 0), SFA and n-6: n-3 ratio in breast muscle and total TG, total cholesterol and malondialdehyde content in plasma. Gene expression analysis in broiler breast muscle revealed that the expression of fatty acid desaturase 1 (FADS1), FADS2, elongase 2 (ELOVL2) and ELOVL5 increased in response to soybean isoflavone supplementation. Similarly, Payne et al. (Payne et al., 2001) observed that low crude protein diets with supplemental crystalline amino acids (CP-AA) and a low concentration of soy isoflavones reduced the weights of abdominal fat pads in 9–52 day-old broilers, which were intermediate between chicks fed the corn–soybean meal diet and low CP-AA diet. Thus, these data suggest that the decreased fatness in broilers may be partially attributed to an increased level of soy isoflavones in these diets.

Effects of isoflavones were also observed on egg-laying and egg lipid composition. Corn–soybean meal-based diet supplementation of genistein at 800 mg/kg feed for 90 days significantly improved the antioxidant indices, feed intake and the egg-laying efficiency of quail (Akdemir and Sahin, 2009). Lv et al. (Lv et al., 2018) demonstrated that a relatively low concentration of genistein (40 mg/kg) in a high-energy and low-choline diet for 64 days significantly increased the hypothalamic mRNA expression of gonadotropin releasing hormone (GnRH) mRNA and raised serum estrogen levels, which were associated with improved egg laying performance. Genistein treatment also reduced liver concentrations of long-chain SFA, MUFA, and the n-6: n-3 PUFA ratio. It was suggested that dietary genistein inhibits the expression of fatty acid synthesis-related genes, SREBP1c, LXRα, FAS, and ACC,

meanwhile promoting the expression of β-oxidation related genes PPARα, PPARδ, ACOT8, ACAD8, and ACADs. There were differing effects in chickens that received a diet with greater concentrations of genistein (400 mg/kg), further reinforcing that a challenge in widespread implementation of dietary supplementation is identifying optimum dose ranges.

Flavonoids may manipulate the intestinal microbiota and in turn be transformed into relatively more or less bioactive polyphenols, or have beneficial effects by modulating the structure of the microbiome as probiotics that enrich for beneficial species of bacteria (Abbas et al., 2017). A well-studied example is the conversion of soybean isoflavone daidzein to equol, which has strong biological activity as a phytoestrogen. One attractive strategy for improving antioxidant status and establishment of a healthy microbial community is in ovo supplementation during embryonic development. It is beyond the scope of this review to discuss in detail, but depending on the day and location of injection and the diluent (e.g., oils, alcohols, etc.), the flavonoid may be absorbed and exert biological effects during critical stages of development, with physiological changes that persist after hatching. Ni et al. (Ni et al., 2012) injected 20 or 100 μg equol into the albumen on embryonic day 7, and at 49 days post-hatch, equol-treated chickens had lower serum TGs and TC, but greater HDL-C concentrations than controls. These changes were accompanied by differences at the molecular level in the liver, including elevated carnitine palmitoyl transferase 1 and reduced FAS mRNAs. These results suggest that early life exposure to equol may induce changes in the liver that lead to increased fatty acid catabolism and reduced synthesis, thereby reducing circulating levels of liver-derived lipids. Similarly, Wei et al. (Wei et al., 2011) observed that in ovo injection of equol affected female broiler meat quality, including decreased redness (a*), cooking loss, and 24 and 48 h drip loss. Further research is needed to determine the practicality of in ovo supplementation of flavonoids in the poultry industry and robustness of physiological effects.

Neoflavonoids

Neoflavonoids are relatively uncommon but are reported to exert a multitude of beneficial health effects. They are distributed in *Coutarea hexandra*, *Calophyllum inophyllum* and *Pityrogrammacalomelanos* var. *aureofiava* (Donnelly and Boland, 2017). Dalbergin is the most common neoflavonoid in the plant kingdom. Neoflavonoids are characterized by a 4-phenylchromen backbone without a hydroxyl group substitution at position 2 of the C ring. These compounds have anti-osteoporosis, anti-androgen, anti-inflammatory, anti-tumor, anti-allergy, anti-oxidation and other biological activities (Liu et al., 2017). There are no reports on the effects of dietary neoflavonoids on livestock, poultry production, or on lipid metabolism and deposition.

CONCLUSIONS AND FUTURE DIRECTIONS

In recent years, dietary flavonoids have received considerable attention in poultry research due to their various beneficial effects on health, growth performance, and meat quality. Given that a vast array of such chemicals exist in nature and many flavonoids are antioxidants with anti-inflammatory and other properties, there are possibilities for developing additives using one or more of these natural and cheap compounds to economically promote production while improving health and meat and egg quality. Dietary supplementation of flavonoids can modulate lipid metabolism and deposition, and in particular alter the fatty acid composition and reduce the cholesterol and TG content of poultry meat and eggs. In adipose tissue, some flavonoids inhibit adipogenesis while promoting lipolysis and apoptosis, which collectively prevent the expansion of adipose tissue. As antioxidants, flavonoids can protect other nutrients from oxidation and contribute to a healthy cellular environment at the gut mucosal layer and in other tissues. The anti-inflammatory properties of flavonoids are also an added benefit because obesity, which is a serious issue in broiler breeders and laying hens, is generally associated with a chronic low-grade inflammation, which eventually leads to a host of comorbidities. A challenge in practically applying results of this research is that many studies yield conflicting results regarding consistent effects of flavonoids on growth and production parameters. It is important to note though, that such studies differ in the form of flavonoid supplemented (extracts vs pure compound vs mixture of compounds), doses in the diet, duration of study, genetic background of bird, and processing of ingredients and diet mixing (as well as remaining composition of diet) which can affect the molecular structure, bioavailability, and bioactivity of the flavonoids and other nutrients in the diet. Additional studies are needed at both the cell culture and whole animal level, especially in poultry adipose tissue, skeletal muscle and the liver, in order to reveal the cellular and molecular mechanisms responsible for the effects of flavonoids on lipid metabolism and fat accretion.

AUTHOR CONTRIBUTIONS

ZT, EG, and MC conceived ideas for the review, ZT wrote and revised the manuscript. BH added information to the manuscript. EG, MC, DL, and BH edited the manuscript.

FUNDING

John Lee Pratt Endowment and Virginia Tech Library Subvention Fund.

REFERENCES

Abbas, M., Saeed, F., Anjum, F. M., Afzaal, M., Tufail, T., Bashir, M. S., et al. (2017). Natural Polyphenols: An Overview. *Int. J. Food Properties* 20 (8), 1689–1699. doi:10.1080/10942912.2016.1220393

Abd El-Hack, M. E., Elnesr, S. S., Alagawany, M., Gado, A., Noreldin, A. E., and Gabr, A. A. (2020). Impact of green tea (Camellia Sinensis) and Epigallocatechin Gallate on Poultry. *World's Poult. Sci. J.* 76 (1), 49–63. doi:10.1080/00439339.2020.1729672

Abdel-Moneim, A. M. E., Shehata, A. M., Alzahrani, S. O., Shafi, M. E., Mesalam, N. M., Taha, A. E., et al. (2020). The Role of Polyphenols in Poultry Nutrition. *J. Anim. PhysiologyAnimal Nutr.* 104 (6), 1851–1866.

Abdel-Azeem, F. J. E. P. S. J. (2005). Green tea Flowers (Camellia Sinensis) as Natural Anti-oxidants Feed Additives in Growing Japanese Quail Diets. *Egypt. Poult. Sci. J.* 25 (3), 569–588.

Aditya, S., Ohh, S.-J., Ahammed, M., and Lohakare, J. (2018). Supplementation of Grape Pomace (Vitis vinifera) in Broiler Diets and its Effect on Growth Performance, Apparent Total Tract Digestibility of Nutrients, Blood Profile, and Meat Quality. *Anim. Nutr.* 4 (2), 210–214. doi:10.1016/j.aninu.2018.01.004

Ahossi, P., Dougnon, J., Kiki, P., and Houessionon, J. (2016). Effects of Tridax Procumbens Powder on Zootechnical, Biochemical Parameters and Carcass Characteristics of Hubbard Broiler Chicken. *J. Anim. Health Productio* 4 (1).,

Akdemir, F., Orhan, C., Sahin, N., Sahin, K., and Hayirli, A. (2012). Tomato Powder in Laying Hen Diets: Effects on Concentrations of Yolk Carotenoids and Lipid Peroxidation. *Br. Poult. Sci.* 53 (5), 675–680. doi:10.1080/00071668.2012.729142

Akdemir, F., and Sahin, K. (2009). Genistein Supplementation to the Quail: Effects on Egg Production and Egg Yolk Genistein, Daidzein, and Lipid Peroxidation Levels. *Poult. Sci.* 88 (10), 2125–2131. doi:10.3382/ps.2009-00004

Al-Harthi, M. J. E. P. S. J. (2004). Responses of Laying Hens to Different Levels of Amoxicillin, Hot Pepper or green tea and Their Effects on Productive Performance, Egg Quality and Chemical Composition of Yolk and Blood Plasma Constituents. *Egypt. Poult. Sci. J.* 24 (4), 845–868.

Amnueysit, P., Tatakul, T., Chalermsan, N., and Amnueysit, K. (2010). Effects of Purple Field Corn Anthocyanins on Broiler Heart Weight. *Asian J. Food Agro-Industry* 3 (3), 319–327.

Ariana, M., Samie, A., Edriss, M. A., and Jahanian, R. J. J. M. P. R. (2011). Effects of Powder and Extract Form of green tea and Marigold, and α-tocopheryl Acetate on Performance, Egg Quality and Egg Yolk Cholesterol Levels of Laying Hens in Late Phase of Production. *J. Med. Plants Res.* 5 (13), 2710–2716.

Awad, W., Aschenbach, J., Setyabudi, F., Razzazi-Fazeli, E., Böhm, J., and Zentek, J. (2007). Environment, Well-Being, and Behavior. *Poult. Sci.* 86, 15–20.

Aziz, M., and Karboune, S. (2018). Natural Antimicrobial/antioxidant Agents in Meat and Poultry Products as Well as Fruits and Vegetables: A Review. *Crit. Rev. Food Sci. Nutr.* 58 (3), 486–511. doi:10.1080/10408398.2016.1194256

Azzini, E., Venneria, E., Ciarapica, D., Foddai, M. S., Intorre, F., Zaccaria, M., et al. (2017). Effect of Red Orange Juice Consumption on Body Composition and Nutritional Status in Overweight/Obese Female: A Pilot Study. *Oxid Med. Cel Longev* 2017, 1672567. doi:10.1155/2017/1672567

Bakalivanova, T., and Kaloyanov, N. (2012). Effect of Taxifolin, Rosemary and Synthetic Antioxidants Treatment on the Poultry Meat Lipid Peroxidation. *Comptes rendus de l'Académie bulgare des Sci. Sci. mathématiques Nat.* 65, 161–168.

Balev, D., Vlahova-Vangelova, D., Mihalev, K., Shikov, V., Dragoev, S., and Nikolov, V. (2015). Application of Natural Dietary Antioxidants in Broiler Feeds. *J. Mountain Agric. Balkans* 18 (2), 224–232.

Bickerstaffe, R., West, C. E., and Annison, E. F. (1970). Lipid Metabolism in the Perfused Chicken Liver. Lipogenesis from Glucose, Acetate and Palmitate. *Biochem. J.* 118 (3), 427–431. doi:10.1042/bj1180427

Bierbach, H., Haag†, G. F., and Holldorf, A. W. (1979). Uptake and Metabolism of Long Chain Fatty Acids in Isolated Chicken Intestinal Epithelial Cells. *Digestion* 19 (6), 392–403. doi:10.1159/000198400

Bigland, C. H., Bennett, E., and Abbott, U. K. (1965). The Effect of Pyrrole-2-Aldehyde Chalcone Derivatives on the Incidence of Blood Spots in Chicken Eggs. *Poult. Sci.* 44, 140–144. doi:10.3382/ps.0440140

Bigland, C. H., Bennett, E. B., and Abbott, U. K. (1964). Decrease in Incidence of Blood Spots in Chicken Eggs by Injection Derivatives of Pyrrole-2-Aldehyde Chalcones into Hens. *Exp. Biol. Med.* 116, 1122–1125. doi:10.3181/00379727-116-29469

Biswas, A. H., and Wakita, M. (2001b). Effect of Dietary Japanese green tea Powder Supplementation on Feed Utilization and Carcass Profiles in Broilers. *J. Poult. Sci.* 38 (1), 50–57. doi:10.2141/jpsa.38.50

Biswas, M. A., and Wakita, M. (2001a). *Comparison of Two Dietary Factors, green tea Powder Feeding and Feed Restriction, Influencing Laying Performance and Egg Quality in Hens*. Tsu, Japan: Bulletin of the Faculty of Bioresources-Mie University.

Butterwith, S. C. (1989). Contribution of Lipoprotein Lipase Activity to the Differential Growth of Three Adipose Tissue Depots in Young Broiler Chickens. *Br. Poult. Sci.* 30 (4), 927–933. doi:10.1080/00071668908417219

Cai, J., Gu, H., Shi, S., and Tong, H. (2013). Effects of High-Dose Daidzein on Laying Performance, Egg Quality and Antioxidation in Laying Hens. *J. Poult. Sci.* 50 (3), 237–241.

Cai, J., Shi, G., Zhang, Y., Zheng, Y., Yang, J., Liu, Q., et al. (2019). Taxifolin Ameliorates DEHP-Induced Cardiomyocyte Hypertrophy via Attenuating Mitochondrial Dysfunction and Glycometabolism Disorder in Chicken. *Environ. Pollut.* 255 (Pt 1), 113155. doi:10.1016/j.envpol.2019.113155

Cain, J. R., Lien, R. J., and Beasom, S. L. (1987). Phytoestrogen Effects on Reproductive Performance of Scaled Quail. *J. Wildl. Manag.* 51, 198–201. doi:10.2307/3801655

Casaschi, A., Rubio, B. K., Maiyoh, G. K., and Theriault, A. G. (2004). Inhibitory Activity of Diacylglycerol Acyltransferase (DGAT) and Microsomal Triglyceride Transfer Protein (MTP) by the Flavonoid, Taxifolin, in HepG2 Cells: Potential Role in the Regulation of Apolipoprotein B Secretion. *Atherosclerosis* 176 (2), 247–253. doi:10.1016/j.atherosclerosis.2004.05.020

Chamorro, S., Viveros, A., Rebolé, A., Arija, I., Romero, C., Alvarez, I., et al. (2017). Addition of Exogenous Enzymes to Diets Containing Grape Pomace: Effects on Intestinal Utilization of Catechins and Antioxidant Status of Chickens. *Food Res. Int.* 96, 226–234. doi:10.1016/j.foodres.2017.02.010

Choct, M., Naylor, A., Hutton, O., and Nolan, J. (2000). Increasing Efficiency of Lean Tissue Composition in Broiler Chickens. A Report for the Rural Industries Research and Development Corporation. Publication No 98/123. rirdc infoservices com au/downloads/98-123 (Accessed September 20, 2013).

Choe, H. S., Song, T. H., Han, O. K., Park, T. I., and Ryu, K. S. (2013). Effect of Barley Containing Different Levels of Anthocyanin on the Performance and Egg Quality of Laying Hens. *J. Life Sci.* 23 (2), 237–241. doi:10.5352/jls.2013.23.2.237

Comalada, M., Ballester, I., Bailón, E., Sierra, S., Xaus, J., Gálvez, J., et al. (2006). Inhibition of Pro-inflammatory Markers in Primary Bone Marrow-Derived Mouse Macrophages by Naturally Occurring Flavonoids: Analysis of the Structure-Activity Relationship. *Biochem. Pharmacol.* 72 (8), 1010–1021. doi:10.1016/j.bcp.2006.07.016

Craig, W. J. (1997). Phytochemicals. *J. Am. Diet. Assoc.* 97 (10), S199–S204. doi:10.1016/s0002-8223(97)00765-7

Cross, A. J., Ferrucci, L. M., Risch, A., Graubard, B. I., Ward, M. H., Park, Y., et al. (2010). A Large Prospective Study of Meat Consumption and Colorectal Cancer Risk: an Investigation of Potential Mechanisms Underlying This Association. *Cancer Res.* 70 (6), 2406–2414. doi:10.1158/0008-5472.can-09-3929

Csernus, B., Biró, S., Babinszky, L., Komlósi, I., Jávor, A., Stündl, L., et al. (2020). Effect of Carotenoids, Oligosaccharides and Anthocyanins on Growth Performance, Immunological Parameters and Intestinal Morphology in Broiler Chickens Challenged with *Escherichia coli* Lipopolysaccharide. *Animals (Basel)* 10 (2). doi:10.3390/ani10020347

D'Mello, J. F. (2000). *Farm Animal Metabolism and Nutrition*. New York, NY: Cabi.

de la Iglesia, R., Milagro, F. I., Campión, J., Boqué, N., and Martínez, J. A. (2010). Healthy Properties of Proanthocyanidins. *Biofactors* 36 (3), 159–168. doi:10.1002/biof.79

Dillard, C. J., and German, J. B. (2000). Phytochemicals: Nutraceuticals and Human Health. *J. Sci. Food Agric.* 80 (12), 1744–1756.

Donnelly, D. M., and Boland, G. (2017). "Neoflavonoids," in *The Flavonoids* (Boca Raton, FL: Routledge), 239–258.

Dulloo, A., Seydoux, J., Girardier, L., Chantre, P., and Vandermander, J. (2000). Green tea and Thermogenesis: Interactions between Catechin-Polyphenols,

Caffeine and Sympathetic Activity. *Int. J. Obes.* 24 (2), 252–258. doi:10.1038/sj.ijo.0801101

Ehrenkranz, J. R. L., Lewis, N. G., Ronald Kahn, C., and Roth, J. (2005). Phlorizin: a Review. *Diabetes Metab. Res. Rev.* 21 (1), 31–38. doi:10.1002/dmrr.532

Ejaz, A., Wu, D., Kwan, P., and Meydani, M. (2009). Curcumin Inhibits Adipogenesis in 3T3-L1 Adipocytes and Angiogenesis and Obesity in C57/BL Mice. *J. Nutr.* 139 (5), 919–925. doi:10.3945/jn.108.100966

El Gharras, H. (2009). Polyphenols: Food Sources, Properties and Applications–A Review. *Int. J. Food Sci. Technol.* 44 (12), 2512–2518.

El-Damrawy, S. (2014). Effect of Grape Seed Extract on Some Physiological Changes in Broilers under Heat Stress. *Egypt. Poult. Sci. J.* 34, 333–343.

Erener, G., Ocak, N., Altop, A., Cankaya, S., Aksoy, H. M., and Ozturk, E. (2011). Growth Performance, Meat Quality and Caecal Coliform Bacteria Count of Broiler Chicks Fed Diet with green tea Extract. *Asian Australas. J. Anim. Sci.* 24 (8), 1128–1135. doi:10.5713/ajas.2011.10434

Farahat, M. H., Abdallah, F. M., Ali, H. A., and Hernandez-Santana, A. (2017). Effect of Dietary Supplementation of Grape Seed Extract on the Growth Performance, Lipid Profile, Antioxidant Status and Immune Response of Broiler Chickens. *Animal* 11 (5), 771–777. doi:10.1017/s1751731116002251

Ferguson, L. R. (2010). Meat and Cancer. *Meat Sci.* 84 (2), 308–313. doi:10.1016/j.meatsci.2009.06.032

Fotakis, C., Lantzouraki, D. Z., Goliomytis, M., Simitzis, P. E., Charismiadou, M., Deligeorgis, S. G., et al. (2017). NMR Metabolomics Investigates the Influence of Flavonoid-Enriched Rations on Chicken Plasma. *J. AOAC Int.* 100 (2), 315–322. doi:10.5740/jaoacint.16-0405

Fouad, A. M., and El-Senousey, H. K. (2014). Nutritional Factors Affecting Abdominal Fat Deposition in Poultry: a Review. *Asian Australas. J. Anim. Sci.* 27 (7), 1057–1068. doi:10.5713/ajas.2013.13702

Frejnagel, S., and Wroblewska, M. (2010). Comparative Effect of green tea, Chokeberry and Honeysuckle Polyphenols on Nutrients and mineral Absorption and Digestibility in Rats. *Ann. Nutr. Metab.* 56 (3), 163–169. doi:10.1159/000278747

Friedrich, M., Petzke, K. J., Raederstorff, D., Wolfram, S., and Klaus, S. (2012). Acute Effects of Epigallocatechin Gallate from green tea on Oxidation and Tissue Incorporation of Dietary Lipids in Mice Fed a High-Fat Diet. *Int. J. Obes. (Lond)* 36 (5), 735–743. doi:10.1038/ijo.2011.136

Furuyashiki, T., Nagayasu, H., Aoki, Y., Bessho, H., Hashimoto, T., Kanazawa, K., et al. (2004). Tea Catechin Suppresses Adipocyte Differentiation Accompanied by Down-Regulation of PPARγ2 and C/EBPα in 3T3-L1 Cells. *Biosci. Biotechnol. Biochem.* 68 (11), 2353–2359. doi:10.1271/bbb.68.2353

Goliomytis, M., Kartsonas, N., Charismiadou, M. A., Symeon, G. K., Simitzis, P. E., and Deligeorgis, S. G. (2015). The Influence of Naringin or Hesperidin Dietary Supplementation on Broiler Meat Quality and Oxidative Stability. *PLoS One* 10 (10), e0141652. doi:10.1371/journal.pone.0141652

Goliomytis, M., Kostaki, A., Avgoulas, G., Lantzouraki, D. Z., Siapi, E., Zoumpoulakis, P., et al. (2018). Dietary Supplementation with orange Pulp (Citrus Sinensis) Improves Egg Yolk Oxidative Stability in Laying Hens. *Anim. Feed Sci. Technology* 244, 28–35. doi:10.1016/j.anifeedsci.2018.07.015

Goliomytis, M., Orfanou, H., Petrou, E., Charismiadou, M. A., Simitzis, P. E., and Deligeorgis, S. G. (2014). Effect of Hesperidin Dietary Supplementation on Hen Performance, Egg Quality and Yolk Oxidative Stability. *Br. Poult. Sci.* 55 (1), 98–104. doi:10.1080/00071668.2013.870328

Goliomytis, M., Tsoureki, D., Simitzis, P. E., Charismiadou, M. A., Hager-Theodorides, A. L., and Deligeorgis, S. G. (2014). The Effects of Quercetin Dietary Supplementation on Broiler Growth Performance, Meat Quality, and Oxidative Stability. *Poult. Sci.* 93 (8), 1957–1962. doi:10.3382/ps.2013-03585

González-Castejón, M., and Rodriguez-Casado, A. (2011). Dietary Phytochemicals and Their Potential Effects on Obesity: a Review. *Pharmacol. Res.* 64 (5), 438–455.

Goodridge, A. G. (1973). Regulation of Fatty Acid Synthesis in Isolated Hepatocytes Prepared from the Livers of Neonatal Chicks. *J. Biol. Chem.* 248 (6), 1924–1931. doi:10.1016/s0021-9258(19)44168-9

Gou, Z. Y., Cui, X. Y., Li, L., Fan, Q. L., Lin, X. J., Wang, Y. B., et al. (2020). Effects of Dietary Incorporation of Linseed Oil with Soybean Isoflavone on Fatty Acid Profiles and Lipid Metabolism-Related Gene Expression in Breast Muscle of Chickens. *Animal* 14 (11), 2414–2422. doi:10.1017/s1751731120001020

Griffin, H. D., Guo, K., Windsor, D., and Butterwith, S. C. (1992). Adipose Tissue Lipogenesis and Fat Deposition in Leaner Broiler Chickens. *J. Nutr.* 122 (2), 363–368. doi:10.1093/jn/122.2.363

Griminger, P. (1986). "Lipid Metabolism," in *Avian Physiology* (Springer), 345–358. doi:10.1007/978-1-4612-4862-0_15

Gross, R., and Mialhe, P. (1984). Effect of Insulin on Free Fatty Acid Uptake by Hepatocytes in the Duck. *J. Endocrinol.* 102 (3), 381–386. doi:10.1677/joe.0.1020381

Guillou, H., Martin, P. G. P., and Pineau, T. (2008). Transcriptional Regulation of Hepatic Fatty Acid Metabolism. *Lipids Health Dis.*, 3–47. doi:10.1007/978-1-4020-8831-5_1

Hager-Theodorides, A. L., Massouras, T., Simitzis, P. E., Moschou, K., Zoidis, E., Sfakianaki, E., et al. (2021). Hesperidin and Naringin Improve Broiler Meat Fatty Acid Profile and Modulate the Expression of Genes Involved in Fatty Acid β-oxidation and Antioxidant Defense in a Dose Dependent Manner. *Foods* 10 (4). doi:10.3390/foods10040739

Hagerman, A. E., and Butler, L. G. (1981). The Specificity of Proanthocyanidin-Protein Interactions. *J. Biol. Chem.* 256 (9), 4494–4497. doi:10.1016/s0021-9258(19)69462-7

Han, C. K., Sung, K. S., Yoon, C. S., Lee, N. H., and Kim, C. S. (1993). Effect of Dietary Lipids on Liver, Serum and Egg Yolk Cholesterol Contents of Laying Hens. *Asian Australas. J. Anim. Sci.* 6 (2), 243–248. doi:10.5713/ajas.1993.243

Hargis, P. S., and Van Elswyk, M. E. (1993). Manipulating the Fatty Acid Composition of Poultry Meat and Eggs for the Health Conscious Consumer. *World's Poult. Sci. J.* 49 (3), 251–264. doi:10.1079/wps19930023

Havenstein, G., Ferket, P., and Qureshi, M. (2003). Growth, Livability, and Feed Conversion of 1957 versus 2001 Broilers when Fed Representative 1957 and 2001 Broiler Diets. *Poult. Sci.* 82 (10), 1500–1508. doi:10.1093/ps/82.10.1500

Havsteen, B. H. (2002). The Biochemistry and Medical Significance of the Flavonoids. *Pharmacol. Ther.* 96 (2-3), 67–202. doi:10.1016/s0163-7258(02)00298-x

He, K., Hu, F. B., Colditz, G. A., Manson, J. E., Willett, W. C., and Liu, S. (2004). Changes in Intake of Fruits and Vegetables in Relation to Risk of Obesity and Weight Gain Among Middle-Aged Women. *Int. J. Obes.* 28 (12), 1569–1574. doi:10.1038/sj.ijo.0802795

Hirai, S., Takahashi, N., Goto, T., Lin, S., Uemura, T., Yu, R., et al. (2010). Functional Food Targeting the Regulation of Obesity-Induced Inflammatory Responses and Pathologies. *Mediators Inflamm.* 2010, 367838. doi:10.1155/2010/367838

Hogan, S., Canning, C., Sun, S., Sun, X., and Zhou, K. (2010). Effects of Grape Pomace Antioxidant Extract on Oxidative Stress and Inflammation in Diet Induced Obese Mice. *J. Agric. Food Chem.* 58 (21), 11250–11256. doi:10.1021/jf102759e

Hrnčár, C., and Bujko, J. (2017). Effect of Different Levels of green tea (Camellia Sinensis) on Productive Performance, Carcass Characteristics and Organs of Broiler Chickens. *Potravinarstvo Slovak J. Food Sci.* 11 (1), 623–628.

Hu, M., Wu, B., and Liu, Z. (2017). Bioavailability of Polyphenols and Flavonoids in the Era of Precision Medicine. *Mol. Pharmaceutics* 14 (9), 2861–2863. doi:10.1021/acs.molpharmaceut.7b00545

Hu, R., He, Y., Arowolo, M., Wu, S., and He, J. (2019). Polyphenols as Potential Attenuators of Heat Stress in Poultry Production. *Antioxidants* 8 (3), 67. doi:10.3390/antiox8030067

Huang, J. B., Zhang, Y., Zhou, Y. B., Wan, X. C., and Zhang, J. S. (2015). Effects of Epigallocatechin Gallate on Lipid Metabolism and its Underlying Molecular Mechanism in Broiler Chickens. *J. Anim. Physiol. Anim. Nutr.* 99 (4), 719–727. doi:10.1111/jpn.12276

Huang, J., Zhang, Y., Zhou, Y., Zhang, Z., Xie, Z., Zhang, J., et al. (2013). Green tea Polyphenols Alleviate Obesity in Broiler Chickens through the Regulation of Lipid-Metabolism-Related Genes and Transcription Factor Expression. *J. Agric. Food Chem.* 61 (36), 8565–8572. doi:10.1021/jf402004x

Hung, P.-F., Wu, B.-T., Chen, H.-C., Chen, Y.-H., Chen, C.-L., Wu, M.-H., et al. (2005). Antimitogenic Effect of green tea (−)-epigallocatechin Gallate on 3T3-L1 Preadipocytes Depends on the ERK and Cdk2 Pathways. *Am. J. Physiology-Cell Physiol.* 288 (5), C1094–C1108. doi:10.1152/ajpcell.00569.2004

Istek, N., and Gurbuz, O. (2017). Investigation of the Impact of Blueberries on Metabolic Factors Influencing Health. *J. Funct. Foods* 38, 298–307.

Jiang, Z. Y., Jiang, S. Q., Lin, Y. C., Xi, P. B., Yu, D. Q., and Wu, T. X. (2007). Effects of Soybean Isoflavone on Growth Performance, Meat Quality, and Antioxidation in Male Broilers. *Poult. Sci.* 86 (7), 1356–1362. doi:10.1093/ps/86.7.1356

Kamboh, A. A., and Zhu, W. Y. (2013). Individual and Combined Effects of Genistein and Hesperidin Supplementation on Meat Quality in Meat-type Broiler Chickens. *J. Sci. Food Agric.* 93 (13), 3362–3367.

Kamboh, A. A., Leghari, R. A., Khan, M. A., Kaka, U., Naseer, M., Sazili, A. Q., et al. (2019). Flavonoids Supplementation - an Ideal Approach to Improve Quality of Poultry Products. *World's Poult. Sci. J.* 75 (1), 115–126. doi:10.1017/s0043933918000703

Kamboh, A. A., Memon, A. M., Mughal, M. J., Memon, J., and Bakhetgul, M. (2018). Dietary Effects of Soy and Citrus Flavonoid on Antioxidation and Microbial Quality of Meat in Broilers. *J. Anim. Physiol. Anim. Nutr.* 102 (1), 235–240. doi:10.1111/jpn.12683

Kamboh, A. A., and Zhu, W.-Y. (2013). Effect of Increasing Levels of Bioflavonoids in Broiler Feed on Plasma Anti-oxidative Potential, Lipid Metabolites, and Fatty Acid Composition of Meat. *Poult. Sci.* 92 (2), 454–461. doi:10.3382/ps.2012-02584

Kaneko, K., Yamasaki, K., Tagawa, Y., Tokunaga, M., Tobisa, M., and Furuse, M. (2001). Effects of Dietary Japanese green tea Powder on Growth, Meat Ingredient and Lipid Accumulation in Broilers. *Jpn. Poult. Sci.* 38 (5), J77–J85. doi:10.2141/jpsa.38.j77

Kara, K., Kocaoğlu Güçlü, B., Şentürk, M., and Konca, Y. (2016). Influence of Catechin (Flavan-3-ol) Addition to Breeder Quail (*Coturnix coturnix* Japonica) Diets on Productivity, Reproductive Performance, Egg Quality and Yolk Oxidative Stability. *J. Appl. Anim. Res.* 44 (1), 436–441. doi:10.1080/09712119.2015.1091337

Kawaguchi, K., Kikuchi, S.-i., Hasunuma, R., Maruyama, H., Yoshikawa, T., and Kumazawa, Y. (2004). A Citrus Flavonoid Hesperidin Suppresses Infection-Induced Endotoxin Shock in Mice. *Biol. Pharm. Bull.* 27 (5), 679–683. doi:10.1248/bpb.27.679

Kersten, S. (2017). Angiopoietin-like 3 in Lipoprotein Metabolism. *Nat. Rev. Endocrinol.* 13 (12), 731–739. doi:10.1038/nrendo.2017.119

Key, T. J. (2011). Fruit and Vegetables and Cancer Risk. *Br. J. Cancer* 104 (1), 6–11. doi:10.1038/sj.bjc.6606032

Kim, H., Hiraishi, A., Tsuchiya, K., and Sakamoto, K. (2010). (−) Epigallocatechin Gallate Suppresses the Differentiation of 3T3-L1 Preadipocytes through Transcription Factors FoxO1 and SREBP1cEpigallocatechin Gallate Suppresses the Differentiation of 3T3-L1 Preadipocytes through Transcription Factors FoxO1 and SREBP1c. *Cytotechnology* 62 (3), 245–255. doi:10.1007/s10616-010-9285-x

Kim, H. K., Jeong, T. S., Lee, M. K., Park, Y. B., and Choi, M. S. (2003). Lipid-lowering Efficacy of Hesperetin Metabolites in High-Cholesterol Fed Rats. *Clin. Chim. Acta* 327 (1-2), 129–137. doi:10.1016/s0009-8981(02)00344-3

King, A. J., Griffin, J. K., and Roslan, F. (2014). *In Vivo* and *In Vitro* Addition of Dried Olive Extract in Poultry. *J. Agric. Food Chem.* 62 (31), 7915–7919. doi:10.1021/jf4050588

Koo, S., and Noh, S. (2007). Green tea as Inhibitor of the Intestinal Absorption of Lipids: Potential Mechanism for its Lipid-Lowering Effect. *J. Nutr. Biochem.* 18 (3), 179–183. doi:10.1016/j.jnutbio.2006.12.005

Krogdahl, Å. (1985). Digestion and Absorption of Lipids in Poultry. *J. Nutr.* 115 (5), 675–685. doi:10.1093/jn/115.5.675

Kumar, R., and Singh, M. (1984). Tannins: Their Adverse Role in Ruminant Nutrition. *J. Agric. Food Chem.* 32 (3), 447–453.

Lee, B., Lee, M., Lefevre, M., and Kim, H.-R. (2014). Anthocyanins Inhibit Lipogenesis during Adipocyte Differentiation of 3T3-L1 Preadipocytes. *Plant Foods Hum. Nutr.* 69 (2), 137–141. doi:10.1007/s11130-014-0407-z

Leitzmann, C. (2016). Characteristics and Health Benefits of Phytochemicals. *Complement. Med. Res.* 23 (2), 69–74. doi:10.1159/000444063

Lesschaeve, I., and Noble, A. C. (2005). Polyphenols: Factors Influencing Their Sensory Properties and Their Effects on Food and Beverage Preferences. *Am. J. Clin. Nutr.* 81 (1), 330S–335S. doi:10.1093/ajcn/81.1.330s

Leusink, G., Rempel, H., Skura, B., Berkyto, M., White, W., Yang, Y., et al. (2010). Growth Performance, Meat Quality, and Gut Microflora of Broiler Chickens Fed with cranberry Extract. *Poult. Sci.* 89 (7), 1514–1523. doi:10.3382/ps.2009-00364

Li, Y., Fu, J., Wang, B., Wang, Y., and Shan, A. (2008). Effect of Flavones of Sea Buckthorn on Carcass Characteristics and Meat Quality of Arbor Acres Broilers. *Chin. J. Anim. Vet. Sci.* 9, 13.

Lien, T. F., Yeh, H. S., and Su, W. T. (2008). Effect of Adding Extracted Hesperetin, Naringenin and Pectin on Egg Cholesterol, Serum Traits and Antioxidant Activity in Laying Hens. *Arch. Anim. Nutr.* 62 (1), 33–43. doi:10.1080/17450390701780318

Lim, H., Yeo, E., Song, E., Chang, Y.-H., Han, B.-K., Choi, H.-J., et al. (2015). Bioconversion ofCitrus Unshiupeel Extracts with Cytolase Suppresses Adipogenic Activity in 3T3-L1 Cells. *Nutr. Res. Pract.* 9 (6), 599–605. doi:10.4162/nrp.2015.9.6.599

Liu, H. N., Liu, Y., Hu, L. L., Suo, Y. L., Zhang, L., Jin, F., et al. (2014). Effects of Dietary Supplementation of Quercetin on Performance, Egg Quality, Cecal Microflora Populations, and Antioxidant Status in Laying Hens. *Poult. Sci.* 93 (2), 347–353. doi:10.3382/ps.2013-03225

Liu, R. H., Lin, S., Zhang, P. Z., Chen, L. Y., Huang, H. L., and Mei, D. Y. (2017). Neoflavonoids and Their Pharmacological Activities in Dalbergia Genus. *Zhongguo Zhong Yao Za Zhi* 42 (24), 4707–4715. doi:10.19540/j.cnki.cjcmm.20170928.013

Liu, Y., Li, Y., Liu, H.-N., Suo, Y.-L., Hu, L.-L., Feng, X.-A., et al. (2013). Effect of Quercetin on Performance and Egg Quality during the Late Laying Period of Hens. *Br. Poult. Sci.* 54 (4), 510–514. doi:10.1080/00071668.2013.799758

Lv, Z., Xing, K., Li, G., Liu, D., and Guo, Y. (2018). Dietary Genistein Alleviates Lipid Metabolism Disorder and Inflammatory Response in Laying Hens with Fatty Liver Syndrome. *Front. Physiol.* 9, 1493. doi:10.3389/fphys.2018.01493

Ma, J. S., Chang, W. H., Liu, G. H., Zhang, S., Zheng, A. J., Li, Y., et al. (2015). Effects of Flavones of Sea Buckthorn Fruits on Growth Performance, Carcass Quality, Fat Deposition and Lipometabolism for Broilers. *Poult. Sci.* 94 (11), 2641–2649. doi:10.3382/ps/pev250

Manach, C., Mazur, A., and Scalbert, A. (2005). Polyphenols and Prevention of Cardiovascular Diseases. *Curr. Opin. Lipidol.* 16 (1), 77–84. doi:10.1097/00041433-200502000-00013

Manach, C., Scalbert, A., Morand, C., Rémésy, C., and Jiménez, L. (2004). Polyphenols: Food Sources and Bioavailability. *Am. J. Clin. Nutr.* 79 (5), 727–747. doi:10.1093/ajcn/79.5.727

McMillan, D. C., Sattar, N., Lean, M., and McArdle, C. S. (2006). Obesity and Cancer. *BMJ* 333 (7578), 1109–1111. doi:10.1136/bmj.39042.565035.be1

Nakao, Y., Yoshihara, H., and Fujimori, K. (2016). Suppression of Very Early Stage of Adipogenesis by Baicalein, a Plant-Derived Flavonoid through Reduced Akt-C/ebpα-GLUT4 Signaling-Mediated Glucose Uptake in 3T3-L1 Adipocytes. *PLoS One* 11 (9), e0163640. doi:10.1371/journal.pone.0163640

Nguyen, P., Leray, V., Diez, M., Serisier, S., Bloc'h, J. L., Siliart, B., et al. (2008). Liver Lipid Metabolism. *J. Anim. Physiol. Anim. Nutr.* 92 (3), 272–283.

Ni, Y. D., Wei, X. J., Zhang, C. X., Zhong, Y., Lu, L. Z., Grossmann, R., et al. (2012). The Effect of Equol Injection in Ovo on Lipid Metabolism and Hepatic Lipogenic Gene Expression in Broilers. *Animal* 6 (9), 1444–1450. doi:10.1017/s1751731112000468

Oelkrug, R., Polymeropoulos, E. T., and Jastroch, M. (2015). Brown Adipose Tissue: Physiological Function and Evolutionary Significance. *J. Comp. Physiol. B* 185 (6), 587–606. doi:10.1007/s00360-015-0907-7

Ogbuewu, I. P., Okoro, V. M., Mbajiorgu, E. F., and Mbajiorgu, C. A. (2019). Beneficial Effects of Garlic in Livestock and Poultry Nutrition: A Review. *Agric. Res.* 8 (4), 411–426. doi:10.1007/s40003-018-0390-y

Omri, B., Chalghoumi, R., Izzo, L., Ritieni, A., Lucarini, M., Durazzo, A., et al. (2019). Effect of Dietary Incorporation of Linseed Alone or Together with Tomato-Red Pepper Mix on Laying Hens' Egg Yolk Fatty Acids Profile and Health Lipid Indexes. *Nutrients* 11 (4). doi:10.3390/nu11040813

Ong, K. C., and Khoo, H.-E. (1996). Insulinomimetic Effects of Myricetin on Lipogenesis and Glucose Transport in Rat Adipocytes but Not Glucose Transporter Translocation. *Biochem. Pharmacol.* 51 (4), 423–429. doi:10.1016/0006-2952(95)02195-7

Oskoueian, E., Ebrahimi, M., Abdullah, N., and Goh, Y. (2013). Manipulation of Broiler Meat Fatty Acid Composition Using Quercetin. *Int. Con Meat Sci. Technol. Icomst*.

Panche, A. N., Diwan, A. D., and Chandra, S. R. (2016). Flavonoids: an Overview. *J. Nutr. Sci.* 5, e47. doi:10.1017/jns.2016.41

Park, H. J., Yang, J.-Y., Ambati, S., Della-Fera, M. A., Hausman, D. B., Rayalam, S., et al. (2008). Combined Effects of Genistein, Quercetin, and Resveratrol in Human and 3T3-L1 Adipocytes. *J. Med. Food* 11 (4), 773–783. doi:10.1089/jmf.2008.0077

Park, S., Hassan, M., Choe, H., Song, T., Park, T., Jeoh, K., et al. (2012). Effect of Two Different Types of Barley on the Performance, Meat Quality and Blood Properties of Broiler Chicken. *J. Anim. Vet. Adv.* 11 (23), 4417–4422.

Payne, R. L., Bidner, T. D., Southern, L. L., and McMillin, K. W. (2001). Dietary Effects of Soy Isoflavones on Growth and Carcass Traits of Commercial Broilers. *Poult. Sci.* 80 (8), 1201–1207. doi:10.1093/ps/80.8.1201

Peña, J., Vieira, S., López, J., Reis, R., Barros, R., Furtado, F., et al. (2008). Ascorbic Acid and Citric Flavonoids for Broilers under Heat Stress: Effects on Performance and Meat Quality. *Braz. J. Poult. Sci.* 10 (2), 125–130.

Pietta, P.-G. (2000). Flavonoids as Antioxidants. *J. Nat. Prod.* 63 (7), 1035–1042. doi:10.1021/np9904509

Pinent, M., Bladé, M. C., Salvadó, M. J., Arola, L., Hackl, H., Quackenbush, J., et al. (2005). Grape-seed Derived Procyanidins Interfere with Adipogenesis of 3T3-L1 Cells at the Onset of Differentiation. *Int. J. Obes.* 29 (8), 934–941. doi:10.1038/sj.ijo.0802988

Pirgozliev, V., Westbrook, C., Woods, S., Karagecili, M. R., Karadas, F., Rose, S. P., et al. (2018). Feeding Dihydroquercetin to Broiler Chickens. *Br. Poult. Sci.*, 1–5. doi:10.1080/00071668.2018.1556387

Puthpongsiriporn, U., Scheideler, S. E., Sell, J. L., and Beck, M. M. (2001). Effects of Vitamin E and C Supplementation on Performance, *In Vitro* Lymphocyte Proliferation, and Antioxidant Status of Laying Hens during Heat Stress. *Poult. Sci.* 80 (8), 1190–1200. doi:10.1093/ps/80.8.1190

Pym, R. A. E., and Solvyns, A. J. (1979). Selection for Food Conversion in Broilers: Body Composition of Birds Selected for Increased Body-weight Gain, Food Consumption and Food Conversion Ratio. *Br. Poult. Sci.* 20 (1), 87–97. doi:10.1080/00071667908416552

Rabie, M. H., and Szilágyi, M. (1998). Effects of L-Carnitine Supplementation of Diets Differing in Energy Levels on Performance, Abdominal Fat Content, and Yield and Composition of Edible Meat of Broilers. *Br. J. Nutr.* 80 (4), 391–400. doi:10.1017/s0007114598001457

Raederstorff, D. G., Schlachter, M. F., Elste, V., and Weber, P. (2003). Effect of EGCG on Lipid Absorption and Plasma Lipid Levels in Rats. *J. Nutr. Biochem.* 14 (6), 326–332. doi:10.1016/s0955-2863(03)00054-8

Rafiei, F., and Khajali, F. (2021). Flavonoid Antioxidants in Chicken Meat Production: Potential Application and Future Trends. *World's Poult. Sci. J.* 77 (2), 347–361. doi:10.1080/00439339.2021.1891401

Rayalam, S., Dellafera, M., and Baile, C. (2008). Phytochemicals and Regulation of the Adipocyte Life Cycle☆. *J. Nutr. Biochem.* 19 (11), 717–726. doi:10.1016/j.jnutbio.2007.12.007

Reue, K. (2011). A Thematic Review Series: Lipid Droplet Storage and Metabolism: from Yeast to Man. *J. lipid Res.* 52 (11), 1865–1868. doi:10.1194/jlr.e020602

Roy, D. M., and Schneeman, B. O. (1981). Effect of Soy Protein, Casein and Trypsin Inhibitor on Cholesterol, Bile Acids and Pancreatic Enzymes in Mice. *J. Nutr.* 111 (5), 878–885. doi:10.1093/jn/111.5.878

Roztočilová, A., Šťastník, O., Mrkvicova, E., and Pavlata, L. (2018). Effect of Purple Wheat RU 687-12 on Performance Parameters of Laying Hens at the End of the Day. *NutriNET Proc. reviewed scientific Pap.*, 92–97.

Stastnik, O., Karasek, F., Roztocilova, A., Dolezal, P., Mrkvicova, E., and Pavlata, L. (2014). The Influence of Feeding Wheat with Purple Grain to Performance and Biochemical Parameters of Broiler Chickens. In: Proceedings of the International Ph d Students Conference on Mendelnet.

Saarela, S., Keith, J. S., Hohtola, E., and Trayhurn, P. (1991). Is the "Mammalian" Brown Fat-specific Mitochondrial Uncoupling Protein Present in Adipose Tissues of Birds? *Comp. Biochem. Physiol. B: Comp. Biochem.* 100 (1), 45–49.

Saeed, M., Babazadeh, D., Arif, M., Arain, M. A., Bhutto, Z. A., Shar, A. H., et al. (2017). Silymarin: a Potent Hepatoprotective Agent in Poultry Industry. *World's Poult. Sci. J.* 73 (3), 483–492. doi:10.1017/s0043933917000538

Saeed, M., Naveed, M., Arain, M. A., Arif, M., Abd El-Hack, M. E., Alagawany, M., et al. (2017). Quercetin: Nutritional and Beneficial Effects in Poultry. *World's Poult. Sci. J.* 73 (2), 355–364. doi:10.1017/s004393391700023x

Sahin, N., Onderci, M., Balci, T. A., Cikim, G., Sahin, K., and Kucuk, O. (2007). The Effect of Soy Isoflavones on Egg Quality and Bone Mineralisation during the Late Laying Period of Quail. *Br. Poult. Sci.* 48 (3), 363–369. doi:10.1080/00071660701341971

Sahin, N., Orhan, C., Tuzcu, M., Sahin, K., and Kucuk, O. (2008). The Effects of Tomato Powder Supplementation on Performance and Lipid Peroxidation in Quail. *Poult. Sci.* 87 (2), 276–283. doi:10.3382/ps.2007-00207

Saito, T., Abe, D., and Sekiya, K. (2009). Flavanone Exhibits PPARγ Ligand Activity and Enhances Differentiation of 3T3-L1 Adipocytes. *Biochem. Biophysical Res. Commun.* 380 (2), 281–285. doi:10.1016/j.bbrc.2009.01.058

Sakuma, S., Sumida, M., Endoh, Y., Kurita, A., Yamaguchi, A., Watanabe, T., et al. (2017). Curcumin Inhibits Adipogenesis Induced by Benzyl Butyl Phthalate in 3T3-L1 Cells. *Toxicol. Appl. Pharmacol.* 329, 158–164. doi:10.1016/j.taap.2017.05.036

Salunkhe, D. (1982). Legumes in Human Nutrition: Current Status and Future Research Needs. *Curr. Sci.* 51 (8), 387–394.

Salunkhe, D. K., Jadhav, S. J., Kadam, S. S., and Chavan, J. K. (1982). Chemical, Biochemical, and Biological Significance of Polyphenols in Cereals and Legumes. *Crit. Rev. Food Sci. Nutr.* 17 (3), 277–305. doi:10.1080/10408398209527350

Santamarina, A. B., Jamar, G., Mennitti, L. V., Cesar, H. d. C., Vasconcelos, J. R., Oyama, L. M., et al. (2020). Obesity-related Inflammatory Modulation by Juçara berry (Euterpe Edulis Mart.) Supplementation in Brazilian Adults: a Double-Blind Randomized Controlled Trial. *Eur. J. Nutr.* 59 (4), 1693–1705. doi:10.1007/s00394-019-02024-2

Santarelli, R. L., Vendeuvre, J.-L., Naud, N., Taché, S., Guéraud, F., Viau, M., et al. (2010). Meat Processing and colon Carcinogenesis: Cooked, Nitrite-Treated, and Oxidized High-Heme Cured Meat Promotes Mucin-Depleted Foci in Rats. *Cancer Prev. Res.* 3 (7), 852–864. doi:10.1158/1940-6207.capr-09-0160

Seo, M.-J., Choi, H.-S., Jeon, H.-J., Woo, M.-S., and Lee, B.-Y. (2014). Baicalein Inhibits Lipid Accumulation by Regulating Early Adipogenesis and M-TOR Signaling. *Food Chem. Toxicol.* 67, 57–64. doi:10.1016/j.fct.2014.02.009

Shomali, T., Mosleh, N., and Nazifi, S. (2012). Two Weeks of Dietary Supplementation with green tea Powder Does Not Affect Performance, D-Xylose Absorption, and Selected Serum Parameters in Broiler Chickens. *Comp. Clin. Pathol.* 21 (5), 1023–1027. doi:10.1007/s00580-011-1220-9

Silva, R. R. d., Oliveira, T. T. d., Nagem, T. J., and Leão, M. A. (2002). Efeito de flavonóides no metabolismo Do ácido araquidônico. *Medicina (Ribeirão Preto)* 35, 127–133. doi:10.11606/issn.2176-7262.v35i2p127-133

Silveira, J. Q., Dourado, G. K. Z. S., and Cesar, T. B. (2015). Red-fleshed Sweet orange Juice Improves the Risk Factors for Metabolic Syndrome. *Int. J. Food Sci. Nutr.* 66 (7), 830–836. doi:10.3109/09637486.2015.1093610

Sivamaruthi, B. S., Kesika, P., and Chaiyasut, C. (2020). The Influence of Supplementation of Anthocyanins on Obesity-Associated Comorbidities: A Concise Review. *Foods* 9 (6). doi:10.3390/foods9060687

Sohaib, M., Butt, M. S., Shabbir, M. A., and Shahid, M. (2015). Lipid Stability, Antioxidant Potential and Fatty Acid Composition of Broilers Breast Meat as Influenced by Quercetin in Combination with α-tocopherol Enriched Diets. *Lipids Health Dis.* 14, 61. doi:10.1186/s12944-015-0058-6

Stastnik, O., Karasek, F., Roztocilova, A., Dolezal, P., Mrkvicova, E., and Pavlata, L. (2016). The Influence of Feeding Wheat with Purple Grain to Performance and Biochemical Parameters of Broiler Chickens. In: International PhD Students Conference on MendelNet.

Stastnik, O., Mrkvicova, E., Karasek, F., Trojan, V., Vyhnanek, T., Hrivna, L., et al. (2014). The Influence of Colored Wheat Feeding on Broiler Chickens Performance Parameters. In: Proceeding of the International PhD Student Conference MendelNet. 196–198.

Steensma, A., Faassen-Peters, M. A. W., Noteborn, H. P. J. M., and Rietjens, I. M. C. M. (2006). Bioavailability of Genistein and its Glycoside Genistin as Measured in the Portal Vein of Freely Moving Unanesthetized Rats. *J. Agric. Food Chem.* 54 (21), 8006–8012. doi:10.1021/jf060783t

S.Ting, S., Yeh, H. S., and Lien, T. F. (2011). Effects of Supplemental Levels of Hesperetin and Naringenin on Egg Quality, Serum Traits and Antioxidant Activity of Laying Hens. *Anim. Feed Sci. Technology* 163 (1), 59–66. doi:10.1016/j.anifeedsci.2010.10.001

Sunil, C., and Xu, B. (2019). An Insight into the Health-Promoting Effects of Taxifolin (Dihydroquercetin). *Phytochemistry* 166, 112066. doi:10.1016/j.phytochem.2019.112066

Theriault, A., Wang, Q., Van Iderstine, S. C., Chen, B., Franke, A. A., and Adeli, K. (2000). Modulation of Hepatic Lipoprotein Synthesis and Secretion by

Taxifolin, a Plant Flavonoid. *J. Lipid Res.* 41 (12), 1969–1979. doi:10.1016/s0022-2275(20)32358-0

Thilakarathna, S., and Rupasinghe, H. (2013). Flavonoid Bioavailability and Attempts for Bioavailability Enhancement. *Nutrients* 5 (9), 3367–3387. doi:10.3390/nu5093367

Tsuda, T., Ueno, Y., Yoshikawa, T., Kojo, H., and Osawa, T. (2006). Microarray Profiling of Gene Expression in Human Adipocytes in Response to Anthocyanins. *Biochem. Pharmacol.* 71 (8), 1184–1197. doi:10.1016/j.bcp.2005.12.042

Tůmová, E., and Teimouri, A. (2010). Fat Deposition in the Broiler Chicken: a Review. *Scientia Agriculturae Bohemica* 41 (2), 121–128.

Vaidya, H. B., and Goyal, R. K. (2010). Exploring Newer Target Sodium Glucose Transporter 2 for the Treatment of Diabetes Mellitus. *Mrmc* 10 (10), 905–913. doi:10.2174/138955710792007213

Varga, T., Czimmerer, Z., and Nagy, L. (2011). PPARs Are a Unique Set of Fatty Acid Regulated Transcription Factors Controlling Both Lipid Metabolism and Inflammation. *Biochim. Biophys. Acta (Bba) - Mol. Basis Dis.* 1812 (8), 1007–1022. doi:10.1016/j.bbadis.2011.02.014

Wang, S. Z., Hu, X. X., Wang, Z. P., Li, X. C., Wang, Q. G., Wang, Y. X., et al. (2012). Quantitative Trait Loci Associated with Body Weight and Abdominal Fat Traits on Chicken Chromosomes 3, 5 and 7. *Genet. Mol. Res.* 11 (2), 956–965. doi:10.4238/2012.april.19.1

Wei, X. J., Ni, Y. D., Lu, L. Z., Grossmann, R., and Zhao, R. Q. (2011). The Effect of Equol Injection in Ovo on Posthatch Growth, Meat Quality and Antioxidation in Broilers. *Animal* 5 (2), 320–327. doi:10.1017/s1751731110001771

Wilson, S. B., Back, D. W., Morris, S. M., Jr., Swierczynski, J., and Goodridge, A. G. (1986). Hormonal Regulation of Lipogenic Enzymes in Chick Embryo Hepatocytes in Culture. Expression of the Fatty Acid Synthase Gene Is Regulated at Both Translational and Pretranslational Steps. *J. Biol. Chem.* 261 (32), 15179–15182. doi:10.1016/s0021-9258(18)66849-8

Wolfram, S., Wang, Y., and Thielecke, F. (2006). Anti-obesity Effects of green tea: from Bedside to Bench. *Mol. Nutr. Food Res.* 50 (2), 176–187. doi:10.1002/mnfr.200500102

Wu, T., Jiang, Z., Yin, J., Long, H., and Zheng, X. (2016). Anti-obesity Effects of Artificial Planting Blueberry (Vaccinium Ashei) Anthocyanin in High-Fat Diet-Treated Mice. *Int. J. Food Sci. Nutr.* 67 (3), 257–264. doi:10.3109/09637486.2016.1146235

Xiao, H.-B., Fang, J., Lu, X.-Y., and Sun, Z.-L. (2012). Kaempferol Improves Carcase Characteristics in Broiler Chickens by regulatingANGPTL3gene Expression. *Br. Poult. Sci.* 53 (6), 836–842. doi:10.1080/00071668.2012.751486

Xiao, Y., Halter, B., Boyer, C., Cline, M. A., Liu, D., and Gilbert, E. R. (2021). Dietary Supplementation of Baicalein Affects Gene Expression in Broiler Adipose Tissue during the First Week Post-hatch. *Front. Physiol.* 12, 697384. doi:10.3389/fphys.2021.697384

Xing, J., Kang, L., Hu, Y., Xu, Q., Zhang, N., and Jiang, Y. (2009). Effect of Dietary Betaine Supplementation on mRNA Expression and Promoter CpG Methylation of Lipoprotein Lipase Gene in Laying Hens. *J. Poult. Sci.* 46 (3), 224–228. doi:10.2141/jpsa.46.224

Yamane, T., Goto, H., Takahashi, D., TakedA, H., Otowaki, K., and Tsuchida, T. (1999). Effects of Hot Water Extracts of tea on Performance of Laying Hens. *Jpn. Poult. Sci.* 36 (1), 31–37. doi:10.2141/jpsa.36.31

Yang, C. J., Yang, I. Y., Oh, D. H., Bae, I. H., Cho, S. G., Kong, I. G., et al. (2003). Effect of green tea By-Product on Performance and Body Composition in Broiler Chicks. *Asian Australas. J. Anim. Sci.* 16 (6), 867–872. doi:10.5713/ajas.2003.867

Yoshida, H., Takamura, N., Shuto, T., Ogata, K., Tokunaga, J., Kawai, K., et al. (2010). The Citrus Flavonoids Hesperetin and Naringenin Block the Lipolytic Actions of TNF-α in Mouse Adipocytes. *Biochem. Biophysical Res. Commun.* 394 (3), 728–732. doi:10.1016/j.bbrc.2010.03.060

Yousaf, S., Butt, M. S., Suleria, H. A. R., and Iqbal, M. J. (2014). The Role of green tea Extract and Powder in Mitigating Metabolic Syndromes with Special Reference to Hyperglycemia and Hypercholesterolemia. *Food Funct.* 5 (3), 545–556. doi:10.1039/c3fo60203f

Zhang, X. Y., Wu, M. Q., Wang, S. Z., Zhang, H., Du, Z. Q., Li, Y. M., et al. (2018). Genetic Selection on Abdominal Fat Content Alters the Reproductive Performance of Broilers. *Animal* 12 (6), 1232–1241. doi:10.1017/s1751731117002658

Zhang, Y., Shi, G., Cai, J., Yang, J., Zheng, Y., Yu, D., et al. (2019). Taxifolin Alleviates Apoptotic Injury Induced by DEHP Exposure through Cytochrome P450 Homeostasis in Chicken Cardiomyocytes. *Ecotoxicology Environ. Saf.* 183, 109582. doi:10.1016/j.ecoenv.2019.109582

Zhao, Y., Huang, W., Wang, J., Chen, Y., Huang, W., and Zhu, Y. (2018). Taxifolin Attenuates Diabetic Nephropathy in Streptozotocin-Induced Diabetic Rats. *Am. J. Transl Res.* 10 (4), 1205–1210.

Zheng, C.-D., Duan, Y.-Q., Gao, J.-M., and Ruan, Z.-G. (2010). Screening for Anti-lipase Properties of 37 Traditional Chinese Medicinal Herbs. *J. Chin. Med. Assoc.* 73 (6), 319–324. doi:10.1016/s1726-4901(10)70068-x

Zhou, Y., Wan, X., Hu, J., Shao, L., and Shang, Y. (2012). Effect of green tea and tea Catechins on the Lipid Metabolism of Caged Laying Hens. *Indian J. Anim. Sci.* 82 (11), 1408–1414.

Zhou, Y., Mao, S., and Zhou, M. (2019). Effect of the Flavonoid Baicalein as a Feed Additive on the Growth Performance, Immunity, and Antioxidant Capacity of Broiler Chickens. *Poult. Sci.* 98 (7), 2790–2799. doi:10.3382/ps/pez071

Conflict of Interest: The authors declare that the research was conducted in the absence of any commercial or financial relationships that could be construed as a potential conflict of interest.

Publisher's Note: All claims expressed in this article are solely those of the authors and do not necessarily represent those of their affiliated organizations, or those of the publisher, the editors, and the reviewers. Any product that may be evaluated in this article, or claim that may be made by its manufacturer, is not guaranteed or endorsed by the publisher.

frontiers | Frontiers in Physiology

ORIGINAL RESEARCH
published: 20 May 2022
doi: 10.3389/fphys.2022.862721

Interaction Between Cecal Metabolites and Liver Lipid Metabolism Pathways During Induced Molting in Laying Hens

Jun Zhang[1,2], *Xiaoqing Geng*[1,2], *Yihui Zhang*[1,2], *Xinlong Zhao*[1,2], *Pengwei Zhang*[1,2], *Guirong Sun*[1,2], *Wenting Li*[1,2], *Donghua Li*[1,2], *Ruili Han*[1,2], *Guoxi Li*[1,2], *Yadong Tian*[1,2], *Xiaojun Liu*[1,2], *Xiangtao Kang*[1,2] *and Ruirui Jiang*[1,2]*

[1]College of Animal Science and Technology, Henan Agricultural University, Zhengzhou, China, [2]Henan Innovative Engineering Research Center of Poultry Germplasm Resource, Henan Agricultural University, Zhengzhou, China

Moult is a normal physiological phenomenon in poultry. Induced molting (IM) is the most widely used and economical molting technique. By inducing moult, the laying hens can grow new feathers during the next laying cycle and improve laying performance. However, the lack of energy supply has a huge impact on both the liver and intestines and acts on the intestines and liver through the "gut-liver axis". More importantly, lipid metabolism in the liver is closely related to the laying performance of laying hens. Therefore, in this study, cecal metabolites and liver transcriptome data during IM of laying hens at the late stage of laying (stop feeding method) were analyzed together to reveal the regulatory mechanism of "gut-liver axis" affecting the laying performance of laying hens from the perspective of lipid metabolism. Transcriptome analysis revealed that 4,796 genes were obtained, among which 2,784 genes had significant differences ($p < 0.05$). Forty-nine genes were associated with lipid metabolism, and five core genes (*AGPAT2*, *SGPL1*, *SPTLC1*, *PISD*, and *CYP51A1*) were identified by WGCNA. Most of these differential genes are enriched in steroid biosynthesis, cholesterol metabolism, drug metabolism—cytochrome P450, synthesis and degradation of ketone bodies, PPAR signaling pathway, and bile secretion. A total of 96 differential metabolites were obtained by correlating them with metabolome data. Induced moult affects laying performance by regulating genes related to lipid metabolism, and the cecal metabolites associated with these genes are likely to regulate the expression of these genes through the "enterohepatic circulation". This experiment enriched the theoretical basis of induced moult and provided the basis for prolonging the feeding cycle of laying hens.

Keywords: induced molting, lipid metabolism, liver, cecum, hens

OPEN ACCESS

Edited by:
Jie Wen,
Institute of Animal Sciences (CAAS), China

Reviewed by:
Ruiqiang Zhang,
Zhejiang A&F University, China
Davina Derous,
University of Aberdeen, United Kingdom

***Correspondence:**
Ruirui Jiang
jrrcaas@163.com

Specialty section:
This article was submitted to Avian Physiology, a section of the journal Frontiers in Physiology

Received: *26 January 2022*
Accepted: *23 March 2022*
Published: *20 May 2022*

Citation:
Zhang J, Geng X, Zhang Y, Zhao X, Zhang P, Sun G, Li W, Li D, Han R, Li G, Tian Y, Liu X, Kang X and Jiang R (2022) Interaction Between Cecal Metabolites and Liver Lipid Metabolism Pathways During Induced Molting in Laying Hens. Front. Physiol. 13:862721. doi: 10.3389/fphys.2022.862721

1 INTRODUCTION

Molting is a natural physiological phenomenon of birds in response to seasonal changes (Abg, 2008). During molting, the ovaries deteriorate and estrogen production decreases, resulting in reduced laying capacity and egg production (Brake, 1993). Natural molting generally needs 4 months and lasts a long time without uniform production time, which seriously affects the economic benefits of operators (Belland, 2003). However, Induced molting (IM) can shorten the molting time,

synchronize egg production, save breeding costs, and improve egg production performance in the next cycle (Breeding et al., 1992; Alodan and Mashaly, 1999; Berry, 2003; Sandhu et al., 2007).

IM refers to the intense and sudden stress response caused by humans to chickens, resulting in nutritional disorders, metabolic disorders, endocrine disorders, and promoting the rapid molting of chickens to resume egg production (Zhang, 2021). There are many ways to force molting, but fasting is the most popular because it is simple and less expensive (Onbaşılar and Erol, 2007).

Studies have shown that when nutrients are deprived, the body's glucose is initially provided from the stores of glycogen, but glycogen is quickly depleted (Furchtgott et al., 2009). If fasting continues, fatty acids become the main source of energy. Lipids break down the produced and released non-esterified fatty acids (NEFAs) and glycerol. NEFAs are oxidized to ketone bodies (ketogenesis) in the liver mitochondria through fatty acid D. Glucose and ketone bodies produced by the liver are the main metabolites of extrahepatic tissues and organs during starvation and exercise (Li et al., 2001; Arai et al., 2003).

During fasting, the gut, as an important place for digestion and nutrient absorption (Dou et al., 2002), loses the supply of nutrients and energy, and then the morphological and physiological characteristics of the gut and the homeostasis of intestinal microbes are greatly changed (Michalsen et al., 2005; Kohl et al., 2014; Gebert et al., 2020), which directly or indirectly affects the health and production performance of animals (Ferraris and Carey, 2000). There are a large number and a wide variety of microbial communities in the gastrointestinal tract of poultry, and the cecum is an important place for the survival and activity of microorganisms in the digestive tract of poultry (Zhen, 2019). The cecum is in an anerobic environment for a prolonged period, making it a fermenter for some anerobic bacteria, so it has the function of preventing the colonization of pathogenic bacteria and promoting intestinal health (Gérard, 2008).

Unlike mammals, lipid metabolism in poultry takes place mainly in the liver (Butler, 1975; Szabo et al., 2005). Although poultry adipose tissue can also esterify a small amount of fatty acids into triglycerides, it is not the main tissue of poultry triglyceride (TG) production (Leveille et al., 1975; Brady et al., 1976; Bedu et al., 2002). In order to meet the high demand for TG and cholesterol during laying, the liver of laying hens is particularly active in fat synthesis (Klasing, 1998) because yolk formation requires the transport of large amounts of hepatic lipoproteins to the developing oocytes of laying hens, whereas the ovaries of laying hens do not synthesize lipids. Fasting reduces fat production in the liver, cutting off the oocyte's fat source.

With the development of multi-omics, transcriptome has been widely used in genetic breeding and nutritional regulation of chicken (Li et al., 2013; Li et al., 2018; Wang, 2019; As, 2021; Luo et al., 2021), however, few researchers have focused on lipid metabolism during IM. On the one hand, numerous studies have shown that intermittent fasting benefits human and animal health through lipid metabolism, significantly improving fatty liver and non-alcoholic fatty liver disease (David, 2014; Patterson et al., 2015). The gut and liver, on the other hand, are closely related in embryonic origin and anatomy and interact through the "gut-liver axis" (Compare et al., 2012; Paolella, 2014; Hussain et al., 2020). Therefore, based on the existing studies, this study analyzed the liver transcriptome and cecal metabolome of laying hens and revealed the interaction between the changes of cecal metabolites induced by hunger and liver lipid metabolism, and the effect of intestinal microbes on the laying performance of laying hens during IM. More importantly, it provides a theoretical reference for the study of IM.

2 MATERIALS AND METHODS

2.1 Experimental Animals and Sampling

Ninety lady chickens at the late stage of laying (500 days of age) were selected and divided into nine replicates with 10 chickens in each replicate. According to the compulsory molting procedure, using the timeline as a control, there are six key time points in this experiment (**Table 1**, namely, F0 (on the day before the first day of feed breaking); F3 (on the third day of feed breaking); F16 (on the 16th day of feed breaking); R6 (on the sixth day of feed resuming); R16 (on the 16th day of feed resuming); and R32 (on the 32nd day of feed resuming). The samples (liver tissue samples and cecal contents) were collected at each treatment period, and sequencing of the liver transcriptome and cecal contents metabolome was commissioned by Gene Denovo Biotechnology Co., Ltd., Guangzhou.

2.2 Transcriptome Analysis

2.2.1 RNA Extraction, cDNA Library Construction, and Sequencing

Total RNA was extracted using a TRIzol reagent kit (Invitrogen, Carlsbad, CA, United States) according to the manufacturer's protocol. RNA quality was assessed on an Agilent 2,100 Bioanalyzer (Agilent Technologies, Palo Alto, CA, United States) and checked using RNase-free agarose gel electrophoresis. After total RNA was extracted, eukaryotic mRNA was enriched by oligo (dT) beads, while prokaryotic mRNA was enriched by removing rRNA by the Ribo-ZeroTM Magnetic Kit (Epicentre, Madison, WI, United States). Then, the enriched mRNA was fragmented into short fragments using fragmentation buffer and reverse-transcripted onto cDNA with random primers. Second-strand cDNA was synthesized by DNA polymerase I, RNase H, dNTP, and buffer. Then, the cDNA fragments were purified with a QiaQuick PCR extraction kit (Qiagen, Venlo, Netherlands), end-repaired, poly(A) added, and ligated to Illumina sequencing adapters. The ligation products were size-selected by agarose gel electrophoresis, PCR-amplified, and sequenced using Illumina HiSeq2500 by Gene Denovo Biotechnology Co. (Guangzhou, China).

2.2.2 Filtering of Clean Reads, Alignment With the Reference Genome, and DEG Analysis

Reads obtained from the sequencer contain adapters or raw reads of low-quality base, which will affect subsequent assembly and analysis. Therefore, for clean reads of high quality, reads that contain the adapter should be removed; reads (N) containing more than 10% unknown nucleotides were removed; low-quality reads containing more than 50% of low-quality ($Q \leq 20$) bases were removed (Chen et al., 2018). The short fragment comparison tool Bowtie2 (Version

TABLE 1 | IM program induced by starvation.

Test period	Treatment			
	Feed	Water	Light	Processing time for each stage
F0	Normal feed	√	16 h	On the day before the test
F3	No feed	×	8 h	On the third day of fasting
F16	No feed	√	10 h	On the 16th day of fasting
R6	Gradually resuming feeding	√	10 h + 0.5 h per day	On the sixth day of recovery
R16		√		On the 16th day of recovery
R32	Normal feed	√	16 h	On the 30th day of recovery

2.2.8) was used to compare short fragments to the ribosomal RNA (rRNA) database. The rRNA mapping read is then removed. The remaining clean reads are further used for assembly and gene abundance calculation. To establish the reference index of the genome and using HISAT2-2.2.4 to clean reads mapped to a reference genome (https://www.ncbi.nlm.nih.gov/assembly/GCF_000002315.6), the other parameter is set to the default. Then, RNA differential expression analysis was performed by DESeq2 (Love et al., 2014) software between two different groups (and by edgeR (Smyth, 2010) between two samples). The genes/transcripts with the parameter of false discovery rate (FDR) below 0.05 and an absolute fold change ≥2 were considered differentially expressed genes/transcripts.

2.2.3 Gene Ontology and Kyoto Encyclopedia of Genes and Genomes Enrichment

Gene Ontology (GO) (Ashburner, 2000) is an international standardized gene functional classification system that offers a dynamic-updated controlled vocabulary and a strictly defined concept to comprehensively describe the properties of genes and their products in any organism. GO has three ontologies: molecular function, cellular component, and biological process. Genes usually interact with each other to play roles in certain biological functions. Pathway-based analysis helps further understand gene biological functions. Kyoto Encyclopedia of Genes and Genomes (KEGG) (Marisa, 2013) is the major public pathway-related database. Pathway enrichment analysis identified significantly enriched metabolic pathways or signal transduction pathways in DEGs compared with the whole genome background.

2.2.4 Weighted Gene Co-Expression Network Analysis Analysis

WGCNA (weighted gene co-expression network analysis) is a systems biology method for describing the correlation patterns among genes across multiple samples. This method finds clusters (modules) of highly correlated genes and relates modules to external sample traits. The gene co-expression network was constructed using the R package WGCNA (Shannon et al., 2003) to identify modules of highly correlated genes based on the filtering data (mean expression level ≥1 and coefficient of variation ≥0.1). The core co-expression modules were visualized using Cytoscape_v3.8.2.

2.3 Metabolome Analysis

2.3.1 Extraction and Detection of Metabolites

First, the samples were freeze-dried in accordance with the same proportion. Then, 1000 uL methanol (−20°C) redissolved lyophilized powder was transferred to a 2-ml centrifuge tube, followed by vortex oscillation for 1 min, and centrifugation at 12,000 rpm at 4°C for 10 min. 450 μL of the supernatant was taken in a 2-ml centrifuge tube and concentrated by a vacuum concentrator until dry. Then, 20 μL was taken from each sample to be tested and mixed into QC samples (QC: quality control, used to correct the deviation of the analysis result of the mixed sample and the error caused by the analysis instrument itself), and the remaining samples were used to be tested for LC-MS detection (Zelena et al., 2009; Dunn et al., 2018).

In chromatographic tests, chromatographic separation was accomplished in a Thermo Ultimate 3,000 system equipped with an ACQUITY UPLC® HSS T3 (150 × 2.1 mm, 1.8 μm, Waters) column maintained at 40°C. The temperature of the autosampler was 8°C. Gradient elution of analytes was carried out with (A) 0.1% formic acid in water and (B) 0.1% formic acid in acetonitrile or (C) 5 mM ammonium formate in water and (D) acetonitrile at a flow rate of 0.25 ml/min. Injection of 2 μL of each sample was administered after equilibration. An increasing linear gradient of solvent B (v/v) was used as follows: 0–1 min, 2% B/D; 1–9 min, 2–50% B/D; 9–12 min, 50–98% B/D; 12–13.5 min, 98% B/D; 13.5–14 min, 98–2% B/D; 14–20 min, 2% D-positive model (14–17 min, 2% B-negative model).

In mass spectrometry, the ESI-MSn experiments were executed on the Thermo Q Exactive mass spectrometer with the spray voltage of 3.8 kV and −2.5 kV in positive and negative modes, respectively. The sheath gas and auxiliary gas were set at 30 and 10 arbitrary units, respectively. The capillary temperature was 325°C. The analyzer scanned over a mass range of m/z 81-1 000 for a full scan at a mass resolution of 70,000. Data-dependent acquisition (DDA) MS/MS experiments were performed with an HCD scan. The normalized collision energy was 30 eV. Dynamic exclusion was implemented to remove some unnecessary information in MS/MS spectra.

2.3.2 Data Processing and Metabolite Identification

The format of raw data files was converted into mzXML format using Proteowizard (v3.0.8789). Using R (v3.3.2) package XCMS (Want, 2006) to perform peak identification, peak filtration, peak alignment for each metabolite, the main parameters were set as

follows: bw = 5, ppm = 15, peak width = c (5, 30), mzwid = 0.01, mzdiff = 0.01, method = "centWave". Then, mass-to-charge ratio (m/z), retention time and intensity, and positive and negative precursor molecules were used for subsequent analysis. The peak intensities were batch-normalized to the total spectral intensity. The identification of metabolites is based on the exact molecular formula (molecular formula error <20 ppm). Then, peaks were matched with the Metlin (http://metlin.scripps.edu) and MoNA(https://mona.fiehnlab.ucdavis.edu//) to confirm annotations for metabolites.

2.4 Trend Analysis

Genes and metabolites expression pattern analysis is used to cluster metabolites of similar expression patterns for multiple samples (at least three in a specific time point, space, or treatment dose size order). To examine the expression pattern of all annotated genes and metabolites, the expression data of each sample (in the order of treatment) were normalized to 0, log2 (v1/v0), and log2 (v2/v0) and then clustered by Short Time-series Expression Miner software (STEM, version 1.3.11) (Ernst and Bar-Joseph, 2006).

The parameters were set as follows:

1) Maximum unit change in model profiles between time points is 1;
2) Maximum output profile number is 20 (similar profiles will be merged).
3) Minimum ratio of the fold change of DEGs is no less than 2.0.

The clustered profiles with a p-value ≤ 0.05 were considered significant profiles. Then, the genes and metabolites in all or each profile were subjected to KEGG pathway enrichment analysis. Through the hypothesis test of the p-value calculation and FDR (Benjamini and Hochberg, 1995) correction, the pathways with Q_value ≤ 0.05 were defined as significantly enriched pathways.

2.5 Integrated Analysis of the Transcriptome and Metabolome

Transcriptome and metabolome data were used to characterize the differences in gene expression and metabolite levels (Bylesjö et al., 2010). However, transcription and metabolism do not occur independently in biological systems. In order to reveal the regulatory influence mechanism between gene expression and metabolites during starvation-induced IM, the association analysis was carried out based on the same or similar change rules of genes or metabolites involved in the same biological process (Csardi and Nepusz, 2006; Kolde, 2015; Bouhaddani et al., 2016). The co-expression network between differential genes and metabolites in lipid metabolism was constructed using Cytoscape_v3.8.2.

3 RESULTS

3.1 Transcriptome Analysis of the Liver of Laying Hens

In this study, we established 18 cDNA libraries with the following designations, RNA-seq generated 44, 786, and 614 to 95, 424, and 152 raw reads for each library. After filtering the low-quality reads, the average number of clean reads was 48, 911, and 475 (99.37%); 69,071, and 206 (99.40%); 62, 071, and 382 (99.40%); 55, 411, and 170 (99.36%); 55, 481, and 584 (99.28%); and 49, 951, and 232 (99.34%) for the F0F0, F3F3, F16F16, R6R6, R16R16, and R32R32 groups, respectively (**Supplementary Table S1**). The clean reads were used for all further analyses, and from them 91.51–92.91% of clean tags from the RNA-seq data mapped uniquely to the genome, while a small proportion of them (<2.93%) were mapped multiple times to the genome (**Supplementary Table S2**).

To demonstrate the source of variance in our data, PCA analysis with two principal components (PC1 and 2) was performed. As shown in **Figure 1A**, PC score plots showed that the contribution of PC1 and 2 was 84.5% and 7.5%, respectively. The three individual samples collected at each time point were clustered closely together which validated the finding of low variance in the present analysis study and showed that the data could be used for the following analysis.

3.2 Differential Gene Expression in the Liver at Different Stages

FPKM was used to estimate the level of gene expression, and DEGSeq was used to examine the differential gene expression profile. The results showed that F0-VS-R32 and R16-VS-R32 had fewer differentially expressed genes, while F0-VS-F16, F0-VS-R6, F16-VS-R32, and R6-VS-R32 groups had more differentially expressed genes. Therefore, in order to further explore the dynamic gene expression pattern during the IM of laying hens, we conducted a study on DEGs in the F0-VS-F16, F0-VS-R6, F16-VS-R32, and R6-VS-R32 groups (**Figure 1B**). The Venn diagram shows the distribution of DEGs in the liver into four groups with 479 genes shared among the four groups (**Figures 1C–F**).

3.3 Gene Ontology Enrichment and Kyoto Encyclopedia of Genes and Genomes Pathway Analysis of DEGs Among the Four Groups

All DEGs in the four groups (F0-VS-F16, F0-VS-R6, F16-VS-R32, and R6-VS-R32) were analyzed using GO term enrichment and KEGG pathway. To investigate the significant pathways and related biological functions of DEGs during IM.

In our study, a total of 1722 DEGs from the F0-vs-F16 group in the liver were used for GO term enrichment (**Supplementary Figure S1**) and KEGG analyses (**Figure 2A**). We selected ten pathways ($p < 0.05$) from GO and KEGG and analyzed them. The GO term was mainly enriched in some pathways related to lipid metabolism, such as lipid metabolic process, lipid localization, lipid homeostasis, lipid biosynthetic process, sterol metabolic process, cholesterol homeostasis, sterol homeostasis, cholesterol metabolic process, and lipid transport. In addition, it was also enriched in the cellular response to chemical stimuli. KEGG was also enriched in some pathways related to lipid metabolism, such as steroid biosynthesis, cholesterol

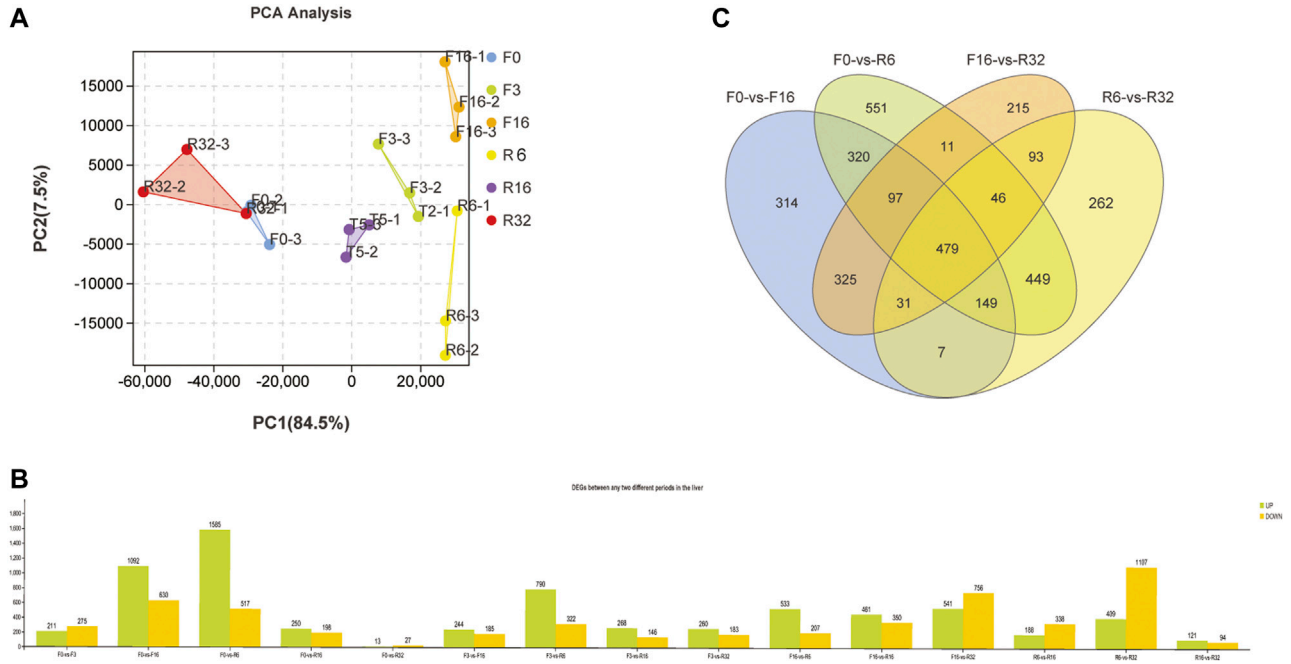

FIGURE 1 | Transcriptome analysis of the liver in six periods during IM. **(A)** PCA analysis was used to understand the repeatability of samples in each period of IM. **(B)** Overall statistics of significantly different genes in each comparison group: green represents upregulation; yellow represents downregulation. **(C)** Difference Venn diagram of the relative comparison group.

metabolism, synthesis, and degradation of ketone bodies. In addition, there were also important pathways such as the PPAR signaling pathway, drug metabolism—other enzymes, and bile secretion.

In the F0-vs-R6 group, a total of 2,102 DEGs in the liver were used to perform GO term (**Supplementary Figure S2**) and KEGG pathway analyses (**Figure 2B**). GO terms ($p < 0.05$) were enriched in cellular response to chemical stimulus, immune system process, and cytokine production, and KEGG was mainly enriched in cholesterol metabolism; valine, leucine, and isoleucine degradation; metabolic pathways; and proteoglycans in cancer.

A total of 1,297 DEGs from the liver of the F16-vs-R32 group were used to perform GO term (**Supplementary Figure S3**). and KEGG pathway analyses (**Figure 2C**). In GO term ($p < 0.05$), most pathways were related to lipid metabolism, including the lipid metabolic process, sterol metabolic process, lipid biosynthetic process, and lipid homeostasis. In addition, there were immune-related pathways, such as the immune system process and regulation of immune system process. The significant KEGG pathways were chemical carcinogenesis, drug metabolism—cytochrome P450, metabolism of xenobiotics by cytochrome P450, cholesterol metabolism, steroid biosynthesis, synthesis, and degradation of ketone bodies.

In the R6-vs-R32 group, the DEGs are mainly enriched in mitotic cell cycle, cell cycle, cell activation, cell cycle process, and cytokine production in GO term analysis (**Supplementary Figure S4**). Moreover, two immune-related pathways were also significant. In KEGG analysis ($p < 0.05$) (**Figure 2D**), cell cycle, cholesterol metabolism, pathways in cancer, and DNA replication were considered significant.

3.4 Co-Expression Network Analysis With Weighted Gene Co-Expression Network Analysis

Between genes have mutual induction and deter expression or synergy; these effects will result in the expression of related gene correlation between the amount, in the case of a large sample, the classification of gene expression was conducted more regularly, In this study, tens of thousands of genes were divided into 19 modules (color-coded) using WGCNA analysis with similar expression patterns, shown by the dendrogram (**Figure 3A**; **Supplementary Figure S5**), in which each tree branch constitutes a module, and each leaf in the branch is one gene. Due to the time-specific expression profile of the characteristic genes, 19 modular characteristic genes from 19 different modules were associated with different types of IM periods (**Figures 3B, C**). Through **Figure 3C**, we found MM. tan, MM. green, and MM. cyan modules that are significantly correlated with specific samples so that corresponding modules can be selected for further research (the module eigenvalue is equivalent to the weighted composite value of all gene expression levels in the module).

KEGG enrichment analysis was conducted for these three modules, focusing only on the lipid metabolism pathway, and

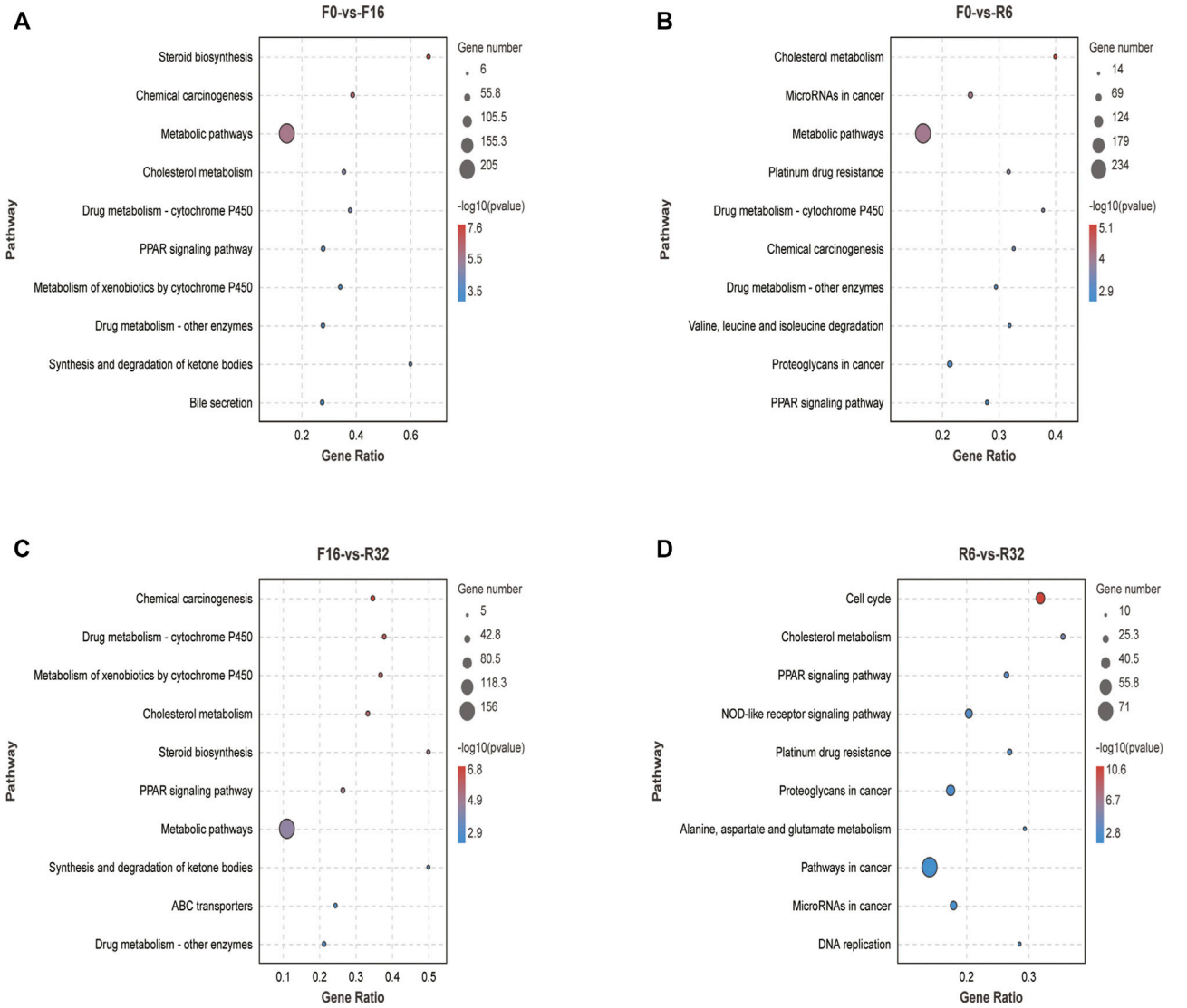

FIGURE 2 | KEGG enrichment analysis of different genes in comparison groups during IM. **(A)** F0-vs-F16. **(B)** F0-vs-R6. **(C)** F16-vs-R32. **(D)** R6-vs-R32.

then all genes (including genes with significant differences and genes with no significant differences) in the lipid metabolism pathway were selected for network interaction analysis, with the purpose of discovering those key genes neglected due to the transient expression. As shown in **Figure 3D**, a total of 43 genes were obtained through interaction. Using Cytoscape software, the connectivity of each gene was calculated. Generally, genes with high connectivity are regarded as hub genes. In the interaction network, the color of the gene gradually deepened as connectivity increased. Among them, AGPAT2F3, SGPL1, SPTLC1, PISD, and CYP51A1 are considered to have high connectivity and are the key genes in the network.

Then, we conducted co-expression network analysis between the selected genes in the module analysis and all the genes involved in lipid metabolism in the IM process (**Figure 4**) so as to dig out more potential core genes, which may have little difference in expression but are consistent with the expression trend of these different genes. We chose the top 10 genes; they were INS, SOAT1, ACSL1, CYP51A1, ACSL4, MSMO1, AGPAT2, Hsd3b7, GPAM, and NSDHL.

Transcriptome data showed significant changes in genes involved in lipid metabolism pathways in the liver of laying hens during IM, and the expression trends of these genes were similar to some extent (**Figure 5**). The expression of some genes (AGPAT2, SGPL1, PISD, CYP51A1, MSMO1, GPAM, and NSDHL) decreased gradually during starvation, with the degree of downregulation of these genes increasing as starvation time extended and gradually returning to their pre-experiment levels when feeding resumed. On the contrary, the expression levels of other genes (SPTLC1, SOAT1, ACSL1, ACSL4, and HSD3B7) were increasingly upregulated with the extension of starvation time and

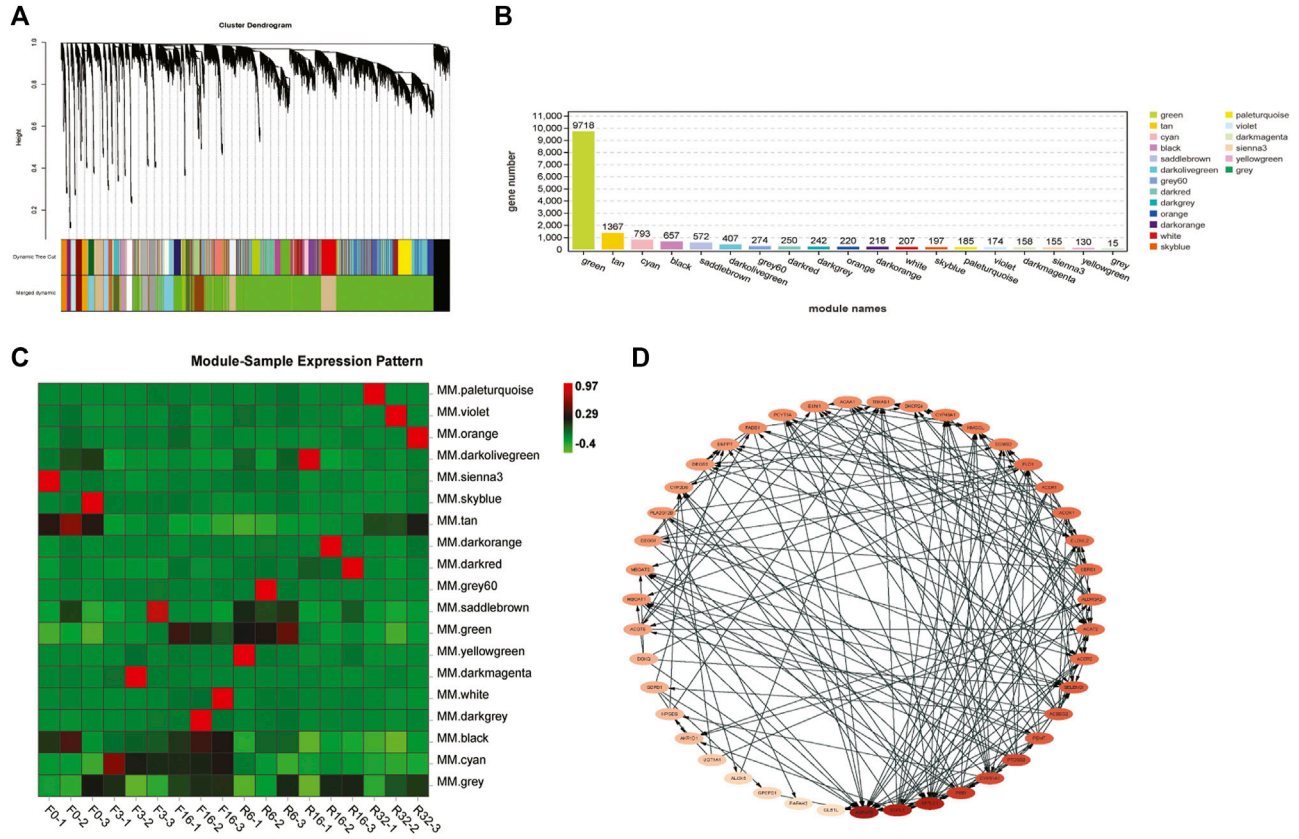

FIGURE 3 | WGCNA of genes in the liver. **(A)** Hierarchical cluster tree showing coexpression modules identified by WGCNA. Each leaf in the tree represents one gene. The major tree branches constitute 19 modules labeled with different colors. **(B)** Number of genes contained in each module. **(C)** Expression patterns of module genes in each sample are displayed by module eigenvalues. The value of module eigenvalues in each sample reflects the comprehensive expression level of all genes in each sample. **(D)** In selected modules, genes related to lipid metabolism interact with each other in the co-expression network, and the darker the color, the stronger the connectivity.

decreased to pre-experiment levels after resuming feeding for a period of time.

3.5 Metabolomics Profiling

Based on the transcriptome results, we selected five important stages (F0, F3, F16, R6, and R32) for cecal content metabolome sequencing of laying hens. Based on the transcriptome results, we selected five important stages (F0, F3, F16, R6, and R32) for cecal content metabolome sequencing of laying hens. The ionization source of LC/MS was electrospray ionization, which included positive (POS) and negative (NEG) ion modes. The QC samples were analyzed to detect the stability and repeatability of the system. The peak retention time (RT) and peak area of total ion chromatograms from all QC samples overlapped well, thereby indicating that the analytical system was stable (**Supplementary Figure S6**). A total of 2016 and 1,597 valid peaks were identified in the POS and the NEG modes, respectively, in metabolomics and matched 1781 (POS) and 1,448 (NEG) metabolites, respectively, in the metabolome based on the in-house MS2 database.

Principal component analysis (PCA) was performed on all samples and QC samples (**Figures 6A, B**), and the stability and reliability of instrumental analysis could be obtained by observing the dispersion between QC samples. Orthogonal least partial square discriminant analysis (OPLS-DA) is a derivative algorithm of PLS-DA. Compared with PLS-DA, OPLS-DA combines two methods of orthogonal signal correction (OSC) and PLS-DA, which can decompose the X matrix information into two types of information related to Y and irrelevant information. By removing the irrelevant differences, the relevant information is concentrated in the first predictive component. The OPLS-DA results were used to analyze subsequent model tests and differential metabolite screening (**Supplementary Figure S7**).

3.6 Differential Metabolite Screening

We combined the VIP value of multivariate statistical analysis OPLS-DA and the *t*-test *p*-value of univariate statistical analysis to screen the significantly differential metabolites between different comparison groups (Saccenti et al., 2014). The threshold for significant difference was VIP≥1 and *t*-test ($p < 0.05$). The

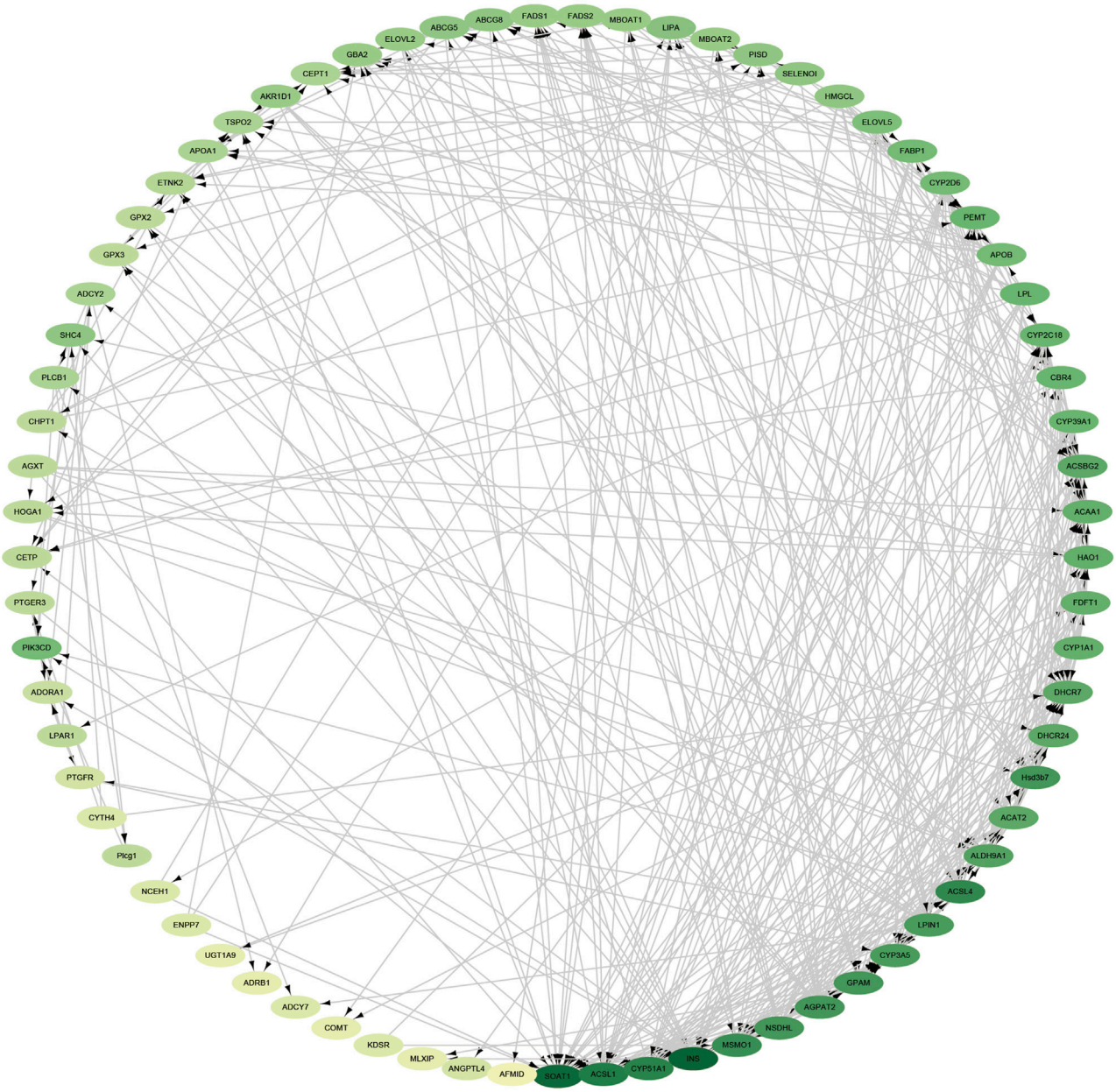

FIGURE 4 | WGCNA of genes associated with lipid metabolism. co-expression network interaction of all lipid metabolism–related genes [including genes derived from module analysis and genes in lipid metabolism-related pathways (did not require $p < 0.05$)], and the darker the color, the stronger the connectivity.

metabolite results with the significant differences are shown in (**Figure 6C**).

Subsequently, KEGG enrichment analysis (**Figure 6D**) was conducted for the differential metabolites, and the results showed that the differential metabolites were mainly enriched in amino acid metabolism, cancers, carbohydrate metabolism, cellular community eukaryotes, digestive system, environmental adaptation, excretory system, global and overview maps, immune system, lipid metabolism, and nervous system.

3.7 Integrated Analysis of the Transcriptome and Metabolome

We correlated all genes associated with lipid metabolism (genes with significant and nonsignificant differences) with metabolome data. As you can see (**Figure 7**), yellow represents genes and pink represents metabolites. The correlations between these genes and metabolites were all greater than 0.88 (both positive and negative). We correlated all genes associated with lipid metabolism (genes with significant and nonsignificant

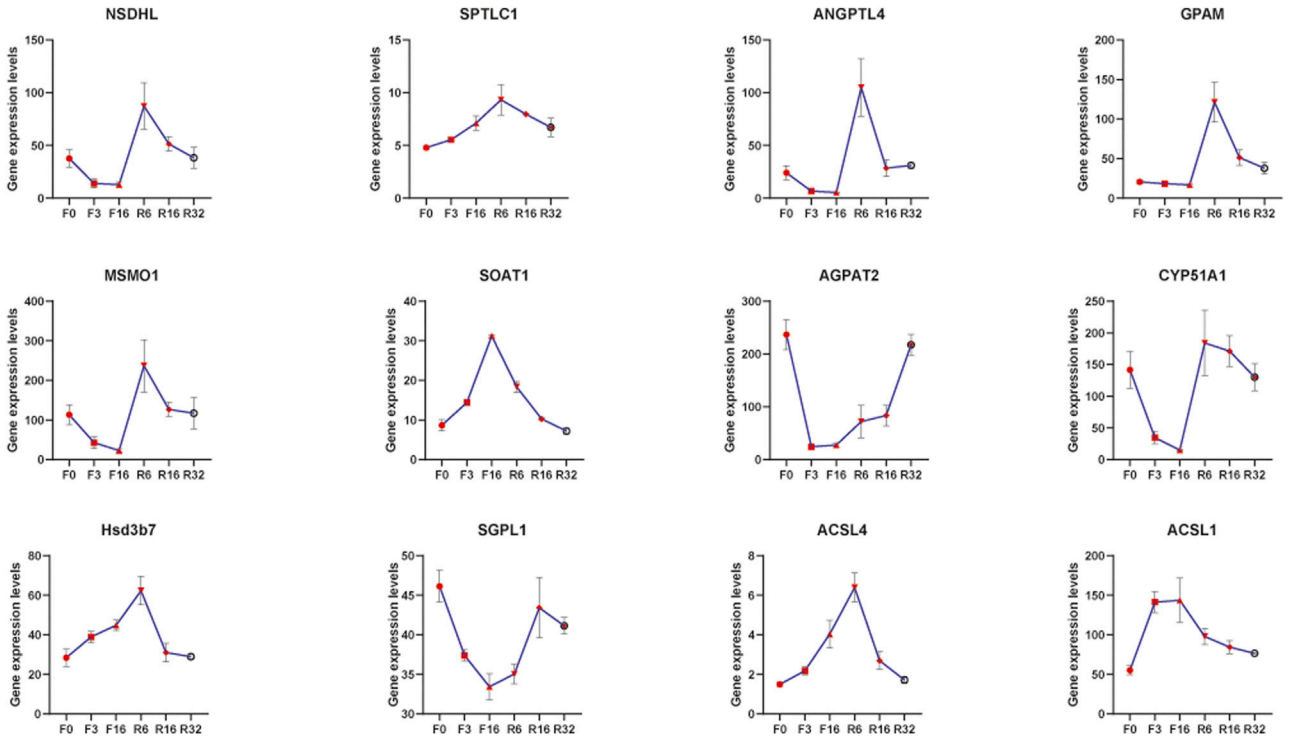

FIGURE 5 | Expression trends of genes related to lipid metabolism during IM.

differences) with metabolome data. We analyzed the connectivity of these genes and metabolites, and the top 20 were CYP2D6, CYP2J21, PISD, N-(5-acetamidopentyl) acetamide, hexamethylene bisacetamide, ABHD4, NDUFC2, SCD, 1-[6-(benzyloxy)-3-(tert-butyl)-2-hydroxyphenyl]Ethan1-one, CYP1A1, estrone, 2-(1,3-benzodioxol-5-yl)-5-(3-methoxybenzyl)-1,3,4-oxadiazole, 4-aminobenzoic_acid, 2-propylglutaric acid, ELOVL2, HSD17B12, PNPLA3, RQH, 5-fluoro-2-[(3S)-1-(2-methylbenzyl)-3-pyrrolidinyl]-1H-benzimidazole, and 2-methoxyestrone (the variation trend of these genes and metabolites during IM is described in **Supplementary Materials**).

4 DISCUSSION

4.1 Induced Molting can Improve the Performance of Laying Hens in the Next Laying Stage by Regulating Lipid Metabolism

Hunger is a physiological imbalance caused by lack of food or nutrition in the body. When the glucose level in the blood drops to the range of hypoglycemia, the body's compensation mechanism will be activated (Staehr et al., 2004). Hunger will increase the production of non-esterified fatty acids (NEFA) in adipose tissue and start the fat mobilization mechanism (Ensling et al., 2011). As an energy substance, fat has many advantages compared with other macromolecules. For example, fat can be stored in adipose tissue in the form of low water content and high energy density. The amount of fat in the body also varies widely (Lindström, 1991; Castellini and Rea, 1992). Lipolysis mainly includes the hydrolysis of triglycerides and the oxidation of fatty acids, in which the hydrolysis of triglycerides into fatty acids and glycerol happens under the joint action of triglyceride lipase, hormone-sensitive esterase, and lipoprotein esterase. Fatty acid oxidation is the formation of fatty acid esters coA under the action of esters coA synthase (ACSL) (Castellini and Rea, 1992). During IM, laying hens experienced long periods of starvation, and in the absence of external energy supplies, the hens used stored body fat to obtain energy; the expression levels of ACSL1 and ACSL4 were significantly upregulated during starvation.

It is well known that lipid metabolism and transport in the liver are closely related to the laying performance of laying hens (Liu et al., 2018). Cholesterol plays an important role in lipid metabolism. CYP51A1 (sterol 14alpha-demethylase) is a late regulator of cholesterol synthesis (Kojima et al., 2000; Degawa, 2006). In this study, the expression level of CYP51A1 decreased significantly in F3 and F16, which is due to the loss of energy supply and the lack of precursor substances in cholesterol synthesis of laying hens. After the energy supply was restored, CYP51A1 expression was significantly upregulated. The expression trend of MSMO1 (methylsterol monooxygenase) and NSDHL (sterol-4alpha-carboxylate 3-dehydrogenase) in the same pathway as CYP51A1 is similar to that of CYP51A1. After IM, the expression level of genes in the steroid biosynthesis

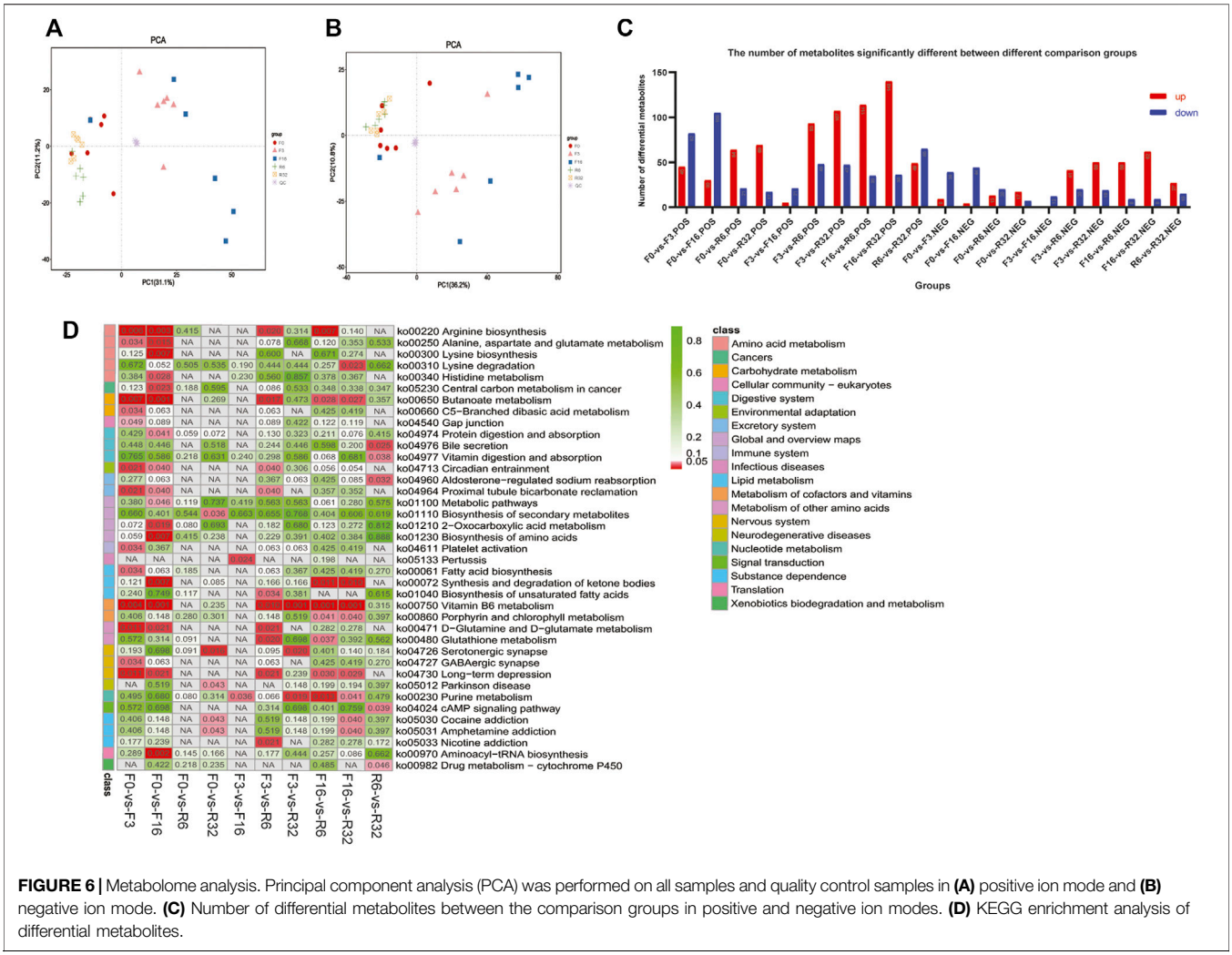

FIGURE 6 | Metabolome analysis. Principal component analysis (PCA) was performed on all samples and quality control samples in **(A)** positive ion mode and **(B)** negative ion mode. **(C)** Number of differential metabolites between the comparison groups in positive and negative ion modes. **(D)** KEGG enrichment analysis of differential metabolites.

pathway was downregulated and increased to the pre-experiment level and tended to exceed the pre-experiment gene expression level (**Figure 8**). Importantly, cholesterol is a precursor to estrogen (the steroid hormone). These results indicated that IM increased the laying rate of laying hens in the second laying cycle at the mRNA level, which was worthy of affirmation.

In addition, PISDs (phosphatidylserine decarboxylases), also known as phosphatidylserine decarboxylase, comprise pyridoxal phosphate and pyruvate. It is a key enzyme in the glycerophospholipid metabolism pathway (Marescaux, 2007). At F3 and F16, the expression of the PISD gene was significantly downregulated. The expression levels of PTDSS2, SELENOI, PEMT, PLD1, PLA2G12B, DGKQ, GPCPD1, GPAM, CEPT1, LPIN1, MBOAT2, and AGPAT2in the same pathway of PISD also showed a similar trend in the starvation stage. This indicates that the body preferentially uses the products of fat mobilization for energy supply (Thouzeau et al., 1997), rather than the production of phospholipids, which protect and regulate metabolism under the condition of long-term starvation. The expression levels of these genes were significantly upregulated when feeding resumed, and the laying hens had enough energy in their bodies. Egg lecithin is a kind of compound phospholipid extracted from egg yolk mainly comprising phosphatidyl choline, PC); phosphatidyl ethanolamine, PE); phosphatidyl inositol, PI); and phasphotidyl serine (PS). From the expression of related genes in the glycerolipid pathway, we can also see that the glycerolipid pathway is significantly active during the recovery stage of IM, possibly in preparation for the formation of egg yolk in the next laying stage.

4.2 Effects of Intestinal Microflora on Laying Performance of Laying Hens Through the"Gut-Liver Axis"

There are a large number of relatively stable microbial communities in the digestive tract of poultry. They play a very important role in maintaining the relative stability of the poultry gastrointestinal tract and nutrient digestion and absorption (Jiangrang, 2003; Ilina, 2016). The cecum is the most developed site of intestinal microorganisms in poultry (Jianhua, 2010; Kang et al., 2021; Pedroso et al., 2021). However, studies have found that gut microbes form a mutualistic symbiosis with their hosts during a long process of coevolution. Gut

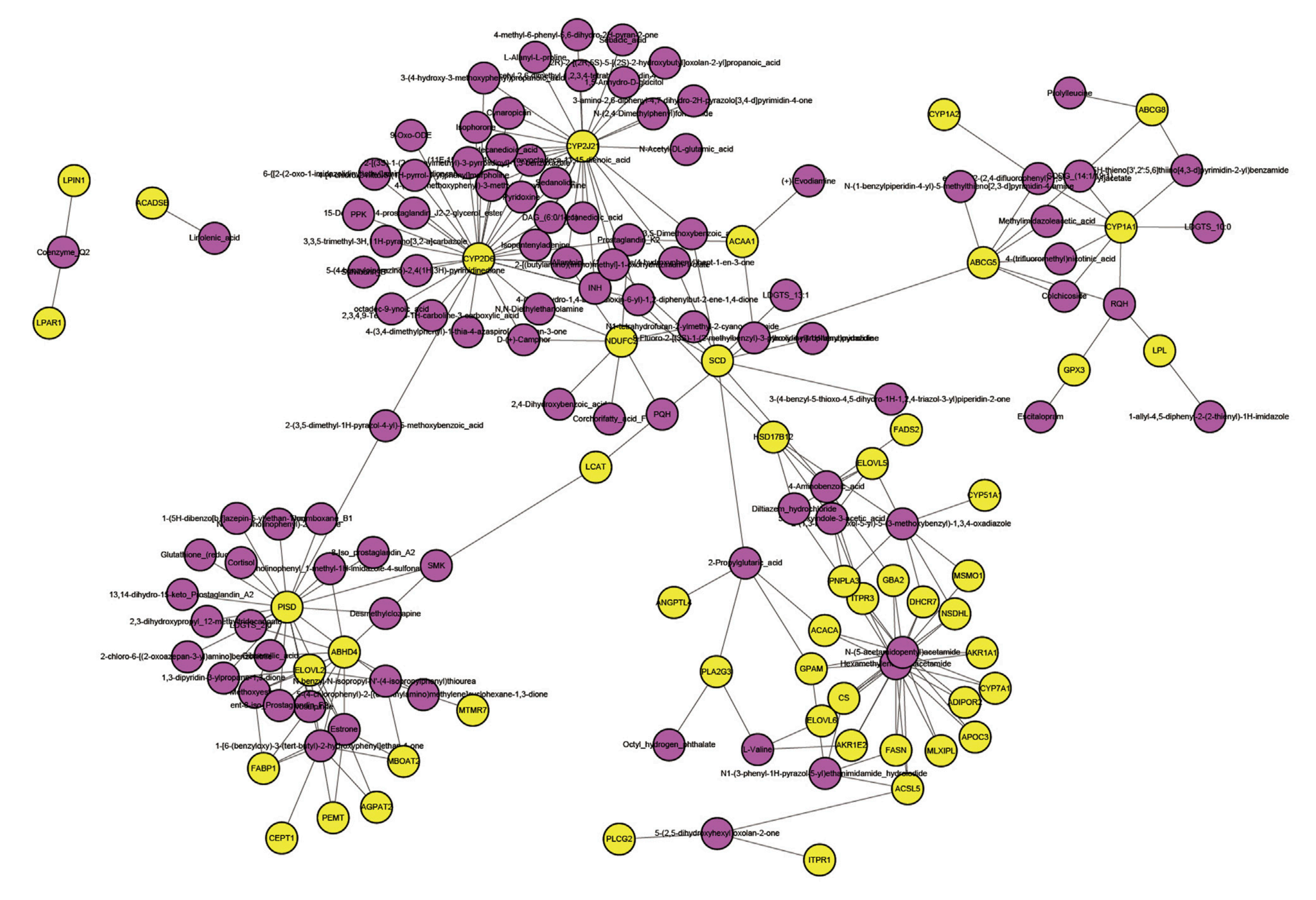

FIGURE 7 | Network interactions of key genes and differential metabolites; yellow represents genes and pink represents metabolites.

microbes can sense changes in the intestinal environment of the host while obtaining nutrients needed for survival, change the gene expression of the host and their own, and establish a mutualistic relationship with the host (Isberg and Barnes, 2002). In human medicine, there is growing evidence that changes in human genetic background, diet, and antibiotic treatment can affect gut microbes, which in turn affect host metabolism (Goodrich et al., 2014; Ting, 2014; Zhang et al., 2015). At present, there are more and more studies on the regulation of intestinal flora on metabolic diseases in the human body. Gut microbiome composition, changes, and imbalances are closely related to host metabolism and can affect a variety of diseases including obesity, type 2 diabetes, and inflammatory bowel disease. In animals, intestinal microorganisms have been confirmed to be closely related to lipid deposition in mice, pigs, and poultry (Guo et al., 2008; Emmanouil et al., 2010; Guo et al., 2010).

Some studies (Pi et al., 2017) have shown that the body and its intestinal microbes can metabolize and produce some small molecules, such as phenols, SCFAs, and bile salts, which play a crucial role in the association of information between host cells and host symbiotic microorganisms and in the health of the body. The metabolites in the cecum are closely related to the life activities and material metabolism of the body.

In this study, we also found significant changes in metabolites in the cecum (**Figure 9**). In our results, colchicine content increased significantly at F3 and F16 but decreased to the pre-experiment level after resuming feeding. In clinical medicine, colchicine is mainly used for the treatment of acute gout, but it has toxic side effects; colchicine can cause liver damage in rats. Colchicine inhibits the expression of nuclear receptor FXR, resulting in the imbalance of bile acid regulation in hepatocytes (Yan-Yan et al., 2018). In this study, the gene associated with colchicine was CYP1A1(cytochrome P450 family 1 subfamily A member 1), and the expression trend of this gene was similar to the change in colchicine content. Studies have shown that CYP1A1 is related to hormone and metabolism of a variety of exogenous toxic substances, such as benzopyrene and dioxins. Moreover, the expression of CYP1A1 gene polymorphism is closely related to the susceptibility of cervical cancer, prostate cancer, childhood acute leukemia, lung cancer, esophageal cancer, and other tumors (Nerurkar et al., 2000). At F3, in terms of the growth rate of colchicine and CYPA1, colchicine content increased faster than CYP1A1 expression. These results indicate that cecal metabolites do affect gene expression in the liver and further demonstrate that intestinal microorganisms and their metabolites play a regulatory role in the metabolic activities of the body.

Furthermore, microorganisms can also regulate lipid metabolism. Angiopoietin-like protein 4 (ANGPTL4)

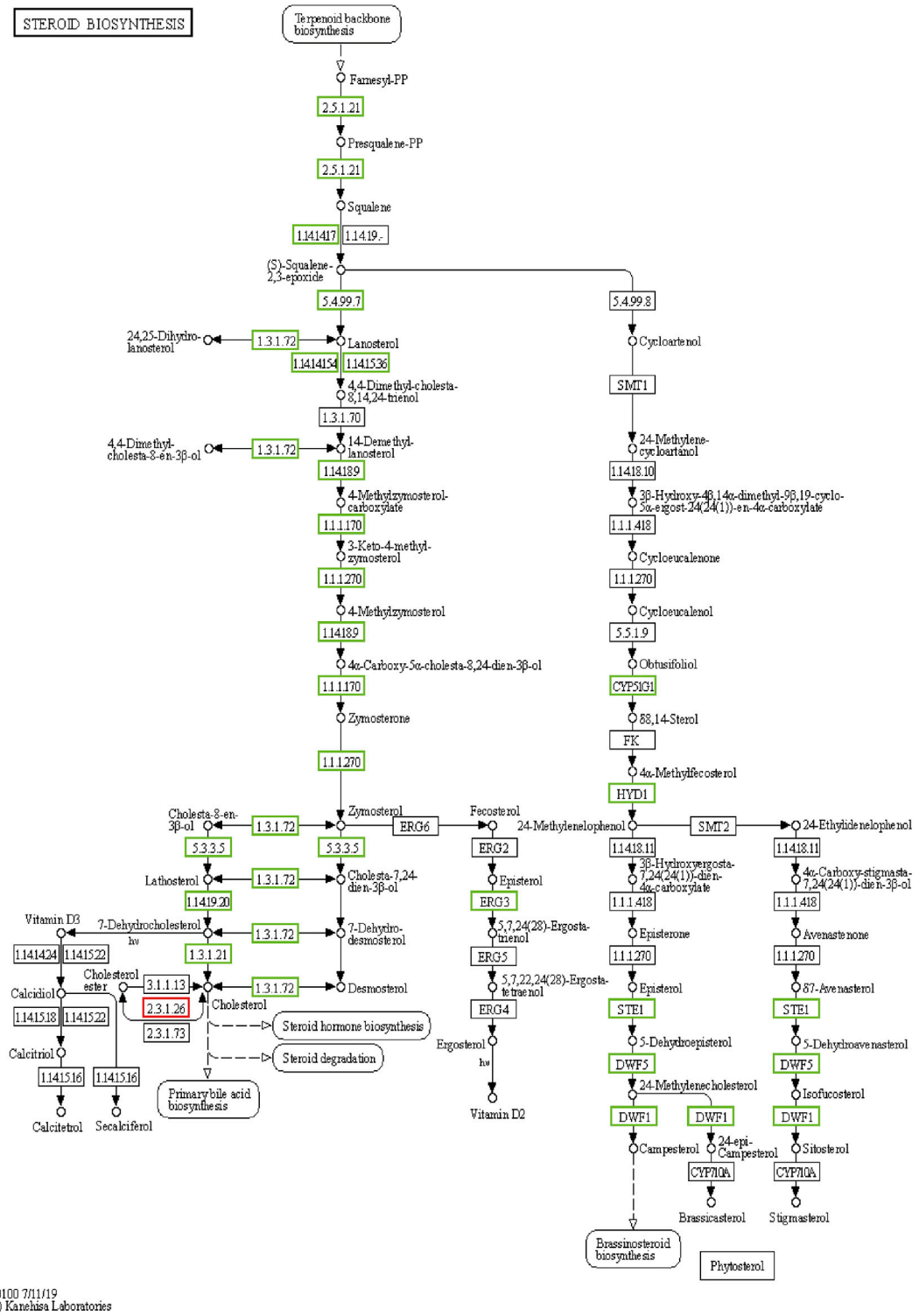

FIGURE 8 | Multiple genes in the F0-VS-F16 steroid biosynthesis pathway were significantly downregulated during IM.

(Aimin, 2005; Alex et al., 2013), also known as fasting inducer factor (FIAF), is a protein closely related to fat metabolism in animals. Studies have shown that overexpression of ANGPTL4 can induce hepatic enlargement and fatty liver formation in mice (Aimin, 2005; Yi, 2016). Some scholars have found that intestinal microorganisms can regulate the expression of

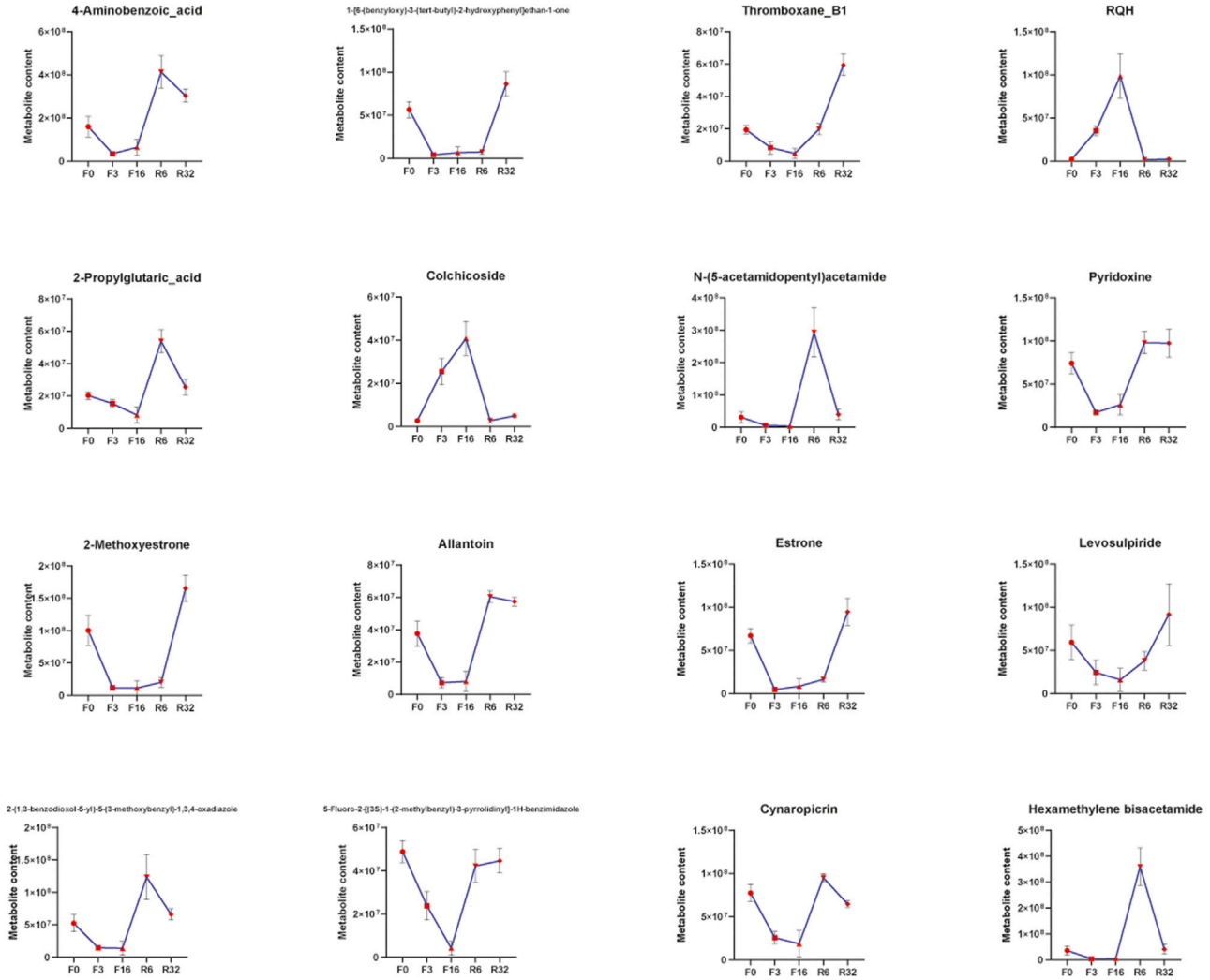

FIGURE 9 | Changes in metabolite content during IM.

ANGPTL4 in intestinal epithelial cells directly or indirectly (metabolites) (Grootaert et al., 2011). Some researchers have also found that intestinal microbial metabolites have a regulatory effect on host ANGPTL4, thus affecting host lipid metabolism (Zhao et al., 2014). In this study, ANGPTL4 was downregulated at F3 and F16 and significantly upregulated and exceeded the expression level at F0 after resuming feeding. The cecal metabolite associated with ANGPTL4 is 2-propyl glutaric acid, and its content variation trend is related to ANGPTL4.

In addition, estrogen content decreased significantly at F3 and F16 and increased significantly at R6 and R16, higher than the level before the test, which was consistent with the expression trend of PISD, AGPAT2, MBOAT2, and PEMT. After 32 days of recovery, the level of estrogen in laying hens was much higher than the level before the experiment. After IM, the level of estrogen was regulated by increasing PISD, AGPAT2, MBOAT2, and PEMT gene expression to stimulate the laying performance of laying hens so as to enter a new reproductive cycle.

In conclusion, intestinal microbes are closely related to metabolic activities, especially lipid metabolism, of their hosts. However, lipid metabolism in poultry liver is closely related to laying performance. Therefore, it is reasonable to believe that microorganisms and their metabolites in the cecum of laying hens are related to laying performance.

5 CONCLUSION

During IM, laying hens had a great influence on the liver and gut, but as to the recovery of food intake, laying hens in the second cycle of egg production rate and egg quality show improvement, and our research results show that in the whole experiment process, laying hens in the cecum metabolites and

genes in the liver do have interaction relations; however, whether this relationship is two-way interaction or one-way regulation remains to be studied, which also points out the direction for our next research.

DATA AVAILABILITY STATEMENT

The original contributions presented in the study are publicly available. This data can be found here BioProject: PRJNA811637. The database connection: https://dataview.ncbi.nlm.nih.gov/object/PRJNA811637.

ETHICS STATEMENT

The animal study was reviewed and approved by the Institutional Animal Care and Use Committee (IACUC) of Henan Agricultural University, China (11-0099). Written informed consent was obtained from the owners for the participation of their animals in this study.

AUTHOR CONTRIBUTIONS

RJ conceived and designed the experiment. YZ, XZ, and PZ contributed to animal breeding and the collection of experimental samples. XG took part in the experiment. GS, WL, and DL provided guidance on data analysis. XL and GL directed this experimental technique. XK, YT, and RH helped revise the manuscript. JZ wrote the manuscript. All authors reviewed and approved the final draft.

FUNDING

This work was supported by China Agriculture Research System of MOF and MARA (CARS-40), the Program for Innovative Research Team (in Science and Technology) in University of Henan Province (21IRTSTHN022), and the Scientific Studio of Zhongyuan Scholars (No. 30601985).

ACKNOWLEDGMENTS

Thanks for my team, Henan Innovative Engineering Research Center of Poultry Germplasm Resource. We are grateful to/thank Guangzhou Genedenovo Biotechnology Co., Ltd. for assisting in sequencing and/or bioinformatics analysis.

SUPPLEMENTARY MATERIAL

The Supplementary Material for this article can be found online at: https://www.frontiersin.org/articles/10.3389/fphys.2022.862721/full#supplementary-material

REFERENCES

Abg, F. (2008). Forced-Molting Methods and Their Effects on the Performance and Egg Quality of Japanese Quails (*Coturnix japonica*) in the Second Laying Cycle. *Braz. J. Poult. Sci.* 10 (1), 53–57. doi:10.1590/S1516-635X2008000100008

Aimin, L. (2005). "Angiopoietin-like Protein 4 Decreases Blood Glucose and Improves Glucose Tolerance but Induces Hyperlipidemia and Hepatic Steatosis in Mice," in Proceedings of the National Academy of Sciences of the United States of America.

Alex, S., Lange, K., Amolo, T., Grinstead, J. S., Haakonsson, A. K., Szalowska, E., et al. (2013). Short-Chain Fatty Acids Stimulate Angiopoietin-like 4 Synthesis in Human Colon Adenocarcinoma Cells by Activating Peroxisome Proliferator-Activated Receptor γ. *Mol. Cell Biol* 33 (7), 1303–1316. doi:10.1128/mcb.00858-12

Alodan, M., and Mashaly, M. (1999). Effect of Induced Molting in Laying Hens on Production and Immune Parameters. *Poult. Sci.* 78 (2), 171–177. doi:10.1093/ps/78.2.171

Arai, M., Yokosuka, O., Chiba, T., Imazeki, F., Kato, M., Hashida, J., et al. (2003). Gene Expression Profiling Reveals the Mechanism and Pathophysiology of Mouse Liver Regeneration. *J. Biol. Chem.* 278, 29813–29818. doi:10.1074/jbc.M212648200

As, A. (2021). Identification and Expression Analysis of MicroRNAs in Chicken Spleen in a Corticosterone-Induced Stress Model. *Res. Vet. Sci.* 136, 287–296. doi:10.1016/j.rvsc.2021.02.023

Ashburner, M. (2000). Gene Ontology: Tool for the Unification of Biology. *Nat. Genet* 25, 25–29. doi:10.1038/75556

Bedu, E., Chainier, F., Sibille, B., Meister, R., Dallevet, G., Garin, D., et al. (2002). Increased Lipogenesis in Isolated Hepatocytes from Cold-Acclimated Ducklings. *Am. J. Physiology-Regulatory, Integr. Comp. Physiol.* 283 (5), R1245–R1253. doi:10.1152/ajpregu.00681.2001

Bell, D. (2003). Historical and Current Molting Practices in the U.S. Table Egg Industry. *Poult. Sci.*82, 965–970.doi:10.1093/ps/82.6.965

Benjamini, Y., and Hochberg, Y. (1995). Controlling the False Discovery Rate: A Practical and Powerful Approach to Multiple Testing. *J. R. Stat. Soc. Ser. B (Methodological)* 57 (1), 289–300. doi:10.1111/j.2517-6161.1995.tb02031.x

Berry, W. (2003). The Physiology of Induced Molting. *Poult. Sci.* 82 (6), 971–980. doi:10.1093/ps/82.6.971

Bouhaddani, S. E., Houwing-Duistermaat, J., Salo, P., Perola, M., Jongbloed, G., Uh, H. W., et al. (2016). Evaluation of O2PLS in Omics Data Integration. *BMC Bioinformatics* 17 (S2), 11. doi:10.1186/s12859-015-0854-z

Brady, L., Romsos, D. R., and Leveille, G. A. (1976). *In Vivo* estimation of Fatty Acid Synthesis in the Chicken (*Gallus domesticus*) Utilizing 3H2O. *Comp. Biochem. Physiol. B: Comp. Biochem.* 54 (3), 403–407. doi:10.1016/0305-0491(76)90265-0

Brake, J. (1993). Recent Advances in Induced Molting. *Poult. Sci.* 72 (5), 929–931. doi:10.3382/ps.0720929

Breeding, S. W., Brake, J., Garlich, J. D., and Johnson, A. L. (1992). Molt Induced by Dietary Zinc in a Low-Calcium Diet. *Poult. Sci.* 71 (1), 168–180. doi:10.3382/ps.0710168

Butler, E. J. (1975). Lipid Metabolism in the Fowl under normal and Abnormal Circumstances. *Proc. Nutr. Soc.* 34 (01), 29–34. doi:10.1079/pns19750007

Bylesjö, M., Eriksson, D., Kusano, M., Moritz, T., and Trygg, J. (2010). Data Integration in Plant Biology: the O2PLS Method for Combined Modeling of Transcript and Metabolite Data. *Plant J.* 52 (6), 1181–1191. doi:10.1111/j.1365-313X.2007.03293.x

Castellini, M. A., and Rea, L. D. (1992). The Biochemistry of Natural Fasting at its Limits. *Experientia* 48 (6), 575–582. doi:10.1007/bf01920242

Chen, S., Zhou, Y., Chen, Y., and Gu, J. (2018). *Fastp : An Ultra-Fast All-In-One FASTQ Preprocessor*. Biorxiv, 274100. doi:10.1101/274100v2

Compare, D., Coccoli, P., Rocco, A., Nardone, O. M., De Maria, S., Cartenì, M., et al. (2012). Gut-Liver Axis: The Impact of Gut Microbiota on Non Alcoholic

Fatty Liver Disease. *Nutr. Metab. Cardiovasc. Dis.* 22 (6), 471–476. doi:10.1016/j.numecd.2012.02.007

Csardi, G., and Nepusz, T. (2006). *The Igraph Software Package for Complex Network Research*. Interjournal Complex Systems, 1695.

David, H. A. (2014). *Novel Therapies in Chronic Liver Disease*. Monash University. Faculty of Medicine, Nursing and Health Sciences. Department of Medicine, Monash Medical Centre.

Degawa, T. M. (2006). Cloning of Chicken Lanosterol 14α-Demethylase (CYP51) cDNA: Discovery of a Testis-specific CYP51 Transcript. *Comp. Biochem. Physiol. A: Mol. Integr. Physiol.* 145 (3), 383–389. doi:10.1016/j.cbpa.2006.07.012

Dou, Y., Gregersen, S., Zhao, J., Zhuang, F., and Gregersen, H. (2002). Morphometric and Biomechanical Intestinal Remodeling Induced by Fasting in Rats. *Dig. Dis. Sci.* 47 (5), 1158–1168. doi:10.1023/a:1015019030514

Dunn, W. B., Broadhurst, D., Begley, P., Zelena, E., Francis-McIntyre, S., Anderson, N., et al. (2018). Procedures for Large-Scale Metabolic Profiling of Serum and Plasma Using Gas Chromatography and Liquid Chromatography Coupled to Mass Spectrometry. *Nat. Protoc.* 67 (67), 1060–1083. doi:10.1038/nprot.2011.335

Emmanouil, A., Didier, R., and Stefan, B. (2010). The Increase of Lactobacillus Species in the Gut Flora of Newborn Broiler Chicks and Ducks Is Associated with Weight Gain. *Plos One* 5 (5), e10463. doi:10.1371/journal.pone.0010463

Ensling, M., Steinmann, W., and Whaley-Connell, A. (2011). Hypoglycemia: A Possible Link between Insulin Resistance, Metabolic Dyslipidemia, and Heart and Kidney Disease (The Cardiorenal Syndrome). *Cardiorenal Med.* 1 (1), 67–74. doi:10.1159/000322886

Ernst, J., and Bar-Joseph, Z. (2006). STEM: a Tool for the Analysis of Short Time Series Gene Expression Data. *Bmc Bioinformatics* 7 (1), 191. doi:10.1186/1471-2105-7-191

Ferraris, R. P., and Carey, H. V. (2000). Intestinal Transport during Fasting and Malnutrition. *Annu. Rev. Nutr.* 20 (1), 195–219. doi:10.1146/annurev.nutr.20.1.195

Furchtgott, L. A., Chow, C. C., and Periwal, V. (2009). A Model of Liver Regeneration. *Biophysical J.* 96 (10), 3926–3935. doi:10.1016/j.bpj.2009.01.061

Gebert, N., Cheng, C.-W., Kirkpatrick, J. M., Di Fraia, D., Yun, J., Schädel, P., et al. (2020). Region-Specific Proteome Changes of the Intestinal Epithelium during Aging and Dietary Restriction. *Cell Rep.* 31 (4), 107565. doi:10.1016/j.celrep.2020.107565

Gérard, P. (2008). Characterization of Cecal Microbiota and Response to an Orally Administered Lactobacillus Probiotic Strain in the Broiler Chicken. *J. Mol. Microbiol. Biotechnol.* 14 (1-3), 115–122. doi:10.1080/10420940600864514

Goodrich, J. K., Waters, J. L., Poole, A. C., Sutter, J. L., Koren, O., Blekhman, R., et al. (2014). Human Genetics Shape the Gut Microbiome. *Cell* 159 (4), 789–799. doi:10.1016/j.cell.2014.09.053

Grootaert, C., Van de Wiele, T., Van Roosbroeck, I., Possemiers, S., Vercoutter-Edouart, A.-S., Verstraete, W., et al. (2011). Bacterial Monocultures, Propionate, Butyrate and H2O2 Modulate the Expression, Secretion and Structure of the Fasting-Induced Adipose Factor in Gut Epithelial Cell Lines. *Environ. Microbiol.* 13 (7), 1778–1789. doi:10.1111/j.1462-2920.2011.02482.x

Guo, X., Xia, X., Tang, R., Zhou, J., Zhao, H., and Wang, K. (2010). Development of a Real-Time PCR Method for Firmicutes and Bacteroidetes in Faeces and its Application to Quantify Intestinal Population of Obese and Lean Pigs. *Lett. Appl. Microbiol.* 47, 367–373. doi:10.1111/j.1472-765X.2008.02408.x

Guo, X., Xia, X., Tang, R., and Wang, K. (2008). Real-time PCR Quantification of the Predominant Bacterial Divisions in the Distal Gut of Meishan and Landrace Pigs. *Anaerobe* 14 (4), 224–228. doi:10.1016/j.anaerobe.2008.04.001

Hussain, M., Umair Ijaz, M., Ahmad, M. I., Khan, I. A., Bukhary, S. U. F., Khan, W., et al. (2020). Gut Inflammation Exacerbates Hepatic Injury in C57BL/6J Mice via Gut-Vascular Barrier Dysfunction with High-Fat-Incorporated Meat Protein Diets. *Food Funct.* 11, 9168–9176. doi:10.1039/d0fo02153a

Ilina, L. A. (2016). Metagenomic Bacterial Community Profiles of Chicken Embryo Gastrointestinal Tract by Using T-RFLP Analysis. *Doklady Biochem. Biophys.* 466 (1), 47–51. doi:10.1134/S1607672916010130

Isberg, R. R., and Barnes, P. (2002). Dancing with the Host. *Cell* 110 (1), 1–4. doi:10.1016/s0092-8674(02)00821-8

Jiangrang (2003). Diversity and Succession of the Intestinal Bacterial Community of the Maturing Broiler Chicken. *Appl. Environ. Microbiol.* 69 (11), 6816–6824. doi:10.1038/85758

Jianhua, G. (2010). 16S rRNA Gene-Based Analysis of Mucosa-Associated Bacterial Community and Phylogeny in the Chicken Gastrointestinal Tracts: from Crops to Ceca. *Fems Microbiol. Ecol.* (1), 147–157. doi:10.1111/j.1574-6941.2006.00193.x

Kang, K., Hu, Y., Wu, S., and Shi, S. (2021). Comparative Metagenomic Analysis of Chicken Gut Microbial Community, Function, and Resistome to Evaluate Noninvasive and Cecal Sampling Resources. *Animals* 11 (6), 1718. doi:10.3390/ani11061718

Klasing, K. C. (1998). Nutritional Modulation of Resistance to Infectious Diseases. *Poult. Sci.* 77 (8), 1119–1125. doi:10.1093/ps/77.8.1119

Kohl, K. D., Amaya, J., Passement, C. A., Dearing, M. D., and McCue, M. D. (2014). Unique and Shared Responses of the Gut Microbiota to Prolonged Fasting: a Comparative Study across Five Classes of Vertebrate Hosts. *FEMS Microbiol. Ecol.* 90 (3), 883–894. doi:10.1111/1574-6941.12442

Kojima, M., Morozumi, T., Onishi, A., and Mitsuhashi, T. (2000). Structure of the Pig Sterol 14 -Demethylase (CYP51) Gene and its Expression in the Testis and Other Tissues. *J. Biochem.* 127 (5), 805–811. doi:10.1093/oxfordjournals.jbchem.a022673

Kolde, R. (2015). *Pheatmap: Pretty Heatmaps*.

Leveille, G. A., Romsos, D. R., Yeh, Y.-Y., and O'Hea, E. K. (1975). Lipid Biosynthesis in the Chick. A Consideration of Site of Synthesis, Influence of Diet and Possible Regulatory Mechanisms. *Poult. Sci.* 54 (4), 1075–1093. doi:10.3382/ps.0541075

Li, D., Wang, X., Fu, Y., Zhang, C., Cao, Y., Wang, J., et al. (2013). Transcriptome Analysis of the Breast Muscle of Xichuan Black-Bone Chickens Under Tyrosine Supplementation Revealed the Mechanism of Tyrosine-Induced Melanin Deposition. *Front. Genet.* 10, 457. doi:10.3389/fgene.2019.00457

Li, H., Gu, Z., Yang, L., Tian, Y., Kang, X., and Liu, X. (2018). Transcriptome Profile Analysis Reveals an Estrogen Induced LncRNA Associated with Lipid Metabolism and Carcass Traits in Chickens (Gallus Gallus). *Cell Physiol Biochem* 50, 1638–1658. doi:10.1159/000494785

Li, W., Liang, X., Leu, J. I., Kovalovich, K., Ciliberto, G., and Taub, R. (2001). Global Changes in Interleukin-6-dependent Gene Expression Patterns in Mouse Livers after Partial Hepatectomy. *Hepatology* 33 (6), 1377–1386. doi:10.1053/jhep.2001.24431

Lindström, Å. (1991). Maximum Fat Deposition Rates in Migrating Birds. *Ornis Scand. (Scandinavian J. Ornithology)* 22 (1), 12–19. doi:10.2307/3676616

Liu, X.-T., Lin, X., Mi, Y.-L., Zeng, W.-D., and Zhang, C.-Q. (2018). Age-Related Changes of Yolk Precursor Formation in the Liver of Laying Hens. *J. Zhejiang Univ. Sci. B* 19 (5), 390–399. doi:10.1631/jzus.B1700054

Love, M. I., Huber, W., and Anders, S. (2014). Moderated Estimation of Fold Change and Dispersion for RNA-Seq Data with DESeq2. *Genome Biol.* 15 (12), 550. doi:10.1186/s13059-014-0550-8

Luo, L., Wang, Q., and Ma, F. (2021). RNA-seq Transcriptome Analysis of Ileum in Taiping Chicken Supplemented with the Dietary Probiotic. *Trop. Anim. Health Prod.* 53 (1), 131. doi:10.1007/s11250-021-02566-w

Marescaux, J. (2007). Surgery without Scars. *Arch. Surg.* 142 (9), 823–826. doi:10.1001/archsurg.142.9.823

Marisa, L. (2013). *KEGG: Kyoto Encyclopedia of Genes and Genomes*. doi:10.1093/nar/27.1.29

Michalsen, A., Riegert, M., Lüdtke, R., Bäcker, M., Langhorst, J., Schwickert, M., et al. (2005). Mediterranean Diet or Extended Fasting's Influence on Changing the Intestinal Microflora, Immunoglobulin A Secretion and Clinical Outcome in Patients with Rheumatoid Arthritis and Fibromyalgia: an Observational Study. *BMC Complement. Altern. Med.* 5, 22. doi:10.1186/1472-6882-5-22

Nerurkar, P. V., Okinaka, L., Aoki, C., Seifried, A., Lum-Jones, A., Wilkens, L. R., et al. (2000). CYP1A1, GSTM1, and GSTP1 Genetic Polymorphisms and Urinary 1-hydroxypyrene Excretion in Non-occupationally Exposed Individuals. *Cancer Epidemiol. Biomarkers Prev.* 9 (10), 1119–1122.

Onbaşılar, E. E., and Erol, H. (2007). Effects of Different Forced Molting Methods on Postmolt Production, Corticosterone Level, and Immune Response to Sheep Red Blood Cells in Laying Hens. *J. Appl. Poult. Res.* 16 (4), 529–536. doi:10.3382/japr.2006-00089

Paolella, G. (2014). Gut-Liver Axis and Probiotics: Their Role in Non-alcoholic Fatty Liver Disease. *World J. Gastroenterol.* doi:10.3748/wjg.v20.i42.15518

Patterson, R. E., Laughlin, G. A., LaCroix, A. Z., Hartman, S. J., Natarajan, L., Senger, C. M., et al. (2015). Intermittent Fasting and Human Metabolic Health. *J. Acad. Nutr. Diet.* 115 (8), 1203–1212. doi:10.1016/j.jand.2015.02.018

Pedroso, A. A., Lee, M. D., and Maurer, J. J. (2021). Strength Lies in Diversity: How Community Diversity Limits Salmonella Abundance in the Chicken Intestine. *Front. Microbiol.* 12, 694215. doi:10.3389/fmicb.2021.694215

Pi, Y., Gao, K., and Zhu, W. (2017). Advances in Host-Microbe Metabolic axis. *Wei Sheng Wu Xue Bao* 57 (2), 161–169. doi:10.13343/j.cnki.wsxb.20160180

Saccenti, E., Hoefsloot, H. C. J., Smilde, A. K., Westerhuis, J. A., and Hendriks, M. M. W. B. (2014). Reflections on Univariate and Multivariate Analysis of Metabolomics Data. *Metabolomics* 10 (3), 361–374. doi:10.1007/s11306-013-0598-6

Sandhu, M. A., Rahman, Z. U., and Rahman, S. U. (2007). Effects of Induced Moking on Some Immunological Parameters in Laying Hens (*Gallus domesticus*). *Archiv fur Geflugelkunde* 71, 110–116.

Shannon, P., Ozier, O., Baliga, N. S., Wang, J. T., Ramage, D., Amin, N., et al. (2003). Cytoscape: A Software Environment for Integrated Models of Biomolecular Interaction Networks. *Genome Res.* 13 (11), 2498–2504. doi:10.1101/gr.1239303

Smyth, G. K. (2010). edgeR: a Bioconductor Package for Differential Expression Analysis of Digital Gene Expression Data. *Bioinformatics* 26 (1), 139. doi:10.1093/bioinformatics/btp616

Staehr, P., Hother-Nielsen, O., and Beck-Nielsen, H. (2004). The Role of the Liver in Type 2 Diabetes. *Rev. Endocr. Metab. Disord.* 5 (2), 105–110. doi:10.1023/b:remd.0000021431.90494.0c

Szabo, A., Febel, H., Mezes, M., Horn, P., Balogh, K., and Romvari, R. (2005). Differential Utilization of Hepatic and Myocardial Fatty Acids during Forced Molt of Laying Hens. *Poult. Sci.* 84 (1), 106–112. doi:10.1093/ps/84.1.106

Thouzeau, C., Massemin, S., and Handrich, Y. (1997). Bone Marrow Fat Mobilization in Relation to Lipid and Protein Catabolism during Prolonged Fasting in Barn Owls. *J. Comp. Physiol. B: Biochem. Systemic, Environ. Physiol.* 167 (1), 17–24. doi:10.1007/s003600050043

Ting, X. U. (2014). Host-gut Microbiota Metabolic Interactions. *Chin. J. Microecology* 336 (6086), 1262–1267. doi:10.1126/science.1223813

Wang, X. (2019). *Combined Transcriptomics and Proteomics Forecast Analysis for Potential Genes Regulating the Columbian Plumage Color in Chickens*.

Want, E. J. (2006). XCMS: Processing Mass Spectrometry Data for Metabolite Profiling Using Nonlinear Peak Alignment, Matching, and Identification. *Anal. Chem.* 78 (3), 779–787. doi:10.1021/ac051437y

Yi, W. (2016). Angiopoietin-like Protein4 Improves Glucose Tolerance and Insulin Resistance but Induces Liver Steatosis in High-Fat-Diet Mice. *Mol. Med. Rep.* 14 (4), 3293. doi:10.3892/mmr.2016.5637

Yan-Yan, Z., Chao-Xu, Z., Yu, L., Xuan, J., Yong-Fang, W., Yang, S., et al. (2018). Development of a Novel Rat Model of Heterogeneous Hepatic Injury by Injection with Colchicine via the Splenic Vein. *World J. Gastroenterol.* 2018 24, 50–57. doi:10.3748/wjg.v24.i44.5005

Zelena, E., Dunn, W. B., Broadhurst, D., Francis-McIntyre, S., Carroll, K. M., Begley, P., et al. (2009). Development of a Robust and Repeatable UPLC–MS Method for the Long-Term Metabolomic Study of Human Serum. *Anal. Chem.* 81 (4), 1357–1364. doi:10.1021/ac8019366

Zhang, C., Yin, A., Li, H., Wang, R., Wu, G., and Shen, J. (2015). Dietary Modulation of Gut Microbiota Contributes to Alleviation of Both Genetic and Simple Obesity in Children. *Ebiomedicine* 10, 968–984. doi:10.1016/j.ebiom.2015.07.007

Zhang, T. (2021). Transcriptomic Analysis of Laying Hens Revealed the Role of Aging-Related Genes during Forced Molting. *Genes (Basel)* 12 (11). doi:10.3390/genes12111767

Zhao, X., Guo, Y., Liu, H., Gao, J., and Nie, W. (2014). Clostridium Butyricum Reduce Lipogenesis through Bacterial wall Components and Butyrate. *Appl. Microbiol. Biotechnol.* 98 (17), 7549–7557. doi:10.1007/s00253-014-5829-x

Zhen, T. (2019). Characterization of the Cecal Microbiome Composition of Wenchang Chickens before and after Fattening. *PloS one* 14 (12), e0225692. doi:10.1371/journal.pone.0225692

Conflict of Interest: The authors declare that the research was conducted in the absence of any commercial or financial relationships that could be construed as a potential conflict of interest.

Publisher's Note: All claims expressed in this article are solely those of the authors and do not necessarily represent those of their affiliated organizations, or those of the publisher, the editors, and the reviewers. Any product that may be evaluated in this article, or claim that may be made by its manufacturer, is not guaranteed or endorsed by the publisher.

Advantages of publishing in Frontiers

OPEN ACCESS
Articles are free to read for greatest visibility and readership

FAST PUBLICATION
Around 90 days from submission to decision

HIGH QUALITY PEER-REVIEW
Rigorous, collaborative, and constructive peer-review

TRANSPARENT PEER-REVIEW
Editors and reviewers acknowledged by name on published articles

Frontiers
Avenue du Tribunal-Fédéral 34
1005 Lausanne | Switzerland

Visit us: www.frontiersin.org
Contact us: frontiersin.org/about/contact

REPRODUCIBILITY OF RESEARCH
Support open data and methods to enhance research reproducibility

DIGITAL PUBLISHING
Articles designed for optimal readership across devices

FOLLOW US
@frontiersin

IMPACT METRICS
Advanced article metrics track visibility across digital media

EXTENSIVE PROMOTION
Marketing and promotion of impactful research

LOOP RESEARCH NETWORK
Our network increases your article's readership